Deciphering Cryptic Stereochemistry in Polyketide Biosynthesis and Functional Characterization of β-processing Domains in Pikromycin Synthase

A DISSERTATION
SUBMITTED TO THE FACULTY OF
UNIVERSITY OF MINNESOTA
BY

Yang Li

IN PARTIAL FULFILLMENT OF THE REQUIREMENTS
FOR THE DEGREE OF
DOCTOR OF PHILOSOPHY

Dr. Robert A. Fecik, Dr. Courtney C. Aldrich

July, 2015

Acknowledgements

Upon finishing my PhD studies, I have so much gratitude to people who have supported me and helped during my PhD candidacy. Firstly, I would like to thank my advisors, Dr. Robert A. Fecik, and Dr. Courtney C. Aldrich. They have been patiently directing me and training me since I entered the lab. From them, I learned how to become a critical thinker, problem solver and independent researcher, which will set a solid foundation for my future career. My committee members, Dr. Rodney Johnson and Dr. Chris Douglas, also deserve many thanks for their insightful suggestions on my research and encouragement of perseverance down this path.

Secondly, I want to express my gratitude to my family. My parents and grandparents offered me unconditional support financially and mentally. My husband always encourages me to chase my dreams no matter how difficult it would be. My parents-in-law are also extremely supportive of my career choices.

I am grateful for past and present Fecik lab members, Dr. Erick Leggans, Dr. Amber Onorato, Dr. Dennis Brown, Dr. Mike Peterson, William Fiers and Bryan Murray. They created a friendly and supportive environment in the lab where I could absorb knowledge, motivation and guidance. Dr. Erick Leggans and Dr. Amber Onorato mentored me on basic skills required for organic chemistry. I am also thankful for Aldrich group members, especially Daniel Wilson and Dr. Ben Duckworth, who have taught me protein expression, biological assay design and LC-MS/MS analysis.

Finally, without the help from our collaborator Dr. Janet Smith (University of Michigan), I could not successfully finish the projects. Especially, I would like to thank

Dr. Steffen Bernard and Greg Dodge for providing me support and insights on the biology section.

Abstract

Combinatorial biosynthesis of polyketides through engineering the respective biosynthetic pathways represents a promising approach to natural products discovery. However, a lack of information on substrate and stereochemical specificity of polyketide synthases (PKS) currently hinders these efforts. Though recent research in the area has provided many mechanistic revelations, a basic-level understanding of kinetic and substrate tolerability is still needed before the full potential of combinatorial biosynthesis can be realized. We have developed a novel set of chemical probes for the study of ketoreductase (KR) and dehydratase (DH) domains of PKS. PKS KRs stereoselectively reduce the β-keto chain intermediate while dictating the orientation of the α-substituent. The DHs of PKS, which generate an α,β-unsaturated bond through dehydration of a β-alcohol, have extremely high stereospecficity towards substrates and can prematurely terminate the nascent polyketide when presented with unnatural substrates.

We have developed a chemical tool-based approach which was verified using KR and DH of pikromycin PKS module 2 (PikKR2) as a model system. Triketide substrate mimics were designed to increase stability (incorporating a non-hydrolyzable thioether linkage) and minimize non-essential functionality (truncating the phosphopantetheinyl arm). The identities of reduction and dehydration products as well as steady-state kinetic parameters were revealed by a LC-MS/MS analysis of synthetic standards. Additionally, the substrate specificity was interrogated with a systematic series of synthetic triketides containing altered stereogenic centers. Furthermore, the mechanism of PikDH2 catalyzed dehydration was investigated by site-directed mutagenesis, evaluation of the pH

dependence of catalytic efficiency (V_{max}/K_M), and through kinetic characterization of a mechanism-based inhibitor.

Table of Contents

List of Schemes

List of Tables

List of Figures

List of Abbreviations

ACP – acyl carrier protein domain
AMPKR1 – amphotericin module 1 ketoreductase domain
AMPKR2 – amphotericin module 2 ketoreductase domain
AMPKR10 - amphotericin module 10 ketoreductase domain
ARO – aromatase
Asp – aspartic acid
AT – acyl transferase domain
AurH – P450 enzyme responsible for C-H oxidation and cyclization in aureothin biosynthesis
AVES – avermectin polyketide synthase
BL21(DE3) – *Escherichia coli* genotype containing T7 gene for heterologous protein expression
CoA – coenzyme A
ChlE3 – first Diels-Alderase in chlorothricin biosynthesis
ChlL – second Diels-Alderase in chlorothricin biosynthesis
CHS – chalcone synthase
m-CPBA – *meta*-chloroperoxybenzoic acid
CurK – the eleventh protein in curacin biosynthesis housing the 6^{th} PKS module in the pathway
CYC – cyclase
DEBS – 6-deoxyerythronolide B polyketide synthase
DH – dehydratase domain
DMAP – 4-dimethylaminopyridine
DMSO – dimethyl sulfoxide
E. coli – gram-negative bacteria *Escherichia coli* used for heterologous protein expression
EpoF – the final module of epothilone polyketide synthase containing the thioesterase domain
ER – enoyl reductase
ERYKR1 – erythronolide module 1 ketoreductase domain
ESI – electrospray ionization
FAS – fatty acid synthase
HEPES – 4-(2-hydroxyethyl)-1-piperazineethanesulfonic acid
His - histidine
HPLC – high-performance liquid chromatography
HRMS – high-resolution mass spectrometry
IBX – 2-iodoxybenzoic acid

IPTG – isopropyl β-D-1-thiogalactopyranoside
KR – ketoreductase domain
KR_c – catalytic sub-domain of a ketoreductase
KR_s – structural sub-domain of a ketoreductase
KS – ketosynthase domain
LC-MS/MS – liquid chromatography tandem mass spectrometry
LDA – lithium diisopropylamine
LIC – ligation-independent cloning
LovB – lovastatin polyketide synthase
Lsd19 – epoxide hydrolase from lasalocid A biosynthesis
LsdA – sub-domain from Lsd19, catalyzing the first cyclization
LsdB – sub-domain from Lsd19, catalyzing the second cyclization
LUMO – lowest unoccupied molecular orbital
MPS – macrophomate synthase
MRM – multiple reaction monitoring, filtration of masses by designated transitions
MS- mass spectrometry
NAC – *N*-acetylcysteamine
$NADP^+$ – nicotinamide adenine dinucleotide phosphate
NADPH - dihydronicotinamide adenine dinucleotide phosphate
NBOM – 2-nitrobenzyloxymethyl ether
NHC – *N*-heterocyclic carbine
NMO – *N*-methylmorpholine *N*-oxide
NMR – nuclear magnetic resonance
NRPS – nonribosomal petide synthetase
OD_{600} – optical density or absorbance at 600 nm wavelength
P450 – oxidative enzyme involved in secondary metabolite biosynthesis
PEG – polyethylene glycol
Phe – phenylalanine
PikAI – pikromycin gene comprised of loading, first and second modules of the PKS
PikDH2 – pikromycin module 2 dehydratase domain
PikKR2 – pikromycin module 2 ketoreductase domain
PikKR2-DH2 – pikromycin module 2 didomain containing a dehydratase and a ketoreductase
PikKR5 – pirkomycin module 5 ketoreductase domain
PIKS – pikromycin polyketide synthase
pLZ51 – cosmid containing the pikromycin polyketide synthase gene sequence
pMCSG7 – plasmid vector containing a ligation independent cloning site
PKS - polyketide synthase
PPG – polypropylene glycol

PPTS –pyridinium *para*-toluenesulfonate
PyrE3 – first Diels-Alderase in pyrroindomycin biosynthesis
PyrI4 – second Diels-Alderase in pyrroindomycin biosynthesis
Rad – radicicol
RAPS – rapamycin polyketide synthase
RifKR10 – rifamycin module 10 ketoreductase domain
SAR – structure-activity relationship
SD – standard deviation
SDS-PAGE – sodium dodecyl sulfate polyacrylamide gel electrophoresis
SpnF – spinosyn A Diels-Alderase
SpnKR3 – spinosyn A module 3 ketoreductase domain
SPS – solanopyranone synthase
TB media – terrific broth culture medium
TBAF – tetra-*N*-butylammonium fluoride
TBS – *tert*-butyldimethylsilyl group
TE – thioesterase domain
TES – triethylsilyl moiety
TESOTf – triethylsilyl trifluoromethanesulfonate
THF- tetrahydrofuran
TIPS – triisopropylsilyl substituent
TLC – thin-layer chromatography
TPAP – tetrapropylammonium perruthenate
Tris – tris(hydroxymethyl)aminomethane or 2-amino-2(hydroxymethyl)-1,3-propanediol
TYLKR1 – tylosin module 1 ketoreductase domain
UV – ultraviolet light
VstJ – versipelostatin Diels-Alderase
Zea – zearalenone

Chapter 1: Introduction and background

1.1. Polyketide natural products

From the earliest records of humankind through the 21st century nature has continued to play a critical role in providing the medicines to treat, prevent, and abolish the myriad of ailments that plague our health.[1] Polyketide natural products are a class of secondary metabolites from plants, animals, bacteria and fungi with a wealth of pharmacological activities, such as antibacterial, antiparasitic, antitumor, cholesterol-lowering and immunosuppressive properties, making them an essential component in novel drug discovery and development.[2] This is clearly showcased by the six blockbuster polyketide-based drugs: lovastatin (**1.1**), pravastatin (**1.2**), simvastatin (**1.3**), sirolimus (**1.4**), clarithromycin (**1.5**) and azithromycin (**1.6**) (Figure 1). As a result of their therapeutic importance, the annual sales of all polyketide-derived pharmaceuticals exceed $20 billion in the US.[3]

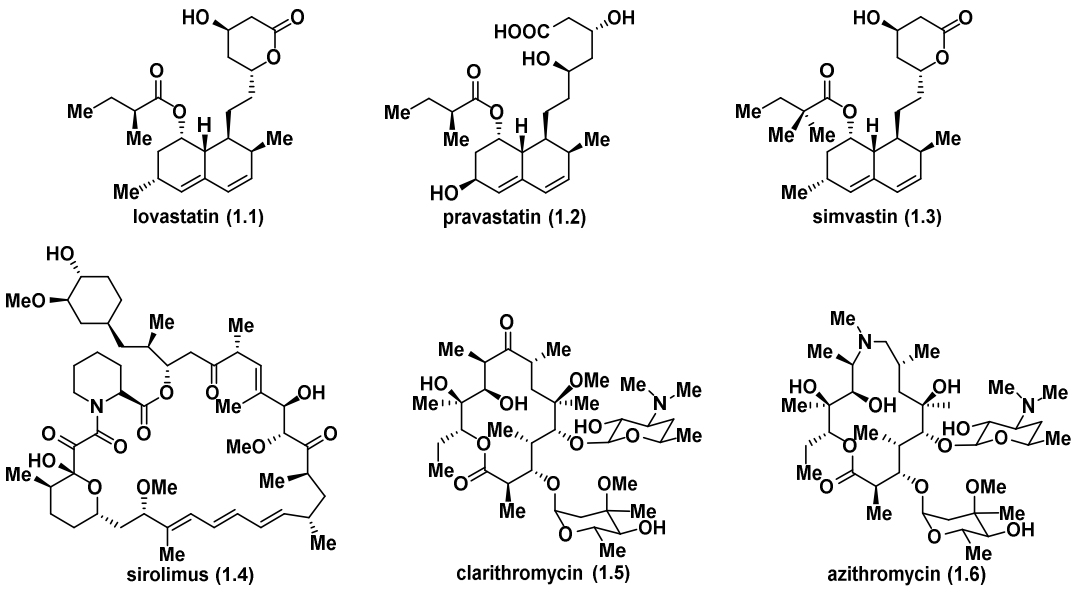

Figure 1. Structures of lovastatin (**1.1**), pravastatin (**1.2**), simvastatin (**1.3**), sirolimus (**1.4**), clarithromycin (**1.5**) and azithromycin (**1.6**).

1.2. Polyketide synthases (PKSs)

Polyketides are also biosynthesized by enzyme complexes known as polyketide synthases (PKSs) through a series of Claisen condensations from simple building blocks, but with more structural and stereochemistry complexity, the mechanism of which resembles that of fatty acid synthases (FASs).[4, 5] Compared with FAS, the PKSs' ability of diversifying the natural product architecture with more diversity is due to three aspects. Firstly, PKSs have the capacity to select more than one extender units, not only malonyl-coenzyme A (CoA) (used by FAS), but also methylmalonyl-, ethylmalonyl-, methoxymalonyl-, hydroxymalonyl-CoA (**1.7**–**1.11**), and others, to produce branched backbone with different substituents (Figure 2). Moreover, a variable combination of processing domains in PKS defines the degree of β-keto reduction, resulting in a variation with a β-alcohol, an α,β-unsaturated olefin and a fully saturated two carbon segments all

possible. Lastly, post-PKS tailoring enzymes further decorate the polyketide framework with more functionality via oxidation, glycosylation, acylation or alkylation.

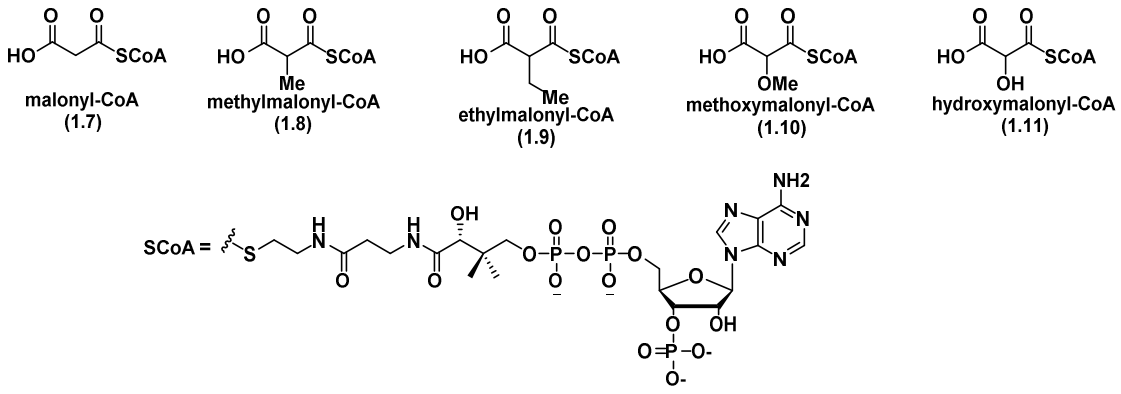

Figure 2. Structures of PKS building blocks.

The nascent polyketide intermediates are covalently bound to a non-catalytic domain, known as acyl carrier protein (ACP) through thioester bonds with the phosphopantetheinyl arm of the ACP domain, which shuttles the growing chain to other catalytic domains.[2] PKSs are classified into three types based on how ACPs exist or connect in the assembly line.[6-8] When ACPs are connected in *cis* with other catalytic domains to form modules, these multi-domain megaenzymes are Type I PKSs. PKS systems with ACPs existing as discrete enzymes and interacting in *trans* with other dissociable protein clusters are categorized as Type II PKSs. Type III PKSs are ACP-independent and utilize CoA as an anchor for chain elongation.

1.2.1. Modular Type I PKSs

Type I PKSs can be further devided into modular and iterative Type I PKSs. Modular type I PKSs are large, multifunctional, modular proteins primarily found in bacteria and protozoans that biosynthesize structurally complicated polyoxygenated natural products.

Two representative classes from this type of PKSs are macrolides, such as erythromycin, pikromycin and tylosin, as well as polyethers, like monensin, nanchangmycin, lasolocid A and salinomycin, generated through cascade oxidative cyclization from linear polyketide polyene.[9]

All modular type I PKSs contain a loading module and several extension modules, each responsible for one round of polyketide chain elongation and β-carbon processing, organized in an assembly line fashion.[2, 4, 6, 10] The loading module recruits a CoA starter unit and covalently tethers it on the ACP domain. Each extension module features a minimal set of three domains responsible for a two-carbon extension of the chain elongation intermediate: non-catalytic ACP, acyltransferase (AT) and ketosynthase (KS) domains (Scheme 1). The AT domain selects the building block, usually L-methylmalonyl- or malonyl-CoA, and transfers it to the ACP domain in the same module. The KS domain accepts the polyketide chain tethered on the ACP arm from the upstream module through transesterification and catalyzes a decarboxylative condensation between the growing chain and the extension unit to complete the two carbon elongation process. After extension, the newly formed β-keto thioester intermediate is frequently followed by sequential β-carbon processing by ketoreductase (KR), dehydratase (DH), and enoylreductase (ER) domains. The KR domain is the most abundant β-carbon processing domain throughout all PKSs. It stereoselectively reduces the newly formed β-ketone to an alcohol with NADPH, and can also control the stereochemistry of the α-substituent through enzymatic epimerization. DH domains remove a water molecule to generate the α,β-unsaturated acyl imtermediate. The geometry of the double bond is usually dependent

on the configuration of the β-hydroxyl group set by the KR domain. The ER domain reduces the α,β-double bond with specific stereo-orientation of the α-substitient by NADPH. As the presence of each β-processing domain is optional, the degree of oxidation is varied in different domains, resulting in unreduced, partially reduced and fully reduced two carbon segments.

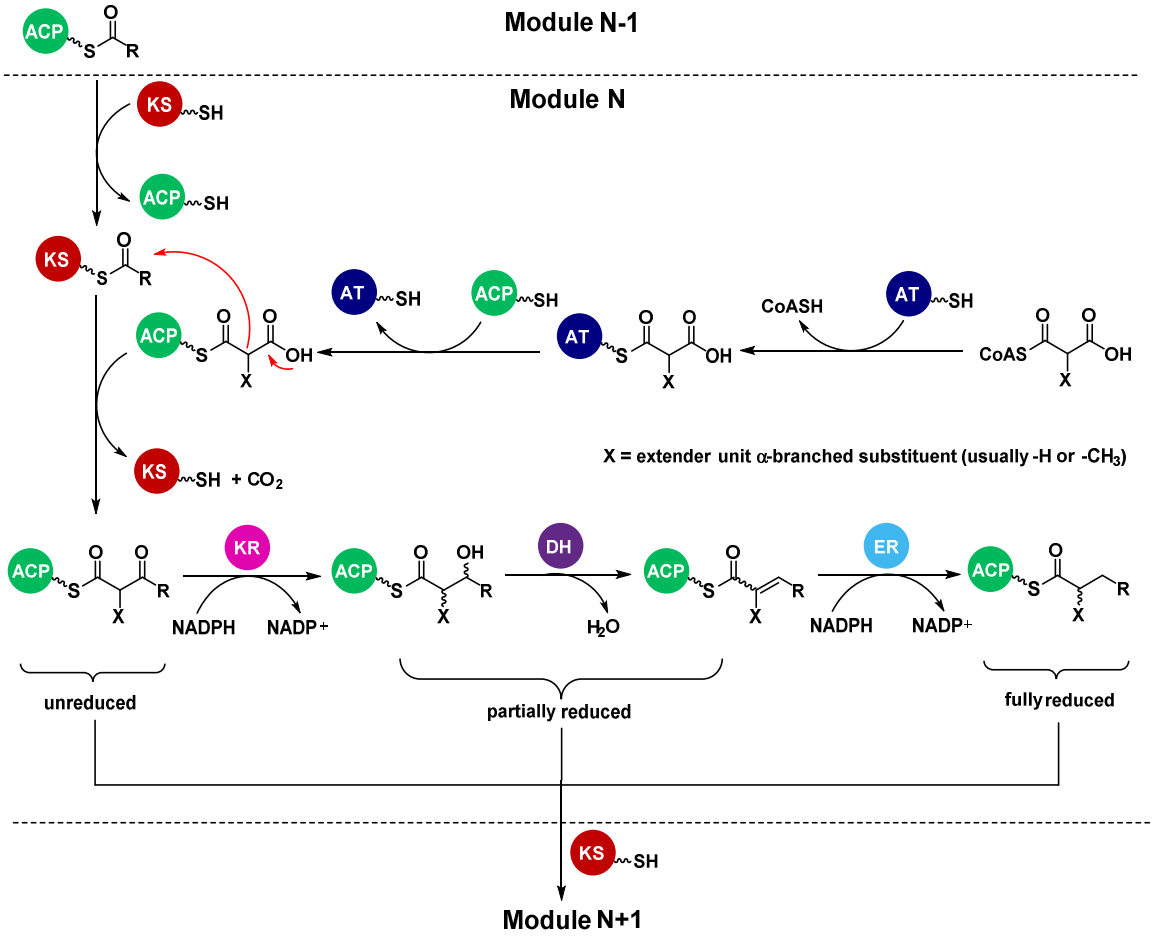

Scheme 1. Modular assembly line in Type I PKSs.

Following multiple rounds of chain elongation and β-carbon processing, a thioesterase (TE) domain translocates the linear polyketide intermediate **1.12** from ACP to its active site and catalyzes an intramolecular cyclization or a hydrolysis to release a

macrolactone **1.14** or carboxylic acid **1.15**, respectively (Scheme 2). The released polyketides are further modified by tailoring enzymes, such as glycosyltransferases, oxygenases, and methyltransferases to afford mature and bioactive natural products.

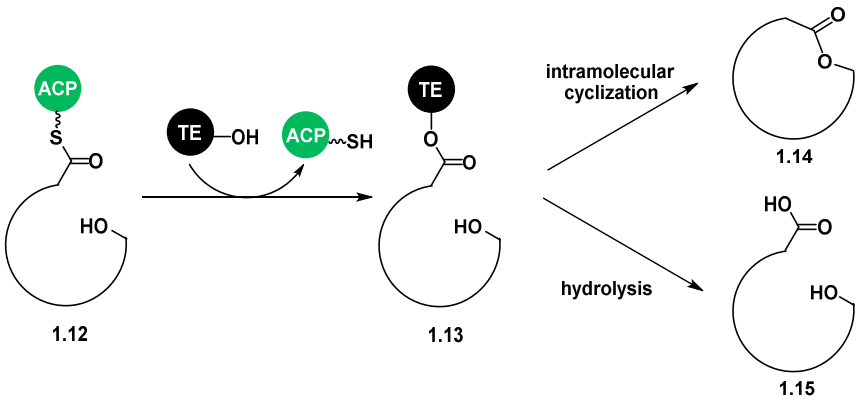

Scheme 2. Macrolactonization or hydrolysis by TE domain.

Modular type I PKSs, such as pikromycin synthase (PIKS) of *Streptomyces venezuelae*, have been well-studied through genome sequence analysis, as well as *in vitro* and *in vivo* recombinant expression for their potential in drug discovery.[11-14] This pathway uses propinoyl CoA as the starter unit which is delivered by ACP to the first extension module (Module 1). Each of the six extension modules adds a two-carbon segment on the polyketide backbone, consuming one malonyl-CoA and five methylmalonyl-CoA building blocks (Figure 3). One unique arbitrate of pikromycin PKS is its ability to produce both 12- and 14-membered macrolactones, including 10-deoxymethynolide (**1.16**), narbonolide (**1.17**), methymycin (**1.18**), and pikromycin (**1.19**). After the fifth extension module, the polyketide chain can either undergo TE-catalyzed macrolactonization or go through another round of chain elongation by module 6 before

macrolactonization. In the end, post-PKS tailoring enzymes, Des VII and PikC stereoselectively install the glycosides and hydroxyl groups on the cyclic polyketides.

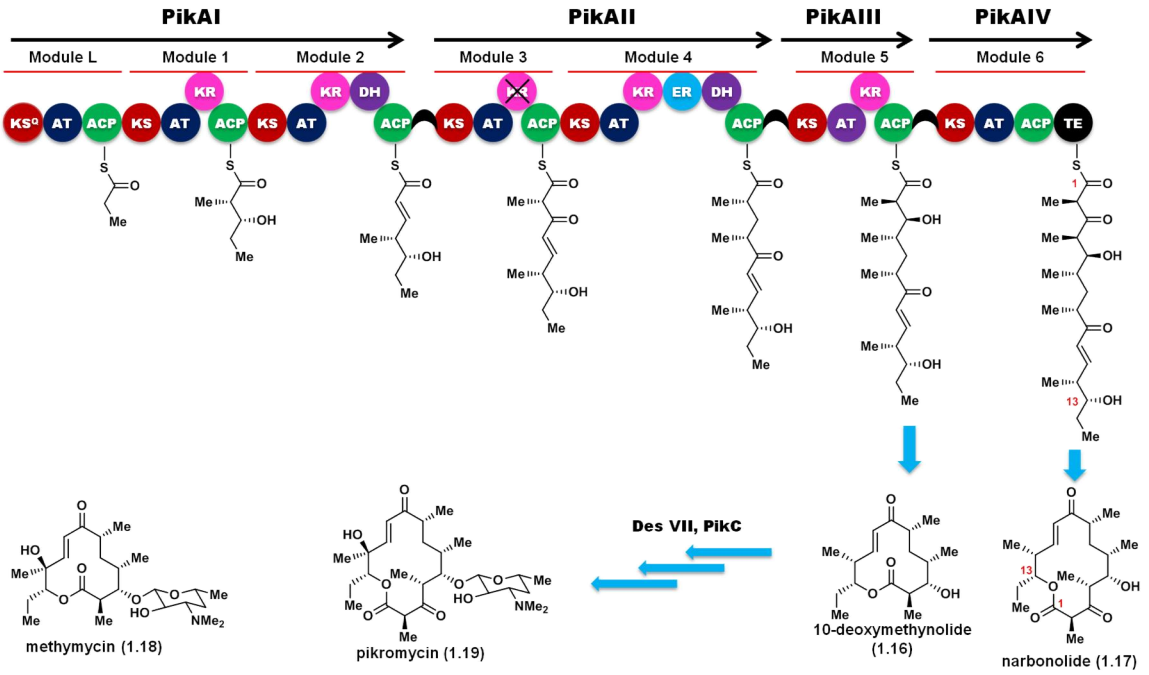

Figure 3. Biosynthetic pathway of pikromycin (**1.18**) and methymycin (**1.19**).

1.2.2. Iterative Type I PKSs

Although iterative Type I PKSs often serve as a hallmark for fungal PKSs, some bacterial PKSs also belong to this type.[7, 8, 15] As seen in modular PKSs, iterative Type I PKSs also contain the characteristic domains, including ACP, KS, AT, and processing domains. However, these extension domains are reused in a cyclic fashion where the KS domain could recapture the growing chain after each chain elongation, rather than a modular assembly line. Orsellinic acid (**1.24**) and (*R*)-mellein (**1.28**) are two representative polyketides biosynthesized by this class (Scheme 3). As the iterative

feature is also seen in Type II PKSs, the detailed mechanism is discussed in the next section.

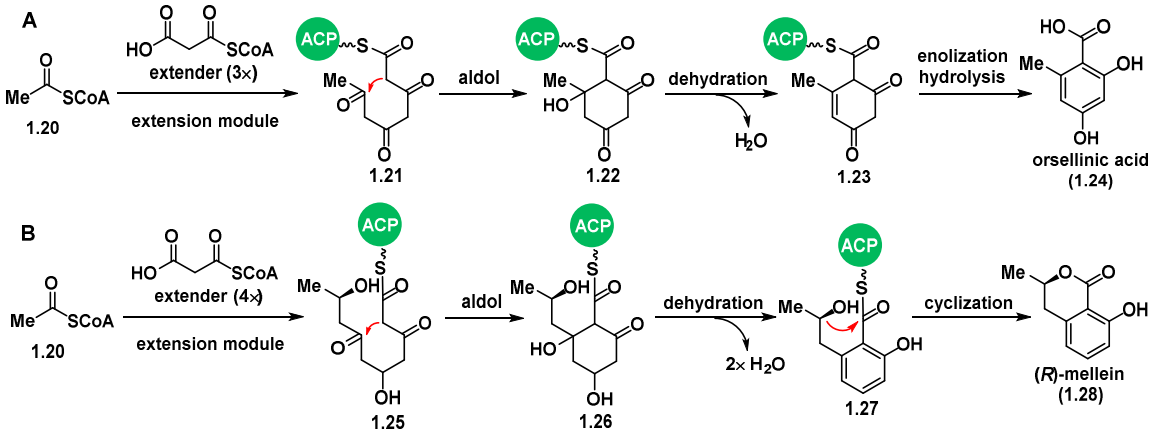

Scheme 3. Iterative Type I PKSs catalyzed biosynthesis of orsellinic acid (**1.24**) and (*R*)-mellein (**1.28**).

1.2.3. Type II PKSs

Type II PKSs are multienzyme complexes that harbor dissociable monofunctional proteins. They are found exclusively in bacteria.[16] Most of Type II PKSs, such as tetracycline PKS, construct polyphenolic rings through iterative decarboxylative condensation of malonyl-CoA extenders.[17] The minimal set of Type II PKSs is comprised by two KS subunits (KS_α and KS_β) and an ACP (Scheme 4). The KS_α subunit is functionally active to form a poly-β-ketone **1.29** while the KS_β seems to facilitate substrate binding, determine the chain length, and control the regiochemistry of the first cyclization. KRs, reducing ketone to secondary alcohol **1.30**, also play an important role in Type II PKS systems. After chain elongation, the regioselective reduction event sets the nascent polyketide chain into a favored conformation to conduct the first aldol

cyclization which indirectly dictates where to make the C-C bond connection. Although spontaneous cyclizations could take place on the linear intermediate, cyclases (CYCs) are found to assist desired aldol reactions by confining the nascent polyketide **1.30** into a specific reaction channel where the random spontaneous cyclization are impeded. In the end, aromatases (AROs) dehydrate the cyclic alcohols into polyphenols and tailoring enzymes, like those in Type I PKSs, further enhance the structural functionality in **1.34** and **1.35**.

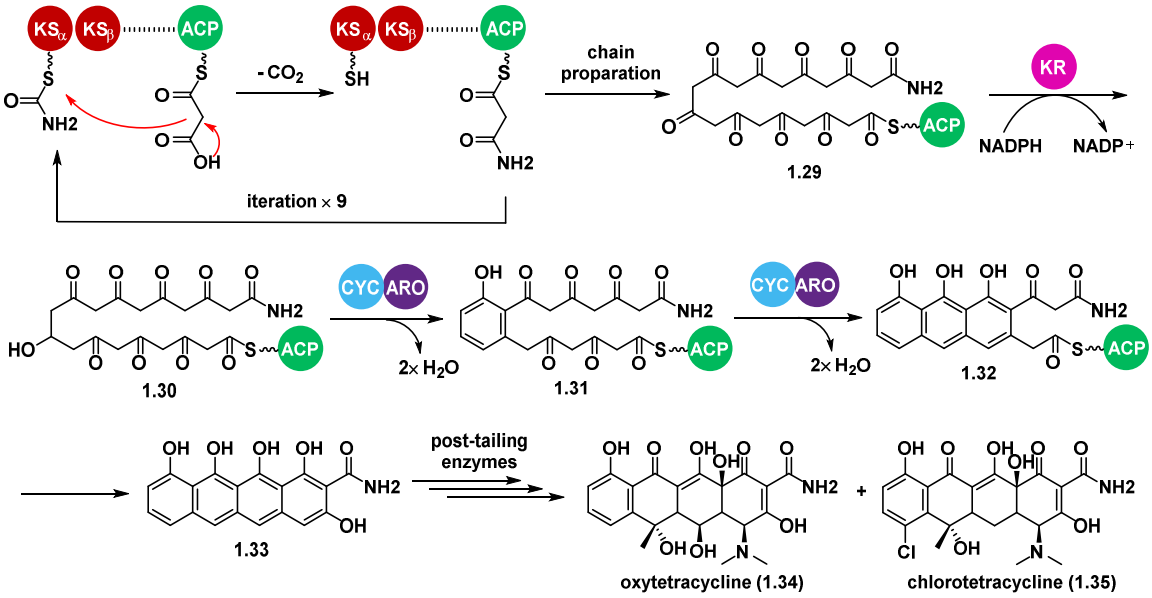

Scheme 4. Biosyntheses of tetracyclines by Type II PKS.

1.2.4. Type III PKSs

Although Type III PKSs are dominantly found in plants, rescent studies have shown their existence in bacteria and fungi.[18] Despite their using CoA instead of ACP as an anchor for the growing chain, Type III PKSs are multi-domain proteins (like Type I), but conduct chain propagation in an iterative manner (like Type II). The most-studied Type

III system is chalcone synthase (CHS) which yields a precursor for flavonoid biosynthesis. CHS exploits 4-coumaroyl-CoA (**1.36**) as a starter unit and catalyzes three sequential Claisen condensations with malonyl-CoA extenders (Scheme 5). As seen in Type II PKSs, the poly-β-keto chain undergoes aldol cyclization and enolization to yield naringenin chalcone (**1.38**). Additionally, this Type III polyketide could be isomerized and diversified by various combinations of post-tailoring reactions, giving rise to more than 6000 flavonoid natural products.[18]

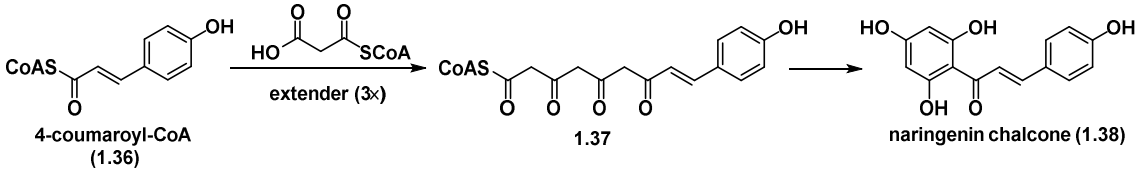

Scheme 5. Biosynthesis of naringenin chalcone (**1.38**) by CHS.

1.3. Combinatorial biosynthesis

As polyketide-derived drugs comprise 20% of the top-selling drugs, scientists have been driven to pursue polyketide analogs with improved therapeutic properties. Although new methodologies and catalysts have greatly improved the efficiency of synthetic polyketide total synthesis,[19-21] the differential oxidation states and numerous oxygenated moieties of polyketides still necessitate multiple redox reactions and careful functional group protection to ensure their successful synthesis. The lengthy synthetic routes towards most polyketides limits their application in pharmaceutical industry due to difficulties in generating natural lead molecules in preparative scale as well as providing large libraries of diverse analogs for SAR studies. Alternatively, combinatorial biosynthesis, genetically engineering the PKS to aid the efficient production of

"unnatural" natural product libraries, has gained in popularity over the past three decades.[22, 23]

1.3.1. Ivermerctin production by combinatorial biosynthesis

Ivermectins (**1.39**), 22,23-dihydrogated version of polyketide avermectins (**1.40**) (Figure 4), are used as antiparasitic agents and for the treatment of river blindness. In addition to regioselective hydrogenation of the naturally produced avermectins (**1.40**), ivermectins (**1.39**) could also be produced by genetic manipulation to yield the desired structures in fermentation.[24] The KR and DH domains in the second module of avermectin polyketide synthase (AVES), responsible for the creation of olefinic and hydroxyl segment at C22-C23 in avermectins, were replaced with a full set of β-processing domains: KR, DH and ER from module 13 of rapamycin-producting PKS. In the fermentation broth, new polyketides with fully reduced C22-C23 segment were isolated and identified, offering a novel approach to afford ivermectin drugs with the technique of combinatorial biosynthesis.

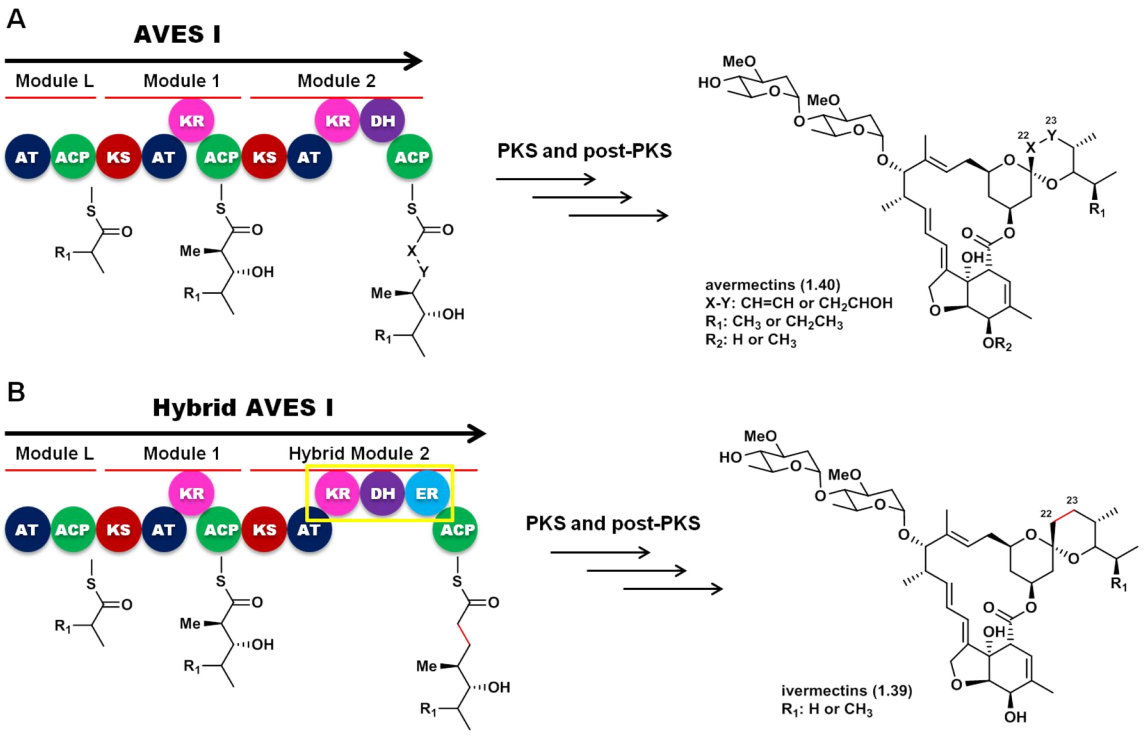

Figure 4. (A) Biosynthetic pathway of avermectins by AVES to install either an unsaturated bond at C22-C23 or a hydroxyl group at C23. (B) Utilization of combinatorial biosynthesis to incorporate a saturated bond at C22-C23 through introducing a full set of reductive domains.

1.3.2. A library of erythromycin analogs

6-Deoxyerythronolide B synthase (DEBS), responsible for biosynthesizing the macrolide in erythromycin, has served as a model modular Type I PKS in studies to understand the mechanism of PKS catalytic events. This pathway was engineered to create a large library of 60 "unnatural" polyketides through combinatorial biosynthesis, which would be impossible by chemical manipulations.[25] This was achieved by altering single and multiple catalytic domains in DEBS, including: replacing the AT domains from DEBS with the counterparts from rapamycin PKS (RAPS) to incorporate unusual

extender units, deleting KR domains to convert functional groups to ketones, and inserting additional β-processing domains from RAPS to tune the degree of β-reduction. Compared to the natural product, 6-deoxyerythronolide B (**1.41**), analogs with one (**1.42**–**1.44**), two (**1.45**–**1.47**) and three (**1.48**–**1.50**) modifications at different carbon centers were biosynthesized to broaden the library (Figure 5). The capacity in constructing diverse unnatural polyketide libraries, demonstrated by combinatorial biosynthesis, is of paramount importance in novel drug discovery and optimization.

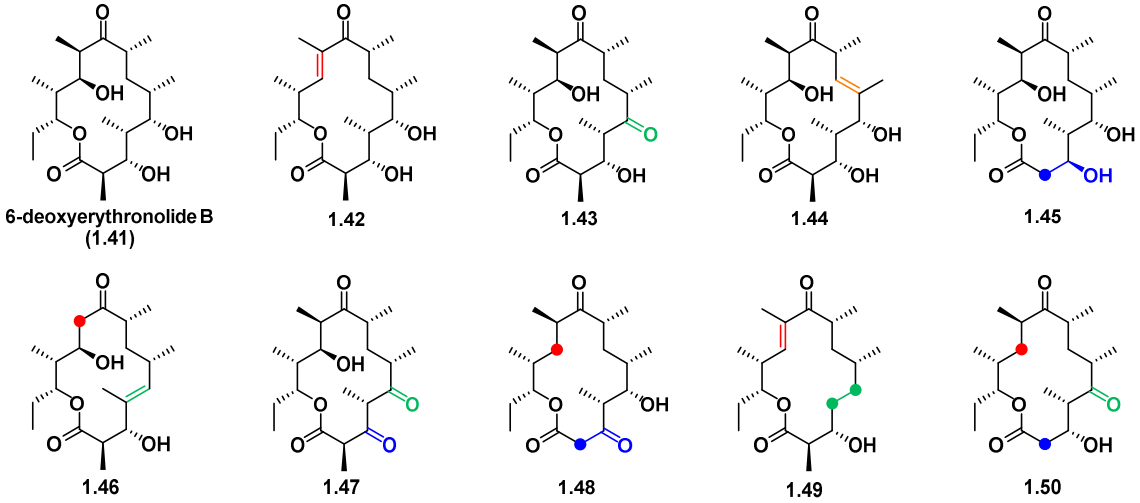

Figure 5. 6-Deoxyerthronolide B (**1.41**) and its representative analogs (**1.42**–**1.50**). Colors indicate the engineered carbon centers originated from module 2 (red), module 4 (orange), module 5 (green) and module 6 (blue).

1.3.3. Challenges in combinatorial biosynthesis

Although tremendous breakthroughs have been made to create libraries of natural product analogs, full exploitation of combinatorial biosynthesis remains a largely unattained goal. One challenging aspect is the loss of specificity and activity of unnatural

substrates or altered domains. For instance, deletion of KR2 in 6-deoxyerythronolide B synthase (DEBS) PKS led to the shutdown of the biosynthesis as module 3 could not accept the nonnative, unreduced β-keto intermediate.[25] In another example, when the stereochemistry of the C2-methyl group established by AmpKR2 was altered by mutagenesis, the polyketide intermediate skipped the ketoreduction step and resulted in an unexpected product due to the competition between the slower, unnatural KR domain and more rapid downstream enzymes.[26] Clearly, prerequisite knowledge of the mechanism, kinetic parameters, stereoselectivity, and substrate specificity of each domain is crucial for applications in combinatorial biosynthesis and metabolic engineering.

1.4. Chemoenzymatic synthesis

Chemoenzymatic synthesis, employing and manipulating enzymes in PKS pathways to conduct chemical reactions and to quickly assemble a natural product skeleton, has gained in popularity among organic chemists, microbiologists, medicinal chemists, and synthetic biologists. Compared to traditional means, chemoenzymatic synthesis boasts a number of advantages. Firstly, nature often designs its enzymatic reactions in an extremely stereoselective manner, ensuring the enantiomeric purity of the outcome products. Secondly, elimination of organic solvents, metal catalysts and chiral ligands is both environmentally and economically friendly. Lastly, transformations that require multiple chemical steps in the laboratory can be performed by enzymes in tandem, which considerably boosts the synthetic efficiency.

1.4.1. TE-catalyzed macrolactonization

A vast amount of polyketides are constrained as macrolides, offering unique cyclic conformations to bind biological targets bestowing diverse bioactivities, such as erythromycin A, epothilone A, amphotericin B, pladienolide B, and others. Synthetic efforts towards an efficient, intramolecular cyclization between an acid and an alcohol have been a persistant goal in natural product total synthesis since 1947.[27] The most common strategy is to transform the carboxylic acid into an activated form including carbodiimides,[28] thioesters,[29] mixed anhydrides,[30, 31] and carbon-phosphorous anhydrides.[32, 33] The alcohol can also be activated for an S_N2 reaction by mesylation[34] or a Mitsunobu reaction.[35] Additionally, new cyclization strategies have emerged, for instance, epoxide opening,[36] C-H activation,[37] and NHC (*N*-heterocyclic carbene)-catalyzed macrocyclization.[38] Despite the development of various chemical macrocyclizations, significant drawbacks cannot be ignored: reaction activity may be hampered by conformational effects of the substituents; acidic, basic conditions or high temperature may be required to overcome the energy barrier to cyclization; nucleophilic groups have to be protected to avoid undesired cyclizations; and substrate epimerization during activation. Therefore, a chemoenzymatic macrolactonization, via a head-to-tail cyclization catalyzed by a PKS TE domain, remains an attractive, alternative approach in the synthesis of natural products and their analogs.

In addition to PKSs, non-ribosomal peptide synthetases (NRPSs) could also fuse linear biosynthetic intermediates into macrocyclic scaffolds through amide, rather than ester bond, formation.[6] Given the abundance of TEs as well as the ease of obtaining

isolated TE domains, which could still retain autonomous catalytic activities, exploitation of TEs to conduct macrocyclization has gained popularity since 2000. The TE domain of tyrocidine synthetase was exploited to promote the macrolactamization reactions of natural and unnatural linear peptides, afforded by solid-phase synthesis, resulting in a library of over 100 cyclic peptide antibiotics.[39, 40]

Inspired by non-ribosomal peptide synthetase (NRPS) TE-catalyzed macrocyclization,[39, 40] a PKS TE domain the terminal module of epothilone biosynthesis (EpoF), was excised to furnish the macrolactone of epothilone C (**1.51**) *in vitro* (Scheme 6).[41] *N*-acetylcysteamine (NAC) was coupled with epothilone C seco-acid to mimic the ACP phosphopantetheine arm of the native TE domain substrate. The linear intermediate **1.52** was loaded onto the TE domain via a transacylation event and nucleophilic attack of the activated ester by C15 hydroxyl group afforded the macrolide **1.51**. The other two hydroxyl groups at C3 and C7 positions remained untouched during the whole process, illustrating the regioselective nature of a chemoenzymatic reaction devoid of functional manipulations. In addition to the macrolide, the hydrolysis product, epothilone C *seco*-acid was also detected, with a partition ratio of 5: 1 between cyclization and hydrolysis at optimal pH. The k_{cat}/K_M value of TE-catalyzed cyclization was 0.41±0.03, more than 7 orders of magnitude faster than the nonenzymatic reaction. Notably, TE also boosted the hydrolysis reaction by 10000-fold with a specificity constant of 0.30±0.07 $min^{-1}mM^{-1}$. The comparable kinetic parameters of the two types of reactions and the dramatic rate enhancement of hydrolysis supports the mechanism that the first step is irreversibly loading the substrate to TE. The regioselectivity, mild reaction condition and facile

procedure of this chemoenzymatic reaction highlight the application of excised TE domains from PKSs.

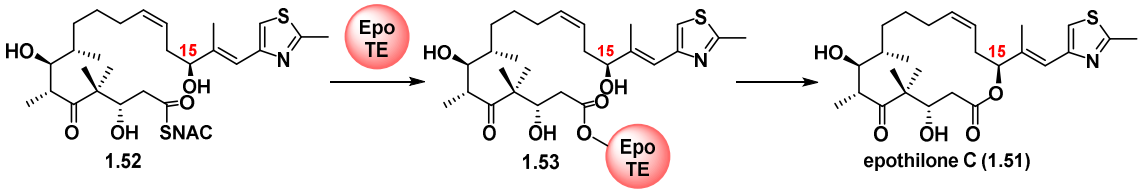

Scheme 6. *In vitro* chemoenzymatic synthesis of epothilone C by Epo TE.

Deeper insight into chemoenzymatic lactonizations have been obtained through close inspection of TEs of PIKS and DEBS.[42-45] A detailed review covering TE-catalyzed macrolactonization in these two PKS systems was published by the Sherman group.[46] These two TEs have the ability to form both 12- and 14-membered macrolactones, and exhibit high preference for their native substrates. Product control, to form either the 12- or 14-membered rings in pikromycin PKS, has currently been achieved through substrate engineering (Scheme 7).[47] The 2-nitrobenzyloxymethyl (NBOM) ether protected NAC-hexaketide **1.54**, substrate mimic for the last module of pikromycin synthase, was submitted to photolysis and was reacted with methyl malonyl-NAC and PikAIV (containing KS, AT, ACP, and TE domains). The linear substrate could either go through a Claisen condensation and subsequent TE-catalyzed cyclization to furnish the 14-membered narbonolide (**1.17**), or to skip the elongation domains and be released directly to convert to the 12-membered, 10-deoxymethynolide (**1.16**). The yields of **1.16** and **1.17** were 52% and 4%, respectively, favoring the formation of the smaller ring **1.16**. However, when the NAC thioester was replaced with the thiophenol thioester in **1.55**, which was previously utilized to improve chemoenzymatic efficiency,[48] the preferred ring size

shifted to the bigger 14-membered macrolactone **1.17** (41% vs 3% of **1.16**). The remarkable selectivity of ring size (greater than 10 to 1 in both cases), dictated by the type of thioester in the substrate, bestows easy product control for chemoenzymatic synthesis. This fascinating finding also indicates the importance of ACP interaction with other domains, which possibly provides information to determine the fate of polyketide intermediates, either direct TE-catalyzed release or submission to another chain elongation cycle by the preceding module.

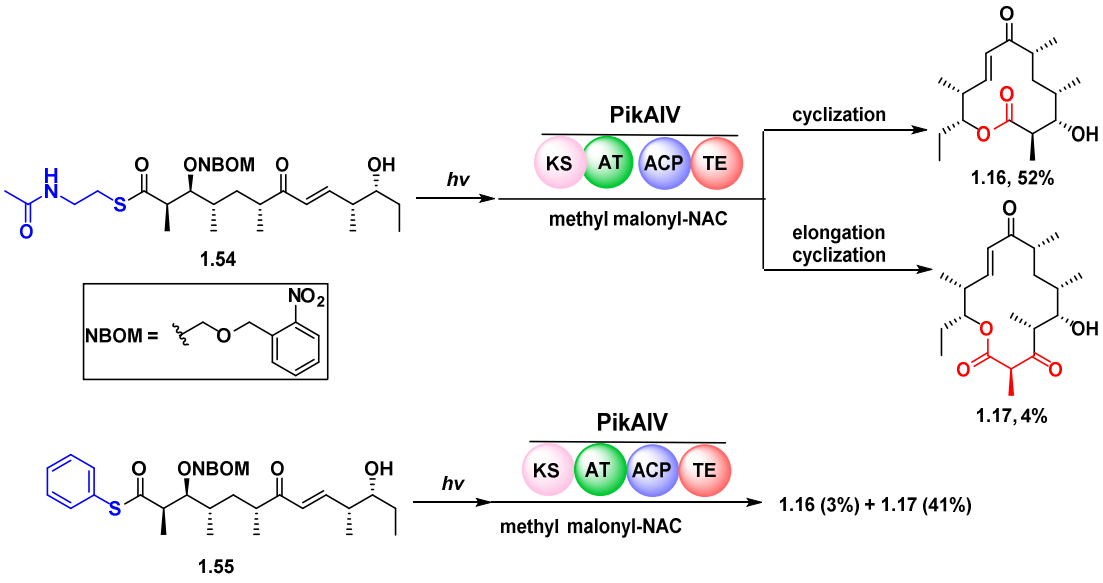

Scheme 7. Chemoenzymatic synthesis of 10-deoxymethynolide (**1.16**) and narbonolide (**1.17**) by PikAIV; the ring size was controlled by the type of thioester present in the substrates.

Although several structurally modified substrates were tolerated by the PKS TEs, the stereochemistry of the nucleophilic hydroxyl group was found crucial for the catalytic activities of many TEs.[49, 50] In contrast, a recent study illustrated the high stereo-permissiveness of two TEs from radicicol (**1.56**) (Rad) and zearalenone (**1.57**) (Zea)

biosynthetic pathways.[51, 52] Both belonging to the resorcylic acid lactone family, radicicol and zearalenone share the same 14-membered phenyl-fused lactone architecture, but with opposite stereochemistry of the nucleophilic alcohols involved in macrocylization (Scheme 8). Excised Rad TE and Zea TE presented with synthetic substrates **1.58** and *ent*-**1.58** in both D- and L-configurations are capable of furnishing macrolactones **1.59** and *ent*-**1.59**, respectively, in spite of the orientation of the nucleophilic alcohols and with comparable kinetic parameters. The two TE domains displayed potential towards employment in chemoenzymatic macrolactonization, based on their broad tolerance for stereochemistry and substituent permutation on the polyketide backbone. Additionally, the TE in vicenistatin biosynthesis, not only possesses the ability to macrolactonize substrates, but can also macrolactamize and even oligomerize, depending on the nucleophilic moiety of the substrate and the length of the linear intermediate.[53, 54]

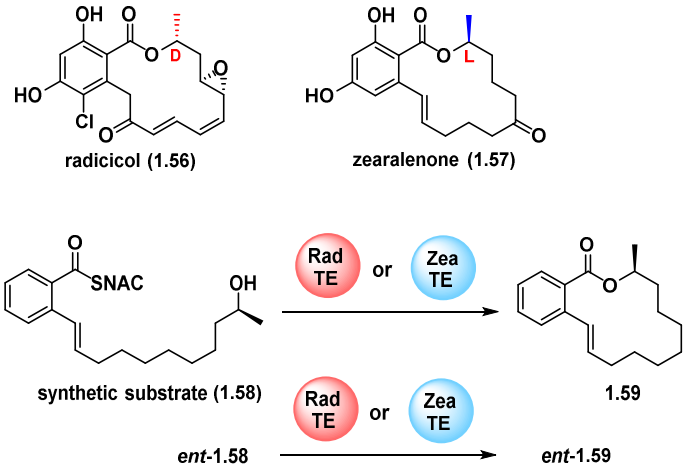

Scheme 8. Structures of radicicol and zearalenone; Rad TE and Zea TE catalyzed macrolactonization from synthetic substrates.

1.4.2. KR-catalyzed stereoselective reduction

KR domains are known to stereoselectively reduce β-keto substrates while dictating the α-substituent orientation through enzymatic epimerization.[26] The resulting α-substituent, β-hydroxyl enzymatic product could serve as a chiral building block in total synthesis, which is often accomplished by different types of aldol reactions. However, the desired level of stereochemistry control is sometimes difficult to achieve by chemical manipulations and stoichiometric amount of chiral auxiliaries is requisite in most cases. Therefore, employment of KRs as a toolbox of biocatalysts to create α,β-substituted chiral compounds is promising and its utility has been explored in 11 isolated KRs from diverse pathways.[55] The screened KRs were incubated with five ketide substrates (**1.60**–**1.64**) harboring different α-substituents and various chain length, respectively (Figure 6). For every reaction, the four potential diastereomeric enzymatic products (two products for substrate **1.60**) were identified and quantitated by authentic standards by chiral HPLC to determine the stereoselectivity of each KR domain. Most of KRs maintained their natural stereocontrol on the reduction products when presented with unnatural substrates. Finally, four KRs, KR in the second module of amphotericin PKS (AmpKR2), KR in the first module of amphotericin PKS (AmpKR1), KR in the first module of tylosin PKS (TylKR1), and KR in the first module of erythromycin PKS (EryKR1) were selected as biocatalysts to afford the chiral α,β-building blocks **1.65**–**1.68**, due to their excellent stereocontrol. Moreover, these chemoenzymatic reaction were conducted on a preparative scale (>100 mg) to yield ~85% of the desired enzymatic products, demonstrating the robustness of this reaction type. The thioester moieties could be easily converted to

carboxylic acids or aldehydes, making the chiral building blocks versatile in total synthesis.

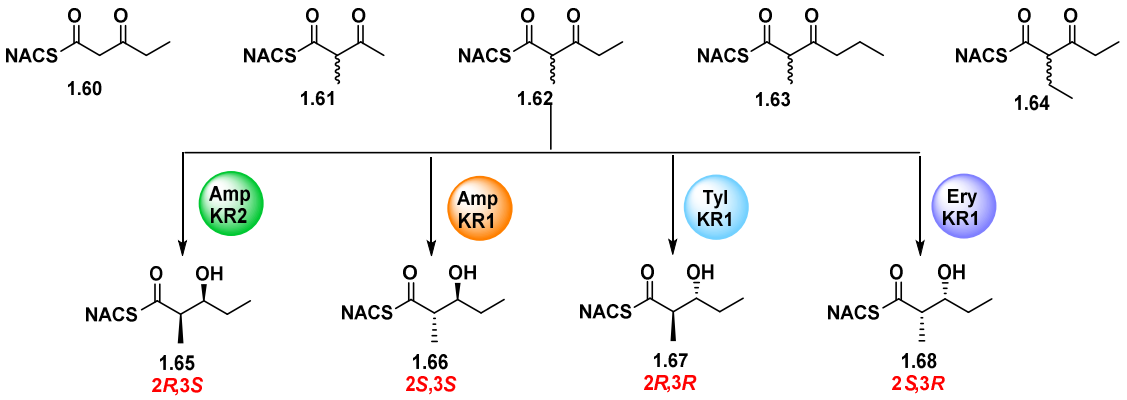

Figure 6. Diketide substrates **1.60–1.64** and chemoenzymatic reductions catalyzed by AmpKR2, AmpKR1, TylKR1 and EryKR2.

1.4.3. Potential Diels-Alderase Catalyzed-[4+2] Cycloaddition

The Diels-Alder reaction, a pericyclic reaction between a conjugated diene and a dienophile through concerted [4+2] cycloaddition with regio- and stereochemical control, has been extensively applied in organic synthesis to provide complex cyclic scaffolds since 1928.[56, 57] However, this reaction is often initiated thermally or via strong Lewis acid, which may be detrimental to existing functional groups often present in total synthesis. In Nature, 6-membered carbocyclic moieties are common in polyketides, alkaloids, and terpenoids, suggesting enzymatic involvement for the construction of cyclohexanes. To date, seven enzymes have been identified as potential Diels-Alderases for their ability to facilitate [4+2] cycloadditions *in vitro*, including macrophomate synthase (MPS),[58, 59] solanopyranone synthase (SPS),[60, 61] lovastatin synthase (LovB),[62, 63] SpnF in spinosyn A biosynthesis,[64, 65] VstJ in versipelostatin biosynthesis,[66] as well as

PyrE3 and PyrI4 in pyrroindomycin biosynthetic pathway,[67] shedding light on the possibility of constructing cyclohexanes under mild conditions.

The biosynthetic pathway of the insecticide spinosyn A (**1.69**) has been elucidated via *in vitro* assays of overexpressed enzymes and synthesized polyketide intermediates.[64] Among these enzymes, SpnF converted keto-intermediate **1.70** to monocyclic macrolactone **1.71** through a transannular [4+2] cycloaddition (Scheme 9). Kinetic parameters illustrated that SpnF could accelerate cyclohexene formation at least 500-fold at 30 °C, compared to the non-enzymatic cyclization (k_{cat} values: 14 ± 1.6 min^{-1} vs 0.0288 ± 0.00041 min^{-1}). Similar rate enhancement has also been observed in engineered antibody catalyzed Diels-Alder reactions.[68] Several explanations have been proposed based on the three-dimesional structure of SpnF: Firstly, hydrogen bonds between the dienophile carbonyl and the active site cause more electron deficiency of the dienophile resulting in a lower lying, more reactive LUMO; secondly, when bound to the active site, the substrate may be oriented and stabilized in a reactive geometry for intramolecular cyclization by bringing the reactive groups into close proximity; lastly, water molecules surrounding the substrate are eliminated.[69] Although the mechanism of this [4+2] cycloaddition, whether a concerted Diels-Alder reaction or a cationic rearrangement, has yet to be determined, the rapid, and clean conversion by SpnF suggests its potential application in chemoenzymatic synthesis.

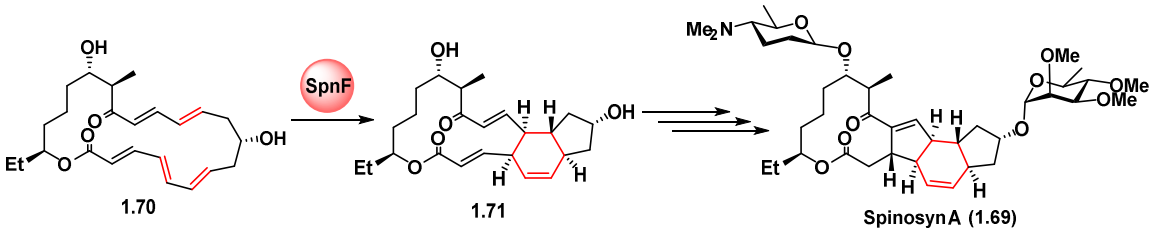

Scheme 9. SpnF-catalyzed [4+2] cycloaddition in spinosyn A (**1.69**) biosynthesis.

The high efficiency of the enzymatic [4+2] cycloaddition was promulgated recently in a discovered cascade reaction where the pentacyclic core of pyrroindomycins (**1.72** and **1.73**) was set via tandem cycloadditions (Scheme 10).[67] Genes *pyrE3* and *pyrI4* were identified as candidates responsible for the two [4+2] cycloaddtions in pyrroindomycin. Intermediate **1.74** was detected and isolated from the culture where *pyrE3* and *pryI4* were inactivated. When treated with overexpressed PyrE3 *in vitro*, polyene **1.74** was enantiomerically transformed to dialkyldecalin **1.75** through a [4+2] cyclozation between diene $\Delta^{10,11}$, $\Delta^{12,13}$ and dienophile $\Delta^{4,5}$. The second intramolecular cycloaddition of terminal $\Delta^{22,23}$-methylene and $\Delta^{18,19}$, $\Delta^{20,21}$ -diene took place in the presence of PyrI4, affording spiro-conjugate **1.76** with the pentacyclic scaffold, which also helped determine the stereochemistry of the aglycone in pyrroindomycins. What is more, *chlE3* and *chlL* in chlorothricin biosynthesis, homologs of *pyrE3* and *pyrI4*, were identified through sequence analysis. These gene products, ChlE3 and ChlL were expressed and evaluated with intermediate **1.74** *in vitro*, where the cascade [4+2] cycloaddition product **1.76** was also detected, despite the structural difference of **1.74** from their natural substrate. This experiment illustrates the generality of cascade cyclases and opens a new door to rapidly create the highly strained pentacyclic skeleton through chemoenzymatic synthesis.

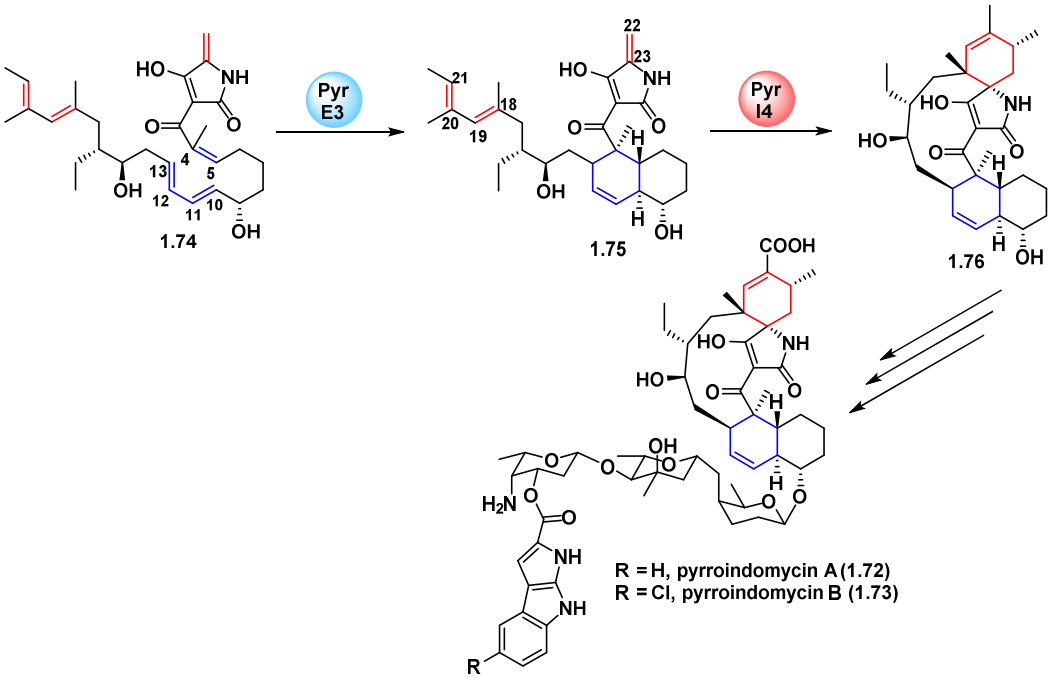

Scheme 10. [4+2] cycloaddtion cascade furnishing pentacyclic core in pyrroindomycins.

In addition to rate acceleration, enzymatic cycloaddition often allows for the formation of cyclohexenes with confirmations difficult to obtain through chemical methods.[70] SPS, a protein in the solanapyrone biosynthetic pathway, has a dual function: oxidizing the linear precursor, alcohol **1.77**, to its corresponding aldehyde, and catalyzing a [4+2] cycloaddition with decent *exo*-selectivity (7:1), furnishing the *trans*-decalin in natural product solanapyrone A (**1.80**), the major isomer in solanapyrone family (Scheme 11A).[61] In contrast, chemical oxidation of **1.77** in various solvents resulted in a non-enzymatic Diels-Alder reaction, but the major product was *cis*-decalin solanapyrone D (**1.81**) through an *endo* transition state (*endo : exo* = 97 : 3).[60, 71] Interestingly, SPS catalyzes the transformation of achiral substrate **1.77** to enantiomerically pure products, a task impossible to match chemically without the aid of a chiral ligand or auxiliary in total synthesis. Similarly, triene **1.82**, an intermediate in lovastatin (**1.1**) biosynthesis, can

undergo Diels-Alder reaction thermally or by Lewis acid catalyst to provide both *exo* and *endo* products, **1.86** and **1.87**, in the absence of enzyme (Scheme 11B).[72] On the contrary, in the reaction catalyzed by cyclase LovB, not only **1.86** and **1.87** were observed, but enzymatic product **1.88** was also found, which maintained the same stereochemistry with the final natural product, lovastatin (**1.1**).[62, 63] The formation of **1.88** was through an *endo* transition state in which the C-6 methyl group occupies the less-favored pseudo-axial position, a pose unattainable by chemical manipulations. The capacity of [4+2] cyclases in generating chemically inaccessible compounds may due to their ability of creating a hydrophobic binding pocket to confine the substrate in a thermally or kinetically disfavored transition state. The high efficiency as well as stereo- and enantioselectivity of enzymatic [4+2] cycloaddition have provided a feasible approach to build mono-, di- or tricyclic scaffolds in total synthesis.[65, 71] Further research on substrate permutation and enzyme engineering may provide promising biocatalysts for chemoenzymatic synthesis.

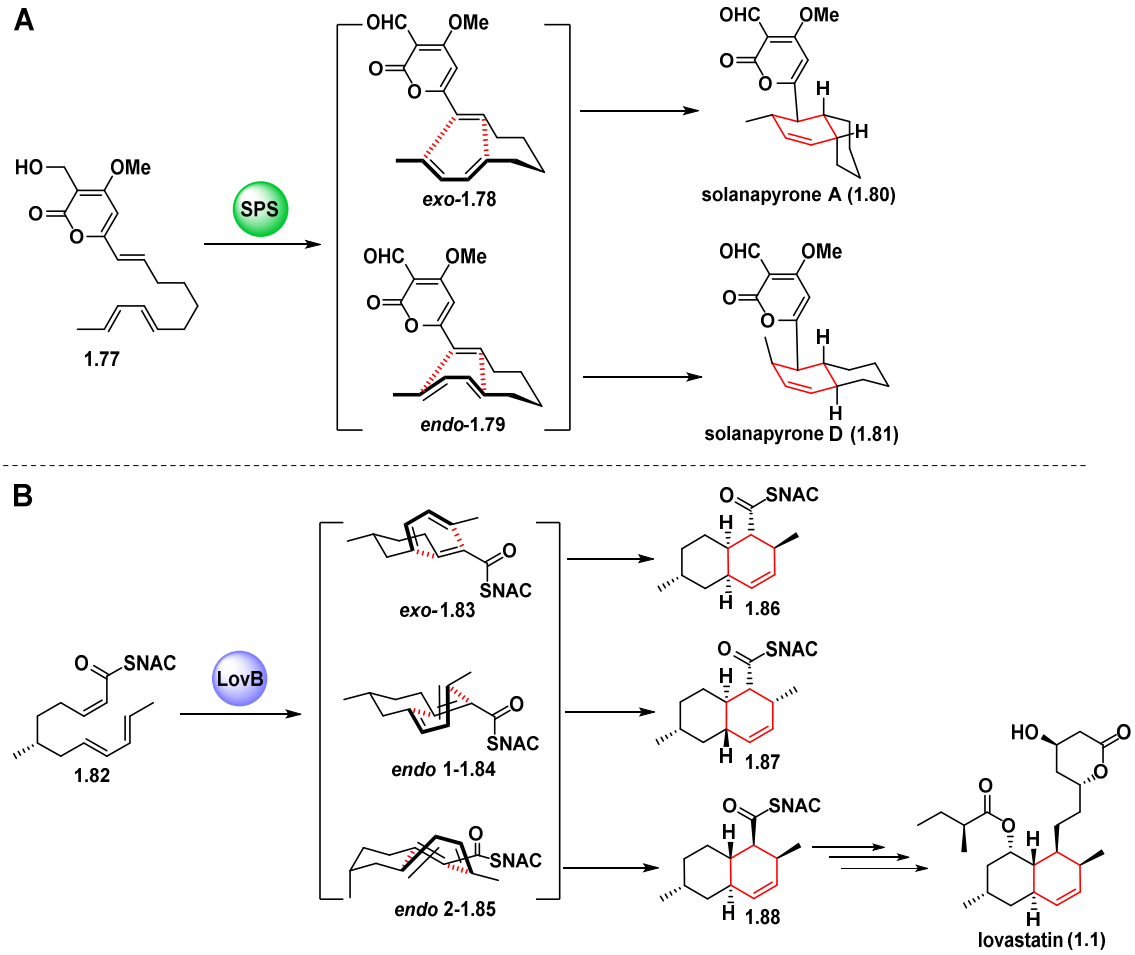

Scheme 11. A) SPS-catalyzed cyclization, favoring *exo*-transition state; while nonenzymatic reaction offered *endo*-product. B) The stereochemistry of the cyclohexene in lovastatin (**1.1**) was only produced by LovB through a sterically disfavored transition state.

1.4.4. Cyclization through epoxide-opening

A myriad of polyketides contain medium-sized cyclic ether moieties, including hydropyrans and hydrofurans, such as in ionophore antibiotics, marine toxins and plant-derived acetogenins. Nature has devised multiple ways to construct these moieties, many of which have inspired biomimetic chemical syntheses.[73-75] The most common approach

is epoxide-opening, proposed by Cane, Celmer and Westley in 1983, whereby the nucleophilic attack of epoxide by hydroxyl or keto-group initiates a cascade of S_N2 reactions, giving rise to polyether formation.[76] This biosynthetic hypothesis was only recently experimentally verified in lasalocid A (**1.89**) biosynthesis (Scheme 12).[77] Synthesized bisepoxyprelasalocid **1.90** was incubated with lasalocid epoxide hydrolase Lsd19 that contains two independent catalytic domains, LsdA and LsdB.[78, 79] Domain dissection and mutagenesis analyses illustrated that LsdA catalyzed the formation of monocyclized intermediate **1.91** through a 5-*exo* cyclization and formed C-O-C bond between C15 and C18. On the other hand, LsdB broke Baldwin's rules by guiding the attack of C-19 hydroxyl group to the epoxide C23 and affording the chemically disfavored 6-*endo* cyclized product, lasalocid A (**1.89**), while non-enzymatic reaction only led to the 5-*exo* cyclization in isolasalocid A (**1.92**). To explain the discrepancy of the enzymatic and the non-enzymatic reactions, co-crystallography of Lsd19 with a bound substrate and computational dockings were completed.[79] It is believed that the interactions provided by acid and base groups in the active site lowered the energy of the 6-*endo* transition state, allowing for the formation of the anti-Baldwin hydropyran ring. In addition to its high regioselectivity and capacity to overcome an unfavorable energy barrier, Lsd19 also demonstrated great promiscuity in terms of substrate preference, making it an attractive agent for chemoenzymatic synthesis.[80] Lsd19 is highly tolerant towards substrate modification in the distal, left-hand portion of the substrate, as the altered substrates demonstrated comparable kinetic parameters to the full-length, native substrate. Although only (22*R*,23*R*)-epoxide was able to afford the 6-*endo* product, the

inversion of the stereochemistry of the C18-C19 epoxide proved to be well tolerated. These intrinsic features of Lsd19 provide insights on substrate design and showcase the potential application of this biocatalyst in total synthesis.

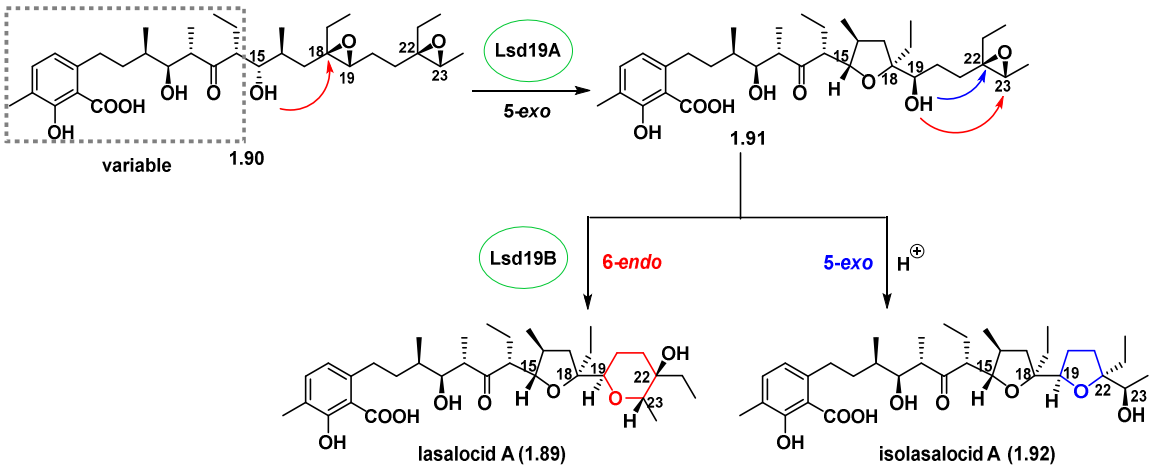

Scheme 12. Lsd19 directed 6-*endo* cyclization in the production of lasalocid A (**1.89**).

1.4.5. P450-Catalyzed Oxidation

Cyclic ether formation may also be catalyzed by cytochrome P450 monooxygenases, an enzymatic family that is traditionally known to conduct many oxidation reactions, including epoxidation, hydroxylation and heteroatom oxidation. AurH, a P450 in aureothin (**1.93**) biosynthesis, was found to perform a regio- and stereoselective hydroxylation at C7 on deoxyaureothin **1.94** to furnish alcohol **1.95**, whose identity was determined by NMR spectroscopic data and Mosher ester analysis of a known standard (Scheme 13).[81] The optically pure alcohol **1.95** was sequentially oxidized by AurH through a heterocyclization to install a C-O bond between C10 and C7 hydroxyl group. Unlike epoxide-opening, this asymmetric biotransformation is impractical to emulate by synthetic manipulations, making the enzymatic, AurH-catalyzed tetrahydrofuran

formation through C-H oxidation the only feasible route. A library of aureothin analogs was constructed through combinatorial biosynthesis via exploitation of the relatively relaxed substrate tolerance of AurH, offering potential therapeutic agents with improved antiproliferative activities.[82] Additionally, the AurH-catalyzed hetero-cyclization reaction is highly stereospecific, only acting on 7*R*-hydroxyl intermediates.[83] This feature was exploited in the preparative synthesis of enantiomerically pure aureothin via AurH-catalyzed kinetic resolution of racemic starting material. Through insights gained from the crystal structure of the enzyme, AurH was genetically altered to hydroxylate C10 methyl group in lieu of C7 in alcohol **1.96** followed by sequential oxidation, resulting carboxylic acid **1.97** as the enzymatic product.[84] The ease of AurH's genetic modification illuminated its prospective usage as a multifunctional catalyst in chemoenzymatic synthesis.

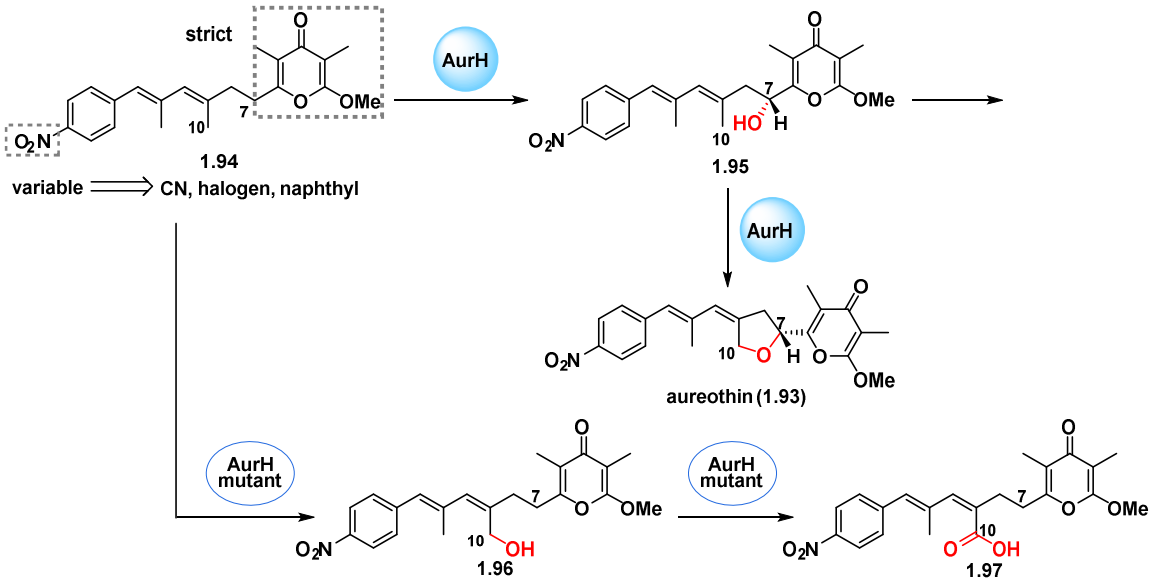

Scheme 13. P450 AurH generated tetrahydrofuran scaffold in aureothin (**1.93**) and its structural fine-tuning to yield carboxylic acid **1.97**.

1.4.6. Perspectives in Chemoenzymatic synthesis

Nature's evolution of various strategies to construct polyketide scaffold has captivated the imagination of chemists to harness their power in total synthesis. Biocatalysts have advanced chemical methodologies in many aspects, including mild reaction conditions, high regio- and stereoselectivity, and eradication of heavy metals or asymmetric ligands. To fully realize the potential of chemoenzymatic synthesis, a thorough understanding of the catalytic mechanism, such as how the active site acts on the substrate and how the conformational change of the enzyme leads to product formation, is of paramount importance. This information is currently being pursued by structural biologists and enzymologists to elucidate the three-dimensional structures of PKS cyclases. The insights gained through these approaches may help design suitable

substrates to be accommodated by the enzyme, predict the stereochemistry outcome, and improve the efficiency of the chemoenzymatic reaction.

One challenge experimentalists must face is limited reaction scope. A practical solution is to screen more promiscuous enzymes that could act on a variety of substrates to finish the biotransformation. A more systematic approach is through enzyme engineering, whereby certain residues in the active site are mutated to permit unnatural substrates, while maintaining the catalytic activity.[85] What is more, enzyme engineering may also promote regio- or stereoselectivity, leading to enantiomerically pure products in synthesis.[86, 87] A combination of structural information and enzyme engineering is key to fully exploit Nature's gift towards the development of chemoenzymatic synthesis.

In order to fully realize the potential of PKS domains as biocatalysts, a critical understanding of their functions, mechanisms and substrate preferences are prerequisite. Therefore, we aim to obtain the knowledge on KR and DH domains as reduction and dehydration reactions are commonly used in total synthesis. The following two charters describe the detailed accounts of the characterization of KR and DH domains from pikromycin synthase and the insights gained from our novel approach.

Chapter 2. Deciphering the cryptic stereochemistry of ketoreductase (KR)[1]

2.1. Backgroud on KRs

2.1.1. Function and structure of KRs

A myriad of polyketides possess complicated structures, harboring multiple stereogenic centers with alkyl and hydroxyl substituents. KR domains play a pivotal role in dictating the stereochemistry of polyketide architecture through stereoselective reduction of the β-keto intermediate and epimerization of the α-substituent. [88] To date, several crystal structures of modular Type I KRs have been elucidated, which reveal two subdomains, the N-terminal KR_S and the C-terminal KR_C.[26, 89-94] The KR_S subdomain is not catalytically active, and only stabilizes KR_C which harbors the binding pockets for the cofactor NADPH and the growing polyketide chain. In the active site, serine and tyrosine residues bind to the β-keto group of the substrate and make the carbonyl carbon more electrophilic, resulting in a transfer of the 4-*pro*-*S*-hydride in NADPH to the β-carbonyl carbon of the polyketide (Figure 7). The catalytic tyrosine donates its proton to the carbonyl oxygen of the substrate, which is promoted by the adjacent lysine to lower the pK_a of the tyrosine residue, to furnish the reductive process.

---

[1] Reproduced in part with permission from Li, Y.; Fiers, W. D.; Bernard, S. M.; Smith, J. L.; Aldrich, C. C.; Fecik, R. A. Polyketide intermediate mimics as probes for revealing cryptic stereochemistry of ketoreductase domains. *ACS Chem. Biol.* **2014,** 9, 2914–2922.

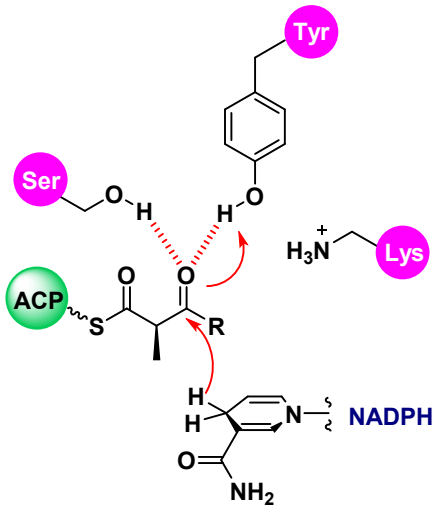

Figure 7. Active site of KR domains and mechanism of KR-catalyzed reduction.

The KS domain catalyzes the Claisen condensation in a stereoselective fashion where the α-substituent is confined in the D-configuration. However, scaffolds bearing an L-alkyl substituent are also common in naturally produced polyketides, suggesting enzymatic epimerization reactions take place during biosynthesis. Recently, $NaBH_4$-trapping and isotope incorporation experiments pinpointed KR domains responsible enzyme for this.[95, 96] It is believed that KR examines the stereochemistry of the α-substituent before performing reduction activity. A KR specific for a D-α-substituent accepts and processes the β-keto intermediate from the KS domain while a KR harboring intrinsic preference for an L-α-substituent epimerizes the substrate into its favored orientation, and then reduces the resulting L-α-alkyl-β-ketone. The characteristic activities executed by KRs can be summarized as a combination of epimerization and reduction driven by a specific epimer.[88]

2.1.2. Classifications of KRs

Based on the stereochemical outcome of the reduction, KRs are divided into three major types: A-type (L-β-alcohols), B-type (D-β-alcohols), and reductase incompetent C-type (β-ketones) (Figure 8). KRs can be further classified into subtypes as they also control the α-substituent orientation. KRs that process substrates with no α-substituent are termed as A0 and B0. The numeral "1" is designated to KRs that generate a D-α-substituted product, such as A1, B1 and C1 while "2" is denoted to the ones which lead to a L-α-substituted product, including A2, B2 and C2.

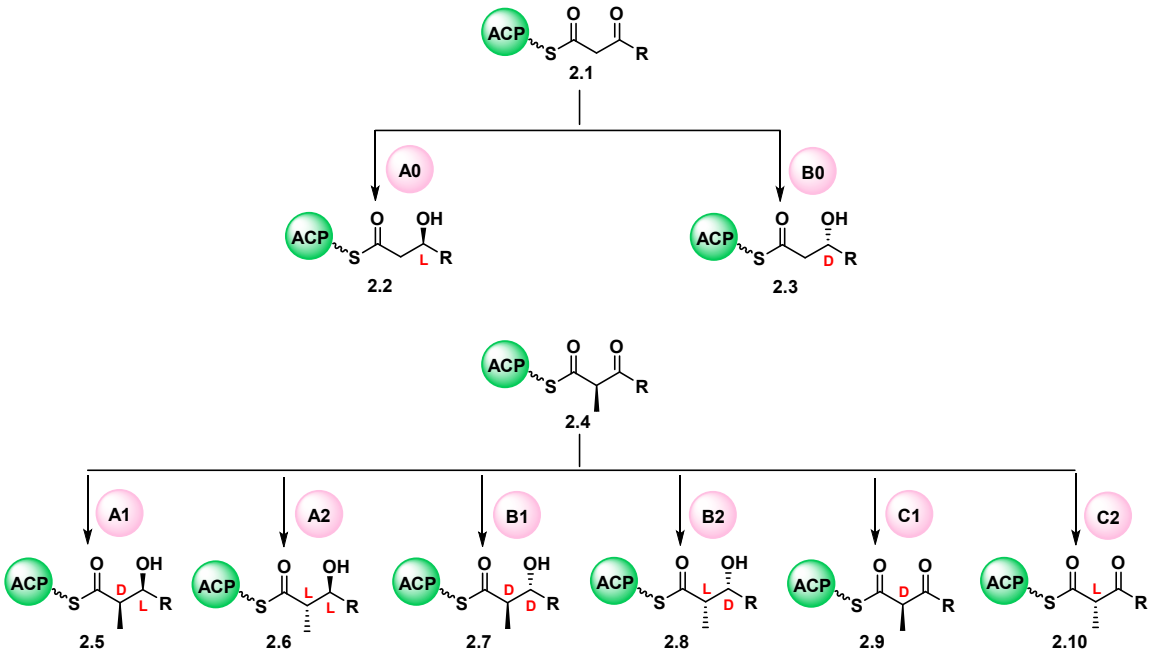

Figure 8. Classifications of KRs and their corresponding products.

Recent research has shown a strong correlation between the amino acid sequence of KR domains and the stereochemistry of the KR products.[90, 97, 98] A-type KRs generating L-hydroxyacyl products contain a highly conserved tryptophan (W motif), located eight

residues N-terminal to the catalytic tyrosine, while in B-type KRs a LDD motif (or often LXD motif) is present at ~57 amino acids before the catalytic tyrosine (Figure 9). Moreover, absolute configuration of an α-substituent can be determined through additional motif indicators. A1- and A2-type KRs are distinguished from each other via the absence or presence of the histidine residue at three amino acids N-terminal to the catalytic tyrosine. Similarly, B2-type KRs possess a proline, 2 residues after the catalytic tyrosine while B1-type KRs do not. C2-type KRs, only bearing epimerase activity, lack the NADPH binding pocket known as the TGGTGXLG motif, and C1-type KRs are insufficient for any catalysis due to the lack of the catalytic tyrosine.

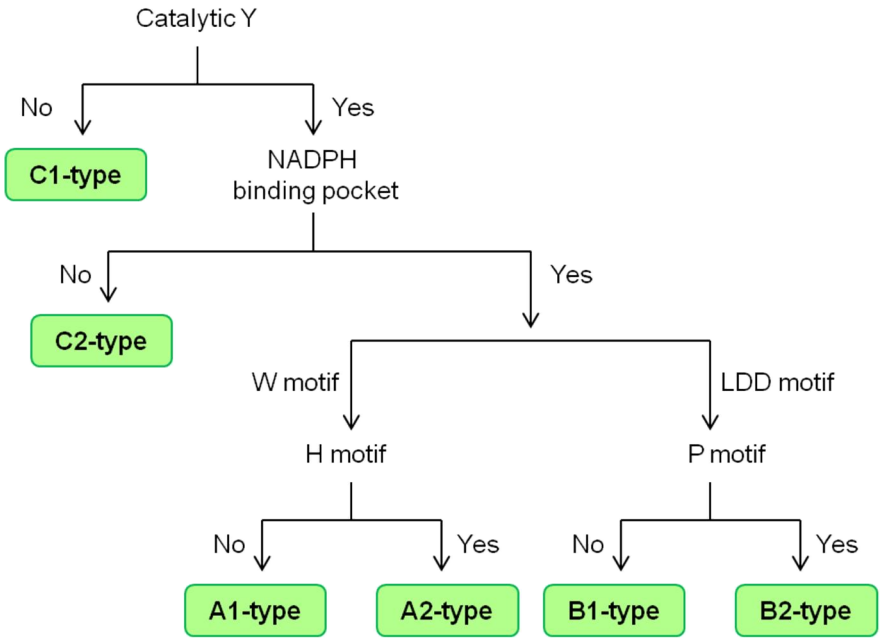

Figure 9. Fingerprint sequences associated with different types of KRs.

To rationalize the relationship between the observed stereochemical outcome and the empirically deduced amino acid motifs, there have been many efforts to obtain the structural information about KR domains. Recent crystallographic studies have shown

that all KRs bind the cofactor NADPH in the same orientation, which transfers the 4-*pro*-*S*-hydride to the β-carbonyl carbon of the polyketide intermediate. As a result, the difference in stereochemical outcome must arise from a reversed presentation of the β-ketoacyl substrate in the active site, exposing *re* or *si* faces of the β-keto group to NADPH in A- and B-type KRs.[90] One hypothesis is that the W motif promotes entry of the polyketide intermediate through the southeast opening of the active site groove in A-type KR (Figure 10A), yielding a product with the L-orientation. In an analogous way, in B-type KRs the LDD motif directs the substrate to access the active site groove from the northwest side to generate the D-hydroxyl product (Figure 10B). However, the W and LDD motifs are not the only factors contributing to stereocontrol based on the distance from the active site (W) and inability to occlude active site openings (LDD).[91, 94, 99] Analysis of crystal structures of both A- and B-type KRs led to a corollary to the direction-of-entry hypothesis by noting that cofactor binding (NADPH or $NADP^+$) in A-type KRs may generate a tight and well-ordered conformation at the active site through a hydrogen bonding network.[94] In this catalysis-ready conformation, Met366 is pushed into the active site to block entry from the northwest. Thus, the substrate could penetrate the active site groove only from the southeast (Figure 10A). In B-type KRs, this cofactor-assisted catalysis-ready state does not exist. Instead, cofactor binding is loose, allowing for polyketide entry through both channel openings. It is proposed that only binding of substrate from the northwest side could set a tight, catalysis-ready conformation in the active site (Figure 10B), leading to the product with D-orientation.[94] Further biochemical

and structural experiments may be needed to better understand the mechanism of the stereoselectivity of KRs.

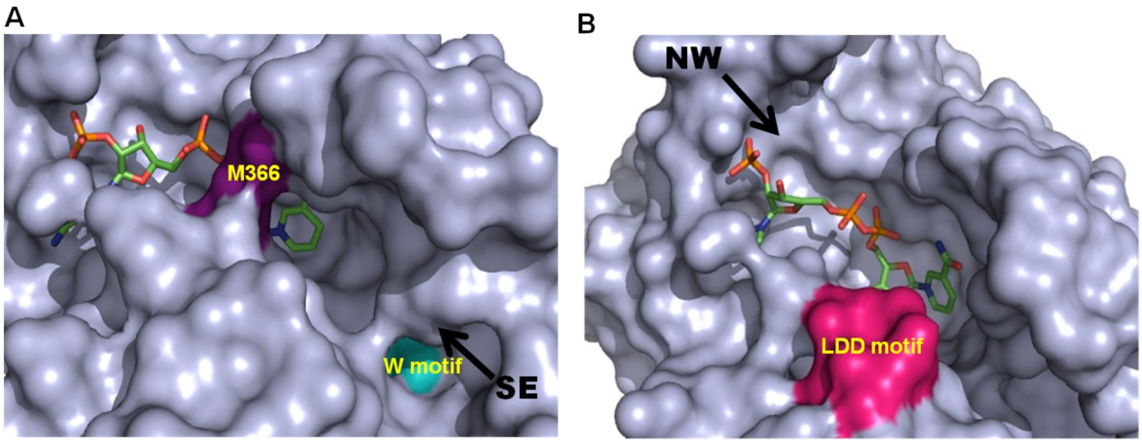

Figure 10. Signature motif comparison of A- and B-type KRs. A) Active site of A-type PlmKR1 with $NADP^+$ bound; W motif shown in cyan; M366 shown in purple. B) Active site of B-type EryKR1 with $NADP^+$ bound; LDD motif shown in pink. Figures 10A and 10B were created in Pymol using PDB codes 4HXY and 2FR0.

2.1.3. KRs' cryptic stereochemistry

Each KR catalyzes its reaction in a highly stereoselective manner. For instance, the initial KR domain of the PIKS (PikKR1) reduces the β-ketone to an alcohol, which establishes the configuration at C-11 of methymycin and C-13 of pikromycin (Figure 3). However, this observational method cannot be utilized for modules that contain a DH domain since the resulting dehydration eliminates the stereogenic center as seen in modules 2 and 4 of the PIKS. This type of "hidden" stereoselectivity, when referral to the mature polyketide gives no implication of the stereochemical outcome of the KR domain of interest, has been termed cryptic stereochemistry.

Although the bioinformatic analysis can provide insight to predict the stereochemistry of uncharacterized KRs, current work has revealed several exceptions. For instance, the KRs in the seventh and tenth modules from the rifamycin PKS, KR7 and RifKR10, do not possess the signature W motif, yet still yield L-alcohol products.[100] Due to the empirical nature of the fingerprint method, the predicted stereochemical outcome of cryptic domains is not absolutely infallible. This highlights the need for novel experimental methods to complement signature sequence methods to decipher cryptic stereochemistry.

2.2. Chemical strategy and rationale

Biochemical and molecular biological approaches have been widely used to provide valuable insights into the mechanism as well as substrate and stereoselectivity of PKS domains, especially KRs.[101-104] Cane and co-workers established the stereochemical outcome of PikKR2 by engineering PIKS module 2 with PikTE and inactivation of PikDH2 by site-directed mutagenesis (Figure 11A).[101] Incubation of diketide thioester **2.11**, methylmalonyl-CoA, and NADPH with this construct produced triketide lactone **2.12** exclusively, establishing the D-configuration of the C3-alcohol. As a general approach, this method may require extensive work on protein expression, mutant construction and product detection. More importantly, most of the substrates used in this and other previous studies are simple diketide analogs, which likely show low affinity and poor stereoselectivity for the study of domains in later, downstream modules due to poor structural similarity to the native substrates.[42] For example, in a recent study with KR domains from the amphotericin, pikromycin, and spinosyn PKSs (AmpKR10,

PikKR5, and SpnKR3), multiple diastereomeric products resulted from use of the simple *N*-acetylcysteamine (NAC)-2-methyl-3-oxobutanethioester as the substrate.[55] Due to the challenges inherent in establishing mechanistic details of polyketide biosynthesis, other complementary approaches to deciphering cryptic domains could be applied broadly.

We sought to employ an alternative, chemical probe-based approach to understand the structural and mechanistic features of KR domains. This novel method entails incubation of synthetic substrate mimics with excised KR domains and observation of enzymatic products by LC-MS/MS (Figure 11B). Compared to previous approaches, we envision our new method offers unique insights in three aspects. Firstly, this method reduces the biochemical and molecular biological workload in studying cryptic stereochemistry since it requires only a single domain versus an entire multimodular PKS protein. Additionally, the substrate is not tethered to the ACP domain; thus neither a TE domain nor a complicated workup procedure is required to release the enzymatic product. Secondly, this intermolecular assay design allows for interrogation of the steady-state kinetic parameters of the individual excised domains. Testing of non-natural substrates enables investigation of substrate-protein interactions. It would also be possible to investigate protein-protein interactions if the probes are linked to an ACP domain. Thirdly, compatibility of substrates is guaranteed. Given that the substrate is specifically designed on the basis of the natural substrate, substrate and stereoselectivity is ensured due to nearly identical steric properties. [91, 94]

In light of previous research (vide supra), we chose PikKR2 to validate this chemical probe-based approach. Both PikKR2 substrate and product mimics were designed and

synthesized (Figure 11B). The substrate mimic designs were based on the natural substrate of PikKR2 (**2.13**) with two modifications. First, truncation of the ACP-phosphopantetheinyl arm to a NAC-based substrate was planned to ease synthetic access to the target molecules. Since the ACP-phosphopantetheinyl arm does not affect the stereocontrol of KRs, NAC thioester derivatives have been widely used as surrogates of natural substrates.[55, 94, 105] Second, since 5-hydroxy triketide thioesters are prone to rapid cyclization to triketide lactones, we sought to replace and mimic the electrophilic thioester of the native PikKR2 intermediate with an amide or thioether bond. In vivo this lactonization is likely prevented by a PKS system by maintaining the nascent polyketide in an extended conformation through interactions with the ACP arm. Thus, two series of substrate mimics with stabilized structures were designed: (1) incorporation of secondary (**2.16**) or tertiary (**2.17**) amides as stable thioester isosteres,[106] and (2) thioether analogs **2.18** and **2.19**, which are based upon previous success of us and others.[107, 108] Although thioethers **2.18** and **2.19** have one- and two-carbon spacers between the C1-carbonyl of the triketide and the NAC group, we anticipated that the long phosphopantetheinyl-binding channel of PikKR2 could accommodate this variance. Additional support for this approach was suggested by prior work of others with malonyl CoA analogs where the thioester was replaced with a ketone. These malonyl CoA analogs, when added to fermentation broths, underwent chain elongation, β-processing, and chain termination to release off-loaded intermediates.[109-113] For analysis of the enzymatic reaction of substrate mimics **2.16**–**2.19**, synthesis of both potential diastereomeric products **2.20**–**2.27** of each substrate mimic was also required. Since thioether substrate mimics **2.18** and **2.19** have

two ketones that could potentially be reduced by PikKR2, we also synthesized diols **2.28**–**2.31** (as diastereomeric mixtures). Diols **2.28**–**2.31** would result from reduction of the C1-ketone (polyketide numbering) instead of expected reduction of the C3-ketone. Since C1-reduction is an unnatural event, and does not occur in the biosynthetic pathway, the C1-epimeric product mixture was deemed sufficient for these studies.

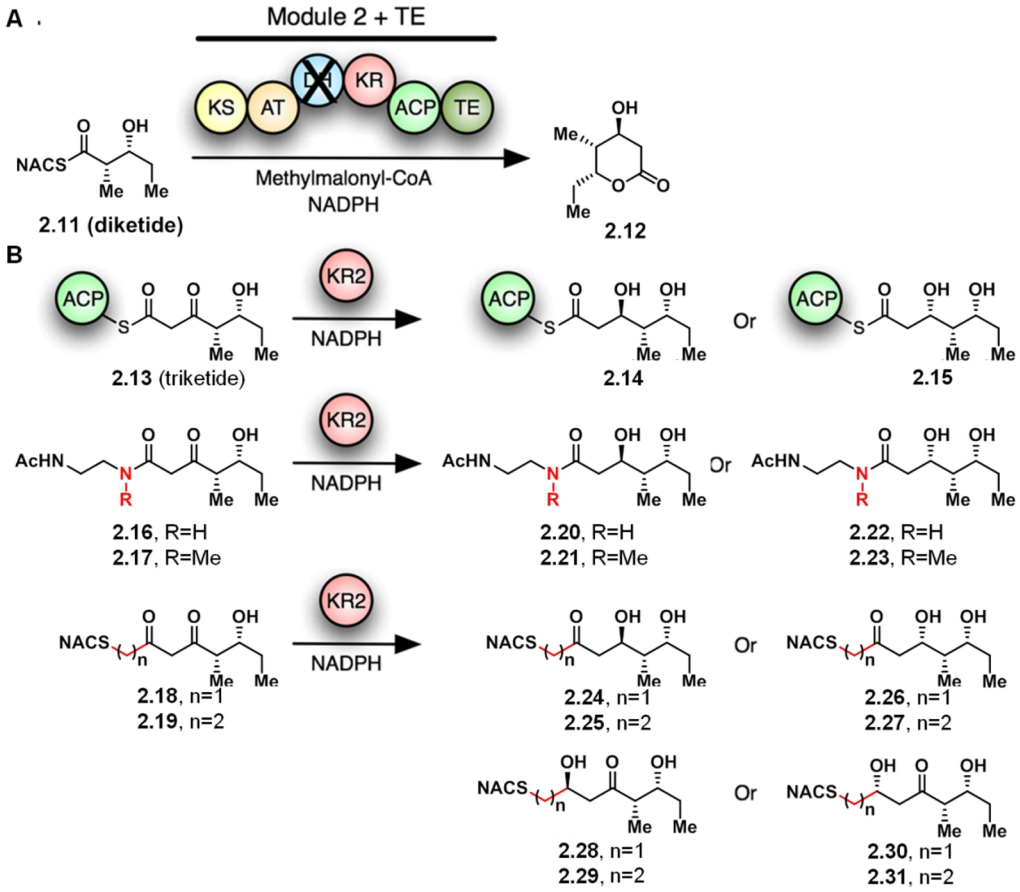

Figure 11. A) Previous approach to determining the cryptic stereochemistry in PikKR2 using an engineered Pik module 2. B) Design of PikKR2 substrate mimics **2.16**–**2.19** and product mimics **2.20**–**2.31** for a KR-based assay to determine cryptic stereochemistry.

2.3. Synthesis of substrate mimics

2.3.1. Synthesis of amide substrates

Synthesis of secondary and tertiary amide substrate analogs **2.16** and **2.17** commenced with with the acetate aldol reaction of thiazolidinethione **2.32**[114, 115] with aldehyde **2.33**[116, 117] to give alcohol **2.34** as the major diastereomer (Scheme 14A). Direct aminolysis of the chiral auxiliary with amine **2.35** or *N*-methylamine **2.36** yielded amide **2.37** and *N*-methylamide **2.38**, respectively. Secondary amine **2.36** was synthesized in three steps from *N*-(2-aminoethyl)acetamide (**2.41**), where the primary amine was protected with 2-nitrobenzenesulfonyl group to conduct mono-methylation in **2.42** (Scheme 14B). TPAP/NMO oxidation and deprotection afforded amide substrate mimics **2.16** and **2.17**. The stereochemistry of aldol product **2.34** was established by deprotection of amide **2.37** and conversion to its acetonide **2.45**, which was subject to Rychnovsky's acetonide analysis (Scheme 14C).[118, 119]

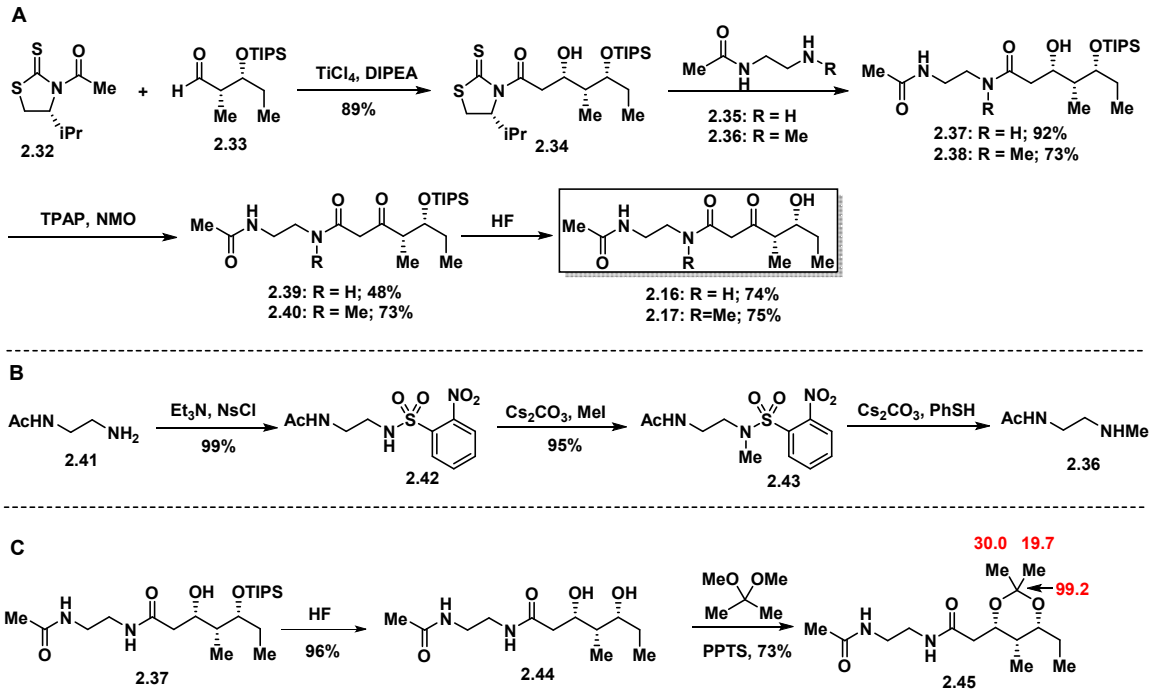

Scheme 14. A) Synthesis of amide substrates **2.16** and **2.17**. B) Synthesis of methylamine **2.36**. C) Acetonide formation to assign relative and absolute stereochemistry.

2.3.2. First attempt to synthesize thioether substrates

For thioether substrate mimics, the synthesis of **2.19** was first explored as a Grignard reaction that could easily install the two carbon spacer in the substrate. Acetate aldol reaction of aldehyde **2.33** with *N*-methoxy-*N*-methylacetamide (**2.46**) gave a separable 2.7:1 diastereomeric mixture of Weinreb amides **2.47** and **2.48** (Scheme 15). The major aldol adduct **2.47** was reacted with excess Grignard reagent to produce vinyl ketone **2.49**, which was elaborated through sequential IBX oxidation, Michael addition of *N*-acetylcysteamine to afford **2.51**.[120] However, under all traditional and non-traditional TIPS deprotection conditions conducted, the desired product **2.19** turned out to exist in the equilibrium of the diketone and hemiketal, which rapidly underwent dehydration to

yield undesired dihydro-4-pyranone **2.52**. After trying numerous attempts, no successful deprotection conditions were found. Therefore, it was decided to choose an alternative protecting group which could be cleaved under mild condition in the end to solve the stability issue of the final product.

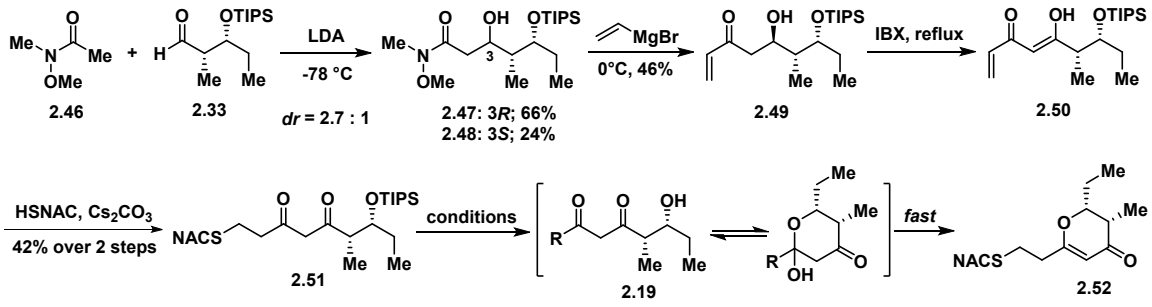

Scheme 15. First attempt to synthesize thioether substrate **2.19**.

2.3.3. Revised syntheses of thioether substrates

To solve the difficulty in final deprotection, a relatively more labile group, triethylsilyl ether, was chosen. *N*-acyl thiazolidinethione **2.53**[117] was protected and reduced to aldehyde **2.55**, followed by acetate aldol reaction with **2.46** to give Weinreb amides **2.56** and **2.57** (dr = 7:3, separated by chromatography) (Scheme 16A). Weinreb amide **2.56** was directly converted to chloromethyl ketone **2.58**, followed by IBX oxidation of the secondary alcohol, S_N2 reaction of the chloromethyl ketone with *N*-acetylcysteamine, and deprotection to afford thioether substrate mimic **2.18**.[120, 121] The synthesis of thioether substrate mimic **2.19** was accomplished in an analogous fashion from Weinreb amide **2.56** by nucleophilic addition of vinyl lithium to produce vinyl ketone **2.61** (Scheme 16B). IBX oxidation, Michael addition of *N*-acetylcysteamine, and deprotection furnished thioether substrate analog **2.19**. The stereochemistry at C-3 of

aldol products **2.56** and **2.57** were determined by conversion to their acetonides followed by Rychnovsky's acetonide analysis (Scheme 16C).[118, 119]

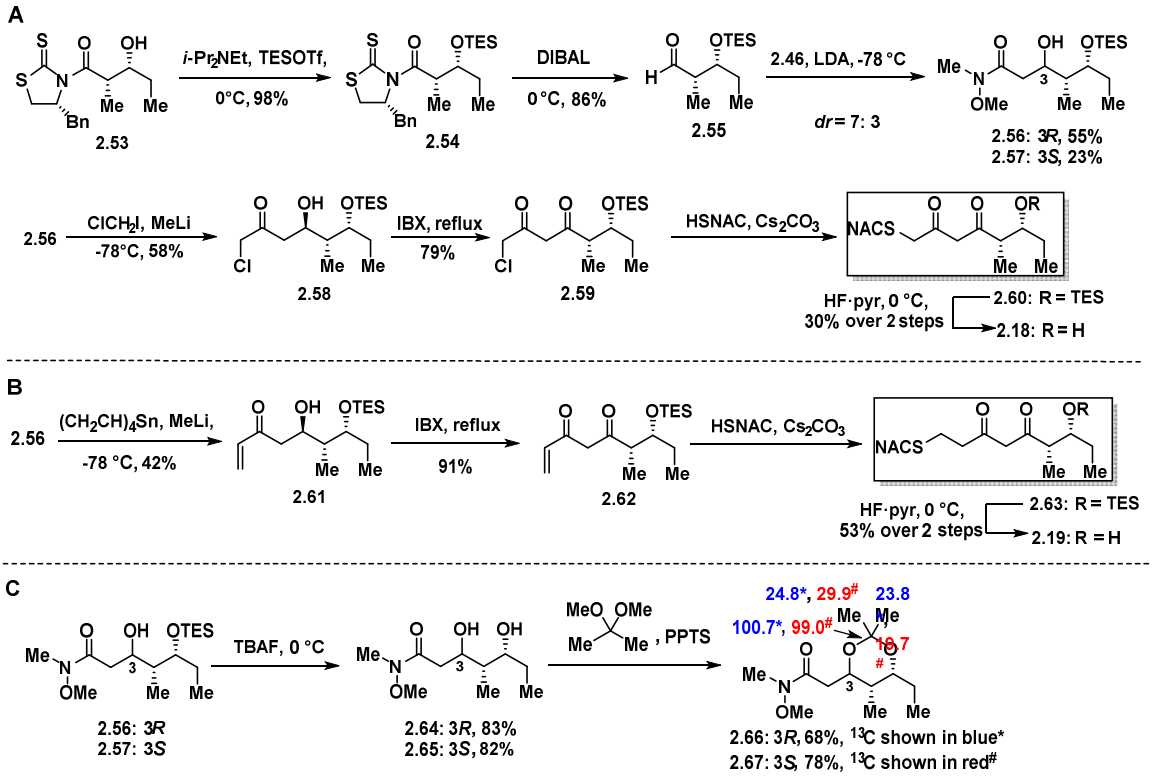

Scheme 16. Syntheses of thioether substrate **2.18** (A), **2.19** (B) and acetonide formation to assign stereochemistry (C).

2.4. Synthesis of potential product mimics

All potential products from PikKR2 reduction of thioether substrate mimics **2.18** and **2.19** were synthesized as authentic standards for analytical comparison to the enzymatic products (Scheme 17). C3-Hydroxy products of substrate mimic **2.18**, diols **2.24** and **2.26**, were synthesized from Weinreb amides **2.56** and **2.57** by protection, conversion of the Weinreb amides to the chloromethyl ketones, S_N2 displacement with *N*-acetylcysteamine, and deprotection (Scheme 17A). Synthesis of the potential products resulting from C1-

reduction of substrate mimic **2.18**, C1-alcohols **2.28** and **2.30**, began with Grignard addition of allyl magnesium bromide to Weinreb amide **2.75**, synthesized in two steps from thiazolidinethione **2.53** to afford allyl ketone **2.76** (Scheme 17B).[122] Non-selective epoxidation of **2.76** with *m*-CPBA, epoxide opening with *N*-acetylcysteamine, and deprotection gave C1-products **2.28**/**2.30** as a distereomeric mixture. The reaction of epoxide **2.77** with *N*-acetylcysteamine was low-yielding due to competitive formation of the C-2 addition product.

The potential C3-reduction products of thioether substrate mimic **2.19**, diols **2.25** and **2.27**, were synthesized from protected Weinreb amides **2.68** and **2.69** in an analogous fashion to **2.25** and **2.27** (Scheme 17C). Synthesis of the potential C1-reduction products of substrate mimic **2.19**, diols **2.29** and **2.31**, began with addition of methylmagesium bromide to Weinreb amide **2.75**, followed by Grignard reaction of the resulting methyl ketone **2.83** with aldehyde **2.84**, coupled from *N*-acetylcysteamine and acrolein, to give alcohol **2.85** (dr = 2:1, inseparable by chromatography), and deprotection to provide diols **2.29**/**2.31** as a diastereomeric mixture (Scheme 17D).

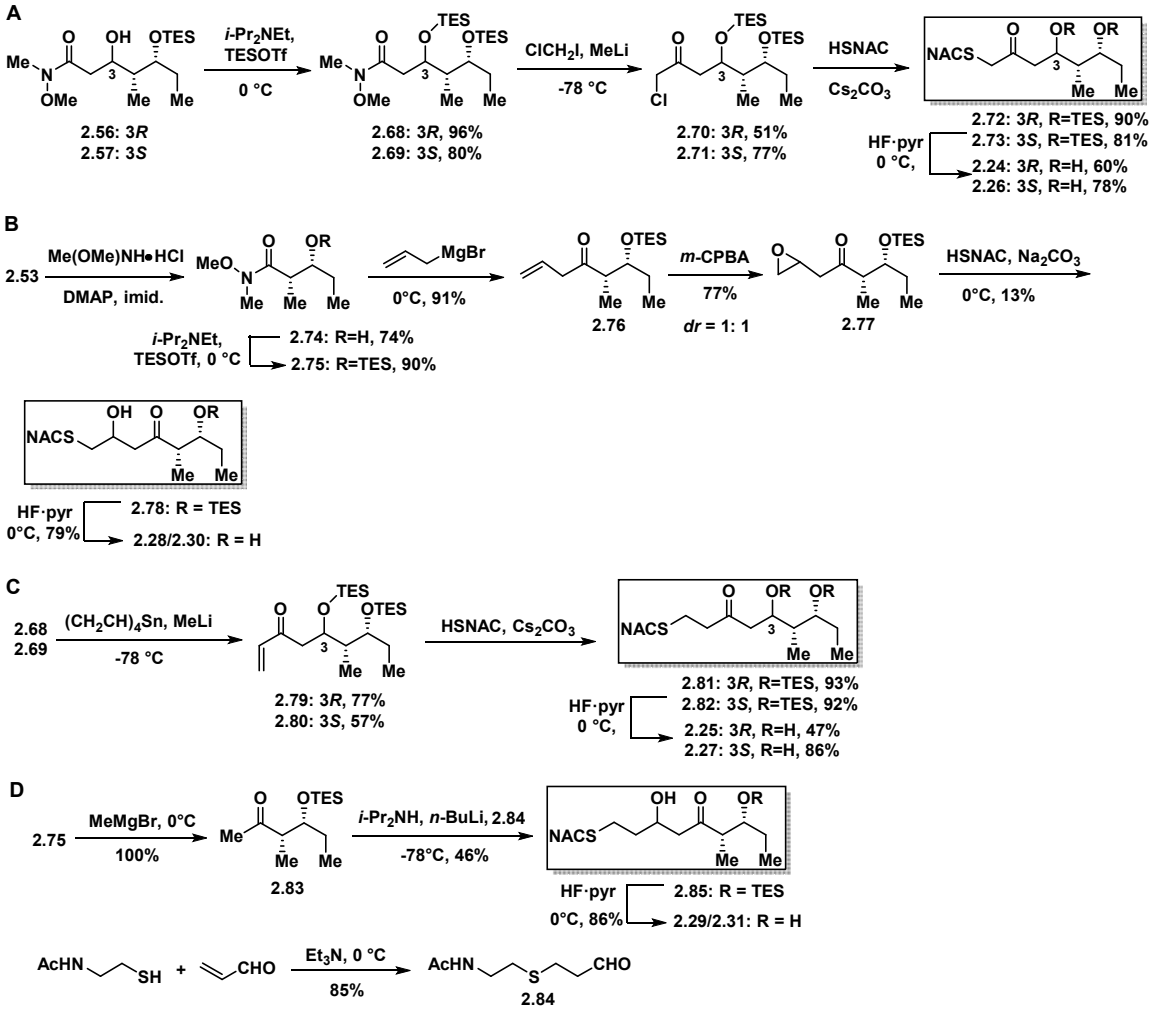

Scheme 17. Synthesis of all possible thioether products **A**) **2.24** and **2.26**, **B**) **2.28**/**2.30**, **C**) **2.25** and **2.27**, and **D**) **2.29**/**2.31**.

2.5. LC-MS/MS analysis of enzymatic products

2.5.1. Cloning, expression, and purification of PikKR2

The KR2 domain of PikAI was identified by sequence comparison with other type I PKS KR domains. The *PikAI* sequence encoding KR2 (residues 3880–4355) was cloned from the cosmid pLZ51 into expression vector pMCSG7 and verified by sequencing.[11, 123] The N-terminal hexa-His tagged protein was overexpressed in *E. coli* BL21(DE3) cells.

The protein was purified by sequential nickel affinity and gel filtration chromatography to afford approximately 45 mg of purified enzyme per liter of culture that was >95% pure as judged by SDS-PAGE (Figure 12). The molecular weight determined by SDS-PAGE is approximately 55 kDa, while the monoisotopic mass of PikKR2 determined by electrospray ionization (ESI) mass spectrometry is 51,430 Da, also consistent with the calculated value from the amino acid sequence of the PikKR2 domain and the histidine tag (51,431 Da). A Superdex 200 gel filtration, calibrated using a Gel Filtration Calibration Kit LMW (GE Healthcare), was used to estimate the molecular weight of the native enzyme as 95 kDa, suggesting the enzyme exists as a homodimer. The cloning, expression and purification of PikKR2-DH2 didomain was conducted in an analogous fashion (SDS-PAGE gel shown in Chapter 3 Figure 27).

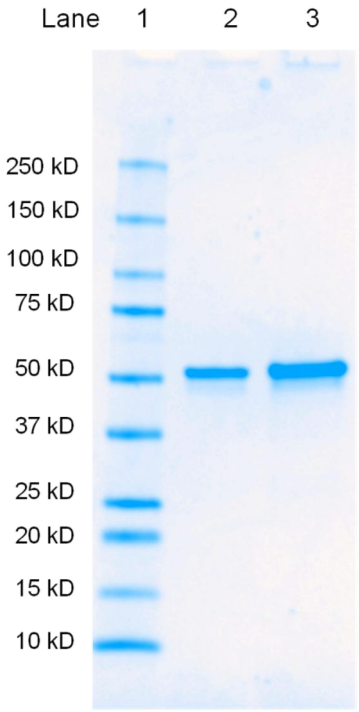

Figure 12. SDS-PAGE gel electrophoresis of purified PikKR2 on BIO-RAD precast gels (Mini-PROTEAN® TGX™ gels) stained by Bio-Safe™ Coomassie G-250 Stain; Lane 1 was loaded with 3 µL Precision Plus Protein Standards (BIO-RAD); Lane 2 was loaded with 1 µg PikKR2; Lane 3 was loaded with 2 µg PikKR2.

2.5.2. Substrate specificity of PikKR2

To initially test whether the synthesized substrate mimics **2.16**–**2.19** were competent substrates, PikKR2 (5 µM) was incubated overnight (12–16 h) with **2.16**, **2.17**, **2.18**, or **2.19** (1 mM) and NADPH (2 mM) in sodium phosphate buffer (100 mM, pH 7.1). After incubation, each enzymatic reaction was quenched via addition of MeCN, and precipitated protein was removed by centrifugation. The supernatant was analyzed by ESI mass spectrometry to detect enzymatic reduction products (as seen by the increase of [M+2] peak), compared to control reaction (either without enzyme or without NADPH).

The reactions of amides **2.16** and **2.17** did not show any appreciable increase of the [M+2] peaks, nor consumption of the parent ion peaks (data not shown). In contrast, thioethers **2.18** and **2.19** demonstrated substantial turnover with large increases of the [M+2] peaks (Figure 13). Exclusion of either NADPH or PikKR2 abolished product formation with **2.18** and **2.19**. This assay indicated that thioethers **2.18** and **2.19** are substrates for PikKR2 while amides **2.16** and **2.17** are not turned over by the enzyme.

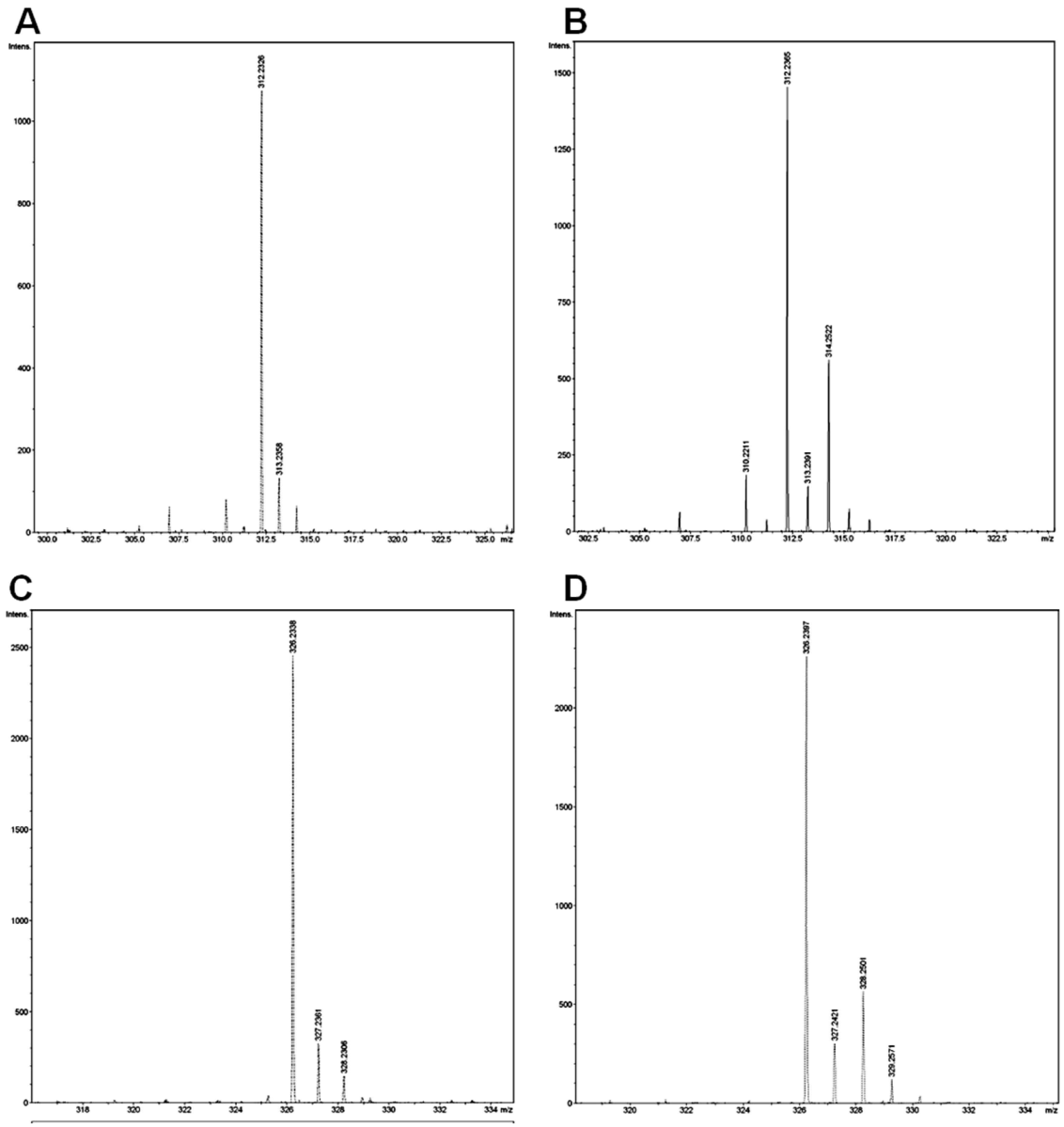

Figure 13. Turnover analysis of substrate **2.18** and **2.19** by ESI-MS. (A) ESI-MS analysis of substrate **2.18** incubation without PikKR2; (B) ESI-MS analysis of substrate **2.18** incubation with PikKR2; (C) ESI-MS analysis of substrate **2.19** incubation without PikKR2; (D) ESI-MS analysis of substrate **2.19** incubation with PikKR2.

Several factors may contribute to the lack of reactivity of amides **2.16** and **2.17**. Unlike the thioester, amides may form either an unfavorable *N*-H hydrogen bond (secondary amide **2.16**) or harbor excess steric bulk (tertiary amide **2.17**), impeding access into the narrow active site channel. The amide linkage's restricted conformations may also not enable the substrate mimics to adopt the required catalytically active conformation. Computational docking by others of a ketide-bound ACP substrate to a KR domain indicated that the thioester linkage may not be planar, lending support to the latter hypothesis.[90]

2.5.3. Confirmation of reaction products by LC-MS/MS

Due to its intrinsic selectivity and sensitivity LC-MS/MS was chosen for assignment of the enzymatic products of PikKR2. We synthesized all plausible constitutional isomer reduction products of thioethers **2.18** and **2.19** as authentic standards. These synthetic standards are readily resolved by LC-MS/MS by their unique HPLC retention times and/or by their parent and daughter ions in MS/MS (Figure 14 and Table 1). Standards **2.25** and **2.27** are observed with two retention times by HPLC (Figure 14), which we hypothesize is caused by the ring-chain equilibration between the open chain keto tautomer and the closed ring lactol tautomer. Standards **2.28/2.30** and **2.29/2.31** are mixtures of two diastereomers, also resulting in two HPLC retention times.

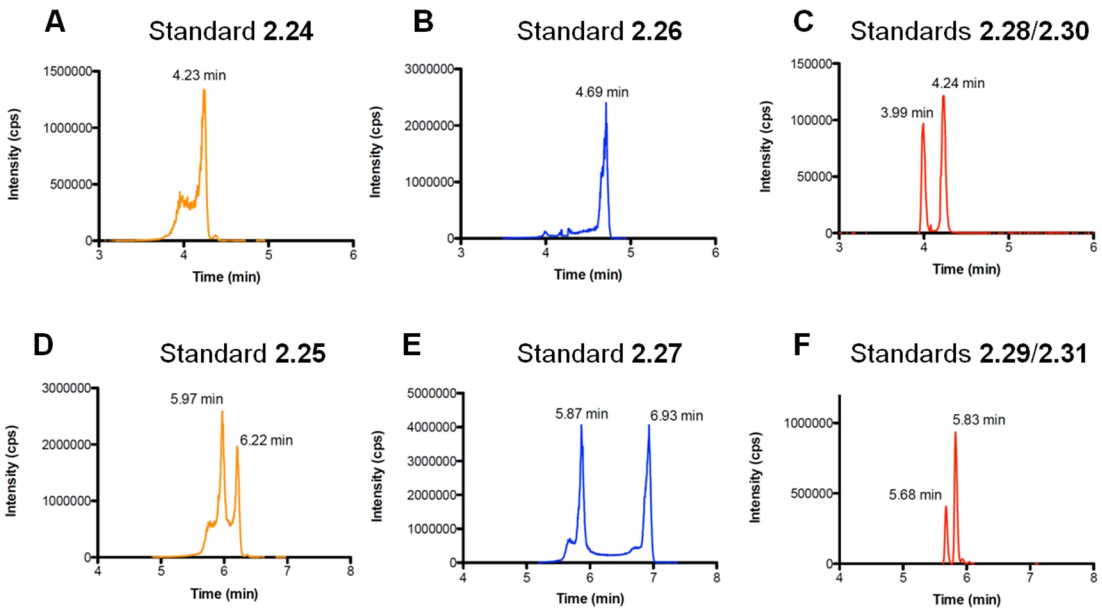

Figure 14. LC–MS/MS analysis of product mimics **2.24**–**2.31**.

Table 1. LC-MS/MS retention times for standards **2.24**–**2.31**.

Standards	Structure	Transition m/z	Retention time (min)
2.24	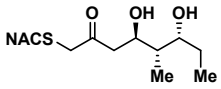	314→198	4.23
2.26	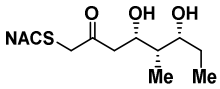	314→198	4.69
2.28/2.30	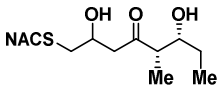	292→216	3.99, 4.23
2.25	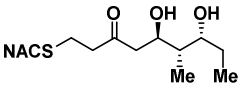	328→212	5.97, 6.22
2.27	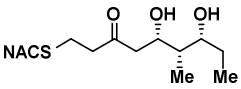	328→212	5.87, 6.93
2.29/2.31	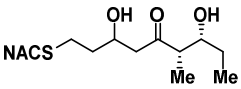	306→230	5.68, 5.83

Incubation of thioether **2.18** with PikKR2 using conditions described above resulted in two reaction products with retention times of 4.00 min (red trace, transition *m/z* 292→216) and 4.70 min (blue trace, transition *m/z* 314→198) corresponding to C1-reduction product (**2.28** or **2.30**) and C3-reduction product **2.26**, respectively (Figure 15A). The normalized product ratio of (**2.28** or **2.30**):**2.26** is 1:4 based on a standard curve generated from the authentic standards. The larger peak for **2.28** or **2.30** at 4.00 min actually represents the minor product, a consequence of its high ionization efficiency. Similarly, incubation of thioether **2.19** with PikKR2 resulted in two reaction products. The peaks at 5.88 and 6.93 min (blue trace, transition *m/z* 328→212) correspond to standard **2.27** while the peak at 5.68 min (red trace, transition *m/z* 306→230) corresponds to one of the diastereomers in standard **2.29**/**2.31** (Figure 15B). The normalized product ratio of (**2.29** or **2.31**):**2.27** is 1:6 based on a standard curve generated from authentic standards. These results indicate that PikKR2 preferentially reduces the C3-ketone in substrates **2.18** and **2.19** with exquisite stereoselectivity to afford the D-configured alcohol products **2.26** and **2.27**, respectively. Intriguingly, only a single peak was observed by LC-MS/MS for C1-reduction products, which corresponds to **2.28** or **2.30** (Figure 15A) and **2.29** or **2.31** (Figure 15B), indicating even the minor reduction (C1-reduction) is conducted in a complete diastereoslective fashion.

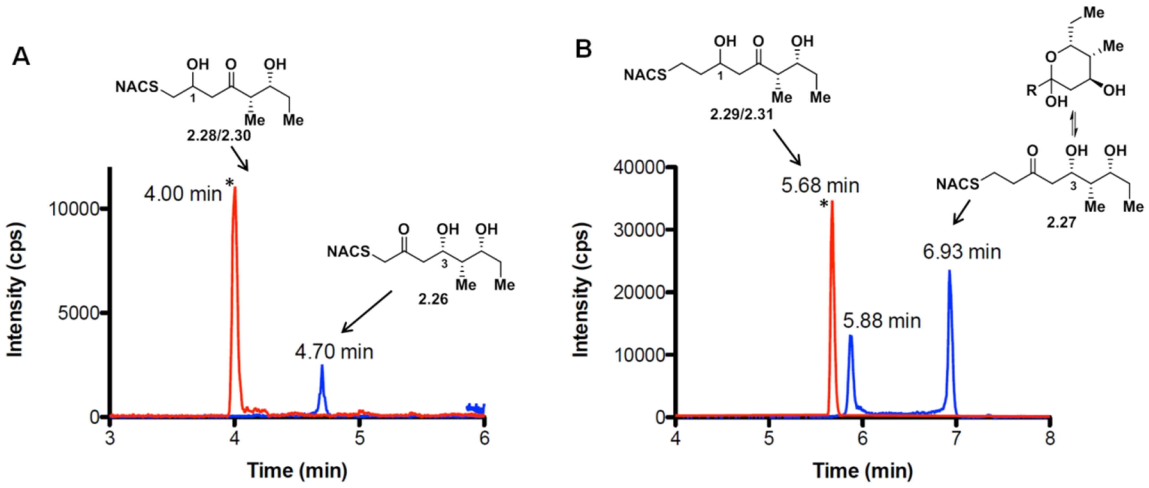

Figure 15. LC-MS/MS analysis of PiKKR2 activity. A) LC-MS/MS enzymatic product analysis of substrate **2.18**; red trace (marked as *) represents MRM (*m/z* 292→216); blue trace represents MRM (*m/z* 314→198). B) LC-MS/MS analysis for enzymatic product of substrate **2.19**; red trace (marked as *) represents MRM (*m/z* 306→230); blue trace represents MRM (*m/z* 328→212).

To investigate the stereoselectivity of KR in a more native context, substrate **2.19** was incubated with the PikKR2-DH2 didomain and analyzed in an analogous way. The LC-MS/MS trace of didomain products showed exactly the same retention times as observed by the single domain, demonstrating the same enzymatic products, D-alcohol at C3-reduction and one single diastereomer at C1-reduction (Figure 16). The ratio of C3-reduction (natural event) to C1-reduction (unnatural event) by PikKR2-DH2 didomain was increased to 18: 1, suggesting that larger portions of PKS module preferably conduct the natural reaction (C3-reduction) over the competitive side reactions (C1-reduction).

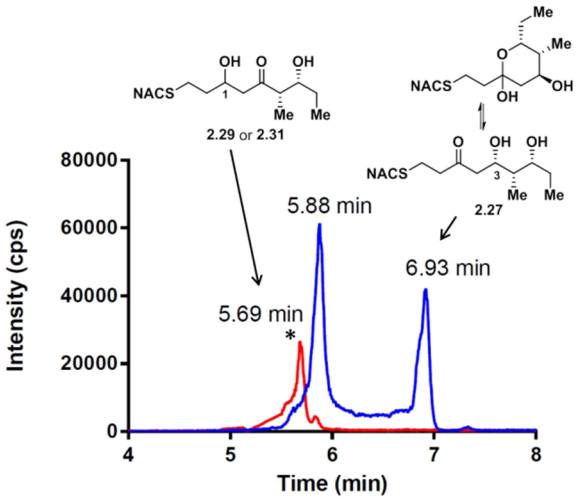

Figure 16. LC-MS/MS analysis for enzymatic products of substrate **2.19** by PikKR2-DH2 didomain; red trace represents MRM (*m/z* 306→230); blue trace represents MRM (*m/z* 328→212); the relative enzymatic product ratio of (**2.29** or **2.31**):**2.27** is 1:18.

2.6. Steady-state kinetic analysis

To study the substrate specificity of PikKR2 the steady-state kinetic parameters of the triketide substrate mimics **2.18** and **2.19**, as well as widely used substrates diketide **2.86** and *trans*-decalone **2.87**, were determined (Table 2 and Figure 17).[124, 125] Incubations were carried out with PikKR2 (5 μM), saturating NADPH (0.5 mM), and varying substrate concentrations under initial velocity conditions. Apparent kinetic parameters for NADPH (Table 2) were determined with 40 mM **2.86** (this is nonsaturating as a result of the limited solubility of this substrate). The initial rates, v_0, at a given [*S*] were determined by single-time point stopped-time incubations at 12 min for **2.18** and **2.19** (the reaction velocity remained linear up to 30 min). The reaction products **2.26** and **2.27** were quantified by LC-MS/MS employing a standard curve generated from synthetic standards. For substrates **2.86** and **2.87**, whose turnover was substantially faster than **2.18**

and **2.19**, we were able to employ a continuous assay that monitors consumption of NADPH by a decrease in absorbance at 340 nm. The enzymatic products of diketide **2.88** were identified as a mixture of D- and L-alcohols, in a ratio of 4 to 1, by chiral HPLC (Figure 18).

Table 2. Steady-state kinetic parameters for PikKR2 substrates.

Substrate	Product	K_M (mM)	k_{cat} (min^{-1})	k_{cat}/K_M ($min^{-1}M^{-1}$)
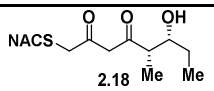 **2.18**	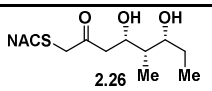 **2.26**	2.4 ± 0.8	0.029 ± 0.004	12.1 ± 5.5
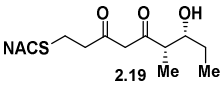 **2.19**	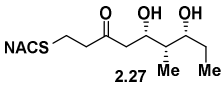 **2.27**	7.8 ± 2.7	0.113 ± 0.023	14.5 ± 7.9
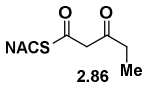 **2.86**	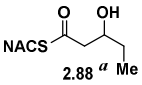 **2.88** [a]	26.1 ± 4.8	1.71 ± 0.16	66 ± 18
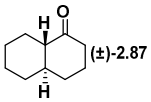 (±)-**2.87**	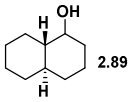 **2.89**	15.2 ± 6.0	10.92 ± 2.62	718 ± 456
NADPH	$NADP^+$	$(65.4 \pm 12.4) \times 10^{-3}$	1.54 ± 0.10	$(23.5 \pm 5.9) \times 10^{3}$

[a] **2.88** was isolated as a 4: 1 mixture of D- and L-alcohols.

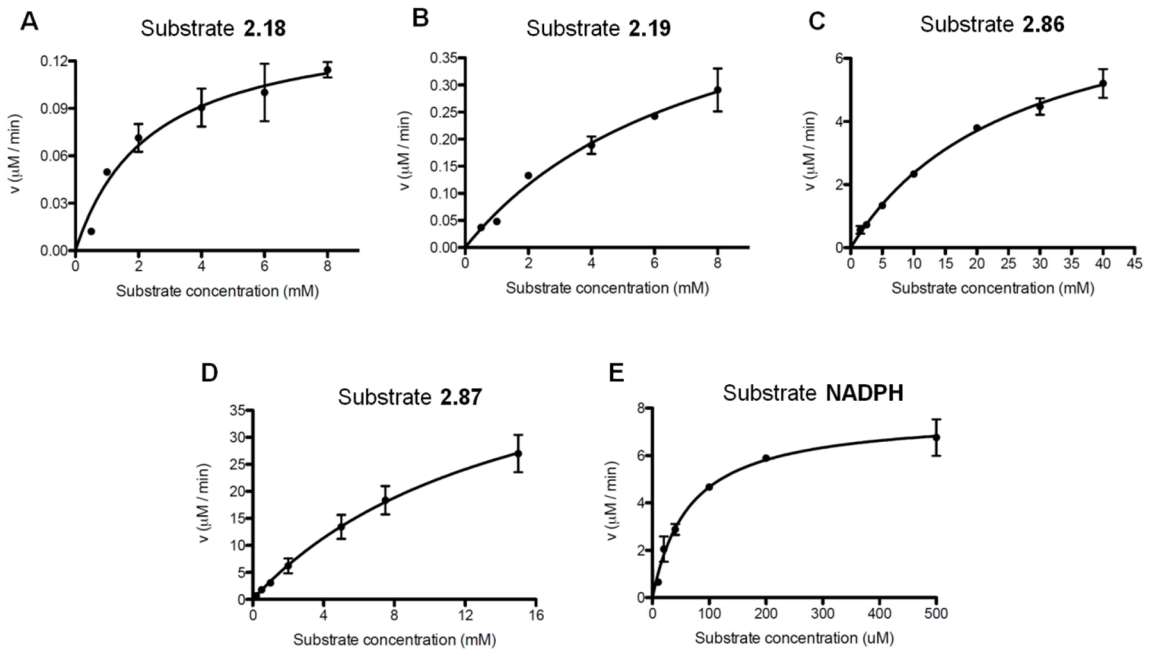

Figure 17. Michaelis-Menton curves of substrates **2.18**, **2.19**, **2.86**, **2.87** and NADPH.

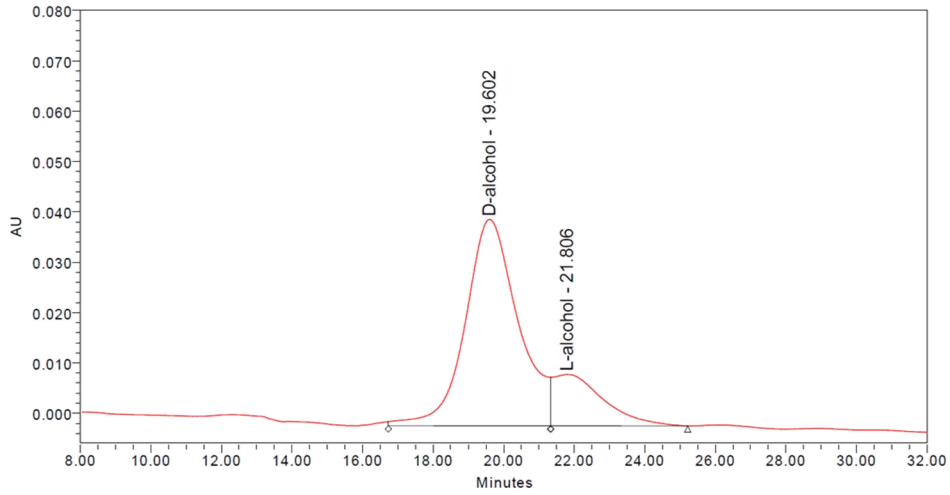

Figure 18. Chiral HPLC trace of enzymatic products of diketide substrate **2.86** by PikKR2.

The specificity constants (k_{cat}/K_M) of the triketide substrate mimics **2.18** and **2.19** are 12.1 and 14.5 $min^{-1}M^{-1}$, respectively while the k_{cat}/K_M values of diketide **2.86** is 66 min-

$^{1}M^{-1}$ and *trans*-decalone **2.87** is 718 $min^{-1}M^{-1}$. Thus, the native substrate mimics **2.18** and **2.19** are processed between 4–60 fold less efficiently than the unnatural substrates **2.86** and **2.87**. Examination of the kinetic parameters reveals that **2.18** and **2.19** possess improved K_M values that are 2–10 fold lower than **2.86** and **2.87**, likely due to their similarity to the natural acyl chain. Consequently, the lower specificity constants for **2.18** and **2.19** are exclusively caused by the greatly reduced turnover of these substrates. Indeed the k_{cat} values for **2.18** and **2.19** are 15–336 fold lower than **2.86** and **2.87**. To explain the slow enzyme turnover of substrate **2.18** and **2.19**, we firstly tested the possibility of product inhibition (see Experimental section). Since this inhibition was not observed, an alternative mechanism for k_{cat} attenuation was considered. We believe the low activity of the thioether substrates **2.18** and **2.19** may be caused by their β-diketone moieties, which exist to a large extent in the nonreducable enol forms (35–85% observed in ^{1}H NMR ($CDCl_3$), see Experimental section) as a result of the greater acidity of this functional group relative to a β-ketothioester.

2.7. Experimental section of chemistry

General chemistry procedures. All commercial reagents were used as provided unless otherwise indicated. THF and CH_2Cl_2 were purified by passage through alumina columns. All reactions were performed under an inert atmosphere of dry N_2 in oven-dried (150 ºC) glassware. Flash chromatography was conducted on silica gel (230–400 mesh) using the indicated solvent systems. TLC was performed on 250 μm, F_{254} silica gel plates, and were visualized by UV and *p*-anisaldehyde stain. Optical rotations were determined on a Rudolph Autopol III polarimeter using the sodium D line (λ = 589 nm) at the temperature

indicated and are reported as follows: $[\alpha]_D^{temp}$, concentration (c = g/100 mL), and solvent. ^1H and ^{13}C NMR spectra were recorded on a Bruker 400 spectrometer at 400 Hz for ^1H NMR and at 100 Hz for ^{13}C NMR. Chemical shifts are reports in ppm from an internal standard of residual $CHCl_3$ (7.26 ppm for ^1H NMR and 77.00 for ^{13}C NMR) or H_2O (4.80 ppm for ^1H NMR). Proton chemical data are reported as follows: chemical shift, multiplicity (s = singlet, d = doublet, t = triplet, q = quartet, m = multiplet, br = broad), coupling constant, and integration. High resolution mass spectra were obtained on a Bruker BioTOF II ESI-TOF/MS using either PEG or PPG standards as high resolution calibrants.

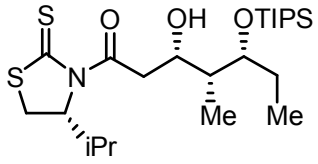

(3*S*,4*R*,5*R*)-3-Hydroxy-1-[(*R*)-4-isopropyl-2-thioxothiazolidin-3-yl]-4-methyl-5-[(triisopropylsilyl)oxy]heptan-1-one (2.34). To a solution of thiazolidinethione **2.32** (574 mg, 2.82 mmol, 1.60 equiv) in CH_2Cl_2 (10 mL) at –40 °C was added $TiCl_4$ (0.33 mL, 3.0 mmol, 1.7 equiv). After stirring at –40 °C or 30 min, *i*-Pr_2NEt (0.52 mL, 3.0 mmol, 1.7 equiv) was added and stirred at –40 °C for 2 h. The reaction mixture was cooled to –78 °C and then aldehyde **2.33** (481 mg, 1.77 mmol, 1.00 equiv) was added, followed by rinsing with CH_2Cl_2 (3 × 0.5 mL). After stirring at –78 °C for 110 min, the reaction was quenched by addition of saturated aqueous NH_4Cl (20 mL). The layers were separated and the aqueous layer was extracted with CH_2Cl_2 (3 × 20 mL). The combined organic layers were dried (Na_2SO_4), filtered, and concentrated under reduced pressure. Purification by flash chromatography (20% EtOAc/hexanes) afforded the title compound (748 mg, 89%) as a yellow oil. R_f = 0.38 (20% EtOAc/hexanes); $[\alpha]_D^{22}$

= –247.0 (*c* 0.42, $CHCl_3$); ^1H NMR ($CDCl_3$, 400 MHz) δ 5.18 (t, *J* = 7.1 Hz, 1H), 4.45–4.37 (m, 1H), 4.02–3.92 (m, 1H), 3.55–3.43 (m, 2H), 3.37 (dd, *J* = 17.3, 9.0 Hz, 1H), 3.28 (d, *J* = 1.5 Hz, 1H), 3.00 (d, *J* = 11.5 Hz, 1H), 2.37 (dq, *J* = 13.6, 6.8 Hz, 1H), 1.72–1.58 (m, 3H), 1.14–1.00 (m, 24H), 0.96 (dt, *J* = 6.8, 4.9 Hz, 6H), 0.82 (t, *J* = 7.4 Hz, 3H); ^{13}C NMR ($CDCl_3$, 100 MHz) δ 202.9, 172.2, 78.7, 71.5, 71.3, 44.1, 39.4, 30.8, 30.6, 27.4, 19.0, 18.2, 17.8, 13.3, 10.0, 6.2; HRMS (ESI-TOF) *m/z*: $[M + Na]^+$ Calcd for $C_{23}H_{45}NO_3S_2SiNa$ 498.2502; Found 498.2512.

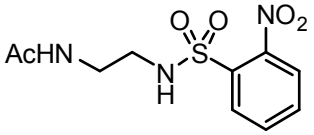

***N*-{2-[(2-Nitrophenyl)sulfonamido]ethyl}acetamide (2.42).** To a solution of *N*-(2-aminoethyl)acetamide (**2.41**) (90%, 0.53 mL, 5.0 mmol, 1.0 equiv) in CH_2Cl_2 (50 mL) at room temperature was added Et_3N (1.05 mL, 7.50 mmol, 1.50 equiv) and 2-nitrobenzenesulfonyl chloride (1.44 g, 6.50 mmol, 1.30 equiv). After stirring at room temperature for 20 min, the reaction was quenched by addition of saturated aqueous NH_4Cl (50 mL). The layers were separated and the aqueous layer was extracted with CH_2Cl_2 (3 × 20 mL). The combined organic layers were dried (Na_2SO_4), filtered, and concentrated under reduced pressure. Purification by flash chromatography (5% MeOH/CH_2Cl_2) afforded the title compound (1.43 g, 99%) as a colorless wax. R_f = 0.24 (5% MeOH/CH_2Cl_2); ^1H NMR ($CDCl_3$, 500 MHz) δ 8.16–8.09 (m, 1H), 7.90–7.85 (m, 1H), 7.80–7.72 (m, 2H), 5.95 (s, 1H), 5.72 (t, *J* = 5.9 Hz, 1H), 3.42 (q, *J* = 5.7 Hz, 2H), 3.25 (q, *J* = 5.8 Hz, 2H), 1.99 (s, 3H); ^{13}C NMR ($CDCl_3$, 100 MHz) δ 171.1, 148.0, 133.8, 133.3, 132.9, 131.0, 125.4, 43.4, 39.5, 23.1; HRMS (ESI-TOF) *m/z*: $[M + Na]^+$ Calcd for $C_{10}H_{13}N_3O_5SNa$ 310.0468; Found 310.0472.

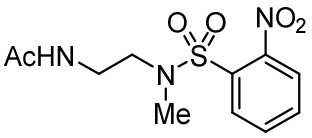

***N*-{2-[(*N*-Methyl-2-nitrophenyl)sulfonamido]ethyl}acetamide (2.43).** To a solution of sulfonamide **2.42** (184 mg, 0.640 mmol, 1.00 equiv) in MeCN (6.4 mL) at room temperature was added Cs_2CO_3 (229 mg, 0.704 mmol, 1.10 equiv). After stirring at room temperature for 15 min, MeI (120 μL, 1.92 mmol, 3.00 equiv) was added. The reaction mixture was stirred at room temperature for an additional 1 h, and quenched by addition of H_2O (10 mL). The layers were separated, the aqueous layer was extracted with CH_2Cl_2 (3 × 10 mL), and the combined organic layers were dried (Na_2SO_4), filtered, and concentrated under reduced pressure. Purification by flash chromatography (5% MeOH/CH_2Cl_2) afforded the title compound (183 mg, 95%) as a colorless oil. R_f = 0.31 (5% MeOH/CH_2Cl_2); ^{1}H NMR ($CDCl_3$, 400 MHz) δ 8.03–7.95 (m, 1H), 7.77–7.67 (m, 2H), 7.67–7.60 (m, 1H), 5.96 (s, 1H), 3.47 (q, J = 5.8 Hz, 2H), 3.38 (t, J = 5.7 Hz, 2H), 2.93 (s, 3H), 1.96 (s, 3H); ^{13}C NMR ($CDCl_3$, 100 MHz) δ 170.7, 148.1, 133.7, 132.0, 131.7, 131.0, 124.2, 49.1, 36.8, 34.7, 23.1; HRMS (ESI-TOF) *m/z*: [M + Na]$^+$ Calcd for $C_{11}H_{15}N_3O_5SNa$ 324.0625; Found 324.0622.

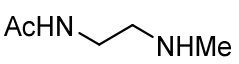

***N*-[2-(Methylamino)ethyl]acetamide (2.36).** To a solution of *N*-methylsulfonamide **2.43** (151 mg, 0.500 mmol, 1.00 equiv) in MeCN (5 mL) at room temperature was added Cs_2CO_3 (326 mg, 1.00 mmol, 2.00 equiv), followed by PhSH (51 μL, 0.50 mmol, 1.0 equiv). The reaction mixture was stirred at room temperature for 5.5 h until no starting material was observed by TLC (5% MeOH/CH_2Cl_2). The resulting solution of the title compound was used as such for the next reaction.

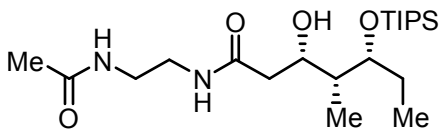

(3*S*,4*R*,5*R*)-*N*-(2-Acetamidoethyl)-3-hydroxy-4-methyl-5-[(triisopropylsilyl)oxy]heptanamide (2.37). To a solution of thiazolidinethione **2.34** (230 mg, 0.483 mmol, 1.00 equiv) in CH_2Cl_2 (3.5 mL) at room temperature was added *N*-(2-aminoethyl)acetamide (**2.35**) (90%, 67 μL, 0.63 mmol, 1.3 equiv), and the reaction mixture immediately turned colorless. After stirring at room temperature for 5 min, the reaction was quenched by addition of saturated aqueous NH_4Cl (10 mL) and extracted with CH_2Cl_2 (3 × 10 mL). The combined organic layers were dried (Na_2SO_4), filtered, and concentrated under reduced pressure. Purification by flash chromatograph (5% MeOH/CH_2Cl_2) afforded the title compound (184 mg, 92%) as a white wax. R_f = 0.26 (5% MeOH/CH_2Cl_2); $[\alpha]_D^{22}$ = –14.8 (*c* 0.80, $CHCl_3$); ^{1}H NMR ($CDCl_3$, 400 MHz) δ 6.78 (s, 1H), 6.38 (s, 1H), 4.21 (d, *J* = 9.9 Hz, 1H), 4.04–3.97 (m, 1H), 3.96 (s, 1H), 3.52–3.28 (m, 4H), 2.49 (dd, *J* = 14.8, 10.1 Hz, 1H), 2.24 (d, *J* = 14.7 Hz, 1H), 1.96 (s, 3H), 1.68–1.57 (m, 3H), 1.18 (s, 21H), 0.92 (d, *J* = 7.0 Hz, 3H), 0.81 (t, *J* = 7.4 Hz, 3H); ^{13}C NMR ($CDCl_3$, 100 MHz) δ 173.6, 170.8, 79.9, 72.9, 42.4, 40.5, 39.4, 39.2, 27.3, 23.2, 18.2, 13.4, 10.0, 5.1; HRMS (ESI-TOF) *m/z*: $[M + Na]^+$ Calcd for $C_{21}H_{44}N_2O_4SiNa$ 439.2963; Found 439.2963.

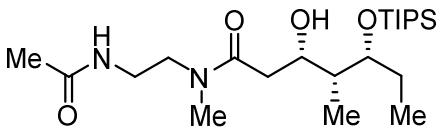

(3*S*,4*R*,5*R*)-*N*-(2-Acetamidoethyl)-3-hydroxy-*N*,4-dimethyl-5-[(triisopropylsilyl)oxy]heptanamide (2.38). To a solution of thiazolidinethione **2.34** (50 mg, 0.11 mmol, 1.0 equiv) in CH_2Cl_2 (2 mL) at room temperature was added *N*-methylamine **2.36** (0.1 M in MeCN, 1.3 mL, 0.13 mmol, 1.2 equiv) dropwise and the yellow color of the reaction mixture immediately faded. The reaction was stirred at room temperature for 1 h and quenched by addition of

saturated aqueous NH_4Cl (5 mL). The layers were separated and the aqueous layer was extracted with CH_2Cl_2 (3 × 5 mL). The combined organic layers were washed with saturated aqueous NaCl (10 mL), dried (Na_2SO_4), filtered, and concentrated under reduced pressure. Purification by flash chromatography (5% MeOH/CH_2Cl_2) afforded the title compound (33 mg, 73%) as a colorless oil. R_f = 0.22 (5% MeOH/CH_2Cl_2); $[\alpha]_D^{22}$ = –22.3 (*c* 0.88, $CHCl_3$); ^{1}H NMR ($CDCl_3$, 400 MHz, approximately 3:1 mixture of rotamers where the integrations have been normalized) δ 6.60 (s, 0.25H), 6.33 (s, 0.75H), 4.41 (d, *J* = 9.7 Hz, 0.25H), 4.27–4.17 (m, 0.75H), 4.06–3.98 (m, 0.25H), 3.97–3.90 (m, 1H), 3.87 (s, 0.75H), 3.80–3.70 (m, 0.25H), 3.64–3.55 (m, 0.75H), 3.54–3.44 (m, 1H), 3.44–3.31 (m, 2H), 3.04 (s, 2.25H), 2.94 (s, 0.75H), 2.79 (dd, *J* = 14.5, 9.8 Hz, 0.25H), 2.56 (dd, *J* = 15.7, 8.8 Hz, 0.75H), 2.45 (dd, *J* = 15.7, 3.8 Hz, 0.75H), 2.22 (dd, *J* = 14.5, 1.9 Hz, 0.25H), 1.96–1.89 (m, 3H), 1.74–1.67 (m, 1H), 1.67–1.55 (m, 2H), 1.07 (s, 21H), 0.99–0.92 (m, 3H), 0.87–0.79 (m, 3H); ^{13}C NMR ($CDCl_3$, 100 MHz) δ Major rotamer: 174.1, 170.6, 78.0, 71.3, 46.9, 40.1, 38.4, 38.3, 36.0, 27.16, 23.2, 18.3, 13.3, 10.1, 7.4; Minor rotamer: 172.2, 170.6, 79.5, 73.6, 48.5, 39.4, 38.2, 37.4, 33.0, 27.23, 22.9, 18.1, 13.4, 10.0, 6.0; HRMS (ESI-TOF) *m/z*: $[M + Na]^+$ Calcd for $C_{22}H_{46}N_2O_4SiNa$ 453.3119; Found 453.3110.

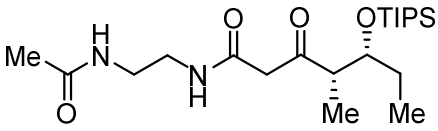

(4*S*,5*R*)-*N*-(2-Acetamidoethyl)-4-methyl-3-oxo-5-[(triisopropylsilyl)oxy]heptanamide (2.39). To a solution of amide **2.37** (31 mg, 0.074 mmol, 1.0 equiv) in CH_2Cl_2 (2 mL) at room temperature was added 4-methylmorpholine *N*-oxide (13 mg, 0.11 mmol, 1.5 equiv) and 4 Å molecular sieves (37 mg), followed by the addition of TPAP (1.3 mg, 0.0037 mmol,

5%). The reaction mixture was stirred at room temperature for 2 h, and then MeCN (0.2 mL) was added. After stirring for an additional 3.5 h, the reaction was concentrated under reduced pressure. Purification by flash chromatography (5% MeOH/CH_2Cl_2) afforded the title compound (15 mg, 48%) as a colorless oil. R_f = 0.32 (5% MeOH/CH_2Cl_2); $[\alpha]_D^{21}$ = 23.2 (*c* 0.50, $CHCl_3$); ^{1}H NMR ($CDCl_3$, 400 MHz) δ 7.43 (s, 1H), 6.34 (s, 1H), 4.21–4.02 (m, 1H), 3.66–3.32 (m, 6H), 2.84–2.67 (m, 1H), 1.97 (s, 3H), 1.66–1.46 (m, 2H), 1.10 (d, *J* = 6.9 Hz, 3H), 1.05 (s, 21H), 0.87 (t, *J* = 7.4 Hz, 3H); ^{13}C NMR ($CDCl_3$, 100 MHz) δ 209.4, 170.8, 167.4, 74.8, 51.6, 47.8, 40.4, 39.6, 27.6, 23.2, 18.2, 12.9, 9.94, 9.85; HRMS (ESI-TOF) *m/z*: $[M + Na]^+$ Calcd for $C_{21}H_{42}N_2O_4SiNa$ 437.2806; Found 437.2805.

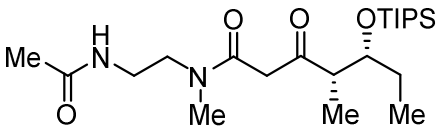

(4*S*,5*R*)-*N*-(2-Acetamidoethyl)-*N*,4-dimethyl-3-oxo-5-[(triisopropylsilyl)oxy]heptanamide (2.40). To a solution of *N*-methylamide **2.38** (33 mg, 0.077 mmol, 1.0 equiv) in CH_2Cl_2 (1 mL) at room temperature was added 4-methylmorpholine *N*-oxide (13 mg, 0.12 mmol, 1.5 equiv) and 4 Å molecular sieves (39 mg), followed by the addition of TPAP (2.7 mg, 0.0077 mmol, 10%). The reaction mixture was stirred at room temperature for 1 h until no starting material was observed by TLC (5% MeOH/CH_2Cl_2). The reaction was concentrated under reduced pressure, and purification by flash chromatography (5% MeOH/CH_2Cl_2) afforded the title compound (25 mg, 76%) as a colorless oil. R_f = 0.30 (5% MeOH/CH_2Cl_2); $[\alpha]_D^{21}$ = 21.3 (*c* 0.60, $CHCl_3$); ^{1}H NMR ($CDCl_3$, 400 MHz, approximately 13:3:4 mixture of major rotamer:minor rotamer:enol where the integrations have been normalized) δ 14.56 (s, 0.2H), 6.42 (s, 1H), 5.15 (s, 0.2H), 4.18–4.04 (m, 1H), 3.83–3.66 (m, 1.6H), 3.65–3.36 (m, 4H), 3.01–2.92 (m, 3H), 2.92–2.88 (m, 0.15H), 2.88–2.81 (m,

0.65H), 2.43–2.36 (m, 0.2H), 2.00 (s, 0.45H), 1.96 (s, 1.95H), 1.93 (s, 0.6H), 1.66–1.43 (m, 2H), 1.16–1.10 (m, 3H), 1.09–1.01 (m, 21H), 0.94–0.84 (m, 3H); ^{13}C NMR ($CDCl_3$, 100 MHz, major rotamer) δ 207.1, 170.9, 168.8, 75.3, 51.5, 49.1, 46.8, 37.6, 36.4, 27.5, 23.2, 18.2, 12.9, 11.1, 10.1; HRMS (ESI-TOF) *m/z*: $[M + Na]^+$ Calcd for $C_{22}H_{44}N_2O_4SiNa$ 451.2963; Found 451.2955.

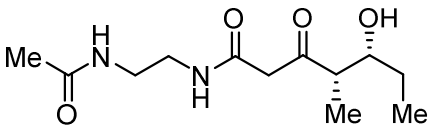

(4*S*,5*R*)-*N*-(2-Acetamidoethyl)-5-hydroxy-4-methyl-3-oxoheptanamide (2.16). To a solution of silyl ether **2.39** (14 mg, 0.034 mmol, 1.0 equiv) in MeCN (0.5 mL) at 0 °C was added a solution of 48% HF in MeCN (2 mL, 11:89). The reaction mixture was allowed to warm up to room temperature and stirred at room temperature for 10 h. The reaction mixture was cooled in an ice bath and quenched by addition of saturated aqueous $NaHCO_3$ until pH 7 was obtained. The mixture was extracted with *n*-butanol (3 × 10 mL). The combined organic layers were dried (Na_2SO_4), filtered, and concentrated under reduced pressure. Purification by flash chromatography (10% MeOH/CH_2Cl_2) afforded the title compound (6.4 mg, 74%) as a colorless oil. R_f= 0.19 (10% MeOH/CH_2Cl_2); $[\alpha]_D^{21}$ = 7.7 (*c* 0.32, $CHCl_3$); ^{1}H NMR ($CDCl_3$, 400 MHz, approximately 3:1 mixture of rotamers where the integrations have been normalized) δ 7.22 (s, 1H), 6.39 (s, 0.25H), 6.30 (s, 0.75H), 3.96 (s, 0.75H), 3.58 (s, 0.25H), 3.59–3.31 (m, 6H), 3.09 (s, 1H), 2.79–2.63 (m, 1H), 1.98 (s, 3H), 1.71–1.37 (m, 2H), 1.11 (d, *J* = 6.6 Hz, 2.25H), 1.07 (d, *J* = 6.7 Hz, 0.75H), 1.02–0.93 (m, 3H); ^{13}C NMR ($CDCl_3$, 100 MHz) δ Major rotamer: 209.6, 171.6, 167.25, 72.6, 51.9, 48.4, 40.0, 39.62, 27.2, 23.17, 10.6, 8.6; Minor rotamer: 210.5, 171.5, 167.27,

75.1, 52.8, 49.6, 39.8, 39.59, 27.4, 23.20, 13.4, 9.4; HRMS (ESI-TOF) *m/z*: $[M + Na]^+$ Calcd for $C_{12}H_{22}N_2O_4SiNa$ 281.1472; Found 281.1471.

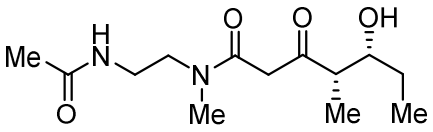

(4*S*,5*R*)-*N*-(2-Acetamidoethyl)-5-hydroxy-*N*,4-dimethyl-3-oxoheptanamide (2.17). To a solution of silyl ether **2.40** (25 mg, 0.058 mmol, 1.0 equiv) in MeCN (1.0 mL) at 0 °C was added a solution of 48% HF in MeCN (3 mL, 11:89). The reaction mixture was allowed to warm up to room temperature and stirred at room temperature for 11.5 h until all the starting material was consumed by TLC (5% $MeOH/CH_2Cl_2$). The reaction mixture was quenched by addition of saturated aqueous $NaHCO_3$ until pH 7, then extracted with *n*-butanol (3 × 10 mL). The combined organic layers were dried (Na_2SO_4), filtered, and concentrated under reduced pressure. Purification by flash chromatography (10% $MeOH/CH_2Cl_2$) afforded the title compound (12 mg, 75%) as a colorless oil. R_f = 0.33 (10% $MeOH/CH_2Cl_2$); $[\alpha]_D^{21}$ = 22.6 (*c* 0.31, $CHCl_3$); ^1H NMR ($CDCl_3$, 400 MHz, approximately 13:3:4 mixture of major rotamer:minor rotamer:enol where the integrations have been normalized) δ 14.90 (s, 0.2H), 6.50 (s, 0.35H), 6.37 (s, 0.65H), 5.13 (s, 0.2H), 4.03–3.87 (m, 0.8H), 3.86–3.61 (m, 1.8H), 3.59–3.31 (m, 4H), 3.03–2.92 (m, 3H), 2.79–2.66 (m, 0.8H), 2.33–2.27 (m, 0.2H), 2.00–1.89 (m, 3H), 1.58–1.36 (m, 2H), 1.19–1.05 (m, 3H), 0.96 (t, *J* = 7.4 Hz, 3H); ^{13}C NMR ($CDCl_3$, 100 MHz, major rotamer) δ 208.4, 170.9, 168.9, 72.9, 51.4, 47.7, 46.9, 37.5, 36.5, 26.9, 23.2, 10.5, 9.1; HRMS (ESI-TOF) *m/z*: $[M + Na]^+$ Calcd for $C_{13}H_{24}N_2O_4SiNa$ 295.1628; Found 295.1629.

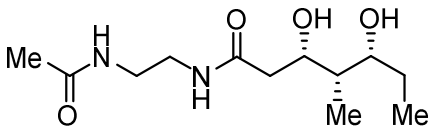

(3*S*,4*S*,5*R*)-*N*-(2-Acetamidoethyl)-3,5-dihydroxy-4-methylheptanamide (2.44). To a solution of silyl ether **2.37** (39 mg, 0.094 mmol, 1.0 equiv) in MeCN (1 mL) at 0 °C was added a solution of 48% HF in MeCN (5 mL, 11:89). After stirring at 0 °C for 5 h, the reaction mixture was cooled in an ice bath and quenched by the addition of saturated aqueous $NaHCO_3$ until pH 7. The mixture was extracted with *n*-butanol (3 × 10 mL), and the combined organic layers were dried (Na_2SO_4), filtered, and concentrated under reduced pressure. Purification by flash chromatography (10% MeOH/CH_2Cl_2) afforded the title compound (23 mg, 96%) as a colorless wax. R_f = 0.16 (10% MeOH/CH_2Cl_2); $[\alpha]_D^{21}$ = –9.8 (*c* 0.50, $CHCl_3$); ^{1}H NMR (D_2O, 400 MHz) δ 4.20–4.09 (m, 1H), 3.74–3.61 (m, 1H), 3.43–3.25 (m, 4H), 2.59–2.38 (m, 2H), 2.00 (s, 3H), 1.66–1.48 (m, 3H), 1.03–0.86 (m, 6H); ^{13}C NMR ($CDCl_3$, 100 MHz) δ 173.6, 171.6, 77.7, 73.5, 41.3, 40.6, 39.83, 39.77, 27.8, 23.1, 10.4, 5.1; HRMS (ESI-TOF) *m/z*: $[M + Na]^+$ Calcd for $C_{12}H_{24}N_2O_4SiNa$ 283.1628; Found 283.1635.

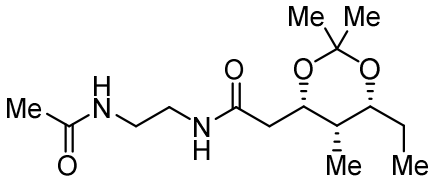

***N*-(2-Acetamidoethyl)-2-[(4*S*,5*S*,6*R*)-6-ethyl-2,2,5-trimethyl-1,3-dioxan-4-yl]acetamide (2.45).** To a solution of diol **2.44** (19 mg, 0.073 mmol, 1.0 equiv) in CH_2Cl_2 (3 mL) at room temperature was added 2,2-dimethoxypropane (0.18 mL, 1.5 mmol, 20 equiv) and a catalytic amount of PPTS. The reaction mixture was stirred at room temperature for 2 h and then quenched by addition of saturated aqueous $NaHCO_3$ (5 mL). The layers were separated and the aqueous layer was extracted with CH_2Cl_2 (3 × 10 mL). The combined organic layers were dried (Na_2SO_4), filtered, and concentrated under

reduced pressure. Purification by flash chromatography (5% MeOH/CH_2Cl_2) afforded the title compound (16 mg, 73%) as colorless oil. R_f = 0.34 (5% MeOH/CH_2Cl_2); $[\alpha]_D^{22}$ = –9.4 (*c* 0.50, $CHCl_3$); ^{1}H NMR ($CDCl_3$, 400 MHz) δ 6.62 (s, 1H), 6.38 (s, 1H), 4.30 (d, *J* = 9.2 Hz, 1H), 3.78 (t, *J* = 6.7 Hz, 1H), 3.45–3.25 (m, 4H), 2.45 (dd, *J* = 14.8, 9.7 Hz, 1H), 2.17 (d, *J* = 14.8 Hz, 1H), 1.97 (s, 3H), 1.59–1.46 (m, 1H), 1.43 (s, 3H), 1.41–1.35 (m, 4H), 0.87 (t, *J* = 7.4 Hz, 3H), 0.83 (d, *J* = 6.8 Hz, 3H); ^{13}C NMR ($CDCl_3$, 100 MHz) δ 172.8, 170.9, 99.2, 74.6, 70.6, 40.7 (ovlp, 2C), 39.4, 34.5, 30.0, 25.4, 23.2, 19.7, 9.6, 4.8; HRMS (ESI-TOF) *m/z*: $[M + Na]^+$ Calcd for $C_{15}H_{28}N_2O_4SiNa$ 323.1941; Found 323.1945.

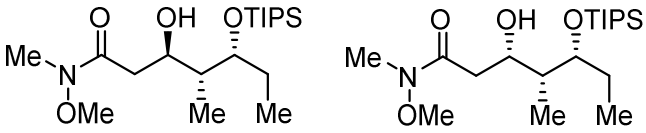

(3*R*,4*R*,5*R*)-3-Hydroxy-*N*-methoxy-*N*,4-dimethyl-5-[(triisopropylsilyl)oxy]heptanamide (2.47) and (3*S*,4*R*,5*R*)-3-hydroxy-*N*-methoxy-*N*,4-dimethyl-5-[(triisopropylsilyl)oxy]heptanamide (2.48). To a solution of distilled *i*-Pr_2NH (0.28 mL, 2.0 mmol, 1.4 equiv) in THF (15 mL) at –78 °C was added *n*-BuLi (2.0 M in THF, 0.92 mL, 1.8 mmol, 1.3 equiv). After stirring at –78 °C for 30 min, *N*-methoxy-*N*-methylacetamide (**2.46**) (0.19 mL, 1.8 mmol, 1.3 equiv) was added. The reaction mixture was stirred at –78 °C for an additional 30 min, followed by the addition of a solution of aldehyde **2.33** (384 mg, 1.41 mmol, 1.00 equiv) in THF (0.5 mL) in a dropwise fashion with the aid of THF (2 × 0.5 mL). The reaction mixture was stirred at –78 °C for and additional 50 min, then quenched by the addition of saturated aqueous NH_4Cl (20 mL). The layers were separated and the aqueous layer was extracted with EtOAc (3 × 20 mL). The combined organic layers were dried (Na_2SO_4), filtered, and concentrated under reduced pressure. Purification by flash chromatography (30%

EtOAc/hexanes) to afford the title compounds **2.47** (347 mg, 66%) and **2.48** (129 mg, 24%) as clear colorless oils (total yield = 90%, dr = 2.7: 1). Compound **2.47**: R_f = 0.41 (30% EtOAc/hexanes); ^{1}H NMR (400 MHz, $CDCl_3$) δ 4.13 (t, *J* = 6.8 Hz, 1H), 4.10–4.02 (m, 2H), 3.69 (s, 3H), 3.19 (s, 3H), 2.68 (d, *J* = 16.0 Hz, 1H), 2.52 (dd, *J* = 15.5, 9.1 Hz, 1H), 1.72 (p, *J* = 7.2 Hz, 1H), 1.60 (p, *J* = 7.3 Hz, 2H), 1.07 (s, 21H), 0.86 (t, *J* = 7.5 Hz, 3H), 0.82 (d, *J* = 7.0 Hz, 3H); ^{13}C NMR ($CDCl_3$, 100 MHz) δ173.8, 74.8, 69.8, 61.2, 41.3, 36.9, 31.9, 27.0, 18.2, 13.0, 10.5, 10.2; Compound **2.48**: R_f = 0.29 (30% EtOAc/hexanes); ^{1}H NMR ($CDCl_3$, 400 MHz) δ 4.23 (td, *J* = 6.9, 6.2, 3.2 Hz, 1H), 3.95 (ddd, *J* = 8.1, 5.1, 2.9 Hz, 1H), 3.71 (d, *J* = 1.7 Hz, 1H), 3.69 (s, 3H), 3.19 (s, 3H), 2.66 (d, *J* = 5.7 Hz, 2H), 1.76–1.69 (m, 1H), 1.66–1.57 (m, 2H), 1.07 (s, 21H), 0.97 (d, *J* = 7.0 Hz, 3H), 0.84 (t, *J* = 7.5 Hz, 3H); ^{13}C NMR ($CDCl_3$, 100 MHz) δ 173.6, 77.9, 70.7, 61.2, 40.1, 36.7, 31.9, 27.2, 18.3, 13.3, 10.1, 7.4.

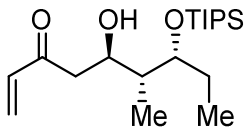

(5*R*,6*R*,7*R*)-5-Hydroxy-6-methyl-7-[(triisopropylsilyl)oxy]non-1-en-3-one (2.49). To a solution of Weinreb amide **2.47** (108 mg, 0.288 mmol, 1.00 equiv) in THF (10 mL) at 0 °C was added vinyl magnesium bromide (0.82 M in Et_2O, 1.2 mL, 1.0 mmol, 3.5 equiv). The reaction mixture was stirred at 0 °C for 45 min, and quenched by the addition of saturated aqueous NH_4Cl (10 mL). The mixture was allowed to warm to room temperature and diluted with EtOAc (10 mL). The layers were separated and the aqueous layer was extracted with EtOAc (3 × 15 mL). The combined organic layers were washed with saturated aqueous NaCl (20 mL), dried (Na_2SO_4), and concentrated under reduced pressure. Purification by flash chromatography (20% EtOAc/hexanes) afforded the title compound (46 mg, 46%) as a

colorless oil. R_f = 0.79 (30% EtOAc/hexanes); ^{1}H NMR ($CDCl_3$, 400 MHz) δ 6.41 (dd, *J* = 17.6, 10.5 Hz, 1H), 6.25 (d, *J* = 17.6 Hz, 1H), 5.85 (d, *J* = 10.5 Hz, 1H), 4.19-4.12 (m, 1H), 4.09–4.03 (m, 1H), 3.85 (d, *J* = 3.0 Hz, 1H), 2.82 (dd, *J* = 16.2, 3.2 Hz, 1H), 2.72 (dd, *J* = 16.3, 8.5 Hz, 1H), 1.82–1.72 (m, 1H), 1.63 (p, *J* = 7.4 Hz, 2H), 1.08 (s, 21H), 0.90 (t, *J* = 7.5 Hz, 3H), 0.83 (d, *J* = 7.0 Hz, 3H); ^{13}C NMR ($CDCl_3$, 100 MHz) δ 201.0, 137.0, 128.6, 76.1, 70.2, 45.1, 41.5, 26.5, 18.2, 12.9, 11.0, 10.7.

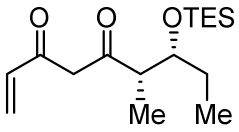

(6*S*,7*R*)-6-Methyl-7-[(triisopropylsilyl)oxy]non-1-ene-3,5-dione (2.50). To a solution of alcohol **2.49** (121 mg, 0.353 mmol, 1.00 equiv) in EtOAc (10 mL) was added IBX (45%, 659 mg, 1.06 mmol, 3.00 equiv). The reaction mixture was heated at reflux for 2 h, cooled to room temperature, and filtered through a 1 cm silica gel. The filtrate was washed with $NaHCO_3$ (4 × 20 mL), concentrated under reduced pressure and afforded the title compound (crude, 114 mg, 95%) as an orange oil without further purification. An analytically pure sample was obtained by purification by flash chromatography (5% EtOAc/hexanes) to afford the pure title compound as a yellow oil. R_f = 0.69 (10% EtOAc/hexanes); ^{1}H NMR ($CDCl_3$, 400 MHz, enol form) δ 15.23 (s, 1H), 6.26 (d, *J* = 17.1 Hz, 1H), 6.14 (dd, *J* = 17.2, 10.3 Hz, 1H), 5.68–5.63 (m, 2H), 4.13 (q, *J* = 4.9 Hz, 1H), 2.63–2.55 (m, 1H), 1.64–1.55 (m, 2H), 1.15 (d, *J* = 6.9 Hz, 3H), 1.04 (s, 21H), 0.88 (t, *J* = 7.4 Hz, 3H); ^{13}C NMR ($CDCl_3$, 100 MHz) δ 204.2, 176.0, 132.7, 125.0, 100.1, 75.3, 47.9, 28., 18.2, 13.0, 10.8, 9.5.

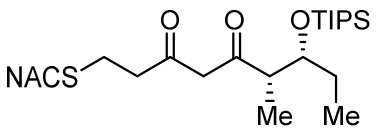

(6*S*,7*R*)-6-Methyl-1-[*N*-(2-acetamidoethyl)thio]-7-[(triethylsilyl)oxy]nonane-3,5-dione (2.51). To a solution of vinyl ketone **2.50** (114 mg, 0.335 mmol, 1.00 equiv) in THF (15 mL) was

added *N*-acetylcysteamine (53 μL, 0.50 mmol, 1.5 equiv) and a catalytic amount of Cs_2CO_3 at room temperature. After stirring at room temperature for 2.5 h, the reaction was quenched by the addition of saturated aqueous NH_4Cl (20 mL). The mixture was extracted with EtOAc (3 × 20 mL), and the combined organic layers were washed with saturated aqueous NaCl (10 mL), dried (Na_2SO_4), filtered, and concentrated under reduced pressure. Purification by flash chromatography (5% MeOH/CH_2Cl_2) afforded the title compound (68 mg, 42%) as a colorless oil. R_f = 0.35 (5% MeOH/CH_2Cl_2); ^{1}H NMR ($CDCl_3$, 400 MHz, enol form) δ 15.47 (s, 1H), 6.10 (s, 1H), 5.60 (s, 1H), 4.11 (q, *J* = 5.6 Hz, 1H), 3.50–3.42 (m, 2H), 2.84–2.76 (m, 2H), 2.72–2.65 (m, 2H), 2.62–2.56 (m, 2H), 2.52–2.44 (m, 1H), 2.01 (s, 3H), 1.59 (p, *J* = 7.3, 6.8 Hz, 2H), 1.12 (d, *J* = 6.9 Hz, 3H), 1.03 (s, 21H), 0.87 (t, *J* = 7.4 Hz, 3H); ^{13}C NMR ($CDCl_3$, 100 MHz) δ 194.9, 193.4, 170.1, 99.6, 75.0, 45.3, 39.0, 38.4, 32.1, 28.0, 26.9, 23.3, 18.2, 13.0, 10.7, 9.4.

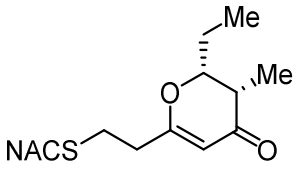

(2*R*,3*S*)-2-Ethyl-6-[*N*-(2-acetamidoethyl)thio]ethyl-3-methyl-2,3-dihydro-4*H*-pyran-4-one (2.52). To a solution of silyl ether **2.51** (41 mg, 0.089 mmol, 1.0 equiv) in MeCN (2 mL) at 0 °C was added a solution of 48% HF: MeCN (11: 89, 6 mL) in a dropwise fashion. The reaction mixture was stirred at 0 °C for 47 h, cooled in an ice bath, then quenched by addition of saturated aqueous $NaHCO_3$ to adjust the mixture to pH 7. The mixture was extracted with EtOAc (3 × 10 mL), and the combined organic layers were washed with saturated aqueous NaCl (20 mL), dried (Na_2SO_4), filtered, and concentrated under reduced pressure. Purification by flash chromatography (5% MeOH/CH_2Cl_2) afforded the title compound (4.5 mg, 18%) as a colorless oil. ^{1}H NMR ($CDCl_3$, 400 MHz) δ 5.89 (s,

1H), 5.27 (s, 1H), 4.22 (ddd, *J* = 8.7, 5.7, 3.2 Hz, 1H), 3.43 (q, *J* = 6.3 Hz, 2H), 2.75 (t, *J* = 7.3 Hz, 2H), 2.68 (t, *J* = 6.5 Hz, 2H), 2.54 (q, *J* = 7.1 Hz, 2H), 2.31 (qd, *J* = 7.3, 3.2 Hz, 1H), 1.99 (s, 3H), 1.92–1.79 (m, 1), 1.65–1.54 (m, 1H), 1.04 (d, *J* = 7.4 Hz, 3H), 1.00 (t, *J* = 7.5 Hz, 3H); ^{13}C NMR ($CDCl_3$, 100 MHz) δ 197.7, 173.9, 170.1, 103.5, 83.5, 42.6, 38.4, 34.7, 31.8, 28.2, 23.3, 9.8, 9.5.

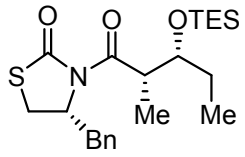

(2*S*,3*R*)-1-[(*R*)-4-Benzyl-2-thioxothiazolidin-3-yl]-3-[(triethylsilyl)oxy]-2-methylpentan-1-one (2.54). To a solution of alcohol **2.53** (702 mg, 2.17 mmol, 1.00 equiv) in CH_2Cl_2 (30 mL) at 0 °C was added *i*-Pr_2NEt (0.68 mL, 3.9 mmol, 1.8 equiv) and TESOTf (0.74 mL, 3.3 mmol, 1.5 equiv). The reaction mixture was stirred at 0 °C for 100 min. The reaction was quenched by the addition of saturated aqueous $NaHCO_3$ (20 mL) and extracted with CH_2Cl_2 (3 × 30 mL). The combined organic layers were washed with saturated aqueous NaCl (40 mL), dried (Na_2SO_4), filtered, and concentrated under reduced pressure. Purification by flash chromatography (20% EtOAc/hexanes) afforded the title compound (928 mg, 98%) as a yellow oil. R_f = 0.57 (20% EtOAc/hexanes); $[\alpha]_D^{22}$ = –106.3 (*c* 1.0, $CHCl_3$); ^{1}H NMR ($CDCl_3$, 400 MHz) δ 7.37–7.26 (m, 5H), 5.40–5.31 (m, 1H), 4.72 (p, *J* = 6.8 Hz, 1H), 4.16 (q, *J* = 5.5 Hz, 1H), 3.33 (dd, *J* = 11.5, 7.2 Hz, 1H), 3.21 (dd, *J* = 13.1, 3.7 Hz, 1H), 3.03 (dd, *J* = 13.0, 10.7 Hz, 1H), 2.86 (dd, *J* = 11.6, 0.9 Hz, 1H), 1.64–1.53 (m, 2H), 1.21 (d, *J* = 7.0 Hz, 3H), 0.98 (t, *J* = 7.9 Hz, 9H), 0.92 (t, *J* = 7.4 Hz, 3H), 0.63 (q, *J* = 8.0 Hz, 6H); ^{13}C NMR ($CDCl_3$, 100 MHz) δ 201.0, 176.9, 136.6, 129.4, 128.9, 127.2, 74.0, 69.1, 43.4, 37.1, 31.6, 28.4, 14.0, 9.6, 7.0, 5.3; HRMS (ESI-TOF) *m/z*: $[M + Na]^+$ Calcd for $C_{22}H_{35}NO_2S_2SiNa$ 460.1771; Found 460.1766.

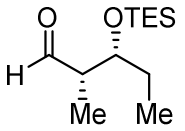

(2*S*,3*R*)-2-Methyl-3-[(triethylsilyl)oxy]pentanal (2.55). To a solution of thiazolidinethione **2.54** (928 mg, 2.12 mmol, 1.00 equiv) in CH_2Cl_2 (50 mL) at – 78 °C was added *i*-Bu_2AlH (1.2 M in PhMe, 2.83 mL, 3.39 mmol, 1.60 equiv). The reaction mixture was stirred at – 78 °C until the bright yellow color faded (<5 min), then immediately quenched by addition of saturated aqueous sodium potassium tartrate (40 mL). The reaction mixture was allowed to warm up to room temperature and stirred for 12 h. The layers were separated and aqueous layer was extracted with CH_2Cl_2 (3 × 30 mL). The combined organic layers were washed with saturated aqueous NaCl (80 mL), dried (Na_2SO_4), filtered, and concentrated under reduced pressure. The residue was dissolved in hexanes (4 mL) and purified by flash chromatography (10% EtOAc/hexanes) to afford the title compound (419 mg, 86%) as a colorless oil. R_f = 0.47 (10% EtOAc/hexanes); $[\alpha]_D^{21}$ = 53.7 (*c* 1.1, $CHCl_3$); ^{1}H NMR ($CDCl_3$, 400 MHz) δ 9.75 (s, 1H); 4.05 (dt, *J* = 6.5, 3.8 Hz, 1H), 2.49–2.37 (m, 1H), 1.60–1.43 (m, 2H), 1.04 (d, *J* = 7.0 Hz, 3H), 0.93 (t, *J* = 7.9 Hz, 9H), 0.88 (t, *J* = 7.4 Hz, 3H), 0.57 (q, *J* = 7.6 Hz, 6H); ^{13}C NMR ($CDCl_3$, 100 MHz) δ 205.3, 73.4, 50.9, 27.5, 10.1, 7.5, 6.8, 5.1; HRMS (ESI-TOF) *m/z*: $[M + Na]^+$ Calcd for $C_9H_{20}O_2SiNa$ 253.1594; Found 253.1605.

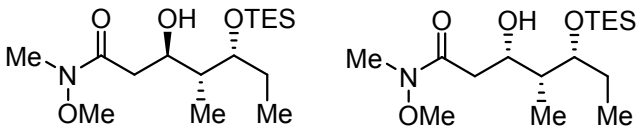

(3*R*,4*R*,5*R*)-3-Hydroxy-*N*-methoxy-*N*,4-dimethyl-5-[(triethylsilyl)oxy]heptanamide (2.56) and (3*S*,4*R*,5*R*)-3-hydroxy-*N*-methoxy-*N*,4-dimethyl-5-[(triethylsilyl)oxy]heptanamide (2.57). To a solution of distilled *i*-Pr_2NH (0.36 mL, 2.6 mmol, 1.4 equiv) in THF (30 mL) at –78 °C was added *n*-BuLi (2.2 M in THF, 1.1 mL, 2.4 mmol, 1.3 equiv). After stirring at –78 °C for 30 min, *N*-methoxy-*N*-

methylacetamide (**2.46**) (0.25 mL, 2.4 mmol, 1.3 equiv) was added. The reaction mixture was stirred at –78 °C for an additional 30 min, followed by the addition of a solution of aldehyde **2.55** (419 mg, 1.82 mmol, 1.00 equiv) in THF (0.5 mL) in a dropwise fashion with the aid of THF (2 × 0.5 mL). The reaction mixture was stirred at –78 °C for and additional 3 h, then quenched by the addition of saturated aqueous NH_4Cl (20 mL). The layers were separated and the aqueous layer was extracted with EtOAc (3 × 20 mL). The combined organic layers were dried (Na_2SO_4), filtered, and concentrated under reduced pressure. Purification by flash chromatography (50% EtOAc/hexanes) to afford the title compounds **2.56** (334 mg, 55%) and **2.57** (140 mg, 23%) as clear colorless oils (total yield = 78%, dr = 7: 3). Compound **2.56**: R_f = 0.42 (50% EtOAc/hexanes); $[\alpha]_D^{22}$ = 36.8 (*c* 1.0, $CHCl_3$); ^{1}H NMR ($CDCl_3$, 400 MHz) δ 4.14 (s, 1H), 4.00 (dt, *J* = 9.0, 2.6 Hz, 1H), 3.93 (dt, *J* = 6.7, 2.1 Hz, 1H), 3.69 (s, 3H), 3.18 (s, 3H), 2.65 (d, *J* = 15.7 Hz, 1H), 2.51 (dd, *J* = 15.6, 9.3 Hz, 1H), 1.72–1.63 (m, 1H), 1.59–1.45 (m, 2H), 0.95 (t, *J* = 7.9 Hz, 9H), 0.86 (t, *J* = 7.4 Hz, 3H), 0.80 (d, *J* = 7.0 Hz, 3H), 0.61 (q, *J* = 7.9 Hz, 6H); ^{13}C NMR ($CDCl_3$, 100 MHz) δ 173.7, 75.0, 70.0, 61.2, 41.8, 36.9, 31.9, 26.6, 10.6, 10.5, 6.9, 5.1; HRMS (ESI-TOF) *m/z*: $[M + Na]^+$ Calcd for $C_{16}H_{35}NO_4SiNa$ 356.2228; Found 356.2223. Compound **2.57**: R_f = 0.32 (50% EtOAc/hexanes); $[\alpha]_D^{22}$ = –32.4 (*c* 1.0, $CHCl_3$); ^{1}H NMR ($CDCl_3$, 400 MHz) δ 4.23–4.16 (m, 1H), 3.83–3.77 (m, 1H), 3.70 (s, 3H), 3.67 (d, *J* = 1.5 Hz, 1H), 3.19 (s, 3H), 2.68–2.58 (m, 2H), 1.67 (tq, *J* = 7.0, 3.7 Hz, 1H), 1.59–1.50 (m, 2H), 0.95 (t, *J* = 8.0 Hz, 9H), 0.94 (d, *J* = 7.0 Hz, 3H), 0.84 (t, *J* = 7.4 Hz, 3H), 0.61 (q, *J* = 7.9 Hz, 6H); ^{13}C NMR ($CDCl_3$, 100 MHz) δ 173.5, 77.2, 70.2, 61.1, 40.3, 36.7, 31.7,

26.8, 9.8, 7.7, 6.8, 5.2; HRMS (ESI-TOF) *m/z*: $[M + Na]^+$ Calcd for $C_{16}H_{35}NO_4SiNa$ 356.2228; Found 356.2223.

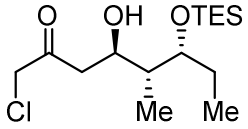

(4*R*,5*R*,6*R*)-1-Chloro-4-hydroxy-5-methyl-6-[(triethylsilyl)oxy]octan-2-one (2.58). To a solution of Weinreb amide **2.56** (144 mg, 0.432 mmol, 1.00 equiv) in THF (25 mL) at –78 °C was added $ClCH_2I$ (0.19 mL, 2.6 mmol, 6.0 equiv) and MeLi (1.6 M in Et_2O, 1.1 mL, 1.7 mmol, 4.0 equiv) dropwise. After stirring at –78 °C for 3 h, the reaction mixture was quenched by the addition of saturated aqueous NH_4Cl (20 mL). The reaction mixture was allowed to warm up to room temperature and the aqueous layer was extracted with EtOAc (3 × 20 mL). The combined organic layers were washed with saturated aqueous NaCl (20 ml), dried (Na_2SO_4), filtered, and concentrated under reduced pressure. Purification by flash chromatography (20% EtOAc/hexanes) afforded the title compound (81 mg, 58%) as a colorless oil. R_f = 0.62 (30% EtOAc/hexanes); $[\alpha]_D^{21}$ = 40.4 (*c* 1.0, $CHCl_3$); ^{1}H NMR ($CDCl_3$, 400 MHz) δ 4.36 (s, 1H), 4.22 (s, 2H), 4.07 (t, *J* = 8.7 Hz, 1H), 3.74 (dt, *J* = 6.3, 2.4 Hz, 1H), 2.70 (dd, *J* = 14.6, 3.1 Hz, 1H), 2.60 (dd, *J* = 14.6, 8.5 Hz, 1H), 1.80–1.67 (m, 1H), 1.53 (p, *J* = 7.1 Hz, 2H), 0.95 (t, *J* = 7.8 Hz, 9H), 0.91 (t, *J* = 7.4 Hz, 3H), 0.79 (d, *J* = 7.1 Hz, 3H), 0.61 (q, *J* = 8.2 Hz, 6H); ^{13}C NMR ($CDCl_3$, 100 MHz) δ 202.2, 78.2, 71.1, 49.6, 45.8, 42.3, 24.7, 12.7, 11.0, 6.8, 5.0; HRMS (ESI-TOF) *m/z*: $[M + Na]^+$ Calcd for $C_{15}H_{31}ClO_3SiNa$ 345.1623; Found 345.1621.

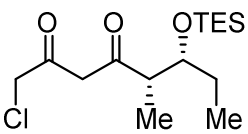

(5*S*,6*R*)-1-Chloro-5-methyl-6-[(triethylsilyl)oxy]octan-2,4-dione (2.59). To a solution of alcohol **2.58** (79 mg, 0.24 mmol, 1.0 equiv) in EtOAc (5 mL) was added IBX (45%, 457 mg, 0.734 mmol, 3.00 equiv). After heating

at reflux for 3.5 h, the reaction mixture was cooled to room temperature and concentrated under reduced pressure. Purification by flash chromatography (10% EtOAc/hexanes) afforded the title compound (62 mg, 79%) as an orange oil. R_f = 0.62 (20% EtOAc/hexanes); $[\alpha]_D^{22}$ = 12.3 (*c* 1.0, $CHCl_3$); ^{1}H NMR ($CDCl_3$, 400 MHz) δ 15.15 (s, 1H), 5.88 (s, 1H), 4.04 (s, 2H), 3.90 (q, *J* = 5.7 Hz, 1H), 2.57–2.43 (m, 1H), 1.60–1.43 (m, 2H), 1.14 (d, *J* = 6.9 Hz, 3H), 0.94 (t, *J* = 7.9 Hz, 9H), 0.89 (t, *J* = 7.4 Hz, 3H), 0.57 (q, *J* = 7.6 Hz, 6H); ^{13}C NMR ($CDCl_3$, 100 MHz) δ 196.2, 188.2, 97.7, 74.8, 46.6, 44.6, 28.0, 11.8, 9.5, 6.9, 5.1; HRMS (ESI-TOF) *m/z*: $[M + Na]^+$ Calcd for $C_{15}H_{29}ClO_3SiNa$ 343.1467; Found 343.1463.

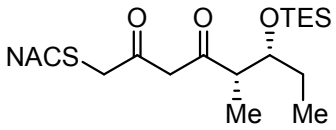

(5*S*,6*R*)-5-Methyl-1-[*N*-(2-acetamidoethyl)thio]-6-[(triethylsilyl)oxy]octane-2,4-dione (2.60). To a solution of chloromethyl ketone **2.59** (66 mg, 0.21 mmol, 1.0 equiv) in THF (5 mL) was added *N*-acetylcysteamine (24 μL, 0.23 mmol, 1.1 equiv) and a catalytic amount of Cs_2CO_3 at room temperature. The reaction mixture was stirred at room temperature for 7.5 h. The reaction was quenched by the addition of saturated aqueous NH_4Cl (10 mL). The layers were separated, and th aqueous layer was extracted with EtOAc (3 × 10 mL). The combined organic layers were washed with saturated aqueous NaCl (20 mL), dried (Na_2SO_4), filtered, and concentrated under reduced pressure to afford the title compound (76 mg) as a crude product. Due to its instability, the crude product was submitted to the next reaction without further purification. An analytically pure sample was obtained by purification by flash chromatography (5% MeOH/EtOAc) to afford the pure title compound as a light yellow oil. R_f = 0.54 (5% MeOH/CH_2Cl_2); $[\alpha]_D^{22}$ = 6.0 (*c* 0.15,

$CHCl_3$); ^1H NMR ($CDCl_3$, 400 MHz, approximately 7:1 mixture of enol:ketone forms where the integrations have been normalized) δ 15.26 (s, 0.88H), 6.02 (s, 1H), 5.69 (s, 0.88H), 3.92–3.84 (m, 1H), 3.51–3.39 (m, 2H), 3.36 (s, 0.25H), 3.24 (s, 1.75H), 2.73 (t, *J* = 6.2 Hz, 1.75H), 2.65 (t, *J* = 6.2 Hz, 0.25H), 2.54–2.40 (m, 1H), 1.99 (s, 3H), 1.59–1.42 (m, 2H), 1.13 (d, *J* = 6.9 Hz, 2.62H), 1.07 (d, *J* = 5.4 Hz, 0.38H), 0.98–0.86 (m, 12H), 0.68–0.50 (m, 6H); ^{13}C NMR ($CDCl_3$, 100 MHz, enol form) δ 194.9, 192.0, 170.1, 99.0, 74.7, 46.3, 38.2, 37.8, 32.5, 28.0, 23.3, 12.0, 9.5, 7.0, 5.1; HRMS (ESI-TOF) *m/z*: $[M + Na]^+$ Calcd for $C_{19}H_{37}NO_4SSiNa$ 426.2105; Found 426.2100.

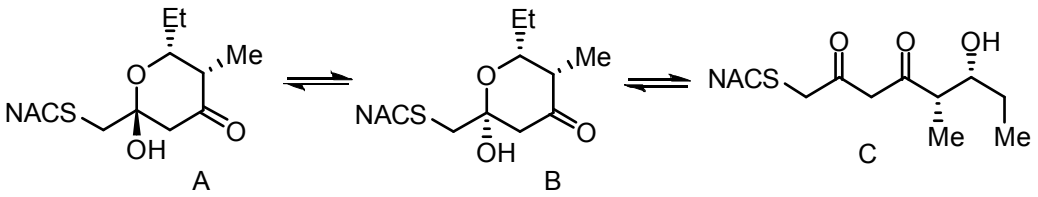

(5*S*,6*R*)-6-Hydroxy-5-methyl-1-[*N*-(2-acetamidoethyl)thio]octane-2,4-dione (2.18). To a solution of crude silyl ether **2.60** (21 mg, 0.052 mmol, 1.0 equiv) in THF (4 mL) at 0 °C was added a solution of 70% HF•pyridine:pyridine:THF (1 mL, 1:2:8) in a dropwise fashion. The reaction mixture was stirred at 0 °C for 13 h until the starting material was consumed by TLC (5% MeOH/EtOAc). The reaction was cooled in an ice bath, quenched by addition of saturated aqueous $NaHCO_3$ to pH 7, and extracted with EtOAc (3 × 10 mL). The combined organic layers were washed with saturated aqueous NaCl (20 mL), dried (Na_2SO_4), filtered, and concentrated under reduced pressure. The residue was dissolved in MeCN (1 mL), and purification by reverse-phase HPLC (Dynamax C_{18}, 10 × 250 mm, Varian) using a gradient elution (20–30% MeCN/H_2O at 0–15 min; 30–60% MeCN/H_2O at 15-28 min; 60–20% MeCN/H_2O at 28–40 min) at a flow rate of 3 mL/min monitoring at 254 nm afforded the title compound (10 mg, 30% over 2 steps) as a

colorless oil. R_f = 0.26 (5% MeOH/EtOAc); Due to the instability of the compound an optical rotation could not be obtained; ^{1}H NMR ($CDCl_3$, 400 MHz, approximately 8:5:7 mixture of A:B:C where the integrations have been normalized) δ 6.65–6.43 (m, 1H), 5.74 (s, 0.35H), 4.35–4.18 (m, 0.6H), 3.97–3.59 (m, 3.7H), 3.54–3.40 (m, 0.4H), 3.33 (d, J = 13.7 Hz, 0.25H), 3.26–3.05 (m, 1.4H), 3.04–2.86 (m, 1.4H), 2.82 (d, J = 14.4 Hz, 0.25H), 2.64–2.27 (m, 2H), 2.22–2.09 (m, 0.35H), 1.99 (s, 3H), 1.78–1.63 (m, 0.5H), 1.59–1.37 (m, 1.5H), 1.17 (d, J = 7.0 Hz, 1.2H), 1.14–1.08 (m, 1.8H), 1.04–0.91 (m, 3H); Due to the instability of the compound a ^{13}C NMR could not be obtained; HRMS (ESI-TOF) *m/z*: $[M + Na]^+$ Calcd for $C_{12}H_{23}NO_4SNa$ 312.1240; Found 312.1244.

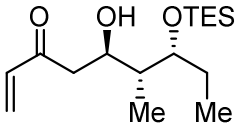

(5*R*,6*R*,7*R*)-5-Hydroxy-6-methyl-7-[(triethylsilyl)oxy]non-1-en-3-one (2.61). To a solution of tetravinyltin (0.12 mL, 0.68 mmol, 1.2 equiv) in THF (10 mL) at –78 °C was added MeLi (1.60 M in Et_2O, 1.43 mL, 2.28 mmol, 4.00 equiv). The reaction mixture was stirred at –78 °C for 30 min, followed by the addition of a solution of Weinreb amide **2.56** (190 mg, 0.570 mmol, 1.00 equiv) in THF (3 mL) in a dropwise fashion. After stirring at –78 °C for an additional 2.5 h, the reaction mixture was quenched by the addition of saturated aqueous NH_4Cl (10 mL) then warmed to room temperature and diluted with EtOAc (10 mL). The layers were separated and the aqueous layer was extracted with EtOAc (3 × 15 mL). The combined organic layers were washed with saturated aqueous NaCl (20 mL), dried (Na_2SO_4), and concentrated under reduced pressure. Purification by flash chromatography (20% EtOAc/hexanes) afforded the title compound (71 mg, 42%) as a colorless oil. R_f = 0.50 (20% EtOAc/hexanes); $[\alpha]_D^{21}$ = 31.4 (*c* 0.80, $CHCl_3$); ^{1}H NMR ($CDCl_3$, 400 MHz) δ 6.40 (dd, J = 17.6, 10.5 Hz, 1H),

6.24 (d, J = 17.6 Hz, 1H), 5.83 (d, J = 11.3 Hz, 1H), 4.14–4.06 (m, 1H), 4.02 (d, J = 2.8 Hz, 1H), 3.84 (dt, J = 6.9, 2.5 Hz, 1H), 2.77 (dd, J = 16.0, 3.4 Hz,1H), 2.68 (dd, J = 16.0, 8.4 Hz, 1H), 1.76–1.67 (m, 1H), 1.59–1.48 (m, 2H), 0.95 (t, J = 7.9 Hz, 9H), 0.88 (t, J = 7.4 Hz, 3H), 0.80 (d, J = 7.0 Hz, 3H), 0.61 (q, J = 7.9 Hz, 6H); ^{13}C NMR ($CDCl_3$, 100 MHz) δ 200.8, 136.9, 128.5, 76.5, 70.4, 45.2, 41.9, 25.8, 11.5, 10.8, 6.8, 5.1; HRMS (ESI-TOF) *m/z*: $[M + Na]^+$ Calcd for $C_{16}H_{32}O_3SiNa$ 323.2013; Found 323.2017.

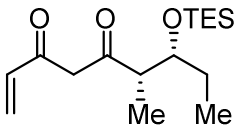

(6*S*,7*R*)-6-Methyl-7-[(triethylsilyl)oxy]non-1-ene-3,5-dione (2.62). To a solution of alcohol **2.61** (65 mg, 0.22 mmol, 1.00 equiv) in EtOAc (5 mL) was added IBX (45%, 404 mg, 0.649 mmol, 3.00 equiv). The reaction mixture was heated at reflux for 2 h, cooled to room temperature, and concentrated under reduced pressure. Purification by flash chromatography (10% EtOAc/hexanes) afforded the title compound (59 mg, 91%) as an orange oil. R_f = 0.69 (20% EtOAc/hexanes); $[\alpha]_D^{22}$ = 15.6 (*c* 0.50, $CHCl_3$); ^{1}H NMR ($CDCl_3$, 400 MHz) δ 15.23 (s, 1H), 6.27 (d, J = 18.5 Hz, 1H), 6.14 (dd, J = 17.2, 10.3 Hz, 1H), 5.67 (d, J = 10.3 Hz, 1H), 5.62 (s, 1H), 3.90 (q, J = 5.7 Hz, 1H), 2.55 (p, J = 6.9 Hz, 1H), 1.57–1.44 (m, 2H), 1.13 (d, J = 7.0 Hz, 3H), 0.94 (t, J = 7.9 Hz, 9H), 0.89 (t, J = 7.4 Hz, 3H), 0.58 (q, J = 7.7 Hz, 6H); ^{13}C NMR ($CDCl_3$, 100 MHz) δ 204.0, 176.3, 132.7, 125.1, 100.3, 75.1, 48.8, 28.1, 12.0, 9.5, 6.9, 5.1; HRMS (ESI-TOF) *m/z*: $[2M - H]^+$ Calcd for $C_{32}H_{59}O_6Si_2$ 595.3856; Found 595.3837.

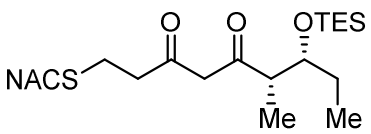

(6*S*,7*R*)-6-Methyl-1-[*N*-(2-acetamidoethyl)thio]-7-[(triethylsilyl)oxy]nonane-3,5-dione (2.63). To a solution of vinyl ketone **2.62** (37 mg, 0.12 mmol, 1.0 equiv) in THF (10 mL) was added *N*-

acetylcysteamine (14 μL, 0.13 mmol, 1.1 equiv) and a catalytic amount of Cs_2CO_3 at room temperature. After stirring at room temperature for 2.5 h, the reaction was quenched by the addition of saturated aqueous NH_4Cl (10 mL). The mixture was extracted with EtOAc (3 × 10 mL), and the combined organic layers were washed with saturated aqueous NaCl (10 mL), dried (Na_2SO_4), filtered, and concentrated under reduced pressure to afford the crude title compound (52 mg) that was used without further purification due to its instability. An analytically pure sample was obtained by flash chromatography (5% MeOH/EtOAc) to afford the pure title compound as a light yellow oil. R_f = 0.34 (5% MeOH/CH_2Cl_2); $[\alpha]_D^{21}$ = 67.2 (*c* 0.25, $CHCl_3$); ^{1}H NMR ($CDCl_3$, 400 MHz, approximately 5:1 mixture of enol:ketone forms where the integrations have been normalized) δ 15.45 (s, 0.83H), 6.05 (s, 0.17H), 5.98 (s, 0.83H), 5.54 (s, 0.83H), 3.88 (q, *J* = 5.6 Hz, 0.83H), 3.72 (d, *J* = 3.2 Hz, 0.17H), 3.45 (q, *J* = 6.1 Hz, 2H), 2.87–2.73 (m, 2.34H), 2.68 (s, 2H), 2.60 (t, *J* = 7.1 Hz, 1.66H), 2.42 (p, *J* = 6.8 Hz, 1H), 1.99 (s, 3H), 1.57–1.41 (m, 2H), 1.11 (d, *J* = 6.9 Hz, 2.5H), 1.05 (d, *J* = 7.0 Hz, 0.5H), 0.93 (t, *J* = 8.0 Hz, 9H), 0.88 (t, *J* = 7.4 Hz, 3H), 0.65–0.53 (m, 6H); ^{13}C NMR ($CDCl_3$, 100 MHz) δ 194.7, 193.6, 170.1, 99.7, 74.8, 46.3, 39.0, 38.4, 32.1, 28.0, 26.8, 23.3, 12.0, 9.4, 6.9, 5.1; HRMS (ESI-TOF) *m/z*: $[M + Na]^+$ Calcd for $C_{20}H_{39}NO_4SSiNa$ 440.2261; Found 440.2264.

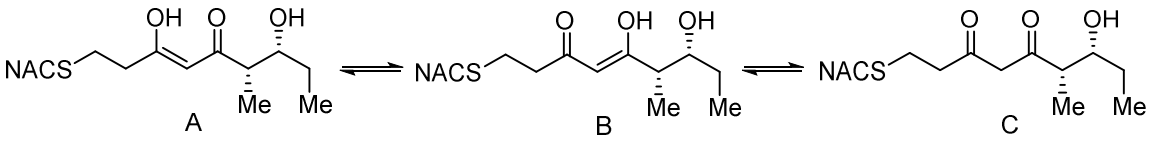

(6*S*,7*R*)-7-Hydroxy-6-methyl-1-[*N*-(2-acetamidoethyl)thio]nonane-3,5-dione (2.19). To a solution of silyl ether **2.63** (52 mg, 0.12 mmol, 1.0 equiv) in THF (8 mL) at 0 °C was added a solution of 70% HF-pyridine:pyridine:THF (1:2:8, 4 mL) in a dropwise

fashion. The reaction mixture was stirred at 0 °C for 8 h, cooled in an ice bath, then quenched by addition of saturated aqueous $NaHCO_3$ to adjust the mixture to pH 7. The mixture was extracted with EtOAc (3 × 10 mL), and the combined organic layers were washed with saturated aqueous NaCl (20 mL), dried (Na_2SO_4), filtered, and concentrated under reduced pressure. The oily residue was dissolved in MeCN (1 mL) and purified by reverse-phase HPLC (Dynamax C_{18}, 10 × 250 mm, Varian). A gradient elution (20–30% MeCN/H_2O at 0–15 min; 30–60% MeCN/H_2O at 15-28 min; 60–20% MeCN/H_2O at 28–40 min) at a flowrate of 3 mL/min with monitoring at 254 nm afforded the title compound (20 mg, 53% over 2 steps) as a colorless oil. R_f = 0.26 (5% MeOH/EtOAc); Due to the instability of the compound the optical rotation could not be obtained; ^{1}H NMR ($CDCl_3$, 400 MHz, approximately 12:5:3 mixture of A:B:C where the integrations have been normalized) δ 15.40 (s, 0.6H), 6.53–6.35 (m, 0.4H), 5.94 (s, 0.6H), 5.62 (s, 0.25H), 5.57 (s, 0.6H), 4.23–4.14 (m, 0.25H), 3.95–3.88 (m, 0.15H), 3.85–3.68 (m, 1.7H), 3.44 (q, J = 6.1 Hz, 1.2H), 3.13–2.95 (m, 0.8H), 2.90–2.76 (m, 2H), 2.73–2.57 (m, 2.4H), 2.51–2.24 (m, 1.8H), 2.03–1.95 (m, 3H), 1.69–1.60 (m, 0.5H), 1.56–1.42 (m, 1.5H), 1.16 (d, J = 7.0 Hz, 1.8H), 1.11 (d, J = 7.0 Hz, 0.45H), 1.08 (d, J = 7.1 Hz, 0.75H), 1.00–0.91 (m, 2.55H), 0.90–0.85 (m, 0.45H); ^{13}C NMR ($CDCl_3$, 100 MHz, major isomer A) δ 197.3, 192.1, 170.2, 99.3, 73.8, 46.7, 38.5 (ovlp, 2C), 32.0, 27.3, 27.1, 23.3, 11.1, 10.4; HRMS (ESI-TOF) *m/z*: $[M + Na]^+$ Calcd for $C_{14}H_{25}NO_4SNa$ 326.1397; Found 326.1408.

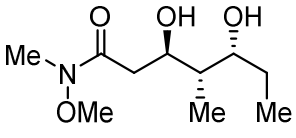

(3*R*,4*S*,5*R*)-3,5-Dihydroxy-*N*-methoxy-*N*,4-dimethylheptanamide (2.64). To a solution of silyl ether **2.56**

(68 mg, 0.20 mmol, 1.0 equiv) in THF (10 mL) at 0 °C was added TBAF (1.0 M in THF, 0.40 mL, 0.40 mmol, 2.0 equiv). The reaction mixture was stirred at 0 °C for 10 min and then quenched by addition of saturated aqueous NH_4Cl (10 mL). The reaction mixture was extracted with EtOAc (3 × 10 mL), and the combined organic layers were washed with saturated aqueous NaCl (20 mL), dried (Na_2SO_4), filtered, and concentrated under reduced pressure. Purification by flash chromatography (5% MeOH/CH_2Cl_2) afforded the title compound (37 mg, 83%) as a colorless oil. R_f = 0.39 (5% MeOH/CH_2Cl_2); $[\alpha]_D^{21}$ = 59.4 (*c* 0.50, $CHCl_3$); ^{1}H NMR ($CDCl_3$, 400 MHz) δ 4.31 (s, 1H), 4.08 (ddd, *J* = 9.6, 6.2, 2.4 Hz, 1H), 3.84–3.77 (m, 1H), 3.70 (s, 3H), 3.20 (s, 3H), 3.16 (s, 1H), 2.72 (d, *J* = 16.4 Hz, 1H), 2.58 (dd, *J* = 16.7, 10.1 Hz, 1H), 1.69–1.60 (m, 1H), 1.60–1.50 (m, 1H), 1.47–1.36 (m, 1H), 0.97 (t, *J* = 7.5 Hz, 3H), 0.95 (d, *J* = 7.1 Hz, 7H); ^{13}C NMR ($CDCl_3$, 100 MHz) δ 173.9, 73.9, 72.0, 61.3, 41.4, 36.3, 31.9, 26.6, 11.3, 10.9; HRMS (ESI-TOF) *m/z*: $[M + Na]^+$ Calcd for $C_{10}H_{21}NO_4Na$ 242.1363; Found 242.1360.

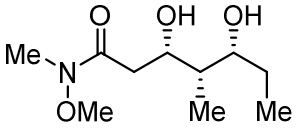

(3*S*,4*S*,5*R*)-3,5-Dihydroxy-*N*-methoxy-*N*,4-dimethylheptanamide (2.65). Identical reaction conditions for the synthesis of diol **2.64** were used, except for the use of silyl ether **2.57** (52 mg, 0.16 mmol, 1.0 equiv). Purification by flash chromatography (5% MeOH/CH_2Cl_2) afforded the title compound (28 mg, 82%) as a colorless oil. R_f = 0.44 (5% MeOH/CH_2Cl_2); $[\alpha]_D^{22}$ = –49.6 (*c* 1.0, $CHCl_3$); ^{1}H NMR ($CDCl_3$, 400 MHz) δ 4.30 (d, *J* = 9.4 Hz, 1H), 4.13 (s, 1H), 3.81 (t, *J* = 6.5 Hz, 1H), 3.70 (s, 3H), 3.30 (s, 1H), 3.20 (s, 3H), 2.69–2.51 (m, 2H), 1.65–1.49 (m, 2H), 1.48–1.36 (m, 1H), 0.95 (d, *J* = 7.2 Hz, 3H), 0.93 (t, *J* = 7.4 Hz, 3H);

^{13}C NMR ($CDCl_3$, 100 MHz) δ 173.9, 77.7, 73.0, 61.3, 40.3, 36.2, 31.9, 27.6, 10.5,5.1; HRMS (ESI-TOF) *m/z*: $[M + Na]^+$ Calcd for $C_{10}H_{21}NO_4Na$ 242.1363; Found 242.1363.

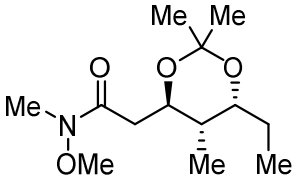

2-[(4*R*,5*S*,6*R*)-6-Ethyl-2,2,5-trimethyl-1,3-dioxan-4-yl]-*N*-methoxy-*N*-methylacetamide (2.66). To a solution of diol **2.64** (35 mg, 0.16 mmol, 1.0 equiv) in CH_2Cl_2 (5 mL) at room temperature was added 2,2-dimethoxypropane (0.20 mL, 1.6 mmol, 10 equiv), followed by the addition of PPTS (8.0 mg, 0.032 mmol, 0.2 equiv). The reaction was stirred at room temperature for 20 h, then quenched with saturated aqueous $NaHCO_3$ (10 mL). The mixture was extracted with CH_2Cl_2 (3 × 10 mL), and the combined organic layers were washed with saturated aqueous NaCl (20 mL), dried (Na_2SO_4), filtered, and concentrated under reduced pressure. Purification by flash chromatography (40% EtOAc/hexanes) afforded the title compound (28 mg, 68%) as a colorless oil. R_f = 0.45 (40% EtOAc/hexanes); $[\alpha]_D^{21} = -11.3$ (*c* 0.30, $CHCl_3$); ^{1}H NMR ($CDCl_3$, 400 MHz) δ 3.83 (ddd, *J* = 9.2, 8.3, 3.2 Hz, 1H), 3.74 (dt, *J* = 8.8, 5.0 Hz, 1H), 3.70 (s, 3H), 3.19 (s, 3H), 2.79 (dd, *J* = 14.7, 9.4 Hz, 1H), 2.45 (dd, *J* = 15.4, 3.2 Hz, 1H), 1.78–1.66 (m, 1H), 1.52–1.34 (m, 2H), 1.37 (s, 3H), 1.31 (s, 3H), 0.92 (t, *J* = 7.3 Hz, 3H), 0.85 (d, *J* = 6.8 Hz, 3H); ^{13}C NMR ($CDCl_3$, 100 MHz) δ 172.0, 100.7, 71.2, 70.7, 61.2, 39.4, 37.0, 32.1, 24.8, 23.8, 23.5, 11.4, 10.6; HRMS (ESI-TOF) *m/z*: $[M + Na]^+$ Calcd for $C_{13}H_{25}NO_4Na$ 282.1676; Found 282.1680.

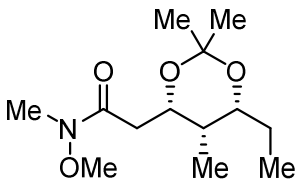

2-[(4*S*,5*S*,6*R*)-6-Ethyl-2,2,5-trimethyl-1,3-dioxan-4-yl]-*N*-methoxy-*N*-methylacetamide (2.67). Identical reaction

conditions for the synthesis of acetonide **2.66** were used, except for the use of diol **2.65** (27 mg, 0.12 mmol, 1.0 equiv). Purification by flash chromatography (5% MeOH/CH_2Cl_2) afforded the title compound (25 mg, 78%) as a colorless oil. R_f = 0.50 (5% MeOH/CH_2Cl_2); $[\alpha]_D^{22}$ = 3.6 (*c* 0.80, $CHCl_3$); ^{1}H NMR ($CDCl_3$, 400 MHz) δ 4.47 (ddd, *J* = 7.7, 6.0, 2.2 Hz, 1H), 3.82 (ddd, *J* = 7.3, 6.9, 2.1 Hz, 1H), 3.70 (s, 3H), 3.18 (s, 3H), 2.75 (dd, *J* = 14.9, 6.0 Hz, 1H), 2.43 (dd, *J* = 15.8, 5.3 Hz, 1H), 1.58–1.48 (m, 2H), 1.45 (s, 3H), 1.42–1.33 (m, 1H), 1.37 (s, 3H), 0.88 (t, *J* = 7.4 Hz, 3H), 0.86 (d, *J* = 6.9 Hz, 3H); ^{13}C NMR ($CDCl_3$, 100 MHz) δ 171.9, 99.0, 74.6, 70.0, 61.3, 35.1, 33.8, 32.0, 29.9, 25.6, 19.7, 9.7, 4.9; HRMS (ESI-TOF) *m/z*: $[M + Na]^+$ Calcd for $C_{13}H_{25}NO_4Na$ 282.1676; Found 282.1681.

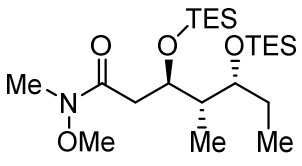

(3*R*,4*S*,5*R*)-*N*-Methoxy-*N*,4-dimethyl-3,5-bis[(triethylsilyl)oxy]heptanamide (2.68). To a solution of alcohol **2.56** (494 mg, 1.48 mmol, 1.00 equiv) in CH_2Cl_2 (30 mL) at 0 °C was added *i*-Pr_2NEt (0.41 mL, 2.4 mmol, 1.6 equiv) and TESOTf (0.54 mL, 2.4 mmol, 1.6 equiv). After stirring at 0 °C for 70 min, the reaction mixture was quenched by the addition of saturated aqueous $NaHCO_3$ (20 mL). The layers were separated and the aqueous layer was extracted with CH_2Cl_2 (3 × 20 mL). The combined organic layers were washed with saturated aqueous NaCl (50 mL), dried (Na_2SO_4), filtered, and concentrated under reduced pressure. Purification by flash chromatography (20% EtOAc/hexanes) afforded the title compound (636 mg, 96%) as a colorless oil. R_f = 0.63 (20% EtOAc/hexanes); $[\alpha]_D^{21}$ = 25.2 (*c* 0.50, $CHCl_3$); ^{1}H NMR ($CDCl_3$, 400 MHz) δ 4.30 (dt, *J* = 9.7, 3.0 Hz, 1H), 3.70 (s, 3H), 3.52 (q, *J* = 5.6 Hz, 1H), 3.17 (s, 3H), 2.79 (d,

J = 13.9 Hz, 1H), 2.20 (dd, J = 14.9, 2.2 Hz, 1H), 1.84–1.75 (m, 1H), 1.60–1.50 (m, 2H), 0.98–0.85 (m, 24H), 0.63–0.54 (m, 12H); ^{13}C NMR ($CDCl_3$, 100 MHz) δ 173.1, 75.2, 71.2, 61.2, 42.9, 34.8, 32.0, 27.7, 8.9, 8.8, 7.0, 6.8, 5.4, 4.9; HRMS (ESI-TOF) *m/z*: [M + Na]$^+$ Calcd for $C_{22}H_{49}NO_4Si_2Na$ 470.3092; Found 470.3094.

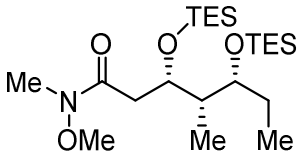

(3*S*,4*S*,5*R*)-*N*-Methoxy-*N*,4-dimethyl-3,5-bis[(triethylsilyl)oxy]heptanamide (2.69). Identical reaction conditions for the synthesis of silyl ether **2.68** were used, except for the use of alcohol **2.57** (403 mg, 1.21 mmol, 1.00 equiv). Purification by flash chromatography (20% EtOAc/hexanes) afforded the title compound (434 mg, 80%) as a colorless oil. R_f = 0.54 (20% EtOAc/hexanes); $[\alpha]_D^{21}$ = –29.2 (*c* 1.0, $CHCl_3$); ^{1}H NMR ($CDCl_3$, 400 MHz) δ 4.29 (dt, J = 8.3, 4.4 Hz, 1H), 3.78 (q, J = 5.6 Hz, 1H), 3.67 (s, 3H), 3.16 (s, 3H), 2.69 (dd, J = 15.2, 7.7 Hz, 1H), 2.54 (dd, J = 15.4, 4.2 Hz, 1H), 1.71–1.62 (m, 1H), 1.59–1.49 (m, 2H), 0.95 (t, J = 8.0 Hz, 9H), 0.92 (t, J = 8.0 Hz, 9H), 0.89 (d, J = 7.0 Hz, 3H), 0.84 (t, J = 7.4 Hz, 3H), 0.59 (q, J = 7.9 Hz, 6H); 0.57 (q, J = 7.9 Hz, 6H); ^{13}C NMR ($CDCl_3$, 100 MHz) δ 173.0, 73.3, 70.6, 61.2, 42.0, 37.3, 32.0, 27.5, 10.1, 9.4, 7.0, 6.9, 5.4, 5.1; HRMS (ESI-TOF) *m/z*: [M + Na]$^+$ Calcd for $C_{22}H_{49}NO_4Si_2Na$ 470.3092; Found 470.3092.

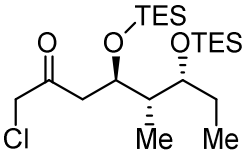

(4*R*,5*S*,6*R*)-1-Chloro-5-methyl-4,6-bis[(triethylsilyl)oxy]octan-2-one (2.70). To a solution of Weinreb amide **2.68** (158 mg, 0.353 mmol, 1.00 equiv) in THF (10 mL) at –78 °C was added $ClCH_2I$ (0.15 mL, 2.1 mmol, 6.0 equiv), followed by the addition of MeLi (1.6 M in Et_2O, 0.88 mL, 1.4 mmol, 4.0 equiv) in a dropwise fashion over 10 min. The reaction was stirred at

–78 °C for 5 h, then quenched by the addition of saturated aqueous NH_4Cl (10 mL). The reaction mixture was allowed to warm to room temperature and extracted with EtOAc (3 × 20 mL). The combined organic layers were washed with saturated aqueous NaCl (20 mL), dried (Na_2SO_4), filtered, and concentrated. Purification by flash chromatography (5% EtOAc/hexanes) afforded the title compound (78 mg, 51%) as a light yellow oil. R_f = 0.59 (10% EtOAc/hexanes); $[\alpha]_D^{23}$ = 45.0 (*c* 0.50, $CHCl_3$); ^{1}H NMR ($CDCl_3$, 400 MHz) δ 4.24 (dt, *J* = 9.7, 2.8 Hz, 1H), 4.14 (d, *J* = 1.6 Hz, 2H), 3.58–3.49 (m, 1H), 2.74 (dd, *J* = 15.1, 9.7 Hz, 1H), 2.52 (dd, *J* = 15.1, 2.2 Hz, 1H), 1.77 (tq, *J* = 7.0, 4.5 Hz, 1H), 1.58–1.47 (m, 2H), 0.94 (t, *J* = 7.9 Hz, 9H), 0.92 (t, *J* = 8.0 Hz, 9H), 0.89 (d, *J* = 6.6 Hz, 3H), 0.85 (t, *J* = 7.4 Hz, 3H), 0.57 (app. p, *J* = 8.0 Hz, 12H); ^{13}C NMR ($CDCl_3$, 100 MHz) δ 201.6, 75.3, 72.0, 50.0, 43.2, 42.4, 27.8, 9.3, 7.6, 7.0, 6.8, 5.4, 4.9; HRMS (ESI-TOF) *m/z*: $[M + Na]^+$ Calcd for $C_{21}H_{45}ClO_3Si_2Na$ 459.2488; Found 437.2491.

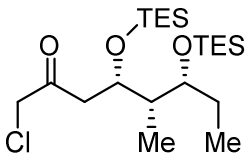

(4*S*,5*S*,6*R*)-1-Chloro-5-methyl-4,6-bis[(triethylsilyl)oxy]octan-2-one (2.71). Identical reaction conditions for the synthesis of chloromethyl ketone **2.70** were used, except for the use of Weinreb amide **2.69** (135 mg, 0.301 mmol, 1.00 equiv). Purification by flash chromatography (5% EtOAc/hexanes) afforded the title compound (101 mg, 77%) as a light yellow oil. R_f = 0.59 (10% EtOAc/hexanes); $[\alpha]_D^{20}$ = –41.6 (*c* 1.0, $CHCl_3$); ^{1}H NMR ($CDCl_3$, 400 MHz) δ 4.22 (ddd, *J* = 7.8, 5.6, 3.8 Hz, 1H), 4.11 (s, 2H), 3.85 (dt, *J* = 6.5, 3.3 Hz 1H), 2.84 (dd, *J* = 15.8, 7.7 Hz, 1H), 2.71 (dd, *J* = 15.8, 3.7 Hz, 1H), 1.69–1.60 (m, 1H), 1.59–1.47 (m, 2H), 0.96 (t, *J* = 8.0 Hz, 9H), 0.93 (t, *J* = 8.0 Hz, 9H), 0.84 (d, *J* =7.0 Hz, 3H), 0.82 (t, *J* = 7.5 Hz, 3H), 0.60 (q, *J* = 7.9 Hz, 6H), 0.57 (q, *J* = 8.0 Hz, 6H); ^{13}C NMR ($CDCl_3$, 100

MHz) δ 201.7, 72.8, 71.0, 49.8, 44.8, 41.5, 27.8, 9.84, 9.80, 7.0, 6.9, 5.5, 5.0; HRMS (ESI-TOF) *m/z*: $[M + Na]^+$ Calcd for $C_{21}H_{45}ClO_3Si_2Na$ 459.2488; Found 437.2489.

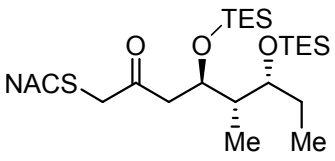

(4*R*,5*R*,6*R*)-5-Methyl-1-[*N*-(2-acetamidoethyl)thio]-4,6-bis[(triethylsilyl)oxy]octan-2-one (2.72). To a solution of chloromethyl ketone **2.70** (78 mg, 0.18 mmol, 1.0 equiv) in THF (10 mL) was added *N*-acetylcysteamine (28 μL, 0.27 mmol, 1.5 equiv) and a catalytic amount of Cs_2CO_3 at room temperature. The reaction was stirred at room temperature for 38 h, then quenched by the addition of saturated aqueous NH_4Cl (10 mL). The layers were separated, and the aqueous layer was extracted with EtOAc (3 × 10 mL). The combined organic layers were washed with saturated aqueous NaCl (40 mL), dried (Na_2SO_4), filtered, and concentrated under reduced pressure. Purification by flash chromatography (5% MeOH/CH_2Cl_2) afforded the title compound (84 mg, 90%) as a colorless oil. R_f = 0.35 (5% MeOH/CH_2Cl_2); $[\alpha]_D^{20}$ = 33.9 (*c* 1.0, $CHCl_3$); ^{1}H NMR ($CDCl_3$, 400 MHz) δ 6.23 (s, 1H), 4.23 (dt, *J* = 9.5, 2.4 Hz, 1H), 3.55–3.48 (m, 1H), 3.46–3.35 (m, 2H), 3.30 (dd, *J* =15.0, 4.3 Hz, 2H), 2.79 (dd, *J* = 15.4, 9.6 Hz, 1H), 2.69–2.56 (m, 2H), 2.51 (dd, *J* = 15.4, 2.2 Hz, 1H), 1.99 (s, 3H), 1.80–1.70 (m, 1H), 1.57–1.43 (m, 2H), 0.96–0.82 (m, 24H), 0.55 (app. p, *J* = 7.8 Hz, 12H); ^{13}C NMR ($CDCl_3$, 100 MHz) δ 205.5, 170.1, 75.2, 71.8, 44.1, 42.5, 42.4, 38.1, 32.1, 27.7, 23.2, 9.2, 7.9, 7.0, 6.9, 5.4, 5.0; HRMS (ESI-TOF) *m/z*: $[M + Na]^+$ Calcd for $C_{26}H_{55}NO_3SSi_2Na$ 542.3126; Found 542.3119.

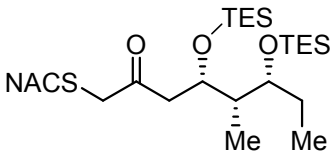

(4*S*,5*R*,6*R*)-5-Methyl-1-[*N*-(2-acetamidoethyl)thio]-4,6-bis[(triethylsilyl)oxy]octan-2-one (2.73). Identical reaction conditions for the synthesis of thioether **2.72** were used, except for the use of chloromethyl ketone **2.71** (50 mg, 0.11 mmol, 1.0 equiv). Purification by flash chromatography (5% MeOH/CH_2Cl_2) afforded the title compound (48 mg, 81%) as a colorless oil. R_f = 0.37 (5% MeOH/CH_2Cl_2); $[\alpha]_D^{22}$ = –28.0 (*c* 1.0, $CHCl_3$); ^{1}H NMR ($CDCl_3$, 400 MHz) δ 6.15 (s, 1H), 4.19 (q, *J* = 5.6 Hz, 1H), 3.82 (q, *J* = 6.2 Hz, 1H), 3.41 (p, *J* = 6.0 Hz, 2H), 3.29 (s, 2H), 2.80 (d, *J* = 5.7 Hz, 2H), 2.63 (t, *J* = 6.2 Hz, 2H), 2.00 (s, 3H), 1.66–1.59 (m, 1H), 1.56–1.48 (m, 2H), 0.96 (t, *J* = 7.9 Hz, 9H), 0.93 (t, *J* = 8.0 Hz, 9H), 0.84 (d, *J* = 6.9 Hz, 3H), 0.82 (t, *J* = 7.5 Hz, 3H), 0.60 (q, *J* = 7.9 Hz, 6H), 0.57 (q, *J* = 8.0 Hz, 6H); ^{13}C NMR ($CDCl_3$, 100 MHz) δ 205.4, 170.1, 72.8, 70.8, 45.9, 42.3, 41.4, 38.1, 32.1, 27.8, 23.2, 9.73, 9.67, 7.02, 6.95, 5.5, 5.1; HRMS (ESI-TOF) *m/z*: $[M + Na]^+$ Calcd for $C_{26}H_{55}NO_3SSi_2Na$ 542.3126; Found 542.3129.

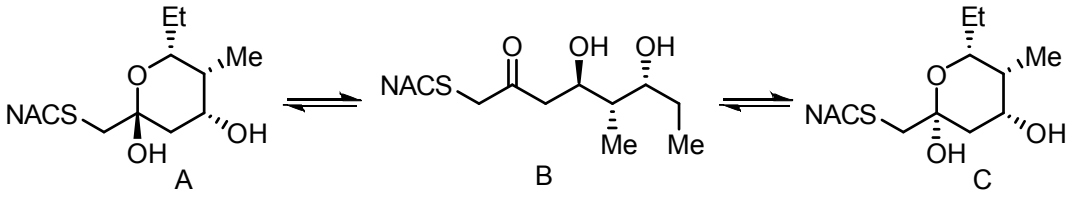

(4*R*,5*R*,6*R*)-4,6-Dihydroxy-5-methyl-1-[*N*-(2-acetamidoethyl)thio]octan-2-one (2.24). To a solution of silyl ether **2.72** (44 mg, 0.085 mmol, 1.0 equiv) in THF (8 mL) at 0 °C was added a solution of 70% HF-pyridine:pyridine:THF (1:2:8, 4 mL). The reaction was stirred at 0 °C for 6 h, then quenched at 0 ºC by the addition of saturated aqueous $NaHCO_3$ until the mixture was pH 7. The layers were separated and the aqueous layer was extracted with EtOAc (3 × 10 mL). The combined organic layers were washed with

saturated aqueous NaCl (20 mL), dried (Na_2SO_4), filtered, and concentrated under reduced pressure. Purification by flash chromatography (5% MeOH/EtOAc) afforded the title compound (15 mg, 60%) as a colorless oil. R_f = 0.31 (5% MeOH/EtOAc); Due to the instability of the compound the optical rotation could not be obtained; ^{1}H NMR ($CDCl_3$, 400 MHz, approximately 17:2:1 mixture of A:B:C where the integrations have been normalized) δ 6.16 (s, 0.1H), 6.10 (s, 0.05H), 5.96 (s, 0.85H), 4.24 (dt, *J* = 11.7, 4.8 Hz, 0.85H), 4.08–3.98 (m, 0.1H), 3.90–3.86 (m, 0.05H), 3.86–3.76 (m, 1H), 3.62 (s, 0.85H), 3.56–3.34 (m, 2.35H), 2.95–2.84 (m, 1.8H), 2.76–2.65 (m, 1.2H), 2.53 (d, *J* = 14.1 Hz, 0.9H), 1.99 (s, 3H), 1.93–1.85 (m, 1H), 1.78 (dd, *J* = 12.4, 4.8 Hz, 1.7H), 1.68–1.46 (m, 1.95H), 1.46–1.31 (m, 1H), 1.11 (d, *J* = 7.2 Hz, 0.15H), 1.05 (t, *J* = 7.1 Hz, 0.15H), 0.98 – 0.93 (m, 0.6H), 0.88 (t, *J* = 7.4 Hz, 2.55H), 0.81 (d, *J* = 6.9 Hz, 2.55H); ^{13}C NMR ($CDCl_3$, 100 MHz, major hemiketal A) δ 206.4, 170.2, 96.2, 73.2, 67.8, 43.5, 38.7, 37.1, 33.2, 25.1, 23.3, 10.4, 3.6; HRMS (ESI-TOF) *m/z*: $[M + Na]^+$ Calcd for $C_{13}H_{25}NO_4SNa$ 314.1397; Found 314.1399.

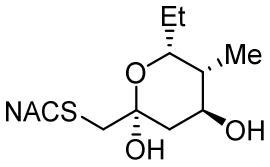

(4*S*,5*R*,6*R*)-4,6-Dihydroxy-5-methyl-1-[*N*-(2-acetamidoethyl)thio]octan-2-one (2.26). Identical reaction conditions for the synthesis of diol **2.24** were used, except for the use of silyl ether **2.73** (48 mg, 0.092 mmol, 1.0 equiv). Purification by flash chromatography (5% MeOH/CH_2Cl_2) afforded the title compound (21 mg, 78%) as a colorless oil. R_f = 0.24 (5% MeOH/EtOAc); Due to the instability of the compound the optical rotation could not be obtained; ^{1}H NMR ($CDCl_3$, 400 MHz) δ 5.95 (s, 1H), 4.45 (d, *J* = 1.7 Hz, 1H), 4.20–4.12 (m, 1H), 3.94–3.85 (m, 1H), 3.61 (d, *J* = 7.9 Hz, 1H),

3.56–3.40 (m, 2H), 2.91–2.82 (m, 2H), 2.78–2.69 (m, 1H), 2.54 (d, J = 14.1 Hz, 1H), 2.00 (s, 3H), 1.92–1.85 (m, 1H), 1.81–1.71 (m, 2H), 1.52 (dq, J = 14.9, 7.5 Hz, 1H), 1.39 (dq, J = 13.8, 7.1 Hz, 1H), 0.91 (t, J = 7.4 Hz, 3H), 0.84 (d, J = 7.1 Hz, 3H); ^{13}C NMR ($CDCl_3$, 100 MHz) δ 170.3, 96.9, 71.2, 68.2, 43.0, 38.7, 36.6, 33.8, 33.3, 25.0, 23.3, 10.3, 10.2; HRMS (ESI-TOF) *m/z*: [M + Na]$^+$ Calcd for $C_{13}H_{25}NO_4SNa$ 314.1397; Found 314.1390.

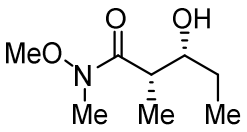

(2*S*,3*R*)-3-Hydroxy-*N*-methoxy-*N*,2-dimethylpentanamide (2.74). To a solution of thiazolidinethione **2.53** (535 mg, 1.65 mmol, 1.00 equiv) in CH_2Cl_2 (5 mL) at room temperature was added *N*,*O*-dimethylhydroxylamine hydrochloride (968 mg, 9.92 mmol, 6.00 equiv) and imidazole (1.35 g, 19.9 mmol, 12.0 equiv), followed by the addition of DMAP (40 mg, 0.33 mmol, 0.20 equiv). The reaction was stirred at room temperature for 24 h until the yellow color disappeared, then quenched by the addition of water (20 mL). The layers were separated and the aqueous layer was extracted with CH_2Cl_2 (3 × 20 mL). The combined organic layers were dried (Na_2SO_4), filtered, and concentrated under reduced pressure. Purification by flash chromatography (5% MeOH/CH_2Cl_2) afforded the title compound (214 mg, 74%) as colorless oil. R_f = 0.34 (5% MeOH.CH_2Cl_2); $[\alpha]_D^{22}$ = 18.6 (*c* 1.0, $CHCl_3$); ^{1}H NMR ($CDCl_3$, 400 MHz) δ 3.77 (ddd, J = 7.9, 5.4, 2.6 Hz, 1H), 3.70 (s, 3H), 3.20 (s, 3H), 2.90 (s, 2H), 1.66–1.51 (m, 1H), 1.45–1.34 (m, 1H), 1.16 (d, J = 7.1 Hz, 3H), 0.96 (t, J = 7.4 Hz, 3H); ^{13}C NMR ($CDCl_3$, 100 MHz) δ 178.1, 73.0, 61.4, 38.2, 31.7, 26.7, 10.2, 10.1; HRMS (ESI-TOF) *m/z*: [M + Na]$^+$ Calcd for $C_8H_{17}NO_3Na$ 198.1101; Found 198.1108.

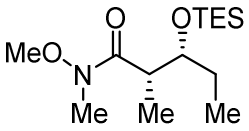

(2*S*,3*R*)-*N*-Methoxy-*N*,2-dimethy-3-[(triethylsilyl)oxy]lpentanamide (2.75). To a solution of alcohol **2.74** (134 mg, 0.765 mmol, 1.00 equiv) in CH_2Cl_2 (10 mL) at 0 °C was added *i*-Pr_2NEt (0.24 mL, 1.4 mmol, 1.8 equiv), followed by the addition of TESOTf (0.26 mL, 1.1 mmol, 1.5 equiv) in a dropwise fashion. The reaction was stirred at 0 °C for 1 h, then quenched by the addition of saturated aqueous $NaHCO_3$ (10 mL). The layers were separated and the aqueous layer was extracted with CH_2Cl_2 (3 × 20 mL). The combined organic layers were dried (Na_2SO_4), filtered, and concentrated under reduced pressure. Purification by flash chromatography (20% EtOAc/hexanes) afforded the title compound (198 mg, 90%) as colorless oil. R_f = 0.37 (20% EtOAc/hexanes); $[\alpha]_D^{22}$ = 4.5 (*c* 0.40, $CHCl_3$); ^{1}H NMR ($CDCl_3$, 400 MHz) δ 3.89 (dt, *J* = 8.5, 4.9 Hz, 1H), 3.68 (s, 3H), 3.17 (s, 3H), 2.98 (s, 1H), 1.59–1.38 (m, 2H), 1.17 (d, *J* = 6.9 Hz, 3H), 0.97 (t, *J* = 7.9 Hz, 9H), 0.89 (t, *J* = 7.5 Hz, 3H), 0.63 (q, *J* = 7.9 Hz, 6H); ^{13}C NMR ($CDCl_3$, 100 MHz) δ 74.7, 61.4, 40.5, 32.1, 28.5, 14.7, 8.8, 7.0, 5.2; HRMS (ESI-TOF) *m/z*: $[M + Na]^+$ Calcd for $C_{14}H_{31}NO_3SiNa$ 312.1965; Found 312.1970.

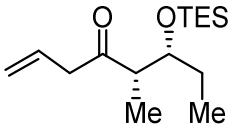

(5*S*,6*R*)-5-Methyl-6-[(triethylsilyl)oxy]oct-1-en-4-one (2.76). To a solution of Weinreb amide **2.75** (69 mg, 0.24 mmol, 1.0 equiv) in THF (5 mL) at 0 °C was added allylmagnesium bromide (1.0 M in Et_2O, 0.38 mL, 0.38 mmol, 1.6 equiv) dropwise. The reaction was stirred at 0 °C for 15 min, then quenched by the addition of saturated aqueous NH_4Cl (5 mL). The layers were separated and the aqueous layer was extracted with EtOAc (3 × 10 mL). The combined organic layers were washed with saturated aqueous NaCl (10 mL), dried (Na_2SO_4), filtered, and concentrated

under reduced pressure. Purification by flash chromatography (10% EtOAc/hexanes) afforded the title compound (58 mg, 91%) as a colorless oil. R_f = 0.49 (10% EtOAc/hexanes); $[\alpha]_D^{21}$ = 42.3 (*c* 1.0, $CHCl_3$); ^{1}H NMR ($CDCl_3$, 400 MHz) δ 5.99–5.86 (m, 1H), 5.18–5.06 (m, 2H), 3.86 (q, *J* = 5.6 Hz, 1H), 3.33 (dd, *J* = 17.7, 6.4 Hz, 1H), 3.23 (dd, *J* = 17.1, 7.0 Hz, 1H), 2.71 (p, *J* = 6.6 Hz, 1H), 1.49 (tq, *J* = 13.4, 7.0 Hz, 1H), 1.36 (dp, *J* = 14.2, 7.1 Hz, 1H), 1.07 (d, *J* = 7.7 Hz, 3H), 0.96 (t, *J* = 7.9 Hz, 9H), 0.87 (t, *J* = 7.4 Hz, 3H), 0.61 (q, *J* = 8.0 Hz, 6H); ^{13}C NMR ($CDCl_3$, 100 MHz) δ 211.2, 130.9, 118.4, 74.9, 50.8, 47.5, 27.5, 12.0, 9.9, 6.9, 5.2; HRMS (ESI-TOF) *m/z*: $[M + Na]^+$ Calcd for $C_{15}H_{30}O_2SiNa$ 293.1907; Found 293.1913.

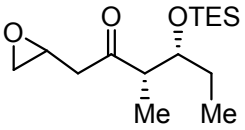

(2*RS*,3*S*,4*R*)-3-Methyl-1-(oxiran-2-yl)-4-[(triethylsilyl)oxy]hexan-2-one (2.77). To a solution of allyl ketone **2.76** (58 mg, 0.21 mmol, 1.0 equiv) in CH_2Cl_2 (2 mL) at room temperature was added *m*-CPBA (77%, 168 mg, 0.75 mmol, 3.5 equiv). The reaction mixture was stirred at room temperature for 14 h, then quenched by the addition of saturated aqueous Na_2HCO_3:$Na_2S_2O_3$ (1:1, 10 mL). The layers were separated and the aqueous layer was extracted with CH_2Cl_2 (3 × 10 mL). The combined organic layers were washed with saturated aqueous NaCl (10 mL), dried (Na_2SO_4), filtered, and concentrated under reduced pressure. Purification by flash chromatography (10% EtOAc/hexanes) afforded the title compound (47 mg, 77%, dr = 1:1) as a colorless oil. R_f = 0.25 (10% EtOAc/hexanes); ^{1}H NMR ($CDCl_3$, 400 MHz) δ 3.90–3.80 (m, 1H), 3.31–3.22 (m, 1H), 2.92 (dd, *J* = 17.5, 5.7 Hz, 0.5H), 2.83 (t, *J* = 4.3 Hz, 1H), 2.75 (dd, *J* = 5.7, 2.3 Hz, 1H), 2.72–2.65 (m, 1H), 2.61 (dd, *J* = 17.5, 5.5 Hz, 0.5H), 2.50–2.44 (m, 1H), 1.49 (tq, *J* =

12.5, 7.0 Hz, 1H), 1.34 (tq, *J* = 14.2, 7.2 Hz, 1H), 1.06 (d, *J* = 7.0 Hz, 3H), 0.96 (t, *J* = 8.0 Hz, 9H), 0.87 (t, *J* = 7.4 Hz, 3H), 0.60 (q, *J* = 7.9 Hz, 6H); ^{13}C NMR ($CDCl_3$, 100 MHz) δ 210.8, 210.7, 75.0, 74.9, 51.7, 51.5, 47.9, 47.8, 46.79, 46.78, 46.0, 45.7, 27.4, 27.3, 11.54, 11.48, 10.00, 9.96, 6.9, 5.1; HRMS (ESI-TOF) *m/z*: $[M + Na]^+$ Calcd for $C_{15}H_{30}O_2SiNa$ 309.1856; Found 309.1858.

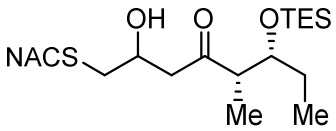

(2*RS*,5*S*,6*R*)-2-Hydroxy-5-methyl-1-[*N*-(2-acetamidoethyl)thio]-6-[(triethylsilyl)oxy]octan-4-one (2.78). To a solution of epoxide **2.77** (47 mg, 0.16 mmol, 1.0 equiv) in MeOH (3 mL) at 0 °C was added *N*-acetylcysteamine (26 μL, 0.25 mmol, 1.5 equiv) and Na_2CO_3 (19 mg, 0.18 mmol, 1.1 equiv). After stirring at 0 °C for 2 h, the reaction was quenched by the addition of saturated aqueous NH_4Cl (5 mL). The layers were separated and the aqueous layer was extracted with EtOAc (3 × 5 mL). The combined organic layers were dried (Na_2SO_4), washed with saturated aqueous NaCl (10 mL), filtered, and concentrated under reduced pressure. Purification by flash chromatography (0–5% MeOH/CH_2Cl_2) afforded the title compound (8.5 mg, 13%) as a colorless oil. R_f = 0.30 (5% MeOH/CH_2Cl_2); ^{1}H NMR ($CDCl_3$, 400 MHz) δ 6.15 (s, 1H), 4.23–4.12 (m, 1H), 3.90–3.79 (m, 1H), 3.54–3.39 (m, 3H), 2.92–2.79 (m, 1H), 2.79–2.64 (m, 5H), 2.63–2.53 (m, 1H), 1.99 (s, 3H), 1.57–1.43 (m, 1H), 1.42–1.28 (m, 1H), 1.07 (app dd, *J* = 7.0, 4.6 Hz, 3H), 0.96 (t, *J* = 7.9 Hz, 9H), 0.88 (t, *J* = 7.4 Hz, 3H), 0.61 (q, *J* = 8.0 Hz, 6H); ^{13}C NMR ($CDCl_3$, 100 MHz) δ 214.2, 213.9, 170.1, 75.04, 75.00, 67.2, 67.1, 52.0, 51.8, 47.93, 47.88, 38.8, 38.3, 38.2, 32.74, 32.72, 27.29, 27.26, 23.24, 11.5, 11.4, 10.1, 10.0, 6.9, 5.1; HRMS (ESI-TOF) *m/z*: $[M + Na]^+$ Calcd for $C_{19}H_{39}NO_4SSiNa$ 428.2261; Found 428.2274.

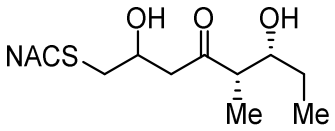

(2*RS*,5*S*,6*R*)-2,6-Dihydroxy-5-methyl-1-[*N*-(2-acetamidoethyl)thio]octan-4-one (2.28/2.30). To a solution of silyl ether **2.78** (8.5 mg, 0.021 mmol, 1.0 equiv) in THF (2 mL) at 0 °C was added a solution of 70% HF-pyridine:pyridine:THF (1:2:8, 1 mL). The reaction mixture was stirred at 0 °C for 5 h, then quenched by addition of saturated aqueous $NaHCO_3$ to adjust the mixture to pH 7. The layers were separated and the aqueous layer was extracted with *n*-butanol (3 × 10 mL). The combined organic layers were dried (Na_2SO_4), filtered, and concentrated under reduced pressure. Purification by flash chromatography (10% MeOH/CH_2Cl_2) afforded the title compound (4.8 mg, 79%) as a colorless oil. R_f = 0.38 (10% MeOH/CH_2Cl_2); ^{1}H NMR ($CDCl_3$, 400 MHz) δ 6.10 (s, 1H), 4.27–4.15 (m, 1H), 3.99–3.85 (m, 1H), 3.61–3.39 (m, 3H), 2.86–2.56 (m, 8H), 1.99 (s, 3H), 1.61–1.35 (m, 2H), 1.12 (app t, J = 7.3 Hz, 3H), 0.96 (t, J = 7.2 Hz, 3H); ^{13}C NMR ($CDCl_3$, 100 MHz) δ 215.1, 214.8, 170.4, 72.8, 72.5, 67.2, 67.0, 51.2, 50.9, 46.80, 46.77, 38.8, 38.5, 38.4, 32.60, 32.57, 27.1, 27.0, 23.3, 10.50, 10.47, 9.3, 9.1; HRMS (ESI-TOF) *m/z*: $[M + Na]^+$ Calcd for $C_{13}H_{25}NO_4SNa$ 314.1397; Found 314.1389.

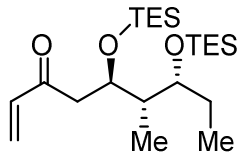

(5*R*,6*S*,7*R*)-6-Methyl-5,7-bis[(triethylsilyl)oxy]non-1-en-3-one (2.79). To a solution of tetravinyltin (41 μL, 0.22 mmol, 1.2 equiv) in THF (5 mL) at –78 °C was added MeLi (1.6 M in Et_2O, 0.46 mL, 0.74 mmol, 4.0 equiv). After stirring at –78 °C for 30 min, Weinreb amide **2.68** (83 mg, 0.19 mmol, 1.0 equiv) was added with the aid of THF (2 mL). The reaction mixture was stirred at –78 °C for 40 min, quenched by the addition of saturated aqueous NH_4Cl (10 mL), and allowed to warm up to room temperature. The layers were separated and the

aqueous layer was extracted with EtOAc (3 × 10 mL). The combined organic layers were washed with saturated aqueous NaCl (20 mL), dried (Na_2SO_4), and concentrated under reduced pressure. Purification by flash chromatography (10% EtOAc/hexanes) afforded the title compound (59 mg, 77%) as a colorless oil. R_f = 0.73 (20% EtOAc/hexanes); $[\alpha]_D^{21}$ = 34.0 (*c* 1.0, $CHCl_3$); ^{1}H NMR ($CDCl_3$, 400 MHz) δ 6.36 (dd, *J* = 17.6, 10.5 Hz, 1H), 6.20 (d, *J* = 17.6 Hz, 1H), 5.80 (d, *J* = 10.5 Hz, 1H), 4.33–4.27 (m, 1H), 3.56–3.50 (m, 1H), 2.86 (dd, *J* = 15.6, 9.3 Hz, 1H), 2.49 (dd, *J* = 15.6, 2.2 Hz, 1H), 1.82–1.72 (m, 1H), 1.58–1.47 (m, 1H), 0.97–0.83 (m, 24H), 0.57 (q, *J* = 7.8 Hz, 6H), 0.54 (q, *J* = 7.8 Hz, 6H); ^{13}C NMR ($CDCl_3$, 100 MHz) δ 200.1, 137.6, 128.0, 75.3, 71.1, 42.82, 42.77, 27.8, 9.2, 8.3, 7.0, 6.9, 5.4, 5.0; HRMS (ESI-TOF) *m/z*: $[M + Na]^+$ Calcd for $C_{22}H_{46}O_3Si_2Na$ 437.2878; Found 437.2881.

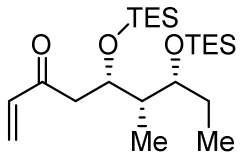

(5*S*,6*S*,7*R*)-6-Methyl-5,7-bis[(triethylsilyl)oxy]non-1-en-3-one (2.80). Identical reaction conditions for the synthesis of vinyl ketone **2.79** were used, except for the use of Weinreb amide **2.69** (62 μL, 0.34 mmol, 1.2 equiv). Purification by flash chromatography (10% EtOAc/hexanes) afforded the title compound (67 mg, 57%) as a colorless oil. R_f = 0.67 (20% EtOAc/hexanes); $[\alpha]_D^{21}$ = –37.6 (*c* 0.50, $CHCl_3$); ^{1}H NMR ($CDCl_3$, 400 MHz) δ 6.36 (dd, *J* = 17.6, 10.5 Hz, 1H), 6.20 (dd, *J* = 17.6, 1.0 Hz, 1H), 5.81 (dd, *J* = 10.5, 1.0 Hz, 1H), 4.30 (dt, *J* = 7.1, 4.7 Hz, 1H), 3.79 (q, *J* = 5.8 Hz, 1H), 2.84 (dd, *J* = 16.1, 7.2 Hz, 1H), 2.76 (dd, *J* = 16.1, 4.4 Hz, 1H), 1.69–1.60 (m, 1H), 1.59–1.49 (m, 2H), 0.96 (t, *J* = 7.9 Hz, 9H), 0.92 (t, *J* = 7.9 Hz, 9H), 0.87 (d, *J* = 7.0 Hz, 3H), 0.84 (t, *J* = 7.5 Hz, 3H), 0.60 (q, *J* = 7.8, 6H); 0.56 (q, *J* = 8.0, 6H); ^{13}C NMR ($CDCl_3$, 100 MHz) δ 200.0, 137.5, 128.0,

73.3, 70.2, 45.1, 41.9, 27.5, 10.0, 9.5, 7.02, 6.95, 5.5, 5.1; HRMS (ESI-TOF) *m/z*: [M + Na]$^+$ Calcd for $C_{22}H_{46}O_3Si_2Na$ 437.2878; Found 437.2881.

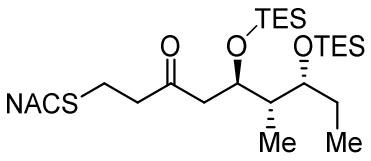

(5*R*,6*R*,7*R*)-6-Methyl-1-[*N*-(2-acetamidoethyl)thio]-5,7-bis[(triethylsilyl)oxy]nonan-3-one (2.81). To a solution of vinyl ketone **2.79** (58 mg, 0.14 mmol, 1.0 equiv) in THF (10 mL) was added *N*-acetylcysteamine (22 μL, 0.21 mmol, 1.5 equiv) and a catalytic amount of Cs_2CO_3. The reaction was stirred at room temperature for 2 h, then quenched by the addition of saturated aqueous NH_4Cl (10 mL). The layers were separated and the aqueous layer was extracted with EtOAc (3 × 10 mL). The combined organic layers were washed with saturated aqueous NaCl (40 mL), dried (Na_2SO_4), filtered, and concentrated under reduced pressure. Purification by flash chromatography (5% MeOH/CH_2Cl_2) afforded the title compound (70 mg, 93%) as a colorless oil. R_f = 0.33 (5% MeOH/CH_2Cl_2); $[\alpha]_D^{21}$ = 29.6 (*c* 0.50, $CHCl_3$); ^{1}H NMR ($CDCl_3$, 400 MHz) δ 6.12 (s, 1H), 4.31–4.20 (m, 1H), 3.55–3.48 (m, 1H), 3.48–3.41 (m, 2H), 2.81–2.68 (m, 4H), 2.68–2.56 (m, 3H), 2.40 (dd, *J* = 15.5, 2.1 Hz, 1H), 2.00 (s, 3H), 1.73 (dq, *J* = 12.5, 7.1 Hz, 1H), 1.57–1.42 (m, 2H), 0.93 (t, *J* = 8.0 Hz, 9H), 0.90 (t, *J* = 8.0 Hz, 9H), 0.87 (d, *J* = 6.9 Hz, 3H), 0.84 (t, *J* = 7.4 Hz, 3H), 0.56 (app p, *J* = 8.0 Hz, 12H); ^{13}C NMR ($CDCl_3$, 100 MHz) δ 208.3, 170.1, 75.2, 71.3, 46.1, 44.4, 42.5, 38.4, 32.3, 27.7, 25.0, 23.2, 9.2, 8.0, 7.0, 6.9, 5.4, 5.0; HRMS (ESI-TOF) *m/z*: [M + Na]$^+$ Calcd for $C_{27}H_{57}NO_3SSi_2Na$ 556.3283; Found 556.3291.

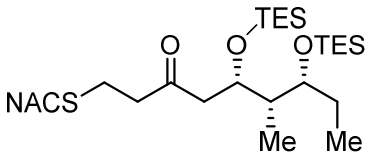

(5*S*,6*R*,7*R*)-6-Methyl-1-[*N*-(2-acetamidoethyl)thio]-5,7-bis[(triethylsilyl)oxy]nonan-3-one (2.82). Identical reaction conditions used for the synthesis of thioether **2.81** were used, except for the use of vinyl ketone **2.80** (66 mg, 0.16 mmol, 1.0 equiv). Purification by flash chromatography (5% MeOH/CH_2Cl_2) afforded the title compound (78 mg, 92%) as a colorless oil. R_f = 0.28 (5% MeOH/CH_2Cl_2); $[\alpha]_D^{21}$ = –22.5 (*c* 0.4, $CHCl_3$); ^{1}H NMR ($CDCl_3$, 400 MHz) δ 6.08 (s, 1H), 4.22 (q, *J* = 5.5 Hz, 1H), 3.83–3.77 (m, 1H), 3.45 (q, *J* = 6.0 Hz, 2H), 2.79–2.61 (m, 8H), 2.00 (s, 3H), 1.66–1.57 (m, 1H), 1.56–1.48 (m, 2H), 0.94 (app dt, *J* = 14.5, 7.9 Hz, 18H), 0.84 (d, *J* = 7.7 Hz, 3H), 0.83 (t, *J* = 7.7 Hz, 3H), 0.57 (app dq, *J* = 12.7, 7.9 Hz, 12H); ^{13}C NMR ($CDCl_3$, 100 MHz) δ 208.1, 170.1, 73.0, 70.2, 48.1, 44.2, 41.5, 38.3, 32.3, 27.7, 25.0, 23.3, 9.9, 9.6, 7.02, 6.96, 5.5, 5.1; HRMS (ESI-TOF) *m/z*: [M + Na]$^+$ Calcd for $C_{27}H_{57}NO_3SSi_2Na$ 556.3283; Found 556.3289.

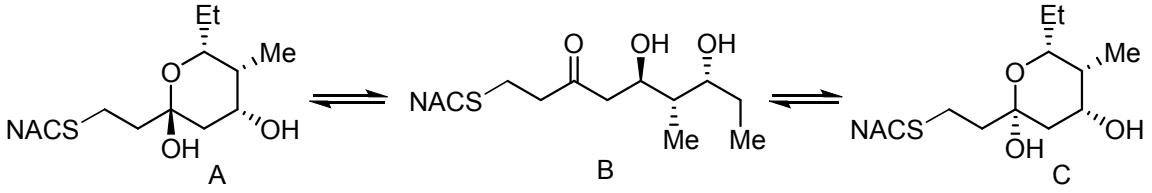

(5*R*,6*R*,7*R*)-5,7-Dihydroxy-6-methyl-1-[*N*-(2-acetamidoethyl)thio]nonan-3-one (2.25). To a solution of silyl ether **2.81** (59 mg, 0.11 mmol, 1.0 equiv) in THF (10 mL) at 0 °C was added a solution of 70% HF-pyridine:pyridine:THF (1:2:8, 4 mL). The reaction was stirred at 0 °C for 6 h, then quenched by the addition of saturated aqueous $NaHCO_3$ to bring the reaction to pH 7, and extracted with EtOAc (3 × 20 mL). The combined organic layers were washed with saturated aqueous NaCl (40 mL), dried (Na_2SO_4), filtered, and

concentrated under reduced pressure. Purification by flash chromatography (10% MeOH/EtOAc) afforded the title compound (16 mg, 47%) as a colorless oil. R_f = 0.26 (10% MeOH/EtOAc); Due to the instability of the compound the optical rotation could not be obtained; ^{1}H NMR ($CDCl_3$, 400 MHz, approximately 6:6:1 mixture of A:B:C where the integrations have been normalized) δ 6.61 (s, 0.08H), 6.08 (s, 0.46H), 5.98 (s, 0.46H), 4.20 (dt, *J* = 11.9, 4.8 Hz, 0.46H), 4.17–4.08 (m, 0.46H), 4.07–4.03 (m, 0.08H), 3.85–3.77 (m, 1H), 3.75–3.69 (m, 0.16H), 3.53–3.34 (m, 1.84H), 3.22–3.13 (m, 0.32H), 2.86–2.58 (m, 5.52H), 1.99 (app d, *J* = 2.0 Hz, 3H), 1.95–1.84 (m, 1.38H), 1.81 (dd, *J* =4.8, 12.5 Hz, 0.46H), 1.65–1.34 (m, 3H), 1.09 (d, *J* = 7.2 Hz, 0.24H), 1.05 (t, *J* = 7.3 Hz, 0.24H), 0.98–0.87 (m, 4.14H), 0.80 (d, *J* = 6.9 Hz, 1.38H); ^{13}C NMR ($CDCl_3$, 100 MHz, major isomers A and B) δ 209.9, 170.4, 170.3, 97.5, 73.8, 72.9, 71.7, 67.6, 48.1, 43.4, 41.4, 41.3, 38.6, 38.3, 37.3, 37.2, 31.9, 31.5, 26.7, 25.2, 25.1, 25.0, 23.3, 23.2, 10.9, 10.8, 10.4, 3.6; HRMS (ESI-TOF) *m/z*: $[M + Na]^+$ Calcd for $C_{14}H_{27}NO_4SNa$ 328.1553; Found 328.1561.

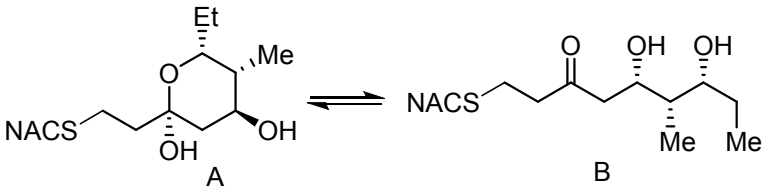

(5*S*,6*R*,7*R*)-5,7-Dihydroxy-6-methyl-1-[*N*-(2-acetamidoethyl)thio]nona n-3-one (2.27). Identical reaction conditions for the synthesis of diol **2.25** were used, except for the use of silyl ether **2.82** (76 mg, 0.14 mmol, 1.0 equiv). Purification by flash chromatography (5% MeOH/CH_2Cl_2) afforded the title compound (37 mg, 86%) as a colorless oil. R_f = 0.42 (10% MeOH/EtOAc); Due to the instability of the compound the

optical rotation could not be obtained; ^{1}H NMR ($CDCl_3$, 400 MHz, 4:1 mixture of hemiketal A:ketone B where the integrations have been normalized) δ 5.92 (s, 1H), 4.67 (s, 0.8H), 4.34 (d, *J* = 9.5 Hz, 0.2H), 4.18–4.07 (m, 0.8H), 3.98–3.88 (m, 0.8H), 3.83–3.76 (m, 0.2H), 3.56 (s, 0.2H), 3.52–3.37 (m, 2H), 3.32 (d, *J* = 6.0 Hz, 0.8H), 2.84 (s, 0.2H), 2.80–2.59 (m, 4.6H), 2.52 (dd, *J* = 16.9, 2.8 Hz, 0.2H), 1.99 (s, 3H), 1.91–1.83 (m, 1.6H), 1.82–1.66 (m, 2.6H), 1.62–1.47 (m, 1H), 1.47–1.32 (m, 1H), 0.97–0.89 (m, 3.5H), 0.84 (d, *J* = 7.1 Hz, 2.5H); ^{13}C NMR ($CDCl_3$, 100 MHz, hemiketal form A) δ 170.2, 97.3, 71.5, 67.6, 41.5, 38.2, 37.0, 34.2, 31.5, 25.1, 24.8, 23.3, 10.4, 10.2; HRMS (ESI-TOF) *m/z*: $[M + Na]^+$ Calcd for $C_{14}H_{27}NO_4SNa$ 328.1553; Found 328.1554.

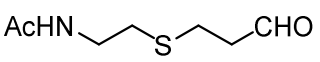

***N*-{2-[(3-Oxopropyl)thio]ethyl}acetamide (2.84).** To a solution of *N*-acetylcystamine (0.11 mL, 1.0 mmol, 1.0 equiv) in CH_2Cl_2 (10 mL) at 0 °C was added Et_3N (28 μL, 0.20 mmol, 0.20 equiv), followed by the addition of acrolein (67 μL, 1.0 mmol, 1.0 equiv). After stirring at 0 °C for 1 h, the reaction was quenched by the addition of saturated aqueous NH_4Cl (5 mL). The layers were separated and the aqueous layer was extracted with CH_2Cl_2 (3 × 10 mL). The combined organic layers were washed with saturated aqueous NaCl (20 mL), dried (Na_2SO_4), filtered, and concentrated under reduced pressure. Purification by flash chromatography (5% MeOH/CH_2Cl_2) afforded the title compound (149 mg, 85%) as colorless oil. R_f = 0.24 (5% MeOH/CH_2Cl_2); ^{1}H NMR ($CDCl_3$, 400 MHz) δ 9.78 (s, 1H), 6.06 (s, 1H), 3.46 (q, *J* = 6.1 Hz, 2H), 2.86–2.74 (m, 4H), 2.69 (t, *J* = 6.4 Hz, 2H), 2.01 (s, 3H); ^{13}C NMR ($CDCl_3$, 100 MHz) δ 200.2, 43.5, 38.4, 32.0, 23.8, 23.2; HRMS (ESI-TOF) *m/z*: $[M + Na]^+$ Calcd for $C_7H_{13}NO_2SNa$ 198.0559; Found 198.0556.

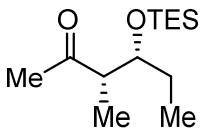

(3*S*,4*R*)-3-Methyl-4-[(triethylsilyl)oxy]hexan-2-one (2.83). To a solution of Weinreb amide **2.75** (404 mg, 1.40 mmol, 1.00 equiv) in THF (20 mL) at 0 °C was added methylmagnesium bromide (3.0 M in Et_2O, 1.86 mL, 5.58 mmol, 4.00 equiv) dropwise. The reaction was stirred at 0 °C for 5 h, then quenched by the addition of saturated aqueous NH_4Cl (20 mL). The layers were separated and the aqueous layer was extracted with EtOAc (3 × 20 mL). The combined organic layers were washed with saturated aqueous NaCl (30 mL), dried (Na_2SO_4), filtered, and concentrated under reduced pressure. Purification by flash chromatography (20% EtOAc/hexanes) afforded the title compound (340 mg, 100%) as a colorless oil. R_f = 0.57 (20% EtOAc/hexanes); $[\alpha]_D^{22}$ = 39.2 (*c* 1.0, $CHCl_3$); ^{1}H NMR ($CDCl_3$, 400 MHz) δ 3.88 (q, *J* = 5.7 Hz, 1H), 2.68–2.57 (m, 1H), 2.18 (s, 3H), 1.53–1.44 (m, 1H), 1.43–1.34 (m, 1H), 1.07 (d, *J* = 7.0 Hz, 3H), 0.96 (t, *J* = 7.9 Hz, 9H), 0.87 (t, *J* = 7.4 Hz, 3H), 0.60 (q, *J* = 8.0 Hz, 6H); ^{13}C NMR ($CDCl_3$, 100 MHz) δ 211.8, 74.8, 51.7, 29.9, 27.5, 11.5, 9.9, 6.9, 5.1; HRMS (ESI-TOF) *m/z*: $[M + Na]^+$ Calcd for $C_{13}H_{28}O_2SiNa$ 267.1751; Found 267.1759.

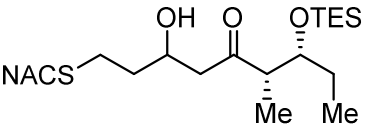

(3*RS*,6*S*,7*R*)-3-Hydroxy-6-methyl-1-[*N*-(2-acetamidoethyl)thio]-7-[(triethylsilyl)oxy]nonan-5-one (2.85). To a solution of distilled *i*-Pr_2NH (0.19 mL, 1.4 mmol, 2.2 equiv) in THF (10 mL) at –78 °C was added *n*-BuLi (1.8 M in THF, 0.78 mL, 1.4 mmol, 2.2 equiv), followed by stirring at –78 °C for 30 min to prepare the LDA solution. To the LDA solution at –78 °C was added methyl ketone **2.83** (316 mg, 1.29 mmol, 2.10 equiv). After stirring at –78 °C for 30 min, aldehyde **2.84** (108 mg, 0.616 mmol, 1.00 equiv) was added with the aid of THF (3 × 0.5 mL), the reaction was stirred at –78 °C for an additional 3 h. The reaction

was quenched by the addition of saturated aqueous NH_4Cl (15 mL) and allowed to warm to room temperature. The layers were separated and the aqueous layer was extracted with EtOAc (3 × 20 mL). The combined organic layers were dried (Na_2SO_4), filtered, and concentrated under reduced pressure. Purification by flash chromatography (5% MeOH/CH_2Cl_2) afforded the title compound (118 mg, 46%, dr = 2:1) as a colorless oil. R_f = 0.31 (5% MeOH/CH_2Cl_2); ^{1}H NMR ($CDCl_3$, 400 MHz) δ 5.97 (s, 1H), 4.22–4.09 (m, 1H), 3.89–3.78 (m, 1H), 3.51–3.39 (m, 2H), 3.36 (d, *J* = 3.2 Hz, 1H), 2.84–2.59 (m, 6.66H), 2.52 (dd, *J* = 18.0, 9.1 Hz, 0.34H), 1.99 (s, 3H), 1.80–1.70 (m, 1H), 1.68–1.58 (m, 1H), 1.55–1.43 (m, 1H), 1.42–1.29 (m, 1H), 1.06 (d, *J* = 6.7, 2H), 1.04 (d, *J* = 7.0, 1H), 0.95 (t, *J* = 7.9 Hz, 9H), 0.87 (t, *J* = 7.4 Hz, 3H), 0.60 (q, *J* = 8.0 Hz, 6H); ^{13}C NMR ($CDCl_3$, 100 MHz) δ 214.9 (major), 214.6 (minor), 170.1, 75.0, 66.2 (major), 66.1 (minor), 51.9 (minor), 51.7 (major), 49.1 (minor), 49.0 (major), 38.4, 36.0, 31.9, 27.7, 27.3, 23.3, 11.6 (minor), 11.4 (major), 10.1 (minor), 10.0 (major), 6.9, 5.1; HRMS (ESI-TOF) *m/z*: $[M + Na]^+$ Calcd for $C_{20}H_{41}NO_4SSiNa$ 442.2418; Found 442.2425.

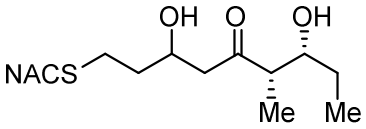

(3*RS*,6*S*,7*R*)-3,7-Dihydroxy-6-methyl-1-[*N*-(2-acetamidoethyl)thio]nonan-5-one (2.29/2.31). To a solution of silyl ether **2.85** (51 mg, 0.12 mmol, 1.0 equiv) in THF (6 mL) at 0 °C was added a solution of 70% HF-pyridine:pyridine:THF (1:2:8, 3 mL). The reaction was stirred at 0 °C for 12 h, then quenched by the addition of saturated aqueous $NaHCO_3$ to adjust the reaction to pH 7. The layers were separated and the aqueous layer was extracted with EtOAc (3 × 10 mL) and *n*-butanol (3 × 10 mL). The combined organic layers were dried (Na_2SO_4), filtered, and concentrated under reduced pressure.

Purification by flash chromatography (5% MeOH/CH_2Cl_2) afforded the title compound (32 mg, 86%) as a colorless oil. R_f = 0.11 (5% MeOH/CH_2Cl_2); ^{1}H NMR ($CDCl_3$, 400 MHz) δ 6.22 (s, 1H), 4.24–4.14 (m, 1H), 3.90 (dt, *J* = 8.1, 4.6 Hz, 0.67H), 3.84 (dt, *J* = 8.1, 4.5 Hz, 0.33H), 3.50–3.34 (m, 2H), 3.10 (s, 2H), 2.78–2.53 (m, 7H), 1.98 (s, 3H), 1.82–1.71 (m, 1H), 1.71–1.61 (m, 1H), 1.55–1.45 (m, 1H), 1.45–1.34 (m, 1H), 1.10 (d, *J* = 8.0 Hz, 1H), 1.08 (d, *J* = 7.3 Hz, 2H), 0.94 (t, *J* = 7.4 Hz, 3H); ^{13}C NMR ($CDCl_3$, 100 MHz) δ 215.7 (minor), 215.3 (major), 170.6, 72.8 (minor), 72.5 (major), 66.5 (major), 66.2 (minor), 51.1 (major), 50.8 (minor), 48.1 (minor), 48.0 (major), 38.5, 36.1 (major), 36.0 (minor), 31.7, 27.6, 27.04 (minor), 27.00 (major), 23.1, 10.47 (major), 10.45 (minor), 9.3 (minor), 9.1 (major); HRMS (ESI-TOF) *m/z*: $[M + Na]^+$ Calcd for $C_{14}H_{27}NO_4SNa$ 328.1553; Found 328.1559.

2.8. Experimental section of biology

General biology procedures. All chemical reagents were purchased from Sigma-Aldrich and were used directly without further purification. *E. coli* BL21(DE3) cells were from New England BioLabs. IPTG was acquired through Gold Biotechnology. His60 Ni Superflow resin was purchased from Clontech Laboratories, Inc. OD_{600} were measured on an Eppendorf BioPhotometer. Gel filtration purification was performed on HiLoad 16/600 Superdex 75 pg column (GE). The protein mass spectra data was obtained by QSTAR XL (AB Sciex) mass spectrometer. NADPH consumption was detected by SpectraMax M5e (Molecular Devices) microplate reader. LC–MS/MS was conducted with AB Sciex QTRAP 5500 mass spectrometer and Shimadzu LC system.

Cloning. The PikKR2 domain was cloned from the cosmid pLZ51 using ligation independent cloning (LIC)-compatible forward: 5'-**TACTTCCAATCCAATGCC**AGCCGCGTCGGCGGG-3'; and reverse: 5'-**TTATCCACTTCCAATGCTA**CGGCCGGGCCCGG-3' primers (LIC-overhangs shown in **bold**; inserted stop codon underlined). The resulting insert was cloned into pMCSG7 vector using a LIC-qualified T4 DNA polymerase (Novagen). The resulting LIC-cloning reaction was directly transform into a chemically competent *E. coli* cell line (XL1Blue). The PikKR2-containing plasmid was isolated from a single colony grown overnight.

Protein expression and purification. Competent *E. coli* BL21 (DE3) cells were transformed with pMCSG7. The cells were grown in Terrific Broth (TB) media with 100 μg/mL ampicillin at 37 °C to an OD_{600} of 1.6. The cultures were cooled to 20 °C and 200 μM IPTG was added to induce protein expression. After overnight expression, cells were harvested by centrifugation at 6000*g* and 4 °C for 10 min, and the resulting cell pellet was frozen (–80 °C, 10 min). The frozen pellet was resuspended in lysis buffer (50 mM HEPES, 300 mM NaCl, 10 mM imidazole, pH 8) and lysed by sonication. The lysate was clarified by centrifuging at 50000*g* and 4 °C for 10 min. The cleared lysate was incubated with His-60 Ni superflow resin (2 mL) at 4 °C for 1 h and then loaded onto a gravity column. The column was washed with 14 mL of wash buffer (10 mM imidazole, 50 mM HEPES, 300 mM NaCl, pH 8.0) and eluted with 2.5 mL elution buffer (500 mM imidazole, 50 mM HEPES, 300 mM NaCl, pH 8.0). The protein was further purified via size exclusion chromatography on a Superdex 200 gel filtration column eluting at 0.5 mL

min^{-1} with 50 mM sodium phosphate (pH 7.1) and 150 mM NaCl. Purified PikKR2 was pooled and concentrated to afford 45 mg of purified enzyme per liter of culture that was greater than 95% pure as judged by SDS-PAGE. For long-term storage, the protein was transferred to storage buffer (20 mM Tris, 150 mM NaCl, 10% (v/v) glycerol, pH 7.5). The enzyme was stored at –80 °C and was stable for at least 6 months. The protein concentration was determined using the Bio-Rad protein assay kit, with bovine serum albumin as the standard. The native molecular weight and oligomeric state was estimated using gel filtration on a column calibrated with Gel Filtration Calibration Kit LMW (GE Healthcare) molecular-weight markers. Exact molecular weight of the purified monomeric protein was measured by ESI mass spectrometry.

Kinetic assay and analysis of PikKR2 reaction products by LC-MS/MS. Substrates **2.18** and **2.19** (1 mM) were incubated with PikKR2 (5 μM), NADPH (2 mM) and sodium phosphate buffer (100 mM, pH 7.2) in a total volume of 100 μL at 25 °C for 12 h. The reaction was quenched with 100 μL MeCN. Following centrifugation, the supernatant was diluted to 100-fold in 1:1 MeCN–100 mM sodium phosphate buffer and analyzed by LC-MS/MS employing a Kinetix reverse-phase C_{18} column (50 mm × 2.1 mm, 2.6 μm, Phenomenex) operated at 0.4 mL min^{-1} with a gradient between mobile phase A (15 mM ammonium acetate in H_2O) and mobile phase B (MeCN or MeOH). For optimal resolution, MeCN was chosen as the mobile phase B for 1-carbon-linker mimics **2.24**, **2.26** and **2.28**/**2.30** while MeOH gave better separation for 2-carbon-linker mimics **2.25**, **2.27** and **2.29**/**2.31**. The gradient program was 0 min, 5% B; 2 min, 5% B; 7 min, 55% B;

8 min, 95% B; 9 min, 95% B; 9.5 min, 5% B, 12 min, 5% B. Retention times were obtained and compared to that of synthetic standards.

In order to carry out kinetic analysis, the enzymatic reactions were carried out in a total volume of 20 μL under initial velocity conditions containing PikKR2 (5 μM), NADPH (0.5 mM), sodium phosphate buffer (100 mM, pH 7.2) and substrates at variable concentrations (0–8 mM). Each reaction was incubated 25 °C for 12 min then quenched by addition of 20 μL MeCN containing an internal standard. Following centrifugation, the supernatant was diluted to 10-fold in precipitated 1:1 MeCN–sodium phosphate reaction buffer and quantified by LC-MS/MS system as described above. Synthetic standards were diluted in reaction buffer and processed as previously mentioned. Standards at varying concentrations were injected with a fixed concentration of an internal standard to generate the standard curves. For the observed product **2.26**, compound **2.25** was used as the internal standard. For the observed product **2.27**, compound **2.24** was used as the internal standard (The calibration curves are shown in the Appendix). The amount of enzymatic products was calculated by plotting the area ratio into the standard curve and converted to initial velocity. The apparent steady-state kinetic parameters were determined as described for the NADPH consumption kinetic assay.

NADPH consumption kinetic assay. PikKR2 activity was measured spectrophotometrically under initial velocity conditions via detection of NADPH consumption at 340 nm (λ_{340} = 6220 M^{-1} cm^{-1}). Each reaction contained PikKR2 (5 μM), NADPH (0.5 mM), sodium phosphate buffer (100 mM, pH 7.2) and substrates (**2.86** and **2.87**) at variable concentrations (0–40 mM) in a total volume of 100 μL. Substrates were

dissolved in DMSO and the final concentration of DMSO was kept constant at 5% (v/v). The enzyme was incubated with NADPH at 25 °C for 15 min before the addition of substrates. The UV absorbance at 340 nm was monitored for 5 min at 15 s intervals. Kinetic parameters for NADPH were determined in a similar manner by pre-incubation with substrate **2.86** (40 mM), followed by addition of various NADPH concentrations (0–500 μM). Each reaction was performed in triplicate. Apparent steady-state kinetic parameters were determined by fitting the normalized v_0 vs [*S*] plots to the Michaelis–Menten equation by nonlinear regression analysis using GraphPad Prism 5.0.

PikKR2 products isolation and seperation by chiral HPLC. Substrates **2.86** (5 mM) was incubated with PikKR2 (25 μM), NADPH (10 mM) and sodium phosphate buffer (100 mM, pH 7.2) in a total volume of 500 μL at 25 °C for 12 h. The reaction was extracted with 5 × 500 μL EtOAc and then concentrated. The extract was dissolved in EtOH (500 μL) and injected to normal-phase HPLC using a ChiralCel OD column (250 × 4.6 mm). An isocratic elution (6: 94 EtOH: hexanes) at a flow rate of 0.8 mL min^{-1} with monitoring at 235 nm was used to afford separation of the enantiomers.

Product inhibition. Product **2.27** (0–0.5 mM) was preincubated with PikKR2 (5 μM) in the reaction buffer described before for 10 min. Cofactor NADPH (2 mM) and substrates **2.19** (1 mM) were added and incubated at 25 °C for 12 h. The reaction mixture was quenched, diluted and analyzed by LC-MS/MS as described before. The amount of enzymatic product formation was calculated by subtracting the amount of the preincubated product.

Chapter 3. Functional characterization of dehydratase (DH)[1]

3.1. Background on DHs

Many polyketides such as the archetypical macrolide antibiotic pikromycin (**3.1**), the antifungal polyene amphotericin B (**3.2**), the linear polyketide discodermolide (**3.3**), and the mixed nonribosomal peptide-polyketide curacin A (**3.4**), contain one or more double bonds that serve as conformational constraints and are essential for biological activity (Figure 19). For instance, the natural products' activities decreased at least 10-fold when the olefin was reduced or the geometry was changed from *cis*- to *trans*-configuration in SAR studies.[126, 127]

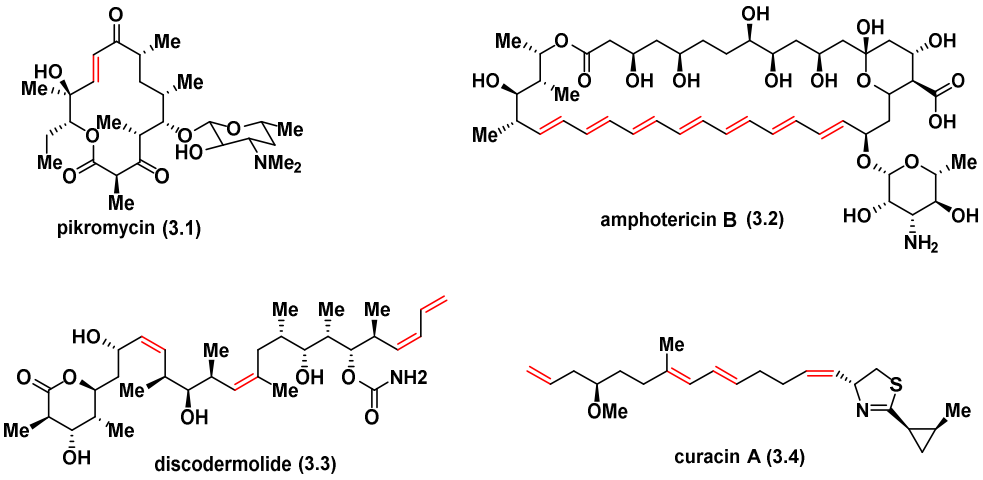

Figure 19. Structures of pikromycin (**3.1**), amphotericin B (**3.2**), discodermolide (**3.3**) and curacin A (**3.4**).

---

[1] Reproduced in part with permission from Li, Y.; Dodge, G. J.; Fiers, W. D.; Fecik, R. A.; Smith, J. L.; Aldrich, C. C. Functional Characterization of a Dehydratase Domain from the Pikromycin Polyketide Synthase. *J. Am. Chem. Soc.* **2015**, 137, 7003–7006. Copyright 2015 American Chemical Society.

The double bonds are formed by DH domains through abstraction of the α-proton and concomitant protonation of the β-hydroxyl group of the nascent β-hydroxyacyl-ACP polyketide intermediate, resulting in loss of one water molecule. As observed in FAS DHs, the characteristic double hotdog fold is also found in PKS DHs to form the active site with two catalytic residues, aspartic acid and histidine.[128-132] The olefin geometry of DH products cannot be predicted through a signature fingerprint as in the KRs since the active site residues appear quite similar in both *cis*- and *trans*-olefin generating DHs.[10, 131] Initial evidence suggested the geometry of a double bond was exclusively dependent on the stereochemistry of the DH substrate, provided by the upstream KR module wherein A-type KR products (L-alcohols) lead to *cis*-double bonds while *trans*-olefins arise from B-type KR products (D-alcohols);[133] although exceptions have recently been observed.[132, 134, 135] To date, no *trans*-olefin has been produced *in vitro* via incubation of a DH domain and its corresponding substrate, leading to the hypothesis that some isomerase may contribute to further obscuring the original olefin geometry.

Steady-state kinetic analysis using simple diffusible NAC thioester precursors, successfully employed to interrogate the substrate specificity of other PKS domains and modules,[101, 105, 136-139] has thus far been ineffective for studying isolated DH domains. This is likely due to the extremely low activity of the excised DH domains, which necessitates overnight incubations to generate sufficient product for detection. Moreover, the simple nature and ready reversibility of the dehydration reaction cannot be easily monitored by conventional radio-TLC or spectrophotometric assays. Cane and co-workers have also shown, at least in one example, that a NAC thioester substrate was not

properly delivered to a DH active site resulting in reversal of diastereospecificity.[132] This result highlights the potential importance of the ACP for chaperoning the polyketide intermediate for proper recognition and processing by DHs. Despite these aforementioned challenges, significant progress has been made in PKS functional characterization using NAC and ACP-bound substrates, which has provided useful insight into the substrate specificity and compelling evidence that (*E*)-unsaturated polyketide intermediates involve a stereospecific *syn*-elimination.[104, 132, 134, 135, 140, 141] To further advance our understanding of DH domains, we report herein the first detailed steady-state kinetic characterization of an individual DH domain through monitoring reaction progress by liquid chromatography-tandem mass spectrometry (LC-MS/MS). The substrate specificity was studied with a systematic series of synthetic triketide analogs to probe the impact of both vicinal and distal stereochemistry and through mutagenesis of active-site residues. The ability to monitor reaction progress also permitted the study of pH dependence on catalytic activity and kinetic characterization of a mechanism-based irreversible inhibitor designed to facilitate co-crystallization and elucidation of substrate-protein interactions.

3.2. Chemoenzymatic synthesis and olefin geometry

The pikromycin biosynthetic pathway is one of the most well-explored type I PKSs and has served as a model system for fundamental investigations of PKS catalysis.[11-14, 101, 138, 139] We selected the DH domain from pikromycin PKS module 2 (PikDH2) for our studies since it is responsible for the *trans*-olefin in pikromycin (Figure 19) and Cane *et al*. revealed that the cryptic β-hydroxy stereochemistry of the triketide substrate possesses

the D-configuration.[101, 142, 143] We predicted a larger, multi-domain portion of the PKS would create a more native context for *in vitro* analysis.[142] The region of *pikAI* encoding the PikKR2-DH2 didomain comprising residues 3579–4365 was cloned into a pMCSG7 expression vector and the resulting protein was overexpressed and purified using standard methods (Supporting Information). Substrate mimics **2.26** and **2.27**, PikKR2 products, for PikDH2 are based on its natural substrate (Figure 20).[142] While maintaining the same stereochemistry on the triketide moiety, they possess two major modifications compared to the natural substrate including replacement of the ACP-phosphopantetheinyl arm with *N*-acetylcysteamine (NAC) and insertion of one or two methylene spacers between the carbonyl and sulfur atom to avoid undesired, intramolecular lactonization. These two modifications were tolerated by PikKR2, instilling confidence that the downstream DH would accept these substrates.[142]

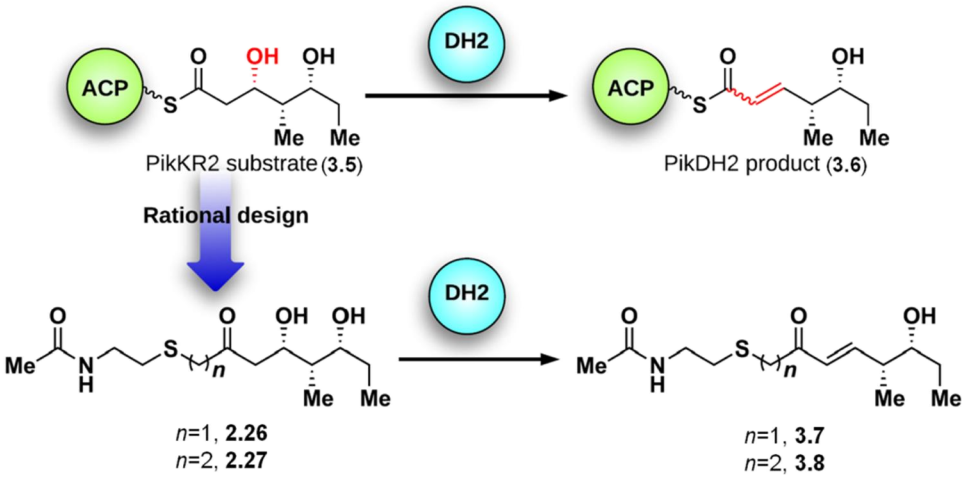

Figure 20. Rational design of PikDH2 substrate mimics **2.26**, **2.27** and their enzymatic products **3.7**, **3.8**.

Overnight incubation of substrates **2.26** and **2.27** with PikKR2-DH2 didomain in relatively large scale generated the corresponding enzymatic products **3.7** and **3.8**, respectively, in slightly more than 50% isolated yield. The structures of **2.26** and **2.27** were unambiguously confirmed by NMR spectroscopy and exhibited diagnostic ^{13}C chemical shifts at 150 and 130 ppm and a $^{3}J_{HH}$ coupling of 16 Hz for the vinyl protons. These results are consistent with the empirical rule that D-alcohols provide *trans*-olefins.

Additionally, we investigated the reason for incomplete reaction. Since most FAS DHs conduct the reverse hydration reactions, enones **3.7** and **3.8** were incubated with PikKR2-DH2 to test the reversibility of the enzymatic reaction. We observed PikKR2-DH2 stereoselectively converted **3.7** and **3.8** exclusively to their hydrated products **2.26** and **2.27**, respectively, whose identities were confirmed by LC-MS/MS with authentic synthetic standards (Figure 21–22). When equilibrium was reached, the ratio of **2.26** to **3.7** was 1:1.2 and the ratio of **2.27** to **3.8** was 1:2, slightly favoring the dehydration products in both cases. In the biosynthetic pathway, this equilibrium is pushed towards dehydration, driven by downstream module activities.

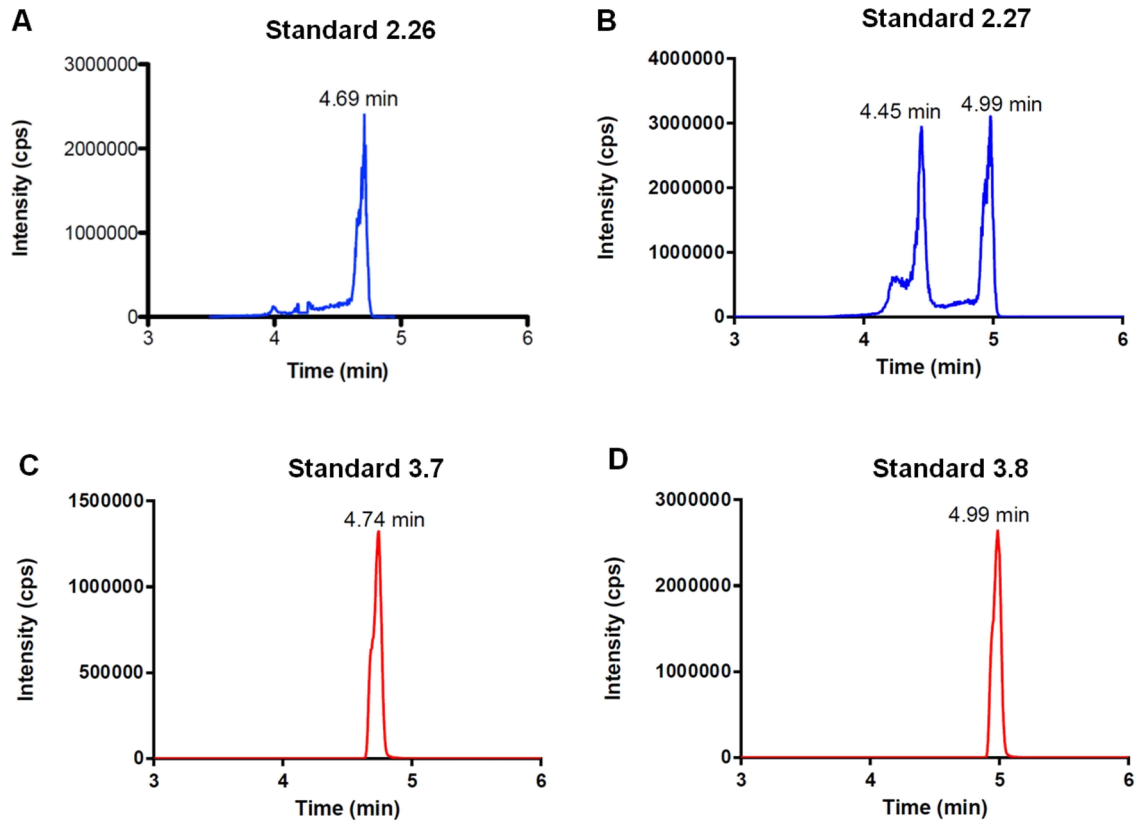

Figure 21. LC-MS/MS analysis of standards. (A) **2.26** (MRM *m*/*z* 314→198); (B) **2.27** (MRM *m*/*z* 328→212); (C) **3.7** (MRM *m*/*z* 274→216); (D) **3.8** (MRM *m*/*z* 288→120).

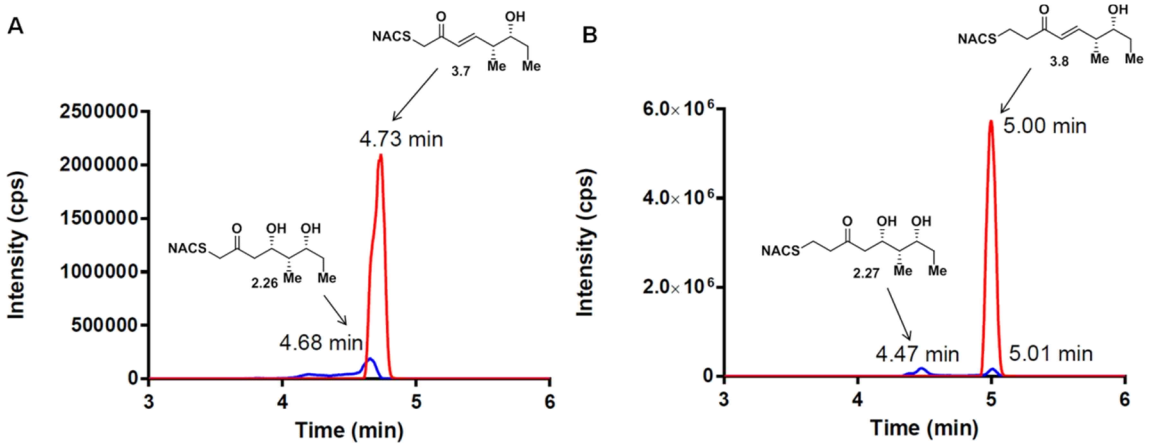

Figure 22. LC-MS/MS traces for hydration reactions of substrate **3.7** (A) and substrate **3.8** (B) by PikKR2-DH2.

3.3. Synthesis of substrate surrogates

To interrogate the stereospecificity of PikDH2, we altered the β-stereocenter of substrates **2.26** and **2.27** as well as every stereogenic center in **2.27** through chemical synthesis resulting in substrate stereoisomers **2.24**, **2.25** (obtained in Chapter 2) and **3.9**–**3.11**.[142] Moreover, racemic diketide **3.12,** similar to widely used diketide substrates to study other DHs,[132, 134] was also synthesized to verify the impact of the distal segment. Anti-aldol product (–)-**3.13**, synthesized using Masamune's chiral auxalliary,[144, 145] was submitted to an acetate aldol reaction with thiazolidinethione **3.14**[114, 115] to yield alcohol **3.15** as the major diastereomer (Scheme 18A). The thiazolidinethione was displaced with *N*,*O*-dimethylhydroxylamine to afford Weinreb amide **3.16**. The TBS protecting group stable in the previous aldol reaction was ultimately problematic in the final deprotection and was therefore replaced with a TES protecting group to facilitate its later removal. This was accomplished by treatment of **3.16** with TBAF to furnish **3.17** and subsequent silylation with TESOTf provided **3.18**. Grignard reaction and Michael addition furnished the NAC-analog **3.20**. A final deprotection under mild conditions furnished the substrate analog **3.9**. Substrate analog **3.10** was also synthesized in an analogous way by using aldehyde (+)-**3.13**. The synthetic route for **3.11** commenced with the acetate aldol reaction of aldehyde **3.21**[142] and *N*-methoxy-*N*-methylacetamide to give Weinreb amide **3.22** as the major diastereomer (dr = 2:1, separated by chromatography) (Scheme 18C). TES protection provided **3.23** that was converted to vinyl ketone **3.24** through Grignard addition of vinylmagnesium bromide. Sequential Michael addition of *N*-acetylcysteamine and silyl deprotection provided substrate analog **3.11.** For the synthesis of substrate

analog (±)-**3.12**, thiazolidinethione **3.26**[142, 146] was subjected to an acetate aldol reaction with propionaldehyde to provide a racemic mixture of **3.27**, followed by displacement with *N*-acetylcysteamine to afford NAC thioester (±)–**3.12** (Scheme 18D).

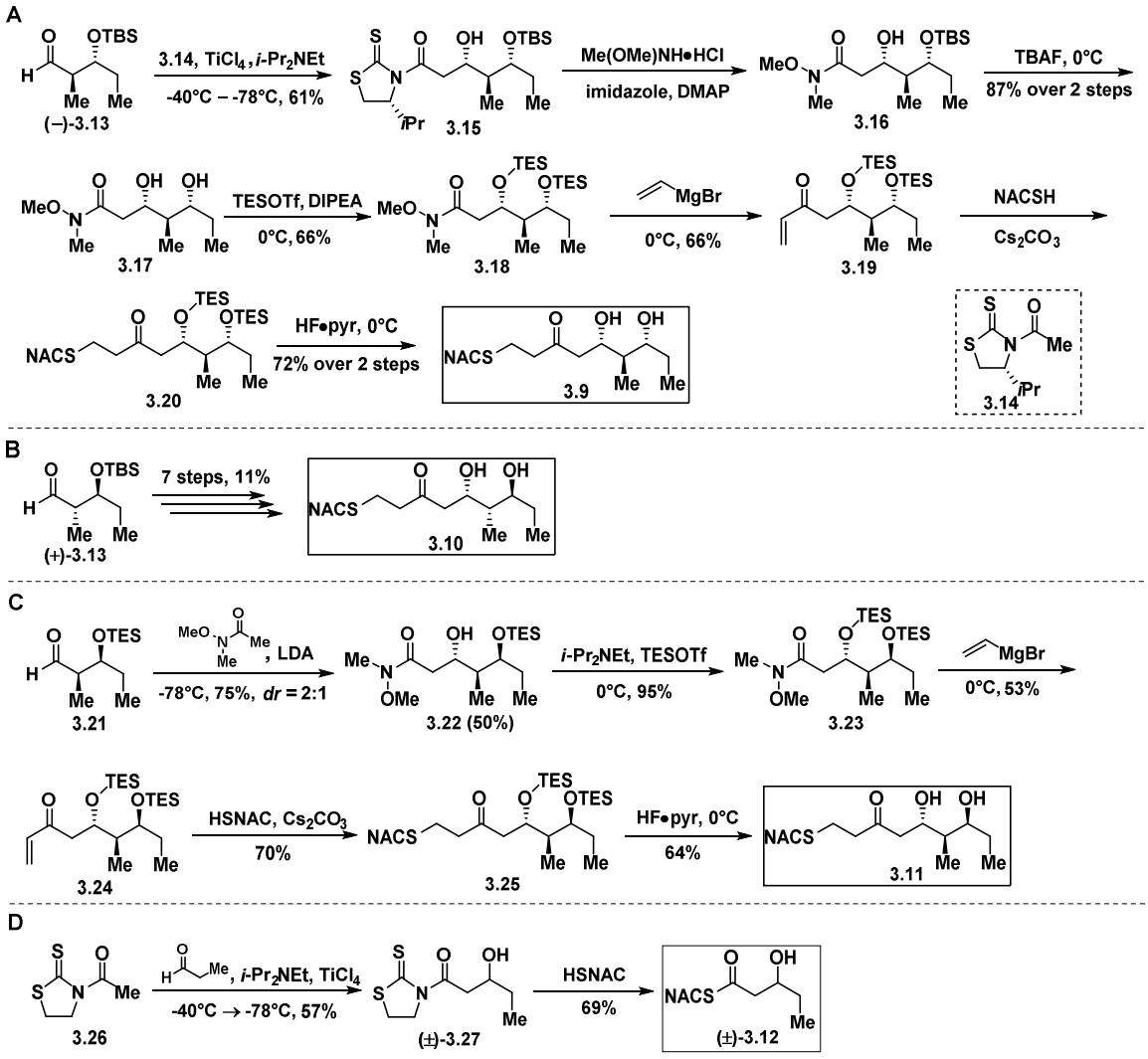

Scheme 18. Synthesis of substrate analogs **3.9** (A), **3.10** (B), **3.11** (C) and (±)-**3.12** (D).

3.4. Interrogation of stereospecificity

As shown before, multi-domain portion of the PKS would create a more native context for *in vitro* analysis. The region of *pikAI* encoding the PikKR2-DH2 didomain

comprising residues 3579–4365 was cloned into a pMCSG7 expression vector and the resulting protein was overexpressed and purified using standard methods.

Since LC-MS/MS showed high sensitivity and selectivity for detection of KR products,[142] we continued using this technique to examine the formation of DH products by their unique fragmentation patterns and/or retention times. Initial velocity was linear up to 40 min with 10 μM PikKR2-DH2 didomain (Figure 23), thus we chose an end-point quench after 15 min incubation for our kinetic studies. The kinetic parameters of all substrates were obtained by fitting the saturation curves to the Michaelis-Menten equation (Table 3).

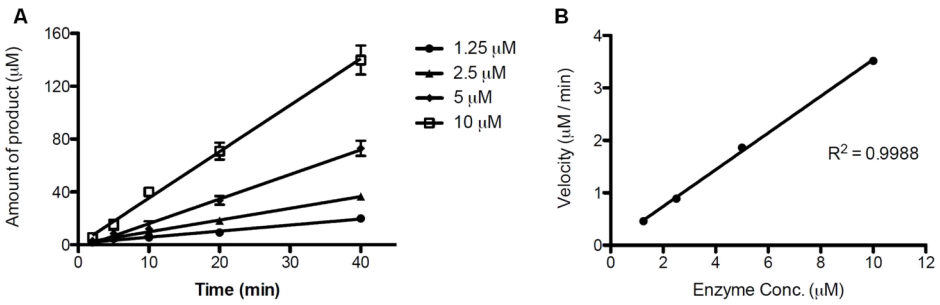

Figure 23. Measurement of initial velocity. (A) Progress curve of PikDH2 dehydration reaction at varying enzyme concentrations (1.25–10 μM); (B) Plot of initial velocity *vs*. enzyme concentration.

Table 3. Structures of substrate analogs **2.24**–**2.27**, **3.9**–**3.12** and their steady state kinetic parameters.

No.	Substrate Structure	K_M (mM)	k_{cat} (min^{-1})	k_{cat}/K_M (min^{-1}M^{-1})
2.26	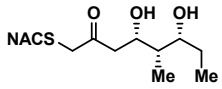	6.9 ± 1.7	0.67 ± 0.11	98 ± 39
2.24	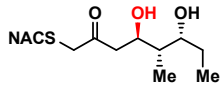	> 8	<0.01	< 1
2.27	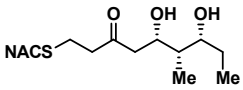	5.7 ± 1.4	1.28 ± 0.19	225 ± 88
2.25	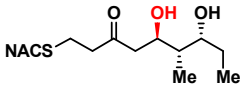	> 8	<0.01	< 1
3.9	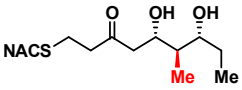	> 8	<0.01	< 1
3.10	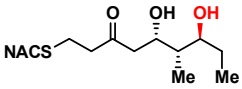	> 8	<0.01	< 1
3.11	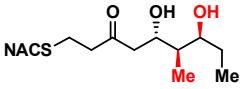	> 8	<0.01	< 1
(±)-3.12	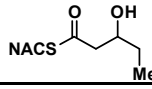	> 8	<0.01	< 1

Substrates **2.26** and **2.27**, maintaining the native stereochemistry, were accepted and processed rapidly by the enzyme. The K_M (6.9 ± 1.7 mM and 5.7 ± 1.4 mM) and k_{cat} values (0.67 ± 0.11 min^{-1} and 1.28 ± 0.19 min^{-1}) were comparable, suggesting the methylene spacer does not adversely impact active site binding and catalysis (Figure 24 and Table 3). Substrates **2.24** and **2.25**, epimeric at the β-position were not processed. This strict substrate specificity has been similarly observed with other DHs.[132, 134, 140] To inspect the sensitivity of PikDH2 to changes in distal stereochemistry, we next investigated substrates **3.9** and **3.10**, epimeric at the γ- and δ-position as well as **3.11** wherein both the γ- and δ-positions are inverted. Enzymatic products of **3.9**–**3.11** were

not detected by LC-MS/MS, indicating an unprecedented degree of discrimination of these distal stereocenters. Moreover, racemic diketide **3.12** was unexpectedly not converted to the corresponding dehydration product. This finding that PikDH2 has strict specificity on all stereogenic centers is of paramount importance in the biosynthesis. As mistakes could be made in the upstream domains, PikDH2, acting as a gatekeeper in the biosynthesis, selects only the correct substrate to catalyze and pass to downstream domains. This mechanism ensures the accuracy of the pathway and enriches the purity of the natural product. Moreover, the information is of great value for enzyme engineering and combinatorinal biosynthesis where unnatural substrates are often presented to diversify the natural product library.

We also compared the kinetic data of PikDH2 with that of PikKR2.[142] The specificity constants of the DH domain with **2.26** and **2.27** were 8–16 fold greater than the corresponding values from the KR domain (**2.26**: 98 *vs*. 12 M^{-1} min^{-1}; **2.27**: 225 *vs*. 14 M^{-1} min^{-1}). As the K_M values were in the same range (2.4–7.8 mM), the increased specificity constants of the DH domain were due to enhanced k_{cat} values suggesting that the KR is the rate-limiting domain in module 2 β-processing events.

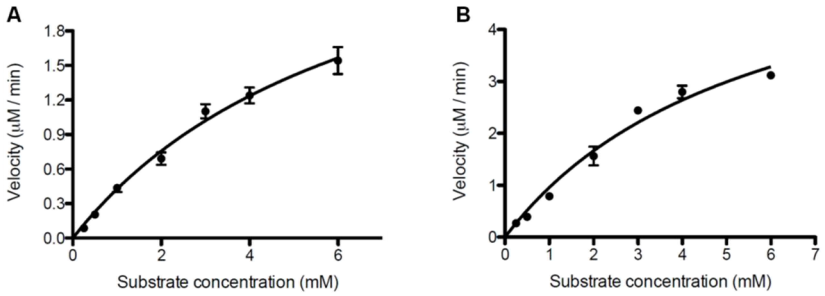

Figure 24. Michaelis-Menton curves of PikDH2. (A) with substrates **2.26**; (B) with substrates **2.27**.

3.5. pH profile

To study the chemical mechanism of PikDH2, the pH dependence of catalytic efficiency (V_{max}/K_M) with substrate **2.27** was obtained from pH 6.6 to 9.0 (Table 4). The hyperbolic curve implicates at least one key ionizable group responsible for binding and catalysis (from either the free enzyme or the free substrate)[147] with a pK_a value of 7.0 ± 0.1 (Figure 25A). The protonation of this ionizable group at low pH values abolished the enzyme activity. The pK_a values for the two hydroxyl groups of substrate **2.27** are expected to be ~14–16. Thus we expect the observed ionizable group is a general base in the enzyme, presumably the conserved histidine residue (His3611), which abstracts the α-proton. An aspartic acid residue protonates the β-hydroxyl group to facilitate the loss of a water molecule (Figure 25B). The slightly perturbed pK_a of 7.0 for the catalytic histidine, compared to pK_a of 6.0 for the free amino acid, indicates the influence of adjacent residues to form a slightly negatively charged cavity.[148]

Table 4. V_{max}/K_M values at varying hydrogen ion concentrations.

pH	V_{max}/K_M ($\times 10^{-3} min^{-1}$)
6.6	0.2606 ± 0.0157
6.7	0.4571 ± 0.0276
7.0	0.6014 ± 0.0147
7.2	0.6675 ± 0.0504
7.5	0.9206 ±0.0345
8.0	0.9154 ± 0.0376
8.5	0.9479 ± 0.0413
9.0	1.112 ± 0.0428

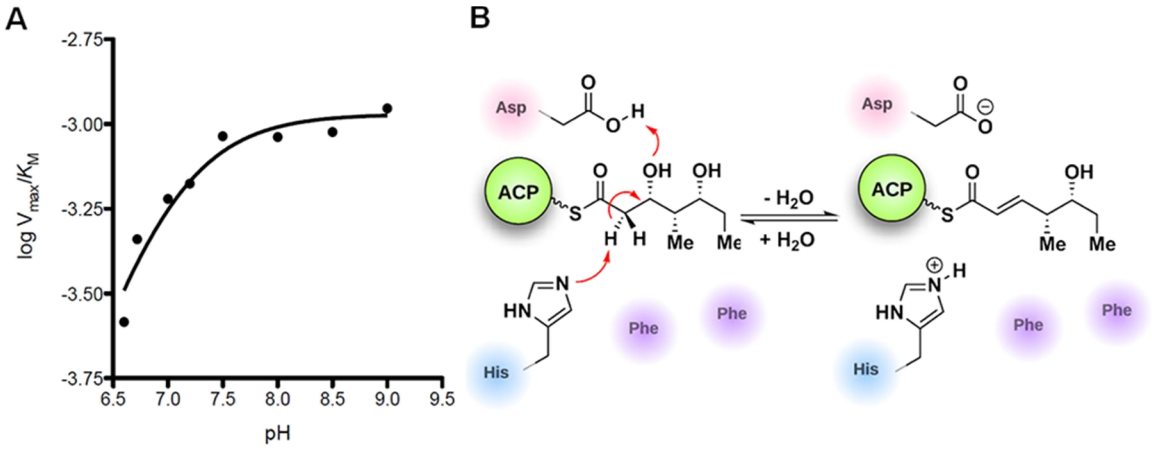

Figure 25. A) pH dependence of logV_{max}/K_M. B) Mechanism and key residues involved in the dehydration reaction.

3.6. Mutagenesis and catalytic activity

In order to understand the basis for the remarkable selectivity of PikDH2 we next aligned the amino acid sequence of PikDH2 with other DHs of known three-dimensional structure.[130-132] Two catalytic residues, the histidine (His3611) in an **H**XXGXXXP motif

and the aspartic acid (Asp3800) in an HPALL**D** motif, are also found in PikDH2. However, the tyrosine in a **Y**GP motif (observed in most DHs), whose role was proposed to assist the protonation of the β-hydroxyl group,[10] is absent in this DH. Instead, a phenylalanine (Phe3746, **F**GP motif) is located only 3.8 Å from the catalytic histidine in a PikDH2 homology model (Figure 26), suggesting that this residue could impact substrate binding at the active site. Another phenylalanine, residue 3750, conserved in most DHs, is also near the catalytic residues (3.2 Å from the aspartic acid) in the homology model. Therefore, F3746L and F3750Y and F3750L point mutants were cloned, overexpressed and characterized analogous to the wild type (Figure 27 and Table 5).

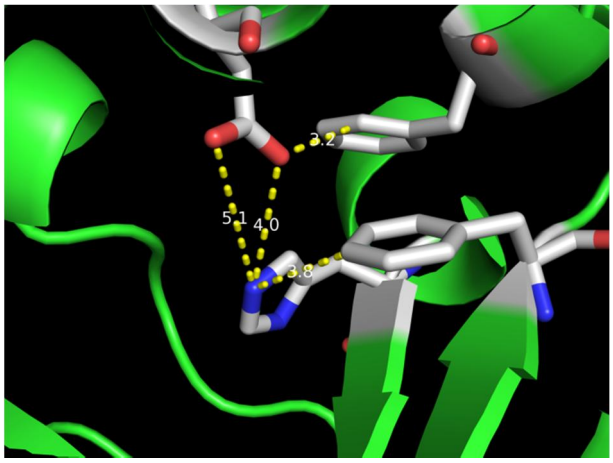

Figure 26. Active site of PikDH2 homology model. Catalytic residues Asp3800 and His3611 as well as hydrophobic residues Phe3746 and Phe3750 have been depicted in detail.

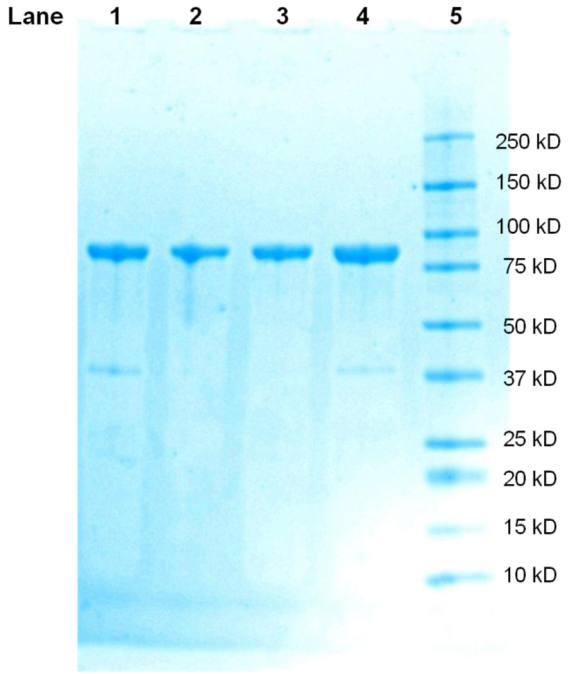

Figure 27. SDS-PAGE gel electrophoresis of purified PikDH2-KR2 and mutants on BIO-RAD precast gels (Mini-PROTEAN® TGX™ gels) stained by Bio-Safe™ Coomassie G-250 Stain; Lane 1 was loaded with PikDH2-KR2 wild type; Lane 2 was loaded with PikDH2-KR2 F3746L; Lane 3 was loaded with PikDH2-KR2 F3750L; Land 4 was loaded with PikDH2-KR2 F3750Y. Lane 5 was loaded with Kaleidoscope Precision Plus Protein Standards (BIO-RAD).

Table 5. Characterization of PikKR2-DH2 and mutants; including calculated molecular weight, monomeric molecular weight (ESI mass spectrometry), and overexpression yield.

Protein	Calculated MW (Da)	Monomeric MW (Da)	Yield (mg/L)
Wild-type	83009	83012	36
F3746L	82975	82975	66
F3750Y	83025	83028	29
F3750L	82975	82978	46

The specificity constant of F3746L dropped to 1/40 of the wild type, indicating the important role this phenylalanine plays for substrate binding (Table 6 and Figure 28). Mutants F3750Y and F3750L had similar K_M values to the wild type, but 15–30-fold decreased k_{cat} values, demonstrating that change of Phe3750 hampers the catalytic activity of PikDH2. We hypothesize that the two phenylalanine residues (F3746 and F3750) may shape a hydrophobic pocket at the active site to position the substrate as well as maintain the catalytically active state.

Table 6. Kinetic parameters of PikDH2 mutants.

Mutants	K_M (mM)	k_{cat} (min^{-1})	k_{cat}/K_M ($min^{-1}M^{-1}$)
Wild	5.7 ± 1.4	1.28 ± 0.19	225 ± 88
F3746L	> 40	N/A	5.2 ± 0.3
F3750Y	4.1 ± 1.4	0.086 ± 0.013	21 ± 9
F3750L	7.1 ± 2.6	0.046 ± 0.011	6.5 ± 3.9

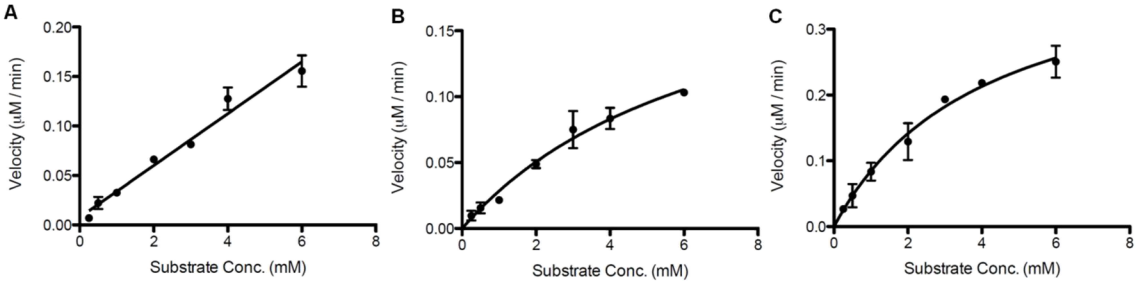

Figure 28. Michaelis-Menten and linear curves of PikDH2 mutants with substrate **2.27**. A) F3746L; B) F3750L; C) F3750Y.

3.7. Mechanism-based inhibitor

Co-crystallography of PKSs is particularly challenging since substrate affinity is often low due to the intramolecular nature of substrate presentation. With the hope of aiding structural studies we set out to screen for a suitable PikDH2 suicide substrate that would covalently react within the enzyme active site. 3-Decynoyl-*N*-acetylcysteamine (**3.28**) developed by Bloch was the first described mechanism-based inhibitor for any enzyme, which coincidentally inactivates FAS DHs.[149, 150] Burkart and co-workers recently developed second-generation DH probes with improved chemical stability and demonstrated these could inactivate functionally and structurally related PKS DHs.[151, 152] Therefore, we evaluated the ability of **3.28** to irreversibly inhibit PikDH2 using our discontinuous assay monitoring the dehydration of substrate **2.27** by LC-MS/MS. Compound **3.28** was shown to exhibit time-dependent inhibition and the kinetic constants for inactivation were determined using the Kitz–Wilson method.[153] The kinetic parameters K_I and k_{inact} were 156 ± 34 μM and 0.36 ± 0.06 min^{-1} (Figure 29B and 29C). Enzyme activity could not be recovered by dialysis and substrate protected PikDH2 from inactivation. Consequently, we expect **3.28** covalently labels PikDH2 in analogy to FAS DHs through abstraction of an α-proton by the catalytic histidine residue of the enzyme to form a reactive allene via propargylic rearrangement, which subsequently undergoes nucleophilic attack by the catalytic histidine (Figure 29A).[154, 155] This tight-binding probe **3.28** could serve as a candidate for the co-crystallographic study of PikDH2 in order to explore the catalytic mechanism. Moreover, the mechanism-based inhibitor could also be

linked to pantetheinamide to further visualize the protein-protein interactions between DH and ACP domain.[152]

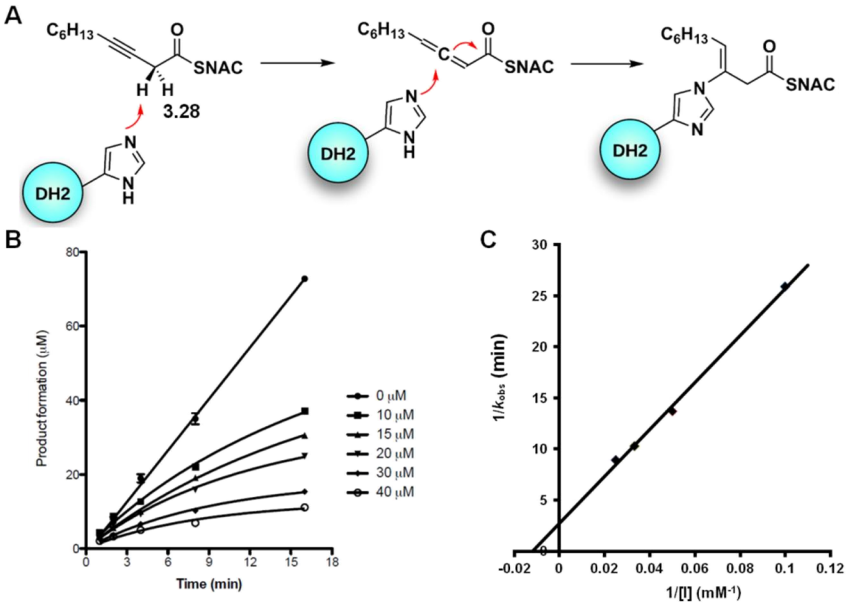

Figure 29. A) Mechanism of DH domain inactivation by 3-decynoyl-*N*-acetylcysteamine (**3.28**). B) Time course of the inactivation of PikDH2 with 10 to 40 μM **3.28**. Symbols represent the mean ± SD from duplicate experiments. C) Kitz and Wilson plot of the inhibition data ($1/k_{obs}$ vs. 1/[I]).

3.8. Experimental Section of Chemistry

General chemistry procedures. All commercial reagents were used as provided unless otherwise indicated. Intermediates **3.13**[144, 145], **3.14**[156, 157], **3.21**[142] and **3.26**[142, 146] were prepared by the published procedures. THF and CH_2Cl_2 were purified by passage through alumina columns. All reactions were performed under an inert atmosphere of dry N_2 in oven-dried (150 ºC) glassware. Flash chromatography was conducted on silica gel (230–400 mesh) using the indicated solvent systems. TLC was performed on 250 μm, F_{254}

silica gel plates, and visualized by UV and *p*-anisaldehyde stain. Optical rotations were determined on a Rudolph Autopol III polarimeter using the sodium D line (λ = 589 nm) at the temperature indicated and are reported as follows: $[\alpha]_D^{temp}$, concentration (*c* = g/100 mL), and solvent. ^{1}H and ^{13}C NMR spectra were recorded on a Bruker 400 spectrometer at 400 Hz for ^{1}H NMR and at 100 Hz for ^{13}C NMR. Chemical shifts are reported in ppm from an internal standard of residual $CHCl_3$ (7.26 ppm for ^{1}H NMR and 77.00 for ^{13}C NMR). Proton chemical data are reported as follows: chemical shift (ppm), multiplicity (s = singlet, d = doublet, t = triplet, q = quartet, quin = quintet, sext = sextet, m = multiplet, br = broad), coupling constant (Hz), and integration. High resolution mass spectra were obtained on a Bruker BioTOF II ESI-TOF/MS using either PEG or PPG standards as high resolution calibrants.

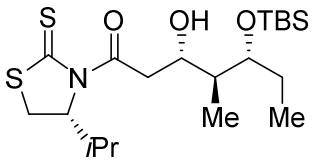

(3*S*,4*S*,5*R*)-5-[(*tert*-Butyldimethylsilyl)oxy]-3-hydroxy-1-[(*R*)-4-isopropyl-2-thioxothiazolidin-3-yl]-4-methylheptan-1-one (3.15). To a solution of thiazolidinethione **3.14** (172 mg, 0.846 mmol, 1.60 equiv) in CH_2Cl_2 (4.2 mL) at –40 °C was added $TiCl_4$ (99 μL, 0.90 mmol, 1.7 equiv). An aliquot of *i*-Pr_2NEt (0.16 mL, 0.90 mmol, 1.7 equiv) was added after stirring at –40 °C for 30 min. The reaction mixture was stirred at –40 °C an additional 2 h, and then cooled to –78 °C. Aldehyde **3.13** (122 mg, 0.529 mmol, 1.00 equiv) was added and rinsed with CH_2Cl_2 (3 × 0.3 mL). The reaction was stirred at –78 °C for 80 min, quenched by addition of saturated aqueous NH_4Cl (20 mL) and allowed to warm to room temperature. The organics were extracted with CH_2Cl_2 (3 × 20 mL), dried (Na_2SO_4), filtered and concentrated under reduced pressure. Purification by

flash chromatography (20% EtOAc/hexanes) afforded the title compound (140 mg, 61%) as a yellow oil: R_f = 0.34 (20% EtOAc/hexanes); $[\alpha]_D^{22}$ = –258 (*c* 1.00, $CHCl_3$); ^{1}H NMR ($CDCl_3$, 400 MHz) δ 5.16 (t, *J* = 6.8 Hz 1H), 4.19–4.11 (m, 1H), 3.75 (q, *J* = 6.0 Hz, 1H), 3.64 (dd, *J* = 17.7, 2.0 Hz, 1H), 3.51 (dd, *J* = 11.5, 8.0 Hz, 1H), 3.15 (dd, *J* = 17.7, 9.9 Hz, 1H), 3.02 (d, *J* = 11.5 Hz, 1H), 2.36 (dq, *J* = 13.5, 6.8 Hz, 1H), 1.85 (sext, *J* = 7.0 Hz, 1H), 1.58–1.40 (m, 2H), 1.06 (d, *J* = 6.8 Hz, 3H), 0.97 (d, *J* = 6.9 Hz, 3H), 0.93–0.83 (m, 15H), 0.06 (s, 3H), 0.05 (s, 3H); ^{13}C NMR ($CDCl_3$, 100 MHz) δ 203.0, 173.4, 75.1, 71.4, 69.4, 43.0, 42.5, 30.8, 30.6, 25.9, 25.6, 19.1, 18.1, 17.8, 11.4, 9.2, -4.4, -4.6; HRMS (ESI-TOF) *m/z*: $[M + Na]^+$ calcd for $C_{20}H_{39}NO_3S_2SiNa$ 456.2033, found 456.2057.

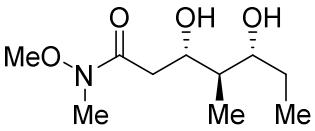

(3*S*,4*R*,5*R*)-3,5-Dihydroxy-*N*-methoxy-*N*,4-dimethylheptanamide (3.17). To a solution of thiazolidinethione **3.15** (136 mg, 0.314 mmol, 1.00 equiv) in CH_2Cl_2 (5 mL) at room temperature was added *N*,*O*-dimethylhydroxylamine hydrochloride (123 mg, 1.26 mmol, 4.00 equiv) and imidazole (171 mg, 2.51 mmol, 8.00 equiv), followed by the addition of DMAP (7.7 mg, 0.063 mmol, 0.20 equiv). The reaction mixture was stirred at room temperature until the bright yellow color faded (24 h), then quenched with water. The layers were separated and the aqueous layer was extracted with CH_2Cl_2 (3 × 10 mL). The combined organic layers were washed with saturated aqueous NaCl (20 mL), dried (Na_2SO_4), filtered and concentrated under reduced pressure to afford the crude **3.16** as a colorless oil, which was used directly in the next reaction without further purification. R_f = 0.41 (30% EtOAc/hexanes).

To a solution of silyl ether **3.16** prepared above (105 mg, 0.314 mmol, 1.00 equiv) in THF (10 mL) at 0 °C was added TBAF (1.0 M in THF, 0.94 mL, 0.94 mmol, 3.0 equiv). The reaction mixture was stirred at 0 °C for 7 h, then quenched by addition of saturated aqueous NH_4Cl (10 mL). The reaction mixture was extracted with EtOAc (3 × 10 mL), and the combined organic layers were washed with saturated aqueous NaCl (20 mL), dried (Na_2SO_4), filtered, and concentrated under reduced pressure. Purification by flash chromatography (5% MeOH/CH_2Cl_2) afforded the title compound (60 mg, 87% over 2 steps) as a colorless oil: R_f = 0.30 (5% MeOH/CH_2Cl_2); $[\alpha]_D^{21}$ = –43.4 (*c* 0.650, $CHCl_3$); ^{1}H NMR ($CDCl_3$, 400 MHz) δ 4.07–3.99 (m, 1H), 3.69 (s, 3H), 3.59 (td, *J* = 7.9, 2.9 Hz, 1H), 3.19 (s, 3H), 2.80 (d, *J* = 16.5 Hz, 1H), 2.51 (dd, *J* = 16.5, 9.8 Hz, 1H), 1.71–1.60 (m, 2H), 1.41 (dquin, *J* = 14.7, 7.4 Hz, 1H), 0.97 (t, *J* = 7.4 Hz, 3H), 0.82 (d, *J* = 6.9 Hz, 3H); ^{13}C NMR ($CDCl_3$, 100 MHz) δ 173.9, 76.3, 72.9, 61.3, 42.8, 36.0, 31.9, 27.1, 12.9, 9.3; HRMS (ESI-TOF) *m/z*: $[M + Na]^+$ calcd for $C_{10}H_{21}NO_4Na$ 242.1363, found 242.1368.

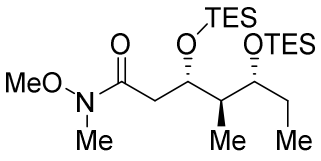

(3*S*,4*R*,5*R*)-*N*-Methoxy-*N*,4-dimethyl-3,5-bis[(triethylsilyl)oxy]heptanamide (3.18). To a solution of alcohol **3.17** (54 mg, 0.25 mmol, 1.0 equiv) in CH_2Cl_2 (10 mL) at 0 °C was added *i*-Pr_2NEt (0.15 mL, 0.89 mmol, 3.6 equiv) and TESOTf (0.18 mL, 0.79 mmol, 3.2 equiv). After stirring at 0 °C for 60 min, the reaction mixture was quenched by the addition of saturated aqueous $NaHCO_3$ (20 mL). The layers were separated and the aqueous layer was extracted with CH_2Cl_2 (3 × 10 mL). The combined organic layers were washed with saturated aqueous NaCl (50 mL), dried (Na_2SO_4),

filtered and concentrated under reduced pressure. Purification by flash chromatography (10% EtOAc/hexanes) afforded the title compound (73 mg, 66%) as a colorless oil: R_f = 0.44 (10% EtOAc/hexanes); $[\alpha]_D^{22}$ = –31.0 (*c* 1.50, $CHCl_3$); ^{1}H NMR ($CDCl_3$, 400 MHz) δ 4.50–4.43 (m, 1H), 3.68 (s, 3H), 3.60 (q, *J* = 5.7 Hz, 1H), 3.16 (s, 3H), 2.76–2.65 (m, 1H), 2.36 (dd, *J* = 15.0, 2.9 Hz, 1H), 1.85–1.77 (m, 1H), 1.58–1.44 (m, 2H), 0.99–0.83 (m, 24H), 0.64–0.52 (m, 12H); ^{13}C NMR ($CDCl_3$, 100 MHz) δ 173.1, 74.5, 69.5, 61.2, 43.7, 35.5, 32.0, 26.4, 10.3, 8.8, 7.0, 6.9, 5.2, 5.0; HRMS (ESI-TOF) *m/z*: $[M + Na]^+$ calcd for $C_{22}H_{49}NO_4Si_2Na$ 470.3092, found 470.3097.

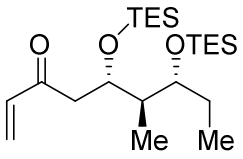

(5*S*,6*R*,7*R*)-6-Methyl-5,7-bis[(triethylsilyl)oxy]non-1-en-3-one (3.19). To a solution of Weinreb amide **3.18** (73 mg, 0.16 mmol, 1.0 equiv) in THF (5 mL) at 0 °C was added vinyl magnesium bromide (1.0 M in THF, 0.48 mL, 0.48 mmol, 3.0 equiv). After stirring at 0 °C for 55 min, the reaction mixture was quenched by the addition of saturated aqueous NH_4Cl (5 mL). The layers were separated and the aqueous layer was extracted with EtOAc (3 × 10 mL). The combined organic layers were washed with saturated aqueous NaCl (20 mL), dried (Na_2SO_4) and concentrated under reduced pressure. Purification by flash chromatography (10% EtOAc/hexanes) afforded the title compound (45 mg, 66%) as a colorless oil: R_f = 0.60 (10% EtOAc/hexanes); $[\alpha]_D^{21}$ = –34.6 (*c* 0.800, $CHCl_3$); ^{1}H NMR ($CDCl_3$, 400 MHz) δ 6.38 (dd, *J* = 17.6, 10.5 Hz, 1H), 6.20 (dd, *J* = 17.6, 1.0 Hz, 1H), 5.79 (dd, *J* = 10.5, 1.1 Hz, 1H), 4.51–4.45 (m, 1H), 3.58 (q, *J* = 5.3 Hz, 1H), 2.77 (q, *J* = 8.8 Hz, 1H), 2.59 (dd, *J* = 15.5, 2.9 Hz, 1H), 1.84–1.76 (m, 1H), 1.57–1.45 (m, 2H), 1.00–0.82 (m, 24H), 0.57 (app. dq, *J* = 19.0, 7.8 Hz, 12H); ^{13}C NMR ($CDCl_3$, 100 MHz) δ 200.0, 137.5, 127.8,

74.6, 69.1, 43.52, 43.46, 26.5, 10.3, 8.6, 7.0, 6.9, 5.2, 5.0; HRMS (ESI-TOF) *m/z*: [M + Na]$^+$ calcd for $C_{22}H_{46}O_3Si_2Na$ 437.2878, found 437.2854.

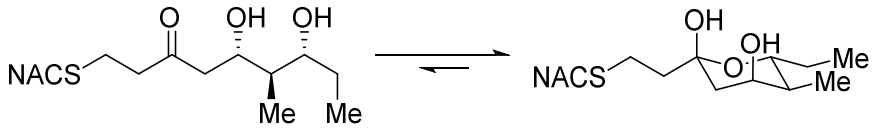

(5*S*,6*R*,7*S*)-5,7-Dihydroxy-6-methyl-1-[*N*-(2-acetamidoethyl)thio]nonan-3-one (3.9). To a solution of vinyl ketone **3.19** (32 mg, 0.078 mmol, 1.0 equiv) in THF (5 mL) was added *N*-acetylcysteamine (12 μL, 0.12 mmol, 1.5 equiv) and a catalytic amount of Cs_2CO_3. The reaction was stirred at room temperature for 40 min, before quenching with saturated aqueous NH_4Cl (5 mL). The layers were separated and the aqueous layer was extracted with EtOAc (3 × 10 mL). The combined organic layers were washed with saturated aqueous NaCl (40 mL), dried (Na_2SO_4), filtered and concentrated under reduced pressure to yield crude **3.20** (35 mg) as a colorless oil, which was used in the next reaction without further purification: R_f = 0.36 (5% MeOH/CH_2Cl_2).

To a solution of crude silyl ether **3.20** prepared above (35 mg, 0.066 mmol, 1.0 equiv) in THF (6 mL) at 0 °C was added a solution of 70% HF-pyridine:pyridine:THF (1:2:8, 3 mL). The reaction was stirred at 0 °C for 3.5 h, then quenched with saturated aqueous $NaHCO_3$ to bring the reaction to pH 7, and extracted with EtOAc (3 × 10 mL). The combined organic layers were washed with saturated aqueous NaCl (40 mL), dried (Na_2SO_4), filtered and concentrated under reduced pressure. Purification by flash chromatography (5% MeOH/CH_2Cl_2) afforded the title compound (17 mg, 72% over 2 steps) as a colorless oil: R_f = 0.20 (5% MeOH/CH_2Cl_2); $[\alpha]_D^{21}$ = 41.1 (*c* 1.00, $CHCl_3$); ^{1}H NMR ($CDCl_3$, 400 MHz) δ 6.10 (s, 1H), 4.98 (s, 1H), 3.97–3.85 (m, 1H), 3.75–3.68 (m,

1H), 3.50–3.36 (m, 3H), 2.78–2.61 (m, 4H), 2.04–1.96 (m, 4H), 1.90–1.81 (m, 2H), 1.71–1.59 (m, 2H), 1.50–1.32 (m, 2H), 0.96–0.90 (m, 6H); ^{13}C NMR ($CDCl_3$, 100 MHz) δ 170.4, 97.1, 70.4, 70.2, 41.4, 39.9, 38.3 (overlap), 31.5, 25.4, 25.0, 23.2, 13.9, 9.3; HRMS (ESI-TOF) *m/z*: $[M + Na]^+$ calcd for $C_{14}H_{27}NO_4SNa$ 328.1553, found 328.1551.

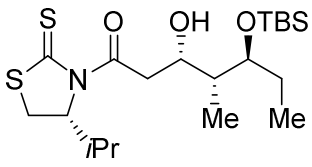

(3*S*,4*R*,5*S*)-5-[(*tert*-Butyldimethylsilyl)oxy]-3-hydroxy-1-[(*R*)-4-isopropyl-2-thioxothiazolidin-3-yl]-4-methylheptan-1-one (4,5-di-*epi*-3.15). The title compound was prepared using otherwise identical conditions as described for the preparation of aldol product **3.15** except for the use of aldehyde (+)–**3.13** (111 mg, 0.482 mmol, 1.00 equiv). Purification by flash chromatography (20% EtOAc/hexanes) afforded the title compound (129 mg, 62%) as a yellow oil: R_f = 0.46 (20% EtOAc/hexanes); $[\alpha]_D^{21}$ = –211 (*c* 2.00, $CHCl_3$); ^{1}H NMR ($CDCl_3$, 400 MHz) δ 5.19–5.13 (m, 1H), 4.66 (d, *J* = 9.4 Hz, 1H), 3.72–3.65 (m, 2H), 3.51 (dd, *J* = 11.4, 8.0 Hz, 1H), 3.42 (dd, *J* = 17.1, 9.3 Hz, 1H), 3.27 (dd, *J* = 17.1, 2.0 Hz, 1H), 3.01 (d, *J* = 11.5 Hz, 1H), 2.40 (dq, *J* = 13.5, 6.7 Hz, 1H), 1.82–1.59 (m, 3H), 1.06 (d, *J* = 6.8 Hz, 3H), 1.01 (d, *J* = 7.1 Hz, 3H), 0.98 (d, *J* = 7.0 Hz, 3H), 0.88 (s, 9H), 0.87 (t, *J* = 7.5 Hz), 0.093 (s, 3H), 0.085 (s, 3H); ^{13}C NMR ($CDCl_3$, 100 MHz) δ 203.0, 172.2, 79.3, 71.6, 66.7, 43.8, 38.0, 30.9, 30.5, 27.5, 25.8, 19.1, 17.9, 17.7, 11.7, 9.5, -4.4, -4.9; HRMS (ESI-TOF) *m/z*: $[M + Na]^+$ calcd for $C_{20}H_{39}NO_3S_2SiNa$ 456.2033, found 456.2052.

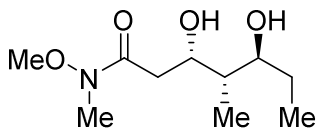

(3*S*,4*S*,5*S*)-3,5-Dihydroxy-*N*-methoxy-*N*,4-dimethylheptanamide (4,5-di-*epi*-3.17). Identical reaction conditions employed for the synthesis of weinreb amide **3.16** were used, except for the

use of thiazolidinethione **4,5-di-*epi*-3.15** (129 mg, 0.297 mmol, 1.00 equiv). The crude product **4,5-di-*epi*-3.16** was used to carry out the next reaction without further purification: R_f = 0.34 (30% EtOAc/hexanes).

The title compound was prepared using otherwise identical conditions as described for the preparation of diol **3.17**, except for the use of of silyl ether **4,5-di-*epi*-3.16** prepared above (99 mg, 0.297 mmol, 1.00 equiv). Purification by flash chromatography (5% MeOH/CH_2Cl_2) afforded the title compound (45 mg, 69% over 2 steps) as a colorless oil: R_f = 0.29 (5% MeOH/CH_2Cl_2); $[\alpha]_D^{22}$ = –40.4 (*c* 1.00, $CHCl_3$); ^{1}H NMR ($CDCl_3$, 400 MHz) δ 4.39 (dt, *J* = 9.8, 2.8 Hz, 1H), 3.69 (s, 4H), 3.55–3.48 (m, 1H), 3.22–3.14 (m, 4H), 2.68–2.49 (m, 2H), 1.72–1.65 (m, 1H), 1.63–1.44 (m, 2H), 1.00–0.91 (m, 6H); ^{13}C NMR ($CDCl_3$, 100 MHz) δ 173.9, 76.1, 69.4, 61.3, 40.6, 34.7, 31.9, 28.1, 11.9, 9.8; HRMS (ESI-TOF) *m/z*: $[M + Na]^+$ calcd for $C_{10}H_{21}NO_4Na$ 242.1363, found 242.1366.

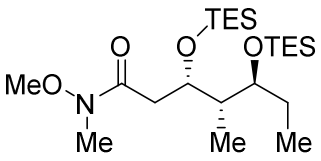

(3*S*,4*S*,5*S*)-*N*-Methoxy-*N*,4-dimethyl-3,5-bis[(triethylsilyl)oxy]heptanamide (4,5-di-*epi*-3.18). The title compound was prepared using otherwise identical conditions as described for the preparation of silylether **3.18**, except for the use of alcohol **4,5-di-*epi*-3.17** (42 mg, 0.19 mmol, 1.0 equiv). Purification by flash chromatography (10% EtOAc/hexanes) afforded the title compound (57 mg, 66%) as a colorless oil: R_f = 0.45 (10% EtOAc/hexanes); $[\alpha]_D^{21}$ = –26.3 (*c* 1.00, $CHCl_3$); ^{1}H NMR ($CDCl_3$, 400 MHz) δ 4.25 (q, *J* = 5.6 Hz, 1H), 3.68 (s, 3H), 3.57 (dt, *J* = 7.9, 3.6 Hz, 1H), 3.16 (s, 3H), 2.66 (dd, *J* = 15.0, 6.7 Hz, 1H), 2.57 (dd, *J* = 15.0, 5.6 Hz, 1H), 1.73–1.65 (m, 1H), 1.55–1.44 (m, 1H),

1.43–1.35 (m, 1H), 1.00–0.85 (m, 24H), 0.60 (app. dq, J = 7.9, 3.5 Hz, 12H); ^{13}C NMR ($CDCl_3$, 100 MHz) δ 172.4, 75.9, 70.8, 61.2, 45.0, 38.8, 32.0, 25.5, 10.4, 9.6, 7.0, 5.2; HRMS (ESI-TOF) *m/z*: $[M + Na]^+$ calcd for $C_{22}H_{49}NO_4Si_2Na$ 470.3092, found 470.3088.

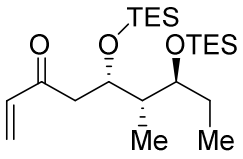

(5*S*,6*S*,7*S*)-6-Methyl-5,7-bis[(triethylsilyl)oxy]non-1-en-3-one (6,7-di-*epi*-3.19). The title compound was prepared using otherwise identical conditions as described for the preparation of enone **3.19**, except for the use Weinreb amide **4,5-di-*epi*-3.18** (42 mg, 0.094 mmol, 1.0 equiv). Purification by flash chromatography (5% EtOAc/hexanes) afforded the title compound (28 mg, 72%) as a colorless oil: R_f = 0.68 (10% EtOAc/hexanes); $[\alpha]_D^{21}$ = –27.0 (*c* 0.650, $CHCl_3$); ^{1}H NMR ($CDCl_3$, 400 MHz) δ 6.37 (dd, J = 17.6, 10.5 Hz, 1H), 6.21 (d, J = 17.6 Hz, 1H), 5.83 (d, J = 10.5 Hz, 1H), 4.28 (q, J = 5.7 Hz, 1H), 3.55 (dt, J = 7.8, 4.0 Hz, 1H), 2.84–2.70 (m, 2H), 1.69–1.61 (m, 1H), 1.53–1.34 (m, 2H), 0.99–0.84 (m, 24H), 0.58 (app. dq, J = 7.9, 4.0 Hz, 12H); ^{13}C NMR ($CDCl_3$, 100 MHz) δ 199.1, 137.1, 128.3, 75.6, 70.2, 46.5, 44.9, 25.6, 10.1, 9.7, 7.00, 5.2; HRMS (ESI-TOF) *m/z*: $[M + Na]^+$ calcd for $C_{22}H_{46}O_3Si_2Na$ 437.2878, found 437.2847.

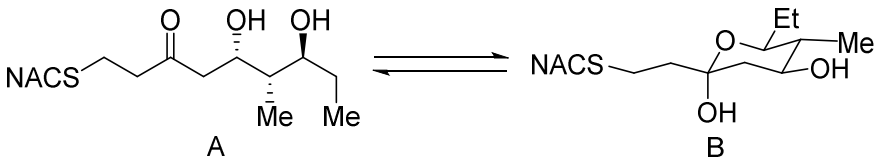

(5*S*,6*S*,7*S*)-5,7-Dihydroxy-6-methyl-1-[*N*-(2-acetamidoethyl)thio]nonan-3-one (3.10). Identical reaction conditions as reported for the synthesis of thioether **3.20** were employed, except for the use of vinyl ketone **6,7-di-**

***epi*-3.19** (14 mg, 0.034 mmol, 1.0 equiv). The crude product **6,7-di-*epi*-3.20** was used to carry out the next reaction without further purification: R_f = 0.45 (5% MeOH/CH_2Cl_2).

The title compound was prepared using otherwise identical conditions as described for the preparation of thioether **3.9**, except for the use of silyl ether **6,7-di-*epi*-3.20** prepared above (18 mg, 0.034 mmol, 1.0 equiv). Purification by flash chromatography (5% MeOH/CH_2Cl_2) afforded the title compound (5.8 mg, 56% over 2 steps) as a colorless oil: R_f = 0.27 (5% MeOH/CH_2Cl_2); Due to the instability of the compound the optical rotation could not be obtained; ^{1}H NMR ($CDCl_3$, 400 MHz, approximately 3:17 mixture of A:B where the integrations have been normalized) δ 6.03 (s, 0.15H), 5.89 (s, 0.85H), 4.45 (dt, J = 10.1, 2.4 Hz, 0.15H), 3.69 (dt, J = 10.7, 4.8 Hz, 0.85H), 3.54–3.36 (m, 3.15H), 3.20 (s, 0.85H), 2.83–2.62 (m, 4.45H), 2.46 (dd, J = 16.4, 2.7 Hz, 0.15H), 2.11 (dd, J = 12.3, 4.8 Hz, 0.85H), 1.99 (s, 3H), 1.95–1.89 (m, 1.7H), 1.76–1.68 (m, 1H), 1.46–1.30 (m, 1.85H), 1.28–1.21 (m, 1H), 1.01–0.87 (m, 6H); ^{13}C NMR ($CDCl_3$, 100 MHz, major isomer B) δ 170.2, 97.3, 74.6, 70.0, 43.2, 43.0, 41.1, 38.2, 31.4, 25.3, 25.2, 23.3, 12.6, 9.6; HRMS (ESI-TOF) *m/z*: $[M + Na]^+$ calcd for $C_{14}H_{27}NO_4SNa$ 328.1553, found 328.1560.

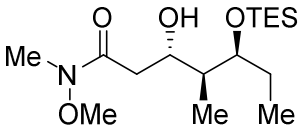

(3*S*,4*S*,5*S*)-3-Hydroxy-*N*-methoxy-*N*,4-dimethyl-5-[(triethylsilyl)oxy]heptanamide (3.22). To a solution of freshly distilled *i*-Pr_2NH (0.21 mL, 1.5 mmol, 1.5 equiv) in THF (30 mL) at –78 °C was added *n*-BuLi (1.2 M in THF, 1.2 mL, 1.4 mmol, 1.4 equiv). After stirring at –78 °C for 30 min, *N*-methoxy-*N*-methylacetamide (0.15 mL, 1.4 mmol, 1.4 equiv) was added. The reaction mixture was stirred at –78 °C for an additional 30 min, followed by the dropwise addition of a solution of aldehyde **3.21** (233 mg, 1.01 mmol, 1.00 equiv) in THF (0.5 mL).

The reaction mixture was stirred at –78 °C for an additional 1 h, then quenched by the addition of saturated aqueous NH_4Cl (20 mL). The layers were separated and the aqueous layer was extracted with EtOAc (3 × 20 mL). The combined organic layers were dried (Na_2SO_4), filtered and concentrated under reduced pressure. Purification by flash chromatography (40% EtOAc/hexanes) afforded the title compound (169 mg, 50%) as a colorless oil (total yield = 75%, dr = 2: 1): $[\alpha]_D^{22} = -32.2$ (*c* 1.00, $CHCl_3$); ^{1}H NMR ($CDCl_3$, 400 MHz) δ 4.16 (d, *J* = 2.9 Hz, 1H), 4.01 (tt, *J* = 9.0, 3.0 Hz, 1H), 3.95 (dt, *J* = 6.8, 2.2 Hz, 1H), 3.70 (s, 3H), 3.20 (s, 3H), 2.66 (d, *J* = 14.3 Hz, 1H), 2.52 (dd, *J* = 15.7, 9.2 Hz, 1H), 1.74–1.63 (m, 1H), 1.60–1.46 (m, 2H), 0.96 (t, *J* = 7.9 Hz, 9H), 0.87 (t, *J* = 7.5 Hz, 3H), 0.81 (d, *J* = 7.0 Hz, 3H), 0.62 (q, *J* = 7.9 Hz, 6H); ^{13}C NMR ($CDCl_3$, 100 MHz) δ 173.7, 75.1, 70.0, 61.2, 41.8, 36.9, 31.9, 26.6, 10.7, 10.6, 6.9, 5.2; HRMS (ESI-TOF) *m/z*: $[M + Na]^+$ calcd for $C_{16}H_{35}NO_4SiNa$ 356.2228, found 356.2226.

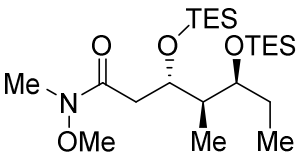

(3*S*,4*R*,5*S*)-*N*-Methoxy-*N*,4-dimethyl-3,5-bis[(triethylsilyl)oxy]heptanamide (3.23). To a solution of alcohol **3.22** (122 mg, 0.366 mmol, 1.00 equiv) in CH_2Cl_2 (10 mL) at 0 °C was added *i*-Pr_2NEt (0.11 mL, 0.66 mmol, 1.8 equiv) and TESOTf (0.13 mL, 0.59 mmol, 1.6 equiv). After stirring at 0 °C for 1 h, the reaction mixture was quenched by the addition of saturated aqueous $NaHCO_3$ (10 mL). The layers were separated and the aqueous layer was extracted with CH_2Cl_2 (3 × 10 mL). The combined organic layers were washed with saturated aqueous NaCl (20 mL), dried (Na_2SO_4), filtered and concentrated under reduced pressure. Purification by flash chromatography (20% EtOAc/hexanes) afforded the title compound (155 mg, 95%) as a colorless oil: R_f = 0.65 (20%

EtOAc/hexanes); $[\alpha]_D^{22} = -28.2$ (*c* 1.00, $CHCl_3$); ^1H NMR ($CDCl_3$, 400 MHz) δ 4.30 (dt, *J* = 9.7, 3.0 Hz, 1H), 3.70 (s, 3H), 3.52 (q, *J* = 5.6 Hz, 1H), 3.17 (s, 3H), 2.87–2.72 (m, 1H), 2.20 (dd, *J* = 14.9, 2.0 Hz, 1H), 1.86–1.74 (m, 1H), 1.61–1.49 (m, 2H), 0.98–0.85 (m, 24H), 0.63–0.54 (m, 12H); ^{13}C NMR ($CDCl_3$, 100 MHz) δ 173.1, 75.2, 71.1, 61.2, 42.9, 34.8, 32.0, 27.7, 8.9, 8.8, 7.0, 6.8, 5.4, 4.9; HRMS (ESI-TOF) *m/z*: $[M + Na]^+$ calcd for $C_{22}H_{49}NO_4Si_2Na$ 470.3092, found 470.3093.

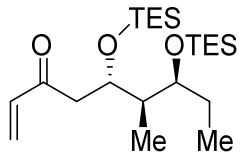

(5*S*,6*R*,7*S*)-6-Methyl-5,7-bis[(triethylsilyl)oxy]non-1-en-3-one (3.24). To a solution of Weinreb amide **3.23** (155 mg, 0.346 mmol, 1.00 equiv) in THF (15 mL) at 0 °C was added vinyl magnesium bromide (1.0 M in THF, 1.04 mL, 1.04 mmol, 3.00 equiv). The reaction mixture was stirred at 0 °C for 70 min, quenched by the addition of saturated aqueous NH_4Cl (10 mL), and allowed to warm up to room temperature. The layers were separated and the aqueous layer was extracted with EtOAc (3 × 20 mL). The combined organic layers were washed with saturated aqueous NaCl (30 mL), dried (Na_2SO_4), and concentrated under reduced pressure. Purification by flash chromatography (10% EtOAc/hexanes) afforded the title compound (77 mg, 53%) as a colorless oil: $R_f = 0.64$ (10% EtOAc/hexanes); $[\alpha]_D^{23} = -34.8$ (*c* 1.00, $CHCl_3$); ^1H NMR ($CDCl_3$, 400 MHz) δ 6.36 (dd, *J* = 17.6, 10.5 Hz, 1H), 6.20 (dd, *J* = 17.6, 1.1 Hz, 1H), 5.81 (dd, *J* = 10.5, 1.1 Hz, 1H), 4.30 (ddd, *J* = 9.2, 3.5, 2.3 Hz, 1H), 3.58–3.50 (m, 1H), 2.86 (dd, *J* = 15.6, 9.3 Hz, 1H), 2.49 (dd, *J* = 15.6, 2.3 Hz, 1H), 1.83–1.73 (m, 1H), 1.57–1.47 (m, 2H), 0.99–0.84 (m, 24H), 0.57 (q, *J* = 7.8 Hz, 6H), 0.54 (q, *J* = 7.8 Hz, 6H); ^{13}C NMR ($CDCl_3$, 100 MHz) δ 200.2, 137.6, 128.1, 75.3, 71.1, 42.82,

42.77, 27.8, 9.2, 8.3, 7.0, 6.9, 5.4, 5.0; HRMS (ESI-TOF) *m/z*: $[M + Na]^+$ calcd for $C_{22}H_{46}O_3Si_2Na$ 437.2878, found 437.2868.

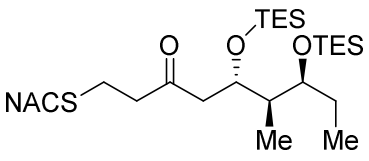

(5*S*,6*R*,7*S*)-6-Methyl-1-[*N*-(2-acetamidoethyl)thio]-5,7-bis[(triethylsilyl)oxy]nonan-3-one (3.25). To a solution of vinyl ketone **3.24** (42 mg, 0.10 mmol, 1.0 equiv) in THF (8 mL) was added *N*-acetylcysteamine (16 μL, 0.15 mmol, 1.5 equiv) and a catalytic amount of Cs_2CO_3. The reaction was stirred at room temperature for 1.5 h, then quenched by the addition of saturated aqueous NH_4Cl (10 mL). The layers were separated and the aqueous layer was extracted with EtOAc (3 × 10 mL). The combined organic layers were washed with saturated aqueous NaCl (40 mL), dried (Na_2SO_4), filtered and concentrated under reduced pressure. Purification by flash chromatography (5% MeOH/CH_2Cl_2) afforded the title compound (38 mg, 70%) as a colorless oil: R_f = 0.37 (5% MeOH/CH_2Cl_2); $[\alpha]_D^{23} = -28.4$ (*c* 1.00, $CHCl_3$); ^{1}H NMR ($CDCl_3$, 400 MHz) δ 6.07 (s, 1H), 4.31–4.20 (m, 1H), 3.54–3.43 (m, 3H), 2.83–2.58 (m, 7H), 2.40 (dd, *J* = 15.5, 1.9 Hz, 1H), 2.01 (s, 3H), 1.78–1.70 (m, 1H), 1.57–1.42 (m, 2H), 1.01–0.81 (m, 24H), 0.56 (app. quin, *J* = 8.0 Hz, 12H); ^{13}C NMR ($CDCl_3$, 100 MHz) δ 208.3, 170.1, 75.2, 71.3, 46.1, 44.4, 42.5, 38.4, 32.3, 27.7, 25.0, 23.2, 9.2, 8.0, 7.0, 6.9, 5.4, 5.0; HRMS (ESI-TOF) *m/z*: $[M + Na]^+$ calcd for $C_{26}H_{55}NO_3SSi_2Na$ 556.3283, found 556.3291.

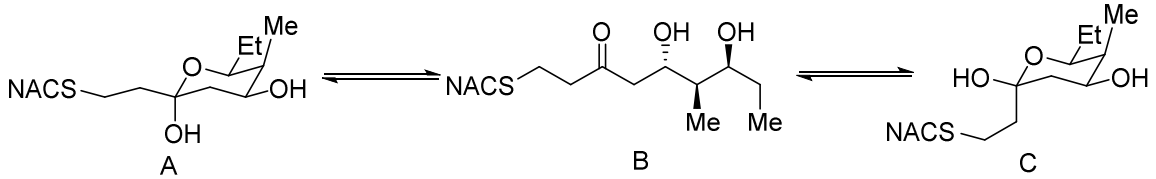

(5*S*,6*R*,7*S*)-5,7-Dihydroxy-6-methyl-1-[*N*-(2-acetamidoethyl)thio]nonan-3-one (3.11).

To a solution of silyl ether **3.25** (44 mg, 0.082 mmol, 1.0 equiv) in THF (6 mL) at 0 °C was added a solution of 70% HF-pyridine:pyridine:THF (1:2:8, 3 mL). The reaction was stirred at 0 °C for 4.5 h, then quenched by the addition of saturated aqueous $NaHCO_3$ to bring the reaction to pH 7, and extracted with *n*-butanol (5 × 20 mL). The combined organic layers were washed with saturated aqueous NaCl (40 mL), dried (Na_2SO_4), filtered, and concentrated under reduced pressure. Purification by flash chromatography (10% MeOH/EtOAc) afforded the title compound (16 mg, 64%) as a colorless oil: R_f = 0.36 (10% MeOH/EtOAc); $[\alpha]_D^{22}$ = –35.5 (*c* 0.52, $CHCl_3$); ^{1}H NMR ($CDCl_3$, 400 MHz, approximately 6:6:1 mixture of A:B:C where the integrations have been normalized) δ 6.61 (s, 0.08H), 6.08 (s, 0.46H), 5.98 (s, 0.46H), 4.20 (dt, *J* = 11.9, 4.8 Hz, 0.46H), 4.17–4.08 (m, 0.46H), 4.07–4.03 (m, 0.08H), 3.85–3.77 (m, 1H), 3.75–3.69 (m, 0.16H), 3.53–3.34 (m, 1.84H), 3.22–3.13 (m, 0.32H), 2.86–2.58 (m, 5.52H), 2.00–1.98 (m, 3H), 1.95–1.84 (m, 1.38H), 1.81 (dd, *J* =4.8, 12.5 Hz, 0.46H), 1.65–1.34 (m, 3H), 1.09 (d, *J* = 7.2 Hz, 0.24H), 1.05 (t, *J* = 7.3 Hz, 0.24H), 0.98–0.87 (m, 4.14H), 0.80 (d, *J* = 6.9 Hz, 1.38H); ^{13}C NMR ($CDCl_3$, 100 MHz, major isomers A and B) δ 209.9, 170.4, 170.3, 97.5, 73.8, 72.9, 71.6, 67.5, 48.1, 43.4, 41.5, 41.3, 38.6, 38.3, 37.3, 37.1, 31.9, 31.4, 26.7, 25.2, 25.1, 25.0, 23.23, 23.21, 10.9, 10.8, 10.3, 3.6; HRMS (ESI-TOF) *m/z*: $[M + Na]^+$ calcd for $C_{14}H_{27}NO_4SNa$ 328.1553, found 328.1560.

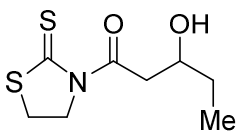

(±)-3-Hydroxy-1-(2-thioxothiazolidin-3-yl)pentan-1-one [(±)-3.27]. To a solution of thiazolidinethione **3.26** (1.06 g, 6.55 mmol, 1.00 equiv) in CH_2Cl_2 (30 mL) at –40 °C was added $TiCl_4$ (0.79 mL, 7.2 mmol, 1.1 equiv). Hünig's base (*i*-Pr_2NEt) (1.37 mL, 7.86 mmol, 1.20 equiv) was added after

stirring at –40 °C for 30 min. The reaction mixture was stirred at –40 °C for another 2 h, and then cooled to –78 °C. Freshly distilled propionaldehyde (0.851 mL, 11.8 mmol, 1.80 equiv) was added. The reaction was stirred at –78 °C for 3 h, quenched by addition of saturated aqueous NH_4Cl (40 mL) and allowed to warm up to room temperature. The organics were extracted with CH_2Cl_2 (3 × 40 mL), dried (Na_2SO_4), filtered, and concentrated under reduced pressure. Purification by flash chromatography (40% EtOAc/hexanes) afforded the title compound (825 mg, 57%) as a yellow oil: R_f = 0.14 (30% EtOAc/hexanes); ^{1}H NMR ($CDCl_3$, 400 MHz) δ 4.66–4.55 (m, 2H), 4.08–3.95 (m, 1H), 3.53 (dd, *J* = 17.6, 2.3 Hz, 1H), 3.35–3.24 (m, 3H), 2.87 (d, *J* = 3.9 Hz, 1H), 1.66–1.49 (m, 2H), 0.98 (t, *J* = 7.4 Hz, 3H); ^{13}C NMR ($CDCl_3$, 100 MHz) δ 201.9, 174.3, 69.5, 55.7, 45.4, 29.4, 28.3, 9.9; HRMS (ESI-TOF) *m/z*: $[M + Na]^+$ calcd for $C_8H_{13}NO_2S_2Na$ 242.0280, found 242.0281.

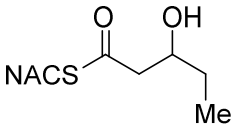

(±)-*S*-(2-Acetamidoethyl)-3-hydroxypentanethioate [(±)-3.12]. To a solution of thiazolidinethione (±)-**3.27** (821 mg, 3.74 mmol, 1.00 equiv) in CH_2Cl_2 (30 mL) at room temperature was added imidazole (763 mg, 11.2 mmol, 3.00 equiv) and *N*-acetylcysteamine (0.44 mL, 4.1 mmol, 1.1 equiv). The reaction was stirred at room temperature for 12 h, then quenched by the addition of saturated aqueous NH_4Cl (30 mL), and extracted with CH_2Cl_2 (3 × 20 mL). The combined organic layers were washed with saturated aqueous NaCl (40 mL), dried (Na_2SO_4), filtered, and concentrated under reduced pressure. Purification by flash chromatography (5% MeOH/CH_2Cl_2) afforded the title compound (566 mg, 69%) as a colorless oil: R_f = 0.24 (5% MeOH/CH_2Cl_2); ^{1}H NMR ($CDCl_3$, 400 MHz) δ 5.79 (s, 1H), 4.04–3.96 (m, 1H),

3.53–3.40 (m, 2H), 3.11–2.98 (m, 2H), 2.77 (dd, J = 15.4, 3.3 Hz, 1H), 2.68 (dd, J = 15.4, 8.7 Hz, 1H), 2.61 (s, 1H), 1.97 (s, 3H), 1.61–1.45 (m, 2H), 0.97 (t, J = 7.4 Hz, 3H); ^{13}C NMR ($CDCl_3$, 100 MHz) δ 199.6, 170.4, 70.1, 50.6, 39.3, 29.6, 28.9, 23.2, 9.8; HRMS (ESI-TOF) *m/z*: $[M + Na]^+$ calcd for $C_9H_{17}NO_3SNa$ 242.0821, found 242.0827.

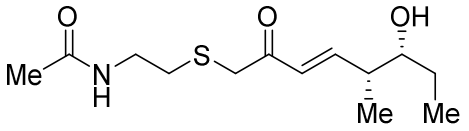

(5*R*,6*R*,*E*)-6-Hydroxy-5-methyl-1-[*N*-(2-acetamidoethyl)thio]oct-3-en-2-one (3.7). The enzymatic reaction was carried out with 4 mM diol **2.26** (5.8 mg, 0.020 mmol, 1.0 equiv, dissolved in 200 µL 1: 1 DMSO: H_2O) in 10% glycerol, 1.5 M NaCl, 0.5 M Tris (pH 8.0) and 40 µM PikKR2-DH2 (16.6 mg, 0.2 µmol, 1 mol%) in a total volume of 5 mL. The reaction mixture was shaken at room temperature at a speed of 150 rpm for 24 h and then extracted with EtOAc (5 × 10 mL). The organic layers were combined, washed with saturated aqueous NaCl (20 mL), dried (Na_2SO_4), filtered, and concentrated under reduced pressure. Since the enzymatic product and starting material had the same R_f values, seperation of enzymatic product was accomplished by converting the starting material to its acetonide. The enzymatic reaction residue was dissolved in CH_2Cl_2 (2 mL) and *O,O*-dimethoxypropane (25 µL) and PPTS (cat.) were added. After stirring at room temperature for 3 h, the reaction was quenched by the addition of saturated aqueous NH_4Cl (2 mL). The layers were separated and the aqueous layer was extracted with CH_2Cl_2 (3 × 5 mL). The combined organic layers were washed with saturated aqueous NaCl (10 mL), dried (Na_2SO_4), filtered and concentrated under reduced pressure. Purification by flash chromatography (5% MeOH/CH_2Cl_2) afforded the title compound (2.8 mg, 51%) as colorless oil: R_f = 0.23 (5% MeOH/CH_2Cl_2); $[\alpha]_D^{22}$ = 20.0 (*c* 0.0900,

$CHCl_3$); ^{1}H NMR ($CDCl_3$, 400 MHz) δ 6.97 (dd, *J* = 15.9, 7.6 Hz, 1H), 6.28 (dd, *J* = 15.9, 1.3 Hz, 1H), 6.04 (s, 1H), 3.58–3.51 (m, 1H), 3.48–3.36 (m, 4H), 2.66 (t, *J* = 6.3 Hz, 2H), 2.55–2.42 (m, 1H), 1.99 (s, 3H), 1.73 (s, 1H), 1.57–1.49 (m, 1H), 1.48–1.38 (m, 1H), 1.11 (d, *J* = 6.8 Hz, 3H), 0.98 (t, *J* = 7.4 Hz, 3H); ^{13}C NMR ($CDCl_3$, 100 MHz) δ 194.8, 170.2, 151.7, 127.9, 75.8, 42.4, 39.0, 38.4, 32.2, 27.4, 23.3, 13.6, 10.4; HRMS (ESI-TOF) *m/z*: $[M + Na]^+$ calcd for $C_{13}H_{23}NO_3SNa$ 296.1291, found 296.1292.

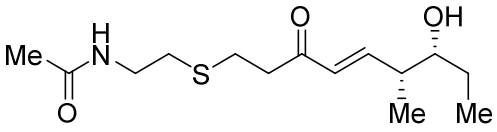

(6*R*,7*R*,*E*)-7-Hydroxy-6-methyl-1-[*N*-(2-acetamidoethyl)thio]non-4-en-3-one (3.8). The enzymatic reaction was carried out with 4 mM diol **2.27** (6.1 mg, 0.020 mmol, 1.0 equiv, dissolved in 200 μL 1: 1 DMSO: H_2O) in 10% glycerol, 1.5 M NaCl, 0.5 M Tris (pH 8.0) and 40 μM PikKR2-DH2 (16.6 mg, 0.2 μmol, 1 mol%) in a total volume of 5 mL. The reaction mixture was shaken at room temperature at a speed of 150 rpm for 24 h. The enzymatic product was extracted with EtOAc (5 × 10 mL) and the combined organic layers were washed with saturated aqueous NaCl (20 mL), dried (Na_2SO_4), filtered, and concentrated under reduced pressure. Purification by flash chromatography (5% MeOH/CH_2Cl_2) afforded the title compound (3.3 mg, 58%) as colorless oil: R_f = 0.21 (5% MeOH/CH_2Cl_2); $[\alpha]_D^{22}$ = 22.0 (*c* 0.100, $CHCl_3$); ^{1}H NMR ($CDCl_3$, 400 MHz) δ 6.94 (dd, *J* = 16.1, 7.6 Hz, 1H), 6.13 (dd, *J* = 16.1, 1.2 Hz, 1H), 6.02 (s, 1H), 3.58–3.50 (m, 1H), 3.45 (q, *J* = 6.3 Hz, 2H), 2.93–2.87 (m, 2H), 2.84–2.78 (m, 2H), 2.67 (t, *J* = 6.5 Hz, 2H), 2.47 (sext, *J* = 6.9 Hz, 1H), 2.02–1.97 (m, 4H), 1.59–1.47 (m, 1H), 1.46–1.35 (m, 1H), 1.09 (d, *J* = 6.8 Hz, 3H), 0.98 (t, *J* = 7.4 Hz, 3H); ^{13}C NMR ($CDCl_3$, 100 MHz) δ 198.5,

170.4, 150.7, 129.8, 75.8, 42.3, 39.7, 38.7, 31.9, 27.3, 25.8, 23.3, 13.5, 10.4; HRMS (ESI-TOF) *m/z*: $[M + Na]^+$ calcd for $C_{14}H_{25}NO_3SNa$ 310.1447, found 310.1438.

3.9. Experimental Section of Biology

General biology procedures. All chemical reagents were purchased from Sigma-Aldrich and were used directly without further purification. *E. coli* BL21(DE3) cells were from New England BioLabs. IPTG was acquired through Gold Biotechnology. His60 Ni Superflow resin was purchased from Clontech Laboratories, Inc. OD_{600} was measured on an Eppendorf BioPhotometer. Sonication was carried out by Branson Sonifier 450. Gel filtration purification was performed on HiLoad 16/600 Superdex 200 pg column (GE). The protein mass spectra data was obtained by Bruker BioTOF II mass spectrometer. LC–MS/MS was conducted with AB Sciex QTRAP 5500 mass spectrometer and Shimadzu LC system.

Cloning and mutagenesis. The PikKR2-DH2 didomain was cloned from the cosmid pLZ51 into the expression vector pMCSG7[158] using ligation independent cloning (LIC). PikKR2-DH2 forward primer: 5'-**TACTTCCAATCCAATGCC**AGCCGCGTCGGCGGG-3'; PikKR2-DH2 reverse primer: 5'-**TTATCCACTTCCAATGCTA**CGGCCGGGCCCGG-3' (LIC-overhangs in **bold**; inserted stop codon underlined). The insert was confirmed via sequencing. Primers for the F3746L, F3750L, and F3750Y variants were designed via the QuickChange primer design tool website (Agilent) (Table 7). Mutagenesis was run using the standard protocol provided with the QuickChange Lightning Site Directed Mutagenesis kit

(Agilent). Mutated codons are underlined below. All mutations were confirmed via sequencing.

Table 7. Primers of mutants F3746L, F3750L, and F3750Y.

Mutant	Primers (5' – 3')
F3746L	gaacagcggacctaaggcgaggccgtt aacggcctcgccttaggtccgctgttc
F3750L	cagcccctgtaacagcggaccgaagg ccttcggtccgctgttacaggggctg
F3750Y	gcgttcagcccctgatacagcggaccgaag cttcggtccgctgtatcaggggctgaacgc

Protein expression and purification. Competent *E. coli* BL21 (DE3) cells were transformed with pMCSG7 containing PikKR2-DH2 and grown in Terrific Broth (TB) media with 100 μg/mL ampicillin at 37 °C until OD_{600} reached to 1.2. The cultures were cooled to 20 °C and 200 μM IPTG was added to induce protein expression. After overnight expression, cells were harvested by centrifugation at 6,000*g* and 4 °C for 10 min. The resulting cell pellet was frozen at –80 °C for 10 min, resuspended in lysis buffer (50 mM HEPES, 300 mM NaCl, 10 mM imidazole, pH 8.0) and lysed by sonication. After centrifuging at 50,000*g* and 4 °C for 10 min, the cleared lysate was incubated with His-60 Ni superflow resin (2 mL) at 4 °C for 1 h and then loaded onto a gravity column. The column was washed with 14 mL of wash buffer (10 mM imidazole, 50 mM HEPES, 300 mM NaCl, pH 8.0) and eluted with 2.5 mL elution buffer (500 mM imidazole, 50 mM HEPES, 300 mM NaCl, pH 8.0). The protein was further purified via size exclusion chromatography on a Superdex 16/600 200pg gel filtration column eluting at 0.5 mL min^{-}

[1] with 50 mM sodium phosphate (pH 7.1) and 150 mM NaCl. Purified protein was stored in storage buffer (50 mM Tris, 150 mM NaCl, 10% (v/v) glycerol, pH 8.0) at –80 °C. Protein concentration was determined using the Bio-Rad protein assay kit with bovine serum albumin as the standard. Exact molecular weight of the purified monomeric protein was determined by ESI mass spectrometry. All the mutants were expressed and purified in an analogous way.

Determination of initial velocity conditions. Substrate **2.27** (6 mM) was incubated with PikDH2-KR2 (1.25–10 μM) and reaction buffer (50 mM Tris, 150 mM NaCl, pH 8.0) in a total volume of 50 μL at 25 °C. At 2, 5, 10, 20 and 40 min time points, 5 μL of the reaction mixture was added to 495 μL of 1:1 MeCN–reaction buffer (100-fold dilution) to quench the reaction. The resulting solution was vortexed, centrifuged. 60 μL of the diluted reaction solution was added to a HPLC vial with 10 μL of internal standard **3.7** (320 nM) and analyzed by LC-MS/MS (Table 8) employing a Kinetix reverse-phase C_{18} column (50 mm × 2.1 mm, 2.6 μm, Phenomenex) operated at 0.4 mL min^{-1} with a gradient between mobile phase A (15 mM ammonium acetate in H_2O) and mobile phase B (MeCN). The gradient program was 0 min, 5% B; 2 min, 5% B; 7 min, 55% B; 8 min, 95% B; 9 min, 95% B; 9.5 min, 5% B; 12 min, 5% B. Standard curve of enzymatic product **3.8** was generated by injecting the authentic standard at varying concentrations with a fixed concentration of an internal standard **3.7**. The amount of enzymatic product formation at each time point was calculated by plotting the area ratio (analyte/internal standard) into the standard curve. Each reaction was performed in duplicate. The progress

curve at varying enzyme concentrations was generated and the initial velocity at each enzyme concentration was obtained.

Table 8. LC-MS/MS analysis of analytes **2.26**, **2.27**, **3.7** and **3.8**.

Analyte	HPLC retention time (min)	Transition	Internal standard
2.26	4.69	314→198	**2.27**
2.27	4.45, 4.99	328→212	**2.26**
3.7	4.74	274→216	**3.8**
3.8	4.99	288→120	**3.7**

Reversibility of the dehydration reaction. Compounds **2.26**, **2.27**, **3.7** and **3.8** (1 mM) were individually added to the reaction buffer (50 mM Tris, 150 mM NaCl, pH 8.0) with PikDH2-KR2 (10 μM) in a total volume of 100 μL, respectively. After 20 h incubation, 5 μL of the reaction mixture was quenched by adding to 495 μL of 1:1 MeCN–reaction buffer (100-fold dilution). 10 μL of the diluted reaction mixture was added to 90 μL of 1:1 MeCN–reaction buffer (10-fold dilution, total 1000-fold dilution). The identities of the enzymatic products were determined by authentic standards and total amount was calculated by standard curve with internal standard added in. Each reaction was performed in duplicate.

Kinetic analysis of dehydration reaction by LC-MS/MS. The enzymatic reactions were carried out in a total volume of 50 μL under initial velocity conditions containing PikDH2-KR2 (5 μM), reaction buffer (50 mM Tris, 150 mM NaCl, pH 8.0) and substrates **2.26** or **2.27** at variable concentrations (0.25, 0.5, 1, 2, 3, 4, 6 mM). The final DMSO concentration was held constant at 3%. After incubation at 25 °C for 15 min, 5

μL of the reaction mixture was added to 495 μL of 1:1 MeCN–reaction buffer (100-fold dilution). The resulting solution was vortexed, centrifuged and analyzed by LC-MS/MS as described above. Control reactions for each concentration of substrate were performed without the addition of enzyme. Each reaction was performed in duplicate. Apparent steady-state kinetic parameters were determined by fitting the normalized v_0 vs [*S*] plots to the Michaelis–Menten equation by nonlinear regression analysis using GraphPad Prism 5.0. Kinetic parameters of PikDH2-KR2 mutants were acquired in an analogous way except in some cases saturation was not achieved and the curve was fit by linear regression to provide specificity constant.

Homology model of PikDH2. The PikDH2 homology model (residues 1-293 of the PikKR2-DH2 didomain) was built in LOMETS[159] using the CurK dehydratase from the curacin pathway as a template (PDB 3KG9).[131] The PikDH2 model has an RMSD of 0.290 Å compared to the template, with a Z-score of 27.3 and 22% sequence identity.

pH dependency profile of PikDH2. The effect of pH on kinetic parameters was obtained by using HEPES (pH 6.6–7.5), Tris (pH 8.0), and bicine (pH 8.5–9.0). At desired pH values, enzymatic reactions were conducted with substrate **2.27** (0–3 mM) under the conditions described above. Kinetic parameters V_{max}/K_M at different pH were obtained via fitting the v_0 vs [*S*] plots to by linear regression analysis. The pK_a value of the ionizable group was obtained through fitting V_{max}/K_M to eq 1:

$$\log\frac{V_{max}}{K_M} = \log\frac{C}{1-[H]^+/K_a} \quad (1)$$

where, C is the pH-independent plateau value, $[H]^+$ is the hydrogen ion concentration, and K_a is the dissociation constant of the acid.[160]

Inhibition assay with mechanism-based inhibitor 3.28. Inhibitor **3.28** (10–40 μM) was incubated with substrate **2.27** (5 mM), PikDH2-KR2 (5 μM), reaction buffer (50 mM Tris, 150 mM NaCl, pH 8.0) in a total volume of 50 μL at 25 °C. At 2, 4, 8, 16 min time points, 5 μL of the reaction mixture was added to 495 μL of 1:1 MeCN–reaction buffer (100-fold dilution). The resulting solution was vortexed, centrifuged and analyzed by LC-MS/MS to detect the enzymatic product formation. Each reaction was conducted in duplicate. Inhibitor **6** showed time-dependent inhibition of PikDH2. The progress curve (Figure 4B) was fit to eq 2 and eq 3 for tight binding time-dependent inhibition:

$$[P] = v_s t + \frac{(1-\gamma)(v_i - v_s)}{\gamma k_{obs}} \ln \frac{1-\exp(-k_{obs} t)}{1-\gamma} \quad (2)$$

$$\gamma = \frac{[E]}{[I]} \left(1 - \frac{v_s}{v_i}\right)^2 \quad (3)$$

where $[P]$ is the concentration of enzymatic product, t is the reaction time, v_i is the initial velocity, v_s is the steady state velocity, and k_{obs} is the observed rate constant of inhibition. Since mechanism-based inhibition is irreversible, the v_s value is equal to 0, thus the γ value is equal to the ratio of enzyme concentration to inhibitor concentration. The secondary plot of $1/k_{obs}$ versus 1/[I] was fit to a Kitz and Wilson plot (Figure 29) to provide $K_{I,app}$ and k_{inact} values. The true K_I value was deduced from eq 4:

$$K_{I,app} = \frac{K_I}{1+[S]/K_M} \quad (4)$$

where [S] is the substrate concentration, and K_M is the Michaelis-Menten constant for the substrate.

References

1. Newman, D. J.; Cragg, G. M. Natural products as sources of new drugs over the 30 years from 1981 to 2010. *J. Nat. Prod.* **2012**, 75, 311–335.

2. Staunton, J.; Weissman, K. J. Polyketide biosynthesis: a millennium review. *Nat. Prod. Rep.* **2001**, 18, 380–416.

3. Weissman, K. J. Chapter 1 introduction to polyketide biosynthesis. In *Methods in Enzymology*, David, A. H., Ed. Academic Press: 2009; Vol. Volume 459, pp 3–16.

4. Smith, S.; Tsai, S.-C. The type I fatty acid and polyketide synthases: a tale of two megasynthases. *Nat. Prod. Rep.* **2007**, 24, 1041–1072.

5. Smith, J. L.; Sherman, D. H. Biochemistry. An enzyme assembly line. *Science* **2008**, 321, 1304–1305.

6. Fischbach, M. A.; Walsh, C. T. Assembly-line enzymology for polyketide and nonribosomal peptide antibiotics: Logic, Machinery, and Mechanisms. *Chem. Rev.* **2006**, 106, 3468–3496.

7. Ben, S.; Yi-Qiang, C.; Steven, D. C.; Hui, J.; Jianhua, J.; Hyung-Jin, K.; Si-Kyu, L.; Wen, L.; Koichi, N.; Jeong-Woo, S.; Wyatt, C. S.; Scott, S.; Gong-Li, T.; Steven Van, L.; Jian, Z. Polyketide biosynthesis beyond the type I, II, and III polyketide synthase paradigms: A progress report. In *Polyketides*, American Chemical Society: 2007; Vol. 955, pp 154–166.

8. Shen, B. Polyketide biosynthesis beyond the type I, II and III polyketide synthase paradigms. *Curr. Opin. Chem. Biol.* **2003**, 7, 285–295.

9. Kwan, D. H.; Schulz, F. The stereochemistry of complex polyketide biosynthesis by modular polyketide synthases. *Molecules* **2011**, 16, 6092–6115.

10. Keatinge-Clay, A. T. The structures of type I polyketide synthases. *Nat. Prod. Rep.* **2012**, 29, 1050–1073.

11. Xue, Y. Q.; Zhao, L. S.; Liu, H. W.; Sherman, D. H. A gene cluster for macrolide antibiotic biosynthesis in Streptomyces venezuelae: Architecture of metabolic diversity. *Proc. Natl. Acad. Sci. U.S.A.* **1998**, 95, 12111–12116.

12. Beck, B. J.; Aldrich, C. C.; Fecik, R. A.; Reynolds, K. A.; Sherman, D. H. Substrate recognition and channeling of monomodules from the pikromycin polyketide synthase. *J. Am. Chem. Soc.* **2003**, 125, 12551–12557.

13. Kittendorf, J. D.; Sherman, D. H. The methymycin/pikromycin pathway: A model for metabolic diversity in natural product biosynthesis. *Bioorg. Med. Chem.* **2009**, 17, 2137–2146.

14. Dutta, S.; Whicher, J. R.; Hansen, D. A.; Hale, W. A.; Chemler, J. A.; Congdon, G. R.; Narayan, A. R. H.; Hakansson, K.; Sherman, D. H.; Smith, J. L.; Skiniotis, G. Structure of a modular polyketide synthase. *Nature* **2014**, 510, 512–517.

15. Zhang, Q.; Pang, B.; Ding, W.; Liu, W. Aromatic polyketides produced by bacterial iterative type I polyketide synthases. *ACS Catal.* **2013**, 3, 1439–1447.

16. Hertweck, C.; Luzhetskyy, A.; Rebets, Y.; Bechthold, A. Type II polyketide synthases: gaining a deeper insight into enzymatic teamwork. *Nat. Prod. Rep.* **2007**, 24, 162–190.

17. Pickens, L. B.; Tang, Y. Decoding and engineering tetracycline biosynthesis. *Metab. Eng.* **2009**, 11, 69–75.

18. Yu, D.; Xu, F.; Zeng, J.; Zhan, J. Type III polyketide synthases in natural product biosynthesis. *IUBMB Life* **2012**, 64, 285–295.

19. Gao, X.; Woo, S. K.; Krische, M. J. Total synthesis of 6-deoxyerythronolide B via C–C bond-forming transfer hydrogenation. *J. Am. Chem. Soc.* **2013**, 135, 4223–4226.

20. Magauer, T.; Smaltz, D. J.; Myers, A. G. Component-based syntheses of trioxacarcin A, DC-45-A1 and structural analogues. *Nat. Chem.* **2013**, 5, 886–893.

21. Woerly, E. M.; Roy, J.; Burke, M. D. Synthesis of most polyene natural product motifs using just twelve building blocks and one coupling reaction. *Nat. Chem.* **2014**, 6, 484–491.

22. Weissman, K. J.; Leadlay, P. F. Combinatorial biosynthesis of reduced polyketides. *Nature Rev. Microbiol.* **2005**, 3, 925–936.

23. Wong, F. T.; Khosla, C. Combinatorial biosynthesis of polyketides--a perspective. *Curr. Opin. Chem. Biol.* **2012**, 16, 117–123.

24. Gaisser, S.; Kellenberger, L.; Kaja, A. L.; Weston, A. J.; Lill, R. E.; Wirtz, G.; Kendrew, S. G.; Low, L.; Sheridan, R. M.; Wilkinson, B.; Galloway, I. S.; Stutzman-Engwall, K.; McArthur, H. A. I.; Staunton, J.; Leadlay, P. F. Direct production of ivermectin-like drugs after domain exchange in the avermectin polyketide synthase of Streptomyces avermitilis ATCC31272. *Org. Biomol. Chem.* **2003**, 1, 2840–2847.

25. McDaniel, R.; Thamchaipenet, A.; Gustafsson, C.; Fu, H.; Betlach, M.; Ashley, G. Multiple genetic modifications of the erythromycin polyketide synthase to produce a library of novel "unnatural" natural products. *Proc. Natl. Acad. Sci. U. S. A.* **1999**, 96, 1846–1851.

26. Zheng, J.; Piasecki, S. K.; Keatinge-Clay, A. T. Structural studies of an A2-type modular polyketide synthase ketoreductase reveal features controlling alpha-substituent stereochemistry. *ACS Chem. Biol.* **2013**, 8, 1964–1971.

27. Hunsdiecker, H.; Erlbach, H. Beiträge zur Kenntnis makrocyclischer Ringsysteme, V, Mitteil.: Eine besonders ergiebige Darstellung der Lactone mit 10-18 Ringgliedern sowie einiger Ketolactone und eines Isoambrettolids. *Chem. Ber.* **1947**, 80, 129–137.

28. Woodward, R. B.; Bader, F. E.; Bickel, H.; Frey, A. J.; Kierstead, R. W. The total synthesis of reserpine. *J. Am. Chem. Soc.* **1956**, 78, 2023–2025.

29. Corey, E. J.; Nicolaou, K. C. Efficient and mild lactonization method for the synthesis of macrolides. *J. Am. Chem. Soc.* **1974**, 96, 5614–5616.

30. Inanaga, J.; Hirata, K.; Saeki, H.; Katsuki, T.; Yamaguchi, M. A rapid esterification by means of mixed anhydride and its application to large-ring lactonization. *Bull. Chem. Soc. Jpn.* **1979**, 52, 1989–1993.

31. Shiina, I.; Kubota, M.; Ibuka, R. A novel and efficient macrolactonization of ω-hydroxycarboxylic acids using 2-methyl-6-nitrobenzoic anhydride (MNBA). *Tetrahedron Lett.* **2002**, 43, 7535–7539.

32. Kaiho, T.; Masamune, S.; Toyoda, T. Macrolide synthesis: narbonolide. *J. Org. Chem.* **1982**, 47, 1612–1614.

33. Corey, E. J.; Hua, D. H.; Pan, B. C.; Seitz, S. P. Total synthesis of aplasmomycin. *J. Am. Chem. Soc.* **1982**, 104, 6818–6820.

34. Kruizinga, W. H.; Kellogg, R. M. Preparation of macrocyclic lactones by ring closure of cesium carboxylates. *J. Am. Chem. Soc.* **1981**, 103, 5183–5189.

35. Kurihara, T.; Nakajima, Y.; Mitsunobu, O. Synthesis of lactones and cycloalkanes. Cyclization of ω-hydroxy acids and ethyl α-cyano-ω-hydroxycarboxylates. *Tetrahedron Lett.* **1976**, 17, 2455–2458.

36. Hoye, T. R.; Hu, M. Macrolactonization via Ti(IV)-mediated epoxy-acid coupling: A total synthesis of (−)-dactylolide [and zampanolide]. *J. Am. Chem. Soc.* **2003**, 125, 9576–9577.

37. Stang, E. M.; Christina White, M. Total synthesis and study of 6-deoxyerythronolide B by late-stage C–H oxidation. *Nat. Chem.* **2009**, 1, 547–551.

38. Lee, K.; Kim, H.; Hong, J. N-Heterocyclic carbene catalyzed oxidative macrolactonization: Total synthesis of (+)-dactylolide. *Angew. Chem. Int. Ed.* **2012**, 51, 5735–5738.

39. Trauger, J. W.; Kohli, R. M.; Mootz, H. D.; Marahiel, M. A.; Walsh, C. T. Peptide cyclization catalysed by the thioesterase domain of tyrocidine synthetase. *Nature* **2000**, 407, 215–218.

40. Kohli, R. M.; Walsh, C. T.; Burkart, M. D. Biomimetic synthesis and optimization of cyclic peptide antibiotics. *Nature* **2002**, 418, 658–661.

41. Boddy, C. N.; Schneider, T. L.; Hotta, K.; Walsh, C. T.; Khosla, C. Epothilone C macrolactonization and hydrolysis are catalyzed by the isolated thioesterase domain of epothilone polyketide synthase. *J. Am. Chem. Soc.* **2003**, 125, 3428–3429.

42. Aldrich, C. C.; Beck, B. J.; Fecik, R. A.; Sherman, D. H. Biochemical investigation of pikromycin biosynthesis employing native penta- and hexaketide chain elongation intermediates. *J. Am. Chem. Soc.* **2005**, 127, 8441–8452.

43. Aldrich, C. C.; Venkatraman, L.; Sherman, D. H.; Fecik, R. A. Chemoenzymatic synthesis of the polyketide macrolactone 10-deoxymethynolide. *J. Am. Chem. Soc.* **2005**, 127, 8910–8911.

44. He, W.; Wu, J.; Khosla, C.; Cane, D. E. Macrolactonization to 10-deoxymethynolide catalyzed by the recombinant thioesterase of the picromycin/methymycin polyketide synthase. *Bioorg. Med. Chem. Lett.* **2006**, 16, 391–394.

45. Mortison, J. D.; Kittendorf, J. D.; Sherman, D. H. Synthesis and biochemical analysis of complex chain-elongation intermediates for interrogation of molecular

specificity in the erythromycin and pikromycin polyketide synthases. *J. Am. Chem. Soc.* **2009**, 131, 15784–15793.

46. Mortison, J. D.; Sherman, D. H. Frontiers and opportunities in chemoenzymatic synthesis. *J. Org. Chem.* **2010**, 75, 7041–7051.

47. Hansen, D. A.; Koch, A. A.; Sherman, D. H. Substrate controlled divergence in polyketide synthase catalysis. *J. Am. Chem. Soc.* **2015**, 137, 3735–3738.

48. Hansen, D. A.; Rath, C. M.; Eisman, E. B.; Narayan, A. R. H.; Kittendorf, J. D.; Mortison, J. D.; Yoon, Y. J.; Sherman, D. H. Biocatalytic synthesis of pikromycin, methymycin, neomethymycin, novamethymycin, and ketomethymycin. *J. Am. Chem. Soc.* **2013**, 135, 11232–11238.

49. Pinto, A.; Wang, M.; Horsman, M.; Boddy, C. N. 6-Deoxyerythronolide B synthase thioesterase-catalyzed macrocyclization is highly stereoselective. *Org. Lett.* **2012**, 14, 2278–2281.

50. Hari, T. P. A.; Labana, P.; Boileau, M.; Boddy, C. N. An evolutionary model encompassing substrate specificity and reactivity of type I polyketide synthase thioesterases. *ChemBioChem* **2014**, 15, 2656–2661.

51. Wang, M.; Zhou, H.; Wirz, M.; Tang, Y.; Boddy, C. N. A thioesterase from an iterative fungal polyketide synthase shows macrocyclization and cross coupling activity and may play a role in controlling iterative cycling through product offloading. *Biochemistry* **2009**, 48, 6288–6290.

52. Heberlig, G. W.; Wirz, M.; Wang, M.; Boddy, C. N. Resorcylic acid lactone biosynthesis relies on a stereotolerant macrocyclizing thioesterase. *Org. Lett.* **2014,** 16, 5858–5861.

53. Kudo, F.; Kitayama, T.; Kakinuma, K.; Eguchi, T. Macrolactam formation catalyzed by the thioesterase domain of vicenistatin polyketide synthase. *Tetrahedron Lett.* **2006**, 47, 1529–1532.

54. Kudo, F.; Asou, Y.; Watanabe, M.; Kitayama, T.; Eguchi, T. Potent oligomerization and macrocyclization activity of the thioesterase domain of vicenistatin polyketide synthase. *Synlett* **2012**, 23, 1843–1846.

55. Piasecki, S. K.; Taylor, C. A.; Detelich, J. F.; Liu, J. N.; Zheng, J. T.; Komsoukaniants, A.; Siegel, D. R.; Keatinge-Clay, A. T. Employing modular polyketide

synthase ketoreductases as biocatalysts in the preparative chemoenzymatic syntheses of diketide chiral building blocks. *Chem. Biol.* **2011**, 18, 1331-1340.

56. Diels, O.; Alder, K. Synthesen in der hydroaromatischen Reihe. *Liebigs Ann.* **1928**, 460, 98–122.

57. Nicolaou, K. C.; Snyder, S. A.; Montagnon, T.; Vassilikogiannakis, G. The Diels–Alder reaction in total synthesis. *Angew. Chem. Int. Ed.* **2002**, 41, 1668–1698.

58. Watanabe, K.; Mie, T.; Ichihara, A.; Oikawa, H.; Honma, M. Detailed reaction mechanism of macrophomate synthase: Extraordinary enzyme catalyzing five-step transformation from 2-pyrones to benzoates.. *J. Biol. Chem.* **2000**, 275, 38393–38401.

59. Ose, T.; Watanabe, K.; Mie, T.; Honma, M.; Watanabe, H.; Yao, M.; Oikawa, H.; Tanaka, I. Insight into a natural Diels-Alder reaction from the structure of macrophomate synthase. *Nature* **2003**, 422, 185–189.

60. Oikawa, H.; Katayama, K.; Suzuki, Y.; Ichihara, A. Enzymatic activity catalysing exo-selective Diels-Alder reaction in solanapyrone biosynthesis. *Chem. Commun.* **1995**, 1321–1322.

61. Kasahara , K.; Miyamoto, T.; Fujimoto, T.; Oguri, H.; Tokiwano , T.; Oikawa, H.; Ebizuka, Y.; Fujii, I. Solanapyrone synthase, a possible Diels–Alderase and iterative type I polyketide synthase encoded in a biosynthetic gene cluster from Alternaria solani. *ChemBioChem* **2010**, 11, 1245–1252.

62. Auclair, K.; Sutherland, A.; Kennedy, J.; Witter, D. J.; Van den Heever, J. P.; Hutchinson, C. R.; Vederas, J. C. Lovastatin nonaketide synthase catalyzes an intramolecular Diels−Alder reaction of a substrate analogue. *J. Am. Chem. Soc.* **2000**, 122, 11519–11520.

63. Ma, S. M.; Li, J. W.-H.; Choi, J. W.; Zhou, H.; Lee, K. K. M.; Moorthie, V. A.; Xie, X.; Kealey, J. T.; Da Silva, N. A.; Vederas, J. C.; Tang, Y. Complete reconstitution of a highly reducing iterative polyketide synthase. *Science* **2009**, 326, 589–592.

64. Kim, H. J.; Ruszczycky, M. W.; Choi, S.-h.; Liu, Y.-n.; Liu, H.-w. Enzyme-catalysed [4+2] cycloaddition is a key step in the biosynthesis of spinosyn A. *Nature* **2011**, 473, 109–112.

65. Kim, H. J.; Choi, S.-h.; Jeon, B.-s.; Kim, N.; Pongdee, R.; Wu, Q.; Liu, H.-w. Chemoenzymatic synthesis of spinosyn A. *Angew. Chem. Int. Ed.* **2014**, 53, 13553–13557.

66. Hashimoto, T.; Hashimoto, J.; Teruya, K.; Hirano, T.; Shin-ya, K.; Ikeda, H.; Liu, H.-w.; Nishiyama, M.; Kuzuyama, T. Biosynthesis of Versipelostatin: Identification of an enzyme-catalyzed [4+2]-cycloaddition required for macrocyclization of spirotetronate-containing polyketides. *J. Am. Chem. Soc.* **2015**, 137, 572–575.

67. Tian, Z.; Sun, P.; Yan, Y.; Wu, Z.; Zheng, Q.; Zhou, S.; Zhang, H.; Yu, F.; Jia, X.; Chen, D.; Mándi, A.; Kurtán, T.; Liu, W. An enzymatic [4+2] cyclization cascade creates the pentacyclic core of pyrroindomycins. *Nat. Chem. Biol.* **2015**, 11, 259–265.

68. Hilvert, D.; Hill, K. W.; Nared, K. D.; Auditor, M. T. M. Antibody catalysis of the Diels-Alder reaction. *J. Am. Chem. Soc.* **1989**, 111, 9261–9262.

69. Fage, C. D.; Isiorho, E. A.; Liu, Y.; Wagner, D. T.; Liu, H.-w.; Keatinge-Clay, A. T. The structure of SpnF, a standalone enzyme that catalyzes [4 + 2] cycloaddition. *Nat. Chem. Biol.* **2015**, 11, 256–258.

70. Vieweg, L.; Reichau, S.; Schobert, R.; Leadlay, P. F.; Sussmuth, R. D. Recent advances in the field of bioactive tetronates. *Nat. Prod. Rep.* **2014**, 31, 1554–1584.

71. Oikawa, H.; Kobayashi, T.; Katayama, K.; Suzuki, Y.; Ichihara, A. Total synthesis of (−)-solanapyrone A via ezymatic Diels−Alder reaction of prosolanapyrone. *J. Org. Chem.* **1998**, 63, 8748–8756.

72. Witter, D. J.; Vederas, J. C. Putative Diels−Alder-catalyzed cyclization during the biosynthesis of lovastatin. *J. Org. Chem.* **1996**, 61, 2613–2623.

73. Hoye, T. R.; Suhadolnik, J. C. Symmetry-assisted synthesis of triepoxide stereoisomers of E,Z,E,-dodeca-2,6,10-trien-1,12-diol and their cascade reactions to 2,5-linked bistetrahydrofurans. *J. Am. Chem. Soc.* **1985**, 107, 5312–5313.

74. Xiong, Z.; Corey, E. J. Simple enantioselective total synthesis of glabrescol, a chiral C2-symmetric pentacyclic oxasqualenoid. *J. Am. Chem. Soc.* **2000**, 122, 9328–9329.

75. Valentine, J. C.; McDonald, F. E.; Neiwert, W. A.; Hardcastle, K. I. Biomimetic synthesis of trans,syn,trans-fused polyoxepanes: Remarkable substituent effects on the

endo-regioselective oxacyclization of polyepoxides. *J. Am. Chem. Soc.* **2005**, 127, 4586–4587.

76. Cane, D. E.; Celmer, W. D.; Westley, J. W. Unified stereochemical model of polyether antibiotic structure and biogenesis. *J. Am. Chem. Soc.* **1983**, 105, 3594–3600.

77. Shichijo, Y.; Migita, A.; Oguri, H.; Watanabe, M.; Tokiwano, T.; Watanabe, K.; Oikawa, H. Epoxide hydrolase Lsd19 for polyether formation in the biosynthesis of lasalocid A: Direct experimental evidence on polyene-polyepoxide hypothesis in polyether biosynthesis. *J. Am. Chem. Soc.* **2008**, 130, 12230–12231.

78. Minami, A.; Migita, A.; Inada, D.; Hotta, K.; Watanabe, K.; Oguri, H.; Oikawa, H. Enzymatic epoxide-opening cascades catalyzed by a pair of epoxide hydrolases in the ionophore polyether biosynthesis. *Org. Lett.* **2011**, 13, 1638–1641.

79. Hotta, K.; Chen, X.; Paton, R. S.; Minami, A.; Li, H.; Swaminathan, K.; Mathews, I. I.; Watanabe, K.; Oikawa, H.; Houk, K. N.; Kim, C.-Y. Enzymatic catalysis of anti-Baldwin ring closure in polyether biosynthesis. *Nature* **2012**, 483, 355–358.

80. Matsuura, Y.; Shichijo, Y.; Minami, A.; Migita, A.; Oguri, H.; Watanabe, M.; Tokiwano, T.; Watanabe, K.; Oikawa, H. Intriguing substrate tolerance of epoxide hydrolase Lsd19 Involved in biosynthesis of the ionophore antibiotic lasalocid A. *Org. Lett.* **2010**, 12, 2226–2229.

81. Richter, M. E. A.; Traitcheva, N.; Knüpfer, U.; Hertweck, C. Sequential asymmetric polyketide heterocyclization catalyzed by a single cytochrome P450 monooxygenase (AurH). *Angew. Chem. Int. Ed.* **2008**, 47, 8872–8875.

82. Werneburg, M.; Busch, B.; He, J.; Richter, M. E. A.; Xiang, L.; Moore, B. S.; Roth, M.; Dahse, H.-M.; Hertweck, C. Exploiting enzymatic promiscuity to engineer a focused library of highly selective antifungal and antiproliferative aureothin analogues. *J. Am. Chem. Soc.* **2010**, 132, 10407–10413.

83. Henrot, M.; Richter, M. E. A.; Maddaluno, J.; Hertweck, C.; De Paolis, M. Convergent asymmetric synthesis of (+)-aureothin employing an oxygenase-mediated resolution step. *Angew. Chem. Int. Ed.* **2012**, 51, 9587–9591.

84. Zocher, G.; Richter, M. E. A.; Mueller, U.; Hertweck, C. Structural fine-tuning of a multifunctional cytochrome P450 monooxygenase. *J. Am. Chem. Soc.* **2011**, 133, 2292–2302.

85. Savile, C. K.; Janey, J. M.; Mundorff, E. C.; Moore, J. C.; Tam, S.; Jarvis, W. R.; Colbeck, J. C.; Krebber, A.; Fleitz, F. J.; Brands, J.; Devine, P. N.; Huisman, G. W.; Hughes, G. J. Biocatalytic asymmetric synthesis of chiral amines from ketones applied to sitagliptin manufacture. *Science* **2010**, 329, 305–309.

86. Coelho, P. S.; Brustad, E. M.; Kannan, A.; Arnold, F. H. Olefin cyclopropanation via carbene transfer catalyzed by engineered cytochrome P450 enzymes. *Science* **2013**, 339, 307–310.

87. Coelho, P. S.; Wang, Z. J.; Ener, M. E.; Baril, S. A.; Kannan, A.; Arnold, F. H.; Brustad, E. M. A serine-substituted P450 catalyzes highly efficient carbene transfer to olefins in vivo. *Nat. Chem. Biol.* **2013**, 9, 485–487.

88. Zheng, J. T.; Keatinge-Clay, A. T. The status of type I polyketide synthase ketoreductases. *Med. Chem. Commun.* **2013**, 4, 34-40.

89. Keatinge-Clay, A. T.; Stroud, R. M. The structure of a ketoreductase determines the organization of the beta-carbon processing enzymes of modular polyketide synthases. *Structure* **2006**, 14, 737–748.

90. Keatinge-Clay, A. T. A tylosin ketoreductase reveals how chirality is determined in polyketides. *Chem. Biol.* **2007**, 14, 898–908.

91. Zheng, J. T.; Taylor, C. A.; Piasecki, S. K.; Keatinge-Clay, A. T. Structural and functional analysis of A-type ketoreductases from the amphotericin modular polyketide synthase. *Structure* **2010**, 18, 913–922.

92. Zheng, J.; Keatinge-Clay, A. T. Structural and functional analysis of C2-type ketoreductases from modular polyketide synthases. *J. Mol. Biol.* **2011**, 410, 105–117.

93. Zheng, J. T.; Gay, D. C.; Demeler, B.; White, M. A.; Keatinge-Clay, A. T. Divergence of multimodular polyketide synthases revealed by a didomain structure. *Nat. Chem. Biol.* **2012**, 8, 615–621.

94. Bonnett, S. A.; Whicher, J. R.; Papireddy, K.; Florova, G.; Smith, J. L.; Reynolds, K. A. Structural and stereochemical analysis of a modular plyketide synthase ketoreductase domain required for the generation of a cis-alkene. *Chem. Biol.* **2013**, 20, 772–783.

95. Valenzano, C. R.; Lawson, R. J.; Chen, A. Y.; Khosla, C.; Cane, D. E. The biochemical basis for stereochemical control in polyketide biosynthesis. *J. Am. Chem. Soc.* **2009**, 131, 18501–18511.

96. Garg, A.; Khosla, C.; Cane, D. E. Coupled methyl group epimerization and reduction by polyketide synthase ketoreductase domains. Ketoreductase-catalyzed equilibrium isotope exchange. *J. Am. Chem. Soc.* **2013**, 135, 16324-16327.

97. Caffrey, P.; Lynch, S.; Flood, E.; Finnan, S.; Oliynyk, M. Amphotericin biosynthesis in Streptomyces nodosus: Deductions from analysis of polyketide synthase and late genes. *Chem. Biol.* **2003**, 10, 93-94.

98. Caffrey, P. Conserved amino acid residues correlating with ketoreductase stereospecificity in modular polyketide synthases. *ChemBioChem* **2003**, 4, 654–657.

99. Kwan, D. H.; Tosin, M.; Schlager, N.; Schulz, F.; Leadlay, P. F. Insights into the stereospecificity of ketoreduction in a modular polyketide synthase. *Org. Biomol. Chem.* **2011**, 9, 2053–2056.

100. You, Y. O.; Khosla, C.; Cane, D. E. Stereochemistry of reductions catalyzed by methyl-epimerizing ketoreductase domains of polyketide synthases. *J. Am. Chem. Soc.* **2013**, 135, 7406–7409.

101. Wu, J. Q.; Zaleski, T. J.; Valenzano, C.; Khosla, C.; Cane, D. E. Polyketide double bond biosynthesis. Mechanistic analysis of the dehydratase-containing module 2 of the picromycin/methymycin polyketide synthase. *J. Am. Chem. Soc.* **2005**, 127, 17393–17404.

102. Castonguay, R.; He, W. G.; Chen, A. Y.; Khosla, C.; Cane, D. E. Stereospecificity of ketoreductase domains of the 6-deoxyerythronolide B synthase. *J. Am. Chem. Soc.* **2007,** 129, 13758–13769.

103. Castonguay, R.; Valenzano, C. R.; Chen, A. Y.; Keatinge-Clay, A.; Khosla, C.; Cane, D. E. Stereospecificity of ketoreductase domains 1 and 2 of the tylactone modular polyketide synthase. *J. Am. Chem. Soc.* **2008**, 130, 11598–11599.

104. Guo, X.; Liu, T. G.; Valenzano, C. R.; Deng, Z. X.; Cane, D. E. Mechanism and stereospecificity of a fully saturating polyketide synthase module: Nanchangmycin synthase module 2 and Its dehydratase domain. *J. Am. Chem. Soc.* **2010**, 132, 14694–14696.

105. Holzbaur, I. E.; Harris, R. C.; Bycroft, M.; Cortes, J.; Bisang, C.; Staunton, J.; Rudd, B. A. M.; Leadlay, P. F. Molecular basis of Celmer's rules: the role of two ketoreductase domains in the control of chirality by the erythromycin modular polyketide synthase. *Chem. Biol.* **1999**, 6, 189–195.

106. Zamudio-Vaazquez, R.; Albericio, F.; Tulla-Puche, J.; Fox, K. R. Thioester bonds of thiocoraline can be replaced with NMe-amide bridges without affecting Its DNA-binding properties. *ACS Med. Chem. Lett.* **2014**, 5, 45–50.

107. Giraldes, J. W.; Akey, D. L.; Kittendorf, J. D.; Sherman, D. H.; Smith, J. L.; Fecik, R. A. Structural and mechanistic insights into polyketide macrolactonization from polyketide-based affinity labels. *Nat. Chem. Biol.* **2006**, 2, 531–536.

108. Leggans, E. K.; Akey, D. L.; Smith, J. L.; Fecik, R. A. A general scheme for synthesis of substrate-based polyketide labels for acyl carrier proteins. *Bioorg. Med. Chem. Lett.* **2010**, 20, 5939-5942.

109. Spiteller, D.; Waterman, C. L.; Spencer, J. B. A method for trapping intermediates of polyketide biosynthesis with a nonhydrolyzable malonyl-coenzyme A analogue. *Angew. Chem. Int. Ed.* **2005,** 44, 7079–7082.

110. Tosin, M.; Spiteller, D.; Spencer, J. B. Malonyl carba(dethia)- and malonyl oxa(dethia)-coenzyme A as tools for trapping polyketide intermediates. *ChemBioChem* **2009**, 10, 1714–1723.

111. Tosin, M.; Betancor, L.; Stephens, E.; Li, W. M. A.; Spencer, J. B.; Leadlay, P. F. Synthetic chain terminators off-load intermediates from a type I polyketide synthase. *ChemBioChem* **2010**, 11, 539–546.

112. Tosin, M.; Demydchuk, Y.; Parascandolo, J. S.; Per, C. B.; Leeper, F. J.; Leadlay, P. F. In vivo trapping of polyketide intermediates from an assembly line synthase using malonyl carba(dethia)-N-acetyl cysteamines. *Chem. Commun.* **2011**, 47, 3460–3462.

113. Tosin, M.; Smith, L.; Leadlay, P. F. Insights into lasalocid A ring formation by chemical chain termination in vivo. *Angew. Chem. Int. Ed.* **2011**, 50, 11930–11933.

114. Nagao, Y.; Hagiwara, Y.; Kumagai, T.; Ochiai, M.; Inoue, T.; Hashimoto, K.; Fujita, E. New C4-chiral 1,3-thiazolidine-2-thiones - Excellent chiral auxiliaries for highly diastereocontrolled aldol-type reactions of acetic-acid and alpha,beta-unsaturated aldehydes. *J. Org. Chem.* **1986**, 51, 2391–2393.

115. Nagao, Y.; Dai, W. M.; Ochiai, M.; Tsukagoshi, S.; Fujita, E. Highly diastereoselective alkylation of chiral tin(II) enolates onto cyclic acyl imines - an efficient asymmetric-synthesis of bicyclic alkaloids bearing a nitrogen atom ring juncture. *J. Org. Chem.* **1990**, 55, 1148–1156.

116. Crimmins, M. T.; King, B. W.; Tabet, E. A.; Chaudhary, K. Asymmetric aldol additions: Use of titanium tetrachloride and (-)-sparteine for the soft enolization of N-acyl oxazolidinones, oxazolidinethiones, and thiazolidinethiones. *J. Org. Chem.* **2001**, 66, 894–902.

117. Crimmins, M. T.; Slade, D. J. Formal synthesis of 6-deoxyerythronolide B. *Org. Lett.* **2006**, 8, 2191–2194.

118. Rychnovsky, S. D.; Skalitzky, D. J. Stereochemistry of alternating polyol chains - C-13 nmr analysis of 1,3-diol acetonides. *Tetrahedron Lett.* **1990**, 31, 945–948.

119. Evans, D. A.; Rieger, D. L.; Gage, J. R. C-13 Nmr chemical-shift correlations in 1,3-diol acetonides -implications for the stereochemical assignment of propionate-derived polyols. *Tetrahedron Lett.* **1990**, 31, 7099–7100.

120. Bartlett, S. L.; Beaudry, C. M. High-yielding oxidation of beta-hydroxyketones to beta-diketones using o-iodoxybenzoic acid. *J. Org. Chem.* **2011**, 76, 9852–9855.

121. Groesbeek, M.; Smith, S. O. Synthesis of 19-fluororetinal and 20-fluororetinal. *J. Org. Chem.* **1997**, 62, 3638–3641.

122. Makino, K.; Nakajima, N.; Hashimoto, S.; Yonemitsu, O. Total synthesis of 16-membered tetraene macrolide hygrolidin. *Tetrahedron Lett.* **1996**, 37, 9077–9080.

123. Donnelly, M. I.; Zhou, M.; Millard, C. S.; Clancy, S.; Stols, L.; Eschenfeldt, W. H.; Collart, F. R.; Joachimiak, A. An expression vector tailored for large-scale, high-throughput purification of recombinant proteins. *Protein Expr. Purif.* **2006**, 47, 446–454.

124. Siskos, A. P.; Baerga-Ortiz, A.; Bali, S.; Stein, V.; Mamdani, H.; Spiteller, D.; Popovic, B.; Spencer, J. B.; Staunton, J.; Weissman, K. J.; Leadlay, P. F. Molecular basis of Celmer's rules: stereochemistry of catalysis by isolated ketoreductase domains from modular polyketide synthases. *Chem. Biol.* **2005**, 12, 1145–1153.

125. Bali, S.; Weissman, K. J. Ketoreduction in mycolactone biosynthesis: Insight into substrate specificity and stereocontrol from studies of discrete ketoreductase domains in vitro. *ChemBioChem* **2006**, 7, 1935–1942.

126. Verdier-Pinard, P.; Lai, J.-Y.; Yoo, H.-D.; Yu, J.; Marquez, B.; Nagle, D. G.; Nambu, M.; White, J. D.; Falck, J. R.; Gerwick, W. H.; Day, B. W.; Hamel, E. Structure-activity analysis of the interaction of curacin A, the potent colchicine site antimitotic agent, with tubulin and effects of analogs on the growth of MCF-7 breast cancer cells. *Mol. Pharmacol.* **1998**, 53, 62–76.

127. Martello, L. A.; LaMarche, M. J.; He, L.; Beauchamp, T. J.; Smith Iii, A. B.; Horwitz, S. B. The relationship between Taxol and (+)-discodermolide: synthetic analogs and modeling studies. *Chem. Biol.* **2001**, 8, 843–855.

128. Leesong, M.; Henderson, B. S.; Gillig, J. R.; Schwab, J. M.; Smith, J. L. Structure of a dehydratase-isomerase from the bacterial pathway for biosynthesis of unsaturated fatty acids: two catalytic activities in one active site. *Structure* **1996**, 4, 253–264.

129. Kimber, M. S.; Martin, F.; Lu, Y.; Houston, S.; Vedadi, M.; Dharamsi, A.; Fiebig, K. M.; Schmid, M.; Rock, C. O. The structure of (3R)-hydroxyacyl-acyl carrier protein dehydratase (FabZ) from Pseudomonas aeruginosa. *J. Biol. Chem.* **2004**, 279, 52593–52602.

130. Keatinge-Clay, A. Crystal structure of the erythromycin polyketide synthase dehydratase. *J. Mo.l Biol.* **2008**, 384, 941–953.

131. Akey, D. L.; Razelun, J. R.; Tehranisa, J.; Sherman, D. H.; Gerwick, W. H.; Smith, J. L. Crystal structures of dehydratase domains from the curacin polyketide biosynthetic pathway. *Structure* **2010**, 18, 94–105.

132. Gay, D.; You, Y. O.; Keatinge-Clay, A.; Cane, D. E. Structure and stereospecificity of the dehydratase domain from the terminal module of the rifamycin polyketide synthase. *Biochemistry* **2013**, 52, 8916–8928.

133. Reid, R.; Piagentini, M.; Rodriguez, E.; Ashley, G.; Viswanathan, N.; Carney, J.; Santi, D. V.; Hutchinson, C. R.; McDaniel, R. A model of structure and catalysis for ketoreductase domains in modular polyketide synthases. *Biochemistry* **2003**, 42, 72–79.

134. Vergnolle, O.; Hahn, F.; Baerga-Ortiz, A.; Leadlay, P. F.; Andexer, J. N. Stereoselectivity of isolated dehydratase domains of the borrelidin polyketide synthase: implications for cis double bond formation. *ChemBioChem* **2011**, 12, 1011–1014.

135. Kandziora, N.; Andexer, J. N.; Moss, S. J.; Wilkinson, B.; Leadlay, P. F.; Hahn, F. Uncovering the origin of Z-configured double bonds in polyketides: intermediate E-double bond formation during borrelidin biosynthesis. *Chem. Sci.* **2014**, 5, 3563–3567.

136. Wu, N.; Kudo, F.; Cane, D. E.; Khosla, C. Analysis of the molecular recognition features of individual modules derived from the erythromycin polyketide synthase. *J. Am. Chem. Soc.* **2000**, 122, 4847–4852.

137. Cane, D. E.; Kudo, F.; Kinoshita, K.; Khosla, C. Precursor-directed biosynthesis: biochemical basis of the remarkable selectivity of the erythromycin polyketide synthase toward unsaturated triketides. *Chem. Biol.* **2002**, 9, 131–142.

138. Lu, H.; Tsai, S. C.; Khosla, C.; Cane, D. E. Expression, site-directed mutagenesis, and steady state kinetic analysis of the terminal thioesterase domain of the methymycin/picromycin polyketide synthase. *Biochemistry* **2002**, 41, 12590–12597.

139. Yin, Y.; Lu, H.; Khosla, C.; Cane, D. E. Expression and kinetic analysis of the substrate specificity of modules 5 and 6 of the picromycin/methymycin polyketide synthase. *J. Am. Chem. Soc.* **2003**, 125, 5671–5676.

140. Valenzano, C. R.; You, Y. O.; Garg, A.; Keatinge-Clay, A.; Khosla, C.; Cane, D. E. Stereospecificity of the dehydratase domain of the erythromycin polyketide synthase. *J. Am. Chem. Soc.* **2010**, 132, 14697–14699.

141. Berkhan, G.; Hahn, F. A dehydratase domain in ambruticin biosynthesis displays additional activity as a pyran-forming cyclase. *Angew. Chem. Int. Ed.* **2014**, 53, 14240–14244.

142. Li, Y.; Fiers, W. D.; Bernard, S. M.; Smith, J. L.; Aldrich, C. C.; Fecik, R. A. Polyketide intermediate mimics as probes for revealing cryptic stereochemistry of ketoreductase domains. *ACS Chem. Biol.* **2014**, 9, 2914–2922.

143. Li, Y.; Dodge, G. J.; Fiers, W. D.; Fecik, R. A.; Smith, J. L.; Aldrich, C. C. Functional characterization of a dehydratase domain from the pikromycin polyketide synthase. *J. Am. Chem. Soc.* **2015**, 137, 7003–7006.

144. Abiko, A.; Liu, J.-F.; Masamune, S. The anti-selective boron-mediated asymmetric aldol reaction of carboxylic esters. *J. Am. Chem. Soc.* **1997**, 119, 2586–2587.

145. Barbier, J.; Jansen, R.; Irschik, H.; Benson, S.; Gerth, K.; Bohlendorf, B.; Hofle, G.; Reichenbach, H.; Wegner, J.; Zeilinger, C.; Kirschning, A.; Muller, R. Isolation and total synthesis of icumazoles and noricumazoles--antifungal antibiotics and cation-channel blockers from Sorangium cellulosum. *Angew. Chem. Int. Ed.* **2012**, 51, 1256–1260.

146. Chung-hsi, L.; Yuen-hwa, Y.; Yao, L.; Yong-jun, L.; Ai-hsueh, C.; Chi-yi, H. 3-aminoacyl-tetrahydrothiazole-2-thione as an active amide for peptide synthesis (I). *Tetrahedron Lett.* **1981**, 22, 3467–3470.

147. Fersht, A. *Structure and Mechanism in Protein Science: A Guide to Enzyme Catalysis and Protein Folding*. W. H. Freeman: 1999.

148. Purich, D. L.; Allison, R. D. *Handbook of Biochemical Kinetics: A Guide to Dynamic Processes in the Molecular Life Sciences*. Elsevier Science: 1999.

149. Brock, D. J.; Kass, L. R.; Bloch, K. Beta-hydroxydecanoyl thioester dehydrase. II. Mode of action. *J. Biol. Chem.* **1967**, 242, 4432–4440.

150. Kass, L. R.; Bloch, K. On the enzymatic synthesis of unsaturated fatty acids in Escherichia coli. *Proc. Natl. Acad. Sci. USA* **1967**, 58, 1168–1173.

151. Ishikawa, F.; Haushalter, R. W.; Burkart, M. D. Dehydratase-specific probes for fatty acid and polyketide synthases. *J. Am. Chem. Soc.* **2012**, 134, 769–772.

152. Ishikawa, F.; Haushalter, R. W.; Lee, D. J.; Finzel, K.; Burkart, M. D. Sulfonyl 3-alkynyl pantetheinamides as mechanism-based cross-linkers of acyl carrier protein dehydratase. *J. Am. Chem. Soc.* **2013**, 135, 8846–8849.

153. Kitz, R.; Wilson, I. B. Esters of methanesulfonic acid as irreversible inhibitors of acetylcholinesterase. *J. Biol. Chem.* **1962**, 237, 3245–3249.

154. Endo, K.; Helmkamp, G. M., Jr.; Bloch, K. Mode of inhibition of beta-hydroxydecanoyl thioester dehydrase by 3-decynoyl-N-acetylcysteamine. *J. Biol. Chem.* **1970**, 245, 4293–4296.

155. Schwab, J. M.; Li, W. B.; Ho, C. K.; Townsend, C. A.; Salituro, G. M. Direct observation by carbon-13 NMR spectroscopy of the regioselectivity and stoichiometry of "suicide" enzyme inactivation. *J. Am. Chem. Soc.* **1984**, 106, 7293–7294.

156. Nagao, Y.; Hagiwara, Y.; Kumagai, T.; Ochiai, M.; Inoue, T.; Hashimoto, K.; Fujita, E. New C-4-chiral 1,3-thiazolidine-2-thiones: excellent chiral auxiliaries for highly diastereo-controlled aldol-type reactions of acetic acid and .alpha.,.beta.-unsaturated aldehydes. *J. Org. Chem.* **1986**, 51, 2391–2393.

157. Nagao, Y.; Dai, W. M.; Ochiai, M.; Tsukagoshi, S.; Fujita, E. Highly diastereoselective alkylation of chiral tin(II) enolates onto cyclic acyl imines. An efficient

asymmetric synthesis of bicyclic alkaloids bearing a nitrogen atom ring juncture. *J. Org. Chem.* **1990**, 55, 1148–1156.

158. Stols, L.; Gu, M.; Dieckman, L.; Raffen, R.; Collart, F. R.; Donnelly, M. I. A new vector for high-throughput, ligation-independent cloning encoding a tobacco etch virus protease cleavage site. *Protein Expr. Purif.* **2002**, 25, 8–15.

159. Wu, S.; Zhang, Y. LOMETS: a local meta-threading-server for protein structure prediction. *Nucleic Acids Res.* **2007**, 35, 3375–3382.

160. Serrano, H.; Blanchard, J. S. Kinetic and isotopic characterization of L-proline dehydrogenase from Mycobacterium tuberculosis. *Biochemistry* **2013**, 52, 5009–5015.

Appendix

Standard curves of **2.26**, **2.27**, **3.7** and **3.8**.

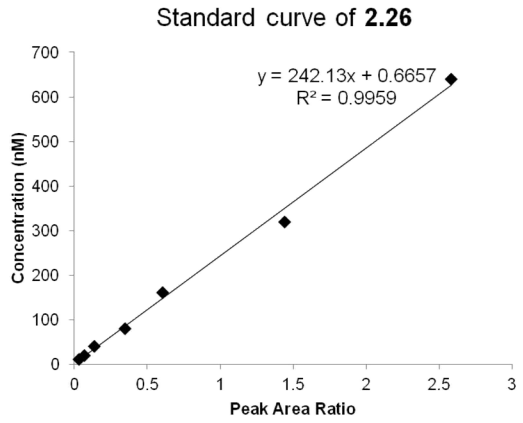

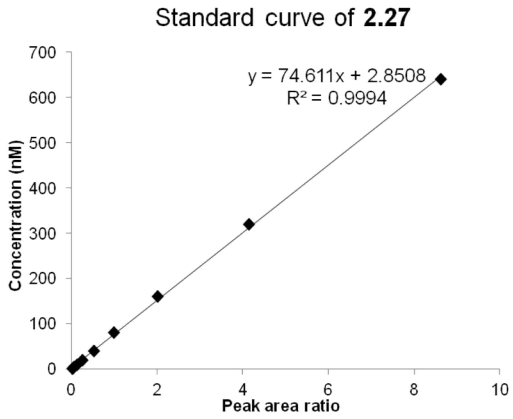

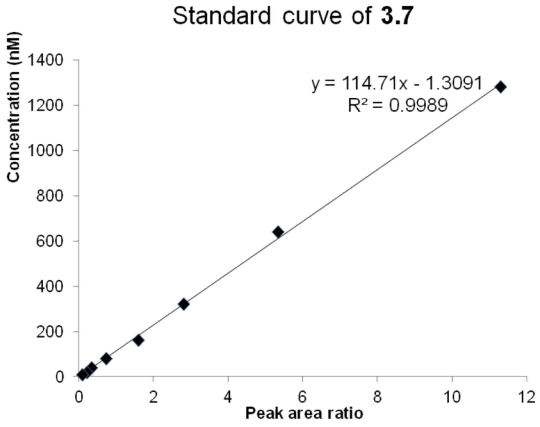

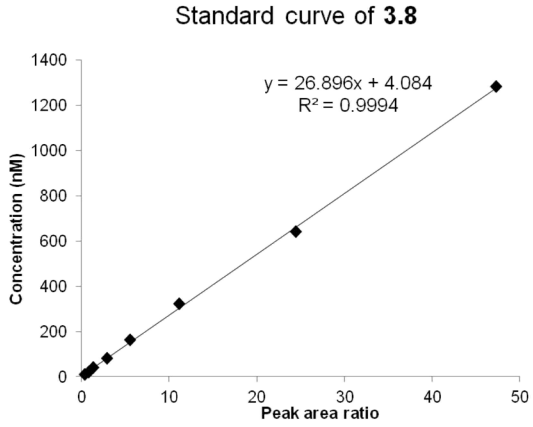

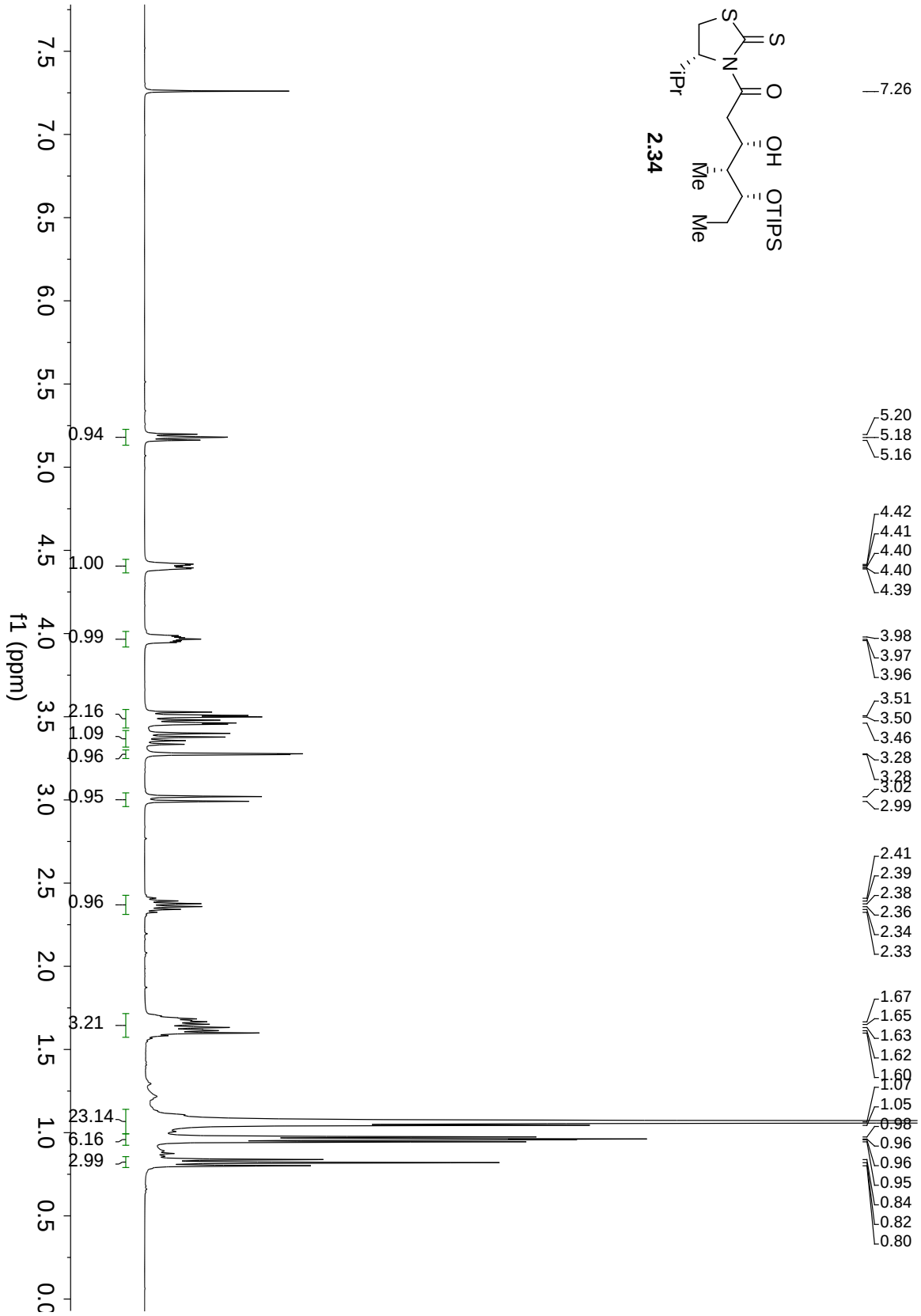
S
S
N
iPr
O
OH
OTIPS
Me
Me
2.34
7.26
5.20
5.18
5.16
4.42
4.41
4.40
4.40
4.39
3.98
3.97
3.96
3.51
3.50
3.46
3.28
3.28
3.02
2.99
2.41
2.39
2.38
2.36
2.34
2.33
1.67
1.65
1.63
1.62
1.60
1.07
1.05
0.98
0.96
0.96
0.95
0.84
0.82
0.80
0.94
1.00
0.99
2.16
1.09
0.96
0.95
0.96
3.21
23.14
6.16
2.99
f1 (ppm)

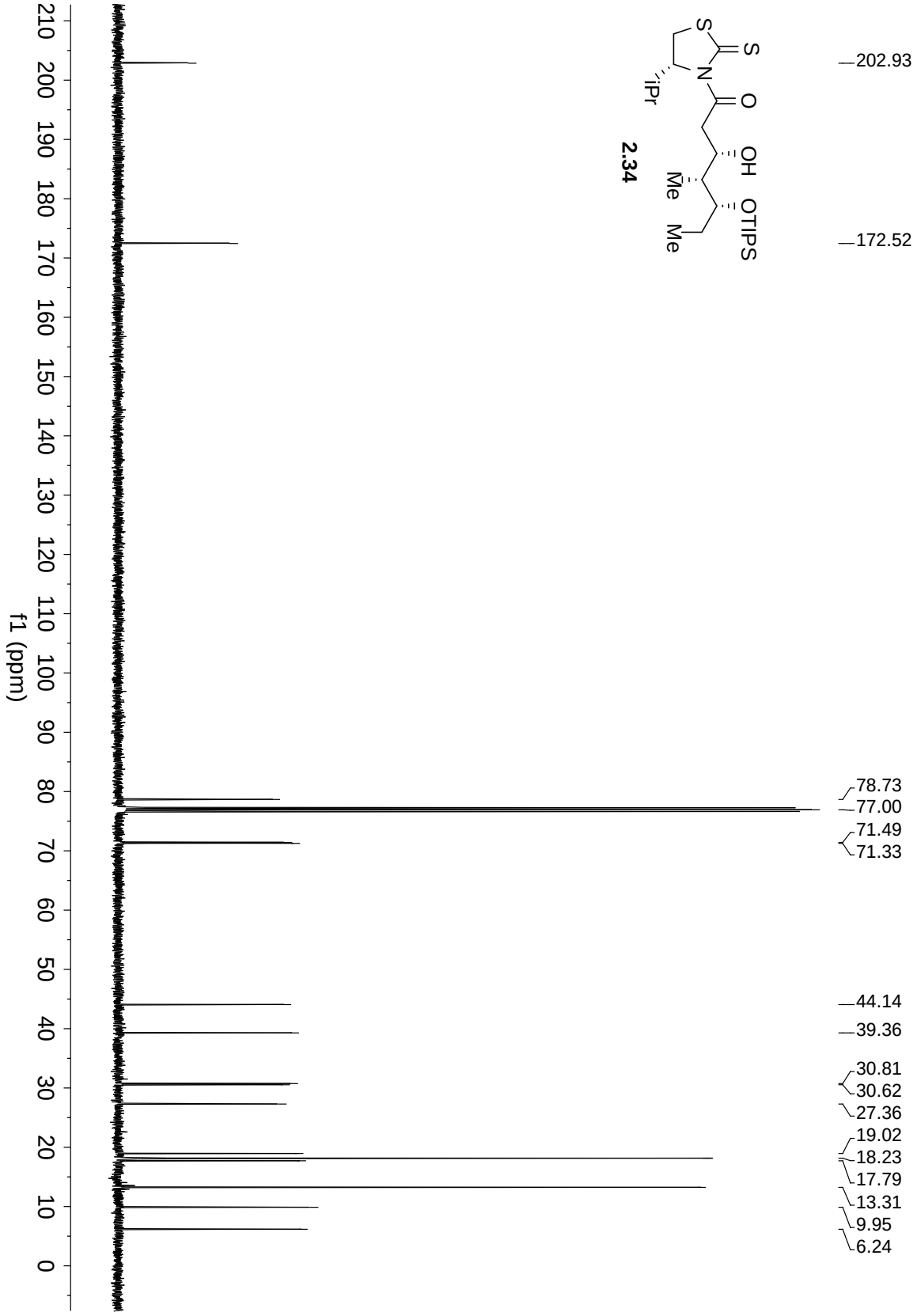
2.34
202.93
172.52
78.73
77.00
71.49
71.33
44.14
39.36
30.81
30.62
27.36
19.02
18.23
17.79
13.31
9.95
6.24
f1 (ppm)

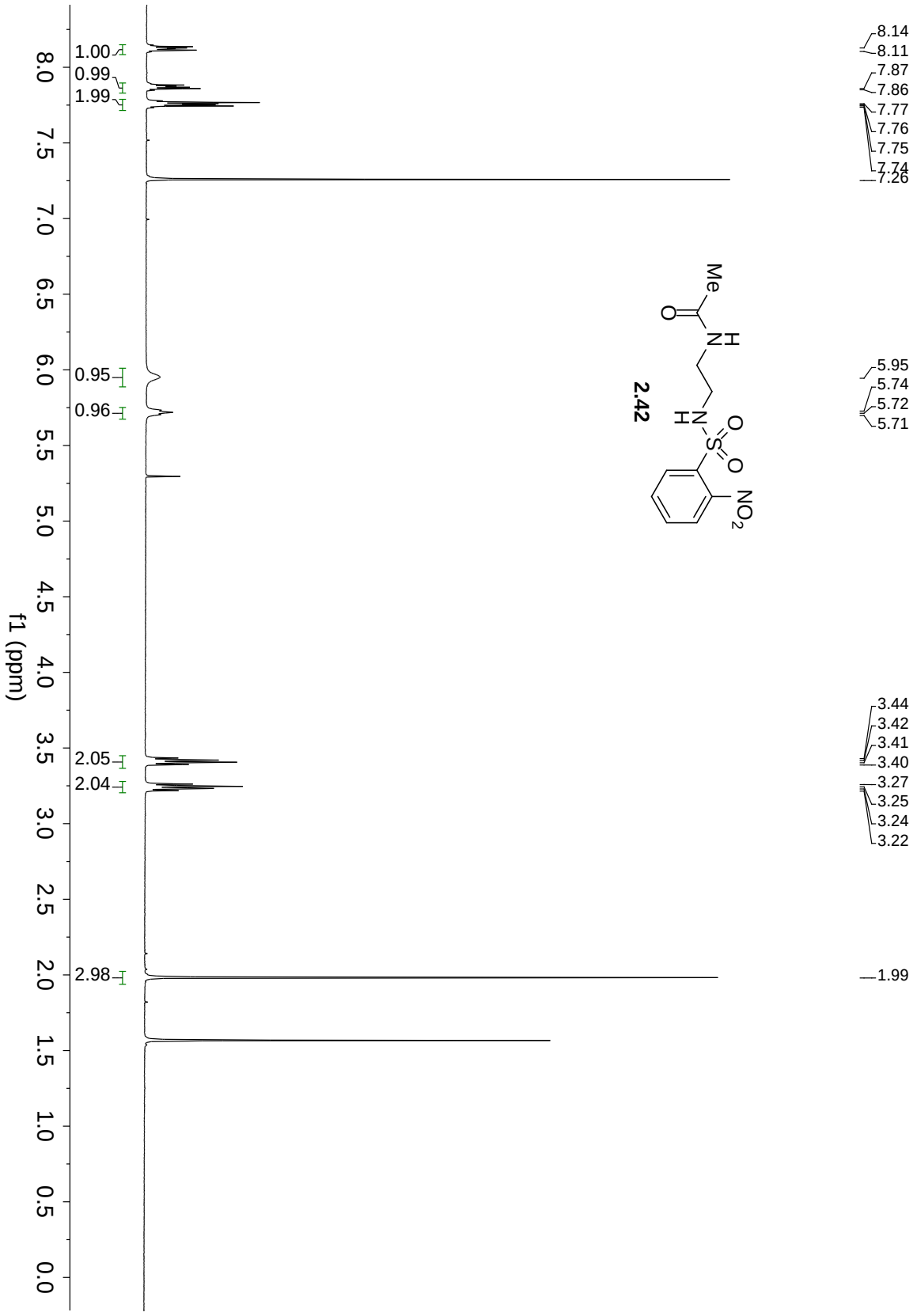
8.14
8.11
7.87
7.86
7.77
7.76
7.75
7.74
7.26
5.95
5.74
5.72
5.71
3.44
3.42
3.41
3.40
3.27
3.25
3.24
3.22
1.99
1.00
0.99
1.99
0.95
0.96
2.05
2.04
2.98
2.42
Me
O
H
N
H
N
S
O
O
O
NO2
f1 (ppm)
8.0
7.5
7.0
6.5
6.0
5.5
5.0
4.5
4.0
3.5
3.0
2.5
2.0
1.5
1.0
0.5
0.0

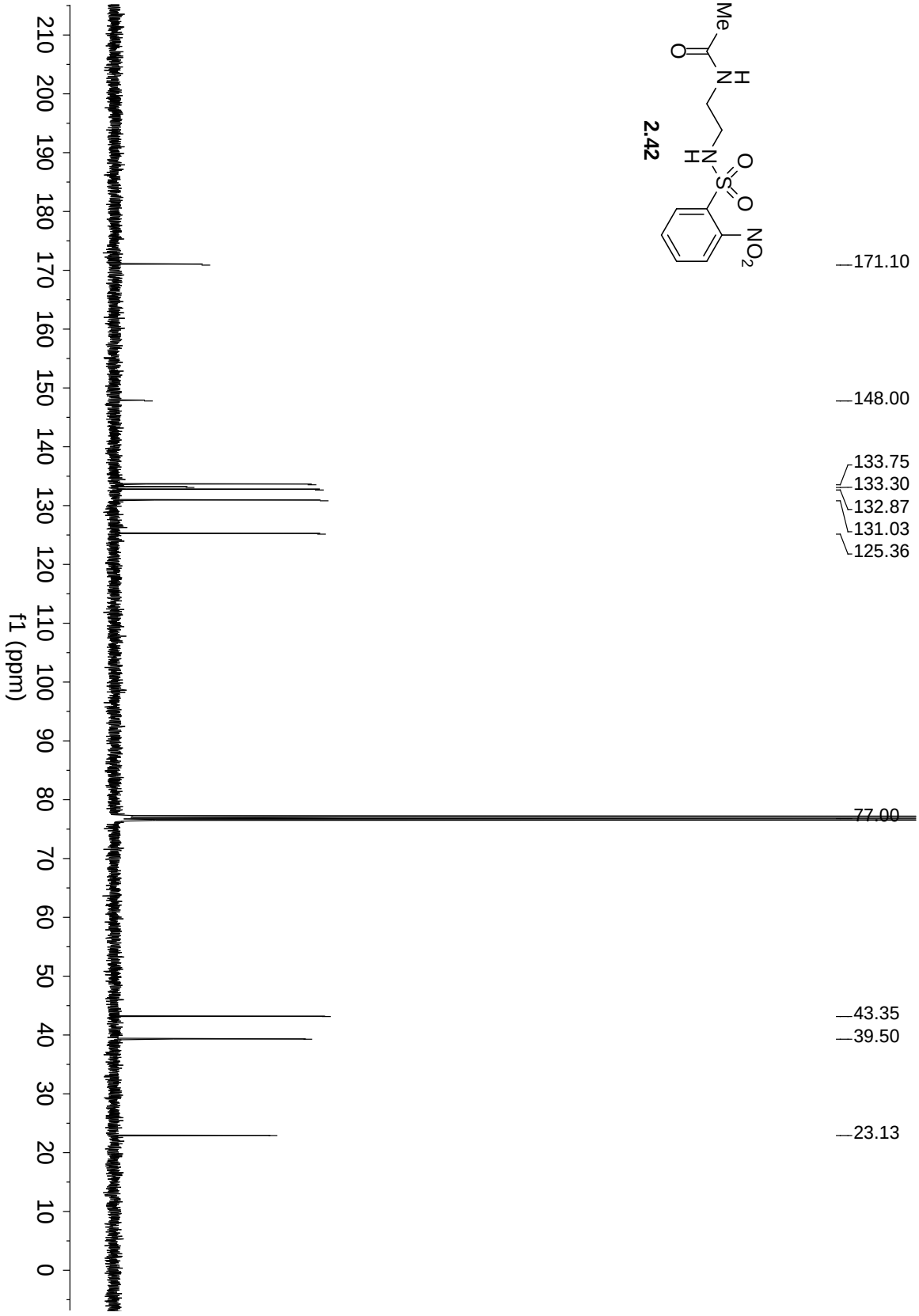
Me
O
N
H
N
H
O
S
O
O
NO2
2.42
171.10
148.00
133.75
133.30
132.87
131.03
125.36
77.00
43.35
39.50
23.13
f1 (ppm)
210
200
190
180
170
160
150
140
130
120
110
100
90
80
70
60
50
40
30
20
10
0

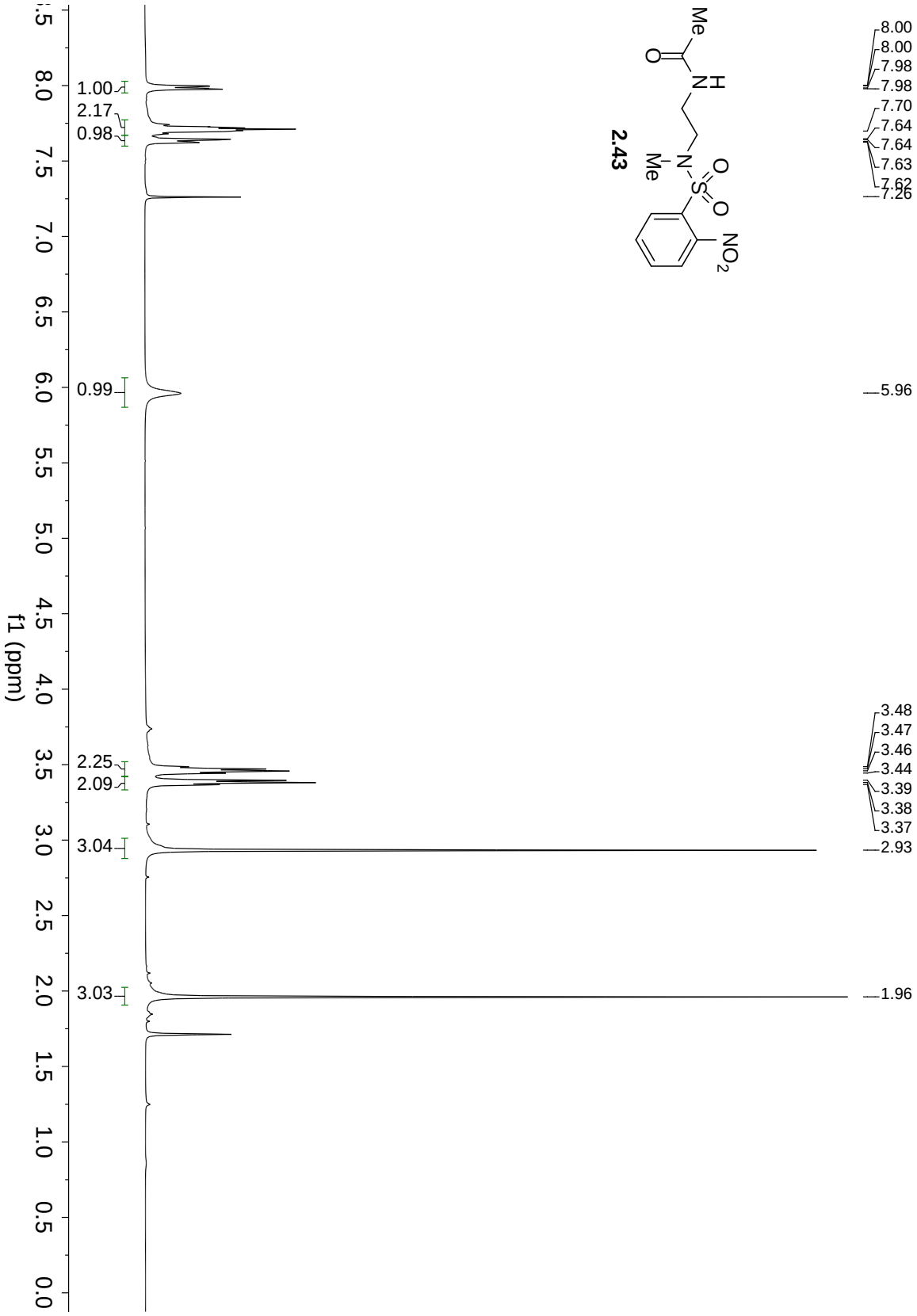
f1 (ppm)
8.5
8.0
7.5
7.0
6.5
6.0
5.5
5.0
4.5
4.0
3.5
3.0
2.5
2.0
1.5
1.0
0.5
0.0
1.00
2.17
0.98
0.99
2.25
2.09
3.04
3.03
2.43
Me
O
H
N
N
Me
O
S
O
NO2
8.00
8.00
7.98
7.98
7.70
7.64
7.64
7.63
7.62
7.26
5.96
3.48
3.47
3.46
3.44
3.39
3.38
3.37
2.93
1.96

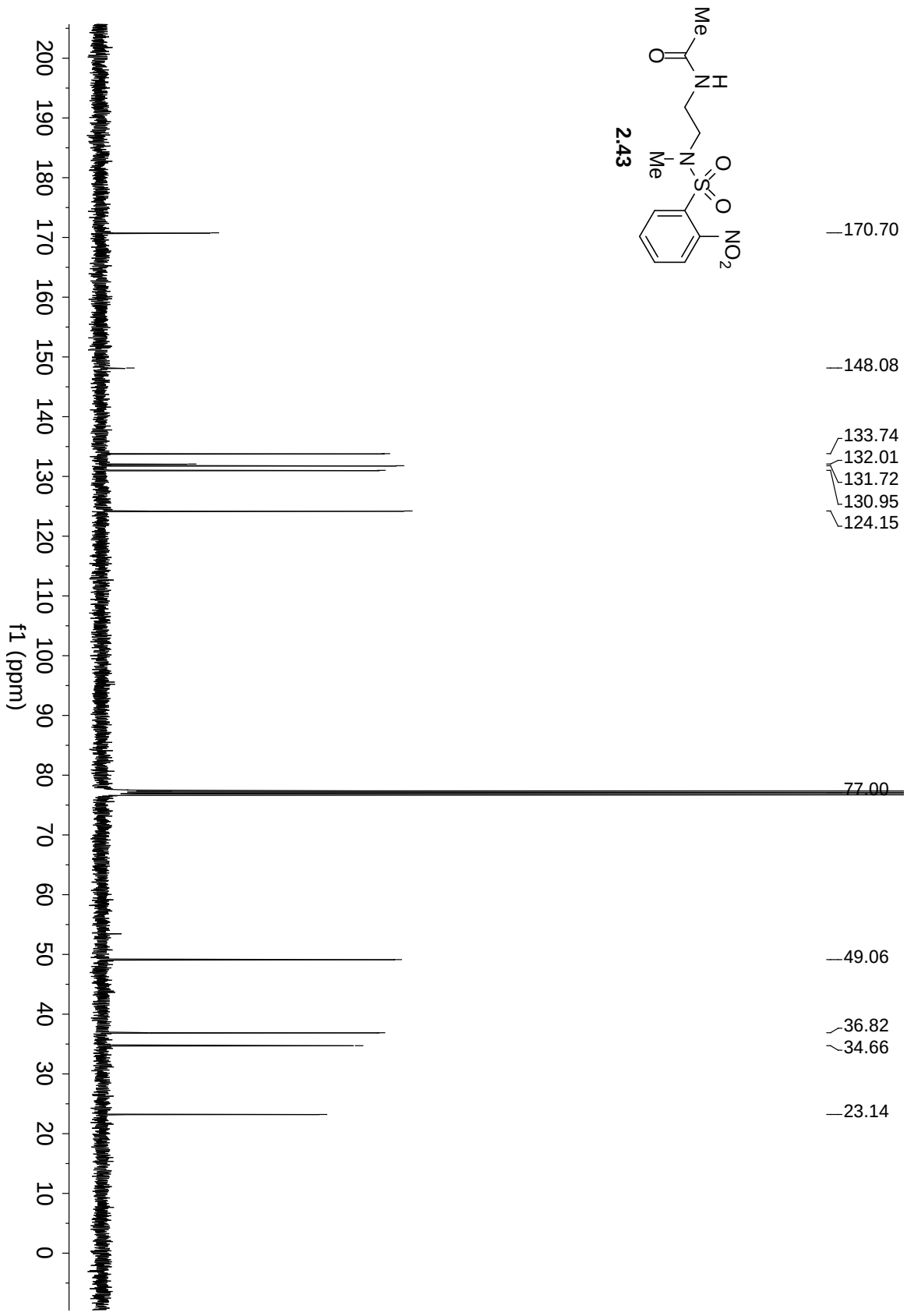
2.43
170.70
148.08
133.74
132.01
131.72
130.95
124.15
77.00
49.06
36.82
34.66
23.14
f1 (ppm)

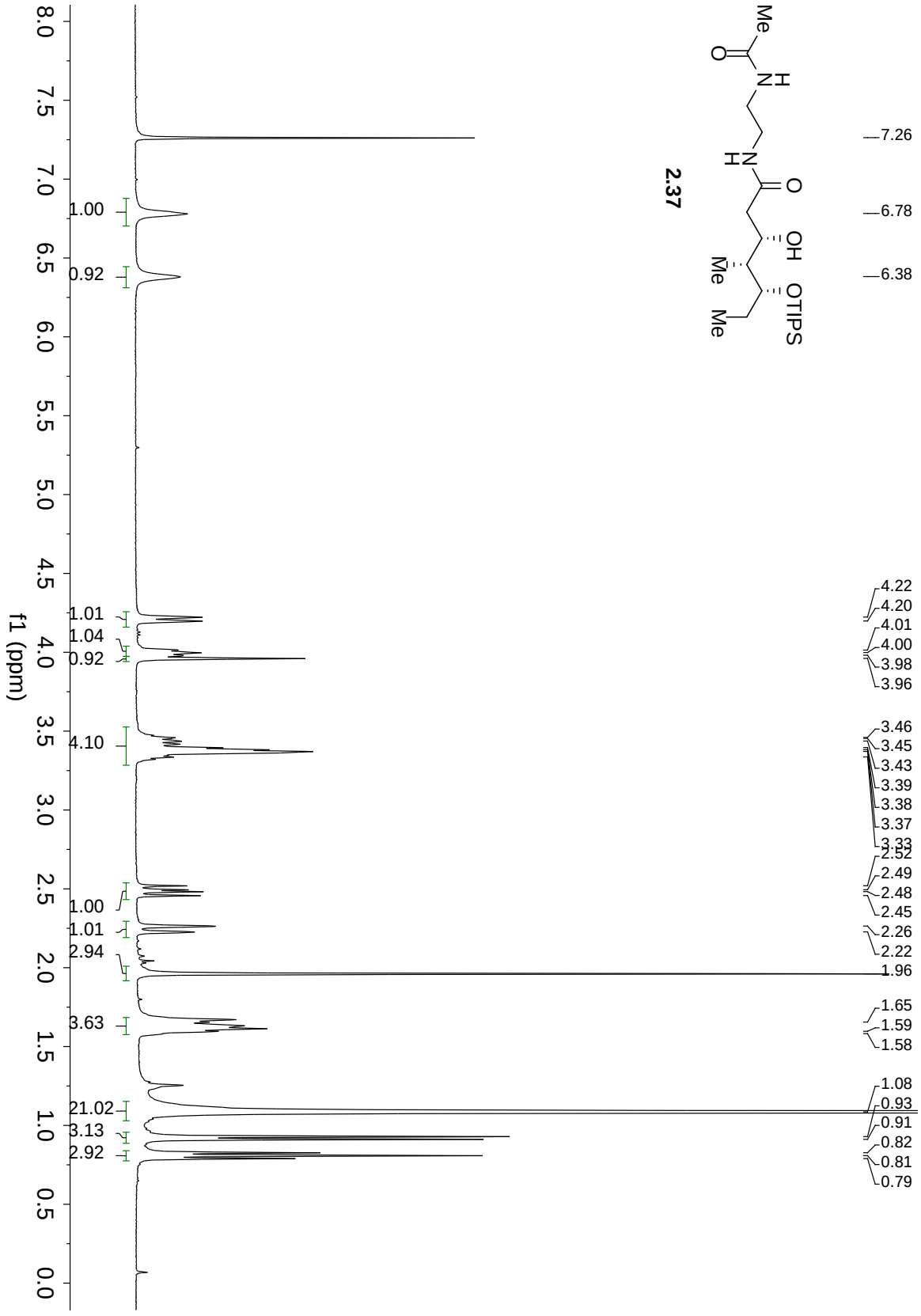
2.37
f1 (ppm)
8.0
7.5
7.0
6.5
6.0
5.5
5.0
4.5
4.0
3.5
3.0
2.5
2.0
1.5
1.0
0.5
0.0
1.00
0.92
1.01
1.04
0.92
4.10
1.00
1.01
2.94
3.63
21.02
3.13
2.92
7.26
6.78
6.38
4.22
4.20
4.01
4.00
3.98
3.96
3.46
3.45
3.43
3.39
3.38
3.37
3.33
2.52
2.49
2.48
2.45
2.26
2.22
1.96
1.65
1.59
1.58
1.08
0.93
0.91
0.82
0.81
0.79

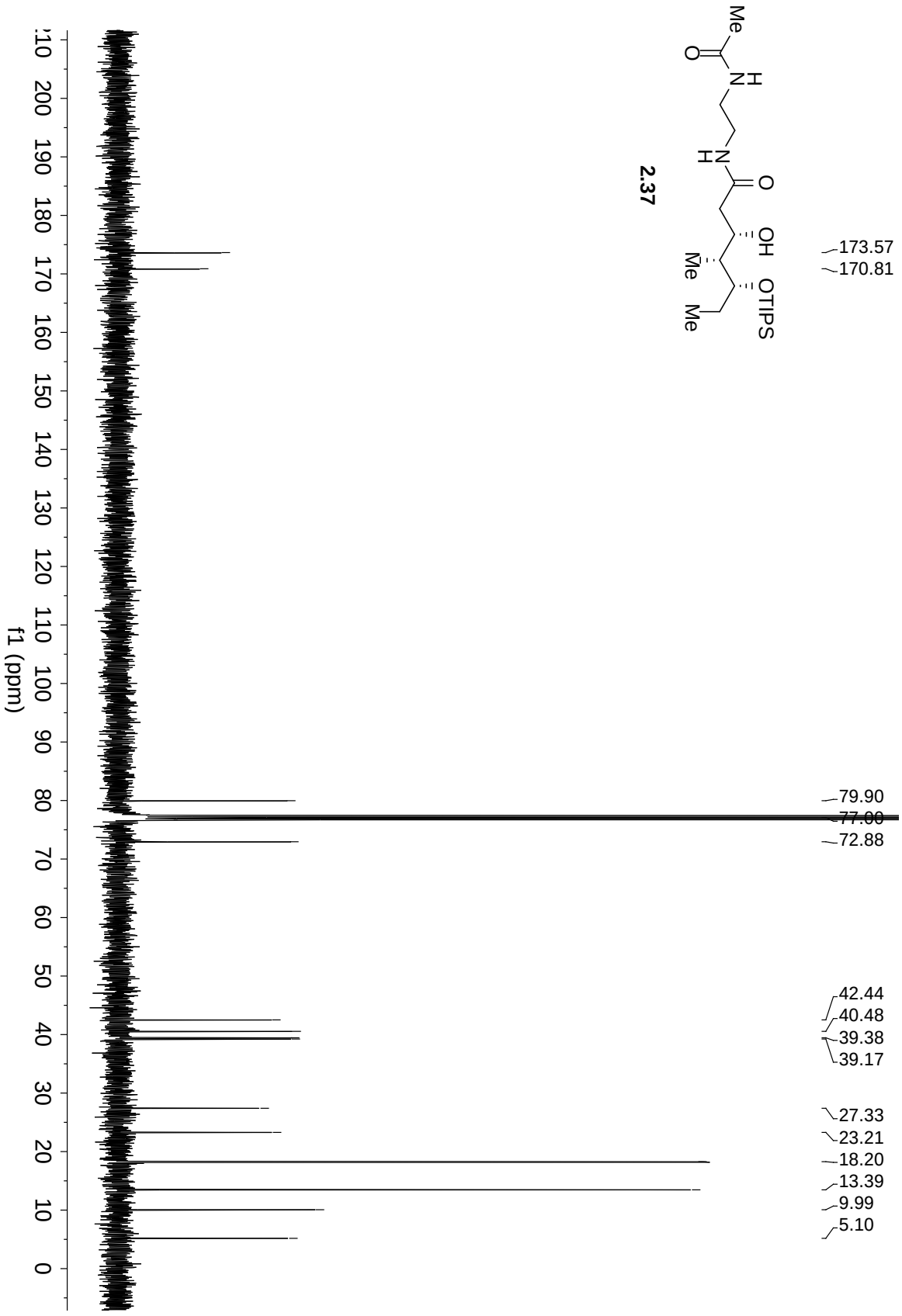
2.37
Me
O
H
N
N
H
O
OH
OTIPS
Me
Me
173.57
170.81
79.90
77.00
72.88
42.44
40.48
39.38
39.17
27.33
23.21
18.20
13.39
9.99
5.10
f1 (ppm)

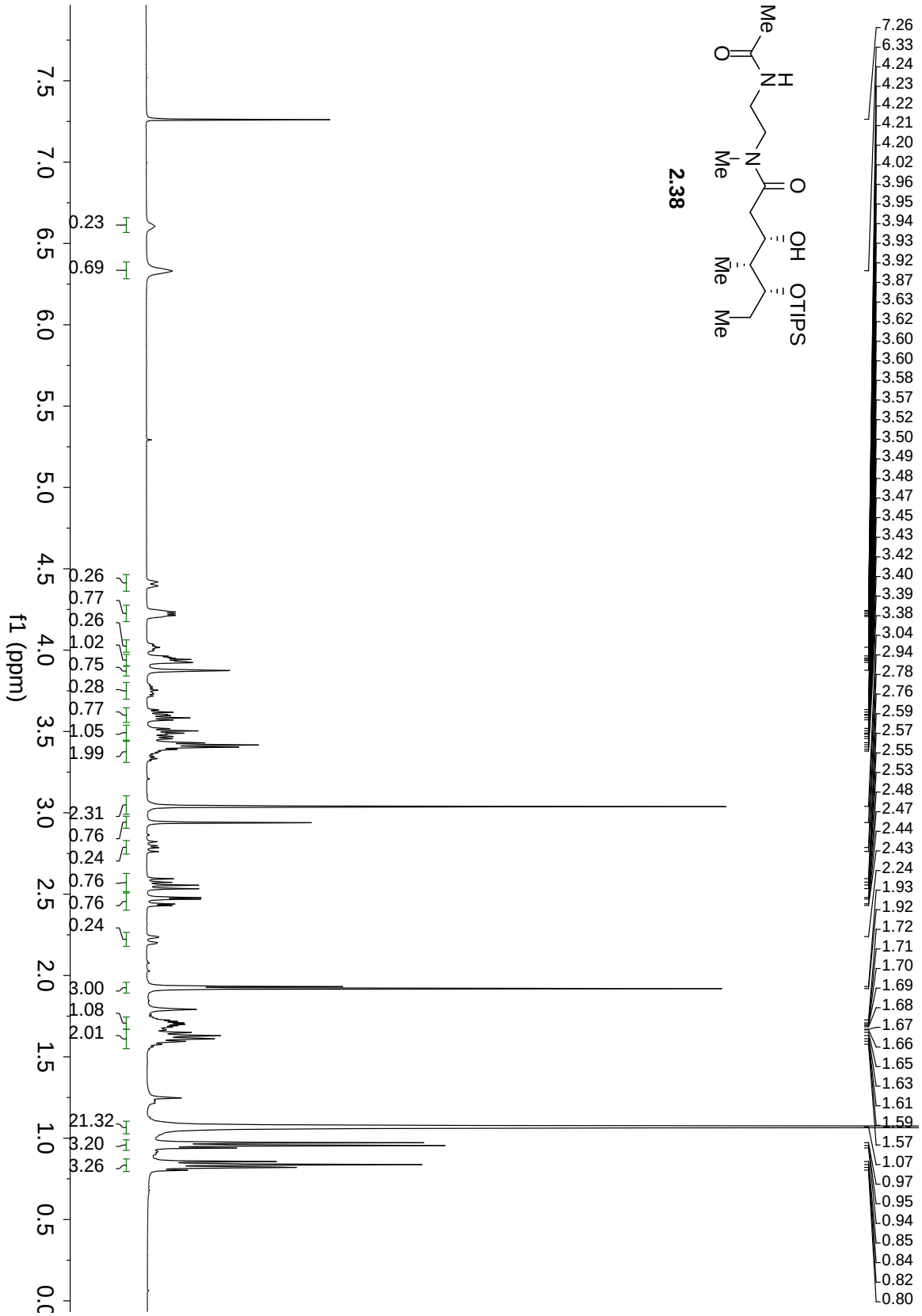
2.38
f1 (ppm)
0.23
0.69
0.26
0.77
0.26
1.02
0.75
0.28
0.77
1.05
1.99
2.31
0.76
0.24
0.76
0.76
0.24
3.00
1.08
2.01
21.32
3.20
3.26

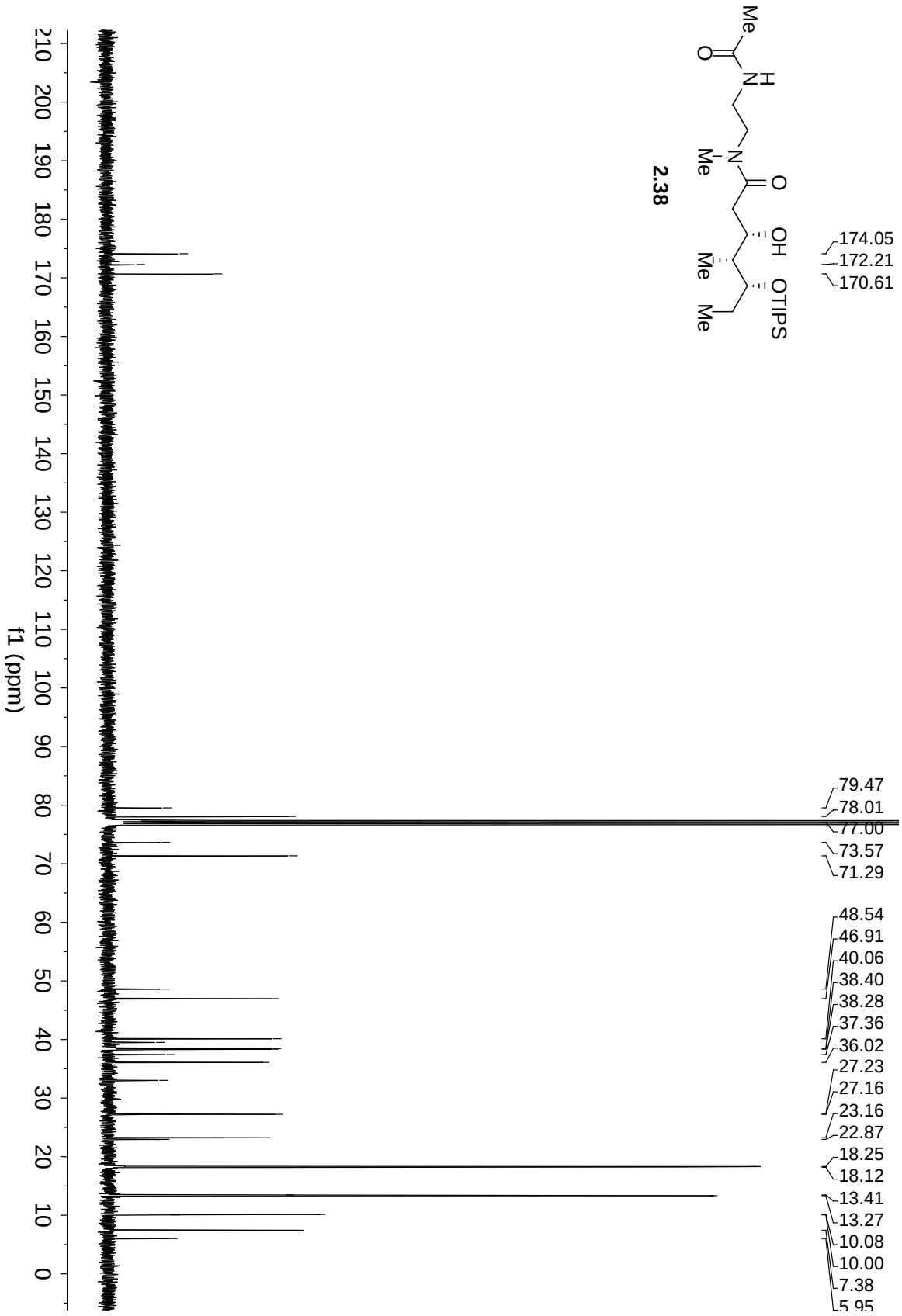
2.38
174.05
172.21
170.61
79.47
78.01
77.00
73.57
71.29
48.54
46.91
40.06
38.40
38.28
37.36
36.02
27.23
27.16
23.16
22.87
18.25
18.12
13.41
13.27
10.08
10.00
7.38
5.95
f1 (ppm)

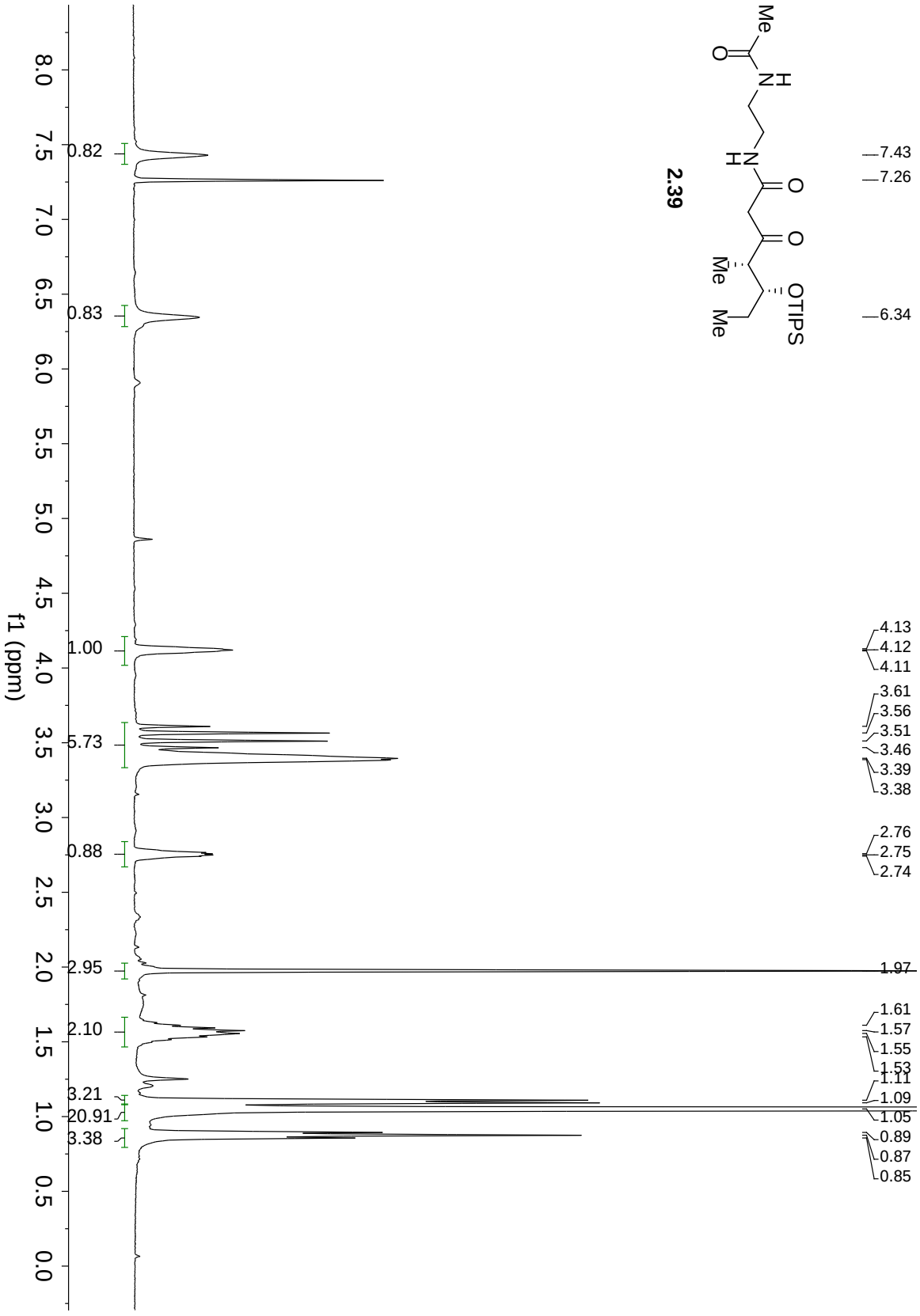
f1 (ppm)
8.0
7.5
7.0
6.5
6.0
5.5
5.0
4.5
4.0
3.5
3.0
2.5
2.0
1.5
1.0
0.5
0.0
0.82
0.83
1.00
5.73
0.88
2.95
2.10
3.21
20.91
3.38
2.39
Me
O
N
H
N
H
O
O
Me
Me
OTIPS
7.43
7.26
6.34
4.13
4.12
4.11
3.61
3.56
3.51
3.46
3.39
3.38
2.76
2.75
2.74
1.97
1.61
1.57
1.55
1.53
1.11
1.09
1.05
0.89
0.87
0.85

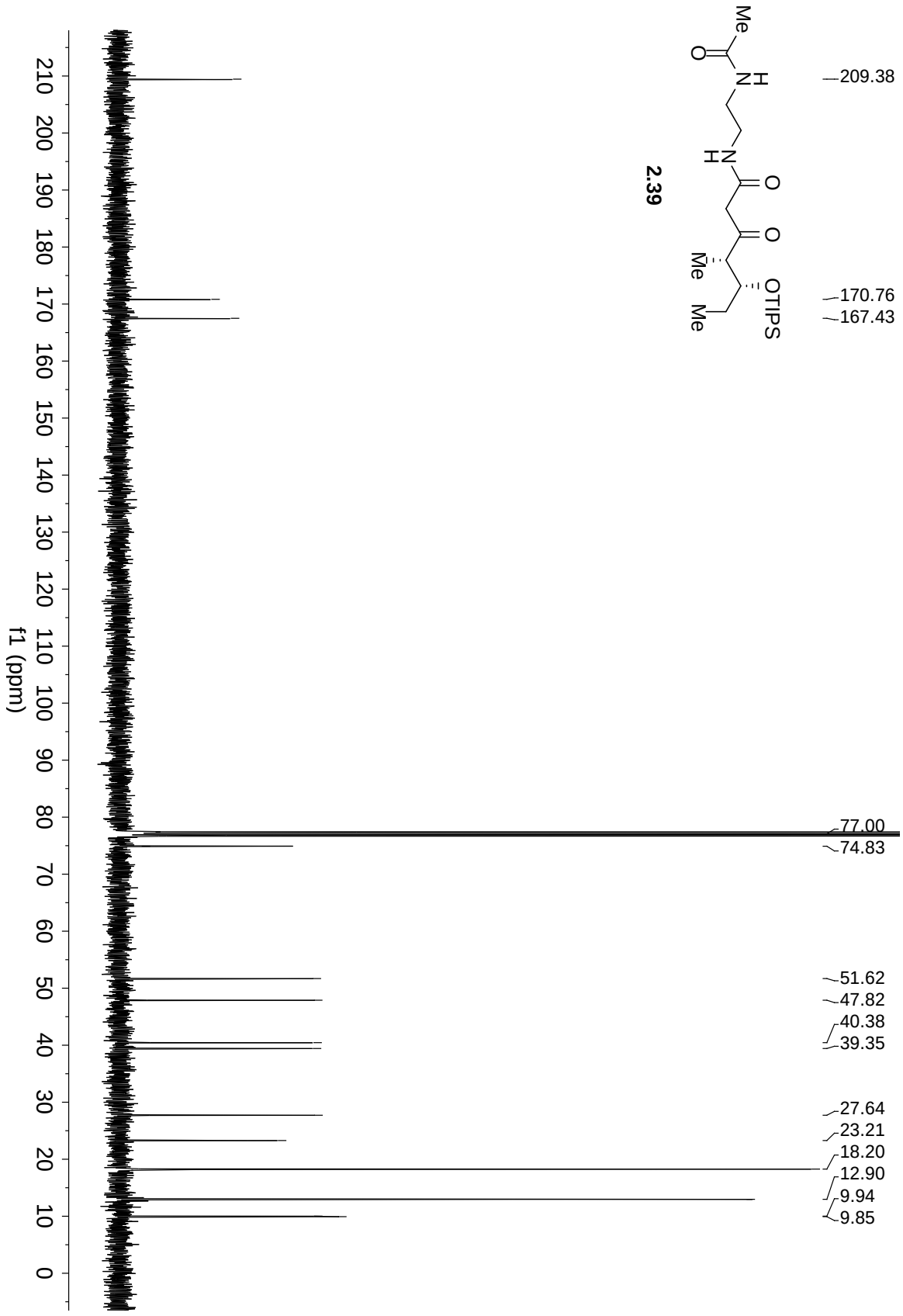
2.39
209.38
170.76
167.43
77.00
74.83
51.62
47.82
40.38
39.35
27.64
23.21
18.20
12.90
9.94
9.85
f1 (ppm)

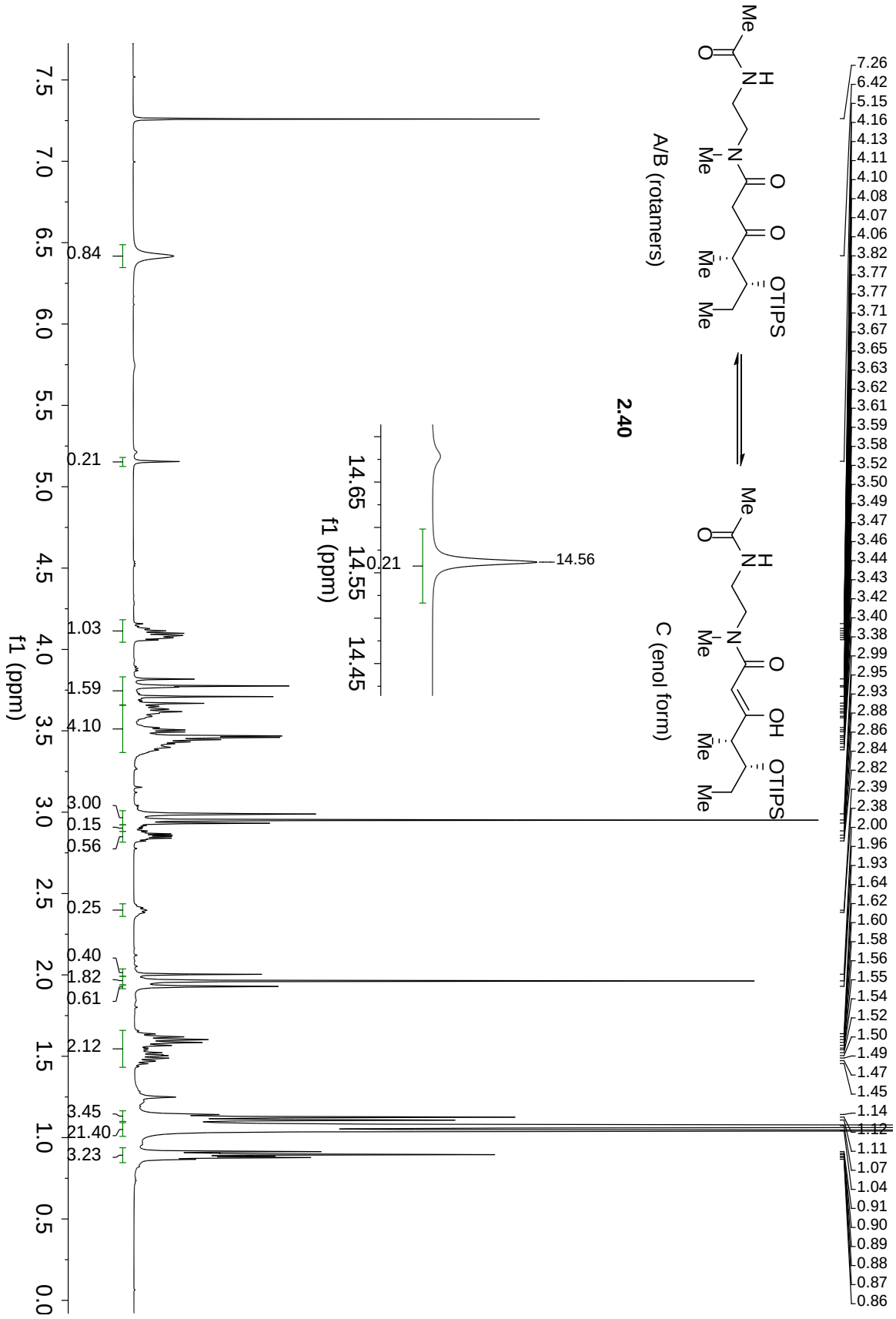
2.40
A/B (rotamers)
C (enol form)
OTIPS
OH
f1 (ppm)
14.56
0.21
0.84
0.21
1.03
1.59
4.10
3.00
0.15
0.56
0.25
0.40
1.82
0.61
2.12
3.45
21.40
3.23

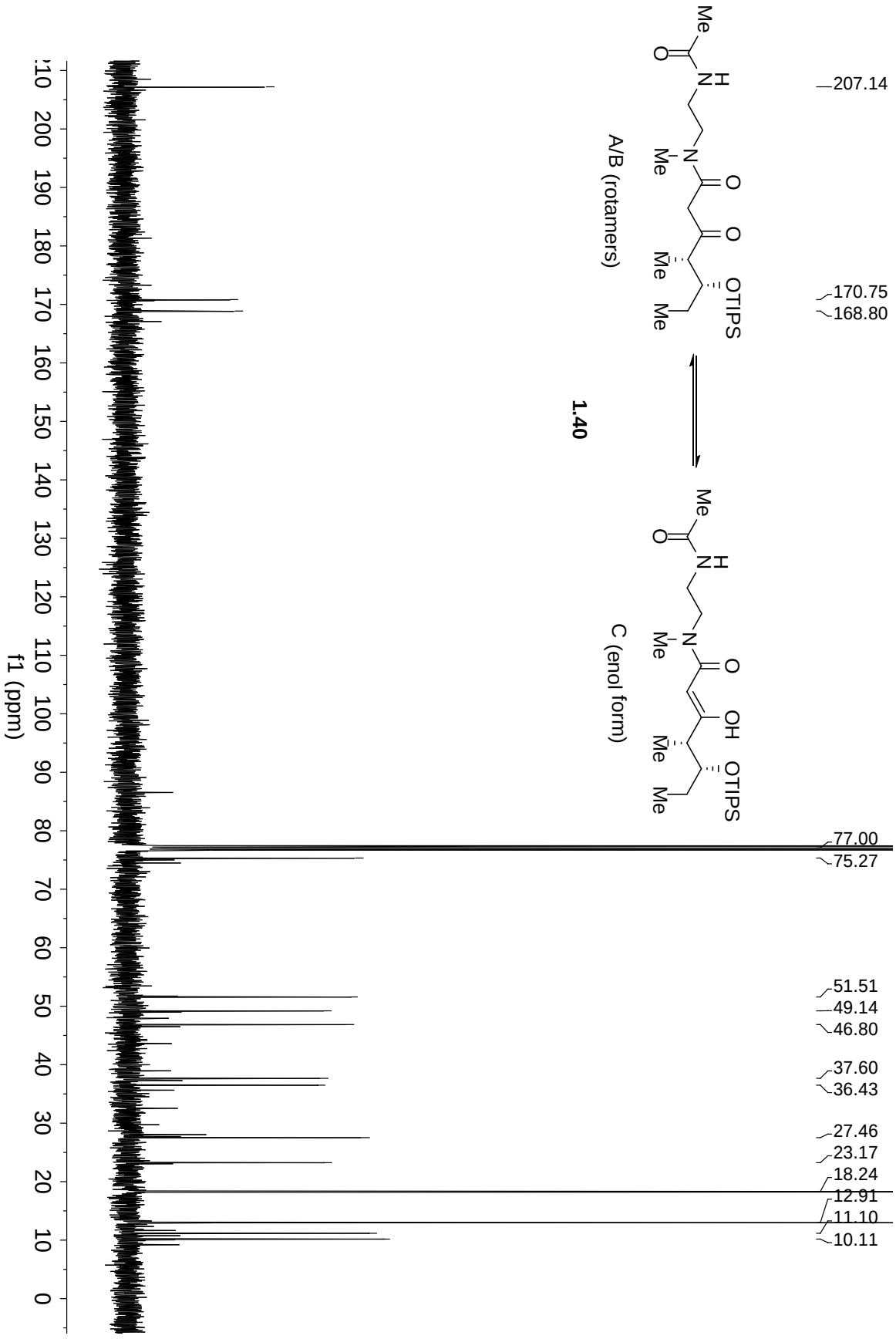
207.14
170.75
168.80
77.00
75.27
51.51
49.14
46.80
37.60
36.43
27.46
23.17
18.24
12.91
11.10
10.11
A/B (rotamers)
C (enol form)
1.40
f1 (ppm)

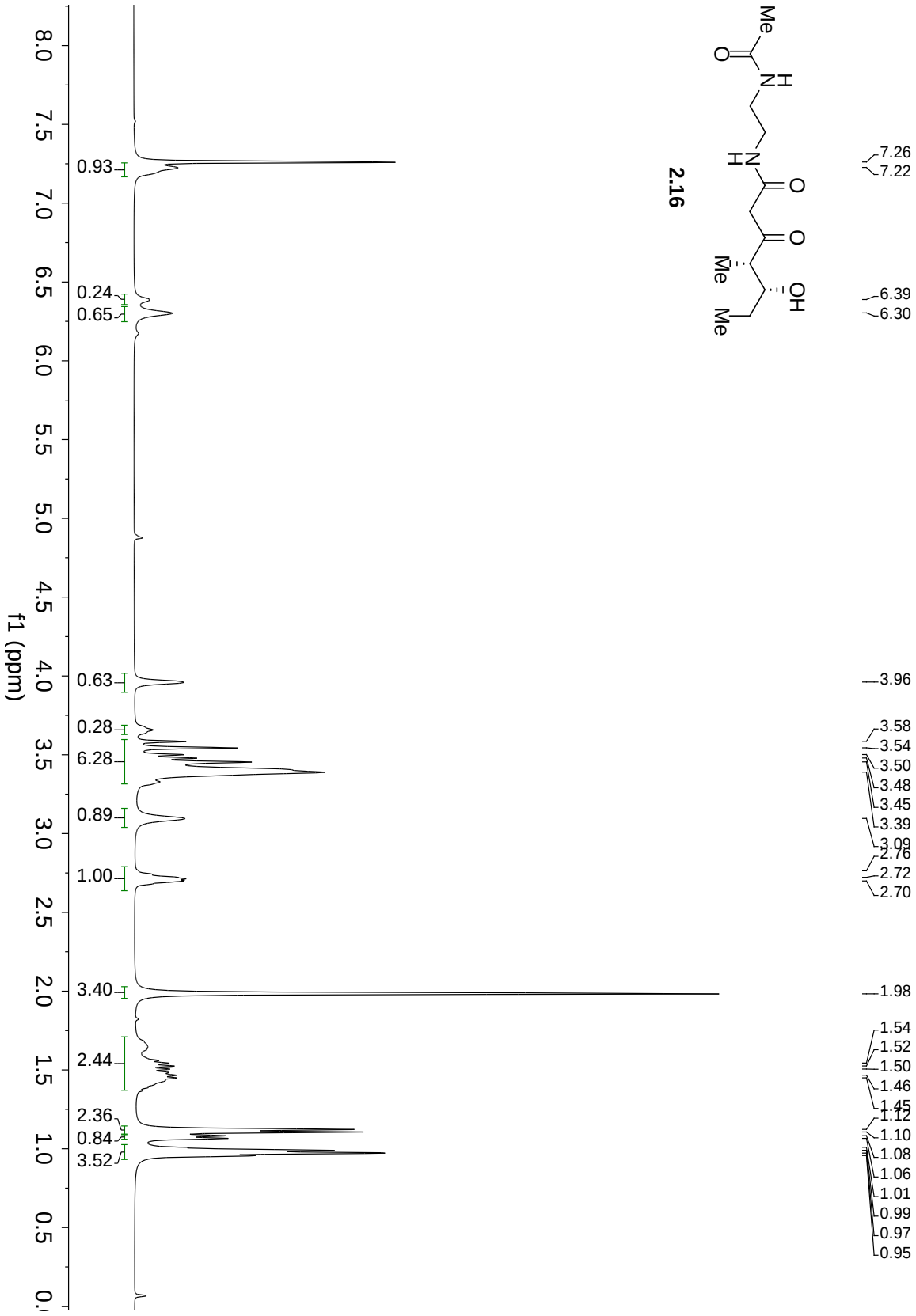
f1 (ppm)
8.0
7.5
7.0
6.5
6.0
5.5
5.0
4.5
4.0
3.5
3.0
2.5
2.0
1.5
1.0
0.5
0.
0.93
0.24
0.65
0.63
0.28
6.28
0.89
1.00
3.40
2.44
2.36
0.84
3.52
2.16
Me
O
H
N
N
H
O
O
OH
Me
Me
7.26
7.22
6.39
6.30
3.96
3.58
3.54
3.50
3.48
3.45
3.39
3.09
2.76
2.72
2.70
1.98
1.54
1.52
1.50
1.46
1.45
1.12
1.10
1.08
1.06
1.01
0.99
0.97
0.95

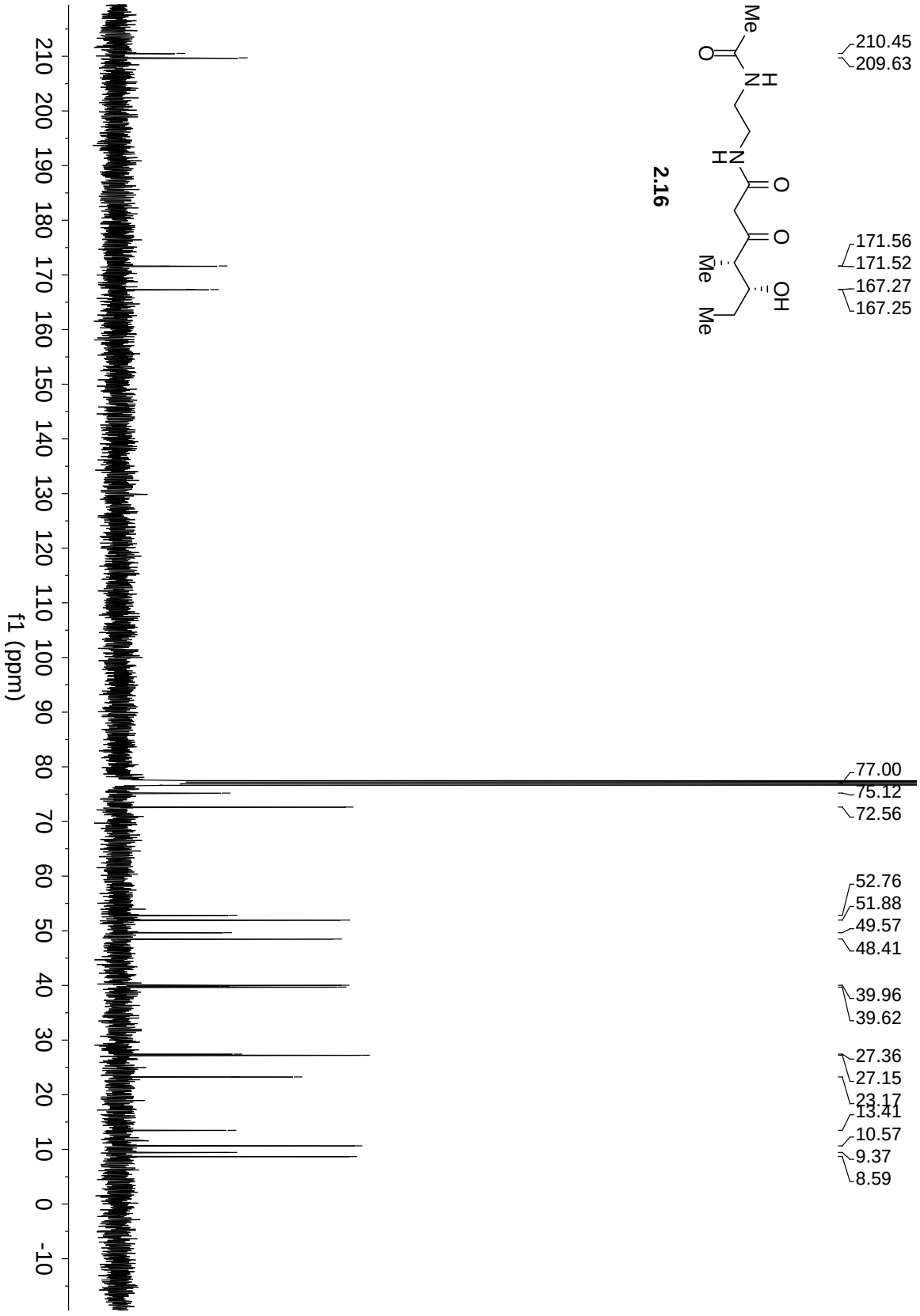
2.16
210.45
209.63
171.56
171.52
167.27
167.25
77.00
75.12
72.56
52.76
51.88
49.57
48.41
39.96
39.62
27.36
27.15
23.17
13.41
10.57
9.37
8.59
f1 (ppm)

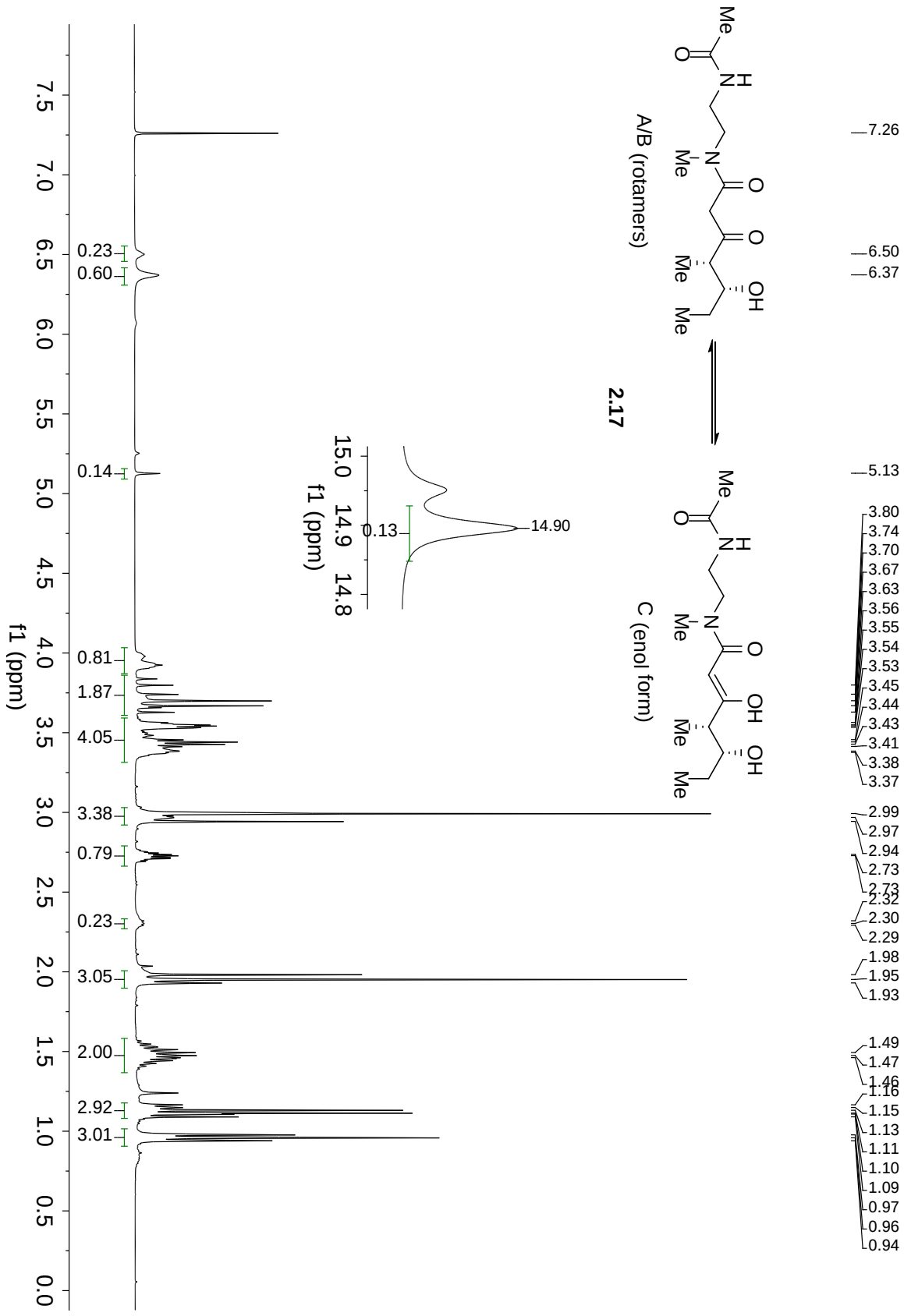
f1 (ppm)
0.23
0.60
0.14
0.81
1.87
4.05
3.38
0.79
0.23
3.05
2.00
2.92
3.01
15.0 14.9 14.8
f1 (ppm)
0.13
14.90
2.17
A/B (rotamers)
C (enol form)
7.26
6.50
6.37
5.13
3.80
3.74
3.70
3.67
3.63
3.56
3.55
3.54
3.53
3.45
3.44
3.43
3.41
3.38
3.37
2.99
2.97
2.94
2.73
2.73
2.32
2.30
2.29
1.98
1.95
1.93
1.49
1.47
1.46
1.16
1.15
1.13
1.11
1.10
1.09
0.97
0.96
0.94

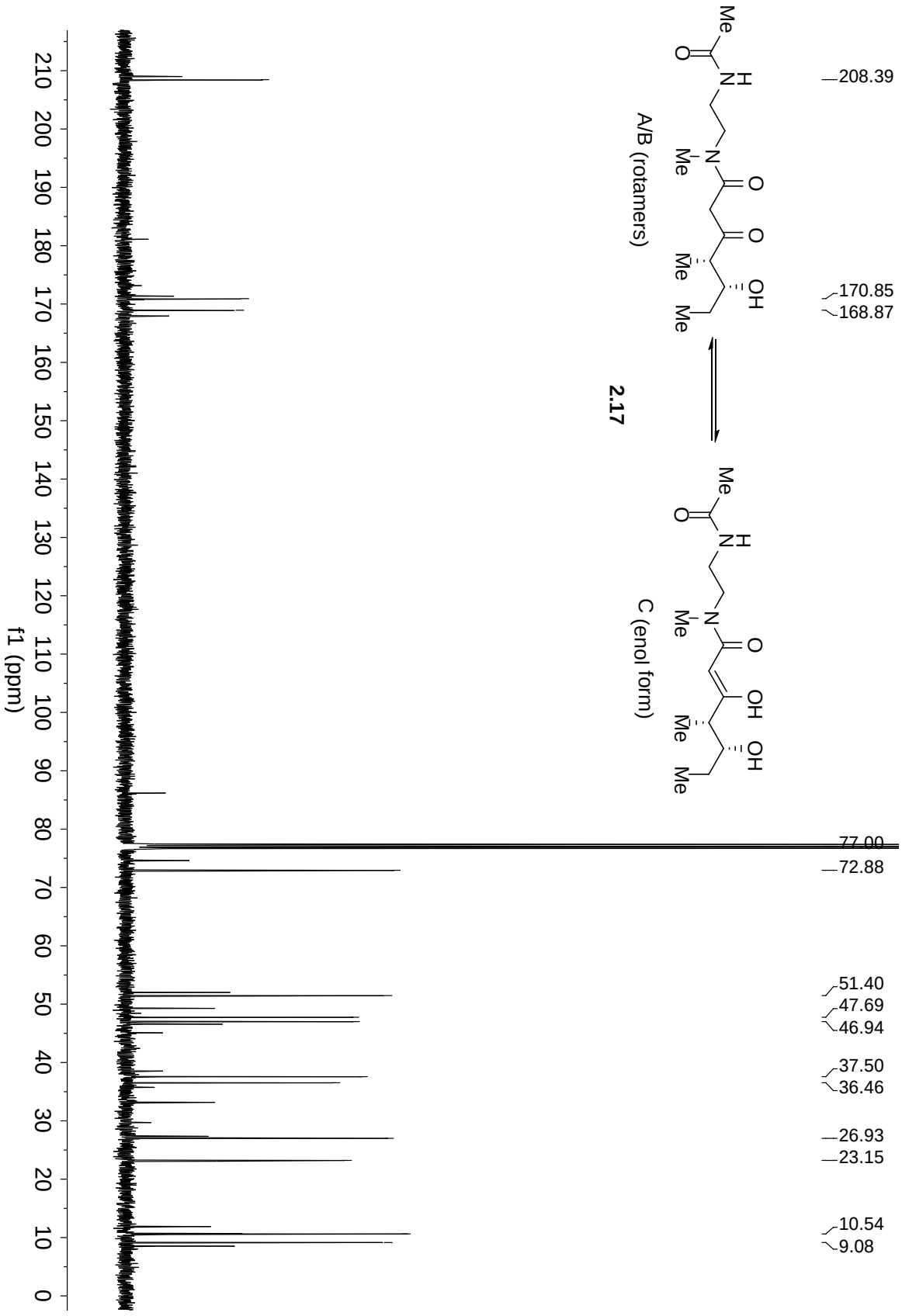
208.39
170.85
168.87
77.00
72.88
51.40
47.69
46.94
37.50
36.46
26.93
23.15
10.54
9.08
A/B (rotamers)
C (enol form)
2.17
f1 (ppm)

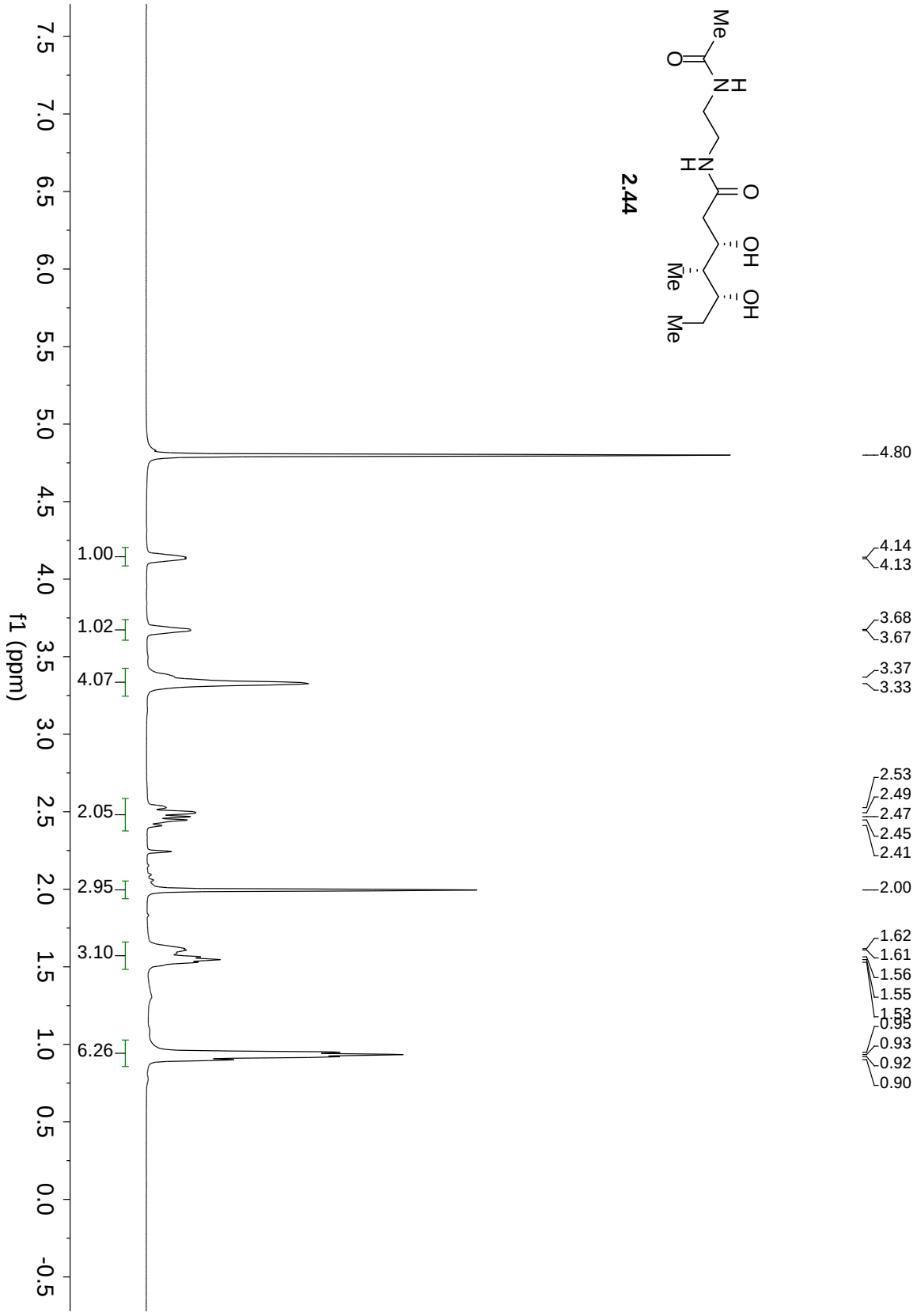
2.44
f1 (ppm)
7.5
7.0
6.5
6.0
5.5
5.0
4.5
4.0
3.5
3.0
2.5
2.0
1.5
1.0
0.5
0.0
-0.5
1.00
1.02
4.07
2.05
2.95
3.10
6.26
4.80
4.14
4.13
3.68
3.67
3.37
3.33
2.53
2.49
2.47
2.45
2.41
2.00
1.62
1.61
1.56
1.55
1.53
0.95
0.93
0.92
0.90

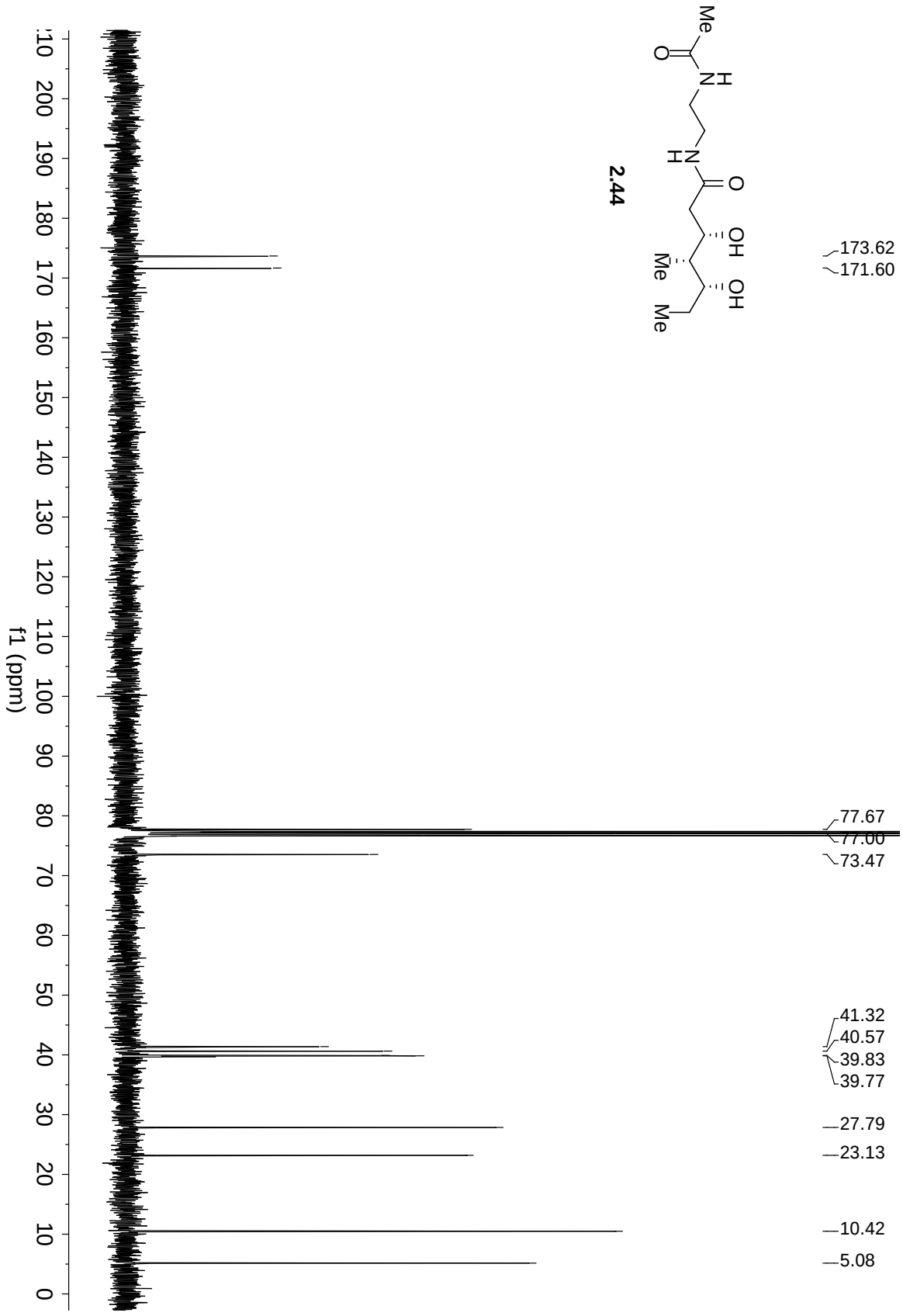
2.44
Me
O
H
N
H
N
O
OH
OH
Me
Me
173.62
171.60
77.67
77.00
73.47
41.32
40.57
39.83
39.77
27.79
23.13
10.42
5.08
f1 (ppm)
210
200
190
180
170
160
150
140
130
120
110
100
90
80
70
60
50
40
30
20
10
0

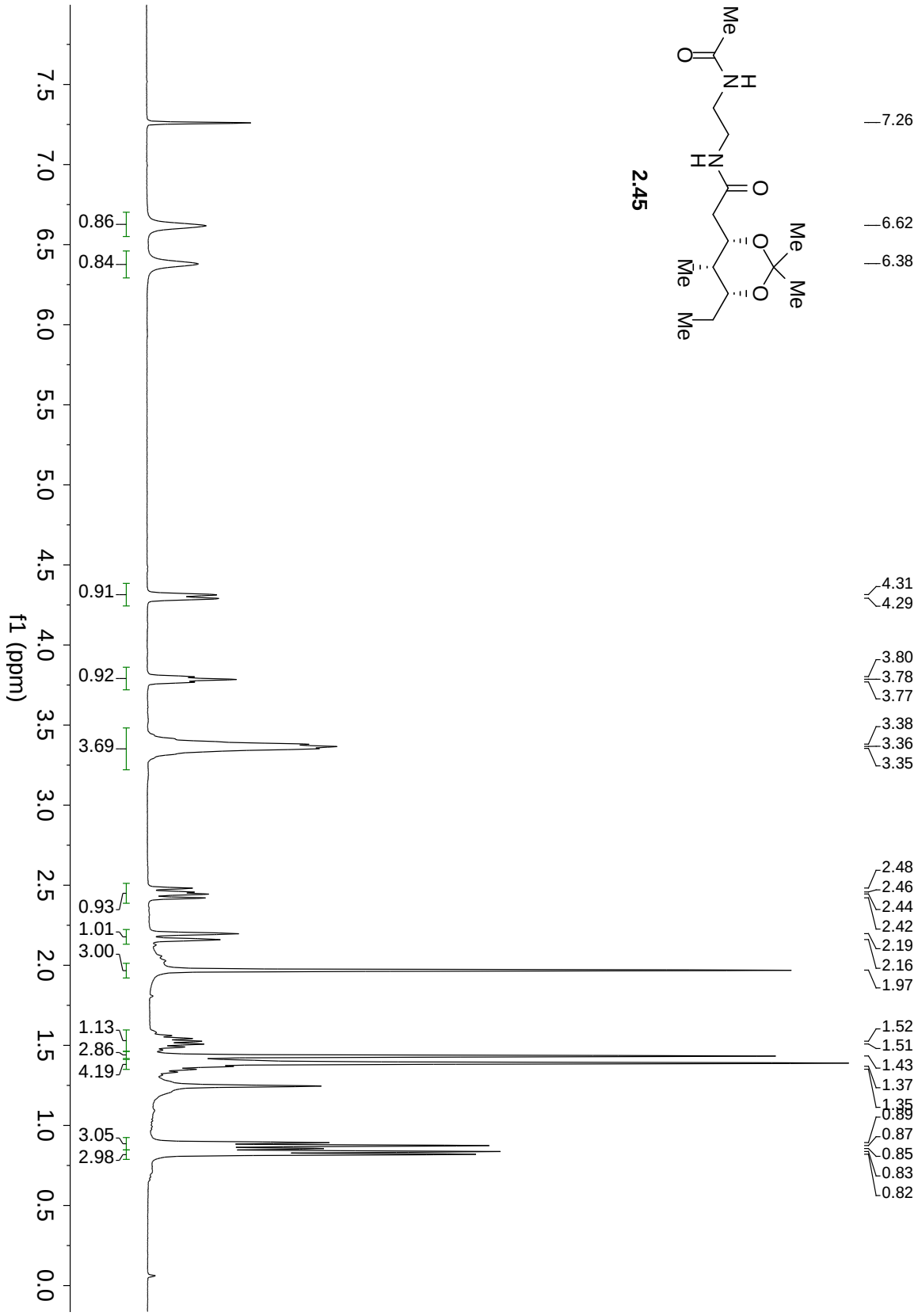
2.45
f1 (ppm)
7.5
7.0
6.5
6.0
5.5
5.0
4.5
4.0
3.5
3.0
2.5
2.0
1.5
1.0
0.5
0.0
0.86
0.84
0.91
0.92
3.69
0.93
1.01
3.00
1.13
2.86
4.19
3.05
2.98
7.26
6.62
6.38
4.31
4.29
3.80
3.78
3.77
3.38
3.36
3.35
2.48
2.46
2.44
2.42
2.19
2.16
1.97
1.52
1.51
1.43
1.37
1.35
0.89
0.87
0.85
0.83
0.82

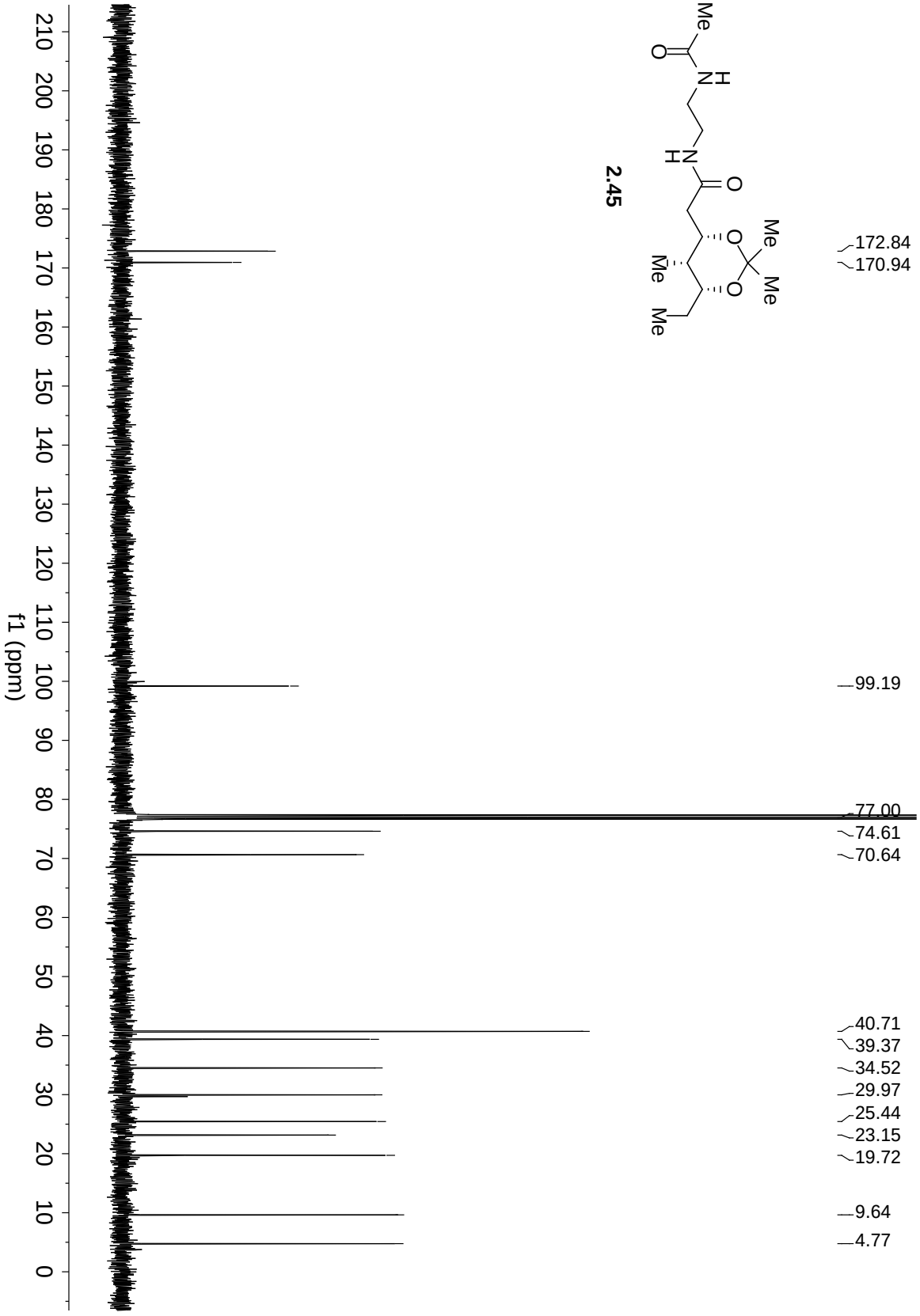
2.45
172.84
170.94
99.19
77.00
74.61
70.64
40.71
39.37
34.52
29.97
25.44
23.15
19.72
9.64
4.77
f1 (ppm)

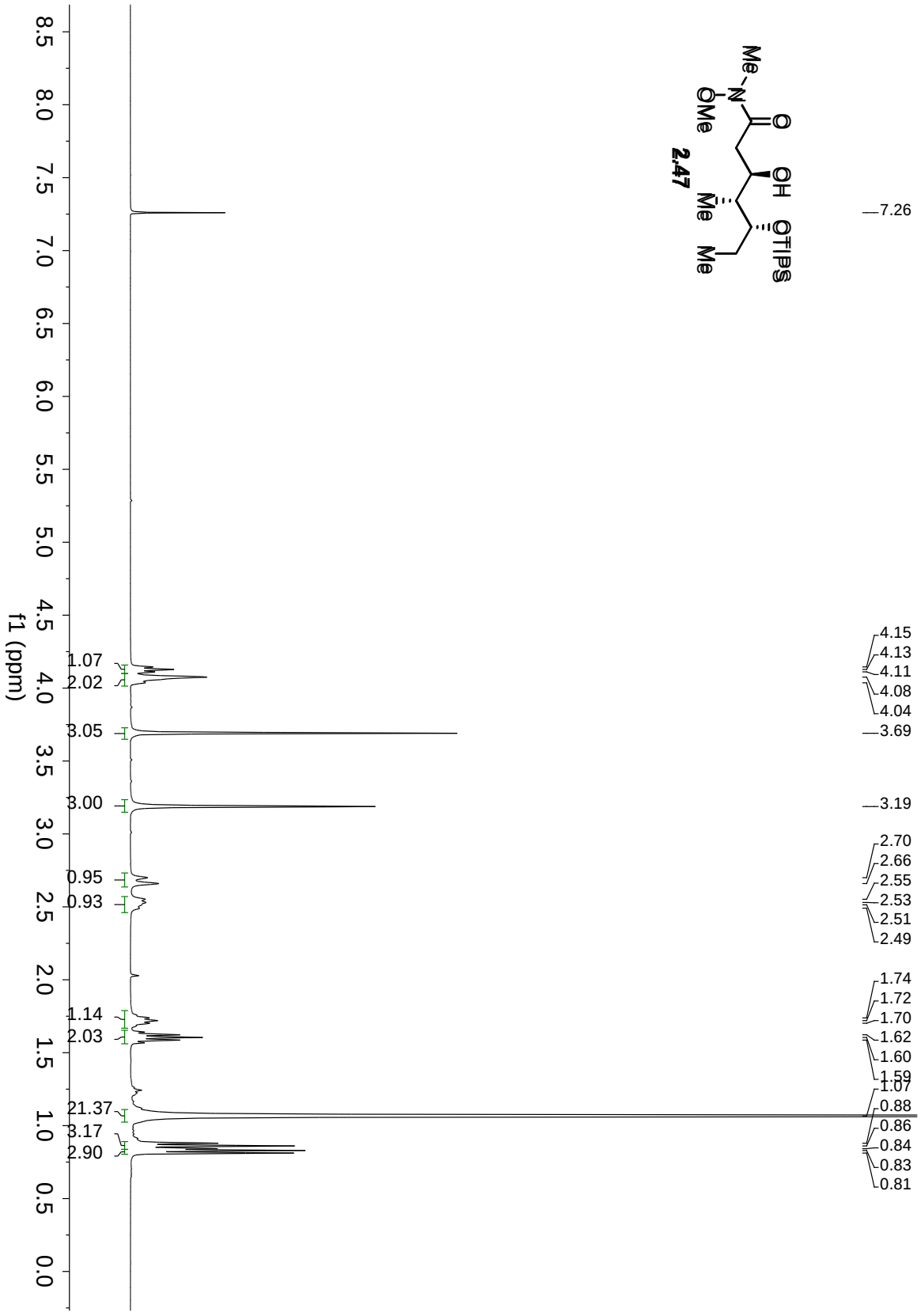
2.47
f1 (ppm)
8.5
8.0
7.5
7.0
6.5
6.0
5.5
5.0
4.5
4.0
3.5
3.0
2.5
2.0
1.5
1.0
0.5
0.0
1.07
2.02
3.05
3.00
0.95
0.93
1.14
2.03
21.37
3.17
2.90
7.26
4.15
4.13
4.11
4.08
4.04
3.69
3.19
2.70
2.66
2.55
2.53
2.51
2.49
1.74
1.72
1.70
1.62
1.60
1.59
1.07
0.88
0.86
0.84
0.83
0.81

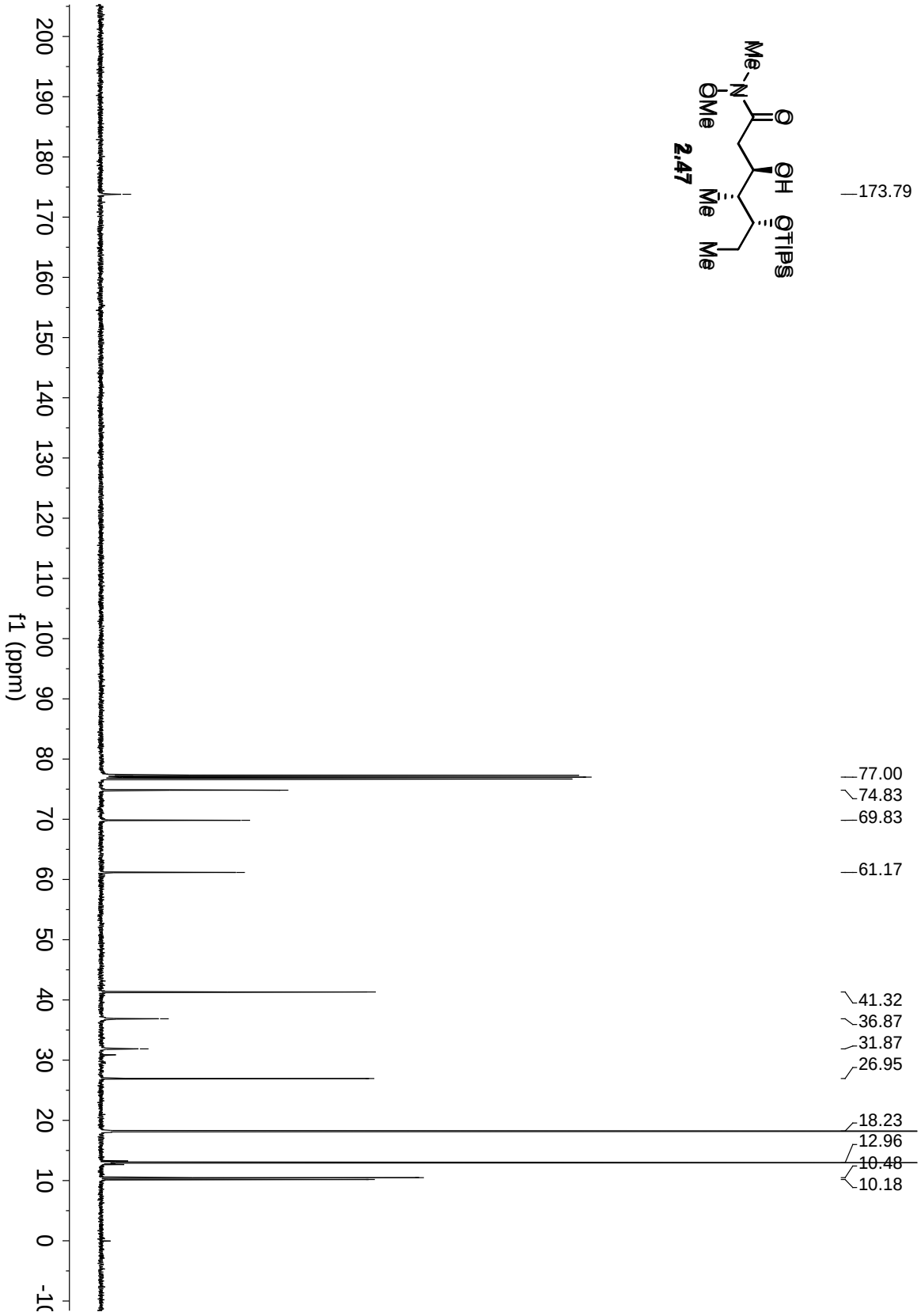
2.47
173.79
77.00
74.83
69.83
61.17
41.32
36.87
31.87
26.95
18.23
12.96
10.48
10.18
f1 (ppm)

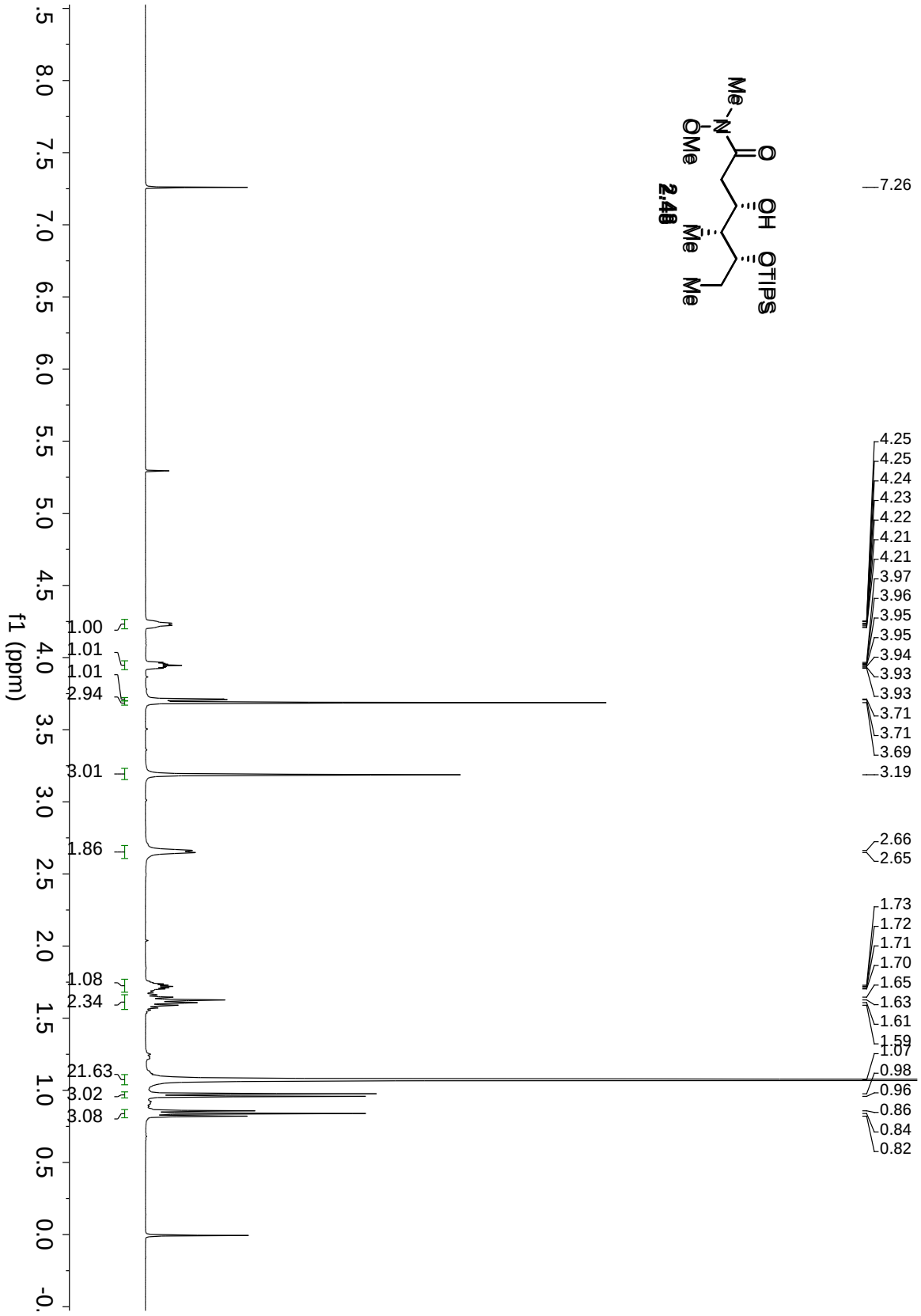
f1 (ppm)
1.00
1.01
1.01
2.94
3.01
1.86
1.08
2.34
21.63
3.02
3.08
7.26
4.25
4.25
4.24
4.23
4.22
4.21
4.21
3.97
3.96
3.95
3.95
3.94
3.93
3.93
3.71
3.71
3.69
3.19
2.66
2.65
1.73
1.72
1.71
1.70
1.65
1.63
1.61
1.59
1.07
0.98
0.96
0.86
0.84
0.82

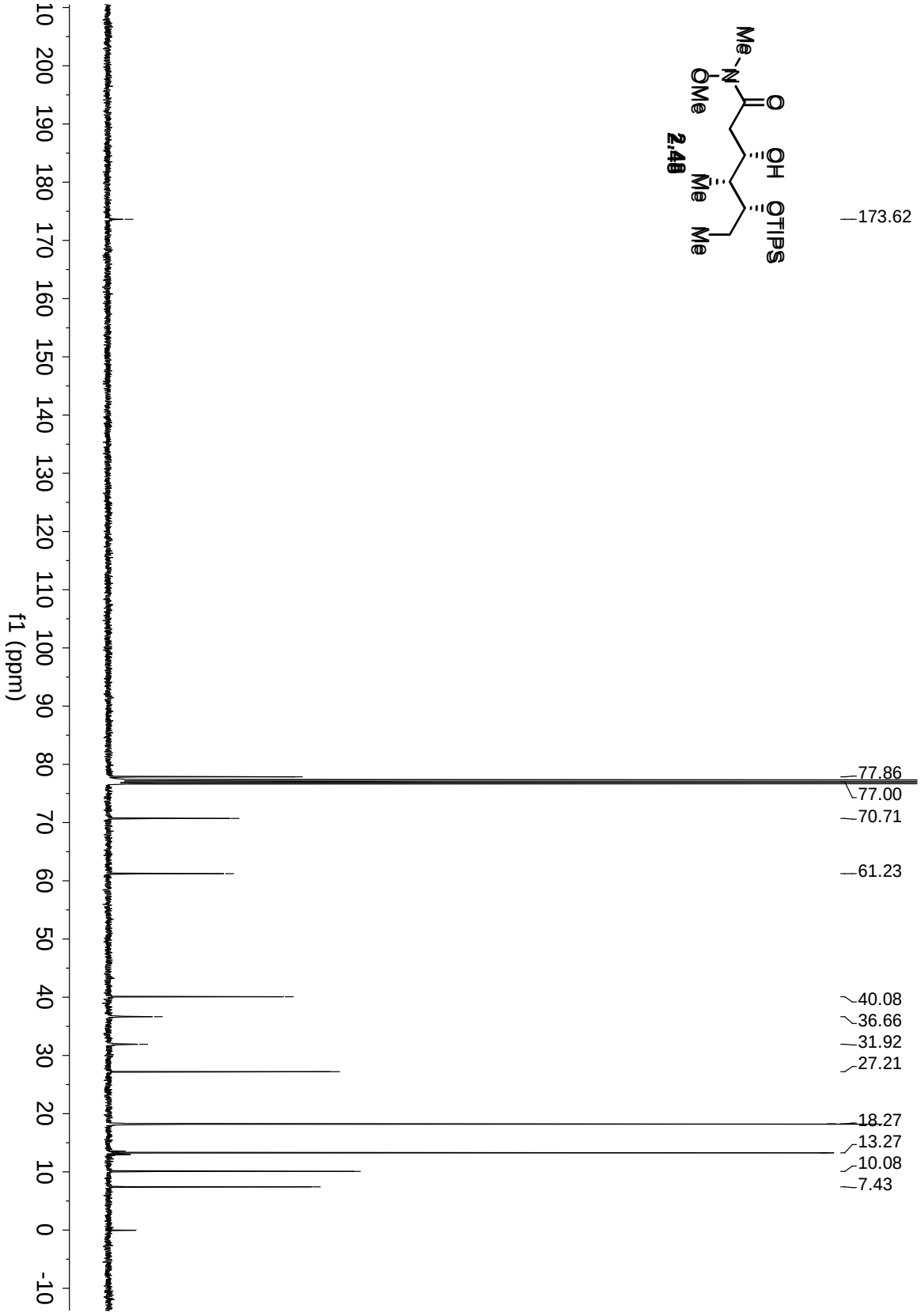
f1 (ppm)
10 200 190 180 170 160 150 140 130 120 110 100 90 80 70 60 50 40 30 20 10 0 -10
Me
N
OMe
O
OH
OTIPS
Me
Me
2,4
173.62
77.86
77.00
70.71
61.23
40.08
36.66
31.92
27.21
18.27
13.27
10.08
7.43

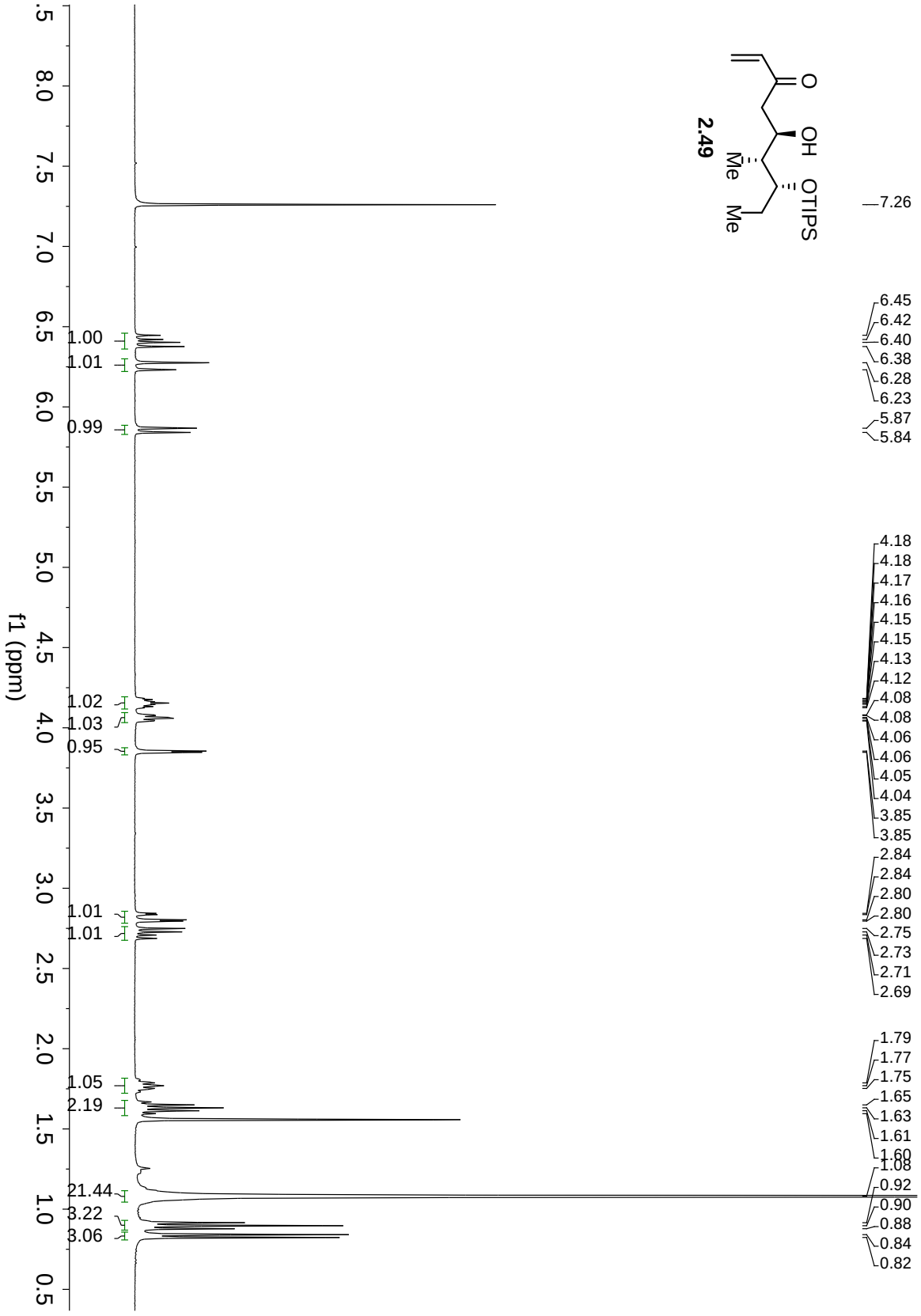
2.49
O
OH
OTIPS
Me
Me
f1 (ppm)
1.00
1.01
0.99
1.02
1.03
0.95
1.01
1.01
1.05
2.19
21.44
3.22
3.06
7.26
6.45
6.42
6.40
6.38
6.28
6.23
5.87
5.84
4.18
4.18
4.17
4.16
4.15
4.15
4.13
4.12
4.08
4.08
4.06
4.06
4.05
4.04
3.85
3.85
2.84
2.84
2.80
2.80
2.75
2.73
2.71
2.69
1.79
1.77
1.75
1.65
1.63
1.61
1.60
1.08
0.92
0.90
0.88
0.84
0.82

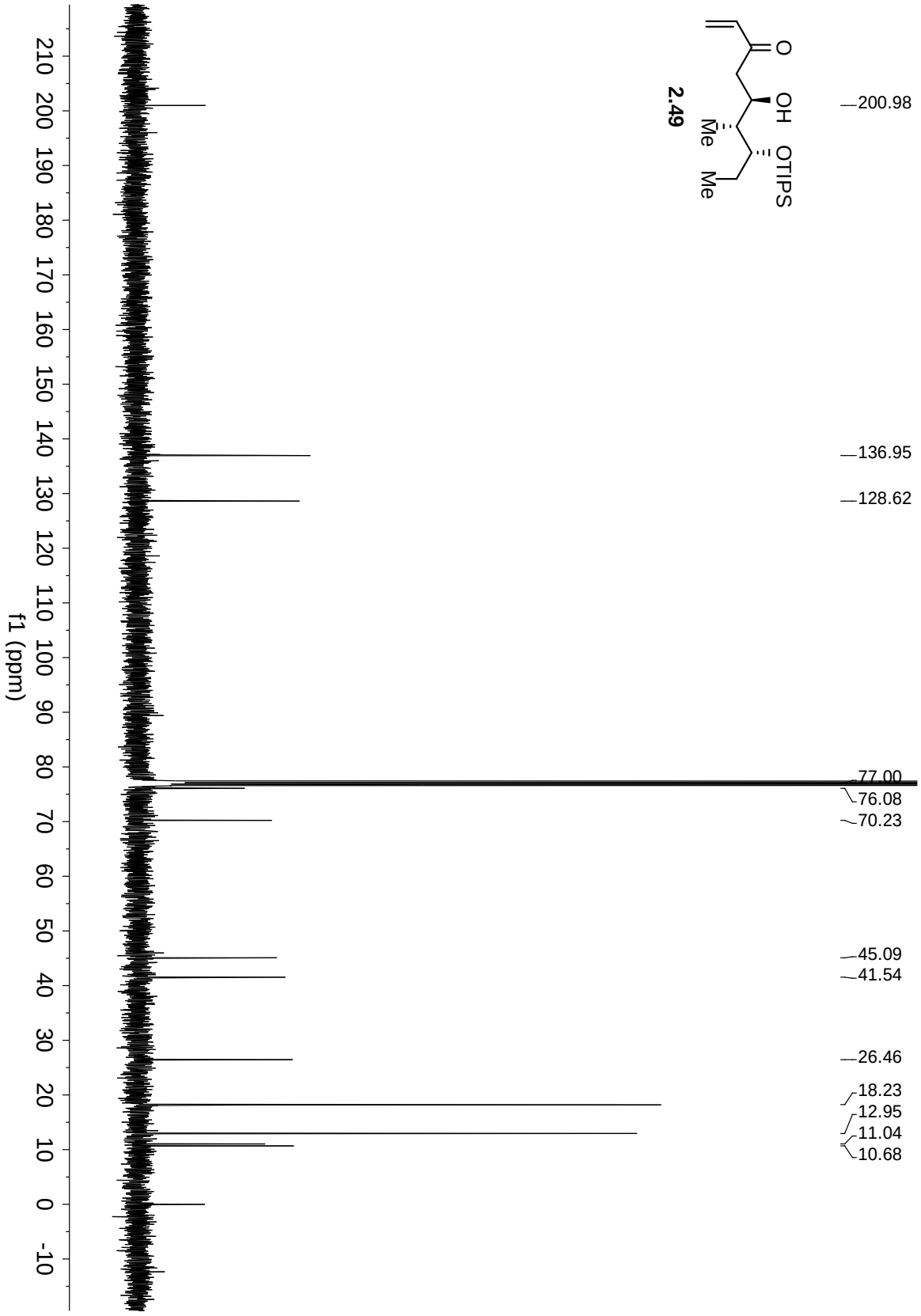
2.49
O
OH
OTIPS
Me
Me
200.98
136.95
128.62
77.00
76.08
70.23
45.09
41.54
26.46
18.23
12.95
11.04
10.68
f1 (ppm)
210
200
190
180
170
160
150
140
130
120
110
100
90
80
70
60
50
40
30
20
10
0
-10

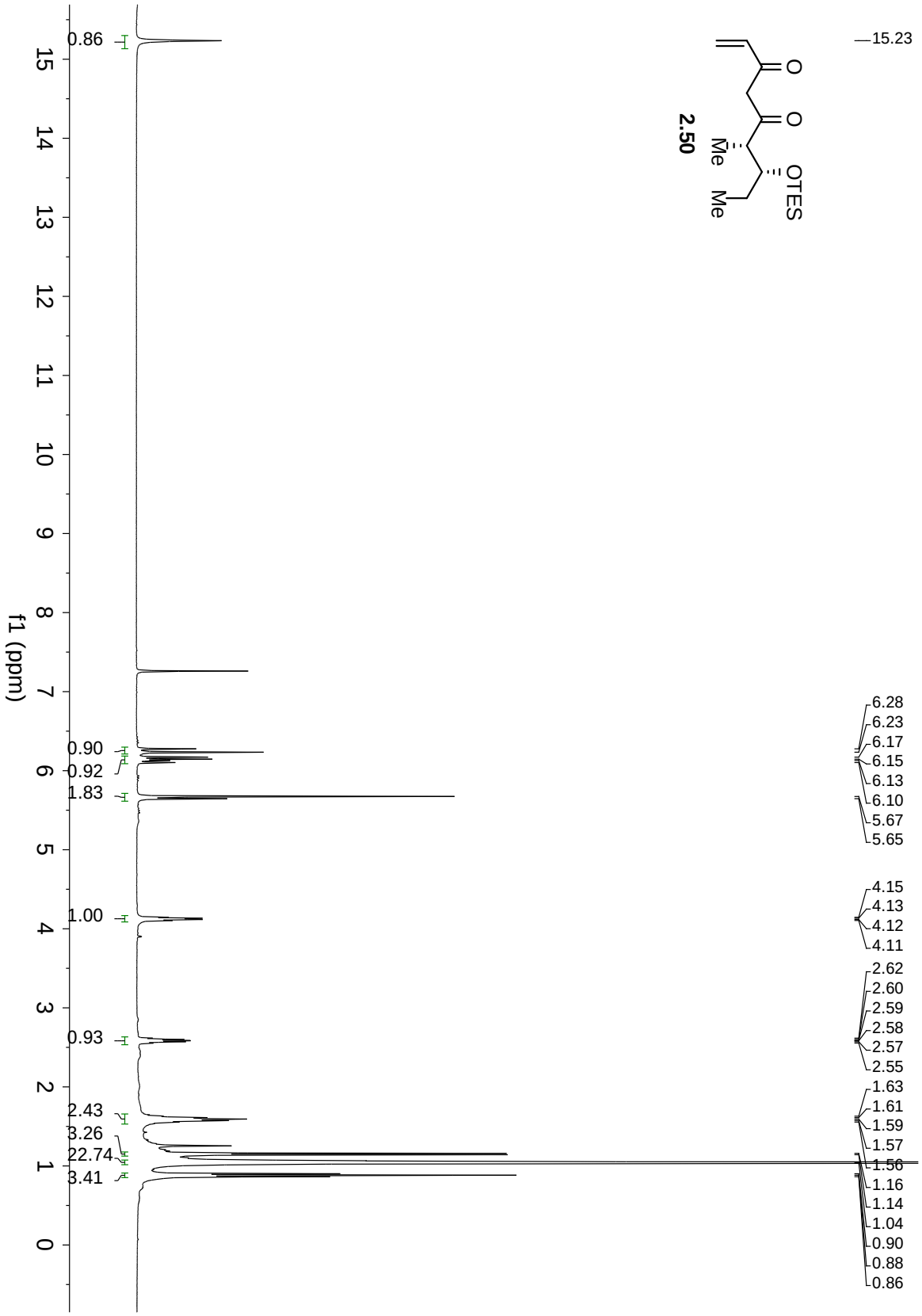
f1 (ppm)
0.86
0.90
0.92
1.83
1.00
0.93
2.43
3.26
22.74
3.41
2.50
O
O
OTES
Me
Me
15.23
6.28
6.23
6.17
6.15
6.13
6.10
5.67
5.65
4.15
4.13
4.12
4.11
2.62
2.60
2.59
2.58
2.57
2.55
1.63
1.61
1.59
1.57
1.56
1.16
1.14
1.04
0.90
0.88
0.86

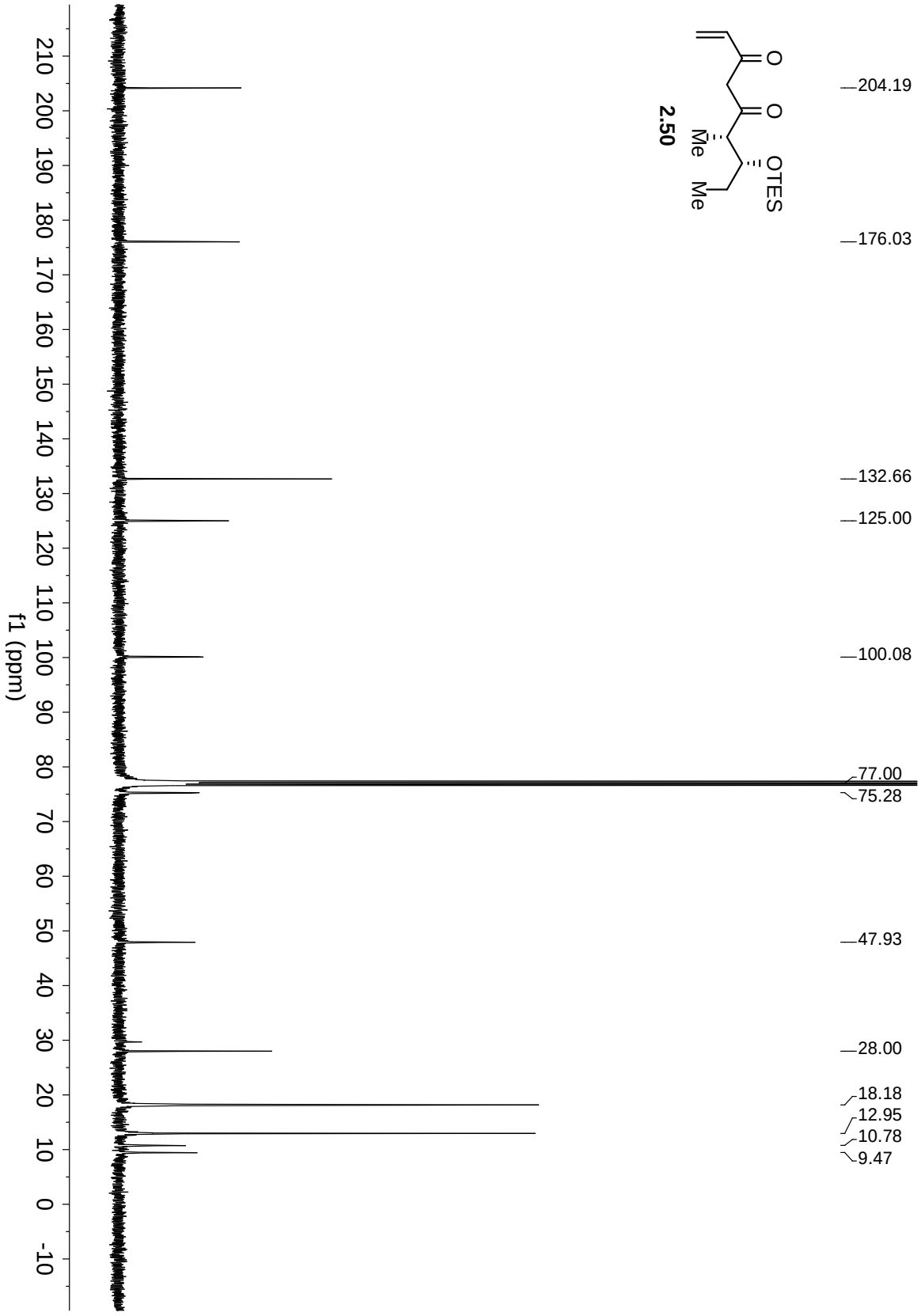
f1 (ppm)
210 200 190 180 170 160 150 140 130 120 110 100 90 80 70 60 50 40 30 20 10 0 -10
204.19
176.03
132.66
125.00
100.08
77.00
75.28
47.93
28.00
18.18
12.95
10.78
9.47
2.50
O
O
OTES
Me
Me

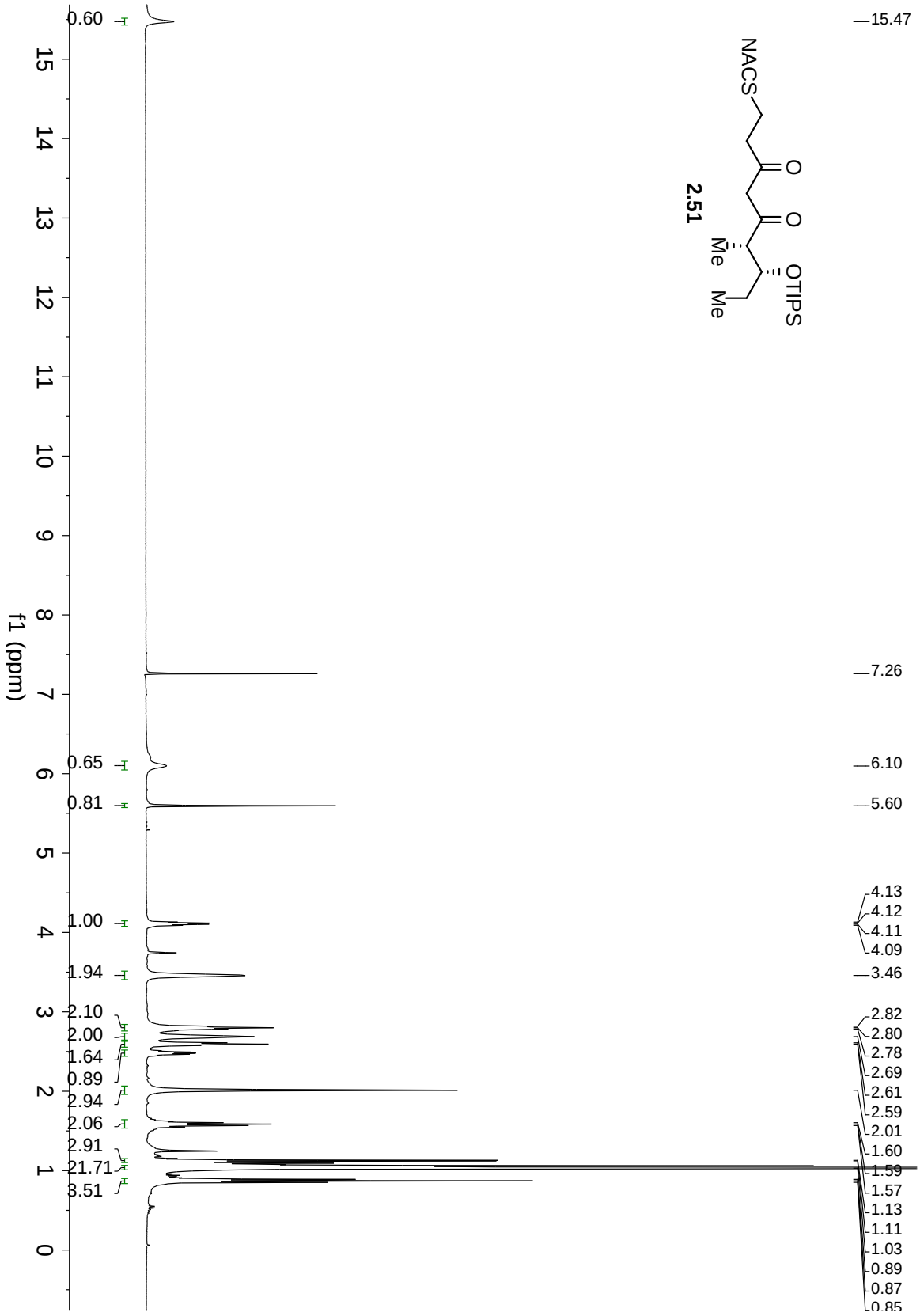
f1 (ppm)
0.60
0.65
0.81
1.00
1.94
2.10
2.00
1.64
0.89
2.94
2.06
2.91
21.71
3.51
15.47
7.26
6.10
5.60
4.13
4.12
4.11
4.09
3.46
2.82
2.80
2.78
2.69
2.61
2.59
2.01
1.60
1.59
1.57
1.13
1.11
1.03
0.89
0.87
0.85
NACS
O
O
OTIPS
Me
Me
2.51

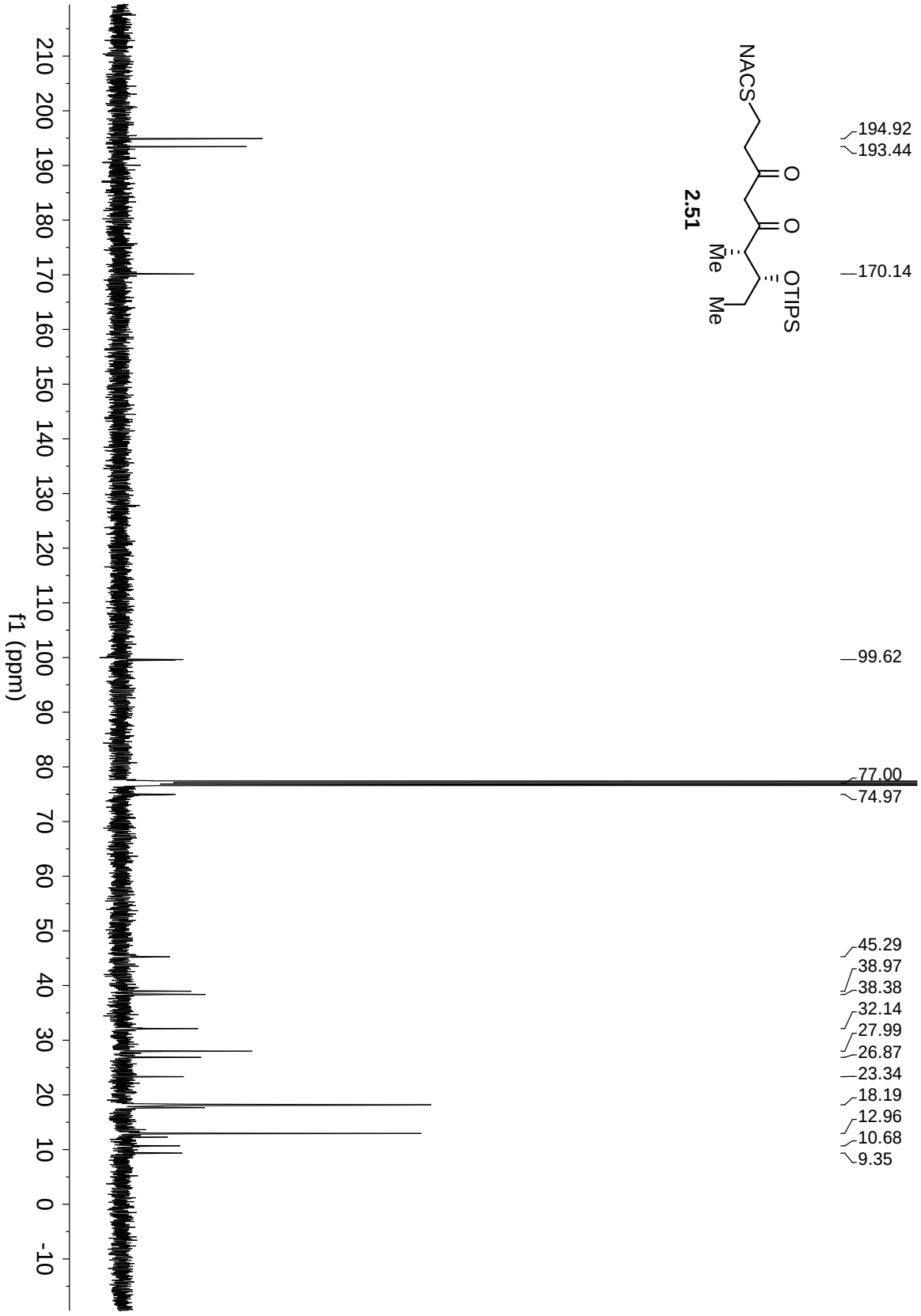
NACS
O
O
OTIPS
Me
Me
2.51
194.92
193.44
170.14
99.62
77.00
74.97
45.29
38.97
38.38
32.14
27.99
26.87
23.34
18.19
12.96
10.68
9.35
f1 (ppm)
210 200 190 180 170 160 150 140 130 120 110 100 90 80 70 60 50 40 30 20 10 0 -10

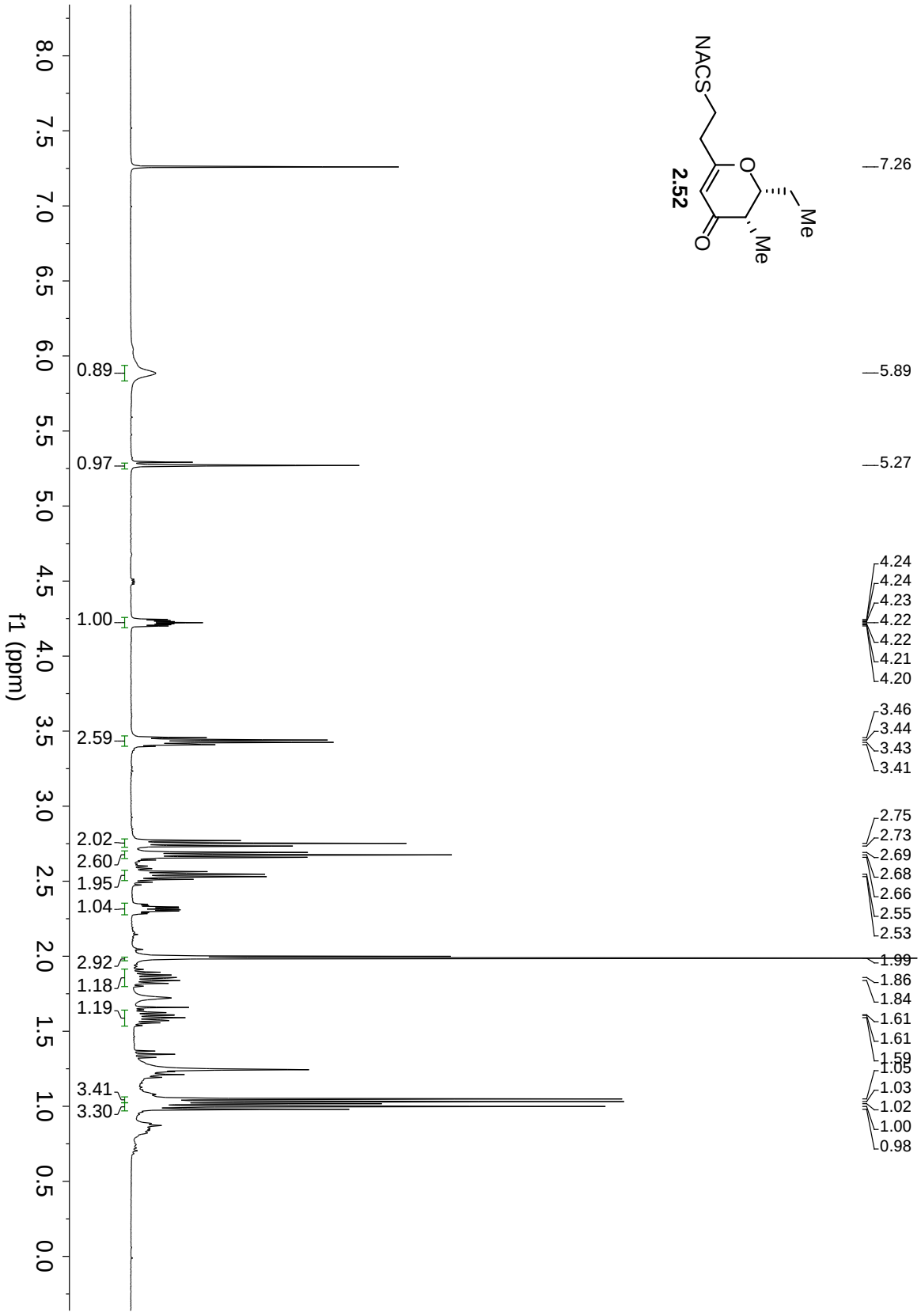
NACS
O
Me
Me
O
2.52
f1 (ppm)
8.0
7.5
7.0
6.5
6.0
5.5
5.0
4.5
4.0
3.5
3.0
2.5
2.0
1.5
1.0
0.5
0.0
0.89
0.97
1.00
2.59
2.02
2.60
1.95
1.04
2.92
1.18
1.19
3.41
3.30
7.26
5.89
5.27
4.24
4.24
4.23
4.22
4.22
4.21
4.20
3.46
3.44
3.43
3.41
2.75
2.73
2.69
2.68
2.66
2.55
2.53
1.99
1.86
1.84
1.61
1.61
1.59
1.05
1.03
1.02
1.00
0.98

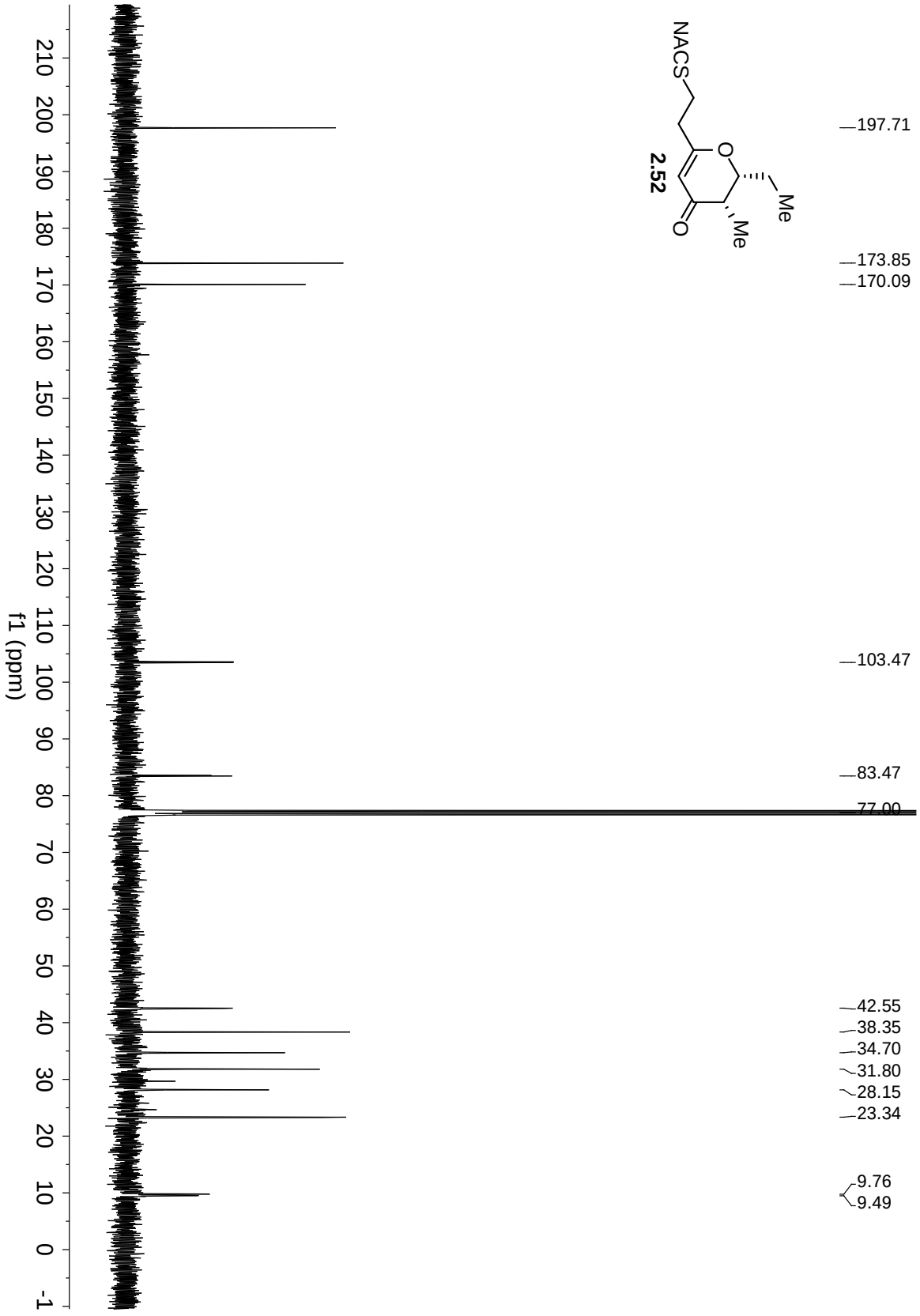
NACS
O
O
Me
Me
2.52
197.71
173.85
170.09
103.47
83.47
77.00
42.55
38.35
34.70
31.80
28.15
23.34
9.76
9.49
f1 (ppm)
210
200
190
180
170
160
150
140
130
120
110
100
90
80
70
60
50
40
30
20
10
0
-1

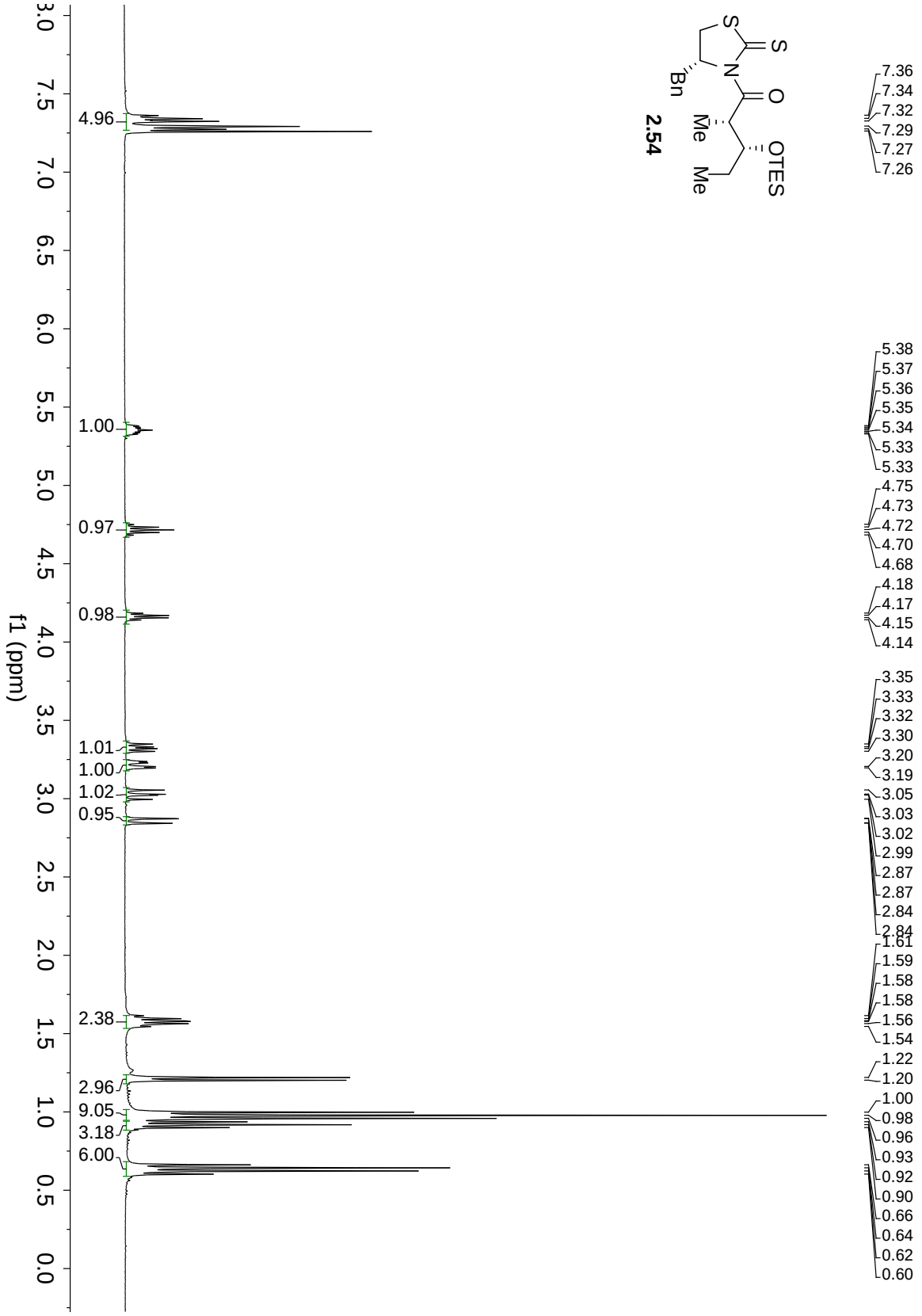
f1 (ppm)
3.0
7.5
7.0
6.5
6.0
5.5
5.0
4.5
4.0
3.5
3.0
2.5
2.0
1.5
1.0
0.5
0.0
4.96
1.00
0.97
0.98
1.01
1.00
1.02
0.95
2.38
2.96
9.05
3.18
6.00
S
S
N
O
OTES
Bn
Me
Me
2.54
7.36
7.34
7.32
7.29
7.27
7.26
5.38
5.37
5.36
5.35
5.34
5.33
5.33
4.75
4.73
4.72
4.70
4.68
4.18
4.17
4.15
4.14
3.35
3.33
3.32
3.30
3.20
3.19
3.05
3.03
3.02
2.99
2.87
2.87
2.84
2.84
1.61
1.59
1.58
1.58
1.56
1.54
1.22
1.20
1.00
0.98
0.96
0.93
0.92
0.90
0.66
0.64
0.62
0.60

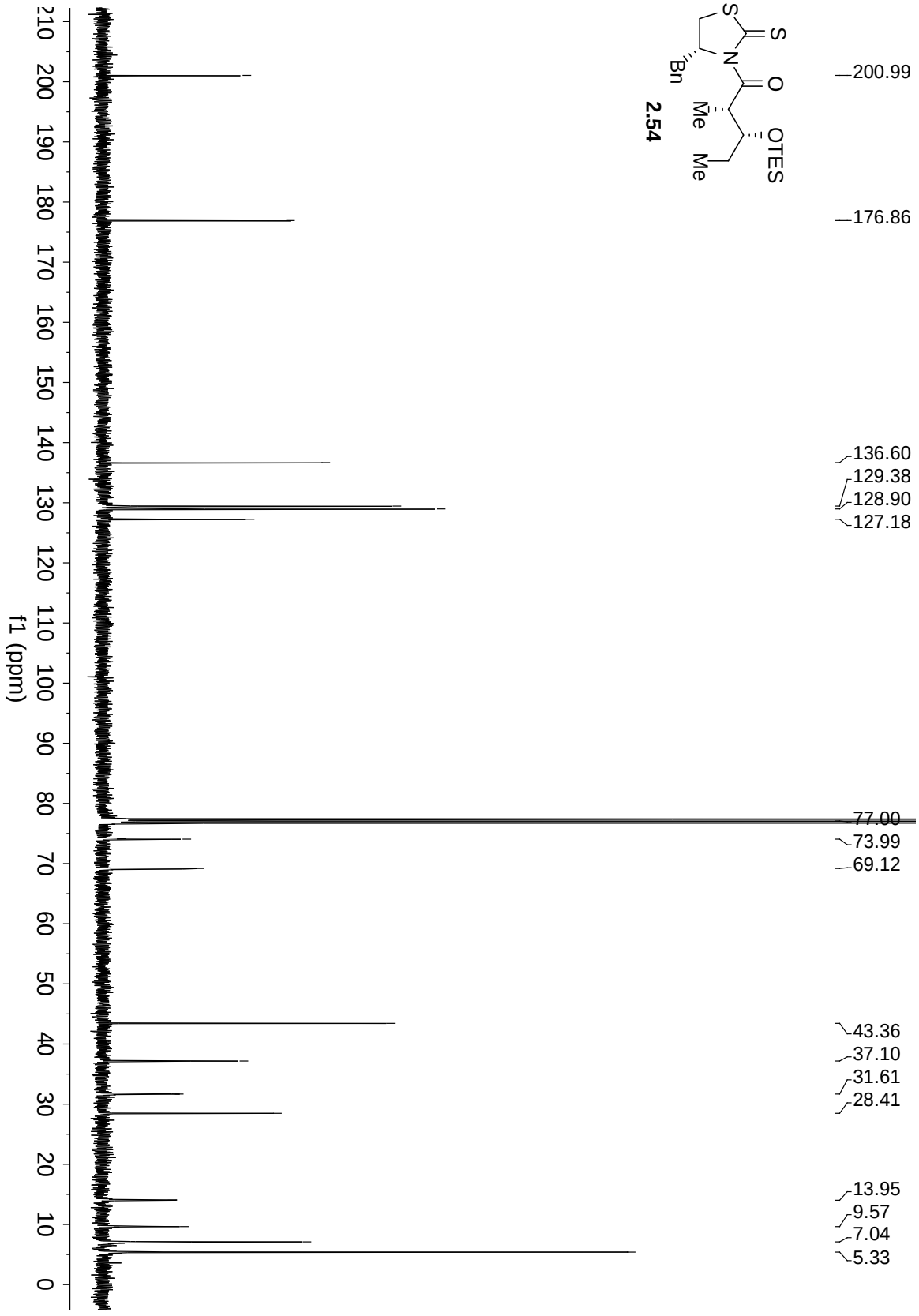
200.99
176.86
136.60
129.38
128.90
127.18
77.00
73.99
69.12
43.36
37.10
31.61
28.41
13.95
9.57
7.04
5.33
f1 (ppm)
2.54

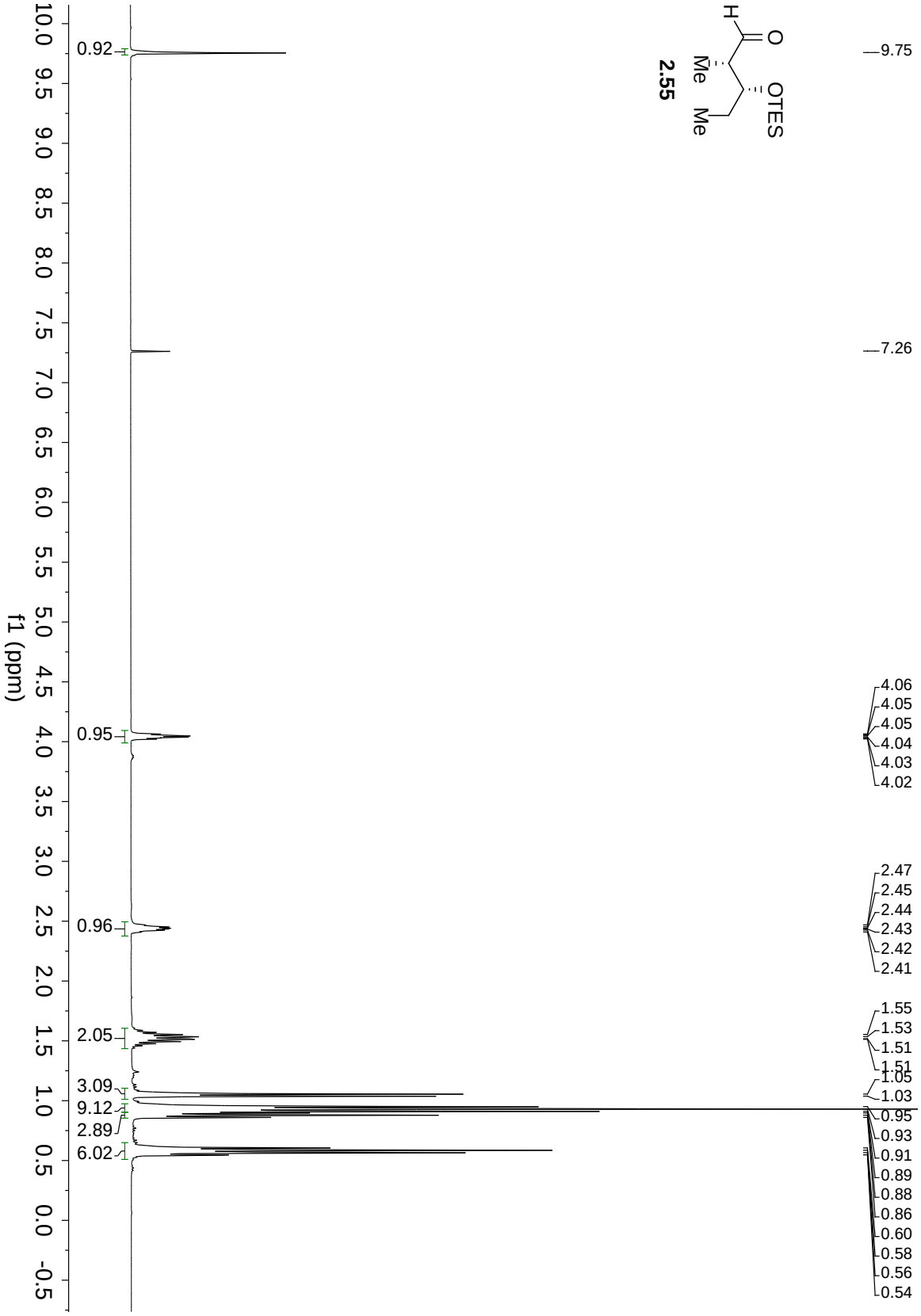
2.55
H
O
OTES
Me
Me
f1 (ppm)
10.0 9.5 9.0 8.5 8.0 7.5 7.0 6.5 6.0 5.5 5.0 4.5 4.0 3.5 3.0 2.5 2.0 1.5 1.0 0.5 0.0 -0.5
0.92
0.95
0.96
2.05
3.09
9.12
2.89
6.02
9.75
7.26
4.06
4.05
4.05
4.04
4.03
4.02
2.47
2.45
2.44
2.43
2.42
2.41
1.55
1.53
1.51
1.51
1.05
1.03
0.95
0.93
0.91
0.89
0.88
0.86
0.60
0.58
0.56
0.54

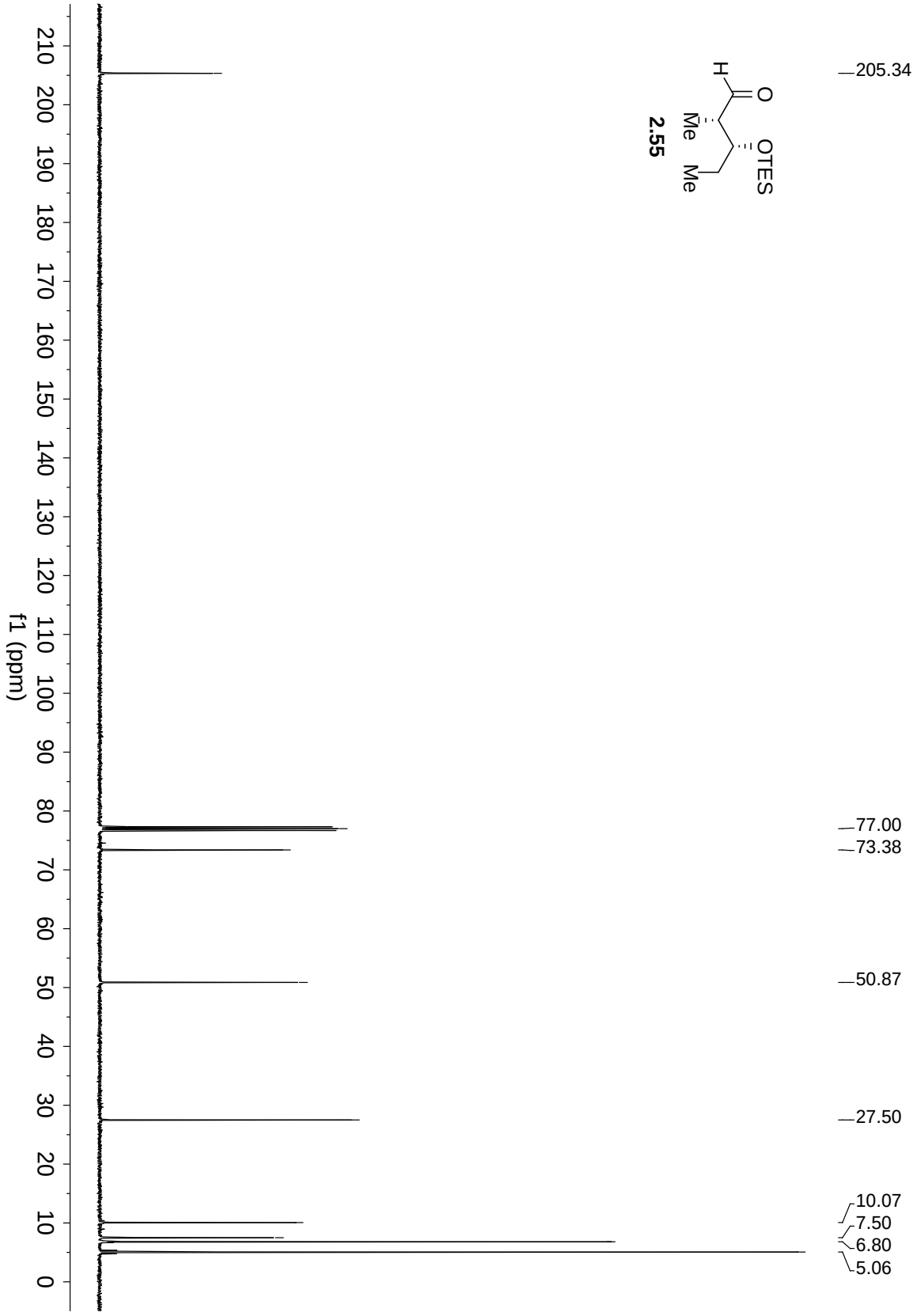
205.34
77.00
73.38
50.87
27.50
10.07
7.50
6.80
5.06
f1 (ppm)
210 200 190 180 170 160 150 140 130 120 110 100 90 80 70 60 50 40 30 20 10 0
H
O
OTES
Me
Me
2.55

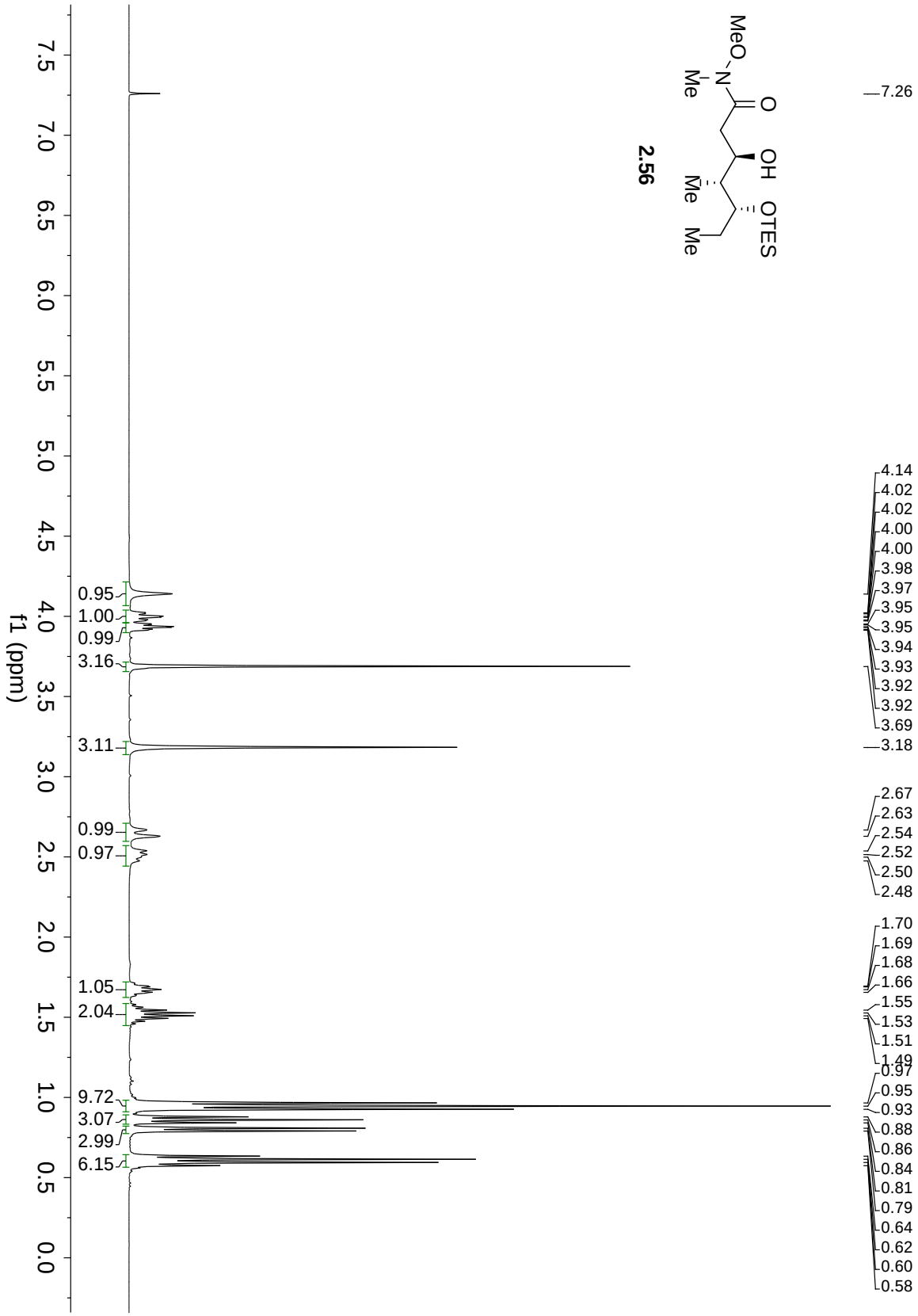
MeO
N
Me
O
OH
OTES
Me
Me
2.56
f1 (ppm)
7.5
7.0
6.5
6.0
5.5
5.0
4.5
4.0
3.5
3.0
2.5
2.0
1.5
1.0
0.5
0.0
0.95
1.00
0.99
3.16
3.11
0.99
0.97
1.05
2.04
9.72
3.07
2.99
6.15
7.26
4.14
4.02
4.02
4.00
4.00
3.98
3.97
3.95
3.95
3.94
3.93
3.92
3.92
3.69
3.18
2.67
2.63
2.54
2.52
2.50
2.48
1.70
1.69
1.68
1.66
1.55
1.53
1.51
1.49
0.97
0.95
0.93
0.88
0.86
0.84
0.81
0.79
0.64
0.62
0.60
0.58

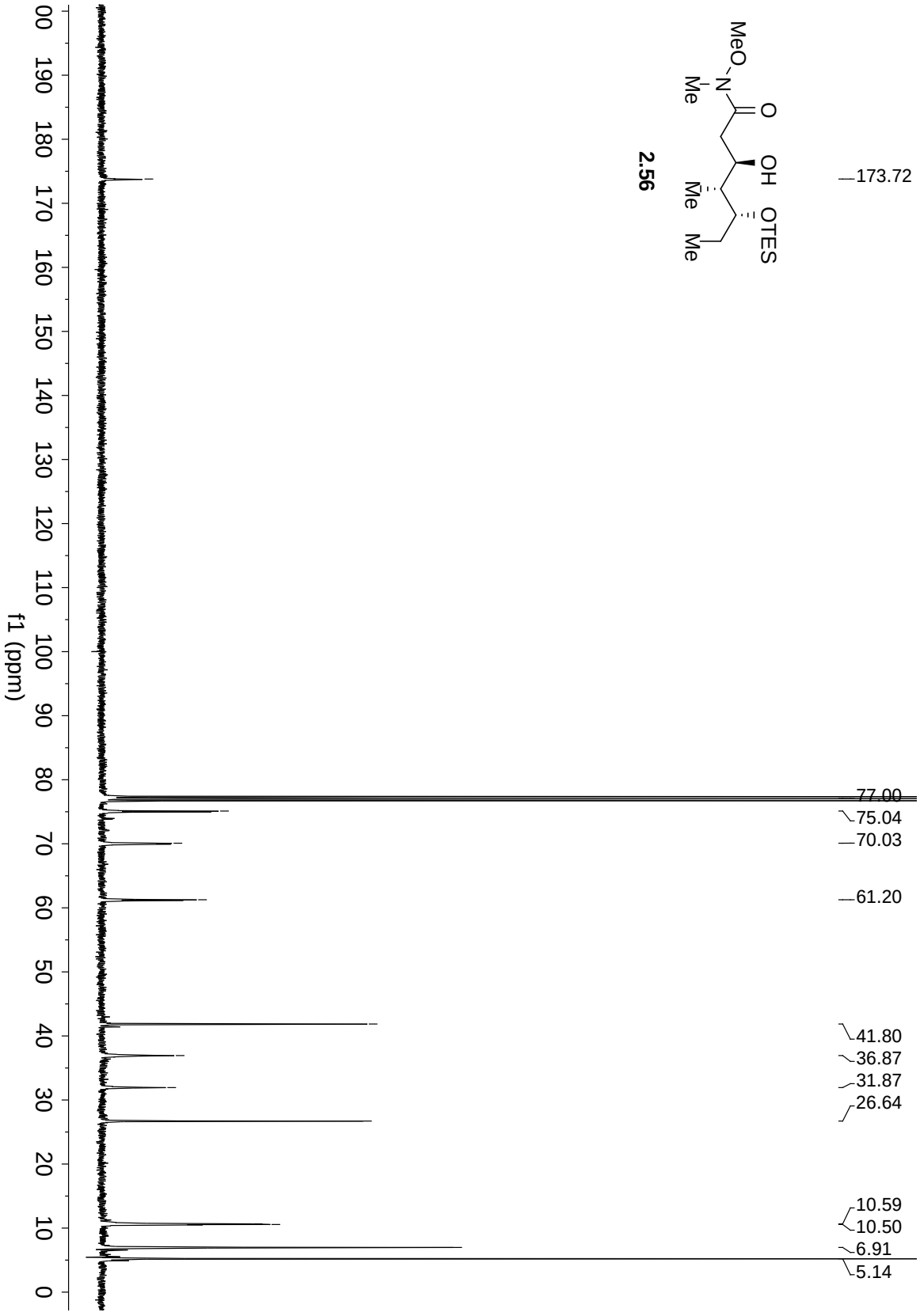
MeO
N
Me
O
OH
OTES
Me
Me
Me
2.56
173.72
77.00
75.04
70.03
61.20
41.80
36.87
31.87
26.64
10.59
10.50
6.91
5.14
f1 (ppm)
200
190
180
170
160
150
140
130
120
110
100
90
80
70
60
50
40
30
20
10
0

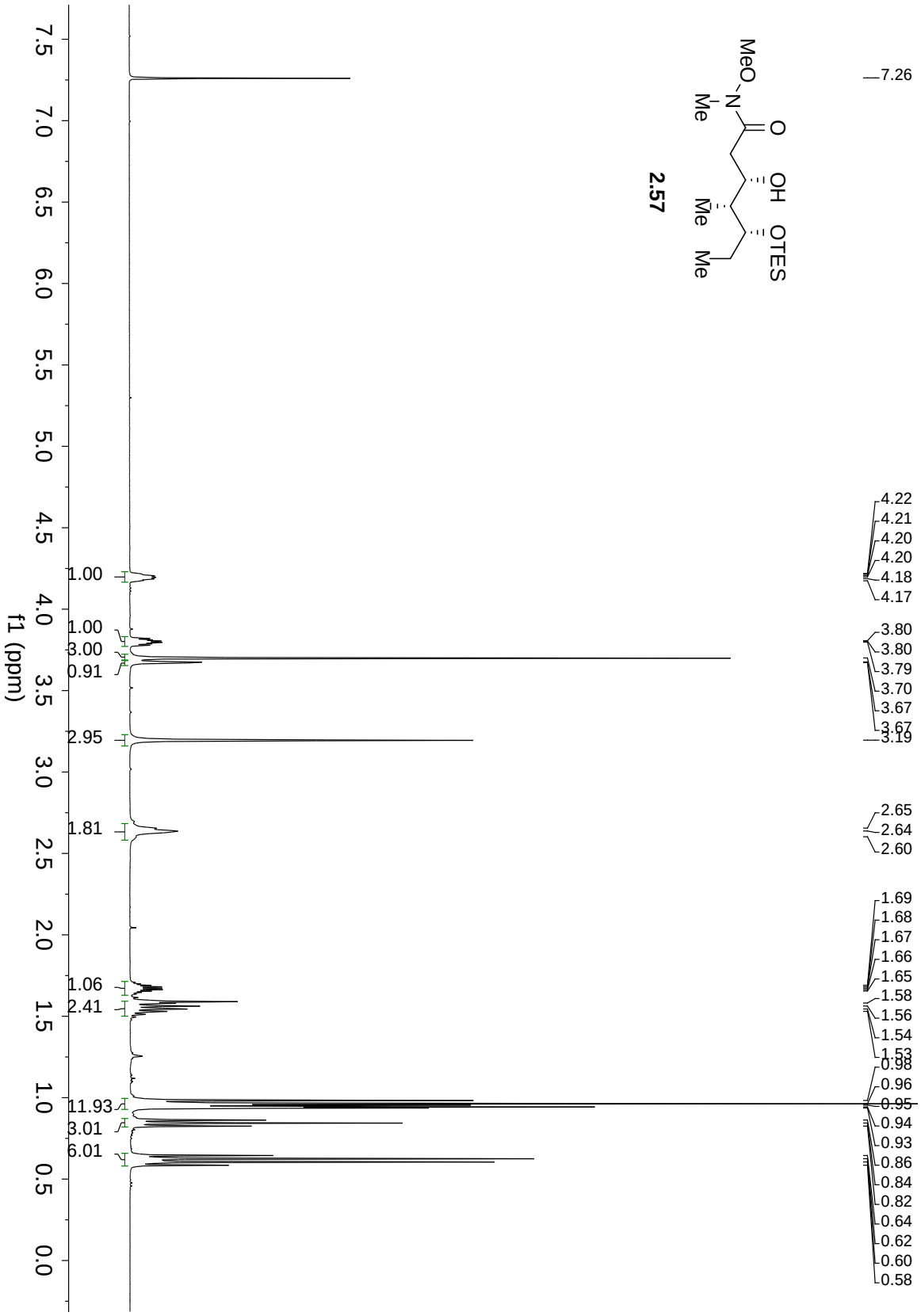
MeO
N
Me
O
OH
OTES
Me
Me
Me
2.57
f1 (ppm)
7.5
7.0
6.5
6.0
5.5
5.0
4.5
4.0
3.5
3.0
2.5
2.0
1.5
1.0
0.5
0.0
1.00
1.00
3.00
0.91
2.95
1.81
1.06
2.41
11.93
3.01
6.01
7.26
4.22
4.21
4.20
4.20
4.18
4.17
3.80
3.80
3.79
3.70
3.67
3.67
3.19
2.65
2.64
2.60
1.69
1.68
1.67
1.66
1.65
1.58
1.56
1.54
1.53
0.98
0.96
0.95
0.94
0.93
0.86
0.84
0.82
0.64
0.62
0.60
0.58

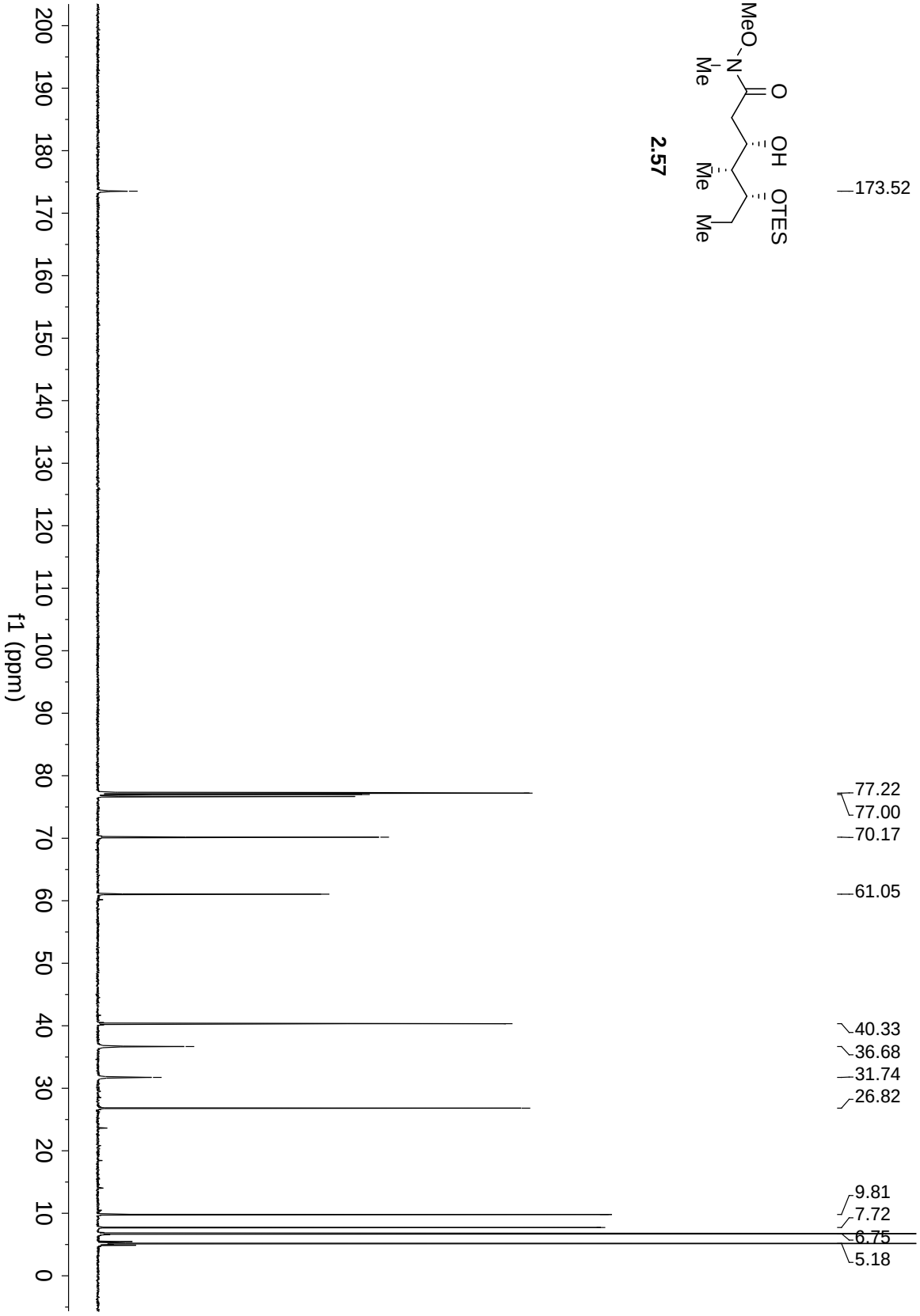
MeO
N
Me
O
OH
OTES
Me
Me
Me
2.57
173.52
77.22
77.00
70.17
61.05
40.33
36.68
31.74
26.82
9.81
7.72
6.75
5.18
f1 (ppm)
200
190
180
170
160
150
140
130
120
110
100
90
80
70
60
50
40
30
20
10
0

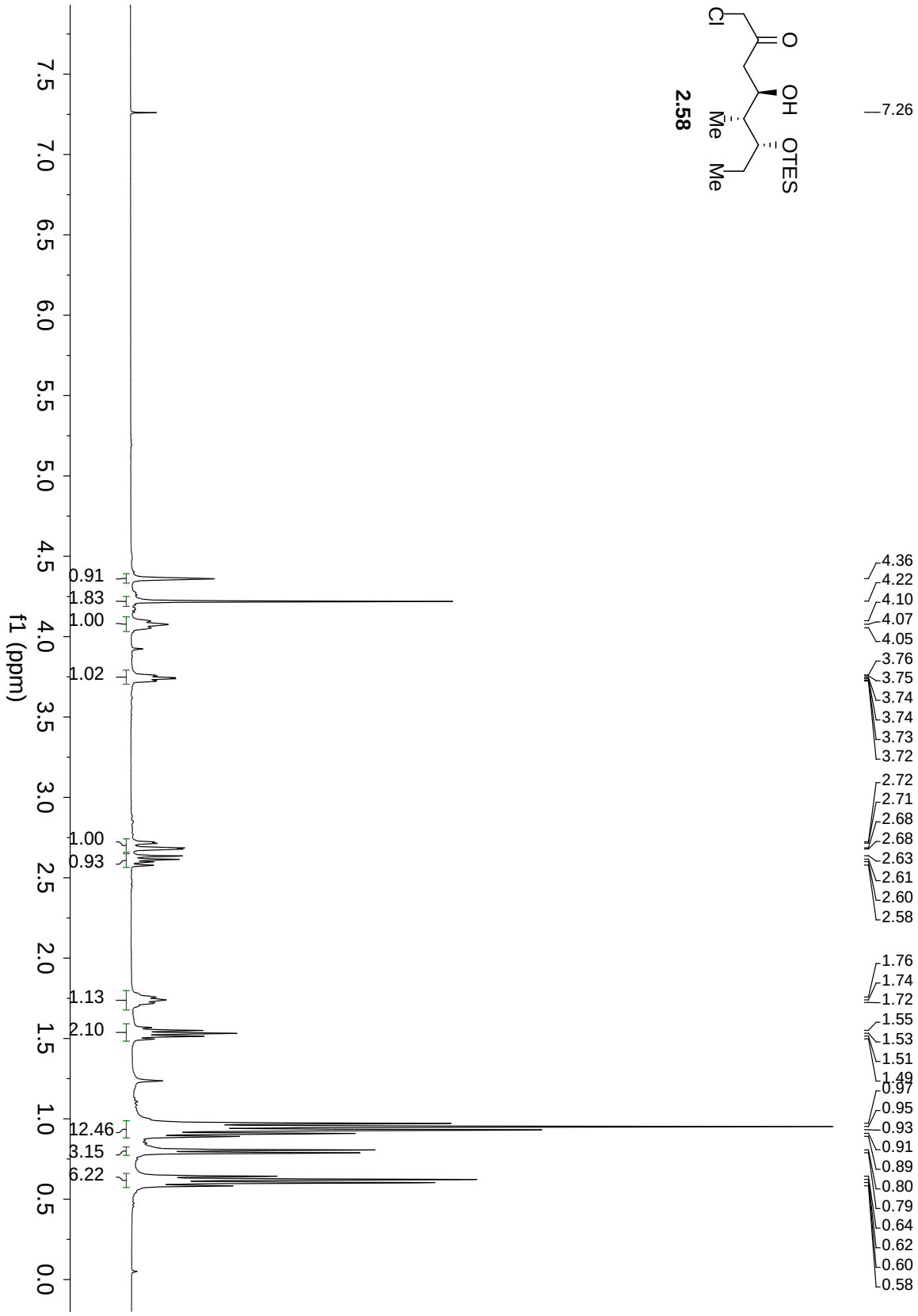
Cl
O
OH
OTES
Me
Me
2.58
7.26
4.36
4.22
4.10
4.07
4.05
3.76
3.75
3.74
3.74
3.73
3.72
2.72
2.71
2.68
2.68
2.63
2.61
2.60
2.58
1.76
1.74
1.72
1.55
1.53
1.51
1.49
0.97
0.95
0.93
0.91
0.89
0.80
0.79
0.64
0.62
0.60
0.58
0.91
1.83
1.00
1.02
1.00
0.93
1.13
2.10
12.46
3.15
6.22
f1 (ppm)
7.5
7.0
6.5
6.0
5.5
5.0
4.5
4.0
3.5
3.0
2.5
2.0
1.5
1.0
0.5
0.0

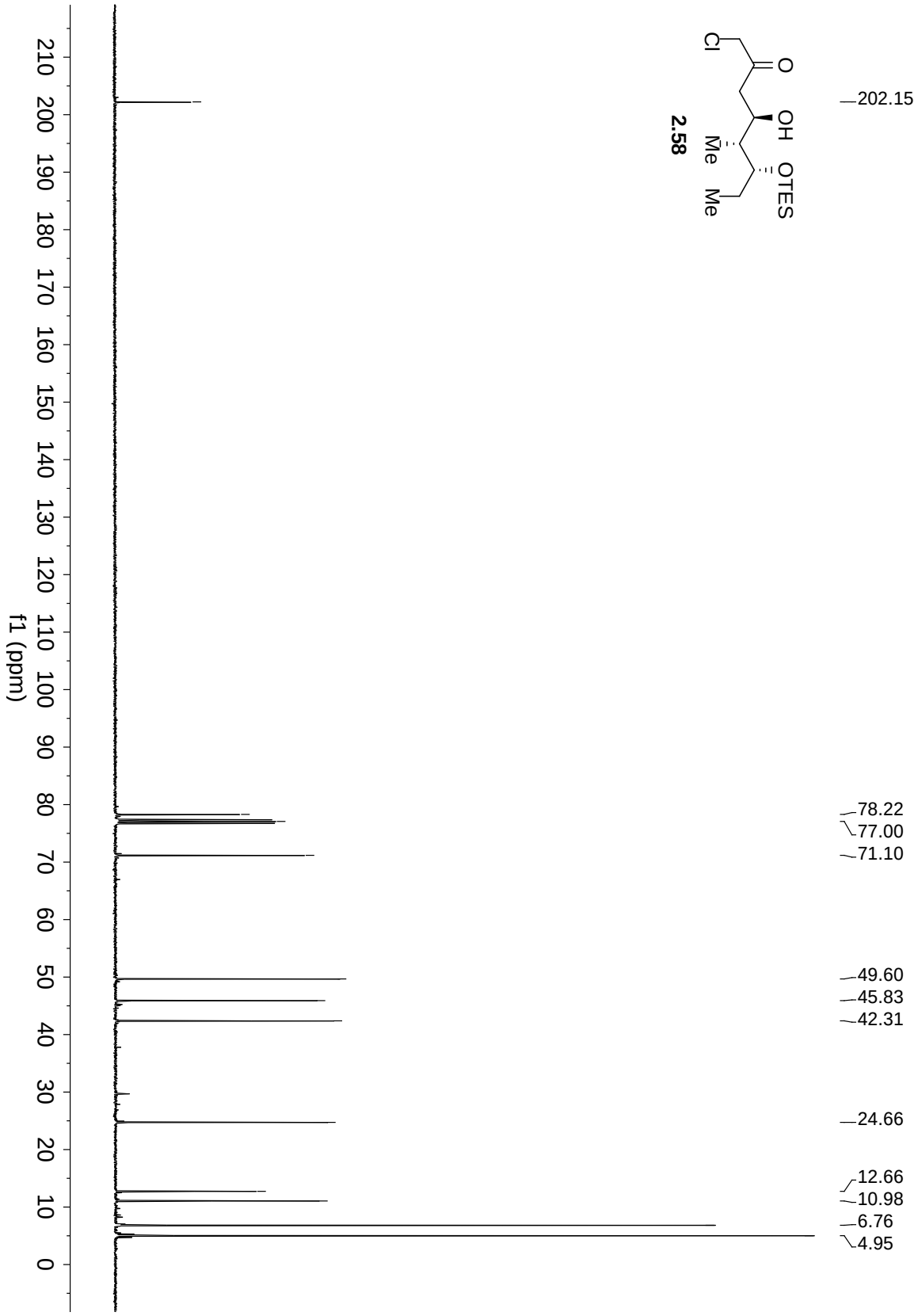
Cl
O
OH
OTES
Me
Me
2.58
f1 (ppm)
210
200
190
180
170
160
150
140
130
120
110
100
90
80
70
60
50
40
30
20
10
0
202.15
78.22
77.00
71.10
49.60
45.83
42.31
24.66
12.66
10.98
6.76
4.95

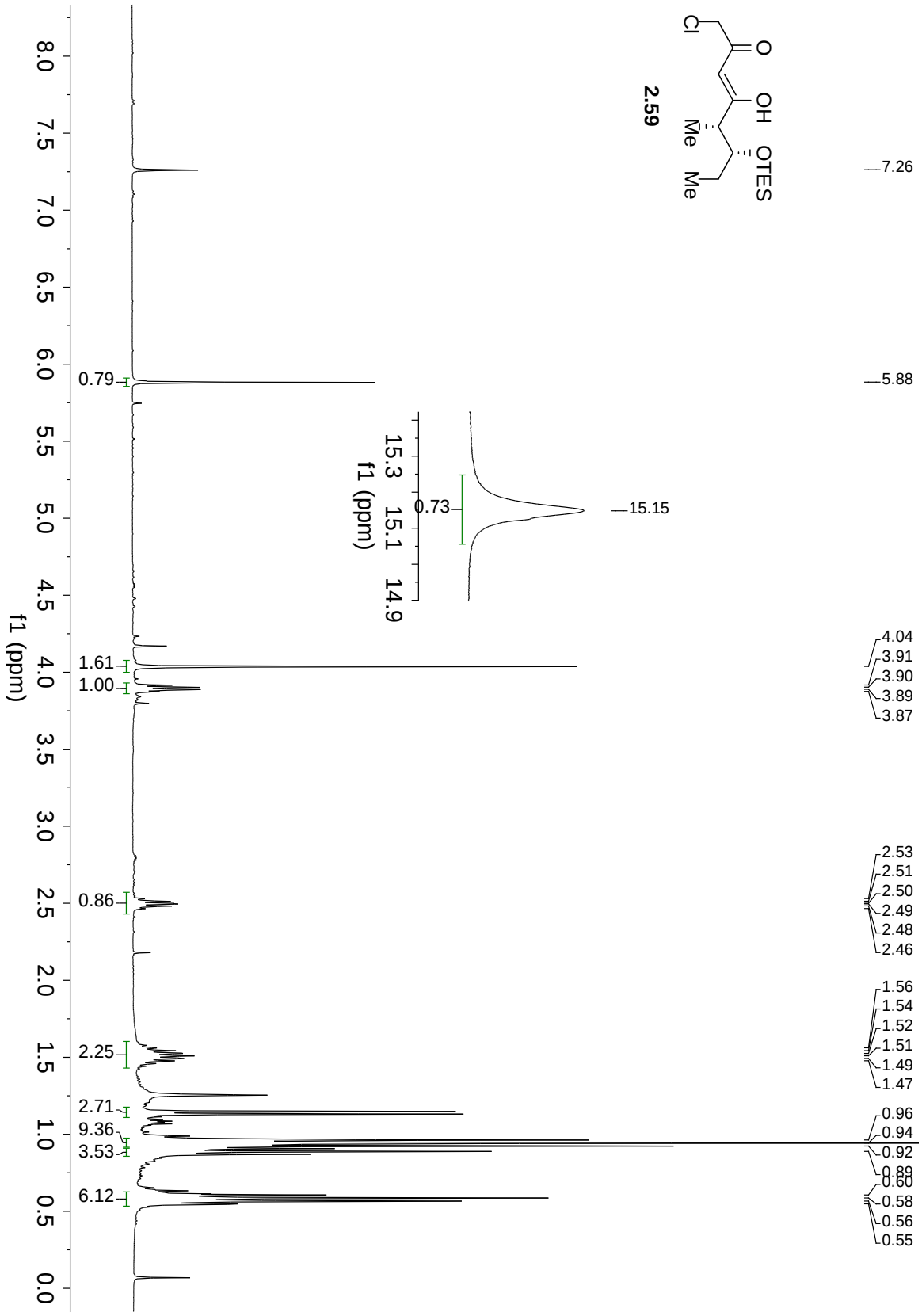
2.59
Cl
O
OH
OTES
Me
Me
f1 (ppm)
8.0
7.5
7.0
6.5
6.0
5.5
5.0
4.5
4.0
3.5
3.0
2.5
2.0
1.5
1.0
0.5
0.0
0.79
1.61
1.00
0.86
2.25
2.71
9.36
3.53
6.12
15.3
15.1
14.9
0.73
15.15
7.26
5.88
4.04
3.91
3.90
3.89
3.87
2.53
2.51
2.50
2.49
2.48
2.46
1.56
1.54
1.52
1.51
1.49
1.47
0.96
0.94
0.92
0.89
0.60
0.58
0.56
0.55

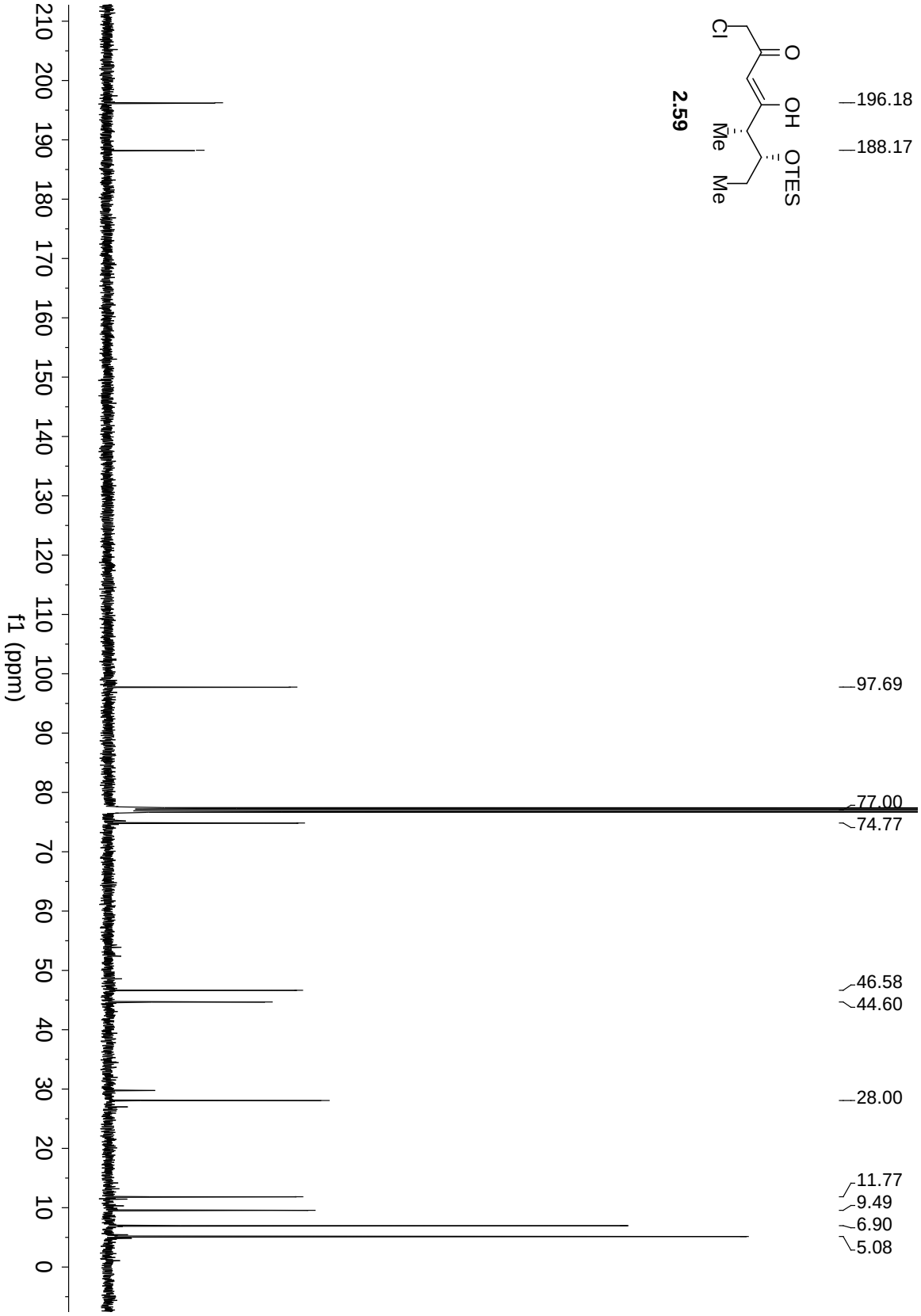
2.59
Cl
O
OH
OTES
Me
Me
196.18
188.17
97.69
77.00
74.77
46.58
44.60
28.00
11.77
9.49
6.90
5.08
f1 (ppm)

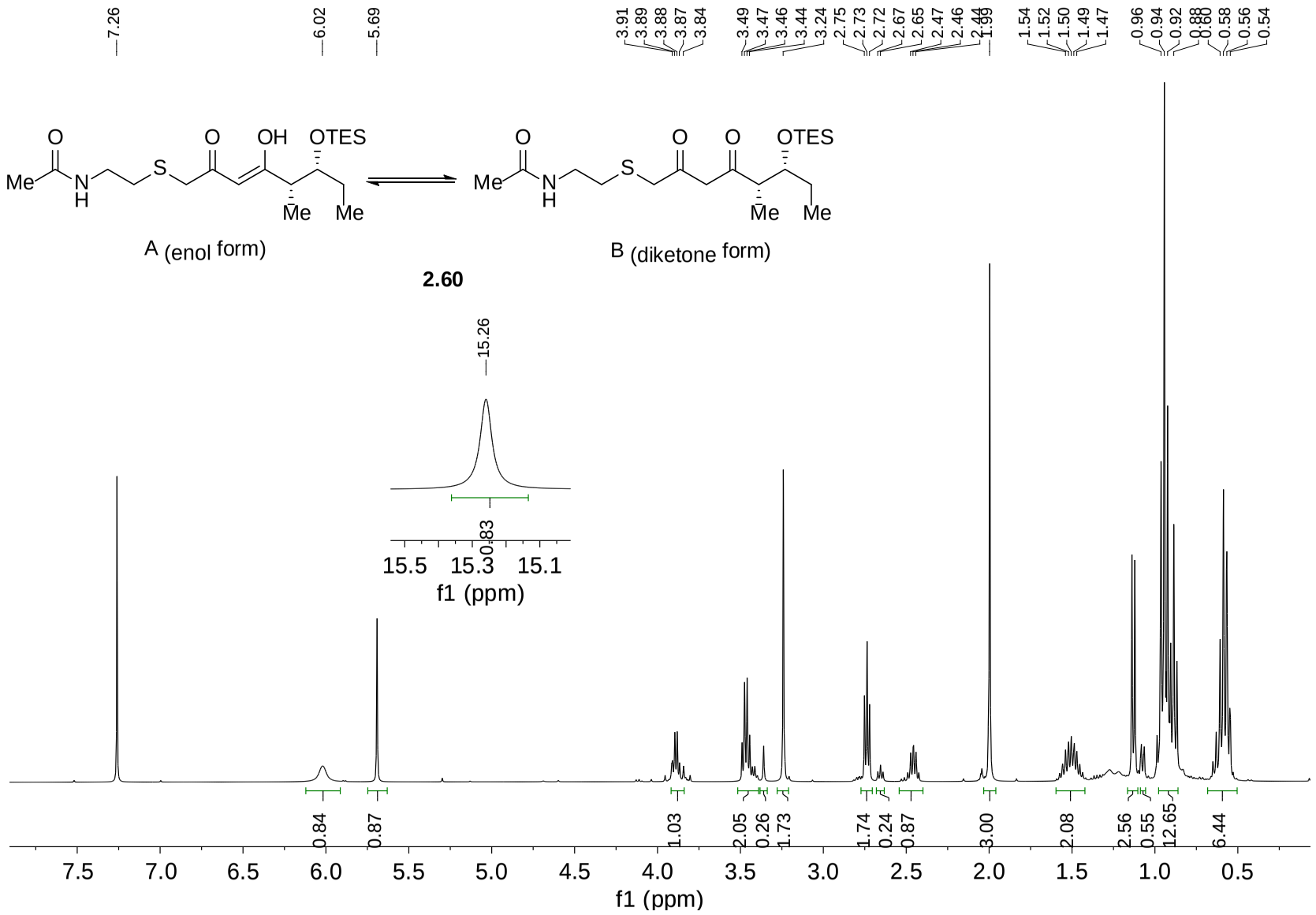
7.26
6.02
5.69
3.91
3.89
3.88
3.87
3.84
3.49
3.47
3.46
3.44
3.24
2.75
2.73
2.72
2.67
2.65
2.47
2.46
2.44
1.99
1.54
1.52
1.50
1.49
1.47
0.96
0.94
0.92
0.88
0.60
0.58
0.56
0.54
A (enol form)
B (diketone form)
2.60
15.26
0.83
15.5
15.3
15.1
f1 (ppm)
0.84
0.87
1.03
2.05
0.26
1.73
1.74
0.24
0.87
3.00
2.08
2.56
0.55
12.65
6.44
7.5
7.0
6.5
6.0
5.5
5.0
4.5
4.0
3.5
3.0
2.5
2.0
1.5
1.0
0.5
f1 (ppm)

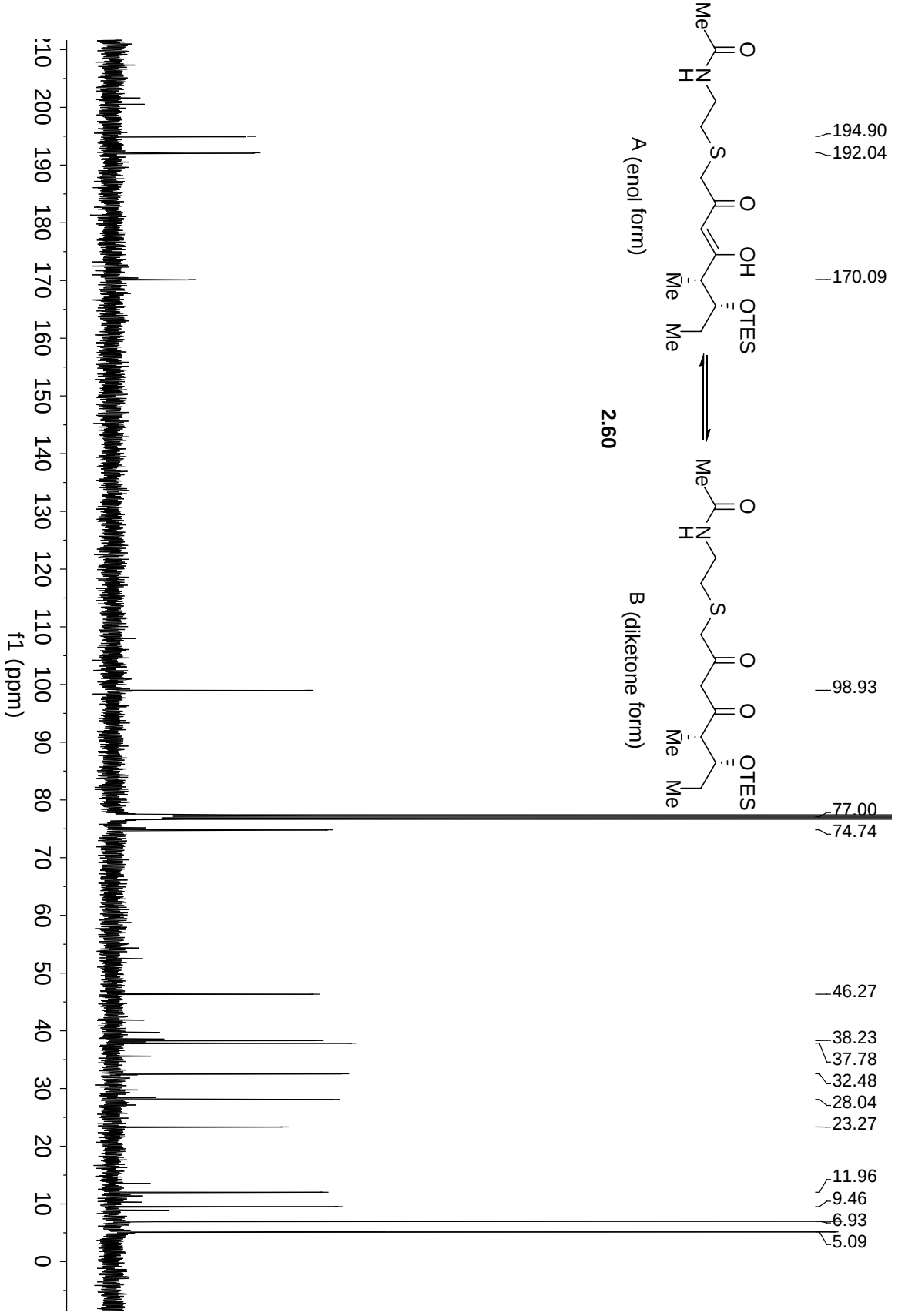
f1 (ppm)
210
200
190
180
170
160
150
140
130
120
110
100
90
80
70
60
50
40
30
20
10
0
194.90
192.04
170.09
98.93
77.00
74.74
46.27
38.23
37.78
32.48
28.04
23.27
11.96
9.46
6.93
5.09
A (enol form)
B (diketone form)
2.60
Me
O
N
H
S
O
OH
OTES
Me
Me

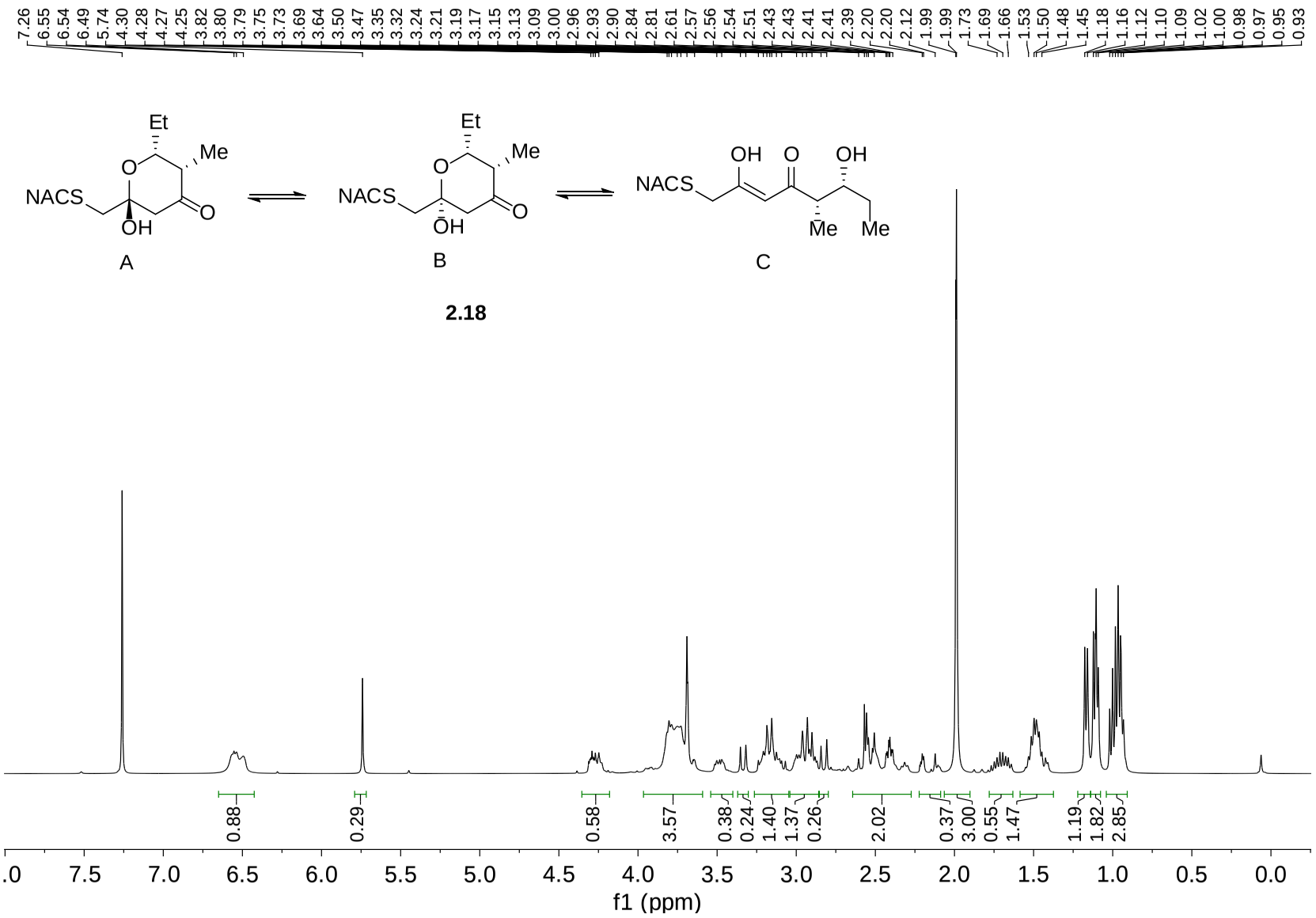
7.26 6.55 6.54 6.49 5.74 4.30 4.28 4.27 4.25 3.82 3.80 3.79 3.75 3.73 3.69 3.64 3.50 3.47 3.35 3.32 3.24 3.21 3.19 3.17 3.15 3.13 3.09 3.00 2.96 2.93 2.90 2.84 2.81 2.61 2.57 2.56 2.54 2.51 2.43 2.43 2.41 2.41 2.39 2.20 2.20 2.12 1.99 1.99 1.73 1.69 1.66 1.53 1.50 1.48 1.45 1.18 1.16 1.12 1.10 1.09 1.02 1.00 0.98 0.97 0.95 0.93
Et
Me
O
NACS
OH
O
A
B
C
OH
O
OH
Me
Me
2.18
0.88
0.29
0.58
3.57
0.38
0.24
1.40
1.37
0.26
2.02
0.37
3.00
0.55
1.47
1.19
1.82
2.85
.0 7.5 7.0 6.5 6.0 5.5 5.0 4.5 4.0 3.5 3.0 2.5 2.0 1.5 1.0 0.5 0.0
f1 (ppm)

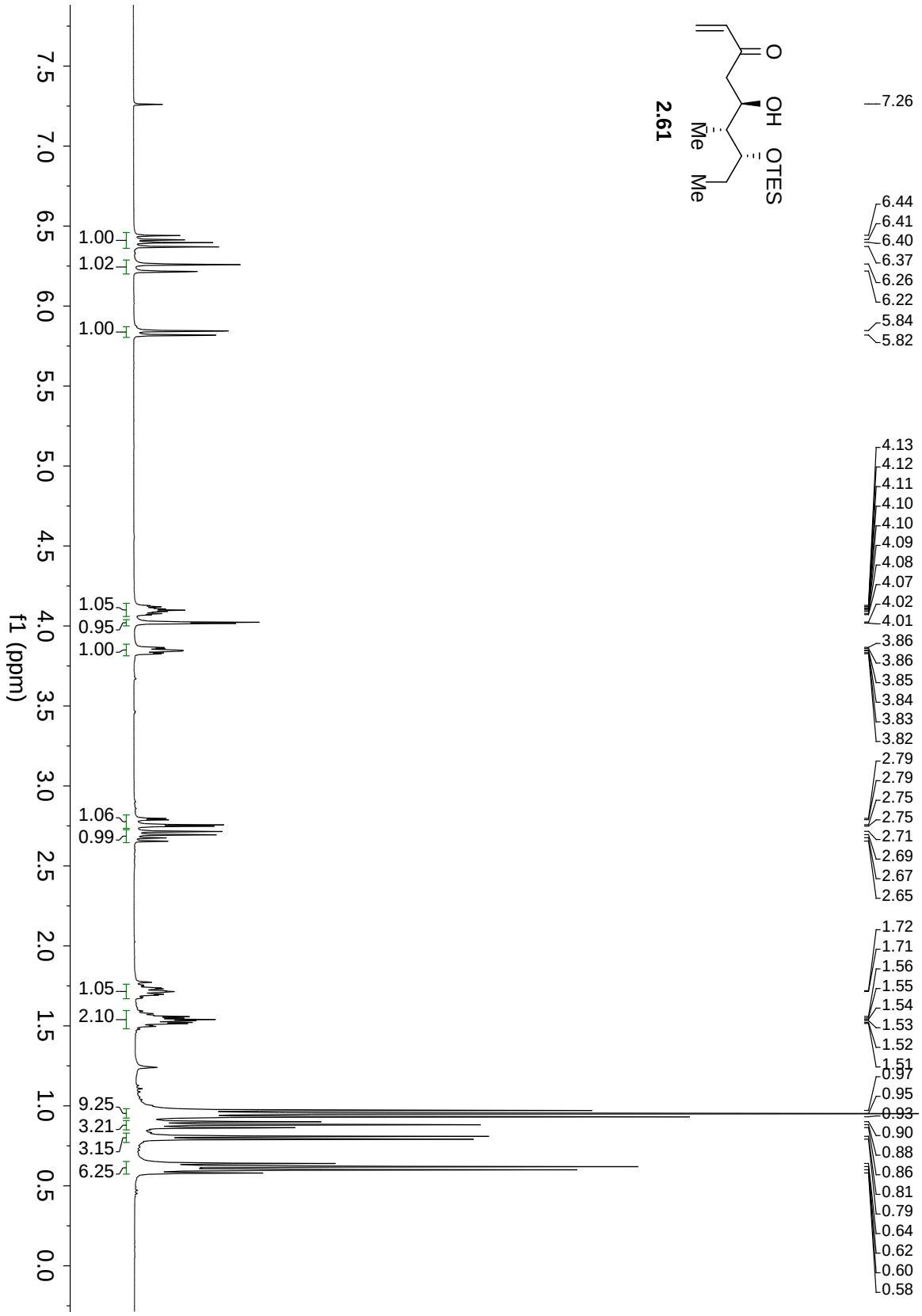
O
OH
OTES
Me
Me
2.61
f1 (ppm)
7.5
7.0
6.5
6.0
5.5
5.0
4.5
4.0
3.5
3.0
2.5
2.0
1.5
1.0
0.5
0.0
1.00
1.02
1.00
1.05
0.95
1.00
1.06
0.99
1.05
2.10
9.25
3.21
3.15
6.25
7.26
6.44
6.41
6.40
6.37
6.26
6.22
5.84
5.82
4.13
4.12
4.11
4.10
4.10
4.09
4.08
4.07
4.02
4.01
3.86
3.86
3.85
3.84
3.83
3.82
2.79
2.79
2.75
2.75
2.71
2.69
2.67
2.65
1.72
1.71
1.56
1.55
1.54
1.53
1.52
1.51
0.97
0.95
0.93
0.90
0.88
0.86
0.81
0.79
0.64
0.62
0.60
0.58

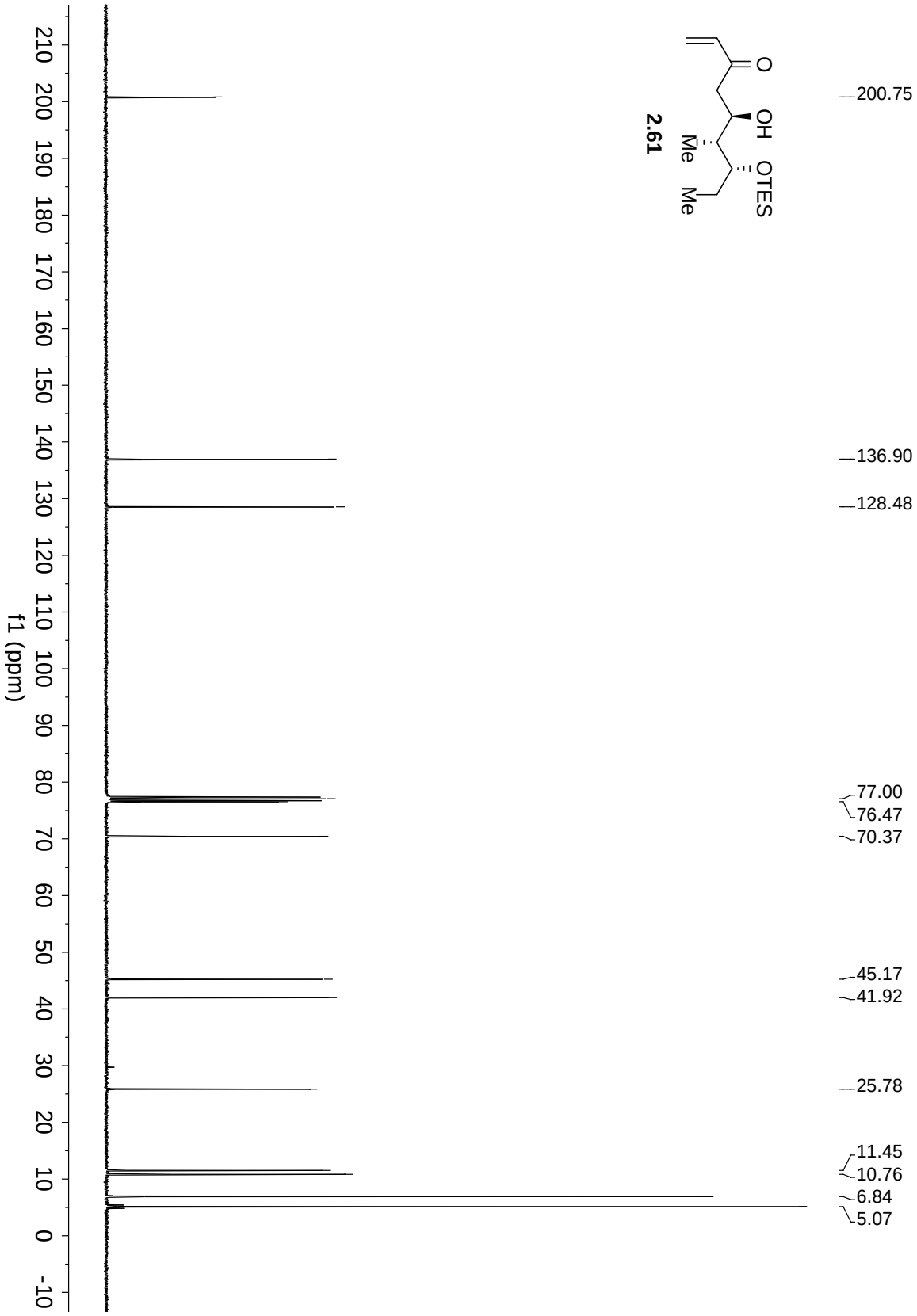
O
OH
OTES
Me
Me
2.61
200.75
136.90
128.48
77.00
76.47
70.37
45.17
41.92
25.78
11.45
10.76
6.84
5.07
f1 (ppm)
210
200
190
180
170
160
150
140
130
120
110
100
90
80
70
60
50
40
30
20
10
0
-10

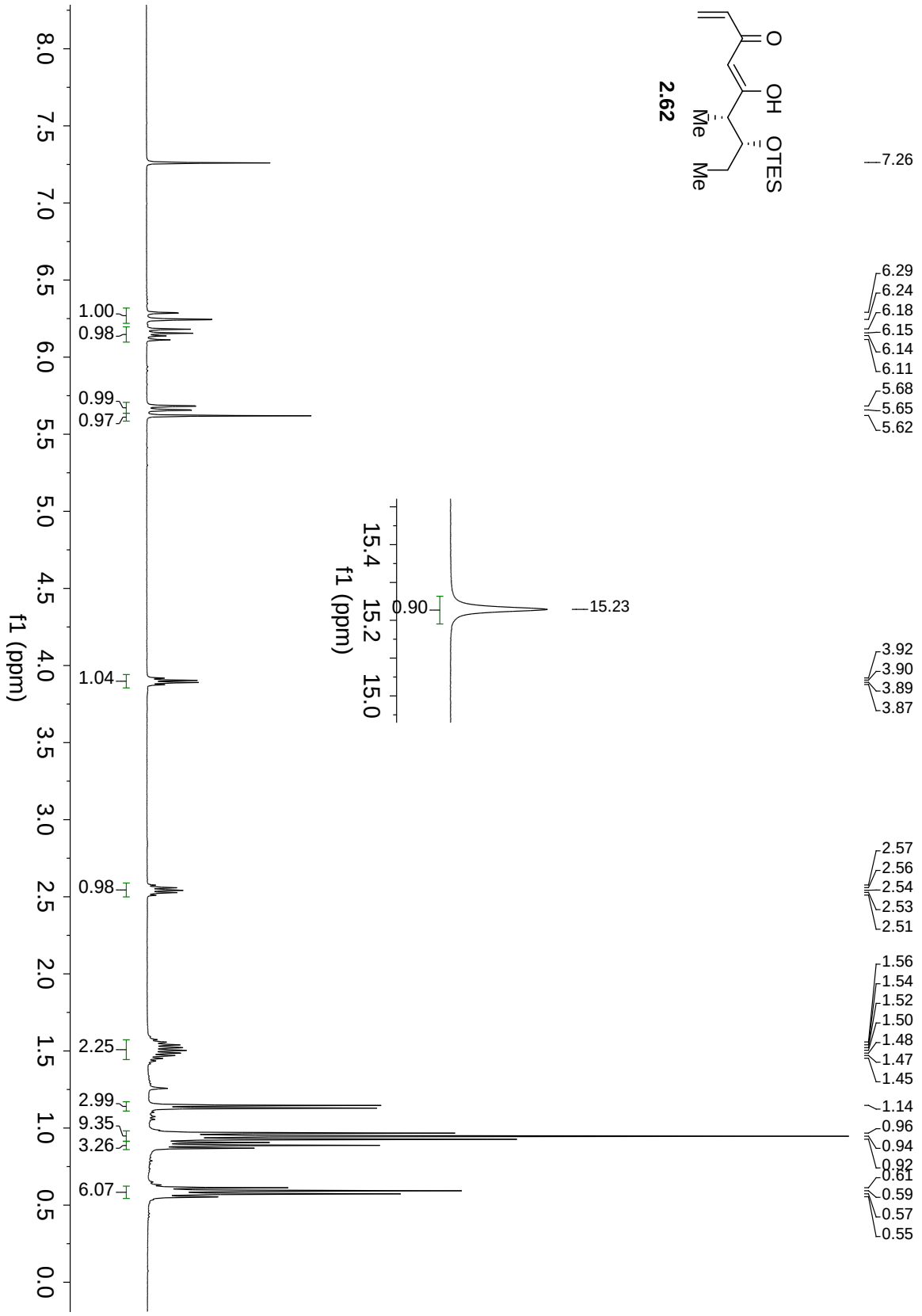
2.62
O
OH
OTES
Me
Me
7.26
6.29
6.24
6.18
6.15
6.14
6.11
5.68
5.65
5.62
3.92
3.90
3.89
3.87
2.57
2.56
2.54
2.53
2.51
1.56
1.54
1.52
1.50
1.48
1.47
1.45
1.14
0.96
0.94
0.92
0.61
0.59
0.57
0.55
1.00
0.98
0.99
0.97
1.04
0.98
2.25
2.99
9.35
3.26
6.07
f1 (ppm)
0.90
15.23
15.4
15.2
15.0
f1 (ppm)

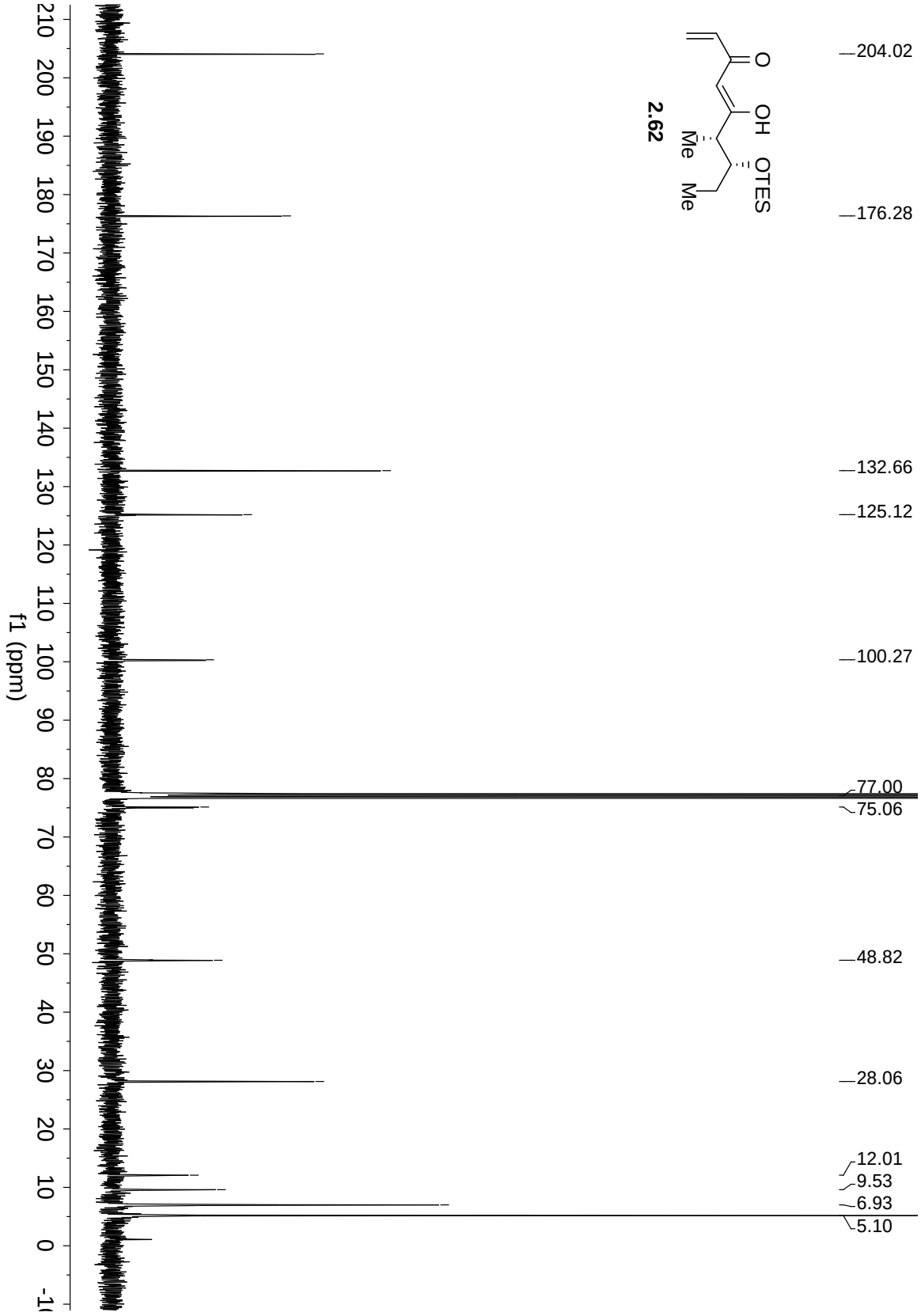
204.02
176.28
132.66
125.12
100.27
77.00
75.06
48.82
28.06
12.01
9.53
6.93
5.10
f1 (ppm)
O
OH
OTES
Me
Me
2.62

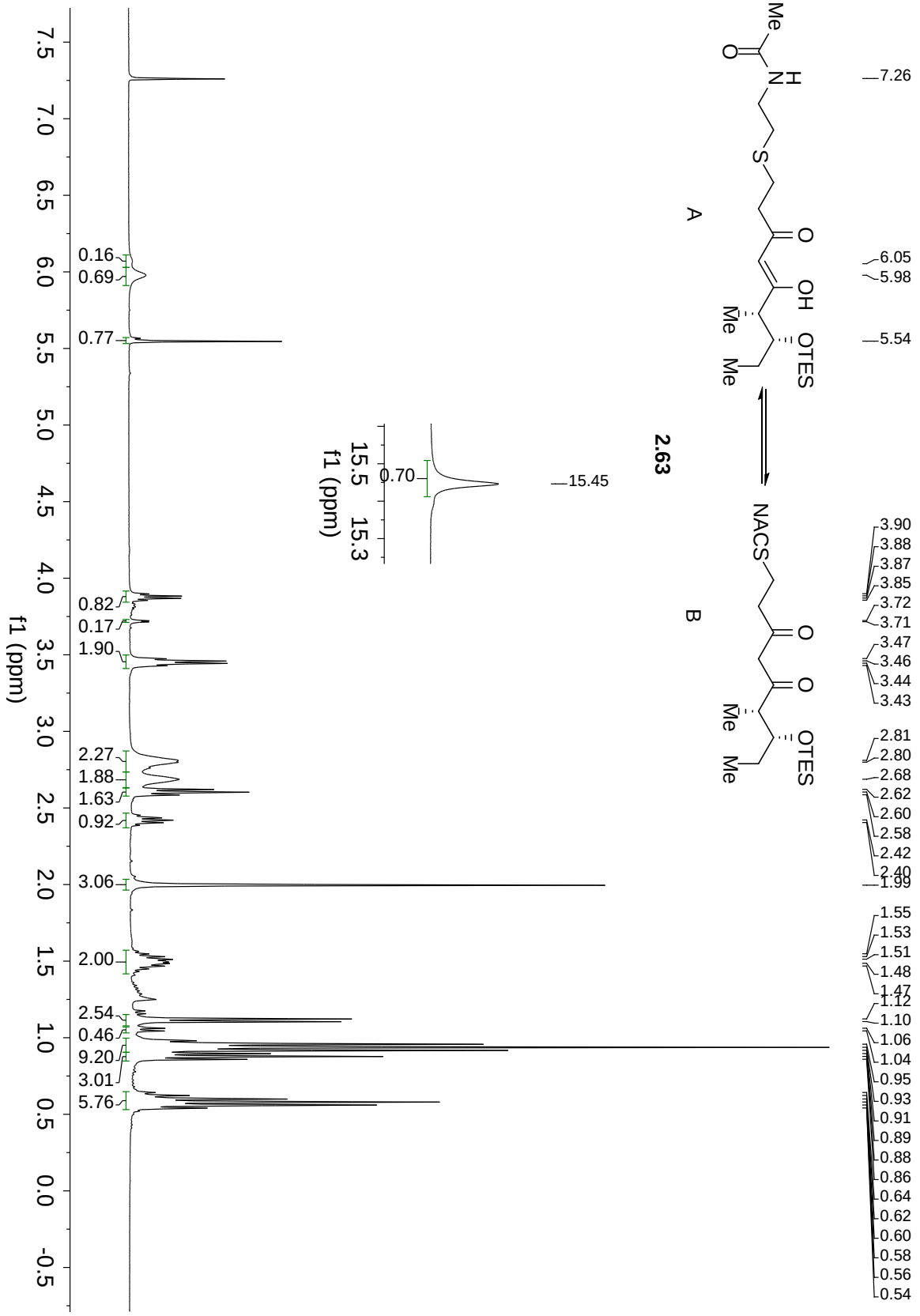
2.63
A
B
Me
O
H
N
S
O
OH
OTES
Me
Me
NACS
O
O
OTES
Me
Me
7.26
6.05
5.98
5.54
3.90
3.88
3.87
3.85
3.72
3.71
3.47
3.46
3.44
3.43
2.81
2.80
2.68
2.62
2.60
2.58
2.42
2.40
1.99
1.55
1.53
1.51
1.48
1.47
1.12
1.10
1.06
1.04
0.95
0.93
0.91
0.89
0.88
0.86
0.64
0.62
0.60
0.58
0.56
0.54
15.45
0.70
15.5
15.3
f1 (ppm)
0.16
0.69
0.77
0.82
0.17
1.90
2.27
1.88
1.63
0.92
3.06
2.00
2.54
0.46
9.20
3.01
5.76
7.5
7.0
6.5
6.0
5.5
5.0
4.5
4.0
3.5
3.0
2.5
2.0
1.5
1.0
0.5
0.0
-0.5
f1 (ppm)

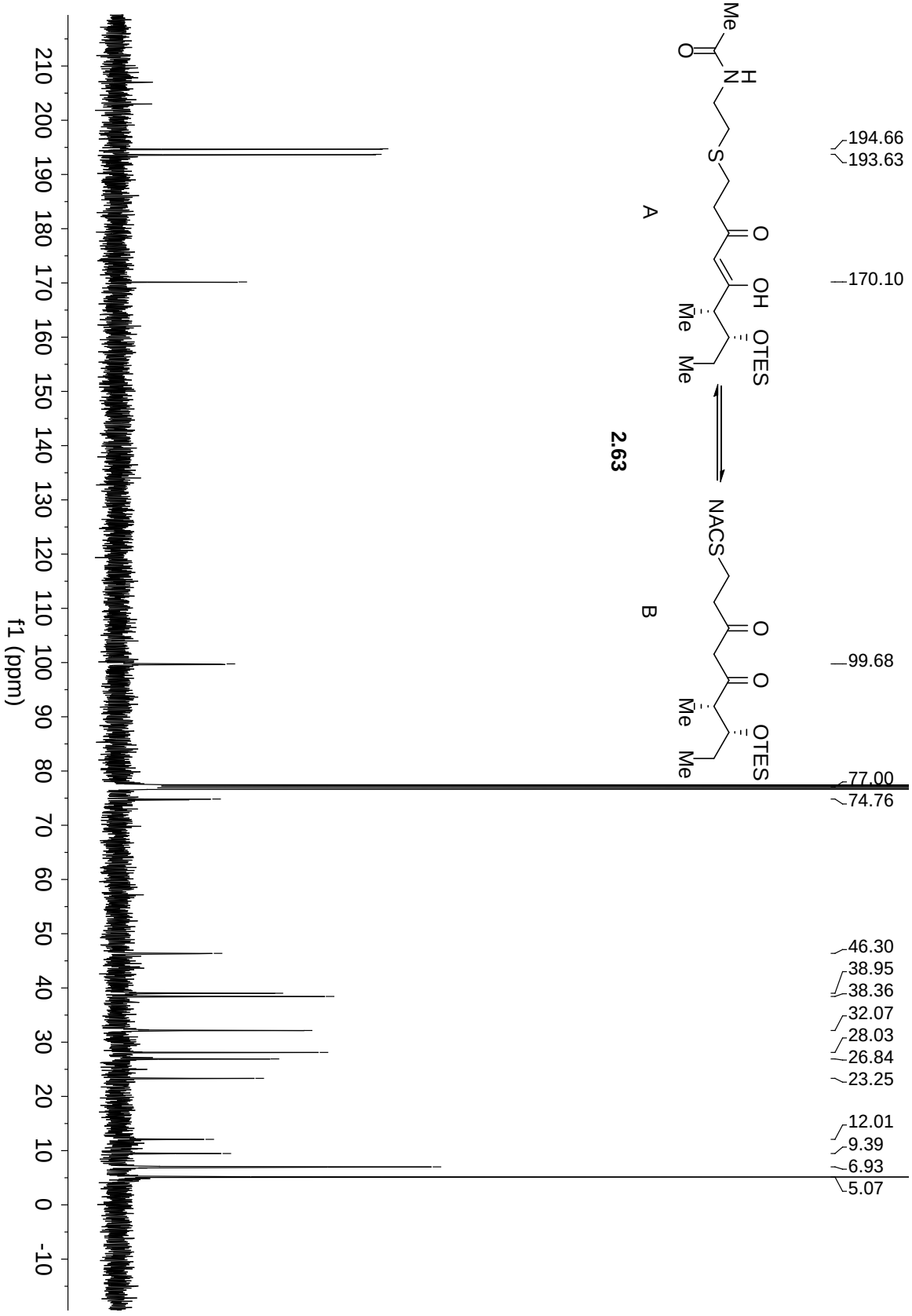
194.66
193.63
170.10
99.68
77.00
74.76
46.30
38.95
38.36
32.07
28.03
26.84
23.25
12.01
9.39
6.93
5.07
f1 (ppm)
2.63
A
B
NACS
OTES
OH
Me
O
S
N
H

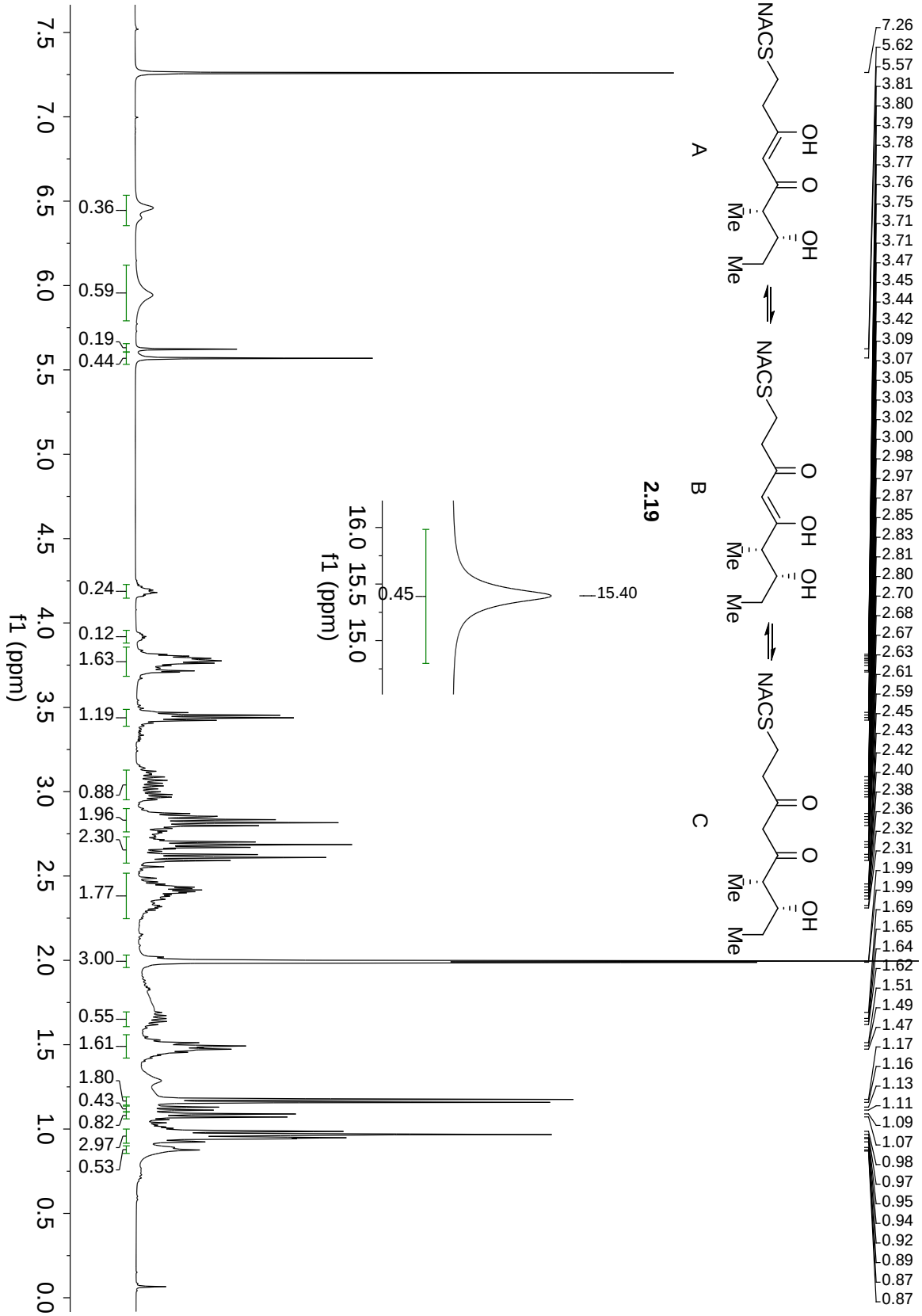
NACS
OH O OH
Me Me
A
B
C
2.19
f1 (ppm)
16.0 15.5 15.0
0.45
15.40
0.36
0.59
0.19
0.44
0.24
0.12
1.63
1.19
0.88
1.96
2.30
1.77
3.00
0.55
1.61
1.80
0.43
0.82
2.97
0.53
7.26
5.62
5.57
3.81
3.80
3.79
3.78
3.77
3.76
3.75
3.71
3.71
3.47
3.45
3.44
3.42
3.09
3.07
3.05
3.03
3.02
3.00
2.98
2.97
2.87
2.85
2.83
2.81
2.80
2.70
2.68
2.67
2.63
2.61
2.59
2.45
2.43
2.42
2.40
2.38
2.36
2.32
2.31
1.99
1.99
1.69
1.65
1.64
1.62
1.51
1.49
1.47
1.17
1.16
1.13
1.11
1.09
1.07
0.98
0.97
0.95
0.94
0.92
0.89
0.87
0.87

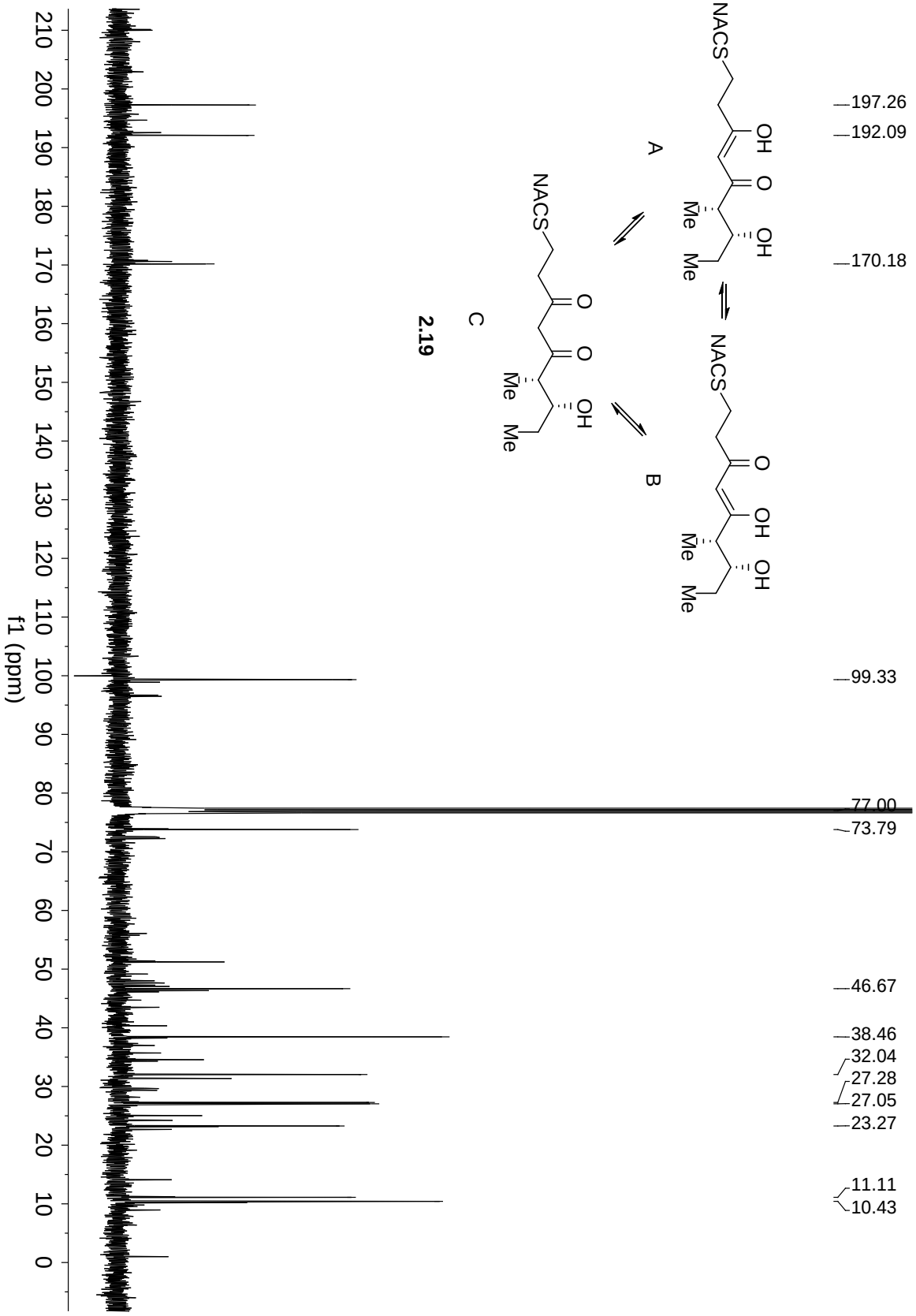
NACS
OH
O
OH
Me
Me
A
B
C
2.19
197.26
192.09
170.18
99.33
77.00
73.79
46.67
38.46
32.04
27.28
27.05
23.27
11.11
10.43
f1 (ppm)

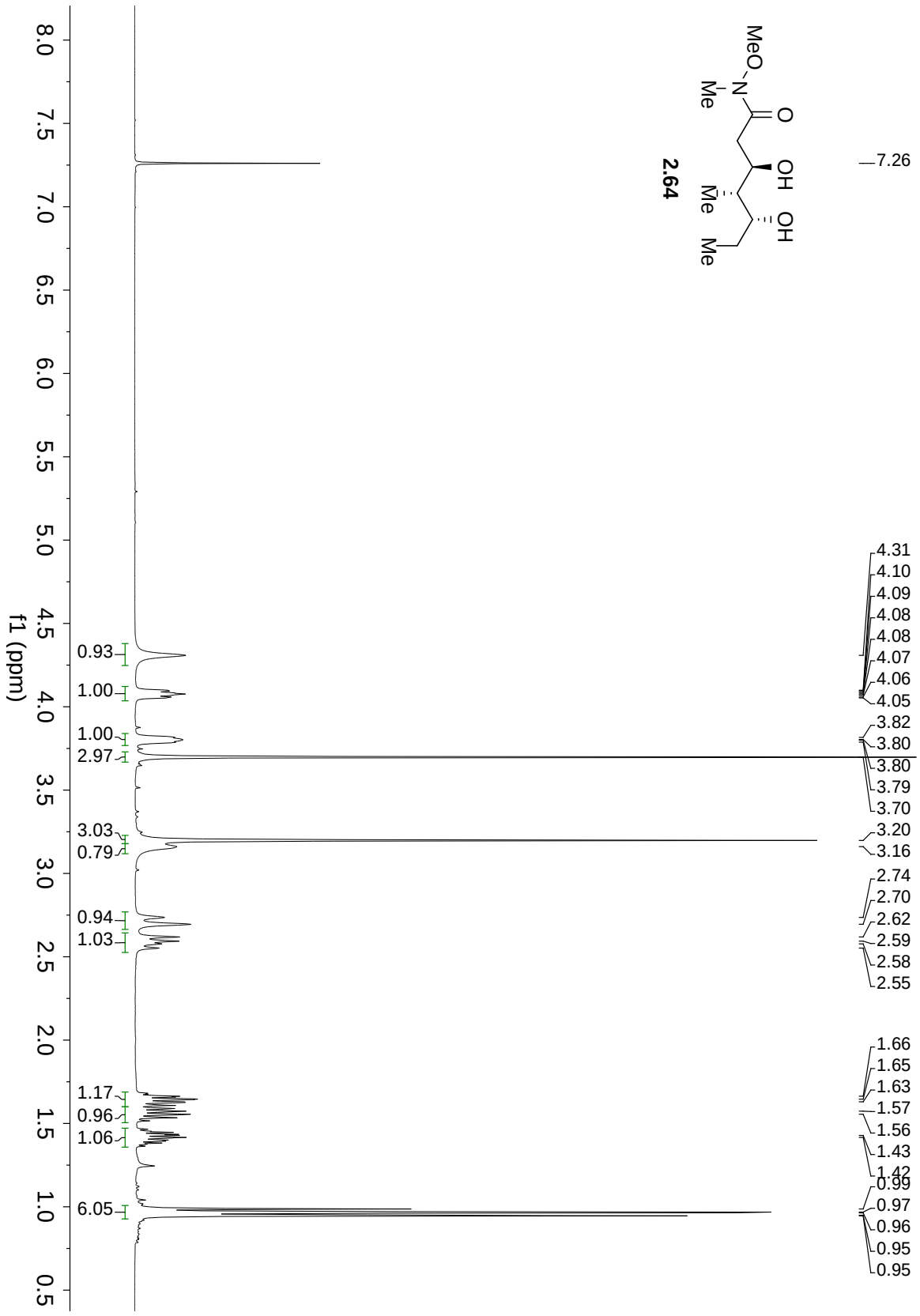
2.64
MeO
N
Me
O
OH
OH
Me
Me
7.26
4.31
4.10
4.09
4.08
4.08
4.07
4.06
4.05
3.82
3.80
3.80
3.79
3.70
3.20
3.16
2.74
2.70
2.62
2.59
2.58
2.55
1.66
1.65
1.63
1.57
1.56
1.43
1.42
0.99
0.97
0.96
0.95
0.95
0.93
1.00
1.00
2.97
3.03
0.79
0.94
1.03
1.17
0.96
1.06
6.05
f1 (ppm)
8.0
7.5
7.0
6.5
6.0
5.5
5.0
4.5
4.0
3.5
3.0
2.5
2.0
1.5
1.0
0.5

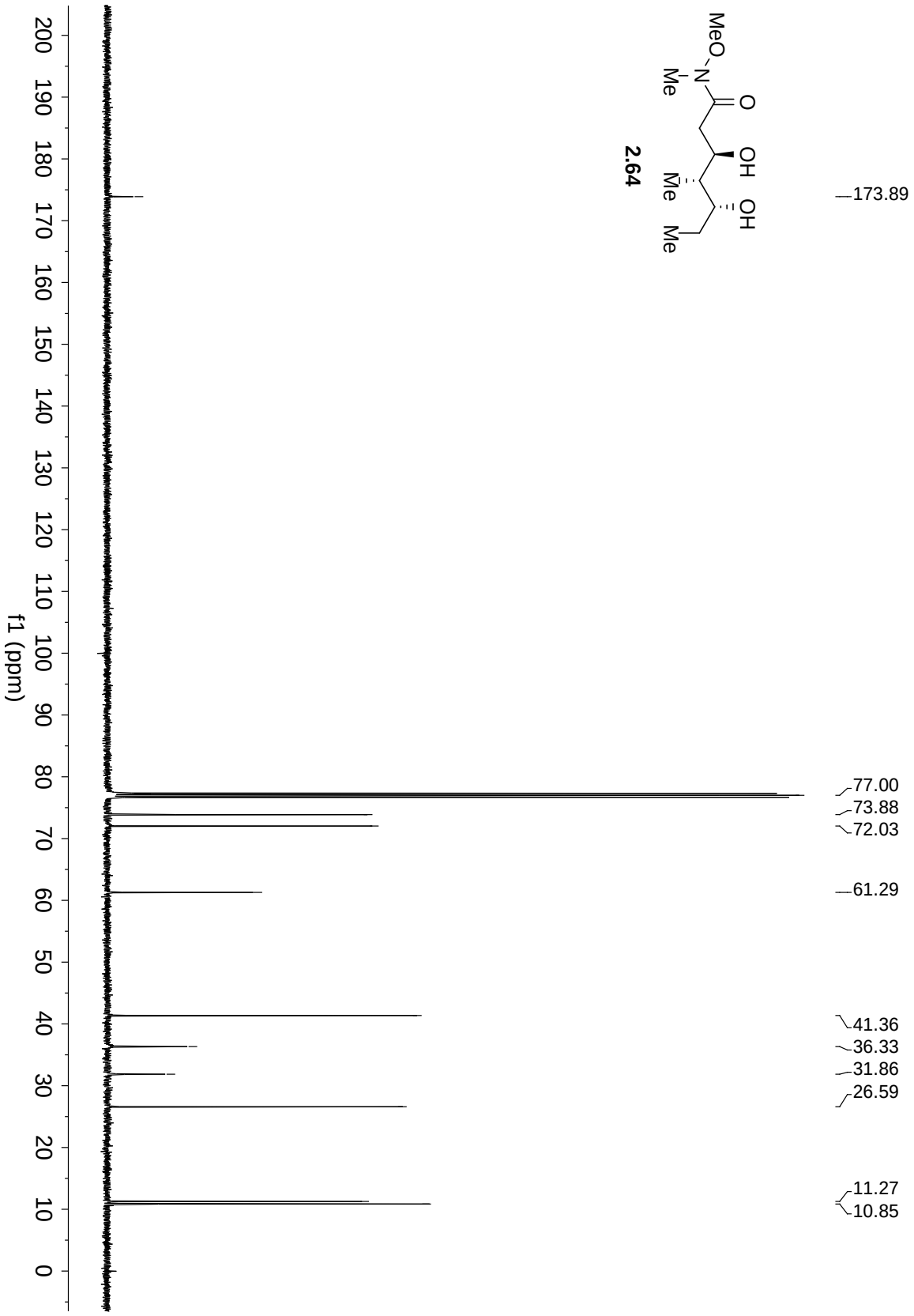
MeO
N
Me
O
OH
OH
Me
Me
2.64
173.89
77.00
73.88
72.03
61.29
41.36
36.33
31.86
26.59
11.27
10.85
f1 (ppm)
200
190
180
170
160
150
140
130
120
110
100
90
80
70
60
50
40
30
20
10
0

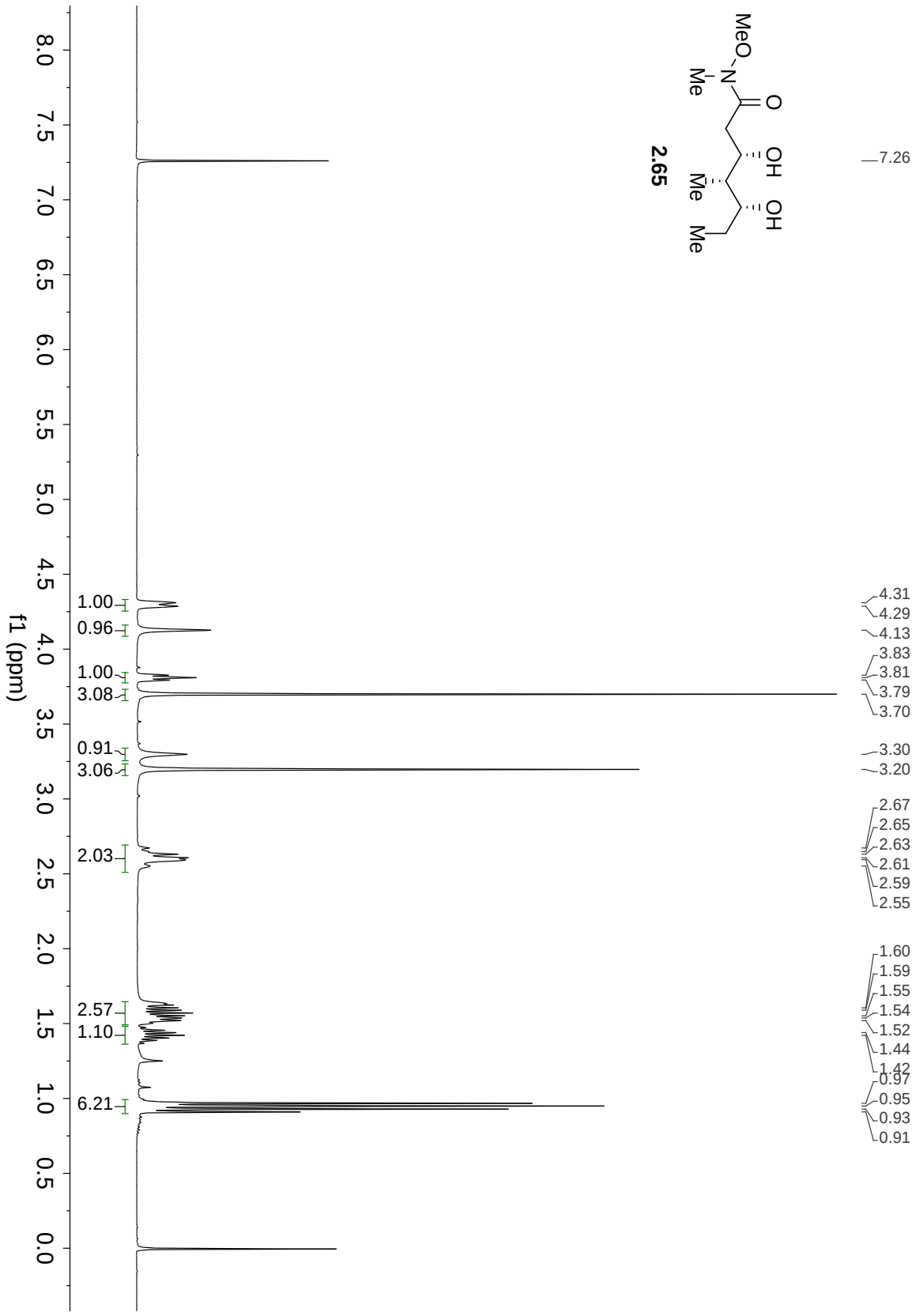
MeO
N
Me
O
OH
OH
Me
Me
2.65
f1 (ppm)
8.0
7.5
7.0
6.5
6.0
5.5
5.0
4.5
4.0
3.5
3.0
2.5
2.0
1.5
1.0
0.5
0.0
1.00
0.96
1.00
3.08
0.91
3.06
2.03
2.57
1.10
6.21
7.26
4.31
4.29
4.13
3.83
3.81
3.79
3.70
3.30
3.20
2.67
2.65
2.63
2.61
2.59
2.55
1.60
1.59
1.55
1.54
1.52
1.44
1.42
0.97
0.95
0.93
0.91

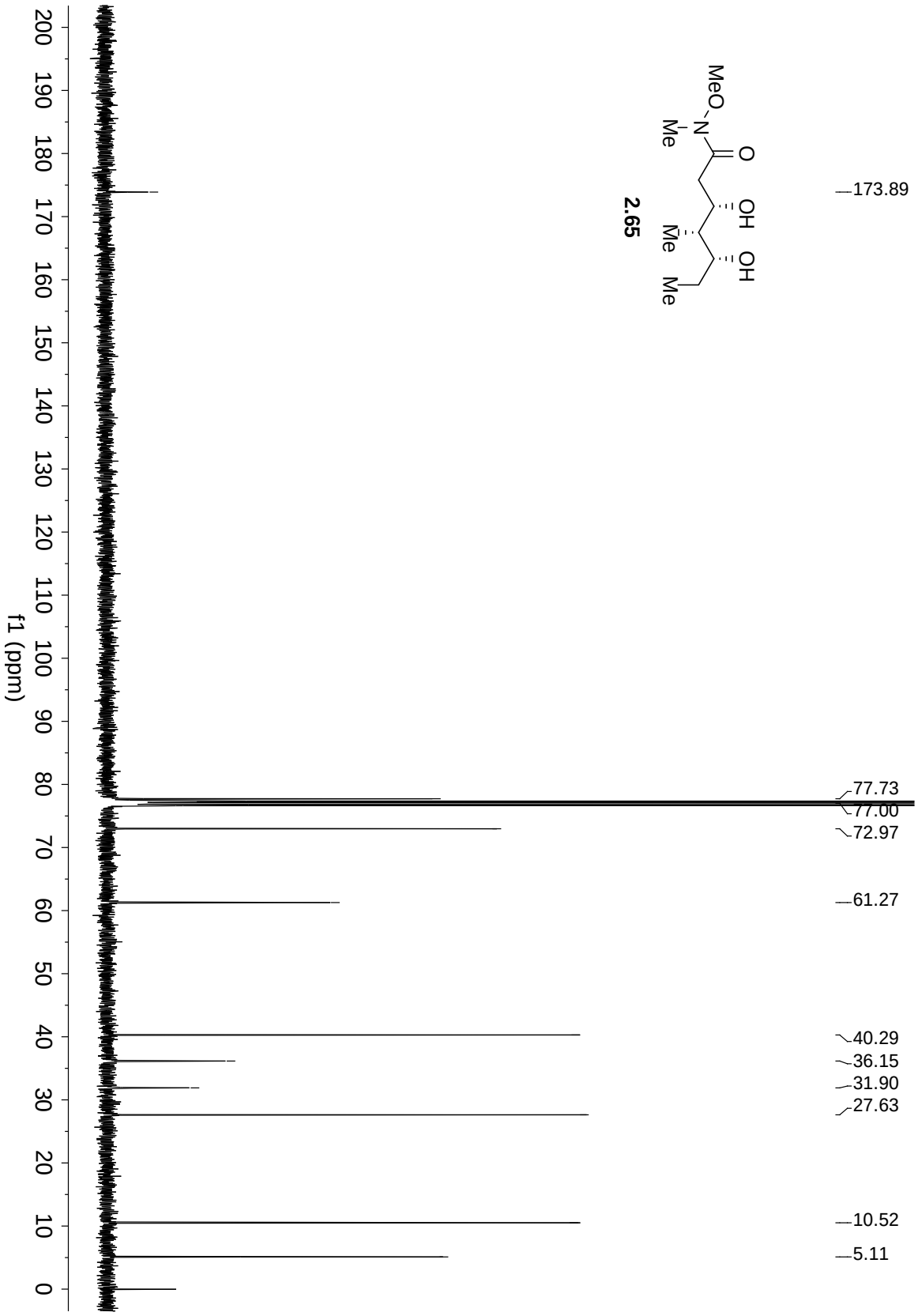
MeO
N
Me
O
OH
OH
Me
Me
2.65
173.89
77.73
77.00
72.97
61.27
40.29
36.15
31.90
27.63
10.52
5.11
f1 (ppm)

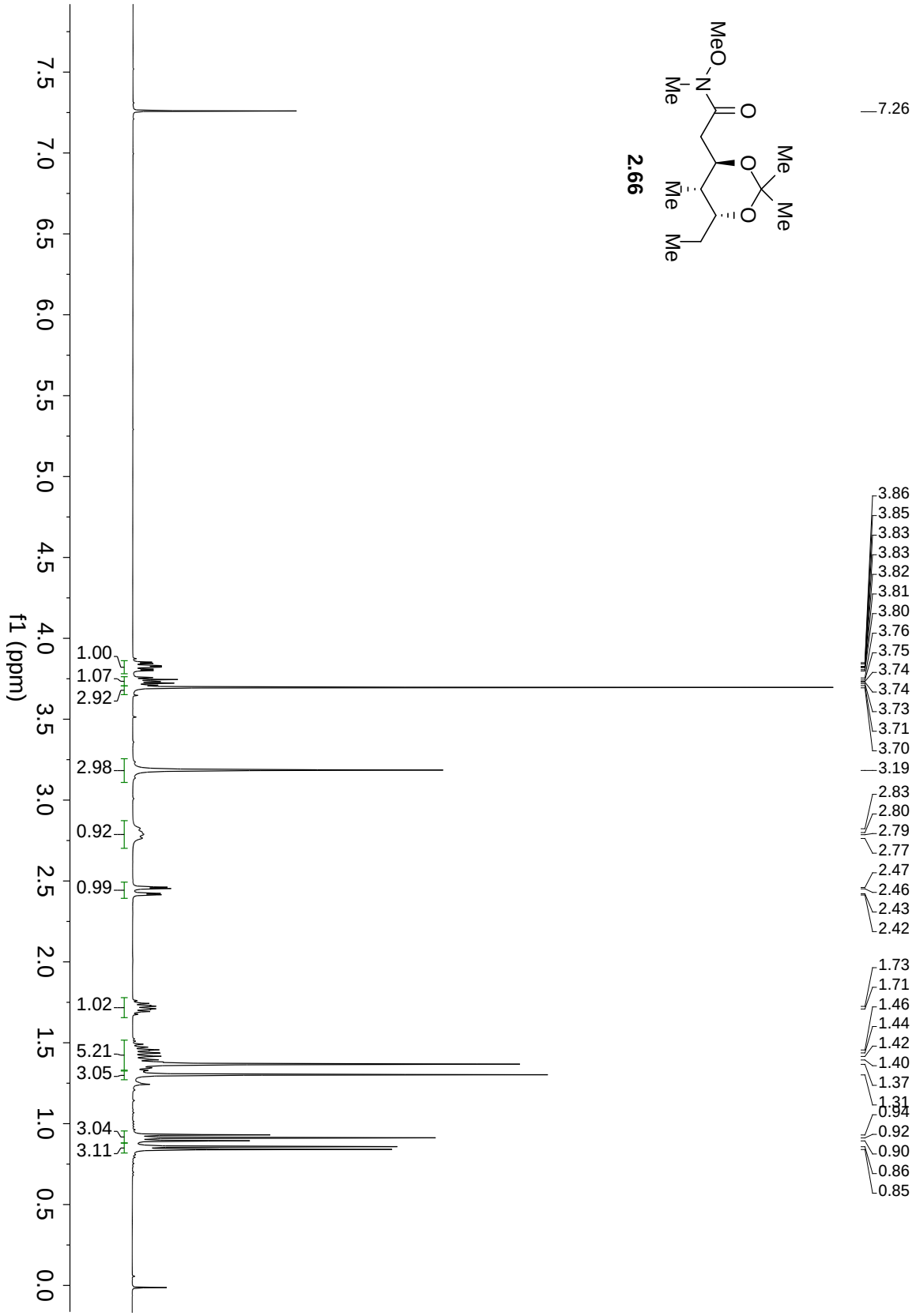
f1 (ppm)
7.5
7.0
6.5
6.0
5.5
5.0
4.5
4.0
3.5
3.0
2.5
2.0
1.5
1.0
0.5
0.0
1.00
1.07
2.92
2.98
0.92
0.99
1.02
5.21
3.05
3.04
3.11
MeO
N
Me
O
Me
Me
O
O
Me
Me
2.66
7.26
3.86
3.85
3.83
3.83
3.82
3.81
3.80
3.76
3.75
3.74
3.74
3.73
3.71
3.70
3.19
2.83
2.80
2.79
2.77
2.47
2.46
2.43
2.42
1.73
1.71
1.46
1.44
1.42
1.40
1.37
1.31
0.94
0.92
0.90
0.86
0.85

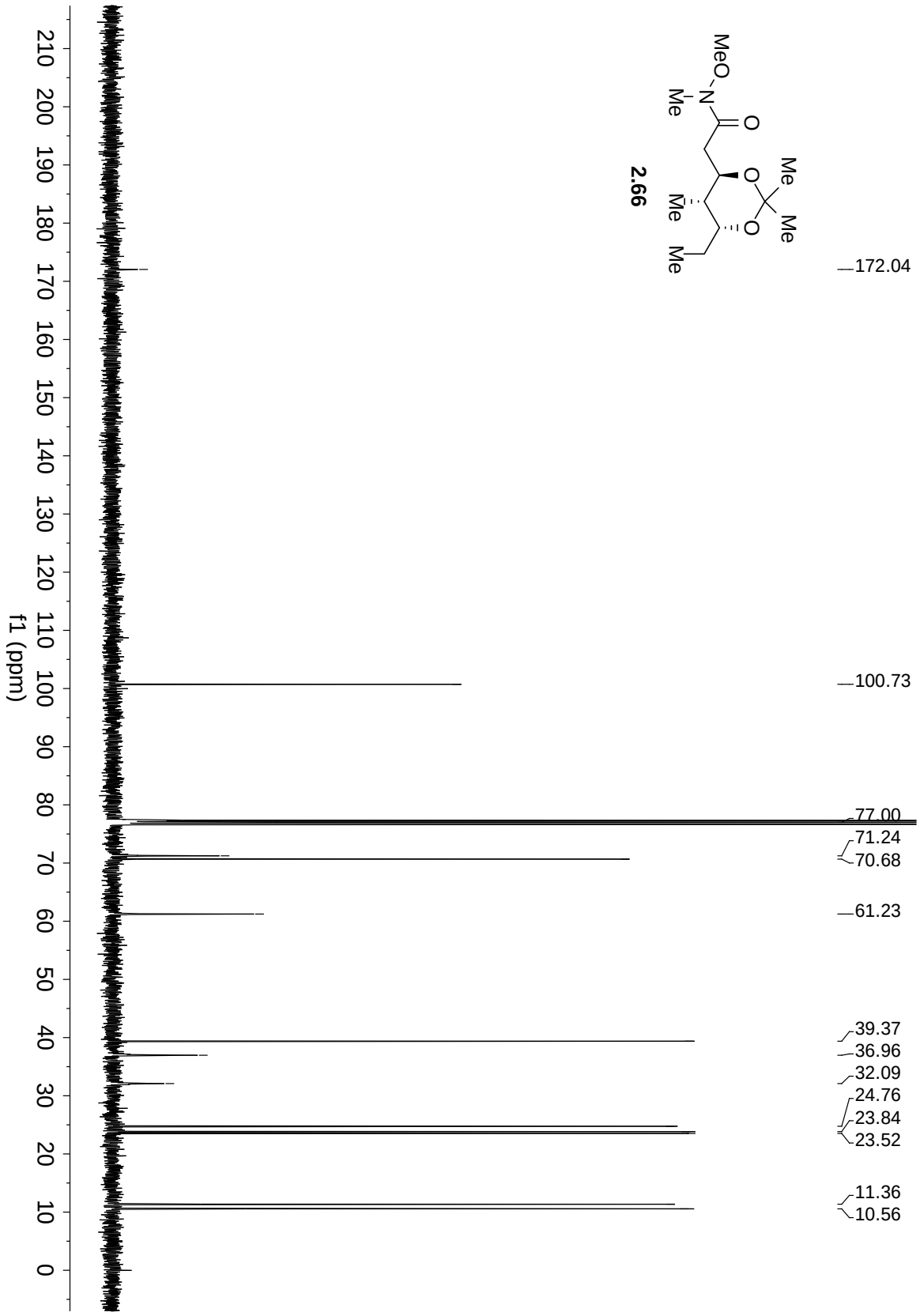
MeO
N
Me
O
O
O
Me
Me
Me
Me
2.66
172.04
100.73
77.00
71.24
70.68
61.23
39.37
36.96
32.09
24.76
23.84
23.52
11.36
10.56
f1 (ppm)

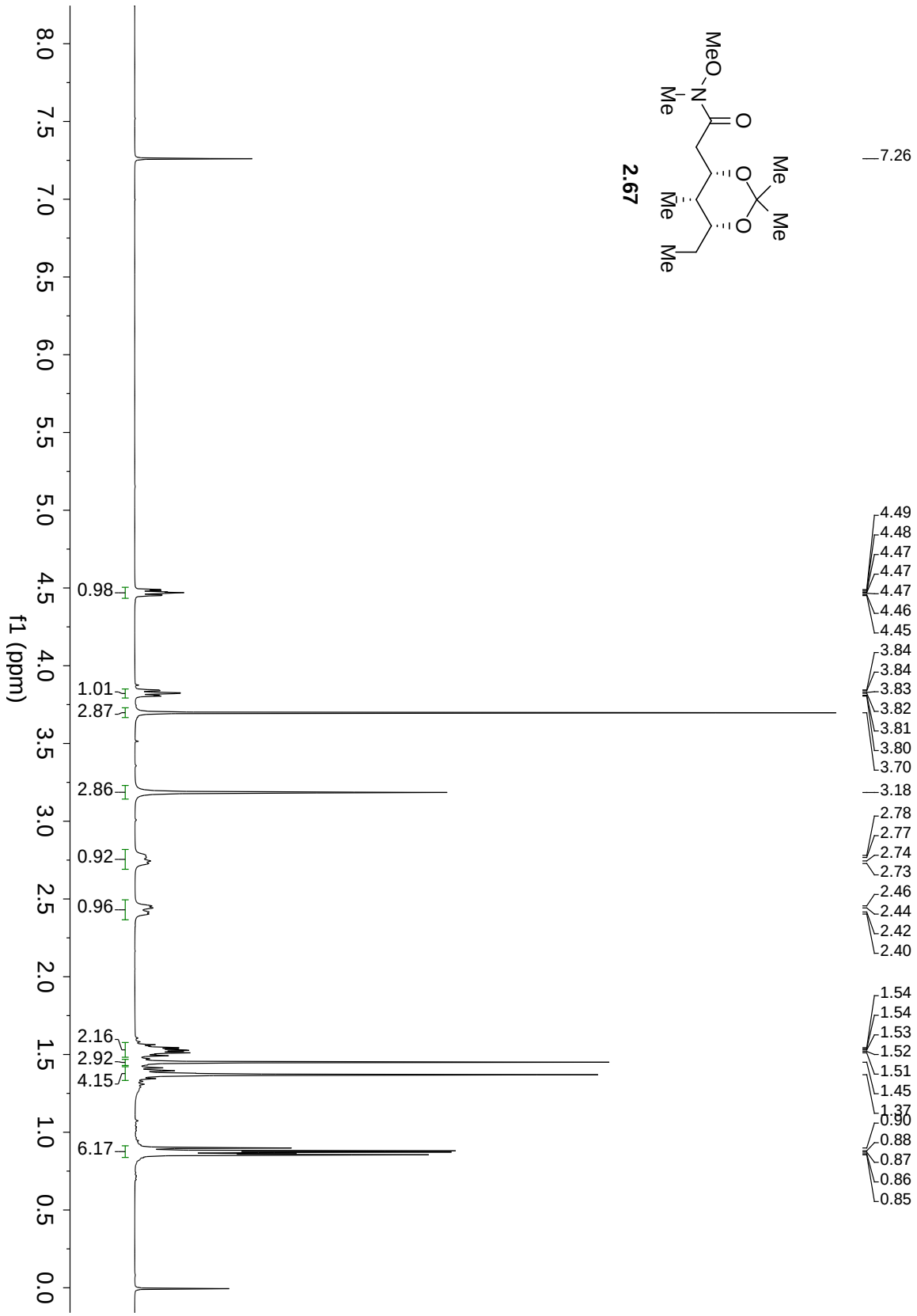
f1 (ppm)
8.0
7.5
7.0
6.5
6.0
5.5
5.0
4.5
4.0
3.5
3.0
2.5
2.0
1.5
1.0
0.5
0.0
0.98
1.01
2.87
2.86
0.92
0.96
2.16
2.92
4.15
6.17
MeO
N
Me
O
Me
Me
O
O
Me
Me
Me
2.67
7.26
4.49
4.48
4.47
4.47
4.47
4.46
4.45
3.84
3.84
3.83
3.82
3.81
3.80
3.70
3.18
2.78
2.77
2.74
2.73
2.46
2.44
2.42
2.40
1.54
1.54
1.53
1.52
1.51
1.45
1.37
0.90
0.88
0.87
0.86
0.85

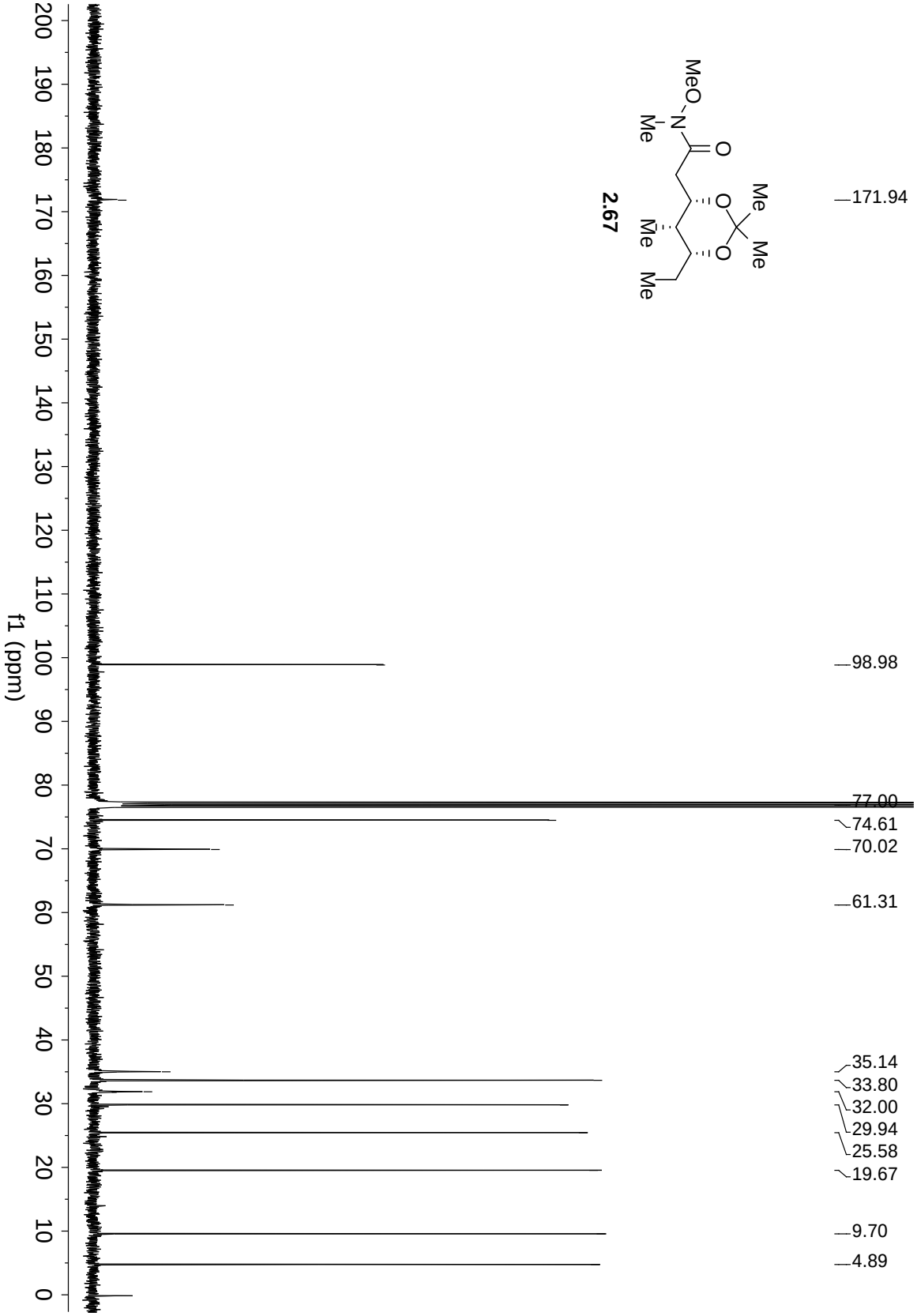
MeO
N
Me
Me
O
O
O
Me
Me
Me
Me
2.67
171.94
98.98
77.00
74.61
70.02
61.31
35.14
33.80
32.00
29.94
25.58
19.67
9.70
4.89
f1 (ppm)
200
190
180
170
160
150
140
130
120
110
100
90
80
70
60
50
40
30
20
10
0

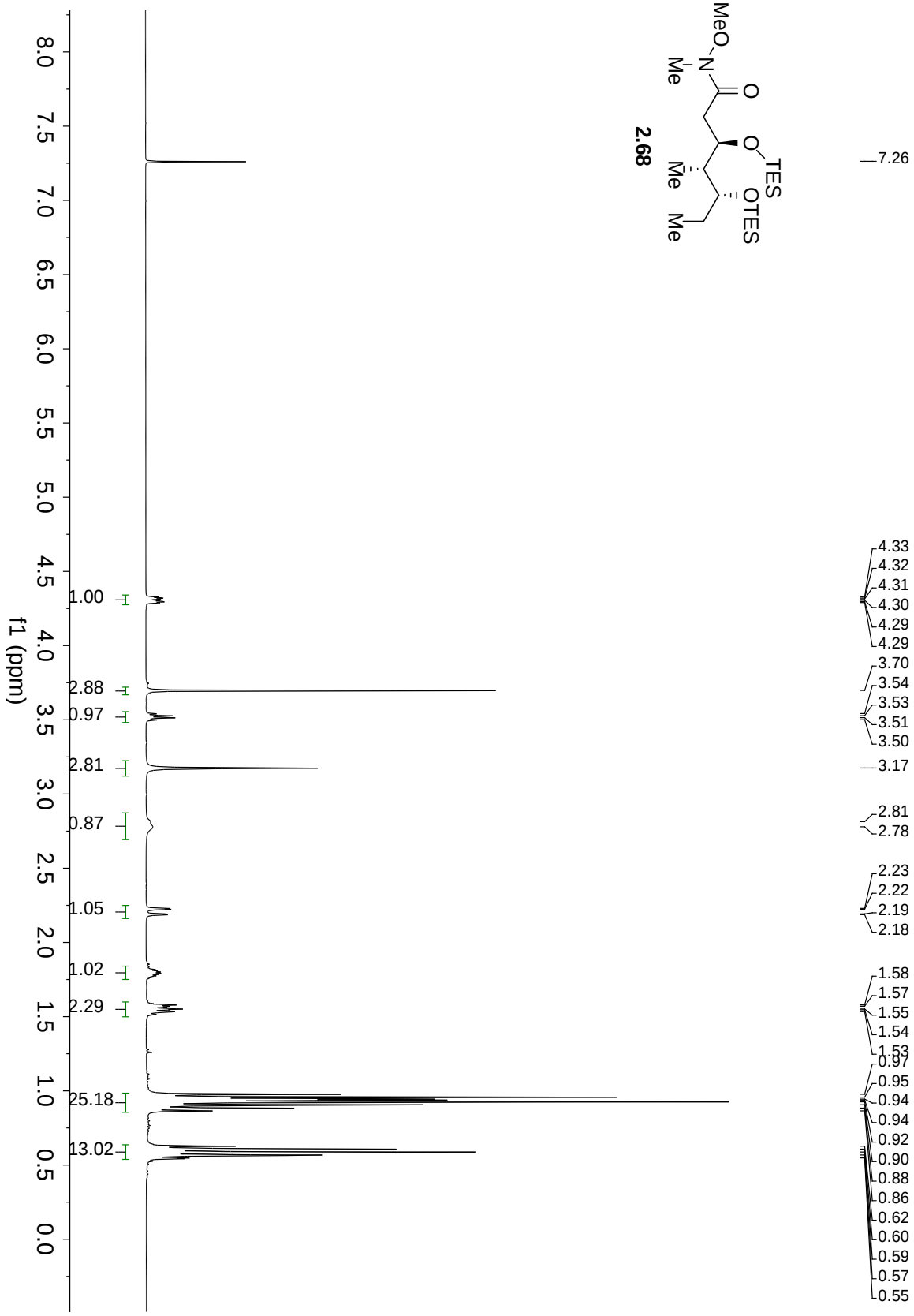
MeO
N
Me
O
O
TES
OTES
Me
Me
Me
2.68
7.26
4.33
4.32
4.31
4.30
4.29
4.29
3.70
3.54
3.53
3.51
3.50
3.17
2.81
2.78
2.23
2.22
2.19
2.18
1.58
1.57
1.55
1.54
1.53
0.97
0.95
0.94
0.94
0.92
0.90
0.88
0.86
0.62
0.60
0.59
0.57
0.55
1.00
2.88
0.97
2.81
0.87
1.05
1.02
2.29
25.18
13.02
f1 (ppm)
8.0
7.5
7.0
6.5
6.0
5.5
5.0
4.5
4.0
3.5
3.0
2.5
2.0
1.5
1.0
0.5
0.0

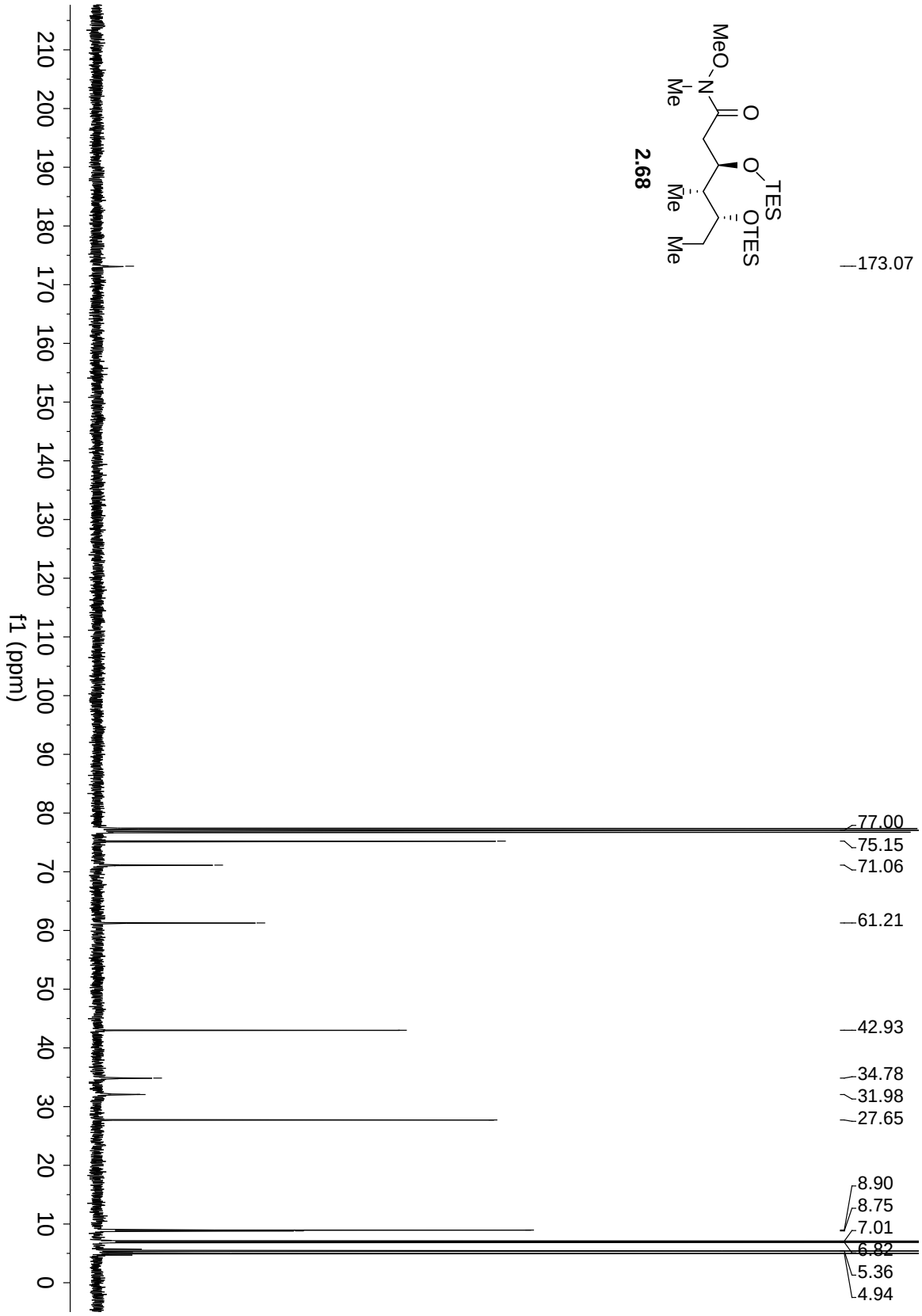
MeO
N
Me
O
O
TES
OTES
Me
Me
2.68
173.07
77.00
75.15
71.06
61.21
42.93
34.78
31.98
27.65
8.90
8.75
7.01
6.82
5.36
4.94
f1 (ppm)

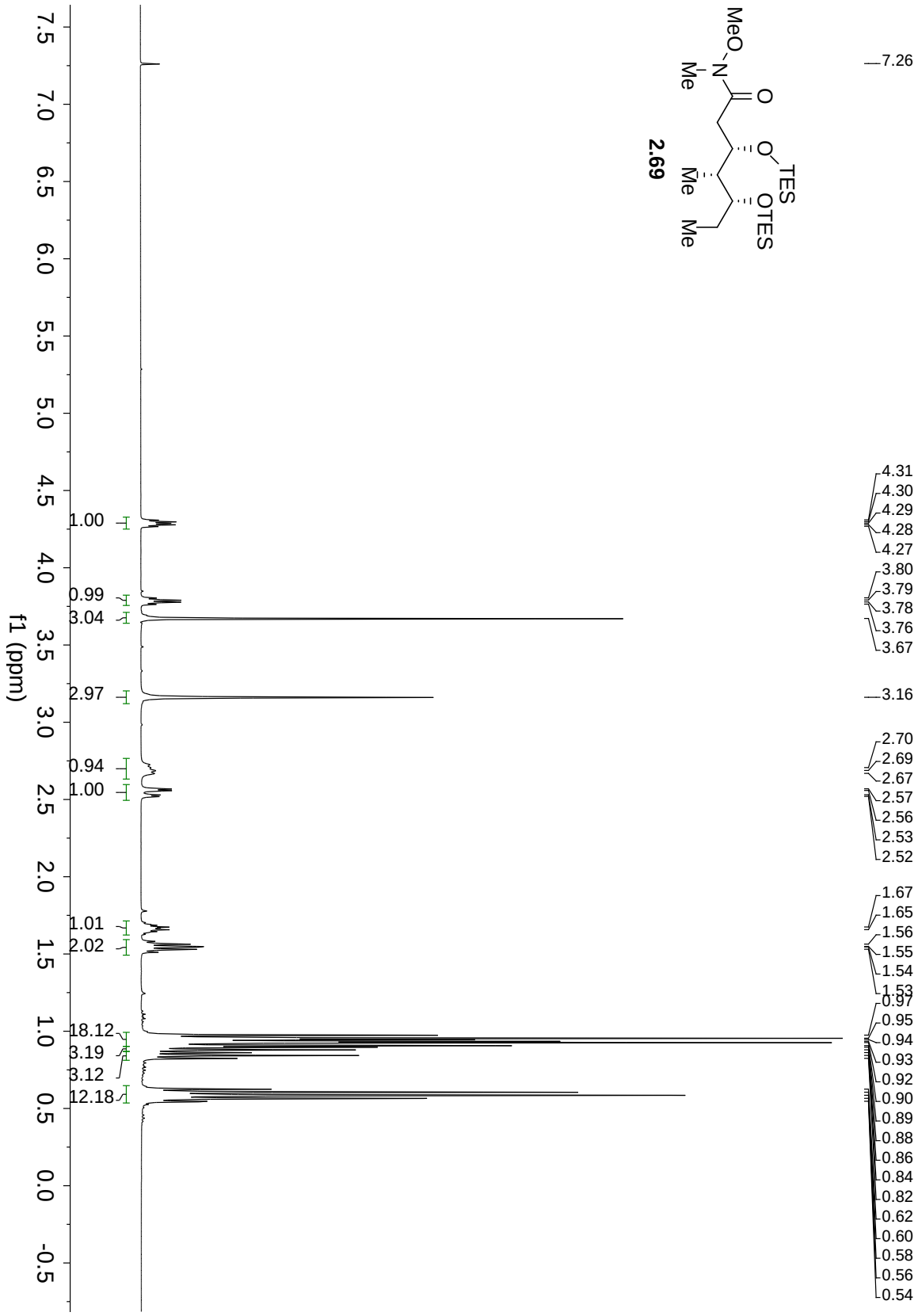
MeO
N
Me
O
O
TES
OTES
Me
Me
2.69
f1 (ppm)
7.5
7.0
6.5
6.0
5.5
5.0
4.5
4.0
3.5
3.0
2.5
2.0
1.5
1.0
0.5
0.0
-0.5
1.00
0.99
3.04
2.97
0.94
1.00
1.01
2.02
18.12
3.19
3.12
12.18
7.26
4.31
4.30
4.29
4.28
4.27
3.80
3.79
3.78
3.76
3.67
3.16
2.70
2.69
2.67
2.57
2.56
2.53
2.52
1.67
1.65
1.56
1.55
1.54
1.53
0.97
0.95
0.94
0.93
0.92
0.90
0.89
0.88
0.86
0.84
0.82
0.62
0.60
0.58
0.56
0.54

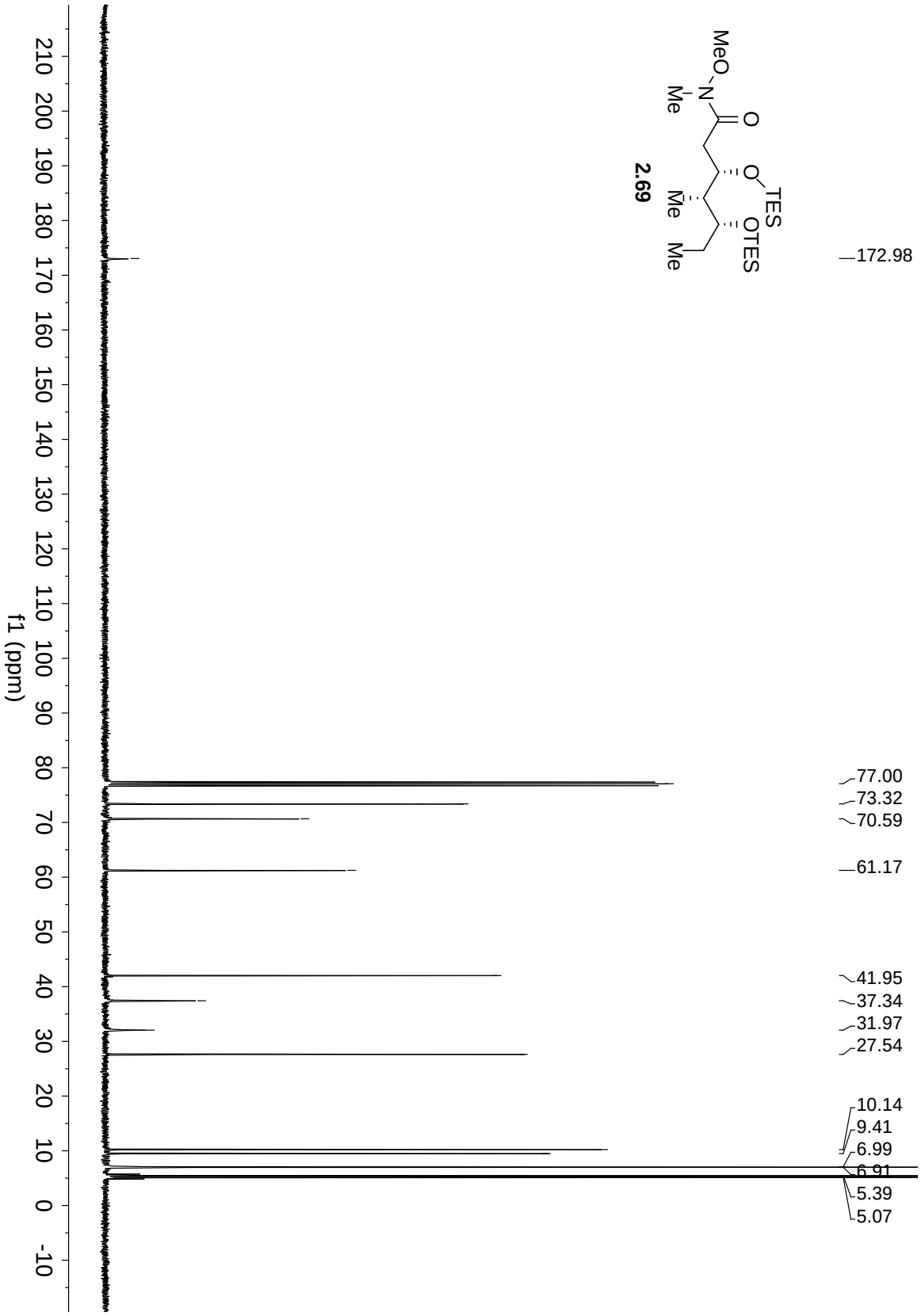
MeO
N
Me
O
O
TES
OTES
Me
Me
2.69
172.98
77.00
73.32
70.59
61.17
41.95
37.34
31.97
27.54
10.14
9.41
6.99
6.91
5.39
5.07
f1 (ppm)
210 200 190 180 170 160 150 140 130 120 110 100 90 80 70 60 50 40 30 20 10 0 -10

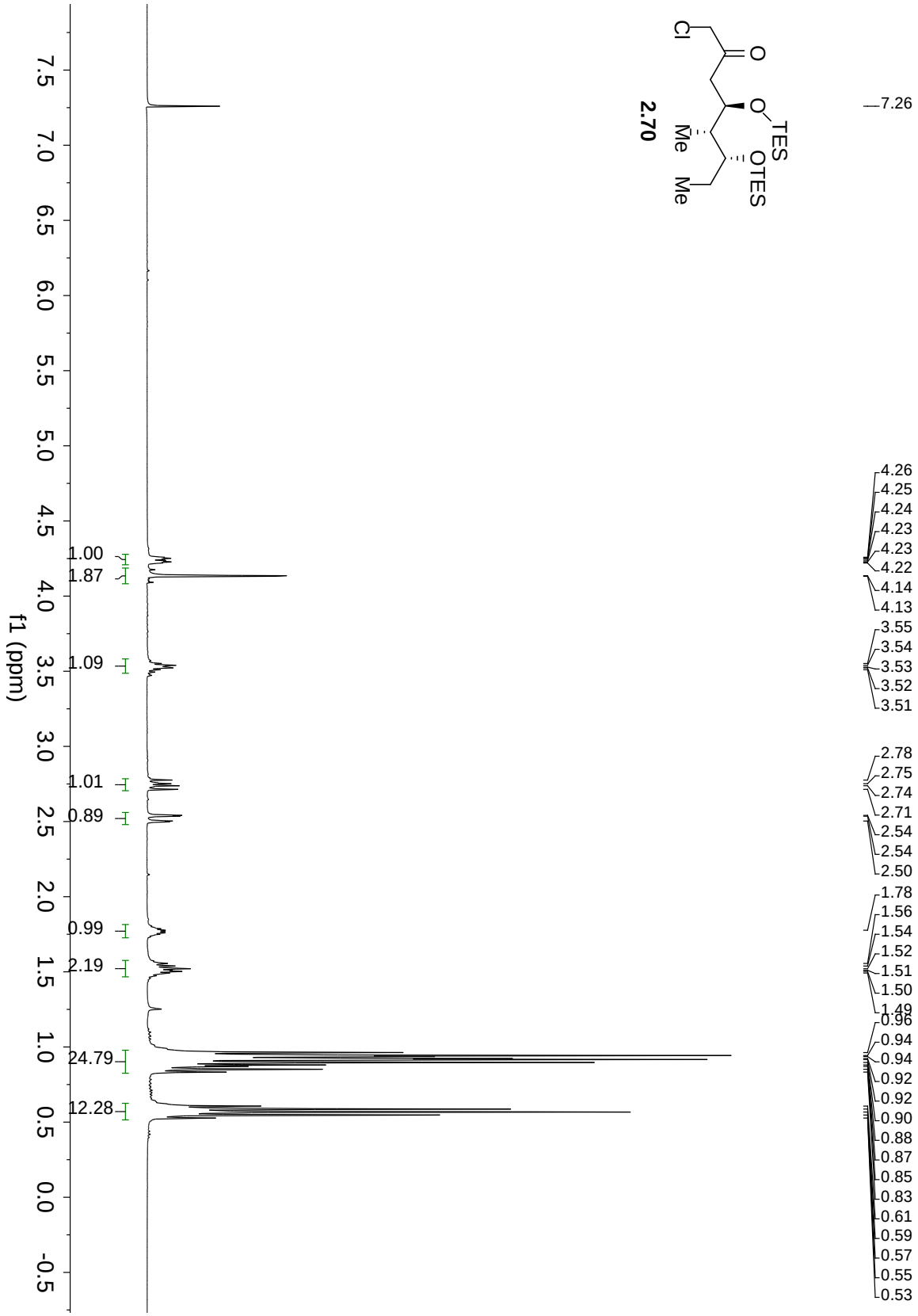
f1 (ppm)
7.5
7.0
6.5
6.0
5.5
5.0
4.5
4.0
3.5
3.0
2.5
2.0
1.5
1.0
0.5
0.0
-0.5
1.00
1.87
1.09
1.01
0.89
0.99
2.19
24.79
12.28
Cl
O
O
TES
OTES
Me
Me
2.70
7.26
4.26
4.25
4.24
4.23
4.23
4.22
4.14
4.13
3.55
3.54
3.53
3.52
3.51
2.78
2.75
2.74
2.71
2.54
2.54
2.50
1.78
1.56
1.54
1.52
1.51
1.50
1.49
0.96
0.94
0.94
0.92
0.92
0.90
0.88
0.87
0.85
0.83
0.61
0.59
0.57
0.55
0.53

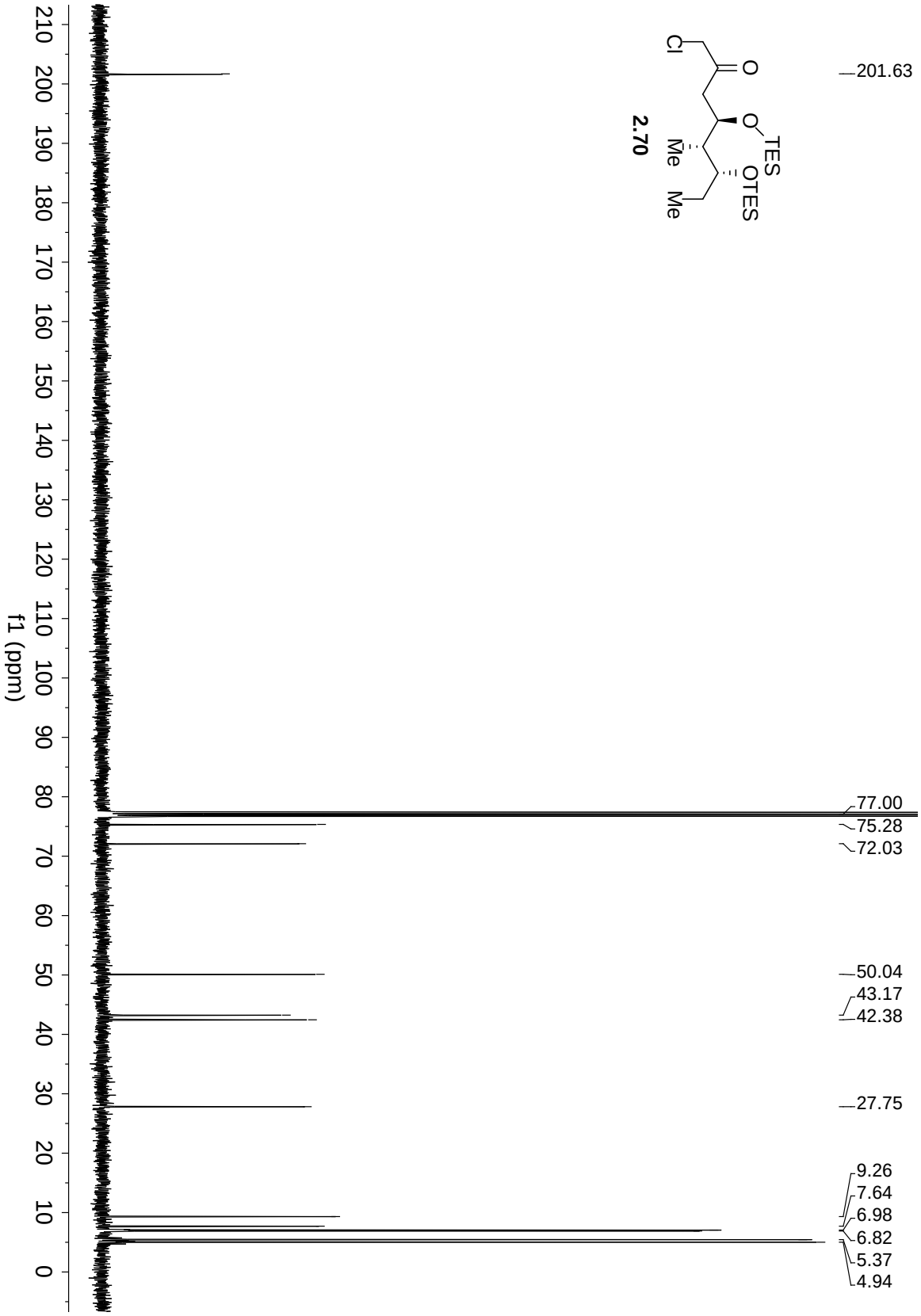
2.70
Cl
O
O
TES
OTES
Me
Me
201.63
77.00
75.28
72.03
50.04
43.17
42.38
27.75
9.26
7.64
6.98
6.82
5.37
4.94
f1 (ppm)
210
200
190
180
170
160
150
140
130
120
110
100
90
80
70
60
50
40
30
20
10
0

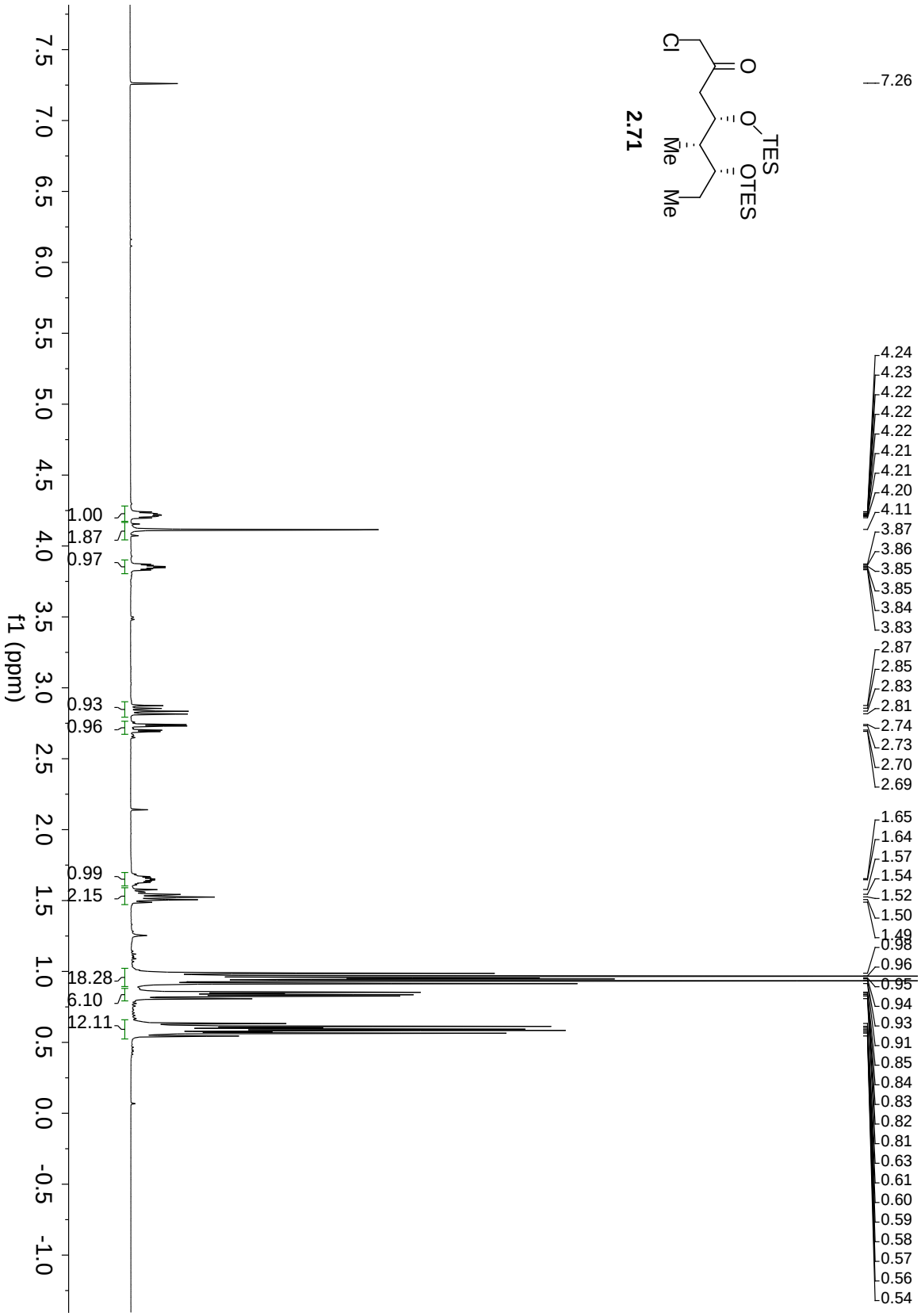
Cl
O
O
TES
OTES
Me
Me
2.71
7.26
4.24
4.23
4.22
4.22
4.22
4.21
4.21
4.20
4.11
3.87
3.86
3.85
3.85
3.84
3.83
2.87
2.85
2.83
2.81
2.74
2.73
2.70
2.69
1.65
1.64
1.57
1.54
1.52
1.50
1.49
0.98
0.96
0.95
0.94
0.93
0.91
0.85
0.84
0.83
0.82
0.81
0.63
0.61
0.60
0.59
0.58
0.57
0.56
0.54
1.00
1.87
0.97
0.93
0.96
0.99
2.15
18.28
6.10
12.11
f1 (ppm)
7.5
7.0
6.5
6.0
5.5
5.0
4.5
4.0
3.5
3.0
2.5
2.0
1.5
1.0
0.5
0.0
-0.5
-1.0

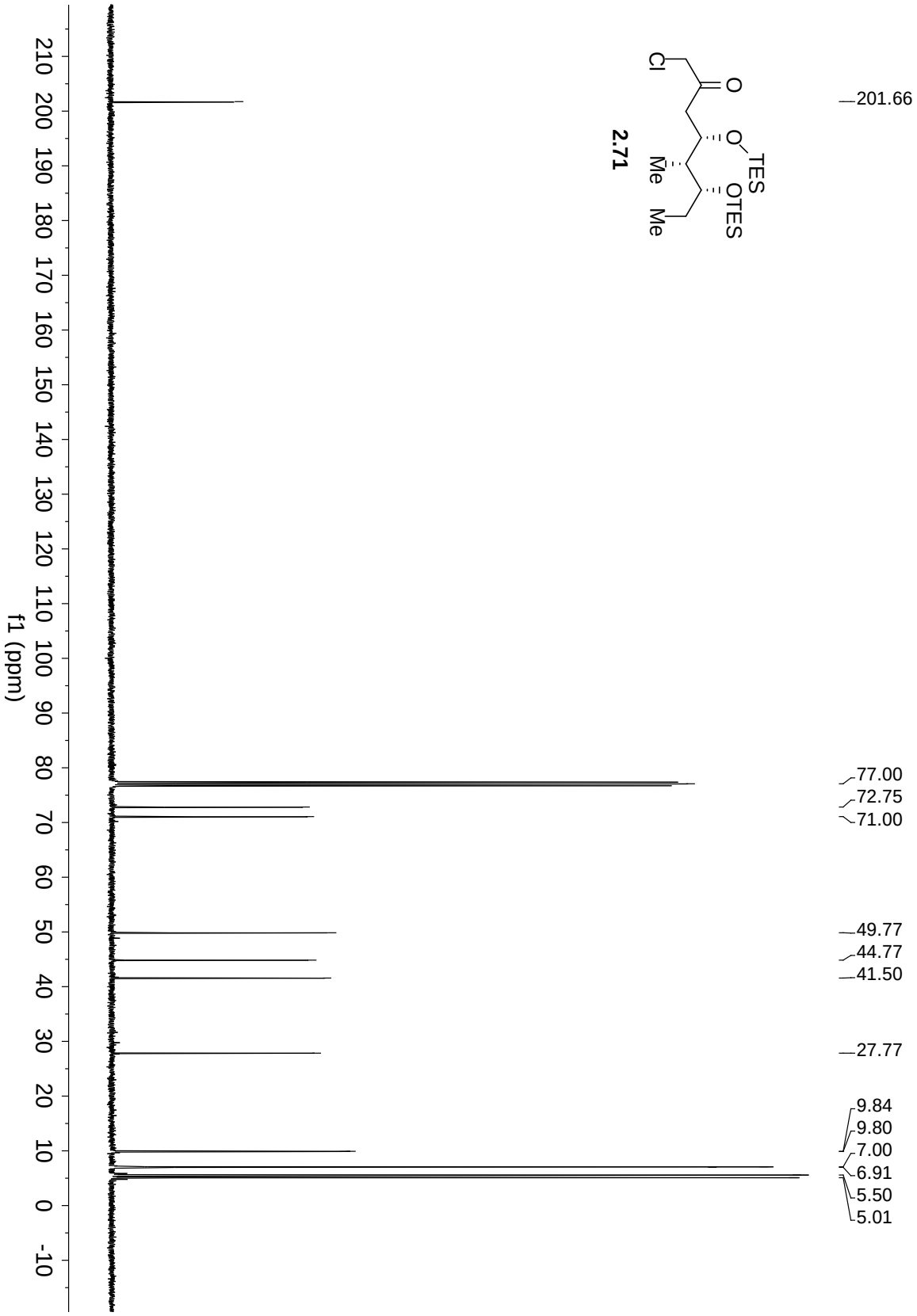
Cl
O
O
TES
OTES
Me
Me
2.71
201.66
77.00
72.75
71.00
49.77
44.77
41.50
27.77
9.84
9.80
7.00
6.91
5.50
5.01
f1 (ppm)
210 200 190 180 170 160 150 140 130 120 110 100 90 80 70 60 50 40 30 20 10 0 -10

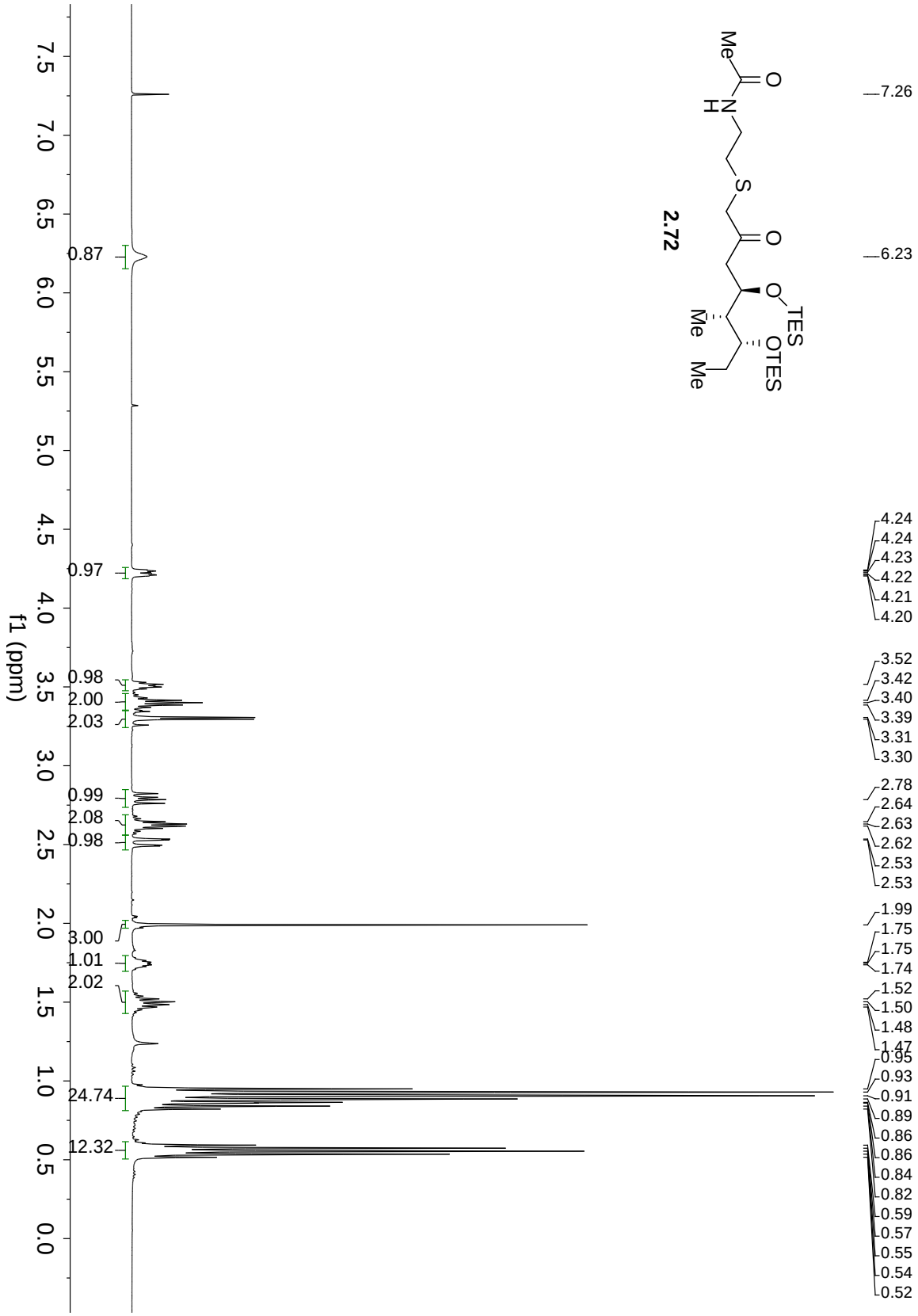
2.72
f1 (ppm)
7.5
7.0
6.5
6.0
5.5
5.0
4.5
4.0
3.5
3.0
2.5
2.0
1.5
1.0
0.5
0.0
0.87
0.97
0.98
2.00
2.03
0.99
2.08
0.98
3.00
1.01
2.02
24.74
12.32
7.26
6.23
4.24
4.24
4.23
4.22
4.21
4.20
3.52
3.42
3.40
3.39
3.31
3.30
2.78
2.64
2.63
2.62
2.53
2.53
1.99
1.75
1.75
1.74
1.52
1.50
1.48
1.47
0.95
0.93
0.91
0.89
0.86
0.86
0.84
0.82
0.59
0.57
0.55
0.54
0.52

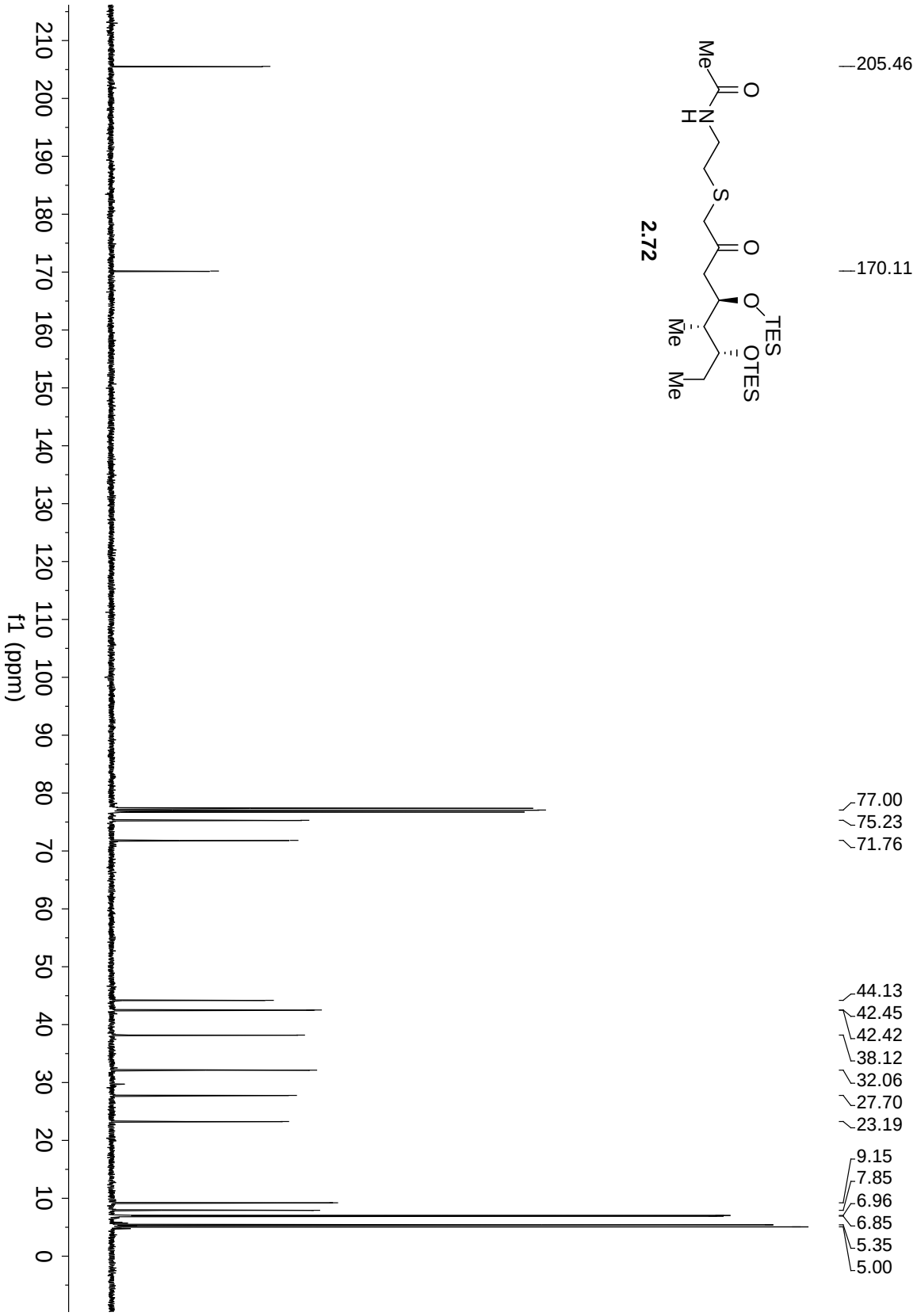
Me
O
N
H
S
O
O
TES
OTES
Me
Me
2.72
205.46
170.11
77.00
75.23
71.76
44.13
42.45
42.42
38.12
32.06
27.70
23.19
9.15
7.85
6.96
6.85
5.35
5.00
f1 (ppm)

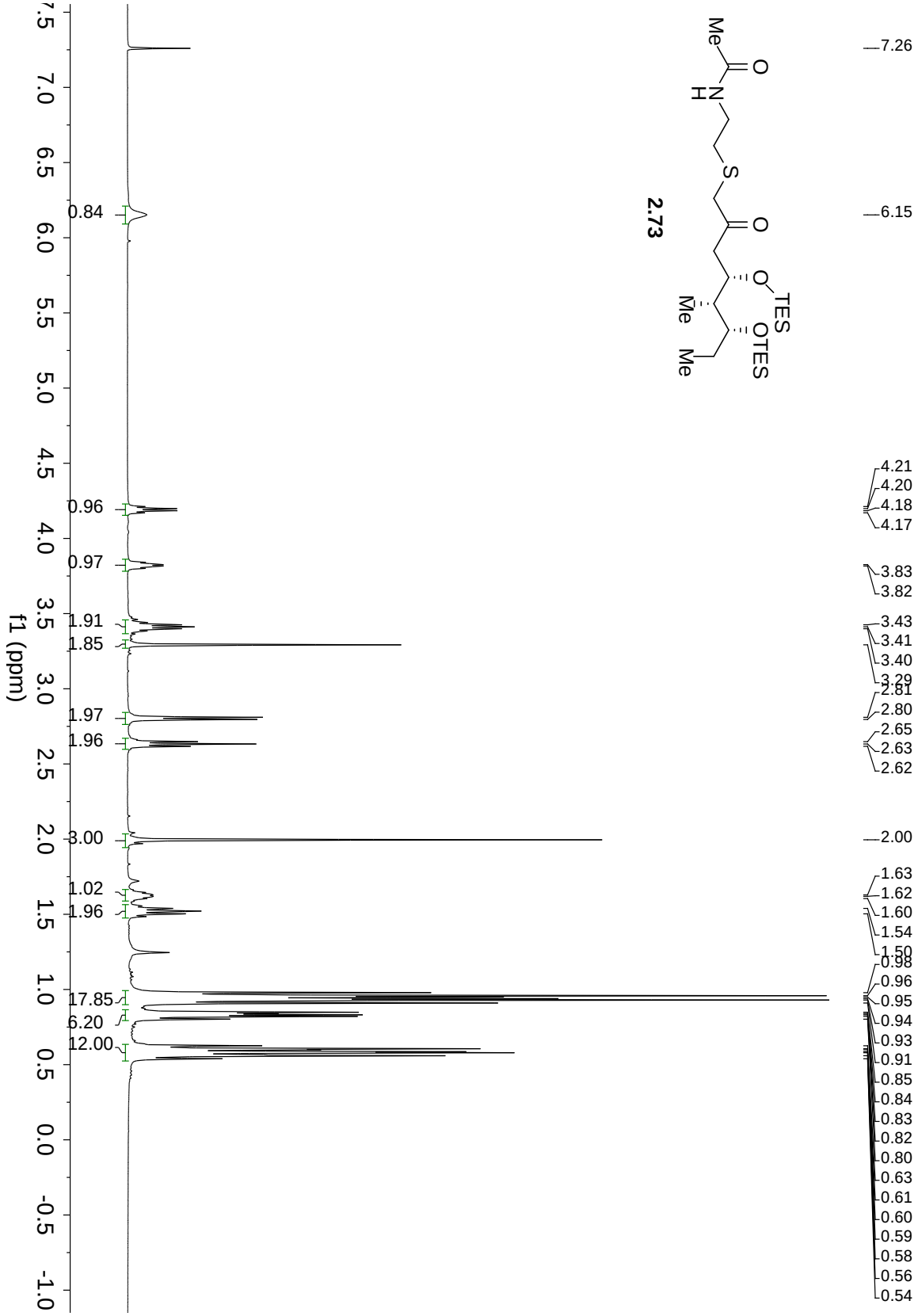
2.73
f1 (ppm)
0.84
0.96
0.97
1.91
1.85
1.97
1.96
3.00
1.02
1.96
17.85
6.20
12.00
7.26
6.15
4.21
4.20
4.18
4.17
3.83
3.82
3.43
3.41
3.40
3.29
2.81
2.80
2.65
2.63
2.62
2.00
1.63
1.62
1.60
1.54
1.50
0.98
0.96
0.95
0.94
0.93
0.91
0.85
0.84
0.83
0.82
0.80
0.63
0.61
0.60
0.59
0.58
0.56
0.54

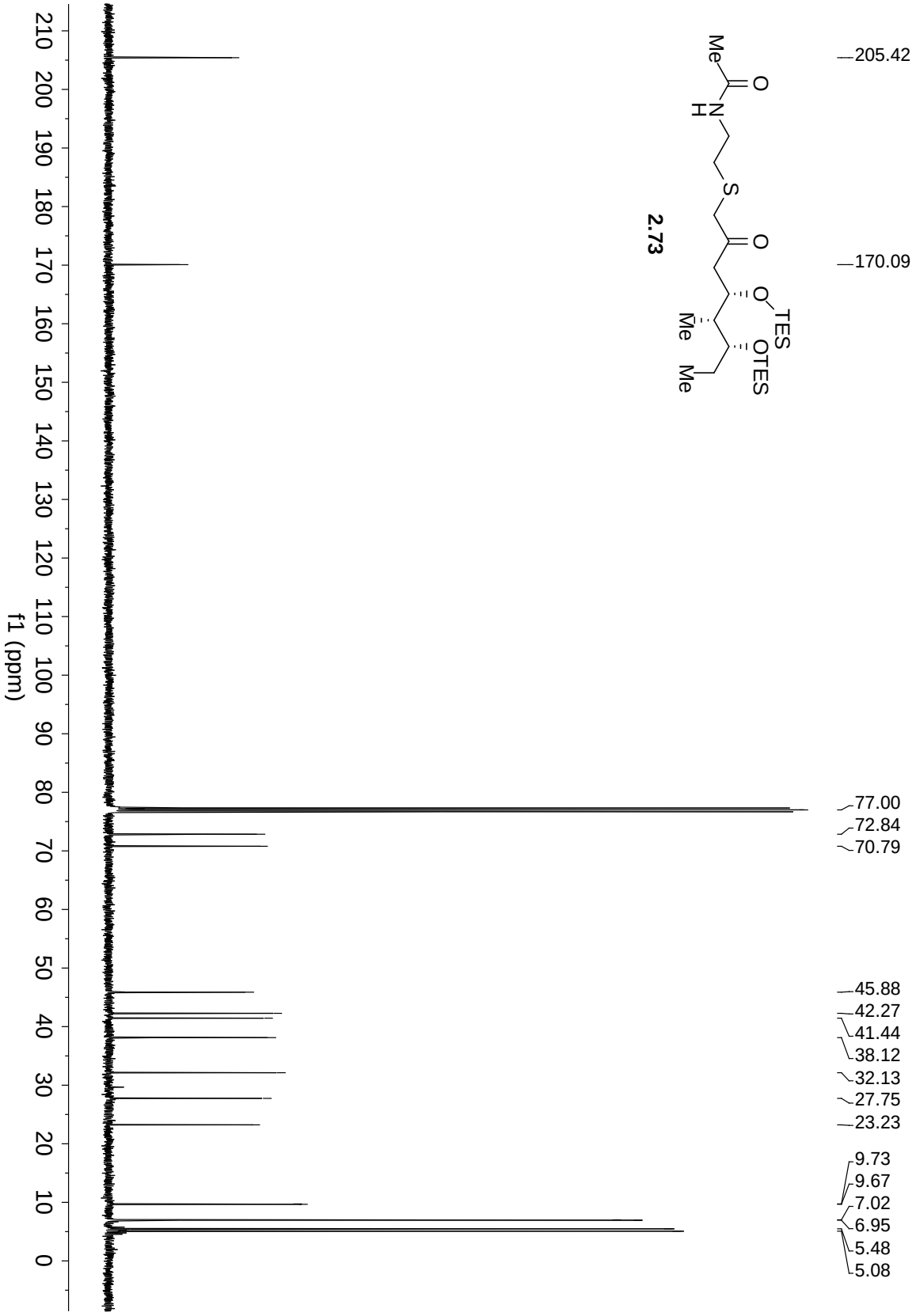
205.42
170.09
77.00
72.84
70.79
45.88
42.27
41.44
38.12
32.13
27.75
23.23
9.73
9.67
7.02
6.95
5.48
5.08
f1 (ppm)
2.73

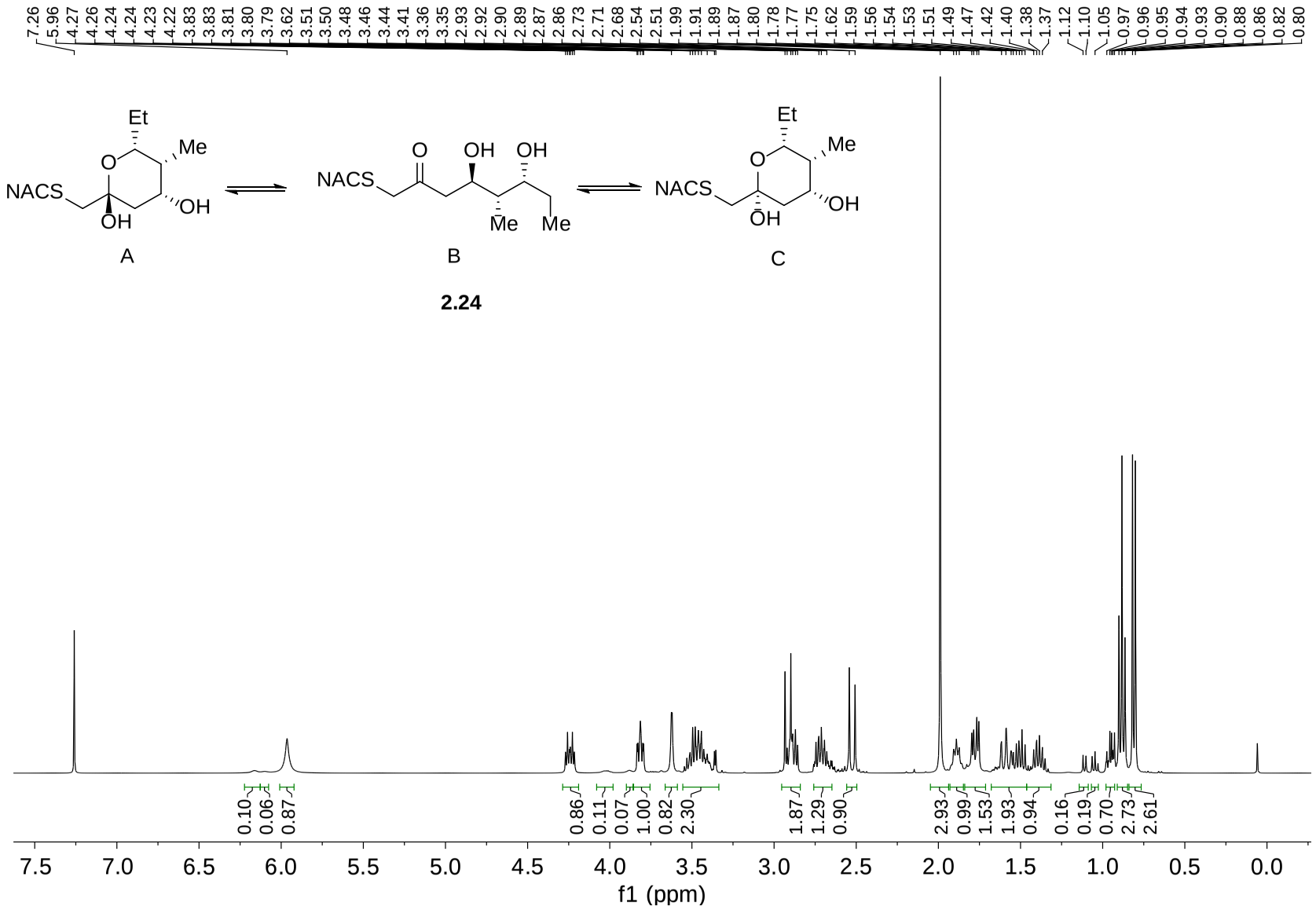
7.26 5.96 4.27 4.26 4.24 4.24 4.23 4.22 3.83 3.83 3.81 3.80 3.79 3.62 3.51 3.50 3.48 3.46 3.44 3.41 3.36 3.35 2.93 2.92 2.90 2.89 2.87 2.86 2.73 2.71 2.68 2.54 2.51 1.99 1.91 1.89 1.87 1.80 1.78 1.77 1.75 1.62 1.59 1.56 1.54 1.53 1.51 1.49 1.47 1.42 1.40 1.38 1.37 1.12 1.10 1.05 0.97 0.96 0.95 0.94 0.93 0.90 0.88 0.86 0.82 0.80
Et
Me
O
NACS
OH
OH
A
O
OH
OH
NACS
Me
Me
B
Et
Me
O
NACS
OH
OH
C
2.24
0.10 0.06 0.87 0.86 0.11 0.07 1.00 0.82 2.30 1.87 1.29 0.90 2.93 0.99 1.53 1.93 0.94 0.16 0.19 0.70 2.73 2.61
7.5 7.0 6.5 6.0 5.5 5.0 4.5 4.0 3.5 3.0 2.5 2.0 1.5 1.0 0.5 0.0
f1 (ppm)

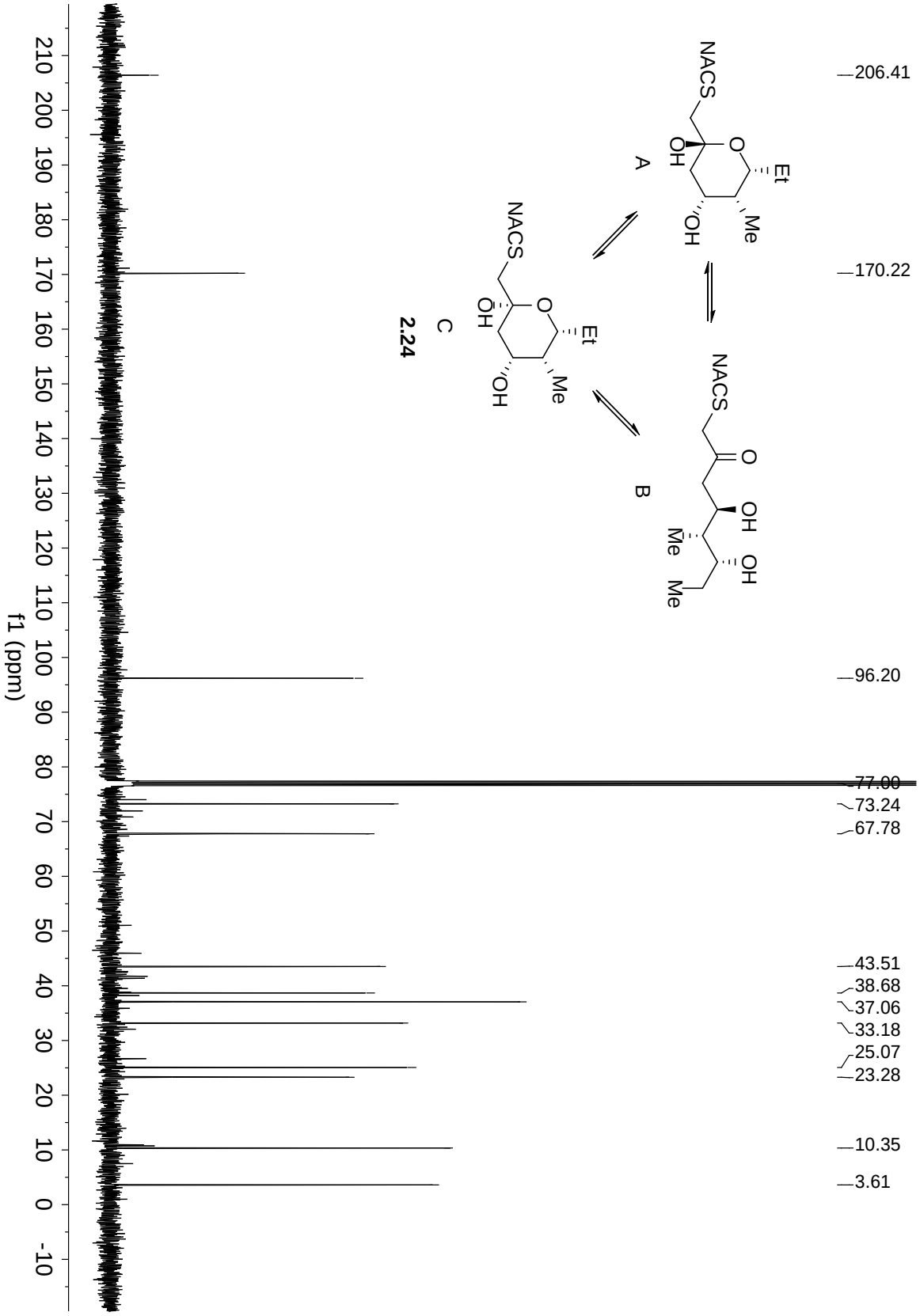
206.41
170.22
96.20
77.00
73.24
67.78
43.51
38.68
37.06
33.18
25.07
23.28
10.35
3.61
f1 (ppm)
NACS
OH
O
Et
Me
OH
A
B
C
2.24

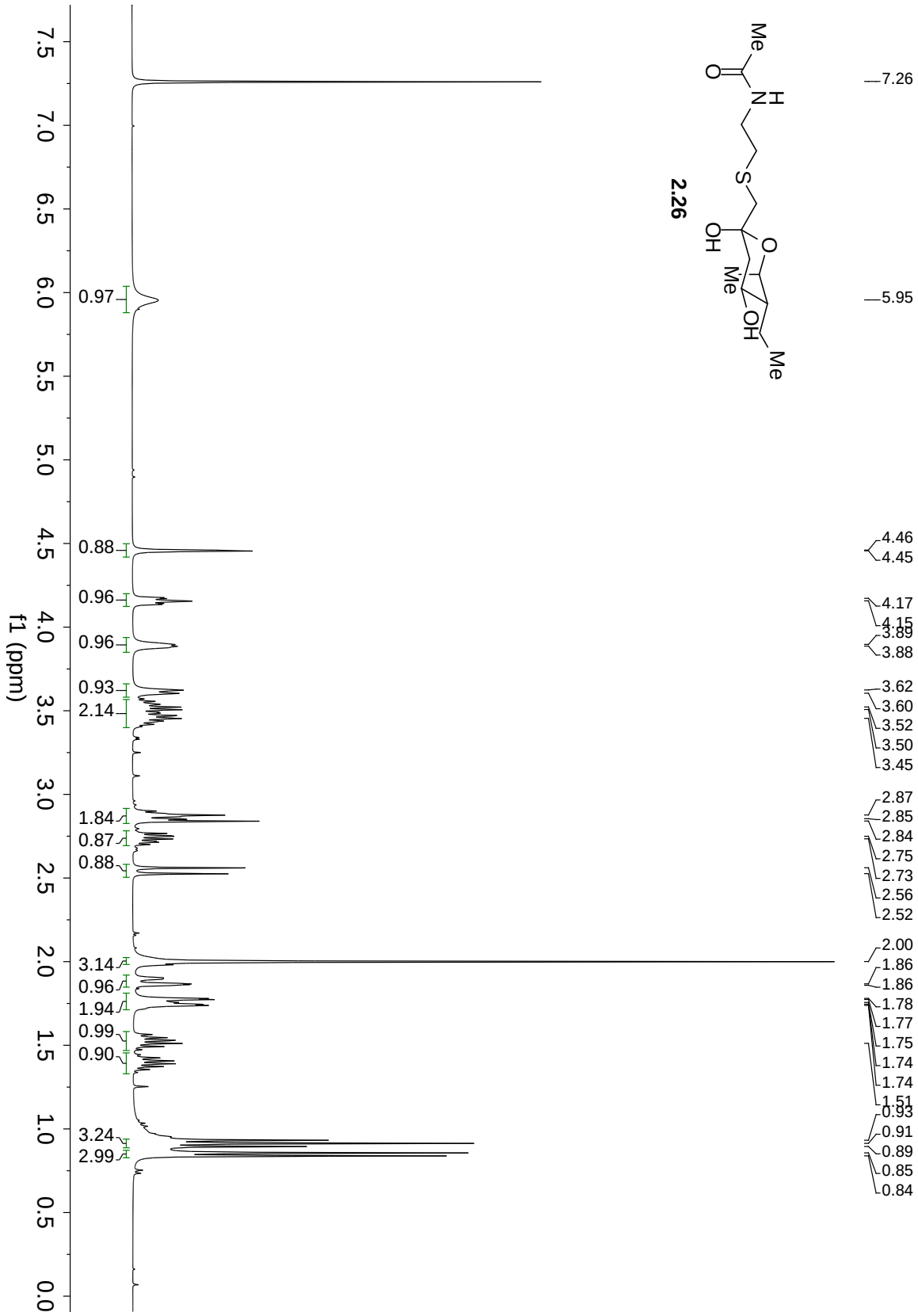
f1 (ppm)
7.5
7.0
6.5
6.0
5.5
5.0
4.5
4.0
3.5
3.0
2.5
2.0
1.5
1.0
0.5
0.0
0.97
0.88
0.96
0.96
0.93
2.14
1.84
0.87
0.88
3.14
0.96
1.94
0.99
0.90
3.24
2.99
Me
O
H
N
S
OH
O
Me
OH
Me
2.26
7.26
5.95
4.46
4.45
4.17
4.15
3.89
3.88
3.62
3.60
3.52
3.50
3.45
2.87
2.85
2.84
2.75
2.73
2.56
2.52
2.00
1.86
1.86
1.78
1.77
1.75
1.74
1.74
1.51
0.93
0.91
0.89
0.85
0.84

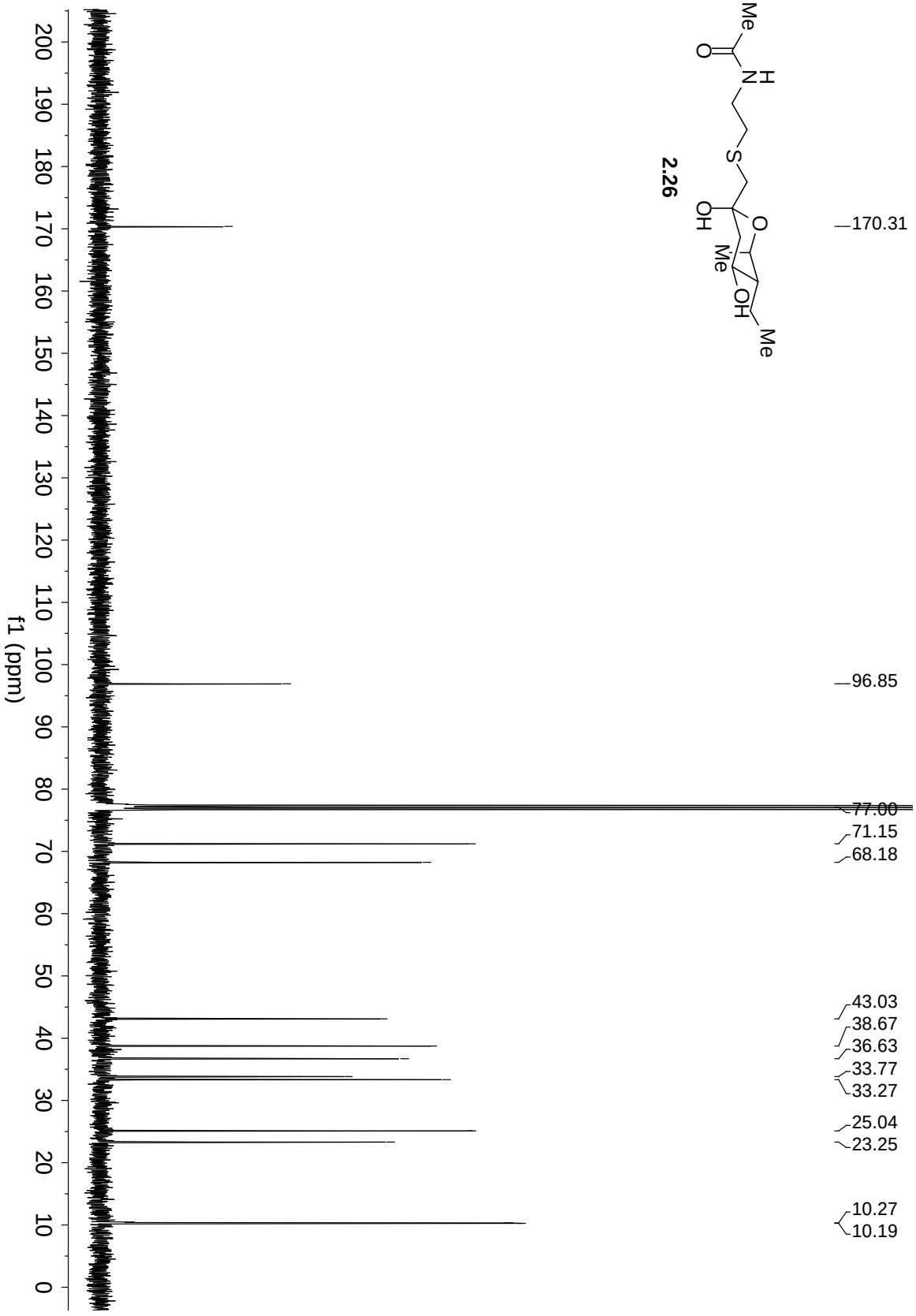
2.26
Me
O
H
N
S
OH
O
Me
OH
Me
170.31
96.85
77.00
71.15
68.18
43.03
38.67
36.63
33.77
33.27
25.04
23.25
10.27
10.19
f1 (ppm)
200
190
180
170
160
150
140
130
120
110
100
90
80
70
60
50
40
30
20
10
0

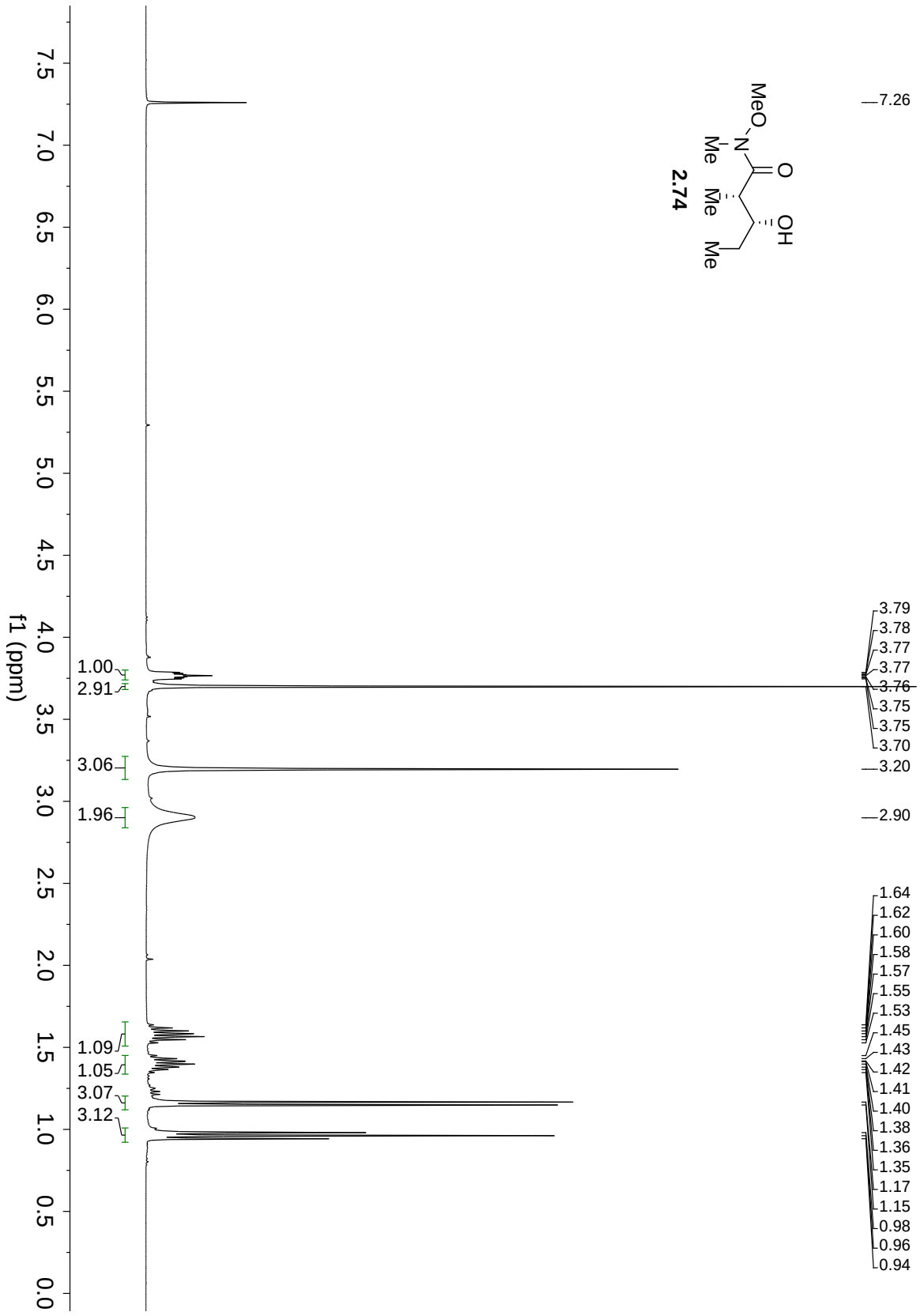
MeO
N
Me
Me
O
OH
Me
Me
Me
2.74
7.26
3.79
3.78
3.77
3.77
3.76
3.75
3.75
3.70
3.20
2.90
1.64
1.62
1.60
1.58
1.57
1.55
1.53
1.45
1.43
1.42
1.41
1.40
1.38
1.36
1.35
1.17
1.15
0.98
0.96
0.94
1.00
2.91
3.06
1.96
1.09
1.05
3.07
3.12
f1 (ppm)
7.5
7.0
6.5
6.0
5.5
5.0
4.5
4.0
3.5
3.0
2.5
2.0
1.5
1.0
0.5
0.0

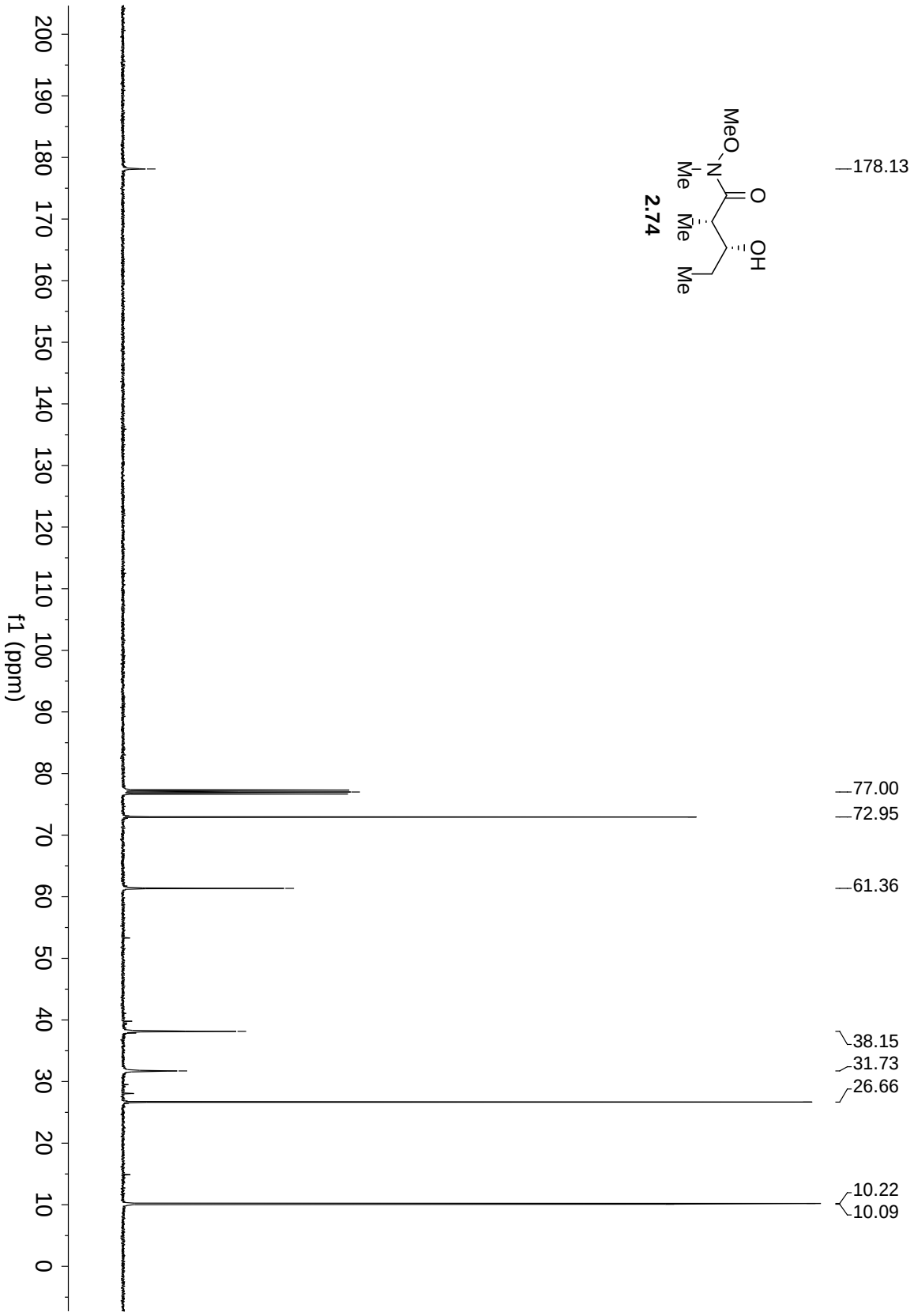
f1 (ppm)
200
190
180
170
160
150
140
130
120
110
100
90
80
70
60
50
40
30
20
10
0
MeO
N
Me
Me
O
OH
Me
2.74
178.13
77.00
72.95
61.36
38.15
31.73
26.66
10.22
10.09

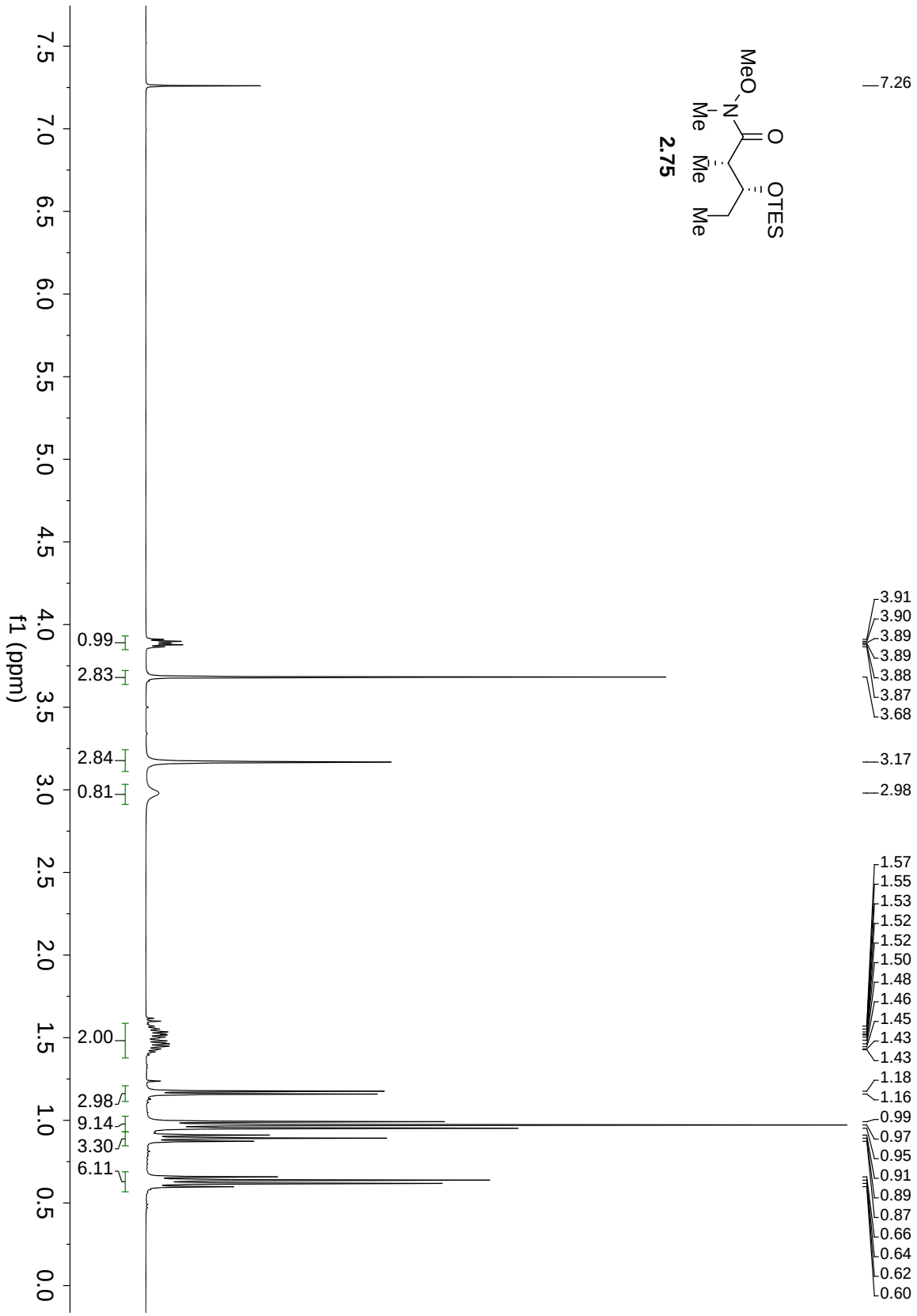
MeO
N
Me
Me
O
OTES
Me
Me
Me
2.75
7.26
3.91
3.90
3.89
3.89
3.88
3.87
3.68
3.17
2.98
1.57
1.55
1.53
1.52
1.52
1.50
1.48
1.46
1.45
1.43
1.43
1.18
1.16
0.99
0.97
0.95
0.91
0.89
0.87
0.66
0.64
0.62
0.60
0.99
2.83
2.84
0.81
2.00
2.98
9.14
3.30
6.11
f1 (ppm)
7.5
7.0
6.5
6.0
5.5
5.0
4.5
4.0
3.5
3.0
2.5
2.0
1.5
1.0
0.5
0.0

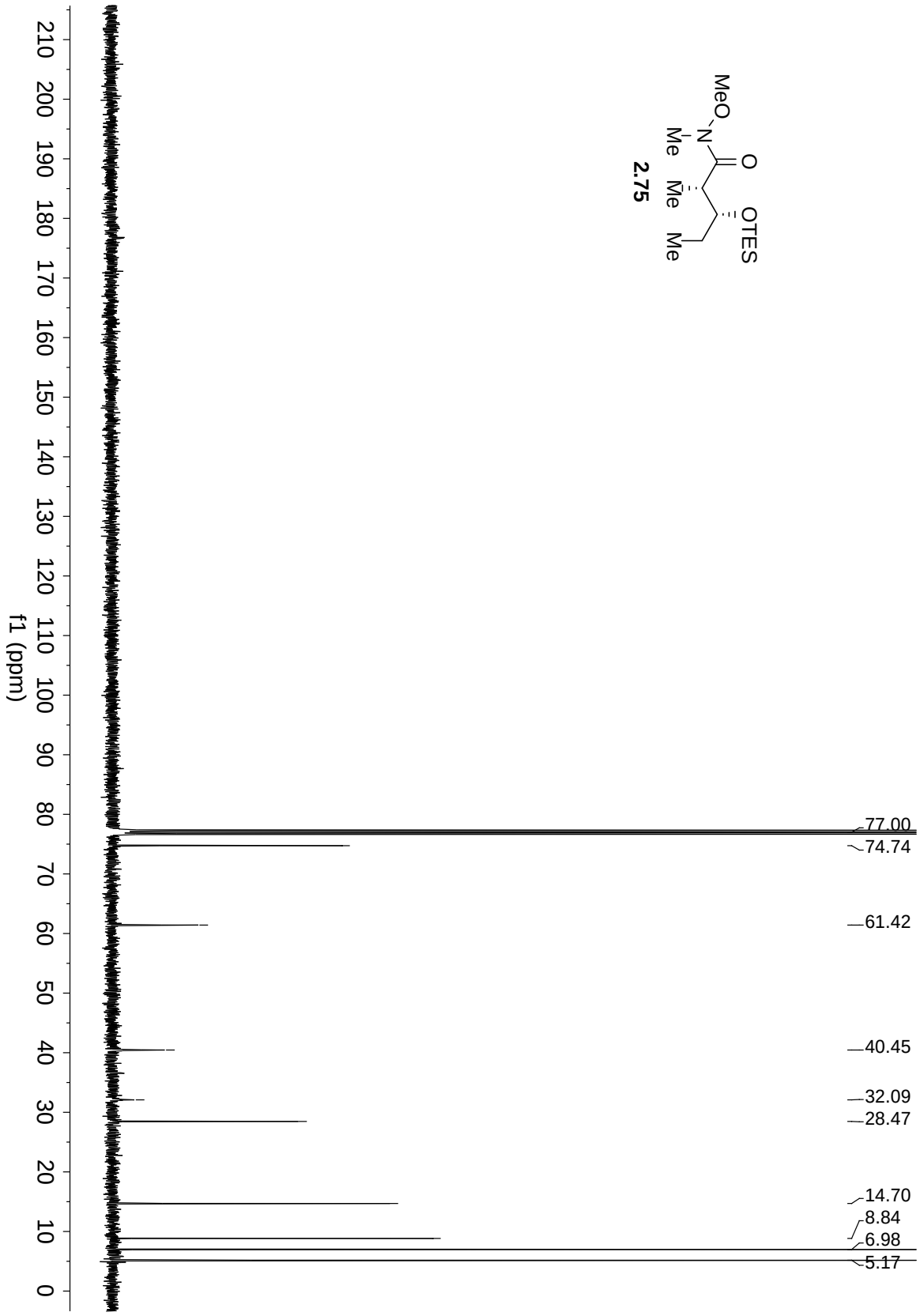
MeO
N
O
OTES
Me
Me
Me
Me
2.75
f1 (ppm)
210
200
190
180
170
160
150
140
130
120
110
100
90
80
70
60
50
40
30
20
10
0
77.00
74.74
61.42
40.45
32.09
28.47
14.70
8.84
6.98
5.17

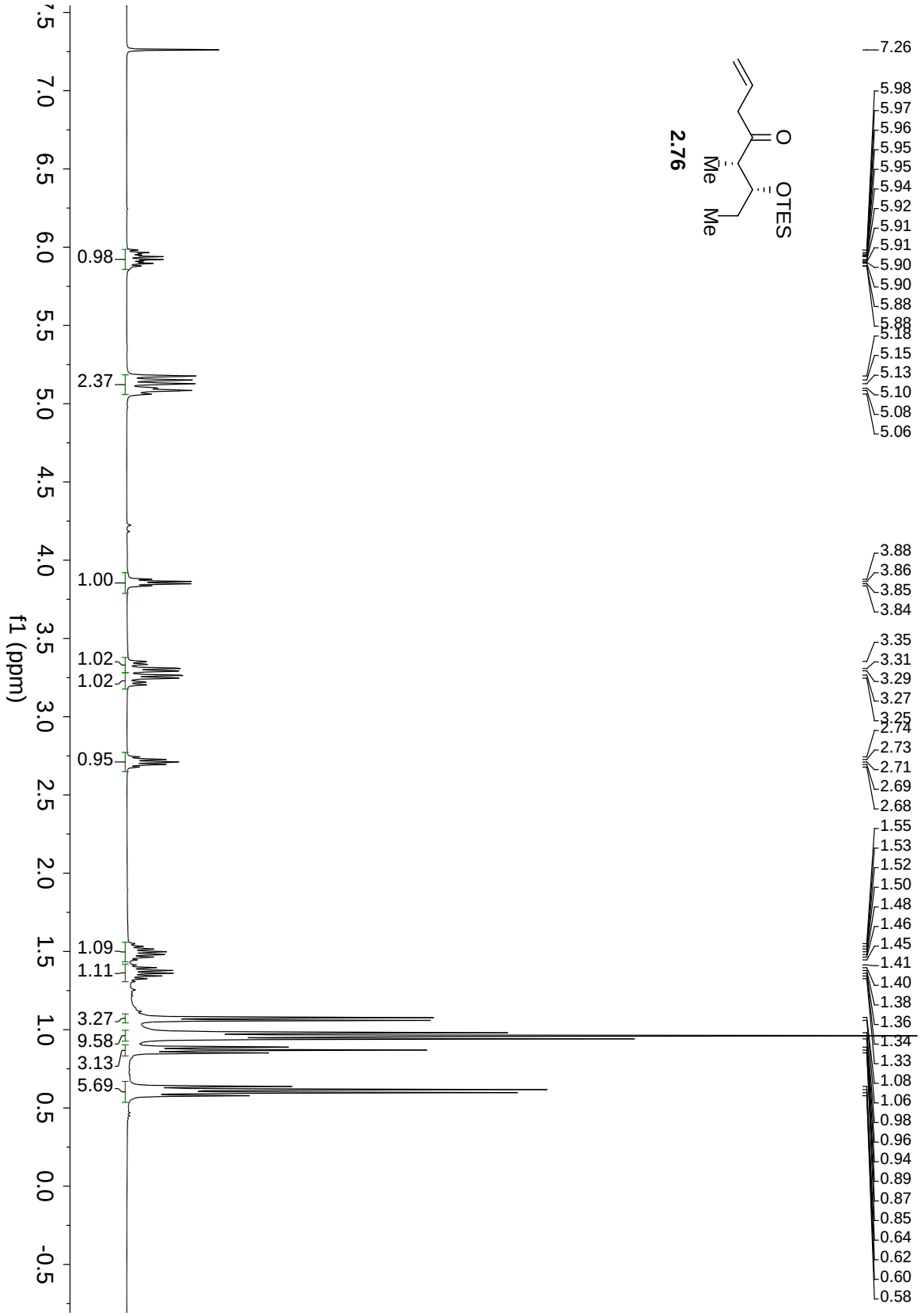
2.76
OTES
Me
Me
f1 (ppm)
0.98
2.37
1.00
1.02
1.02
0.95
1.09
1.11
3.27
9.58
3.13
5.69
7.26
5.98
5.97
5.96
5.95
5.95
5.94
5.92
5.91
5.91
5.91
5.90
5.90
5.88
5.88
5.18
5.15
5.13
5.10
5.08
5.06
3.88
3.86
3.85
3.84
3.35
3.31
3.29
3.27
3.25
2.74
2.73
2.71
2.69
2.68
1.55
1.53
1.52
1.50
1.48
1.46
1.45
1.41
1.40
1.38
1.36
1.34
1.33
1.08
1.06
0.98
0.96
0.94
0.89
0.87
0.85
0.64
0.62
0.60
0.58

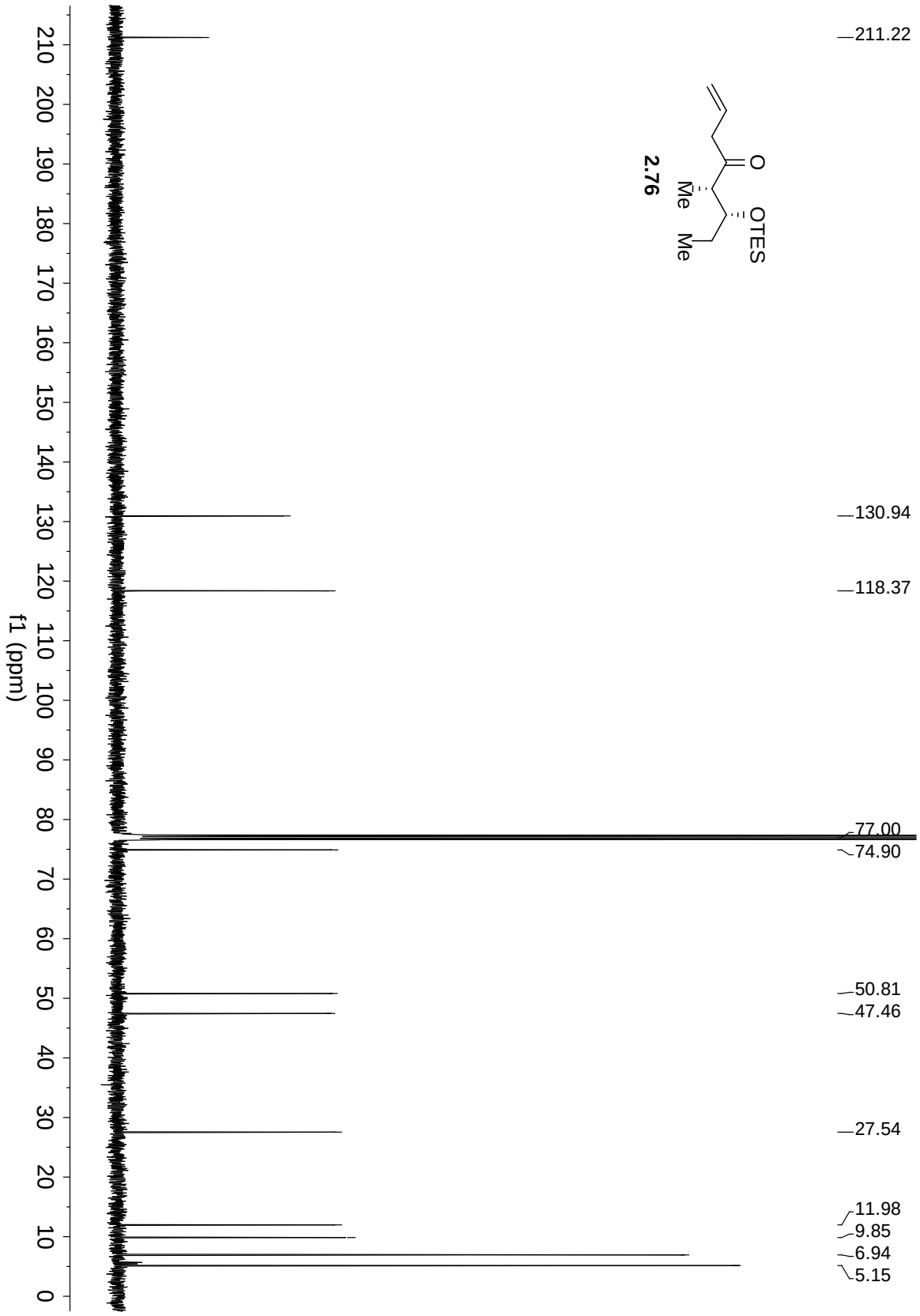
211.22
130.94
118.37
77.00
74.90
50.81
47.46
27.54
11.98
9.85
6.94
5.15
f1 (ppm)
O
OTES
Me
Me
2.76

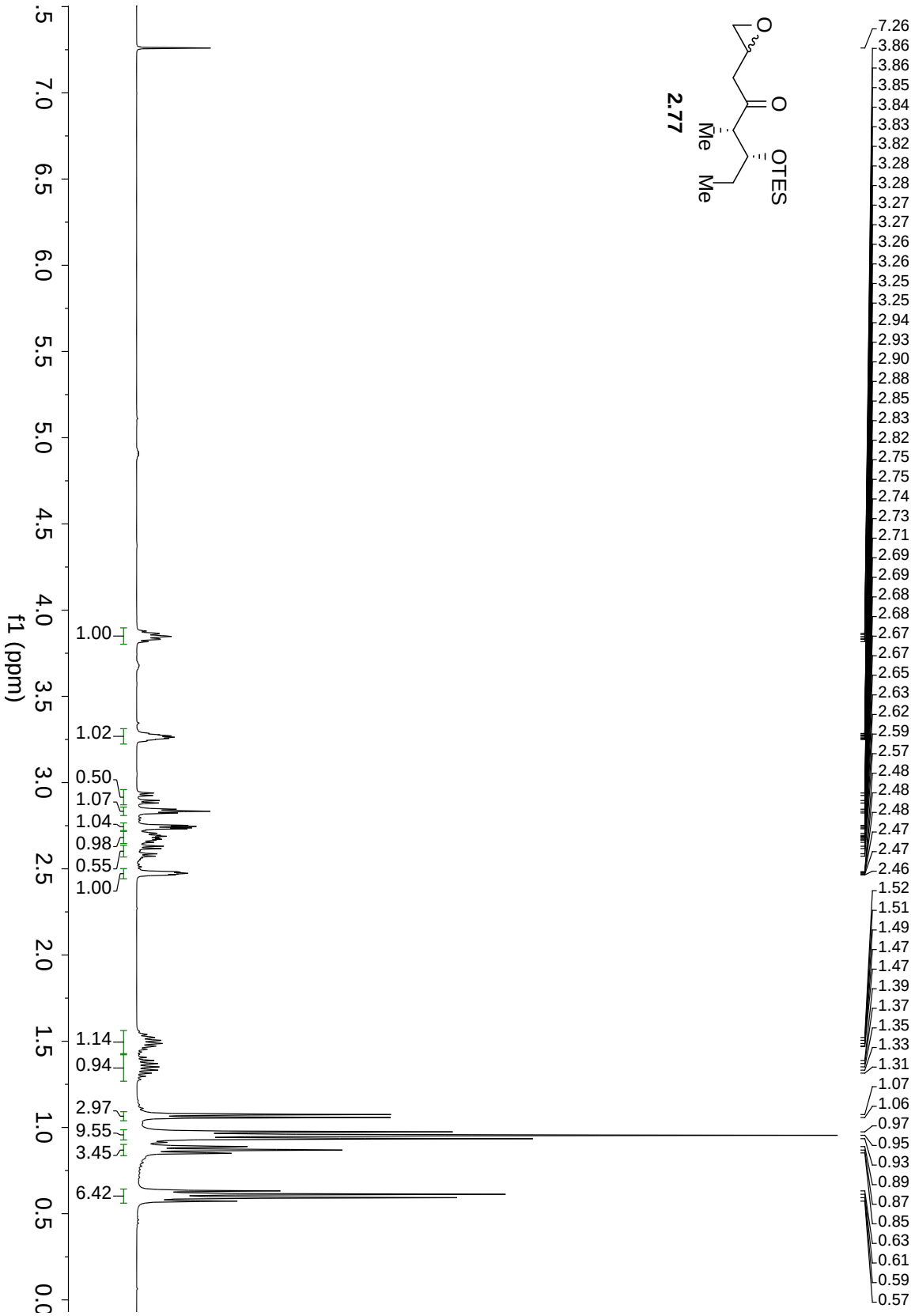
2.77
OTES
Me
Me
f1 (ppm)
1.00
1.02
0.50
1.07
1.04
0.98
0.55
1.00
1.14
0.94
2.97
9.55
3.45
6.42
7.26
3.86
3.86
3.85
3.84
3.83
3.82
3.28
3.28
3.27
3.27
3.26
3.26
3.25
3.25
2.94
2.93
2.90
2.88
2.85
2.83
2.82
2.75
2.75
2.74
2.73
2.71
2.69
2.69
2.68
2.68
2.67
2.67
2.65
2.63
2.62
2.59
2.57
2.48
2.48
2.48
2.47
2.47
2.46
1.52
1.51
1.49
1.47
1.47
1.39
1.37
1.35
1.33
1.31
1.07
1.06
0.97
0.95
0.93
0.89
0.87
0.85
0.63
0.61
0.59
0.57

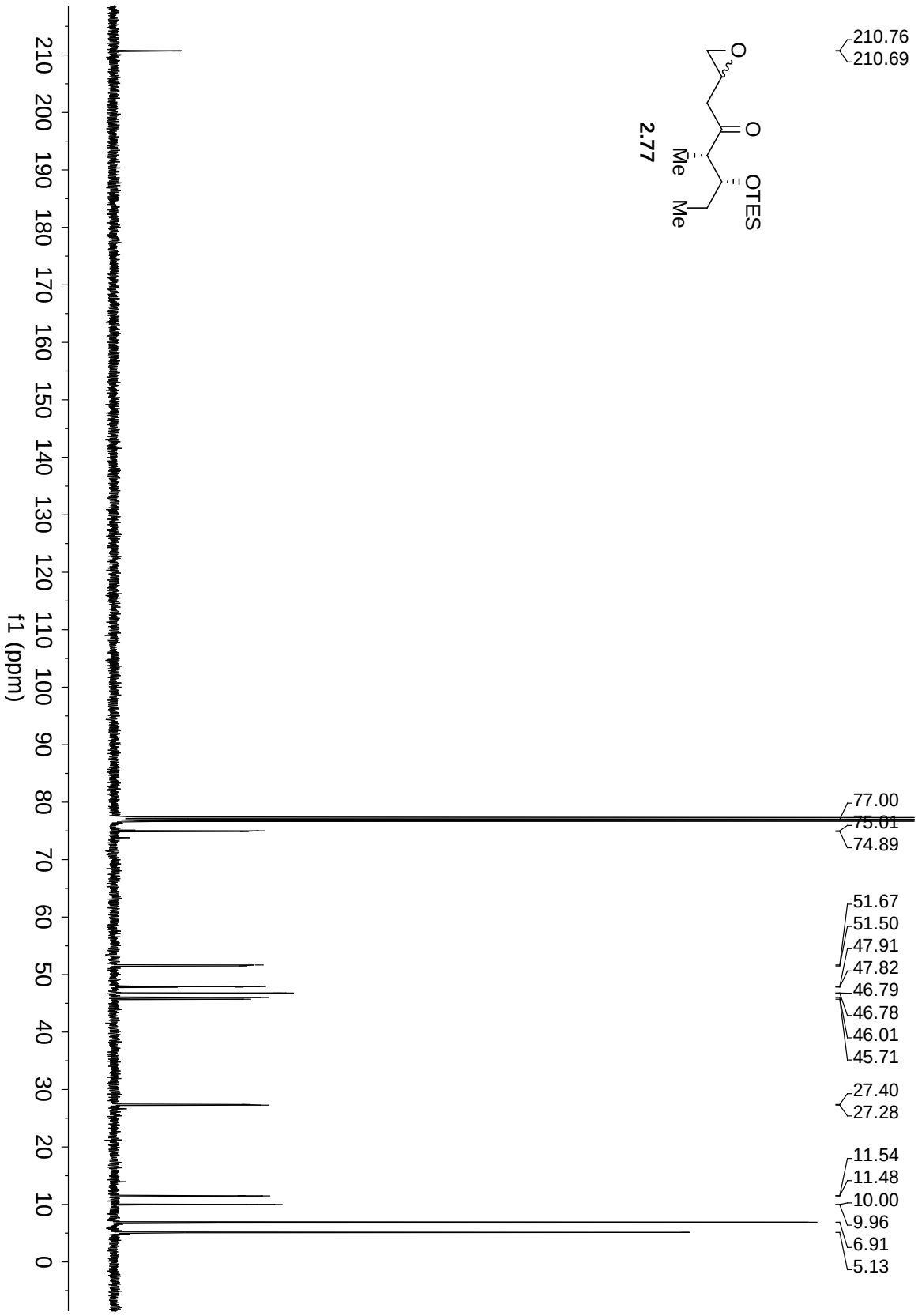
210.76
210.69
77.00
75.01
74.89
51.67
51.50
47.91
47.82
46.79
46.78
46.01
45.71
27.40
27.28
11.54
11.48
10.00
9.96
6.91
5.13
f1 (ppm)
2.77

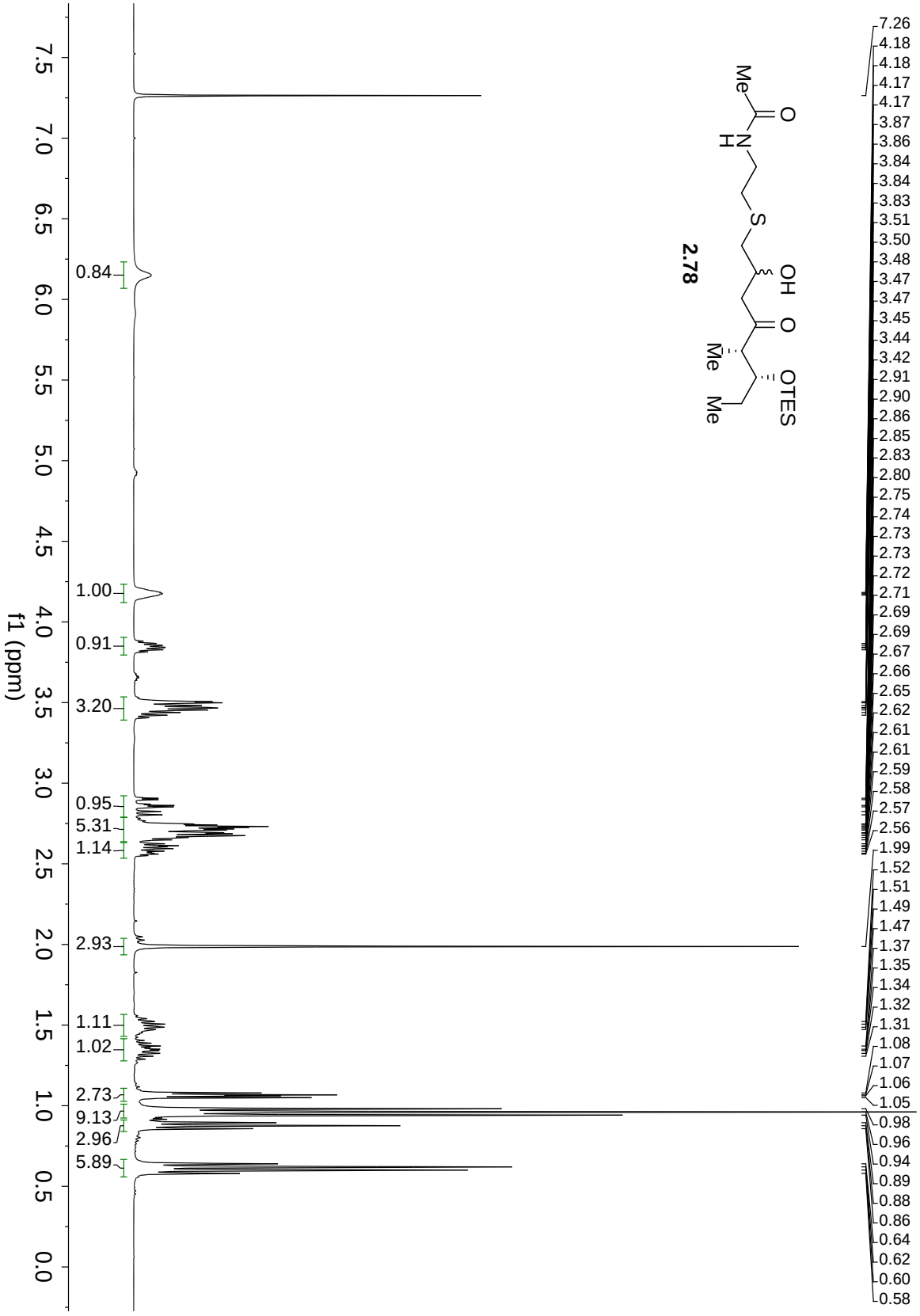
f1 (ppm)
7.5
7.0
6.5
6.0
5.5
5.0
4.5
4.0
3.5
3.0
2.5
2.0
1.5
1.0
0.5
0.0
0.84
1.00
0.91
3.20
0.95
5.31
1.14
2.93
1.11
1.02
2.73
9.13
2.96
5.89
Me
O
N
H
S
OH
O
OTES
Me
Me
2.78
7.26
4.18
4.18
4.17
4.17
3.87
3.86
3.84
3.84
3.83
3.51
3.50
3.48
3.47
3.47
3.45
3.44
3.42
2.91
2.90
2.86
2.85
2.83
2.80
2.75
2.74
2.73
2.73
2.72
2.71
2.69
2.69
2.67
2.66
2.65
2.62
2.61
2.61
2.59
2.58
2.57
2.56
1.99
1.52
1.51
1.49
1.47
1.37
1.35
1.34
1.32
1.31
1.08
1.07
1.06
1.05
0.98
0.96
0.94
0.89
0.88
0.86
0.64
0.62
0.60
0.58

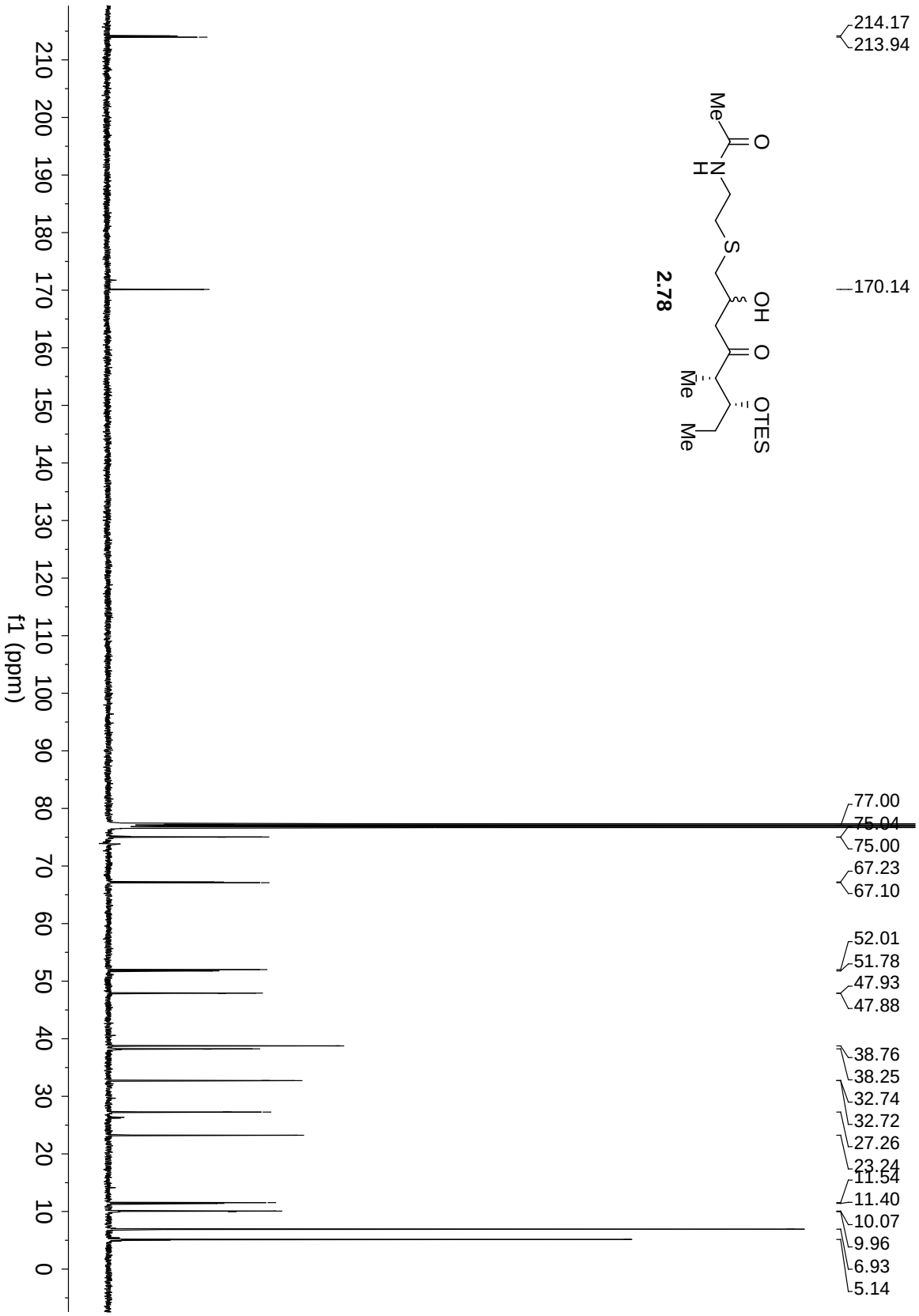
214.17
213.94
170.14
77.00
75.04
75.00
67.23
67.10
52.01
51.78
47.93
47.88
38.76
38.25
32.74
32.72
27.26
23.24
11.54
11.40
10.07
9.96
6.93
5.14
f1 (ppm)
2.78

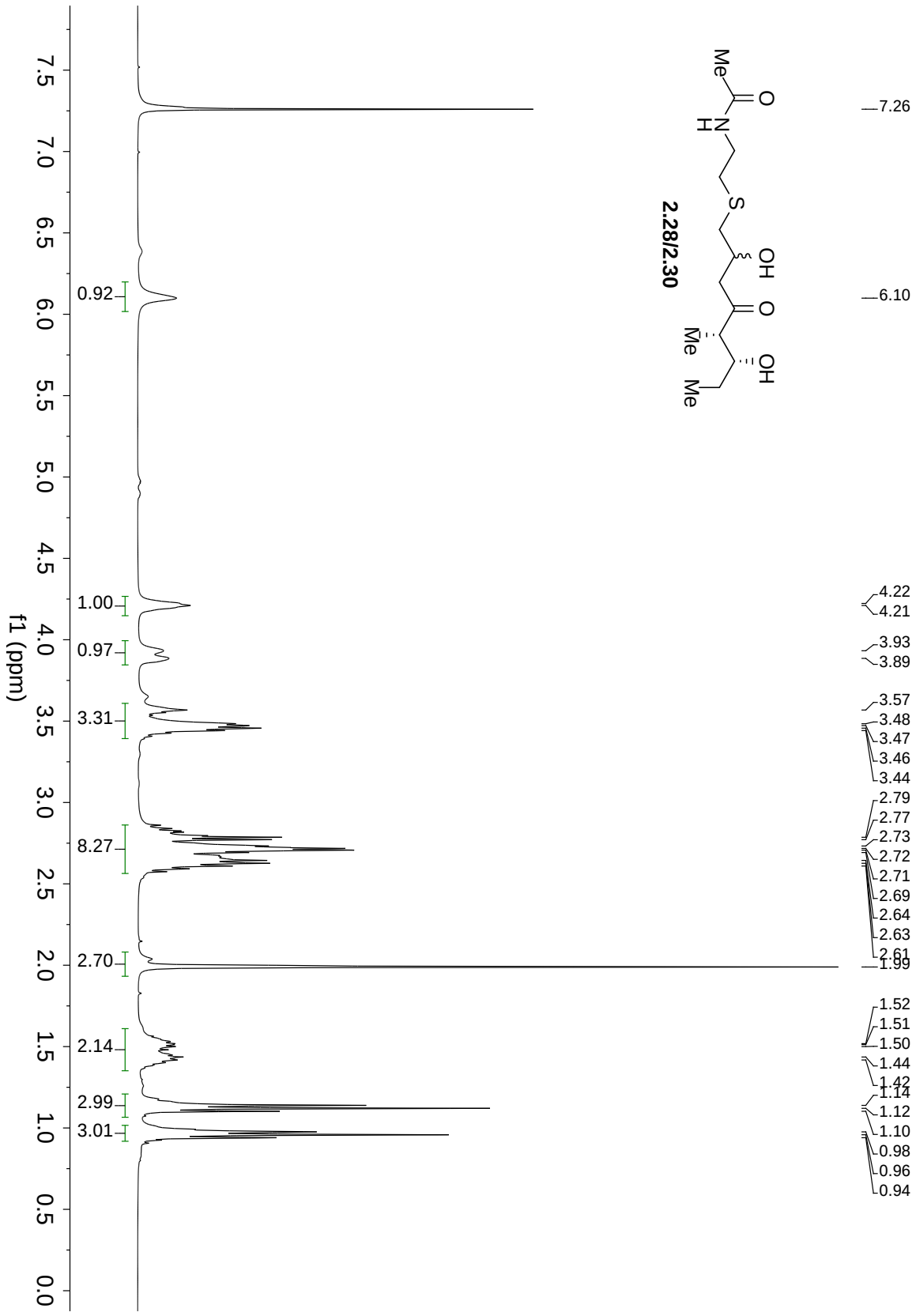
f1 (ppm)
7.5
7.0
6.5
6.0
5.5
5.0
4.5
4.0
3.5
3.0
2.5
2.0
1.5
1.0
0.5
0.0
0.92
1.00
0.97
3.31
8.27
2.70
2.14
2.99
3.01
2.28/2.30
Me
O
N
H
S
OH
O
OH
Me
Me
7.26
6.10
4.22
4.21
3.93
3.89
3.57
3.48
3.47
3.46
3.44
2.79
2.77
2.73
2.72
2.71
2.69
2.64
2.63
2.61
1.99
1.52
1.51
1.50
1.44
1.42
1.14
1.12
1.10
0.98
0.96
0.94

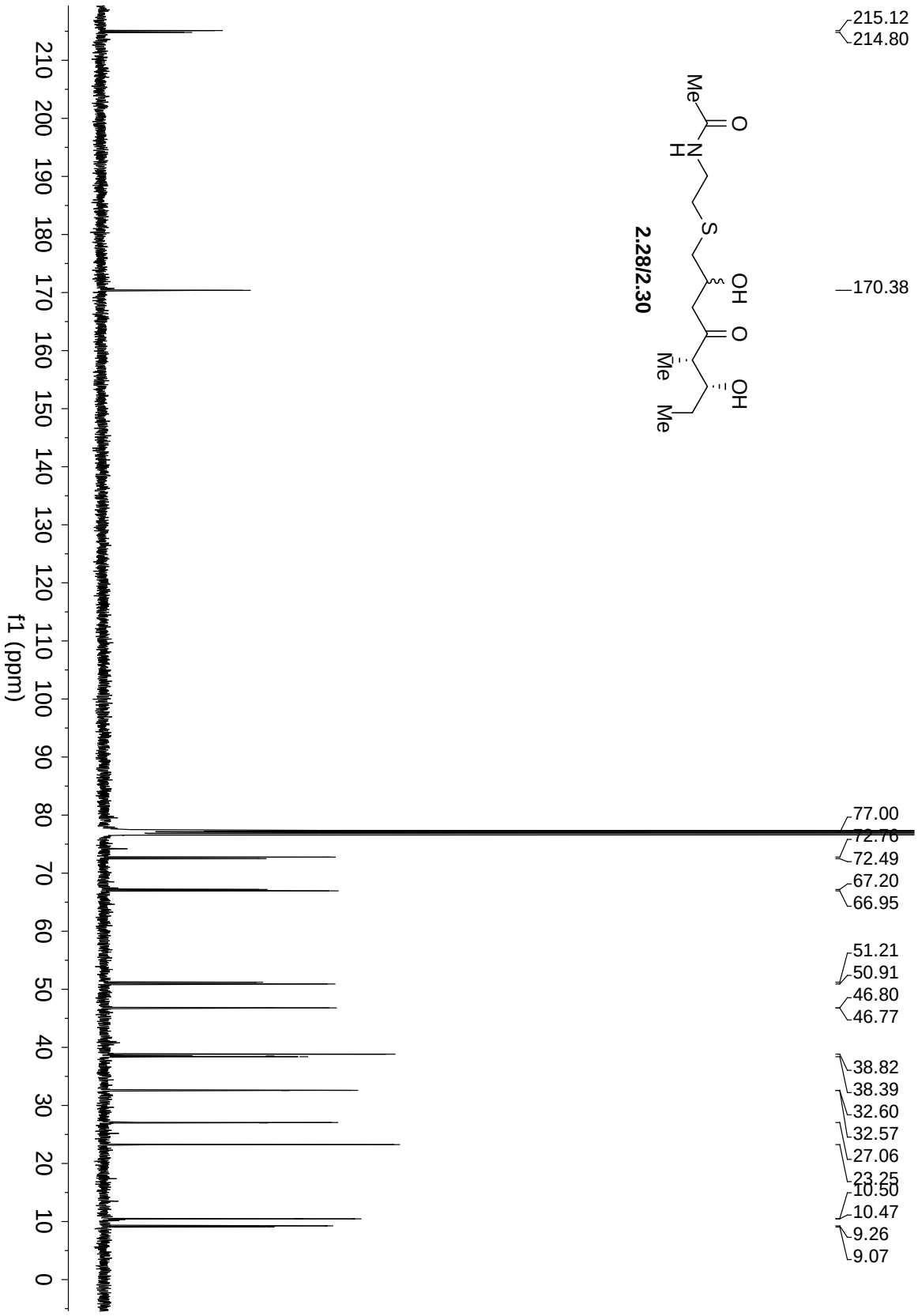
215.12
214.80
170.38
77.00
72.76
72.49
67.20
66.95
51.21
50.91
46.80
46.77
38.82
38.39
32.60
32.57
27.06
23.25
10.50
10.47
9.26
9.07
f1 (ppm)
2.28/2.30

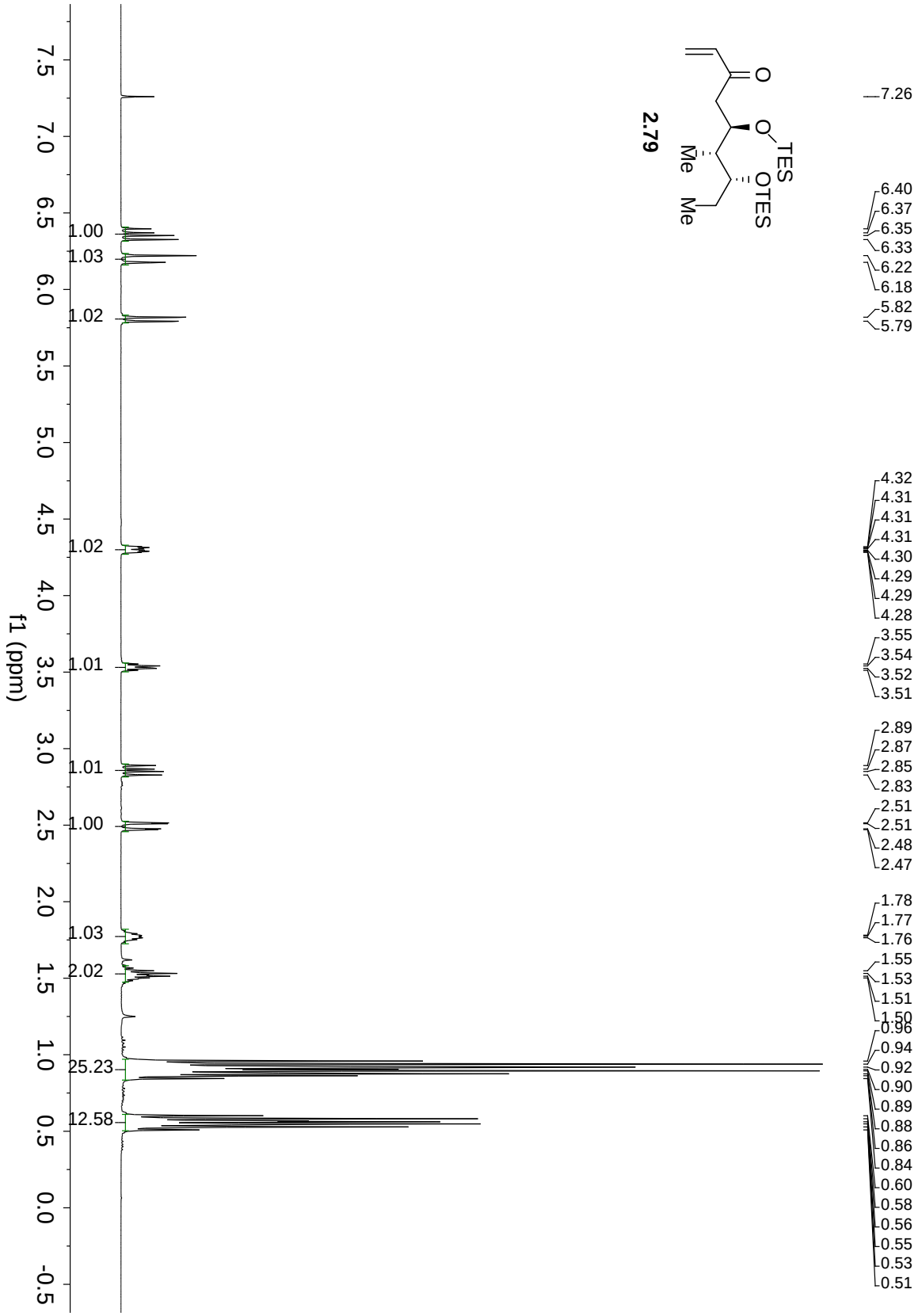
2.79
TES
OTES
Me
Me
7.26
6.40
6.37
6.35
6.33
6.22
6.18
5.82
5.79
4.32
4.31
4.31
4.31
4.30
4.29
4.29
4.28
3.55
3.54
3.52
3.51
2.89
2.87
2.85
2.83
2.51
2.51
2.48
2.47
1.78
1.77
1.76
1.55
1.53
1.51
1.50
0.96
0.94
0.92
0.90
0.89
0.88
0.86
0.84
0.60
0.58
0.56
0.55
0.53
0.51
1.00
1.03
1.02
1.02
1.01
1.01
1.00
1.03
2.02
25.23
12.58
f1 (ppm)
7.5
7.0
6.5
6.0
5.5
5.0
4.5
4.0
3.5
3.0
2.5
2.0
1.5
1.0
0.5
0.0
-0.5

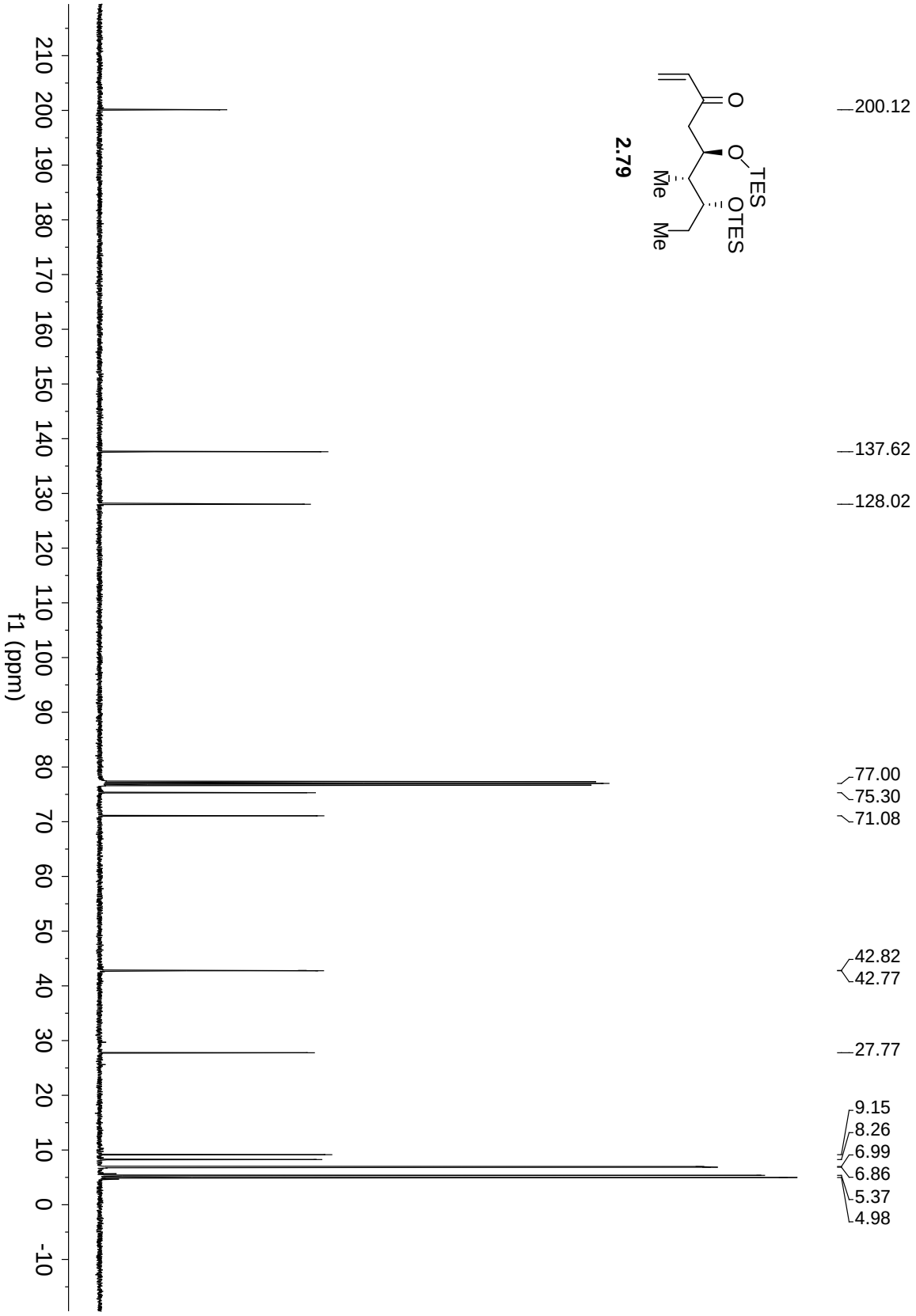
200.12
137.62
128.02
77.00
75.30
71.08
42.82
42.77
27.77
9.15
8.26
6.99
6.86
5.37
4.98
f1 (ppm)
210 200 190 180 170 160 150 140 130 120 110 100 90 80 70 60 50 40 30 20 10 0 -10
O
O
TES
OTES
Me
Me
2.79

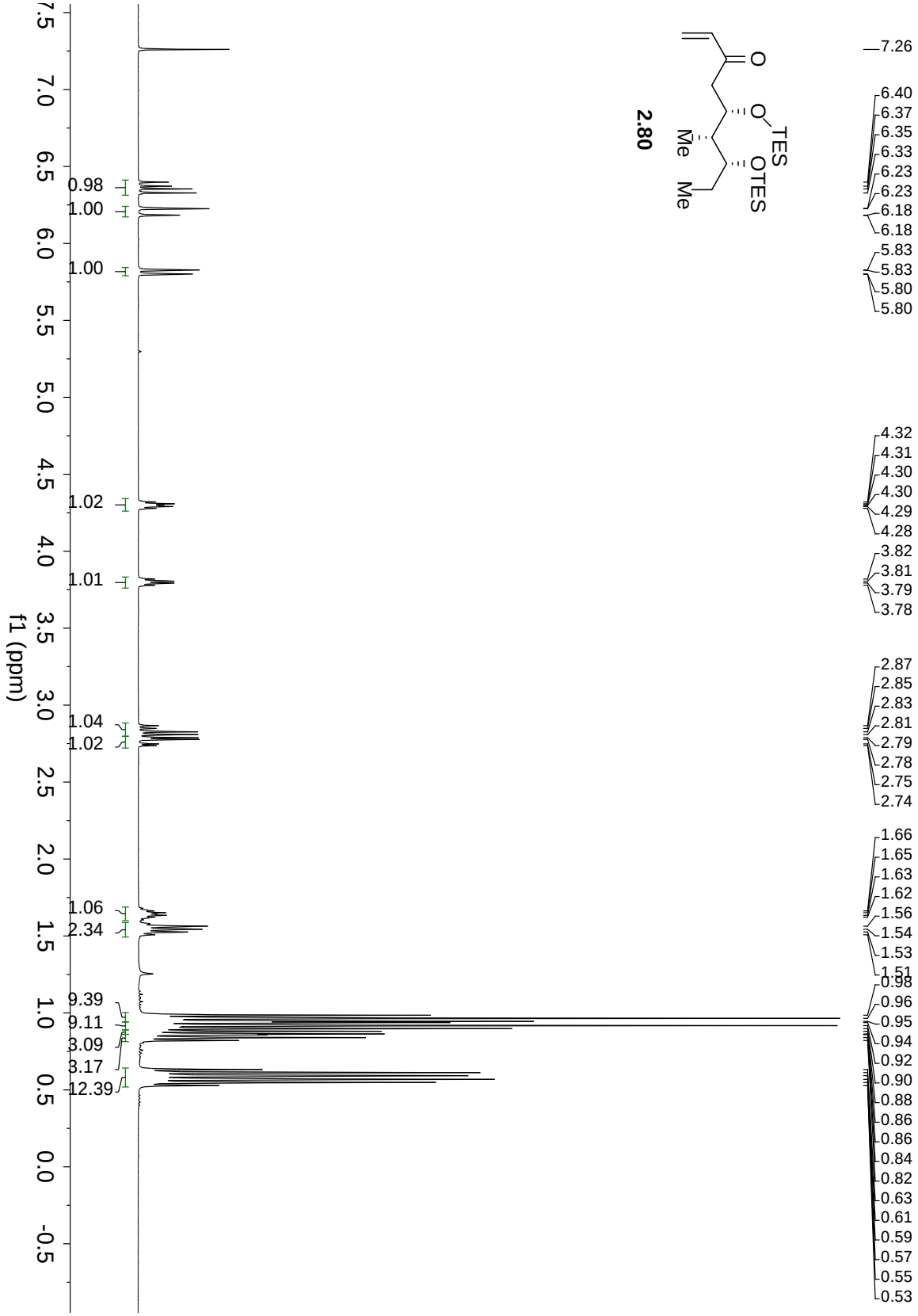
2.80
TES
OTES
Me
Me
f1 (ppm)
7.5
7.0
6.5
6.0
5.5
5.0
4.5
4.0
3.5
3.0
2.5
2.0
1.5
1.0
0.5
0.0
-0.5
0.98
1.00
1.00
1.02
1.01
1.04
1.02
1.06
2.34
9.39
9.11
3.09
3.17
12.39
7.26
6.40
6.37
6.35
6.33
6.23
6.23
6.18
6.18
5.83
5.83
5.80
5.80
4.32
4.31
4.30
4.30
4.29
4.28
3.82
3.81
3.79
3.78
2.87
2.85
2.83
2.81
2.79
2.78
2.75
2.74
1.66
1.65
1.63
1.62
1.56
1.54
1.53
1.51
0.98
0.96
0.95
0.94
0.92
0.90
0.88
0.86
0.86
0.84
0.82
0.63
0.61
0.59
0.57
0.55
0.53

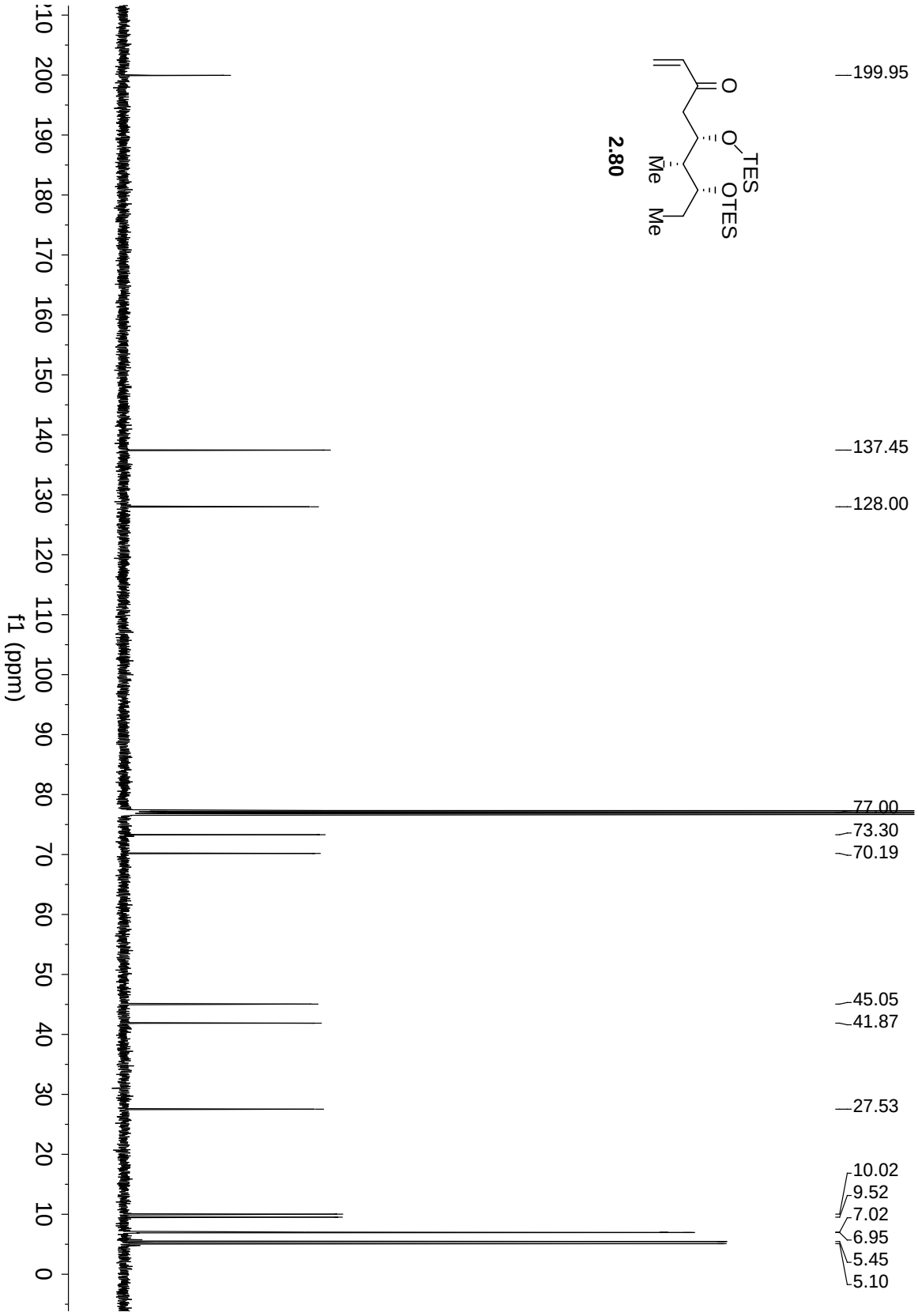
2.80
O
O
TES
OTES
Me
Me
199.95
137.45
128.00
77.00
73.30
70.19
45.05
41.87
27.53
10.02
9.52
7.02
6.95
5.45
5.10
f1 (ppm)

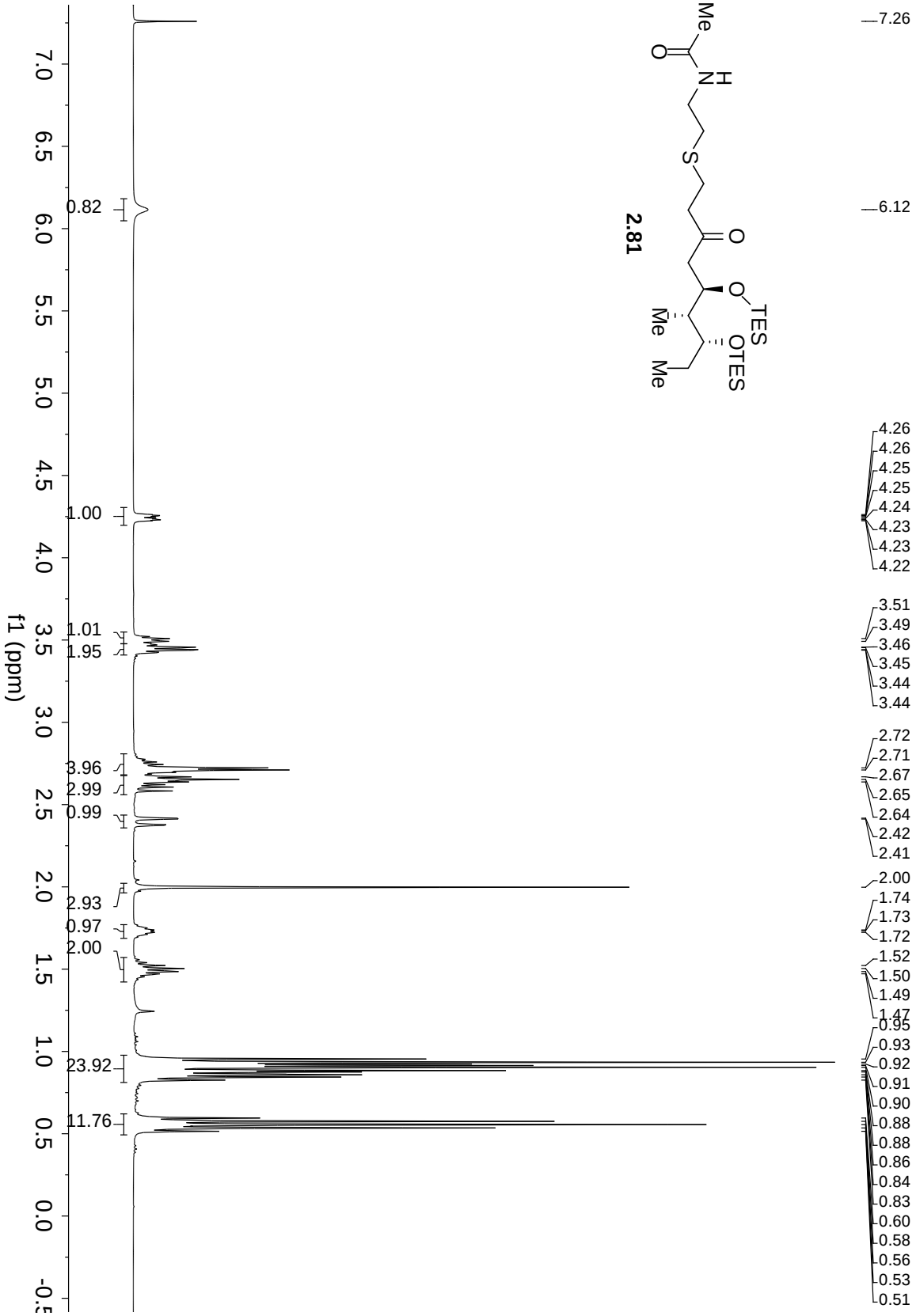
2.81
f1 (ppm)
0.82
1.00
1.01
1.95
3.96
2.99
0.99
2.93
0.97
2.00
23.92
11.76
7.26
6.12
4.26
4.26
4.25
4.25
4.24
4.23
4.23
4.22
3.51
3.49
3.46
3.45
3.44
3.44
2.72
2.71
2.67
2.65
2.64
2.42
2.41
2.00
1.74
1.73
1.72
1.52
1.50
1.49
1.47
0.95
0.93
0.92
0.91
0.90
0.88
0.88
0.86
0.84
0.83
0.60
0.58
0.56
0.53
0.51

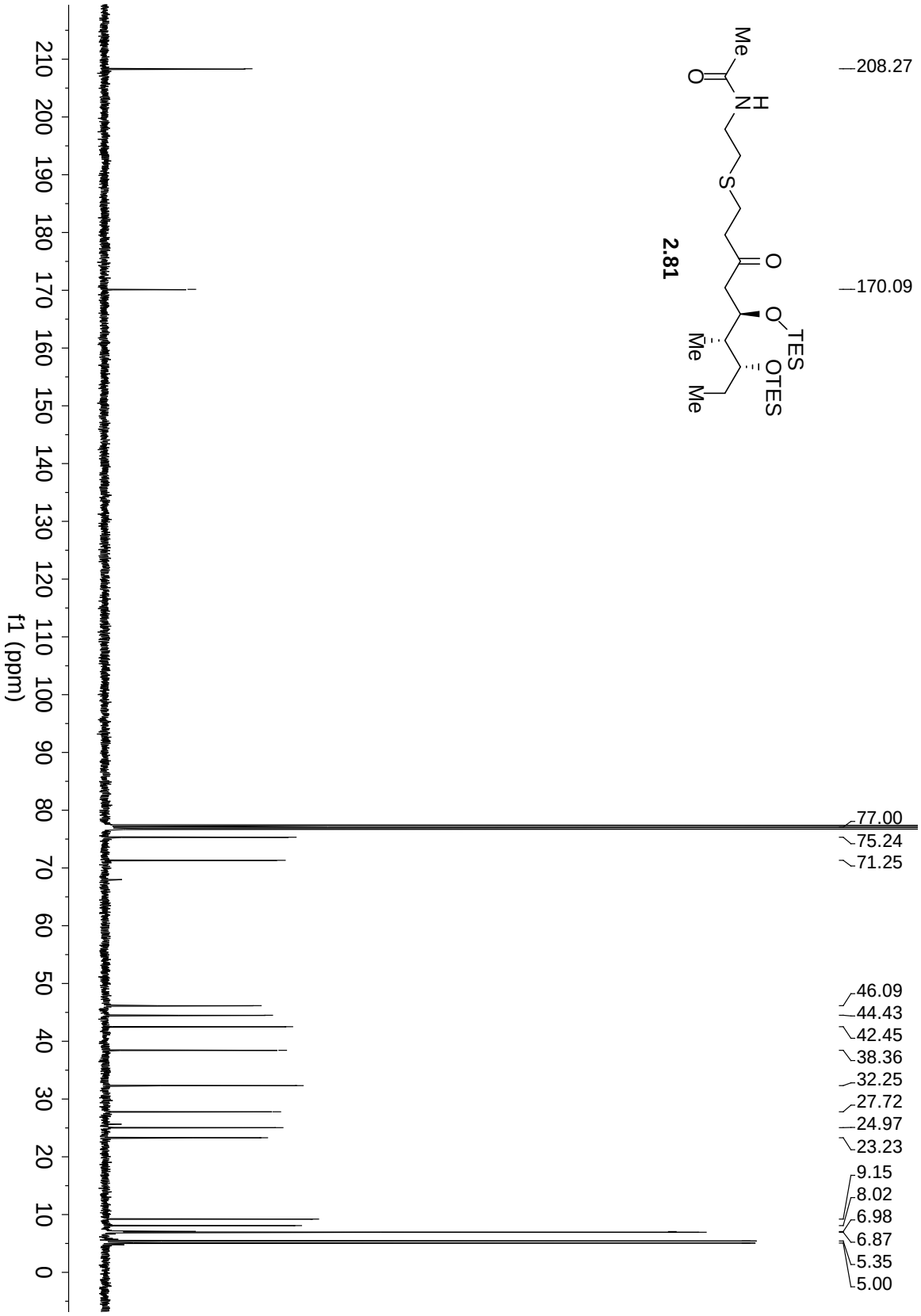
2.81
208.27
170.09
77.00
75.24
71.25
46.09
44.43
42.45
38.36
32.25
27.72
24.97
23.23
9.15
8.02
6.98
6.87
5.35
5.00
f1 (ppm)

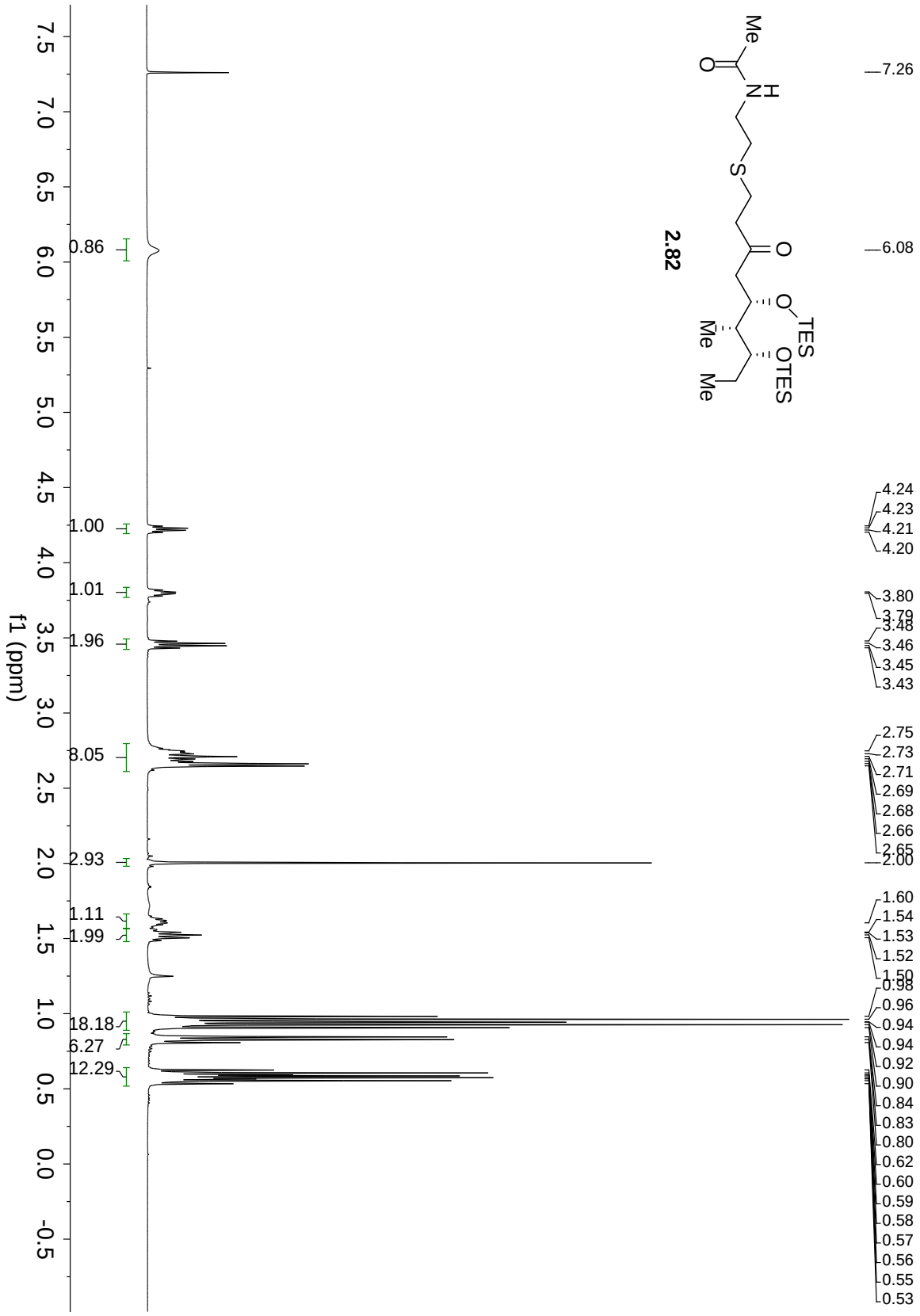
f1 (ppm)
7.5
7.0
6.5
6.0
5.5
5.0
4.5
4.0
3.5
3.0
2.5
2.0
1.5
1.0
0.5
0.0
-0.5
0.86
1.00
1.01
1.96
8.05
2.93
1.11
1.99
18.18
6.27
12.29
Me
O
H
N
S
O
O
TES
OTES
Me
Me
2.82
7.26
6.08
4.24
4.23
4.21
4.20
3.80
3.79
3.48
3.46
3.45
3.43
2.75
2.73
2.71
2.69
2.68
2.66
2.65
2.00
1.60
1.54
1.53
1.52
1.50
0.98
0.96
0.94
0.94
0.92
0.90
0.84
0.83
0.80
0.62
0.60
0.59
0.58
0.57
0.56
0.55
0.53

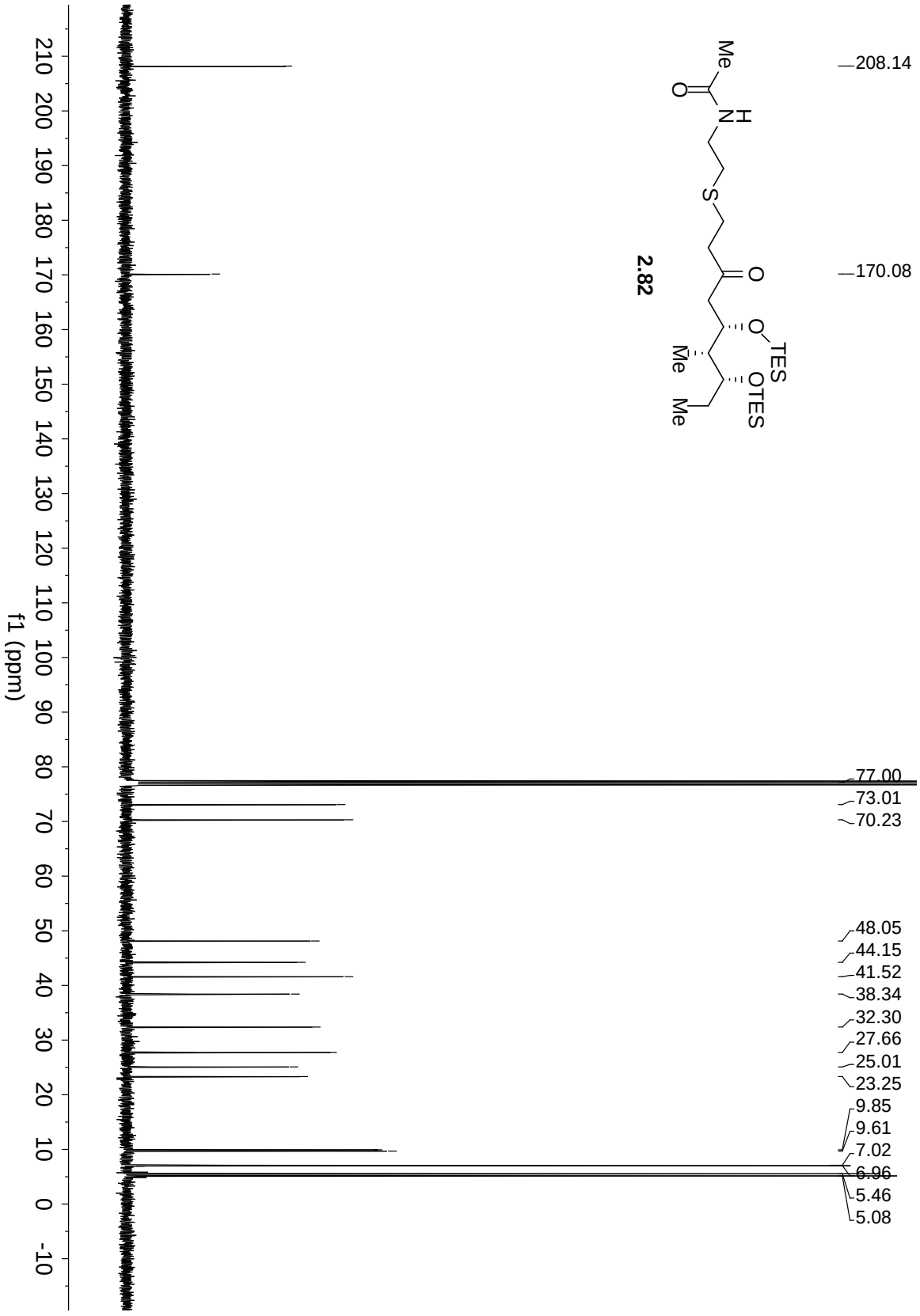
f1 (ppm)
210 200 190 180 170 160 150 140 130 120 110 100 90 80 70 60 50 40 30 20 10 0 -10
Me
O
N
H
S
O
O
TES
Me
Me
OTES
2.82
208.14
170.08
77.00
73.01
70.23
48.05
44.15
41.52
38.34
32.30
27.66
25.01
23.25
9.85
9.61
7.02
6.96
5.46
5.08

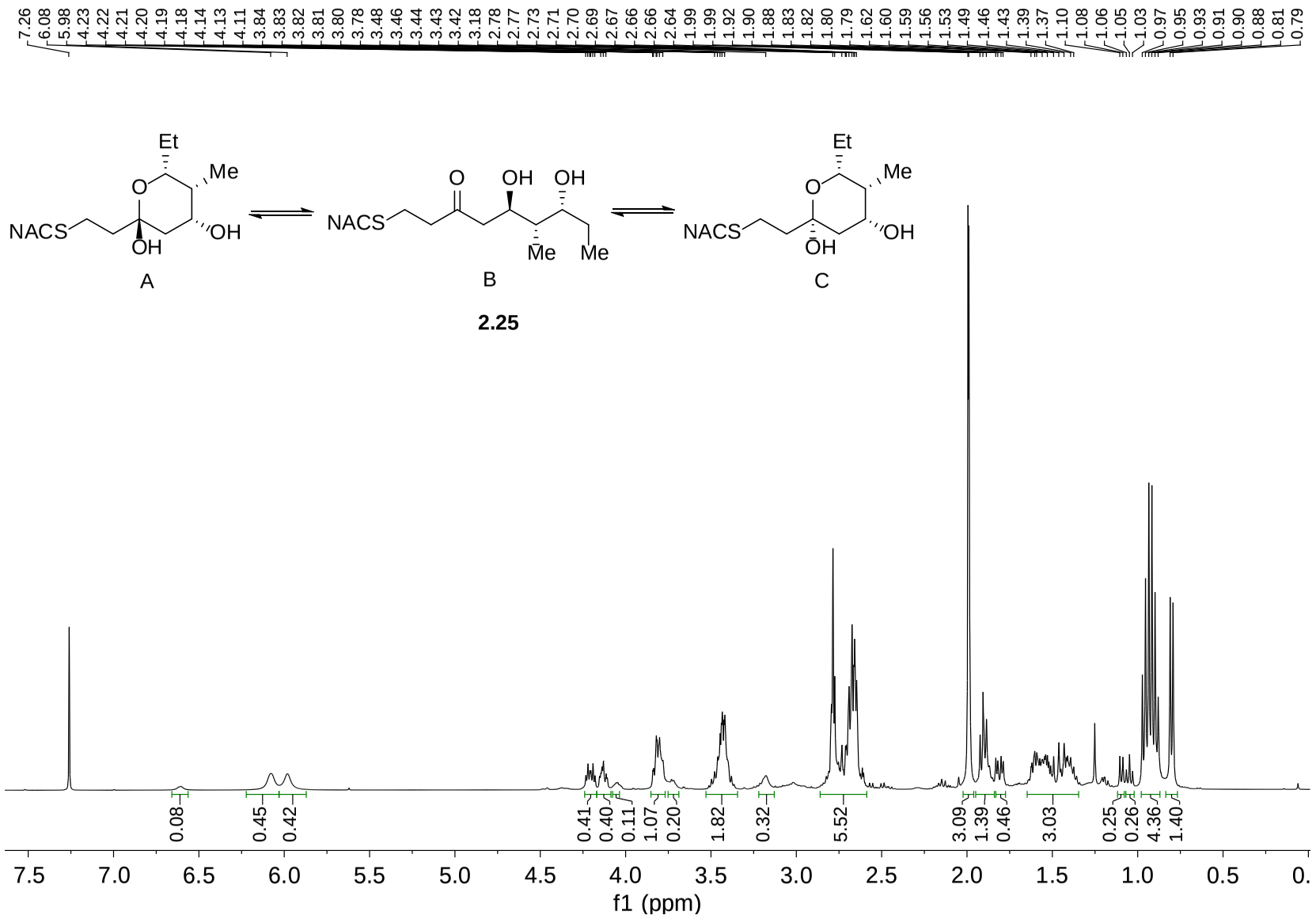
7.26 6.08 5.98 4.23 4.22 4.21 4.20 4.19 4.18 4.14 4.13 4.11 3.84 3.83 3.82 3.81 3.80 3.78 3.48 3.46 3.44 3.43 3.42 3.18 2.78 2.77 2.73 2.71 2.70 2.69 2.67 2.66 2.66 2.64 1.99 1.99 1.92 1.90 1.88 1.83 1.82 1.80 1.79 1.62 1.60 1.59 1.56 1.53 1.49 1.46 1.43 1.39 1.37 1.10 1.08 1.06 1.05 1.03 0.97 0.95 0.93 0.91 0.90 0.88 0.81 0.79
Et
Me
O
OH
NACS
OH
A
O
OH
OH
NACS
Me
Me
B
Et
Me
O
OH
NACS
OH
C
2.25
0.08 0.45 0.42 0.41 0.40 0.11 1.07 0.20 1.82 0.32 5.52 3.09 1.39 0.46 3.03 0.25 0.26 4.36 1.40
7.5 7.0 6.5 6.0 5.5 5.0 4.5 4.0 3.5 3.0 2.5 2.0 1.5 1.0 0.5 0.
f1 (ppm)

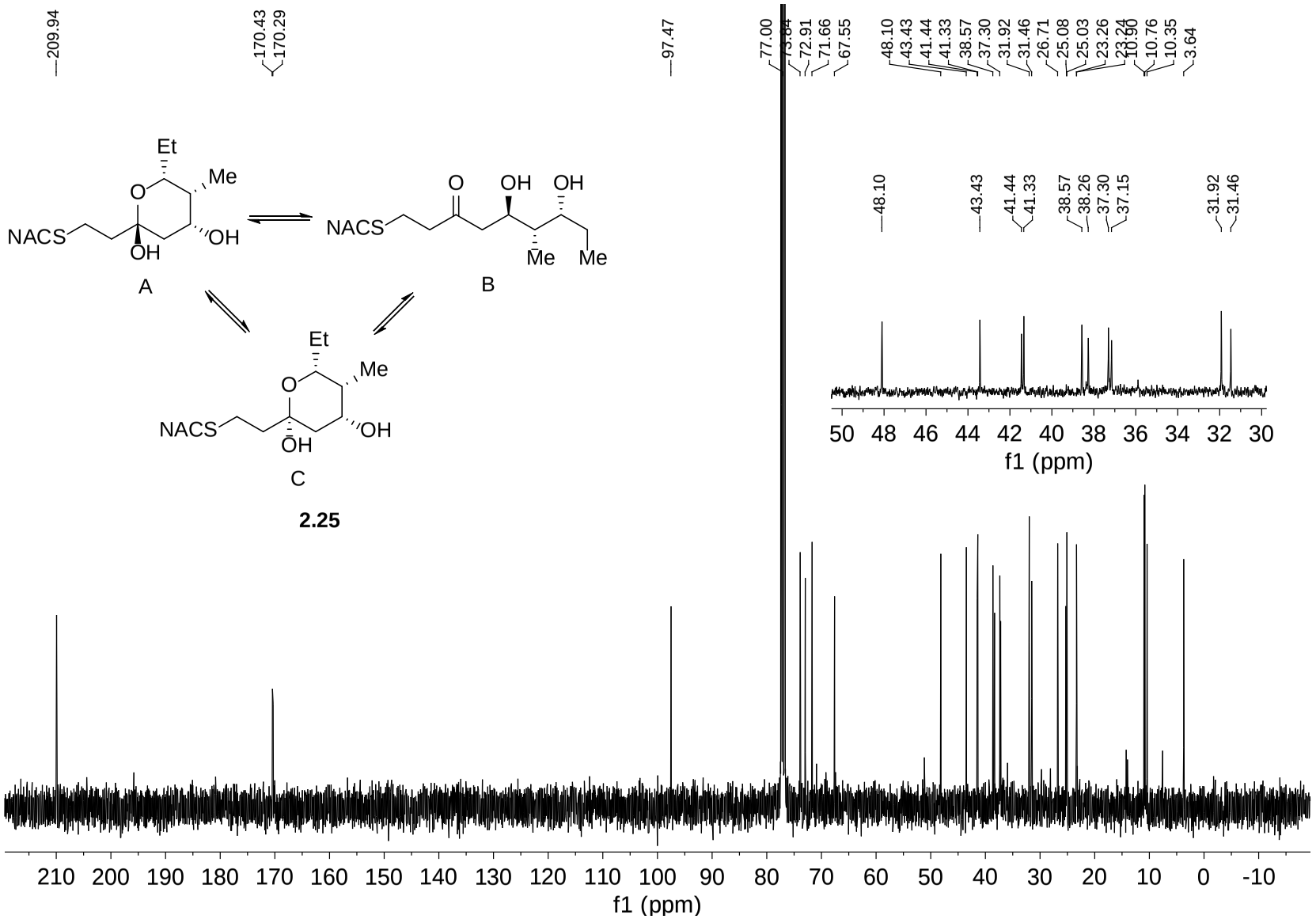
209.94
170.43
170.29
97.47
77.00
73.84
72.91
71.66
67.55
48.10
43.43
41.44
41.33
38.57
37.30
31.92
31.46
26.71
25.08
25.03
23.26
23.24
10.90
10.76
10.35
3.64
Et
Me
O
OH
NACS
OH
A
O
OH
OH
NACS
Me
Me
B
Et
Me
O
NACS
OH
OH
C
2.25
48.10
43.43
41.44
41.33
38.57
38.26
37.30
37.15
31.92
31.46
50 48 46 44 42 40 38 36 34 32 30
f1 (ppm)
210 200 190 180 170 160 150 140 130 120 110 100 90 80 70 60 50 40 30 20 10 0 -10
f1 (ppm)

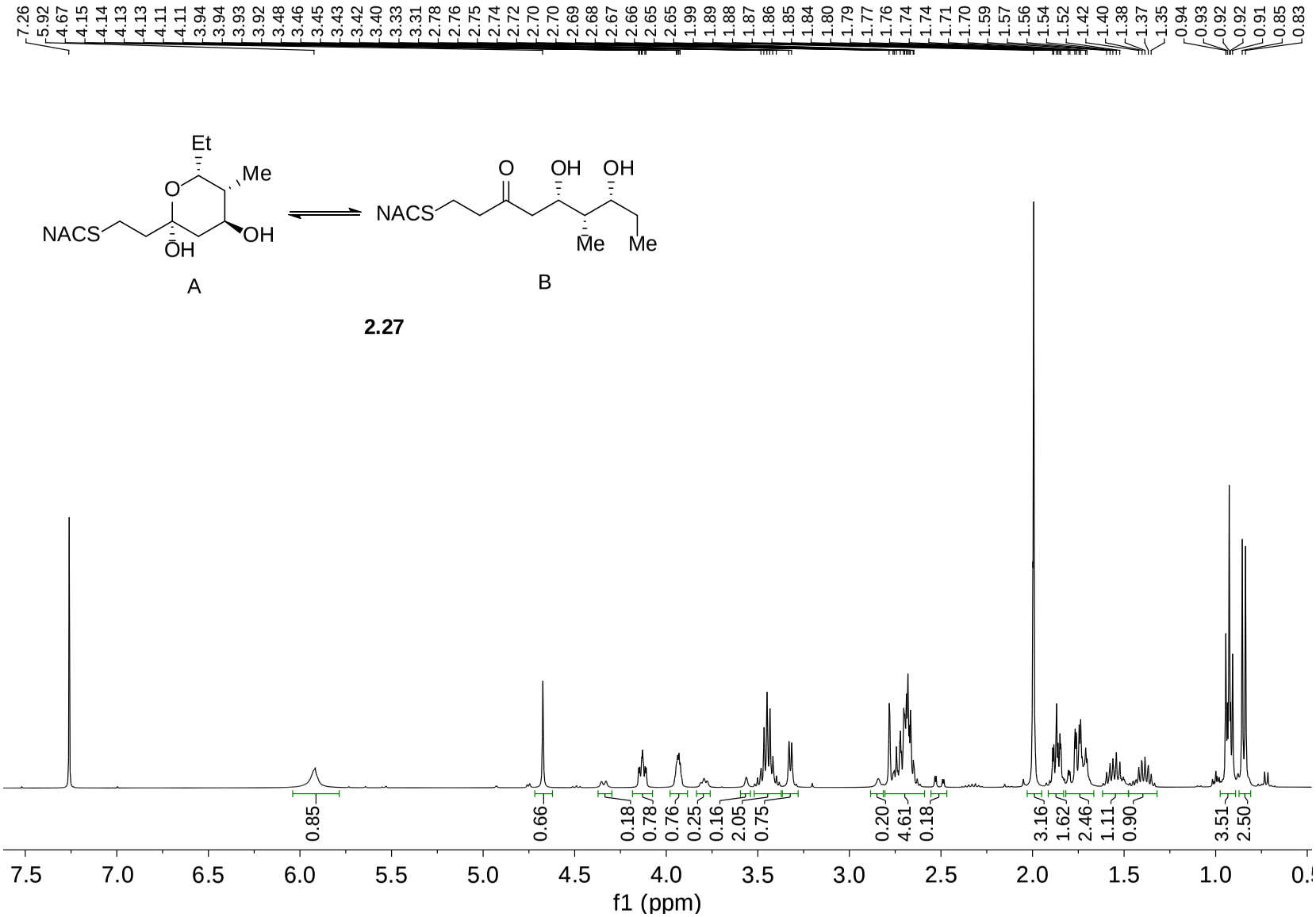
7.26 5.92 4.67 4.15 4.14 4.13 4.13 4.11 4.11 3.94 3.94 3.93 3.92 3.48 3.46 3.45 3.43 3.42 3.40 3.33 3.31 2.78 2.76 2.75 2.74 2.72 2.70 2.70 2.69 2.68 2.67 2.66 2.65 2.65 1.99 1.89 1.88 1.87 1.86 1.85 1.84 1.80 1.79 1.77 1.76 1.74 1.74 1.71 1.70 1.59 1.57 1.56 1.54 1.52 1.42 1.40 1.38 1.37 1.35 0.94 0.93 0.92 0.92 0.91 0.85 0.83
Et
Me
O
NACS
OH
OH
A
O
OH
OH
NACS
Me
Me
B
2.27
0.85 0.66 0.18 0.78 0.76 0.25 0.16 2.05 0.75 0.20 4.61 0.18 3.16 1.62 2.46 1.11 0.90 3.51 2.50
7.5 7.0 6.5 6.0 5.5 5.0 4.5 4.0 3.5 3.0 2.5 2.0 1.5 1.0
f1 (ppm)

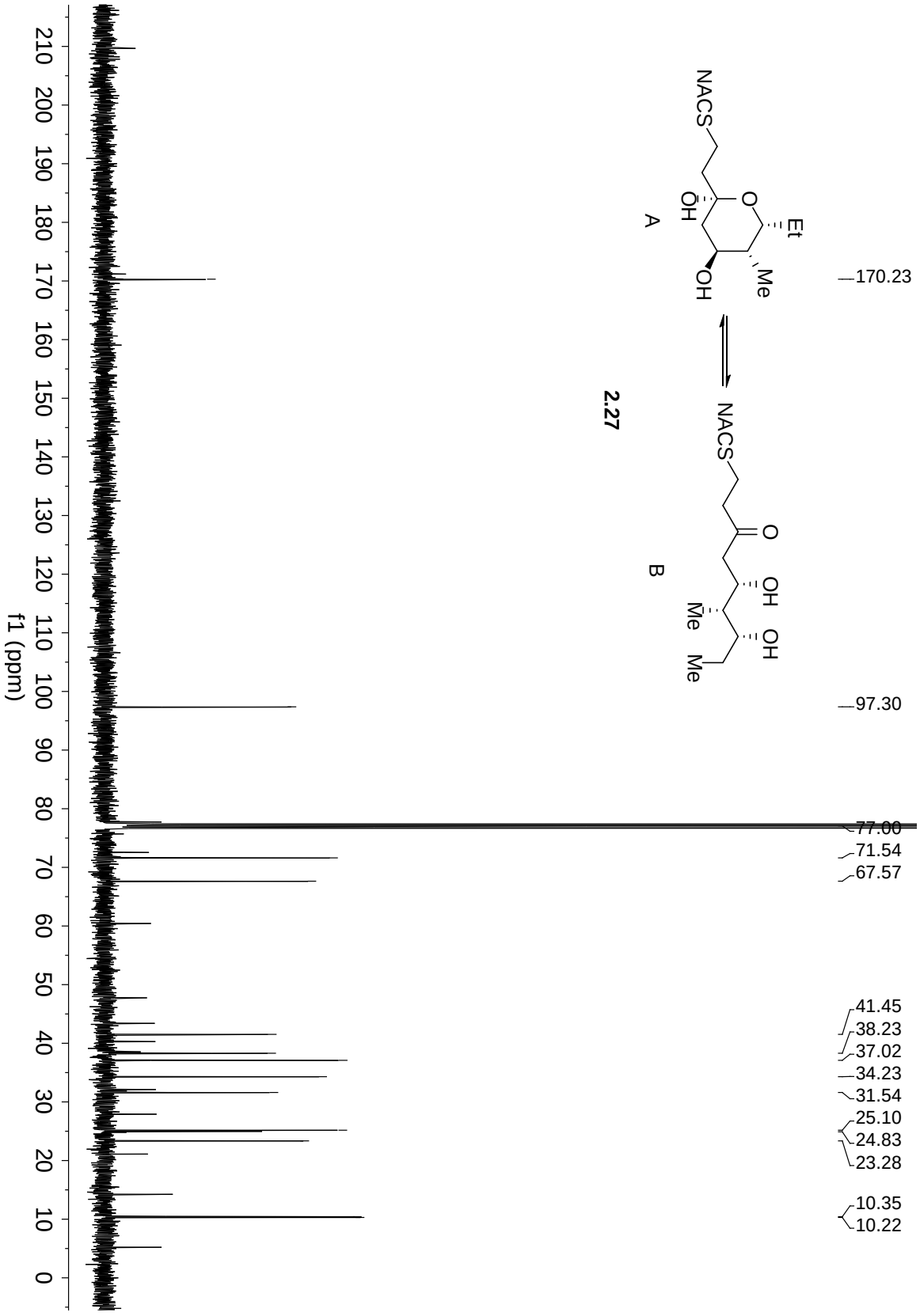
f1 (ppm)
210 200 190 180 170 160 150 140 130 120 110 100 90 80 70 60 50 40 30 20 10 0
NACS
OH
O
Et
Me
OH
A
2.27
NACS
O
OH OH
Me
Me
B
170.23
97.30
77.00
71.54
67.57
41.45
38.23
37.02
34.23
31.54
25.10
24.83
23.28
10.35
10.22

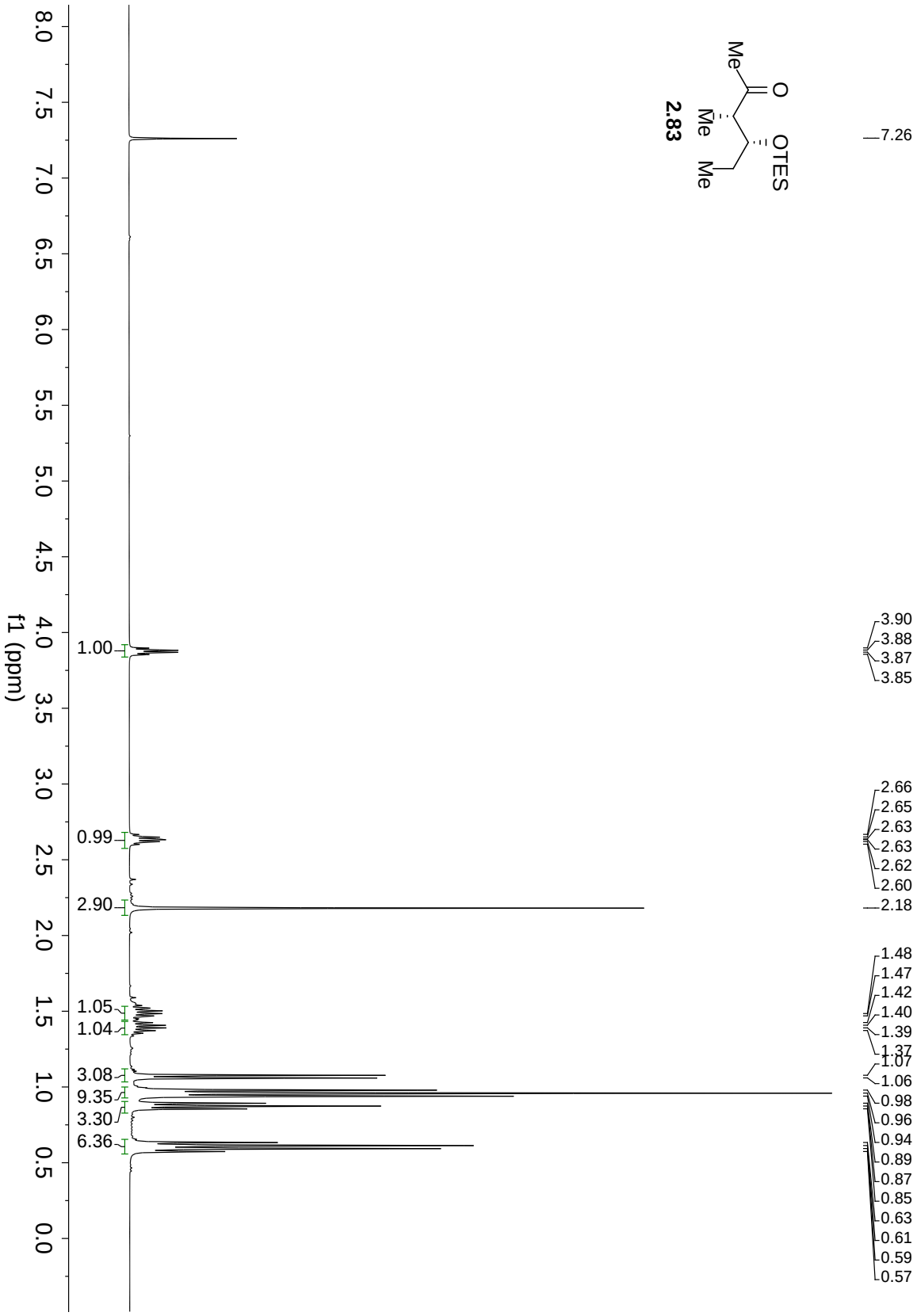
2.83
Me
O
OTES
Me
Me
f1 (ppm)
8.0
7.5
7.0
6.5
6.0
5.5
5.0
4.5
4.0
3.5
3.0
2.5
2.0
1.5
1.0
0.5
0.0
1.00
0.99
2.90
1.05
1.04
3.08
9.35
3.30
6.36
7.26
3.90
3.88
3.87
3.85
2.66
2.65
2.63
2.63
2.62
2.60
2.18
1.48
1.47
1.42
1.40
1.39
1.37
1.07
1.06
0.98
0.96
0.94
0.89
0.87
0.85
0.63
0.61
0.59
0.57

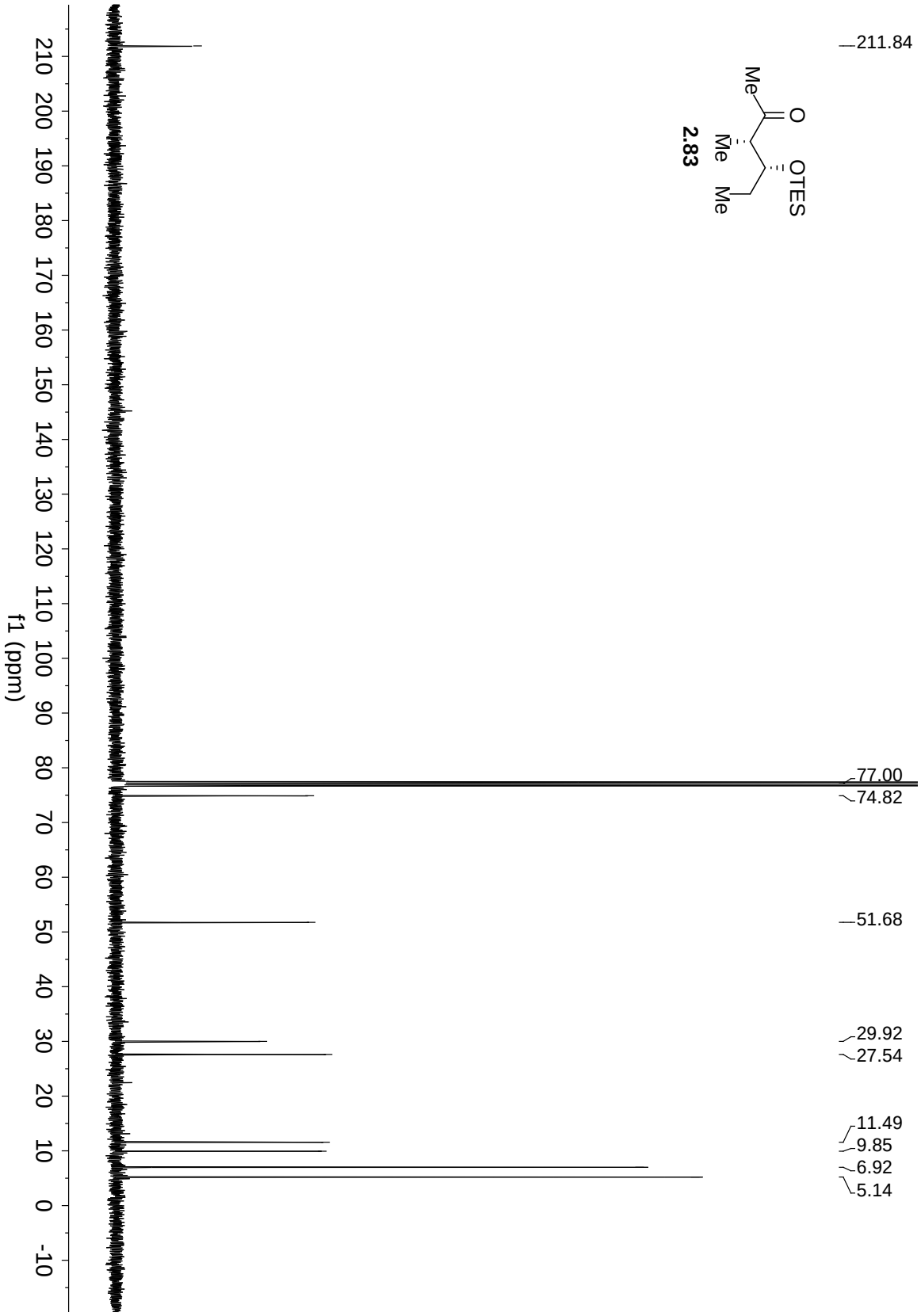
211.84
77.00
74.82
51.68
29.92
27.54
11.49
9.85
6.92
5.14
f1 (ppm)
210 200 190 180 170 160 150 140 130 120 110 100 90 80 70 60 50 40 30 20 10 0 -10
Me
O
OTES
Me
Me
2.83

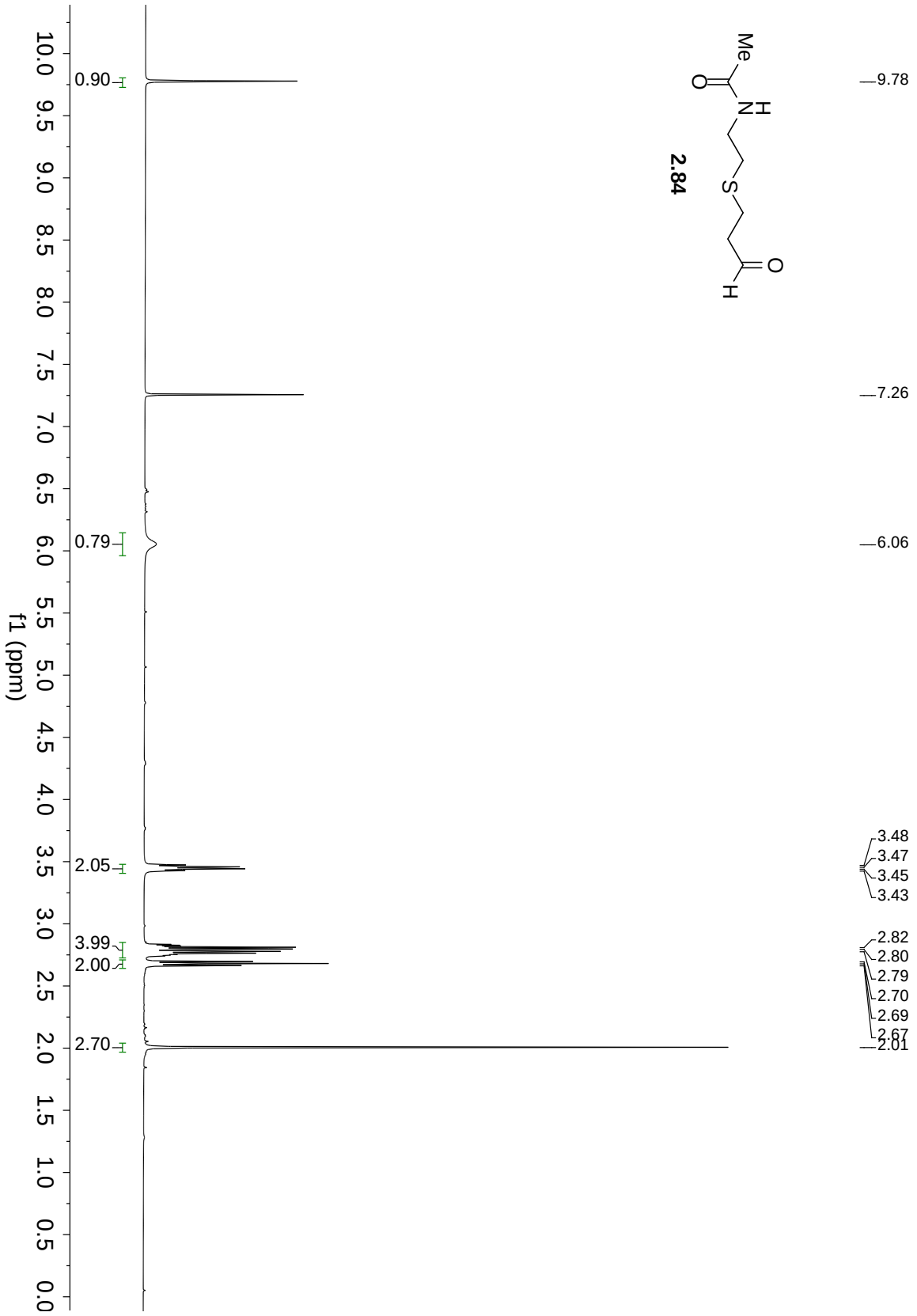
f1 (ppm)
10.0
9.5
9.0
8.5
8.0
7.5
7.0
6.5
6.0
5.5
5.0
4.5
4.0
3.5
3.0
2.5
2.0
1.5
1.0
0.5
0.0
0.90
0.79
2.05
3.99
2.00
2.70
Me
O
H
N
S
O
H
2.84
9.78
7.26
6.06
3.48
3.47
3.45
3.43
2.82
2.80
2.79
2.70
2.69
2.67
2.01

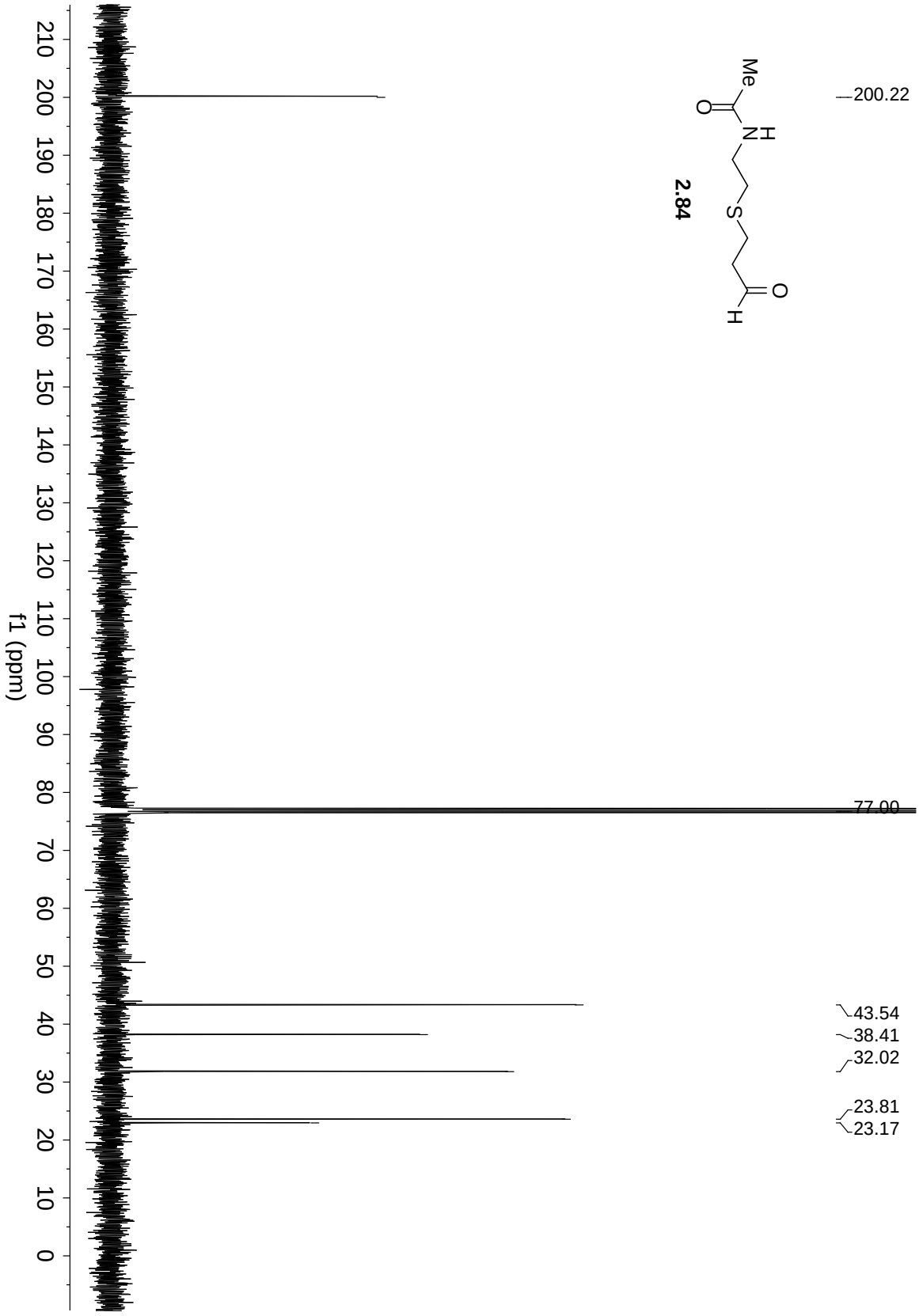
f1 (ppm)
210
200
190
180
170
160
150
140
130
120
110
100
90
80
70
60
50
40
30
20
10
0
Me
O
H
N
S
O
H
2.84
200.22
77.00
43.54
38.41
32.02
23.81
23.17

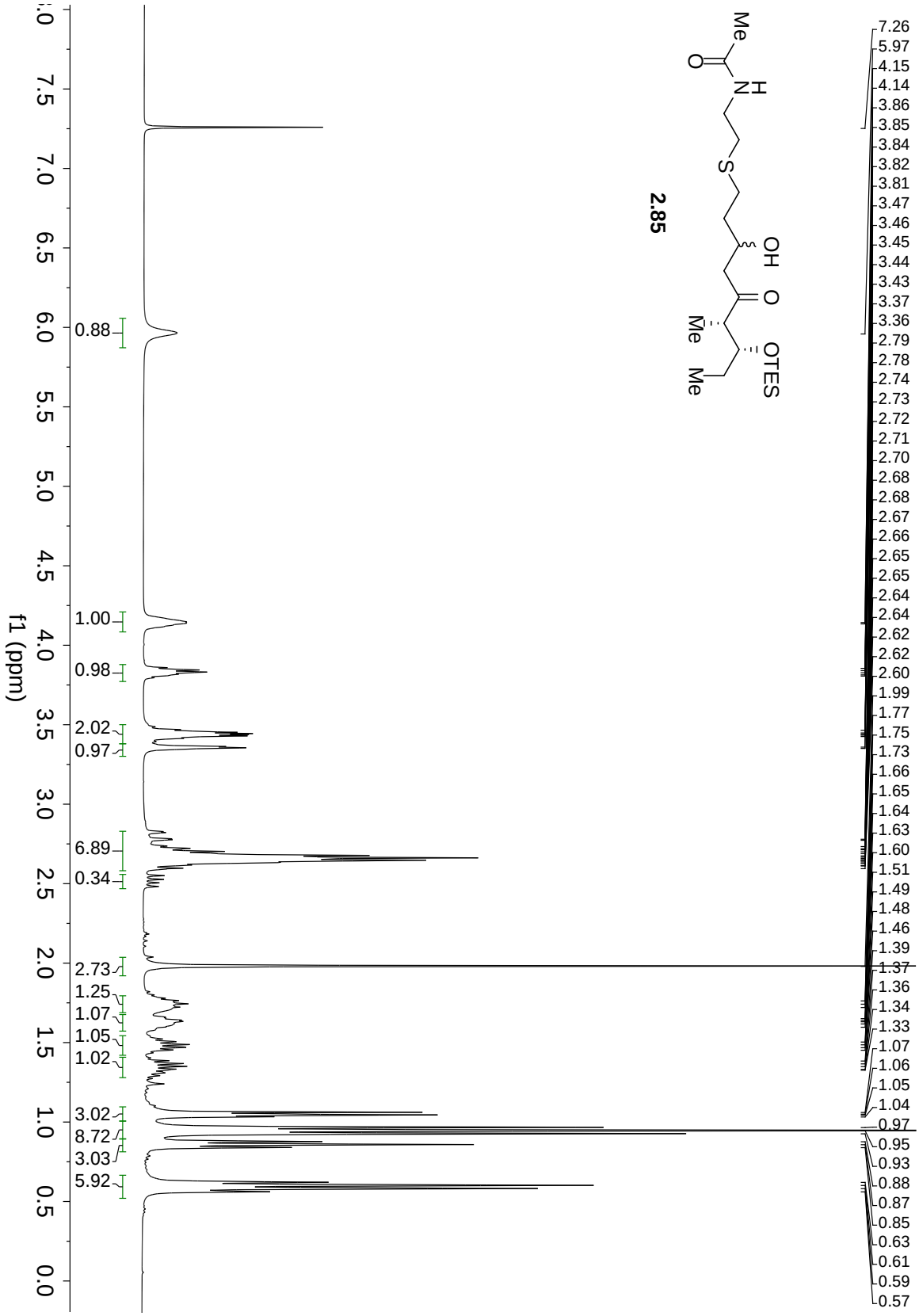
f1 (ppm)
0.88
1.00
0.98
2.02
0.97
6.89
0.34
2.73
1.25
1.07
1.05
1.02
3.02
8.72
3.03
5.92
2.85
Me
O
H
N
S
OH
O
OTES
Me
Me
7.26
5.97
4.15
4.14
3.86
3.85
3.84
3.82
3.81
3.47
3.46
3.45
3.44
3.43
3.37
3.36
2.79
2.78
2.74
2.73
2.72
2.71
2.70
2.68
2.68
2.67
2.66
2.65
2.65
2.64
2.64
2.62
2.62
2.60
1.99
1.77
1.75
1.73
1.66
1.65
1.64
1.63
1.60
1.51
1.49
1.48
1.46
1.39
1.37
1.36
1.34
1.33
1.07
1.06
1.05
1.04
0.97
0.95
0.93
0.88
0.87
0.85
0.63
0.61
0.59
0.57

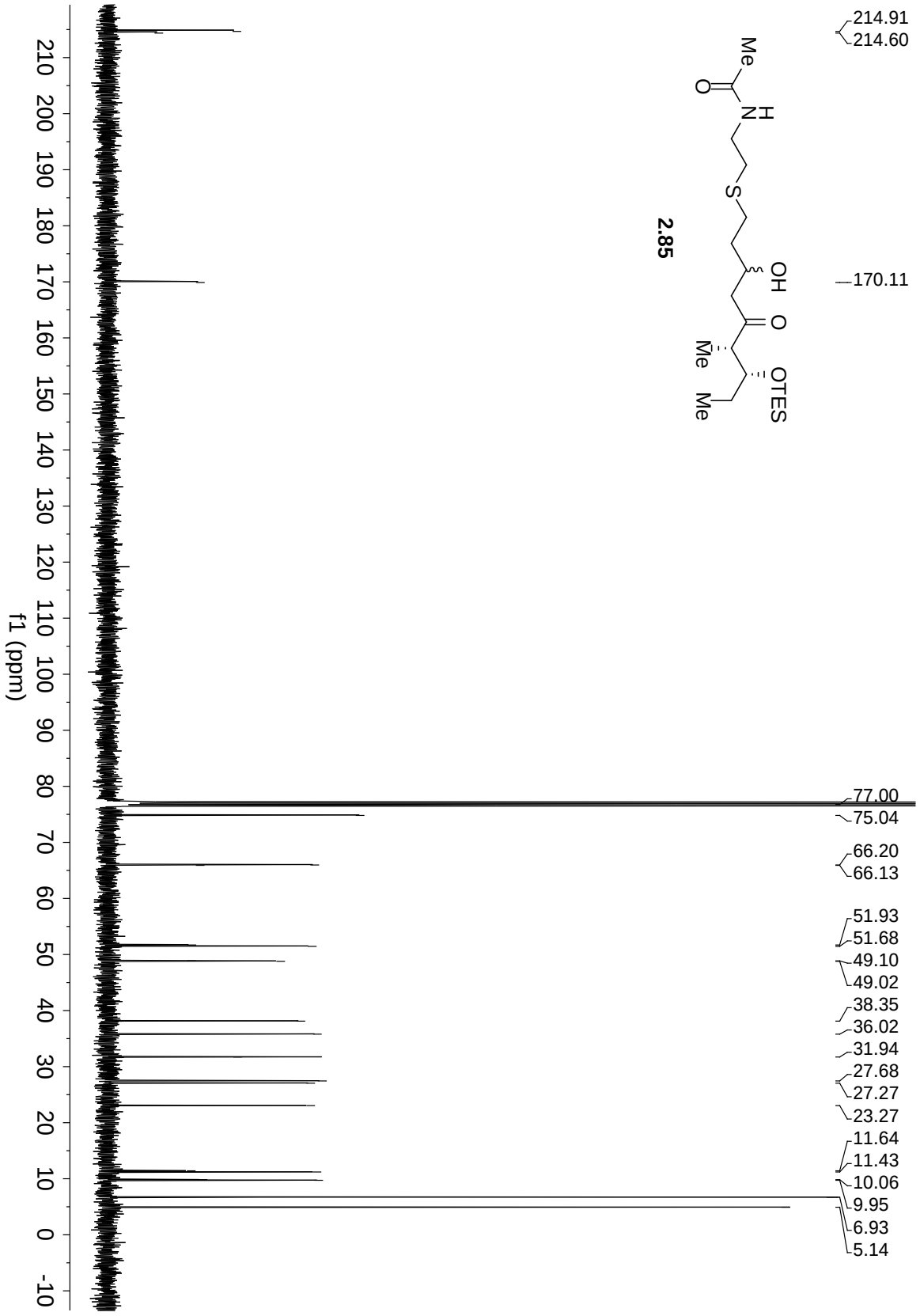
214.91
214.60
170.11
77.00
75.04
66.20
66.13
51.93
51.68
49.10
49.02
38.35
36.02
31.94
27.68
27.27
23.27
11.64
11.43
10.06
9.95
6.93
5.14
2.85
f1 (ppm)

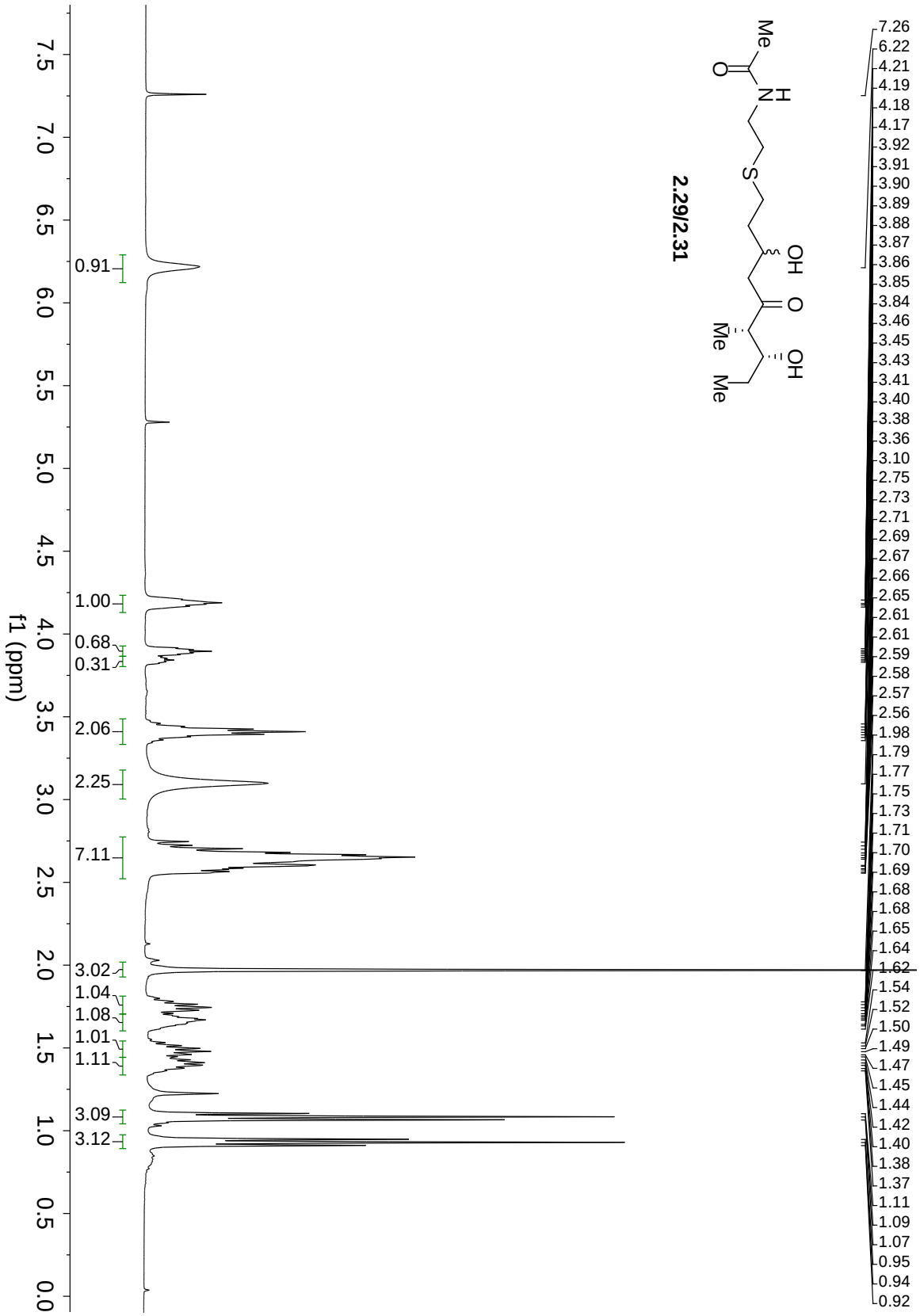
f1 (ppm)
7.5
7.0
6.5
6.0
5.5
5.0
4.5
4.0
3.5
3.0
2.5
2.0
1.5
1.0
0.5
0.0
0.91
1.00
0.68
0.31
2.06
2.25
7.11
3.02
1.04
1.08
1.01
1.11
3.09
3.12
2.29/2.31
Me
O
H
N
S
OH
O
OH
Me
Me
7.26
6.22
4.21
4.19
4.18
4.17
3.92
3.91
3.90
3.89
3.88
3.87
3.86
3.85
3.84
3.46
3.45
3.43
3.41
3.40
3.38
3.36
3.10
2.75
2.73
2.71
2.69
2.67
2.66
2.65
2.61
2.61
2.59
2.58
2.57
2.56
1.98
1.79
1.77
1.75
1.73
1.71
1.70
1.69
1.68
1.68
1.65
1.64
1.62
1.54
1.52
1.50
1.49
1.47
1.45
1.44
1.42
1.40
1.38
1.37
1.11
1.09
1.07
0.95
0.94
0.92

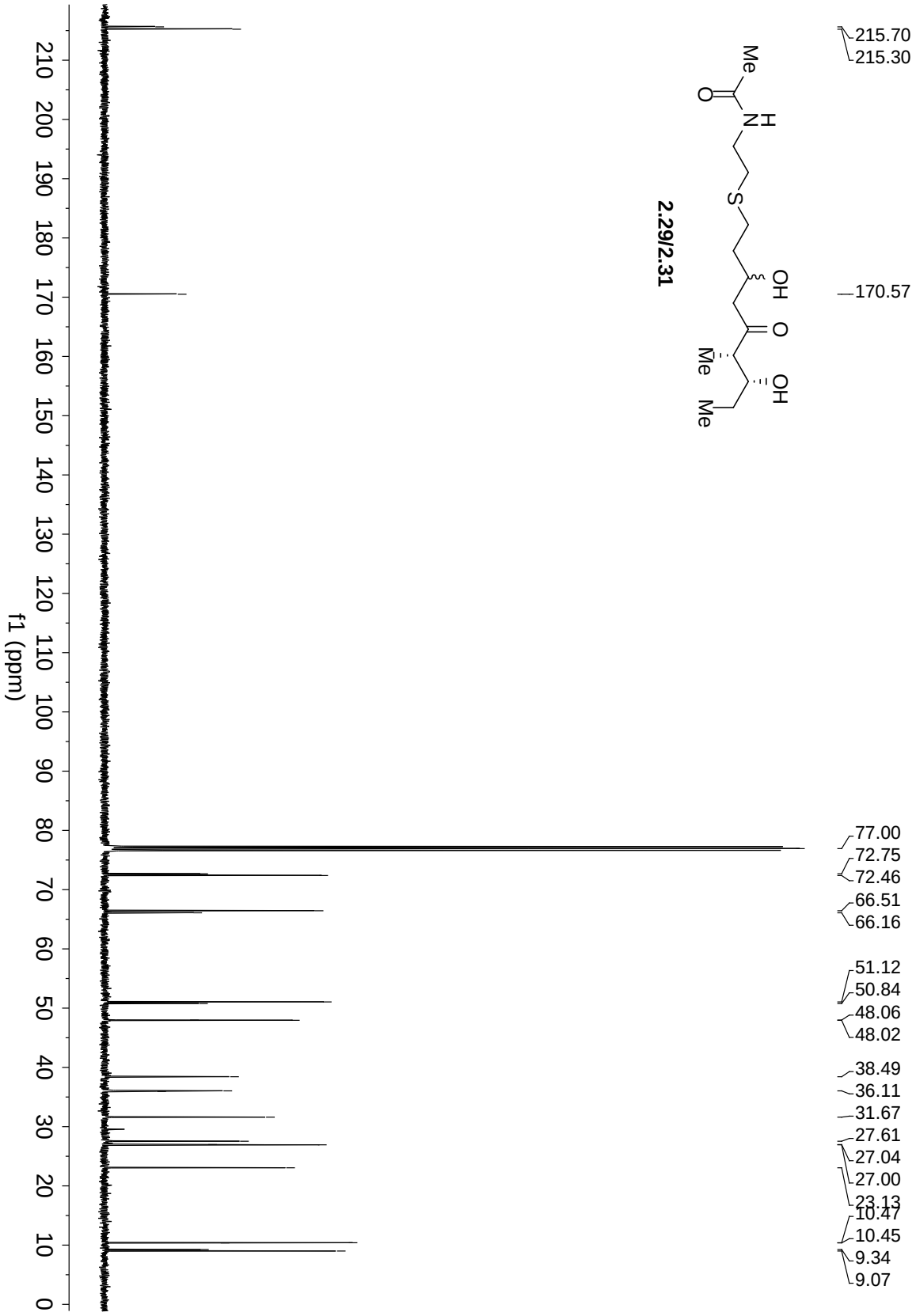
215.70
215.30
170.57
77.00
72.75
72.46
66.51
66.16
51.12
50.84
48.06
48.02
38.49
36.11
31.67
27.61
27.04
27.00
23.13
10.47
10.45
9.34
9.07
2.29/2.31
f1 (ppm)

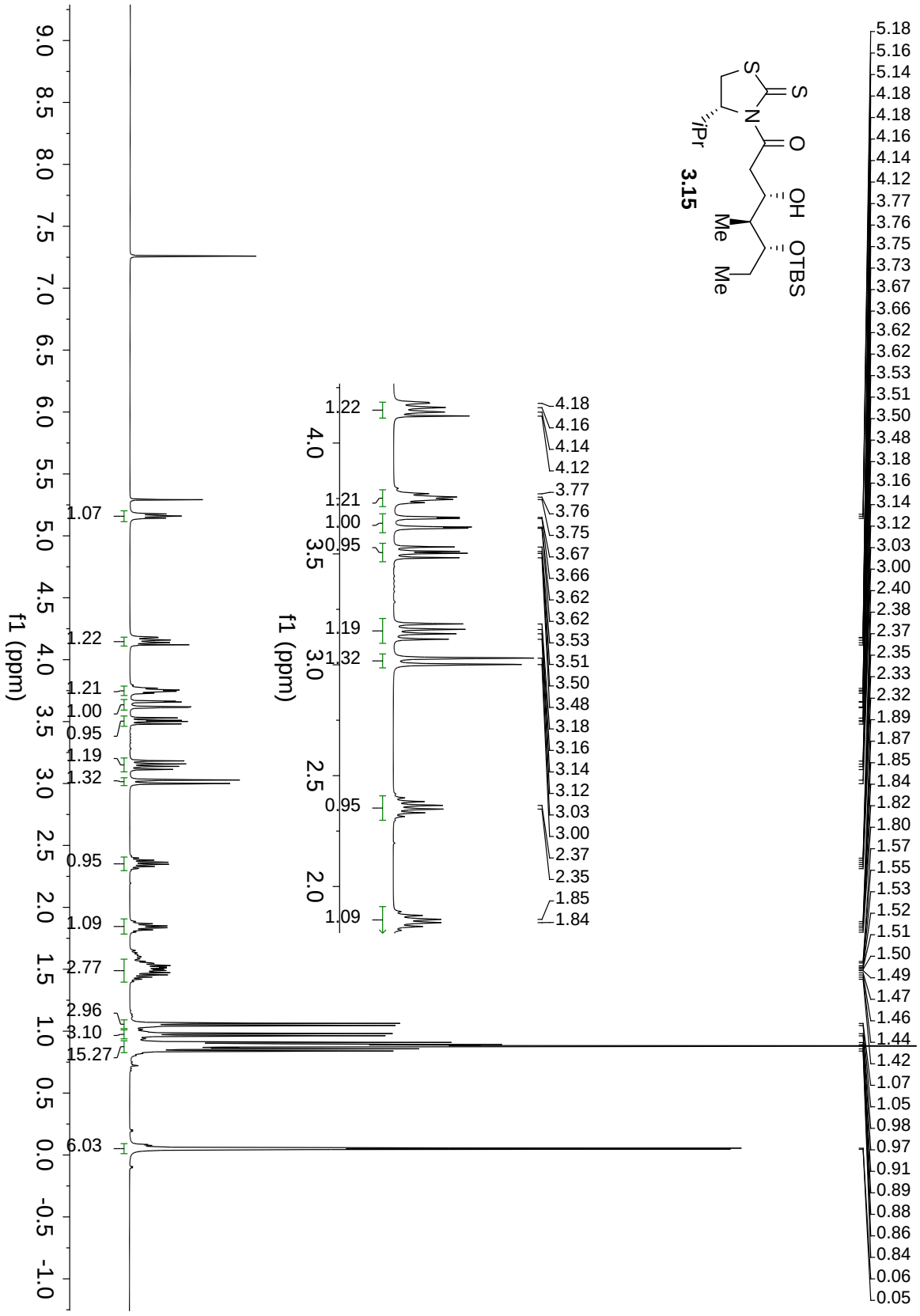
S
O
OH
OTBS
Me
Me
iPr
3.15
f1 (ppm)

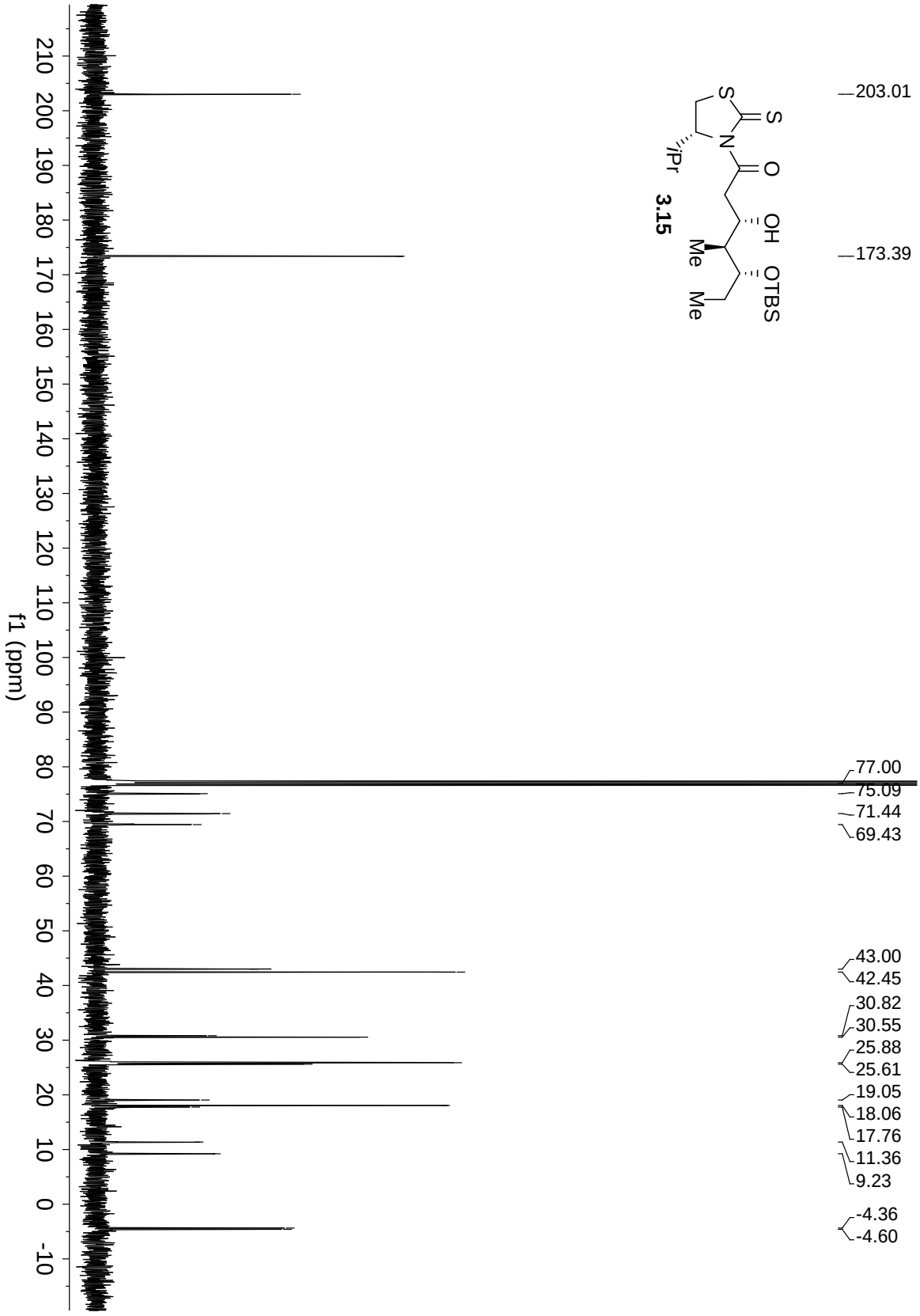
203.01
173.39
77.00
75.09
71.44
69.43
43.00
42.45
30.82
30.55
25.88
25.61
19.05
18.06
17.76
11.36
9.23
-4.36
-4.60
f1 (ppm)
3.15

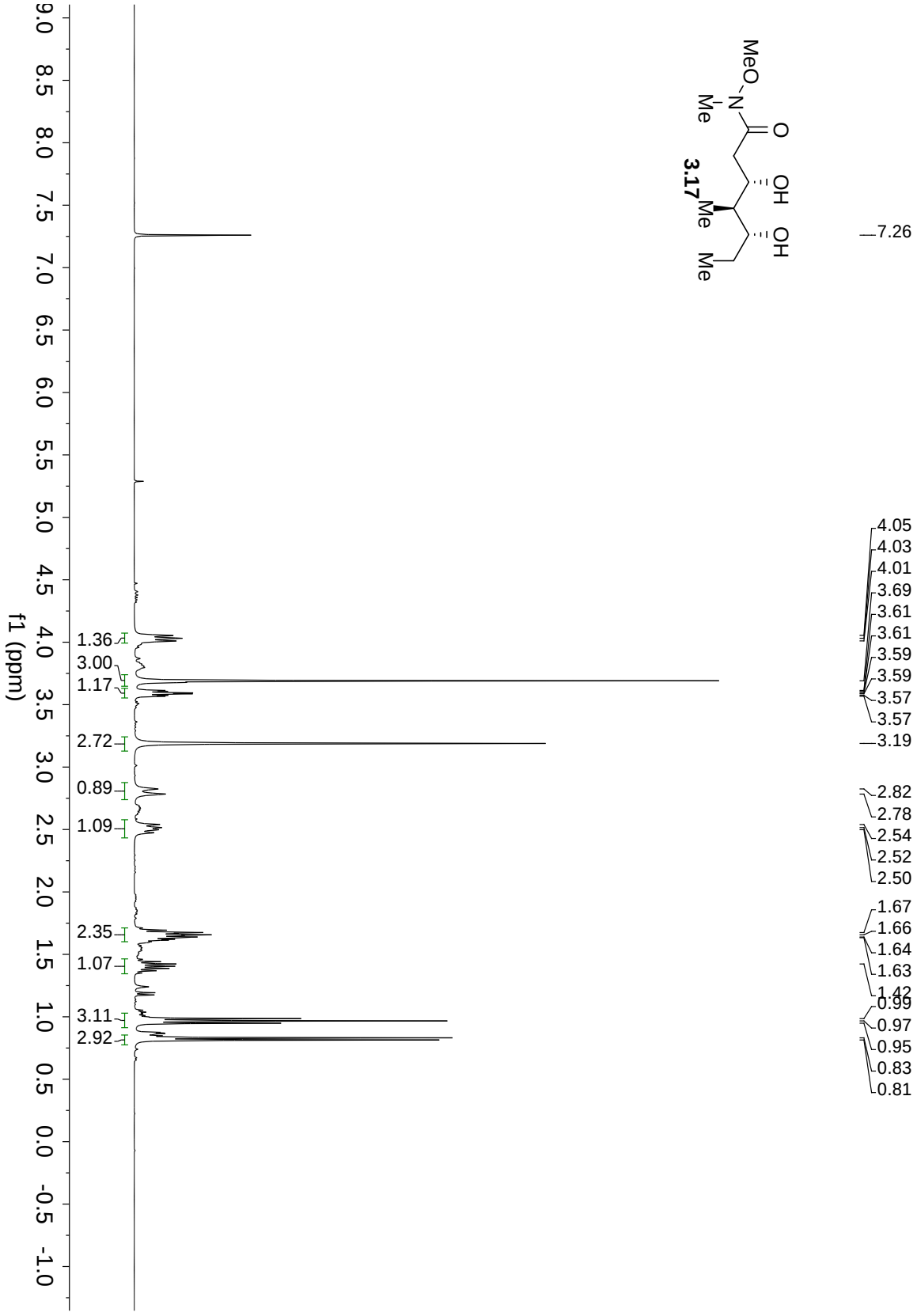
MeO
N
Me
O
OH
OH
3.17
Me
Me
7.26
4.05
4.03
4.01
3.69
3.61
3.61
3.59
3.59
3.57
3.57
3.19
2.82
2.78
2.54
2.52
2.50
1.67
1.66
1.64
1.63
1.42
0.99
0.97
0.95
0.83
0.81
1.36
3.00
1.17
2.72
0.89
1.09
2.35
1.07
3.11
2.92
f1 (ppm)
9.0
8.5
8.0
7.5
7.0
6.5
6.0
5.5
5.0
4.5
4.0
3.5
3.0
2.5
2.0
1.5
1.0
0.5
0.0
-0.5
-1.0

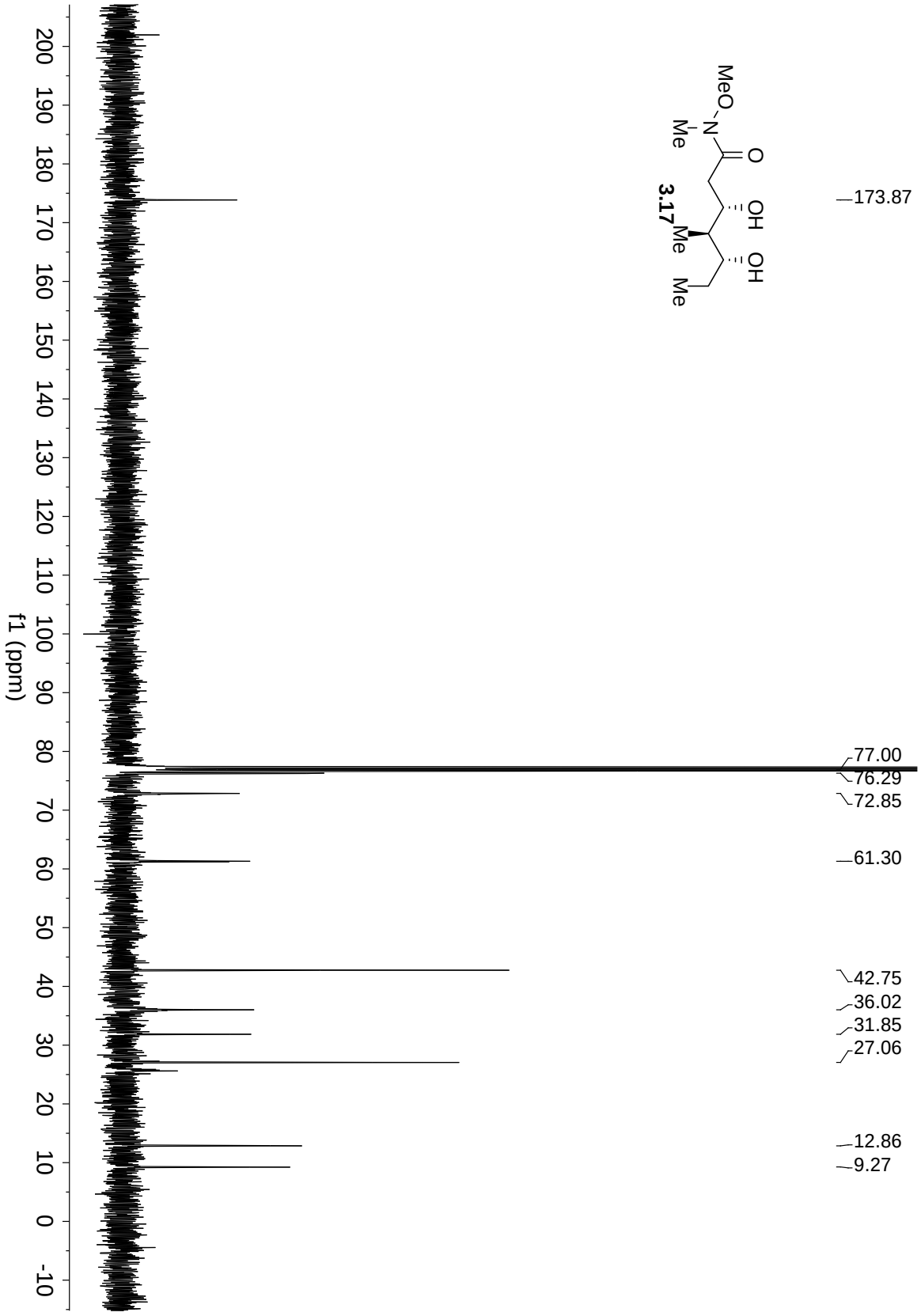
MeO
N
Me
O
OH
OH
Me
Me
3.17
173.87
77.00
76.29
72.85
61.30
42.75
36.02
31.85
27.06
12.86
9.27
f1 (ppm)
200
190
180
170
160
150
140
130
120
110
100
90
80
70
60
50
40
30
20
10
0
-10

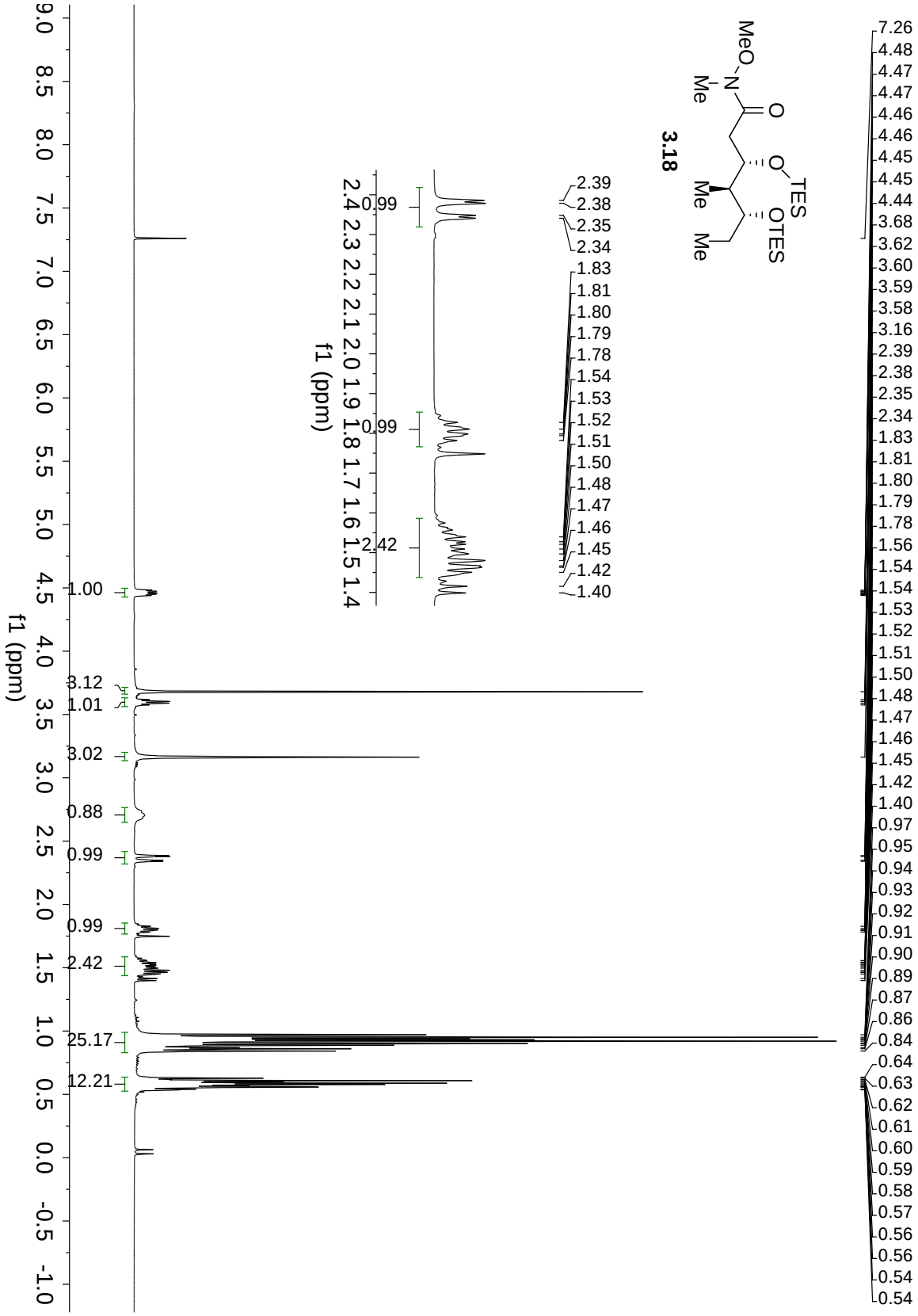
3.18
MeO
N
Me
O
O
TES
OTES
Me
Me
f1 (ppm)
f1 (ppm)
1.00
3.12
1.01
3.02
0.88
0.99
0.99
2.42
25.17
12.21
0.99
0.99
2.42
2.39
2.38
2.35
2.34
1.83
1.81
1.80
1.79
1.78
1.54
1.53
1.52
1.51
1.50
1.48
1.47
1.46
1.45
1.42
1.40
7.26
4.48
4.47
4.47
4.46
4.46
4.45
4.45
4.44
3.68
3.62
3.60
3.59
3.58
3.16
2.39
2.38
2.35
2.34
1.83
1.81
1.80
1.79
1.78
1.56
1.54
1.54
1.53
1.52
1.51
1.50
1.48
1.47
1.46
1.45
1.42
1.40
0.97
0.95
0.94
0.93
0.92
0.91
0.90
0.89
0.87
0.86
0.84
0.64
0.63
0.62
0.61
0.60
0.59
0.58
0.57
0.56
0.56
0.54
0.54

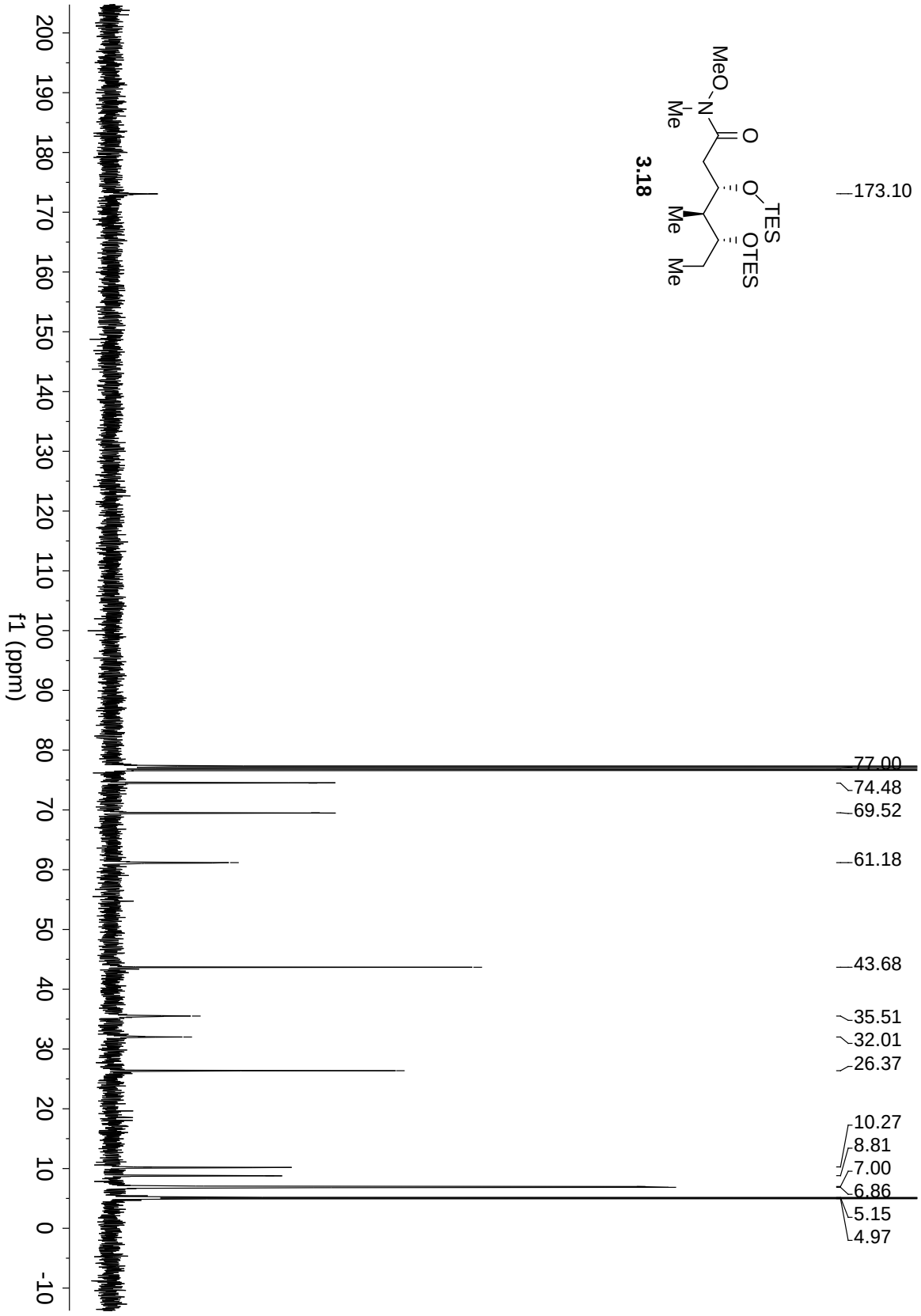
MeO
N
Me
O
O
TES
OTES
Me
Me
3.18
173.10
77.00
74.48
69.52
61.18
43.68
35.51
32.01
26.37
10.27
8.81
7.00
6.86
5.15
4.97
f1 (ppm)
200
190
180
170
160
150
140
130
120
110
100
90
80
70
60
50
40
30
20
10
0
-10

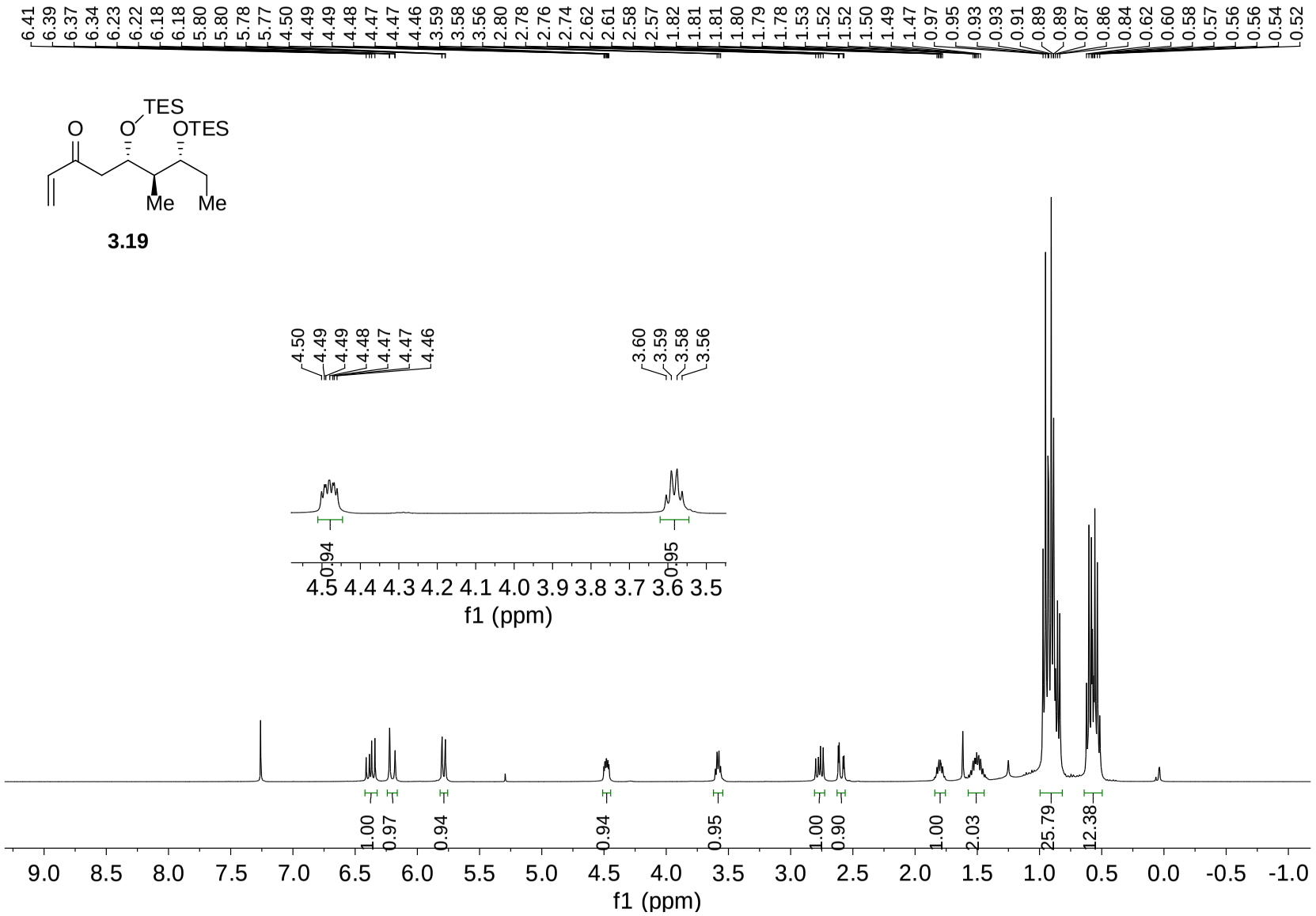
6.41 6.39 6.37 6.34 6.23 6.22 6.18 6.18 5.80 5.80 5.78 5.77 4.50 4.49 4.49 4.48 4.47 4.47 4.46 3.59 3.58 3.56 2.80 2.78 2.76 2.74 2.62 2.61 2.58 2.57 1.82 1.81 1.81 1.80 1.79 1.78 1.53 1.52 1.52 1.50 1.49 1.47 0.97 0.95 0.93 0.93 0.91 0.89 0.89 0.87 0.86 0.84 0.62 0.60 0.58 0.57 0.56 0.56 0.54 0.52
TES
O
O
OTES
Me
Me
3.19
4.50 4.49 4.49 4.48 4.47 4.47 4.46
3.60 3.59 3.58 3.56
0.94
0.95
4.5 4.4 4.3 4.2 4.1 4.0 3.9 3.8 3.7 3.6 3.5
f1 (ppm)
1.00 0.97 0.94 0.94 0.95 1.00 0.90 1.00 2.03 25.79 12.38
9.0 8.5 8.0 7.5 7.0 6.5 6.0 5.5 5.0 4.5 4.0 3.5 3.0 2.5 2.0 1.5 1.0 0.5 0.0 -0.5 -1.0
f1 (ppm)

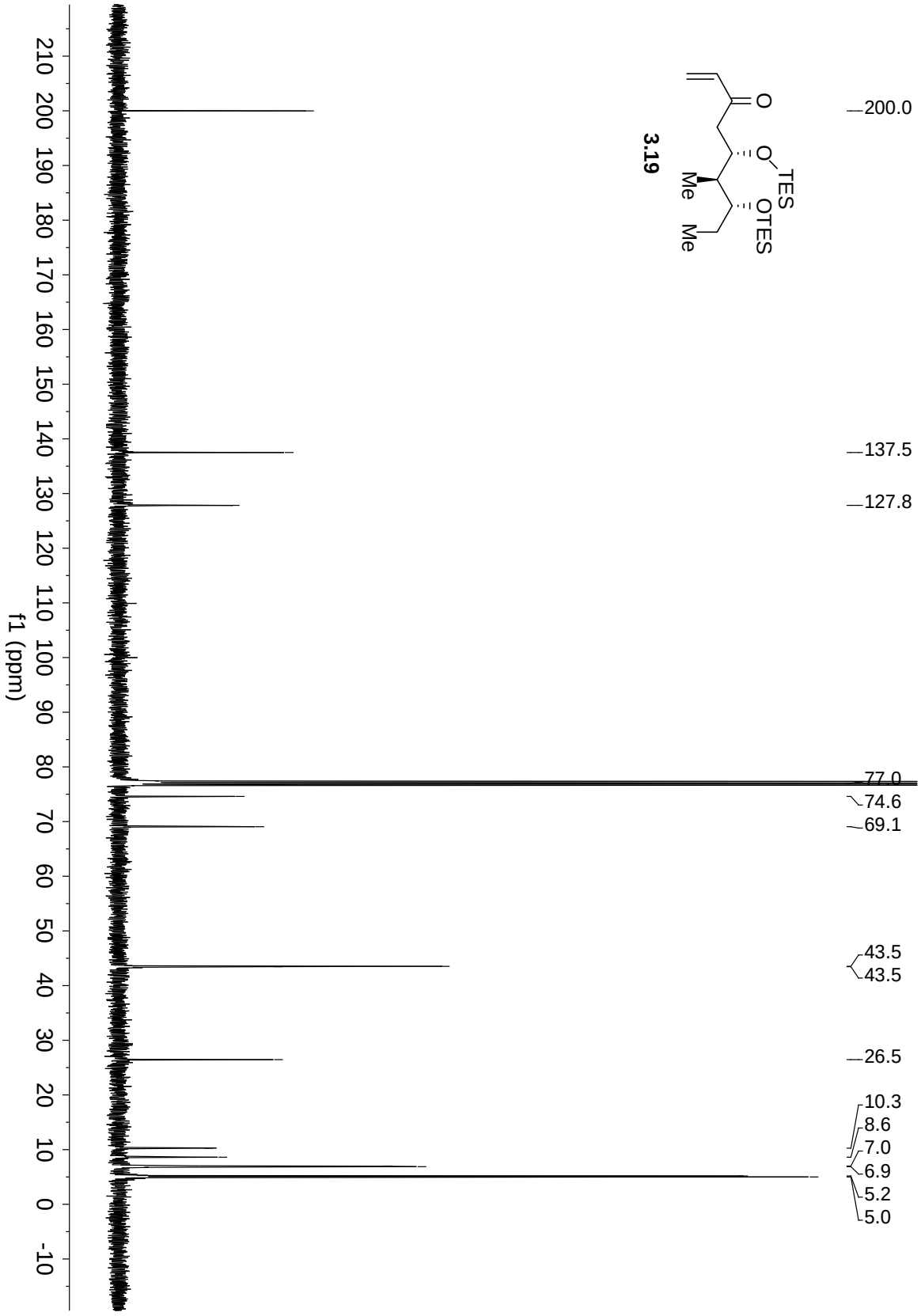
3.19
O
O
TES
OTES
Me
Me
200.0
137.5
127.8
77.0
74.6
69.1
43.5
43.5
26.5
10.3
8.6
7.0
6.9
5.2
5.0
f1 (ppm)
210 200 190 180 170 160 150 140 130 120 110 100 90 80 70 60 50 40 30 20 10 0 -10

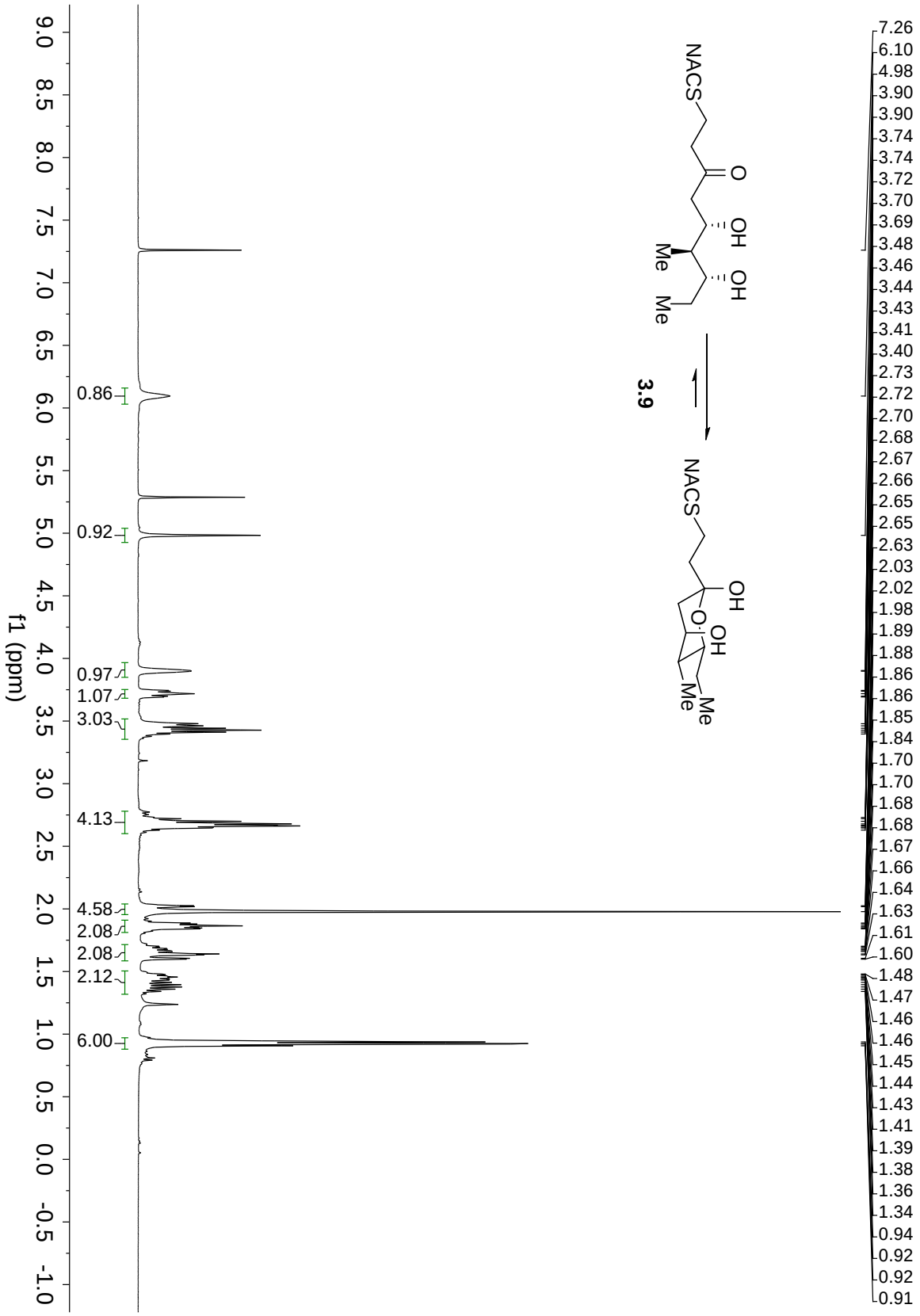
NACS
O
OH
OH
Me
Me
3.9
NACS
OH
O
OH
Me
Me
f1 (ppm)
9.0
8.5
8.0
7.5
7.0
6.5
6.0
5.5
5.0
4.5
4.0
3.5
3.0
2.5
2.0
1.5
1.0
0.5
0.0
-0.5
-1.0
0.86
0.92
0.97
1.07
3.03
4.13
4.58
2.08
2.08
2.12
6.00
7.26
6.10
4.98
3.90
3.90
3.74
3.74
3.72
3.70
3.69
3.48
3.46
3.44
3.43
3.41
3.40
2.73
2.72
2.70
2.68
2.67
2.66
2.65
2.65
2.63
2.03
2.02
1.98
1.89
1.88
1.86
1.86
1.85
1.84
1.70
1.70
1.68
1.68
1.67
1.66
1.64
1.63
1.61
1.60
1.48
1.47
1.46
1.46
1.45
1.44
1.43
1.41
1.39
1.38
1.36
1.34
0.94
0.92
0.92
0.91

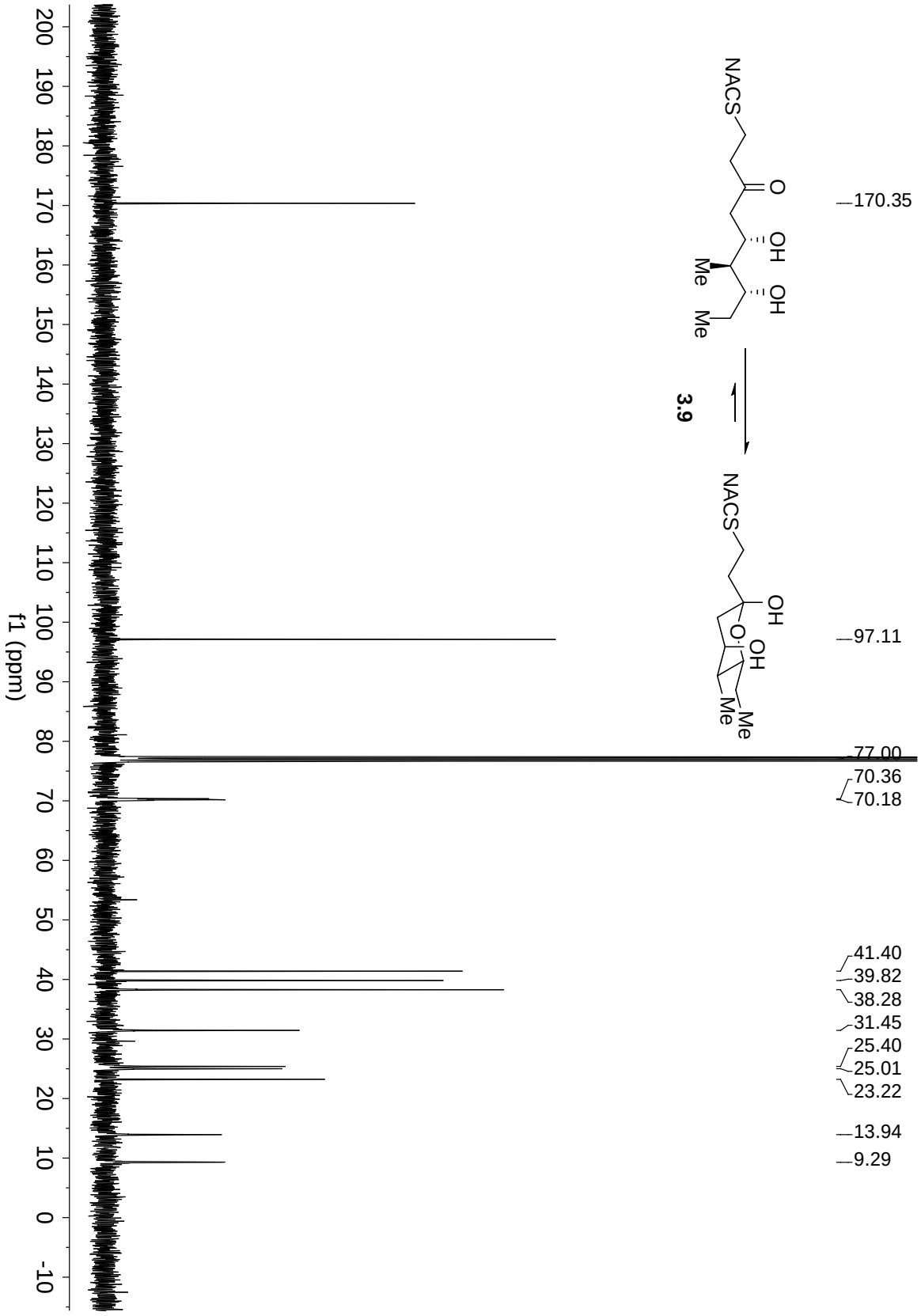
f1 (ppm)
200
190
180
170
160
150
140
130
120
110
100
90
80
70
60
50
40
30
20
10
0
-10
NACS
O
OH
OH
Me
Me
3.9
NACS
OH
O
OH
Me
Me
170.35
97.11
77.00
70.36
70.18
41.40
39.82
38.28
31.45
25.40
25.01
23.22
13.94
9.29

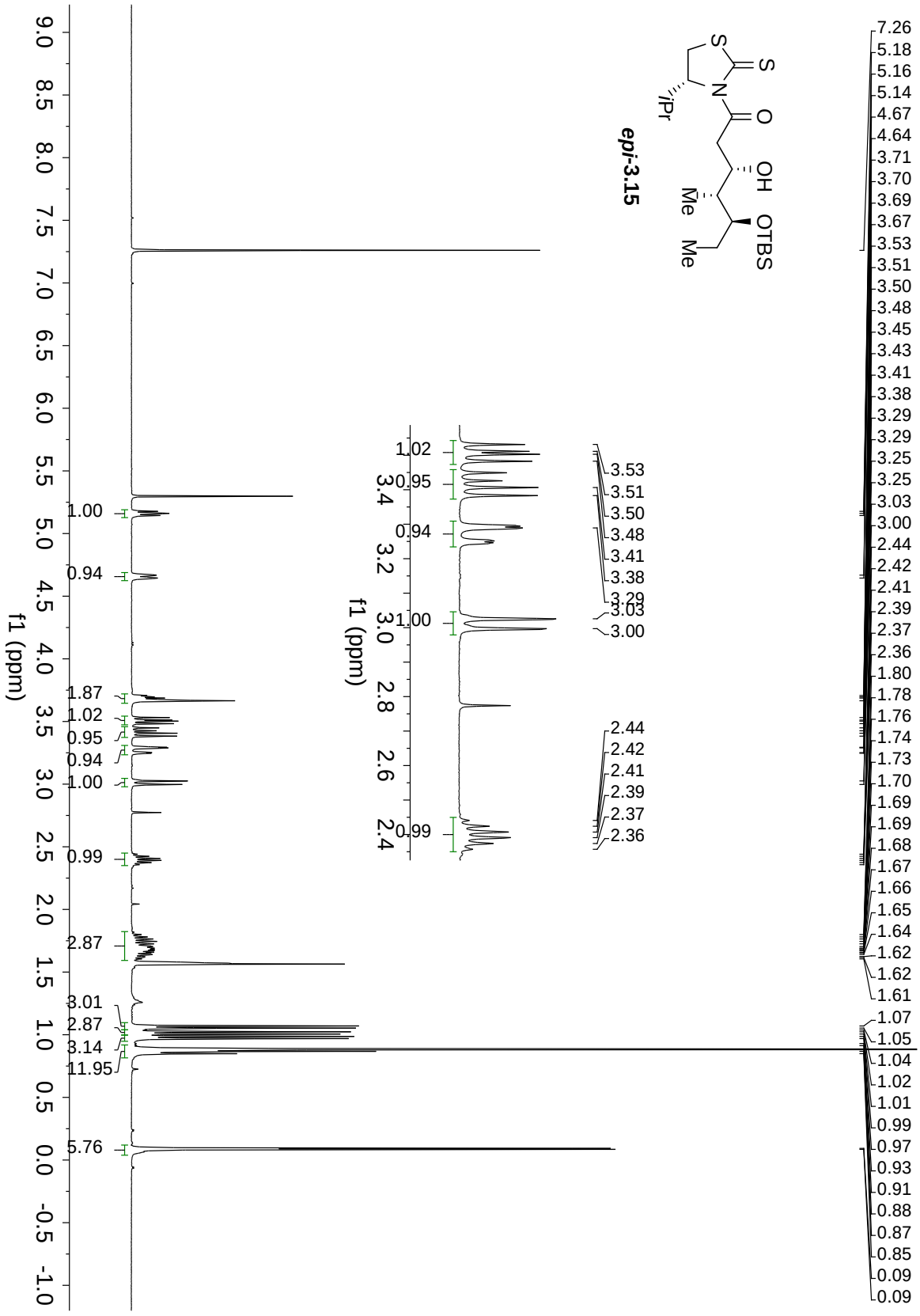
epi-3.15
S
O
OH
OTBS
Me
Me
iPr
f1 (ppm)
9.0 8.5 8.0 7.5 7.0 6.5 6.0 5.5 5.0 4.5 4.0 3.5 3.0 2.5 2.0 1.5 1.0 0.5 0.0 -0.5 -1.0
1.00
0.94
1.87
1.02
0.95
0.94
1.00
0.99
2.87
3.01
2.87
3.14
11.95
5.76
3.4 3.2 3.0 2.8 2.6 2.4
1.02
0.95
0.94
1.00
0.99
3.53
3.51
3.50
3.48
3.41
3.38
3.29
3.03
3.00
2.44
2.42
2.41
2.39
2.37
2.36
7.26
5.18
5.16
5.14
4.67
4.64
3.71
3.70
3.69
3.67
3.53
3.51
3.50
3.48
3.45
3.43
3.41
3.38
3.29
3.29
3.25
3.25
3.03
3.00
2.44
2.42
2.41
2.39
2.37
2.36
1.80
1.78
1.76
1.74
1.73
1.70
1.69
1.69
1.68
1.67
1.66
1.65
1.64
1.62
1.62
1.61
1.07
1.05
1.04
1.02
1.01
0.99
0.97
0.93
0.91
0.88
0.87
0.85
0.09
0.09

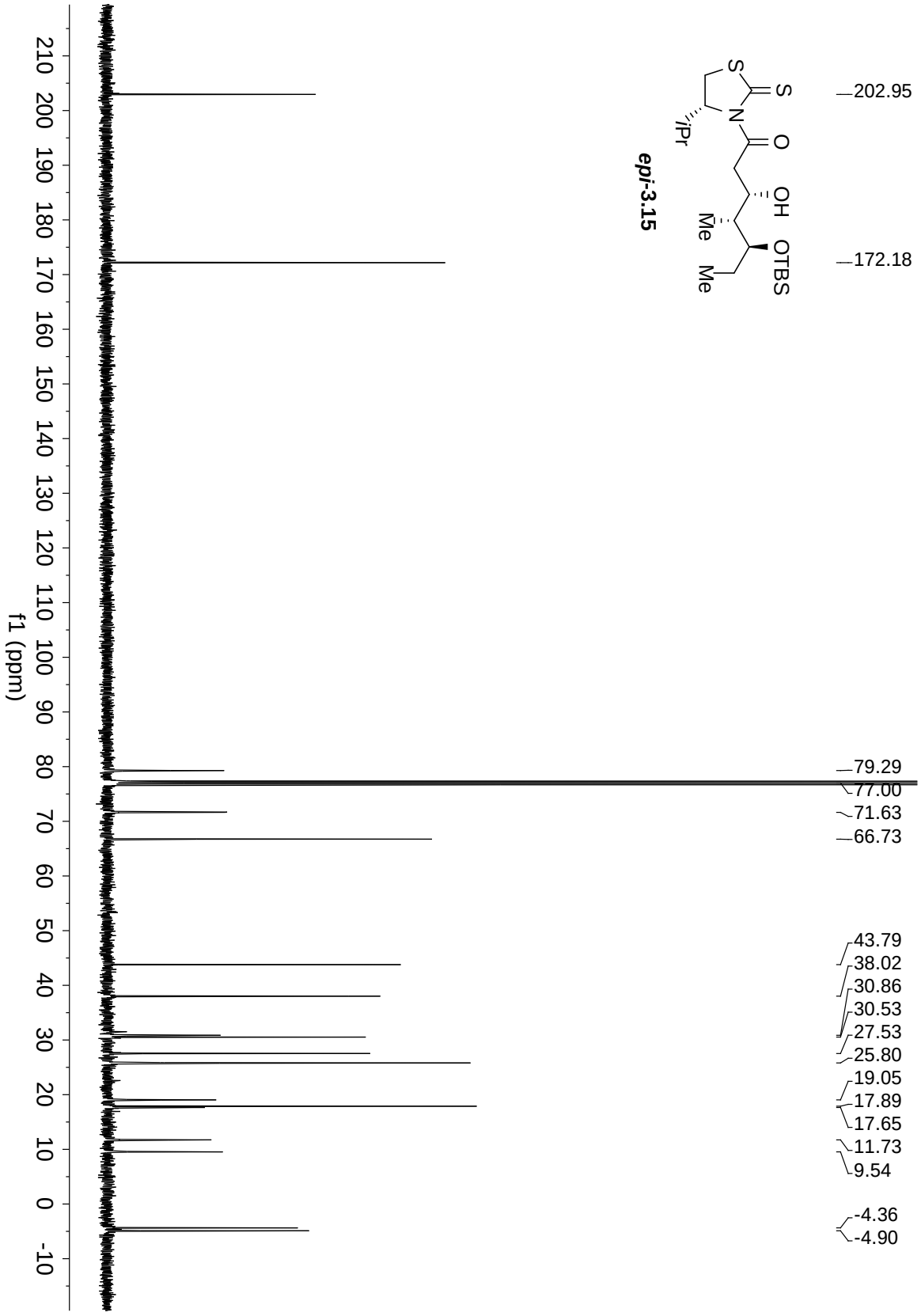
f1 (ppm)
210 200 190 180 170 160 150 140 130 120 110 100 90 80 70 60 50 40 30 20 10 0 -10
epi-3.15
S
S
N
iPr
O
OH
Me
Me
OTBS
202.95
172.18
79.29
77.00
71.63
66.73
43.79
38.02
30.86
30.53
27.53
25.80
19.05
17.89
17.65
11.73
9.54
-4.36
-4.90

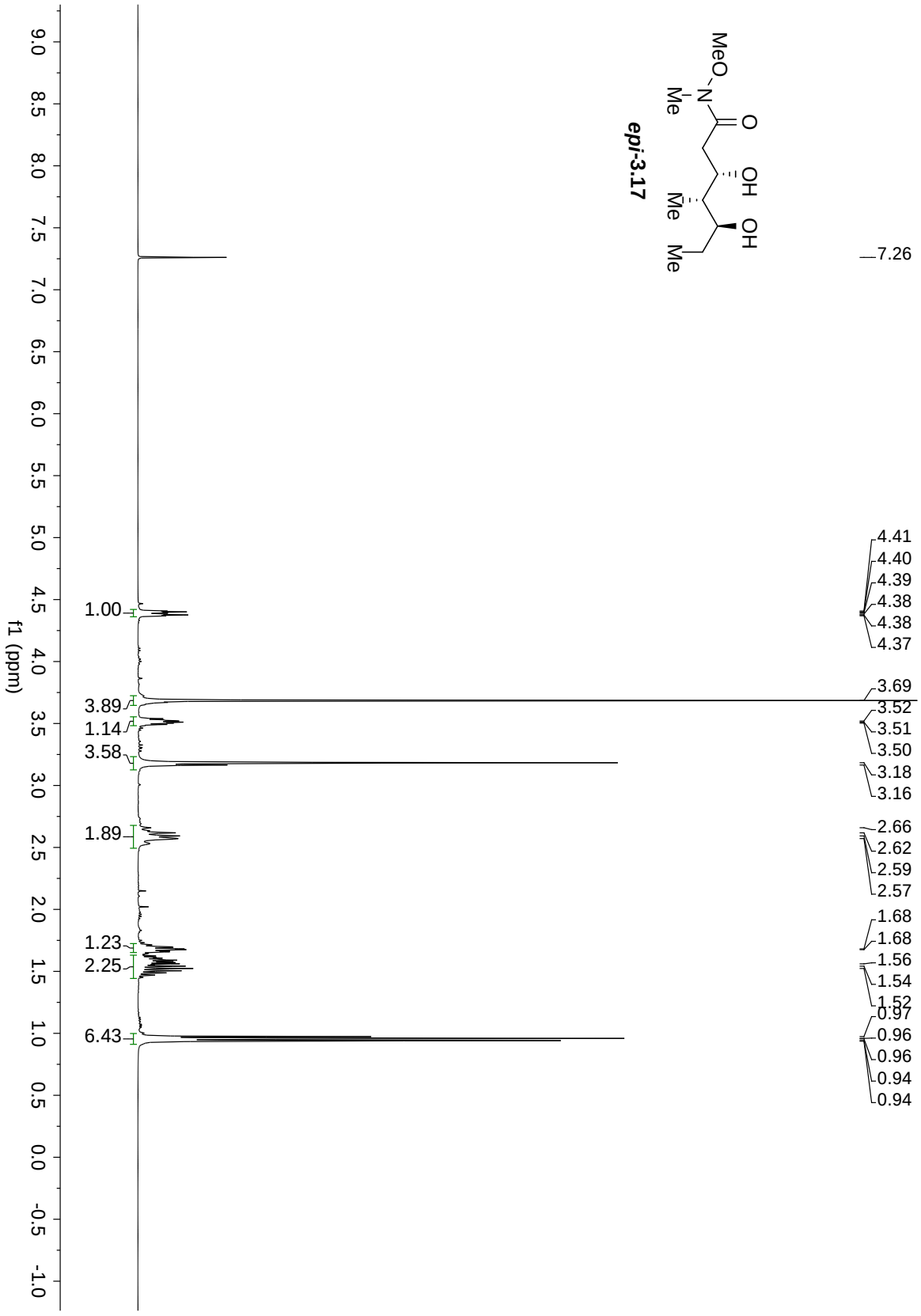
epi-3.17
MeO
N
Me
O
OH
OH
Me
Me
7.26
4.41
4.40
4.39
4.38
4.38
4.37
3.69
3.52
3.51
3.50
3.18
3.16
2.66
2.62
2.59
2.57
1.68
1.68
1.56
1.54
1.52
0.97
0.96
0.96
0.94
0.94
1.00
3.89
1.14
3.58
1.89
1.23
2.25
6.43
f1 (ppm)
9.0
8.5
8.0
7.5
7.0
6.5
6.0
5.5
5.0
4.5
4.0
3.5
3.0
2.5
2.0
1.5
1.0
0.5
0.0
-0.5
-1.0

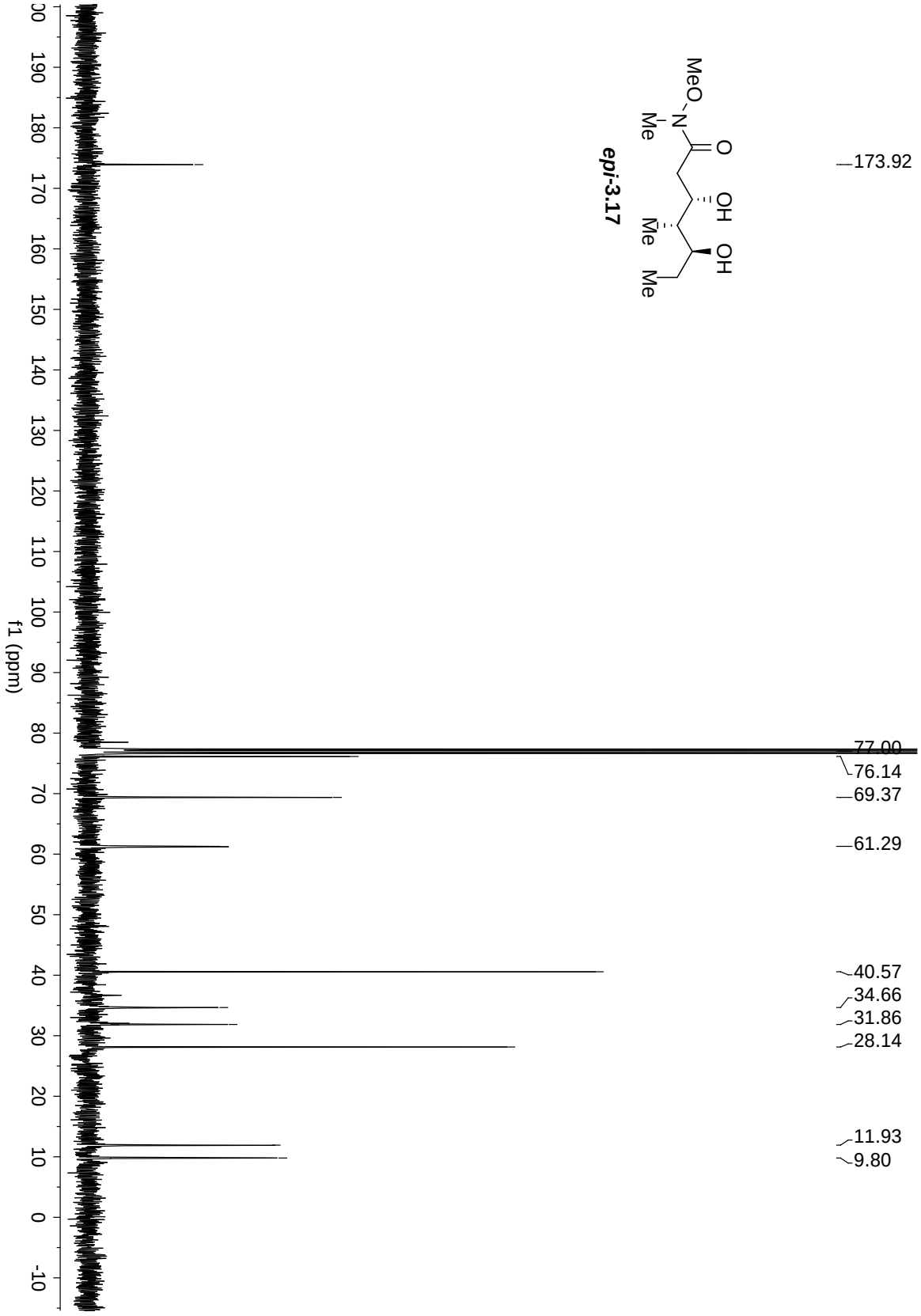
epi-3.17
MeO
N
Me
O
OH
OH
Me
Me
173.92
77.00
76.14
69.37
61.29
40.57
34.66
31.86
28.14
11.93
9.80
f1 (ppm)

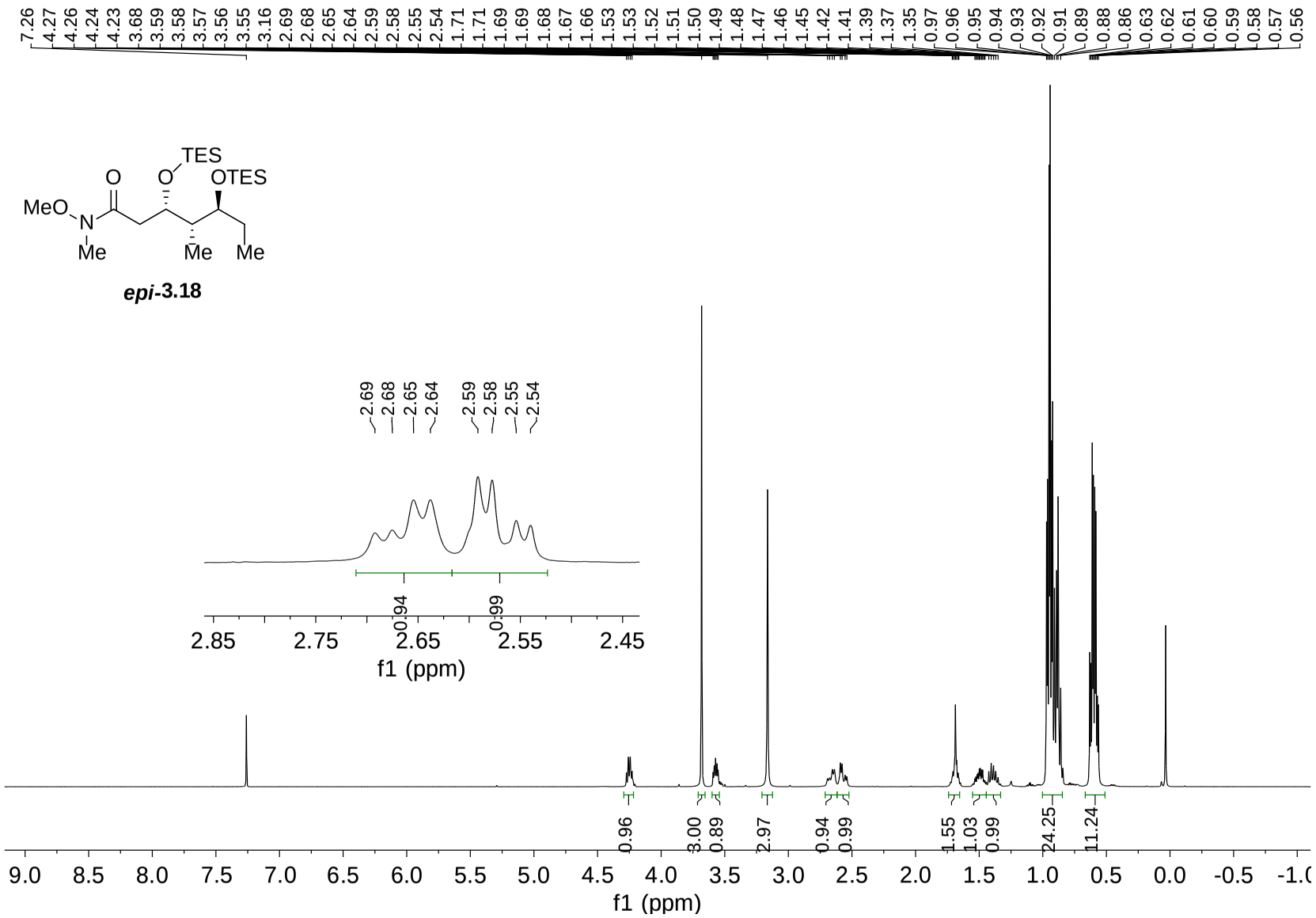
7.26 4.27 4.26 4.24 4.23 3.68 3.59 3.58 3.57 3.56 3.55 3.16 2.69 2.68 2.65 2.64 2.59 2.58 2.55 2.54 1.71 1.71 1.69 1.69 1.68 1.67 1.66 1.53 1.53 1.52 1.51 1.50 1.49 1.48 1.47 1.46 1.45 1.42 1.41 1.39 1.37 1.35 0.97 0.96 0.95 0.94 0.93 0.92 0.91 0.89 0.88 0.86 0.63 0.62 0.61 0.60 0.59 0.58 0.57 0.56
TES
O
O
OTES
MeO
N
Me
Me
Me
Me
epi-3.18
2.69 2.68 2.65 2.64 2.59 2.58 2.55 2.54
0.94
0.99
2.85 2.75 2.65 2.55 2.45
f1 (ppm)
0.96 3.00 0.89 2.97 0.94 0.99 1.55 1.03 0.99 24.25 11.24
9.0 8.5 8.0 7.5 7.0 6.5 6.0 5.5 5.0 4.5 4.0 3.5 3.0 2.5 2.0 1.5 1.0 0.5 0.0 -0.5 -1.0
f1 (ppm)

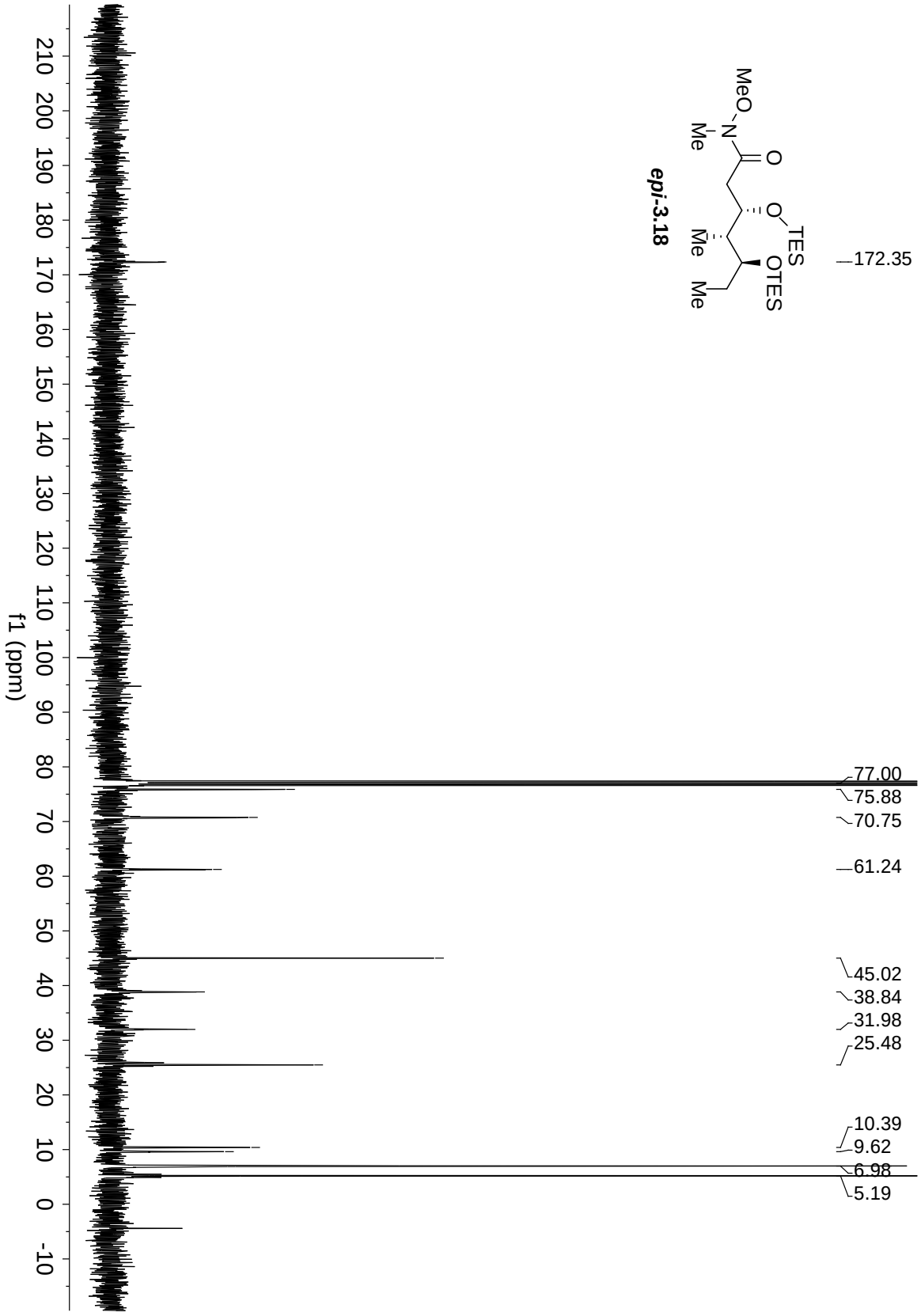
MeO
N
Me
O
O
TES
OTES
Me
Me
Me
epi-3.18
172.35
77.00
75.88
70.75
61.24
45.02
38.84
31.98
25.48
10.39
9.62
6.98
5.19
f1 (ppm)

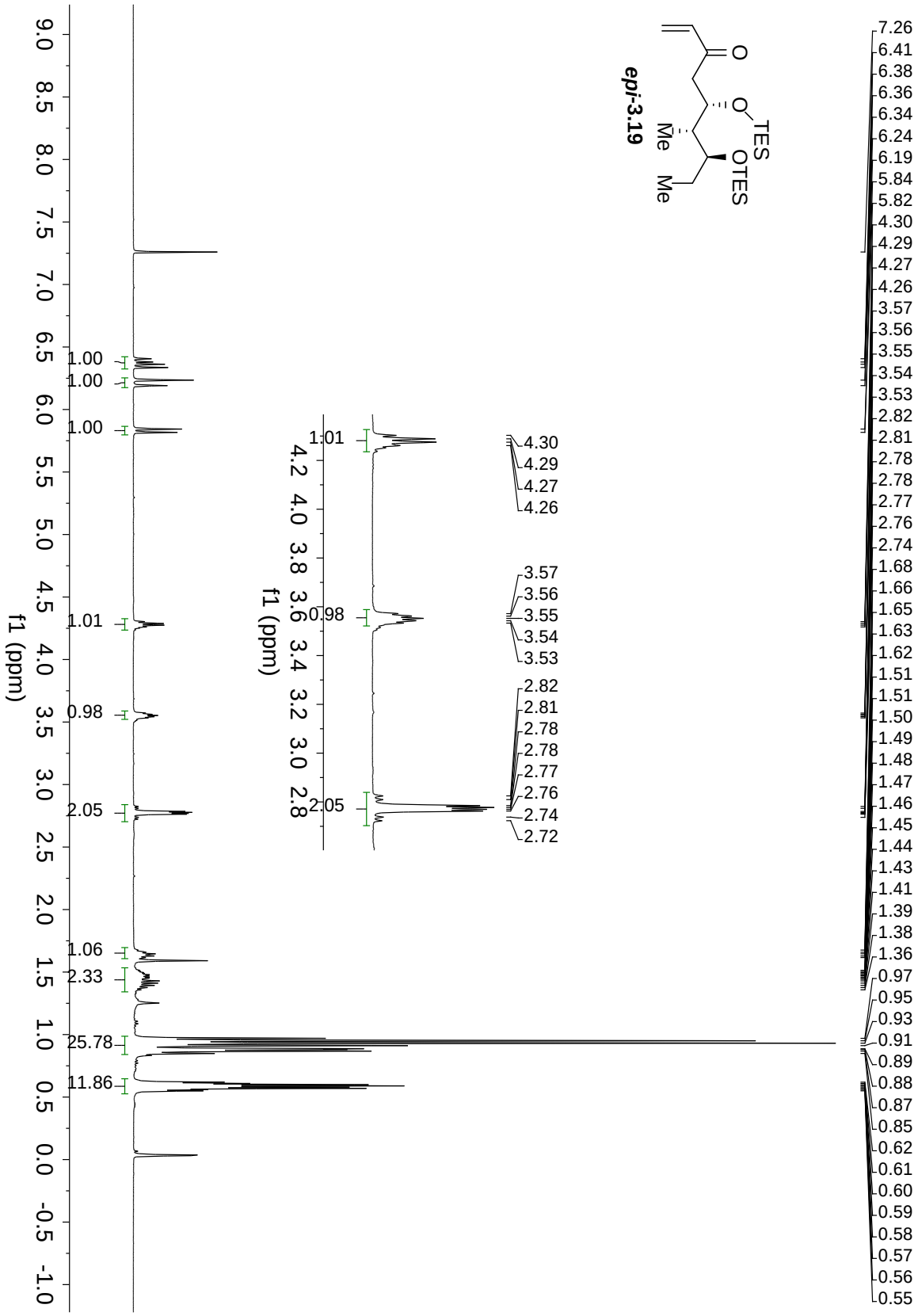
O
O
TES
OTES
Me
Me
epi-3.19
f1 (ppm)
1.00
1.00
1.00
1.01
0.98
2.05
1.06
2.33
25.78
11.86
1.01
0.98
2.05
4.30
4.29
4.27
4.26
3.57
3.56
3.55
3.54
3.53
2.82
2.81
2.78
2.78
2.77
2.76
2.74
2.72
7.26
6.41
6.38
6.36
6.34
6.24
6.19
5.84
5.82
4.30
4.29
4.27
4.26
3.57
3.56
3.55
3.54
3.53
2.82
2.81
2.78
2.78
2.77
2.76
2.74
2.72
1.68
1.66
1.65
1.63
1.62
1.51
1.51
1.50
1.49
1.48
1.47
1.46
1.45
1.44
1.43
1.41
1.39
1.38
1.36
0.97
0.95
0.93
0.91
0.89
0.88
0.87
0.85
0.62
0.61
0.60
0.59
0.58
0.57
0.56
0.55

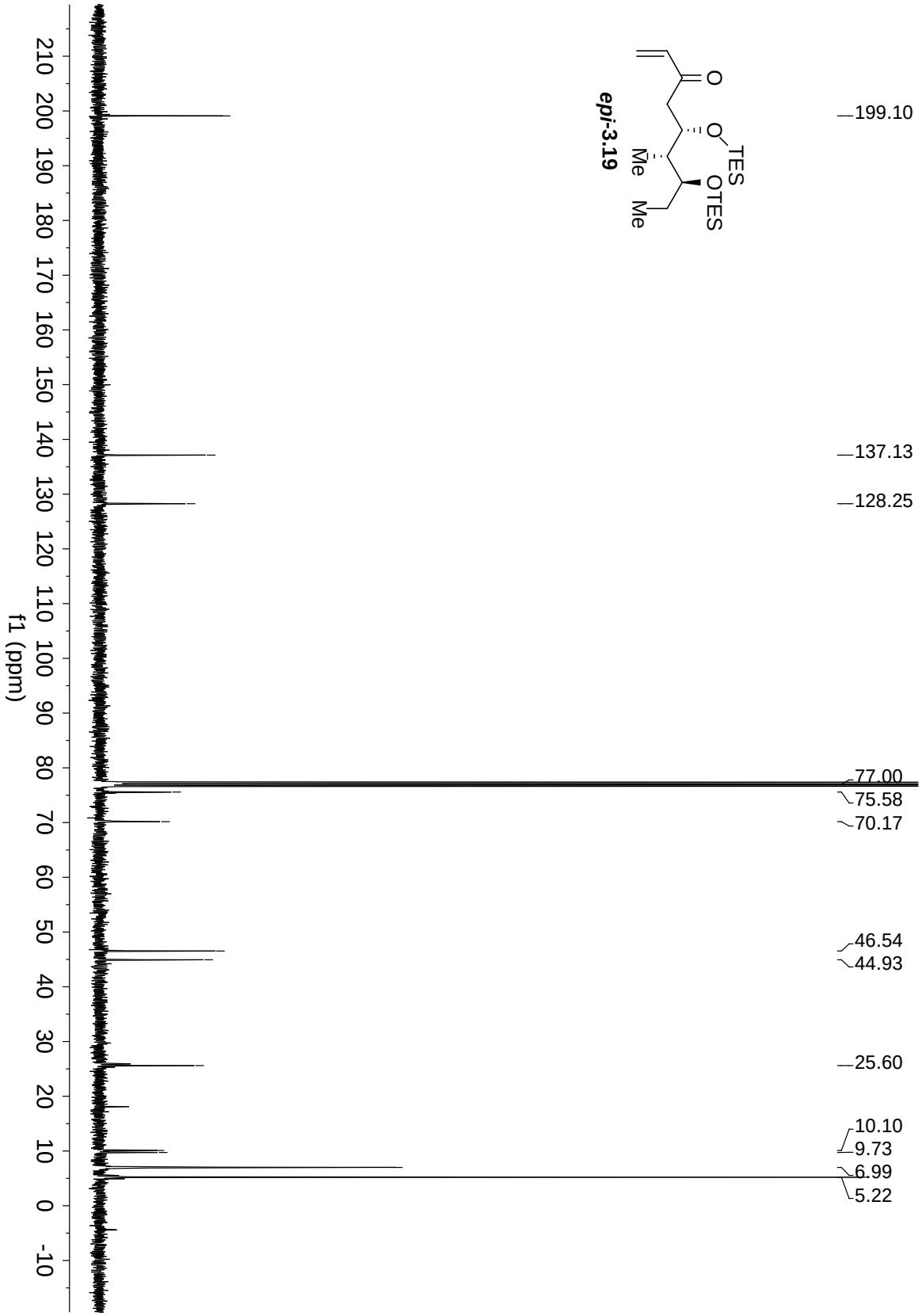
epi-3.19
O
O
TES
OTES
Me
Me
199.10
137.13
128.25
77.00
75.58
70.17
46.54
44.93
25.60
10.10
9.73
6.99
5.22
f1 (ppm)

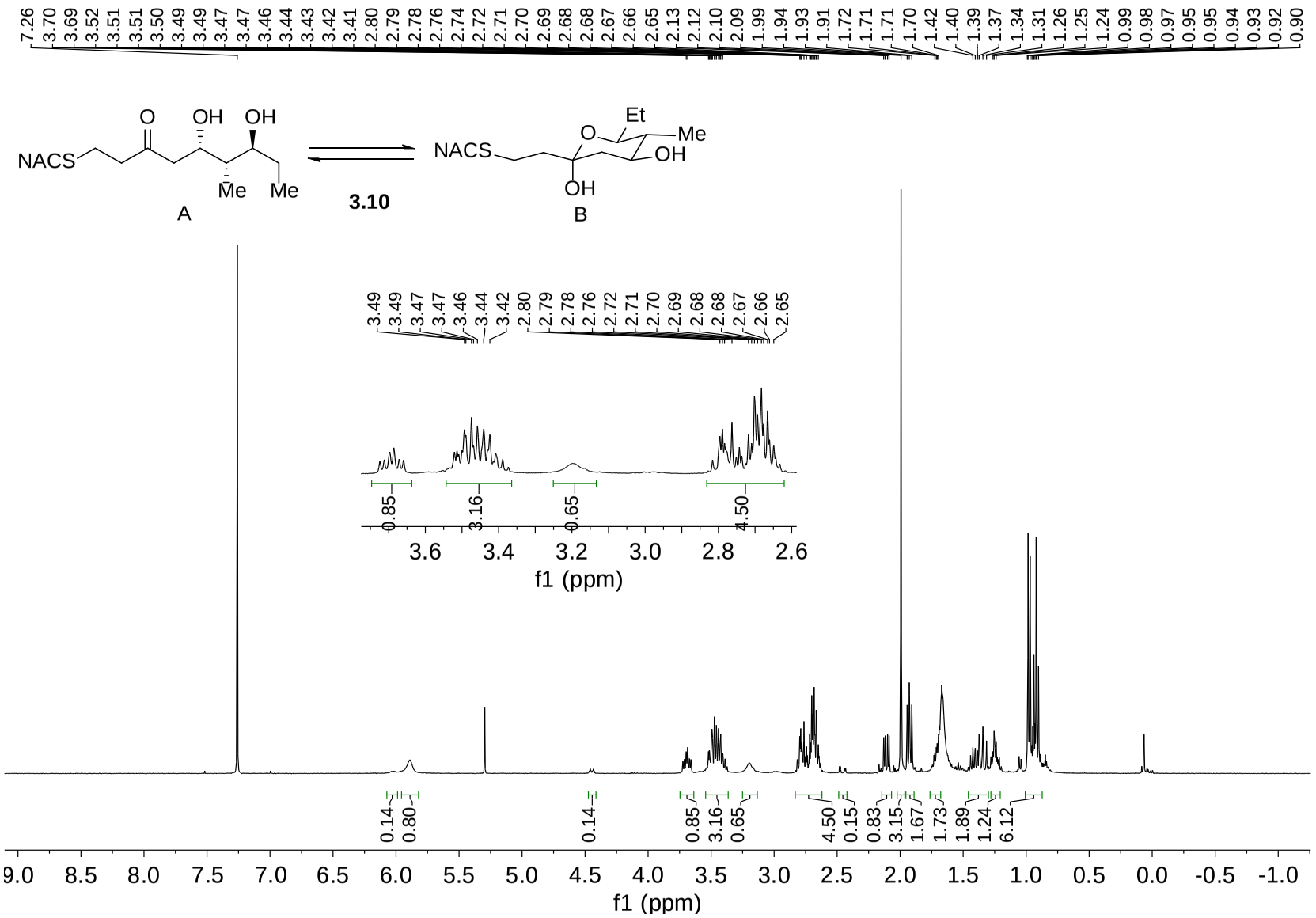
7.26 3.70 3.69 3.52 3.51 3.51 3.50 3.49 3.49 3.47 3.47 3.46 3.44 3.43 3.42 3.41 2.80 2.79 2.78 2.76 2.74 2.72 2.71 2.70 2.69 2.68 2.68 2.67 2.66 2.65 2.13 2.12 2.10 2.09 1.99 1.94 1.93 1.91 1.72 1.71 1.71 1.70 1.42 1.40 1.39 1.37 1.34 1.31 1.26 1.25 1.24 0.99 0.98 0.97 0.95 0.95 0.94 0.93 0.92 0.90
O
OH
OH
NACS
Me
Me
A
3.10
Et
O
Me
NACS
OH
OH
B
3.49 3.49 3.47 3.47 3.46 3.44 3.42 2.80 2.79 2.78 2.76 2.72 2.71 2.70 2.69 2.68 2.68 2.67 2.66 2.65
0.85
3.16
0.65
4.50
3.6 3.4 3.2 3.0 2.8 2.6
f1 (ppm)
0.14 0.80 0.14 0.85 3.16 0.65 4.50 0.15 0.83 3.15 1.67 1.73 1.89 1.24 6.12
9.0 8.5 8.0 7.5 7.0 6.5 6.0 5.5 5.0 4.5 4.0 3.5 3.0 2.5 2.0 1.5 1.0 0.5 0.0 -0.5 -1.0
f1 (ppm)

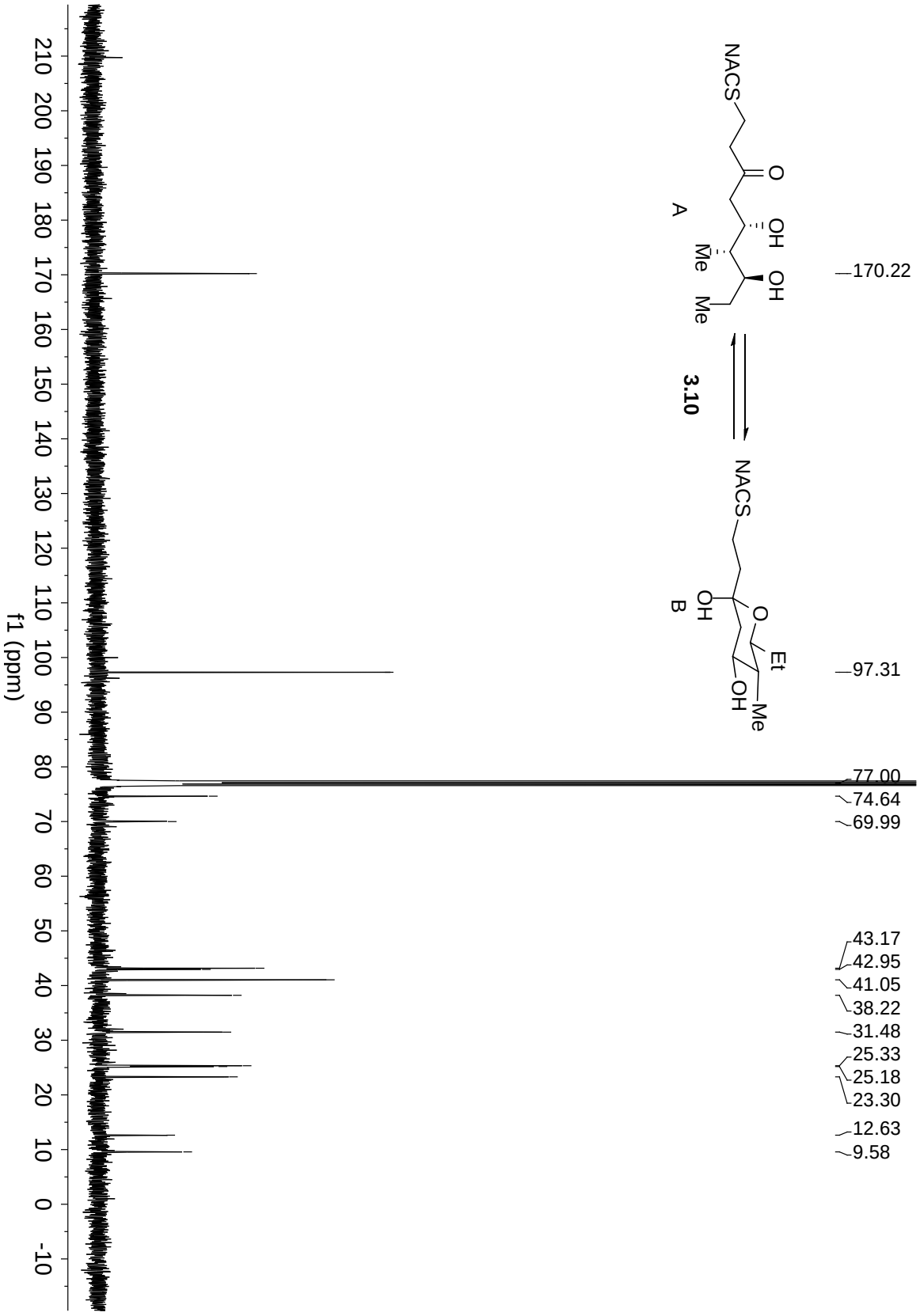
NACS
O
OH
OH
Me
Me
A
3.10
NACS
OH
B
O
Et
OH
Me
170.22
97.31
77.00
74.64
69.99
43.17
42.95
41.05
38.22
31.48
25.33
25.18
23.30
12.63
9.58
f1 (ppm)

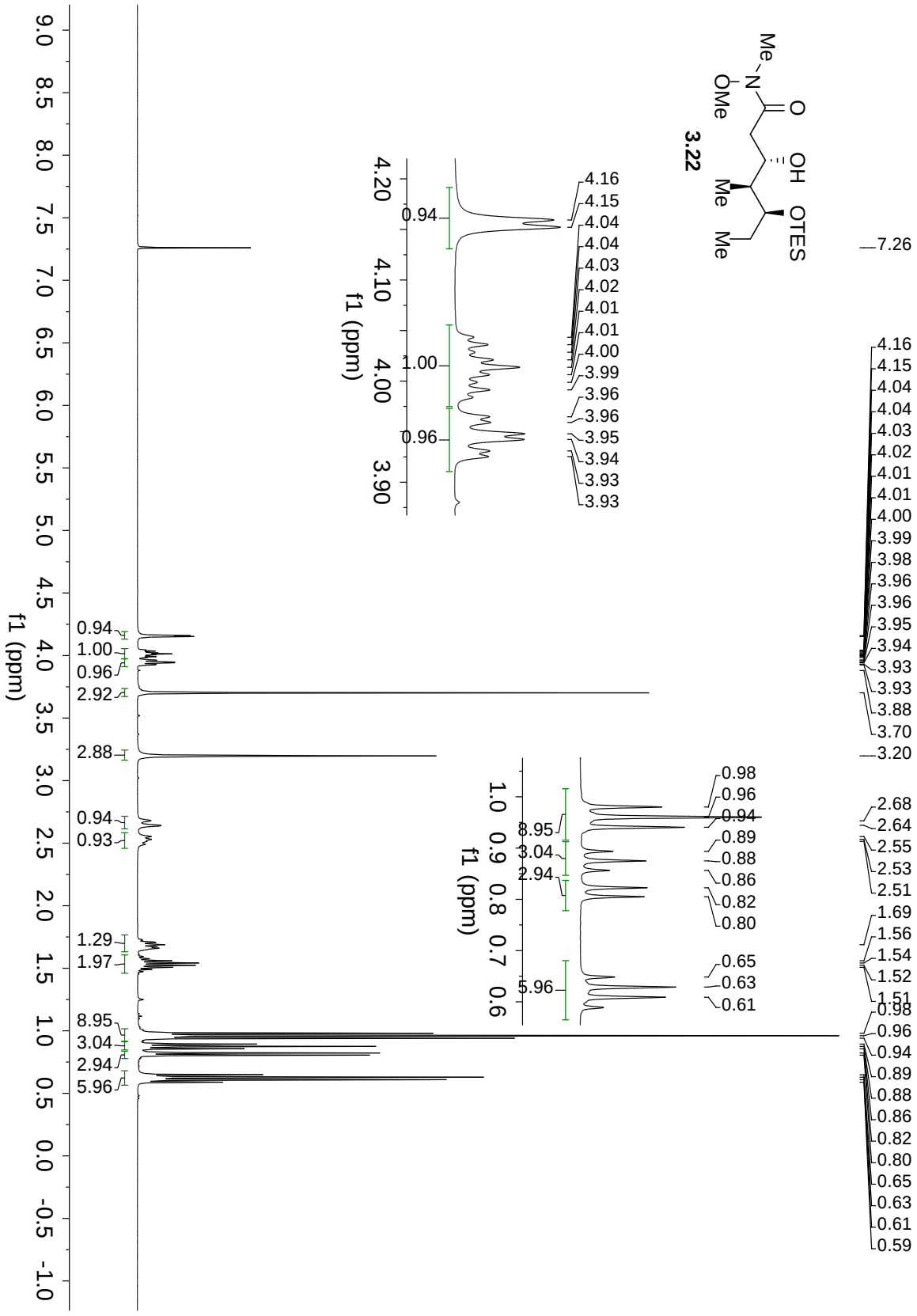
3.22
Me
N
OMe
O
OH
OTES
Me
Me
f1 (ppm)
9.0 8.5 8.0 7.5 7.0 6.5 6.0 5.5 5.0 4.5 4.0 3.5 3.0 2.5 2.0 1.5 1.0 0.5 0.0 -0.5 -1.0
0.94
1.00
0.96
2.92
2.88
0.94
0.93
1.29
1.97
8.95
3.04
2.94
5.96
4.20 4.10 4.00 3.90
0.94
1.00
0.96
4.16
4.15
4.04
4.04
4.03
4.02
4.01
4.01
4.00
3.99
3.96
3.96
3.95
3.94
3.93
3.93
1.0 0.9 0.8 0.7 0.6
8.95
3.04
2.94
5.96
0.98
0.96
0.94
0.89
0.88
0.86
0.82
0.80
0.65
0.63
0.61
7.26
4.16
4.15
4.04
4.04
4.03
4.02
4.01
4.01
4.00
3.99
3.98
3.96
3.96
3.95
3.94
3.93
3.93
3.88
3.70
3.20
2.68
2.64
2.55
2.53
2.51
1.69
1.56
1.54
1.52
1.51
0.98
0.96
0.94
0.89
0.88
0.86
0.82
0.80
0.65
0.63
0.61
0.59

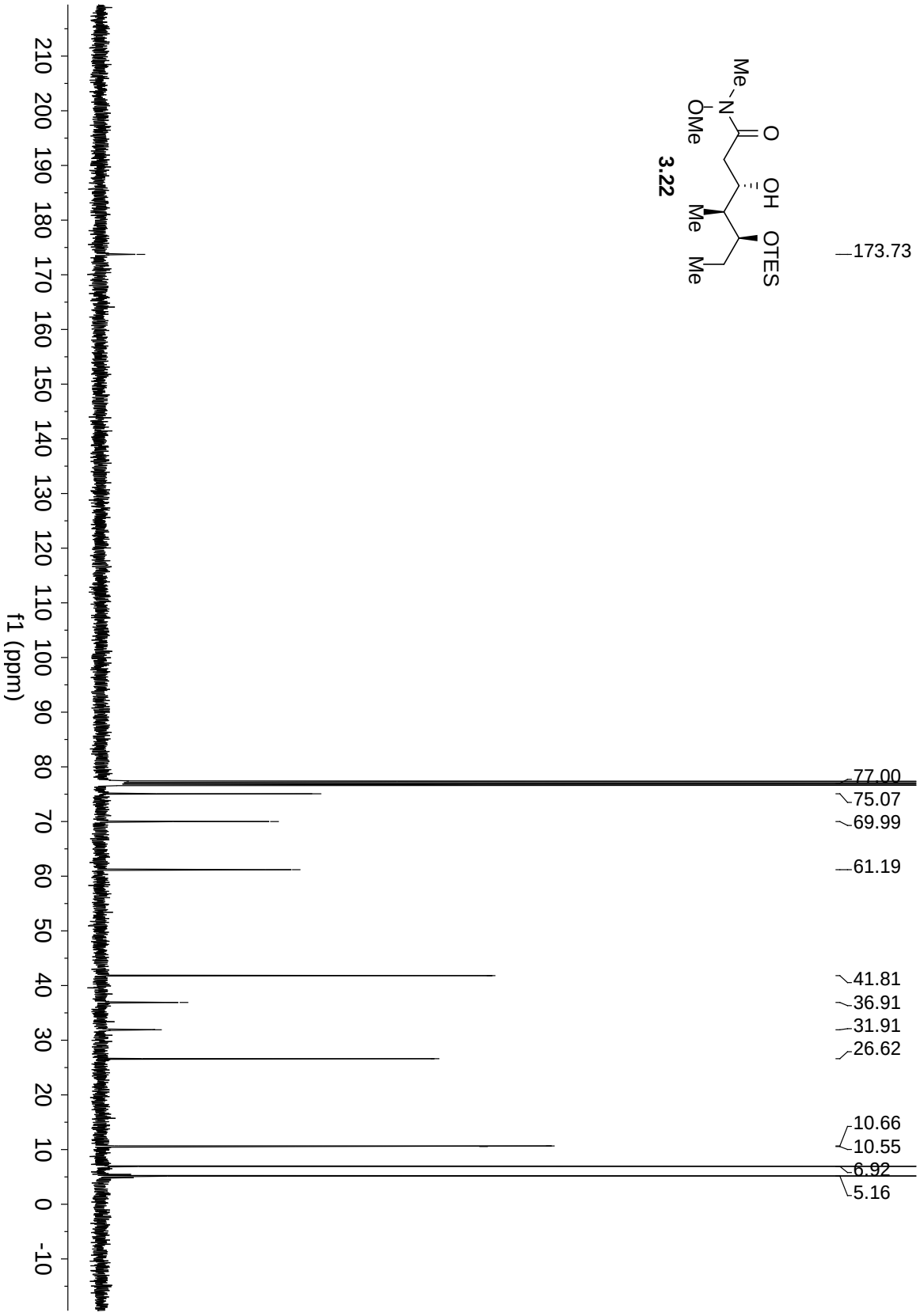
3.22
Me
N
OMe
O
OH
OTES
Me
Me
173.73
77.00
75.07
69.99
61.19
41.81
36.91
31.91
26.62
10.66
10.55
6.92
5.16
f1 (ppm)
210 200 190 180 170 160 150 140 130 120 110 100 90 80 70 60 50 40 30 20 10 0 -10

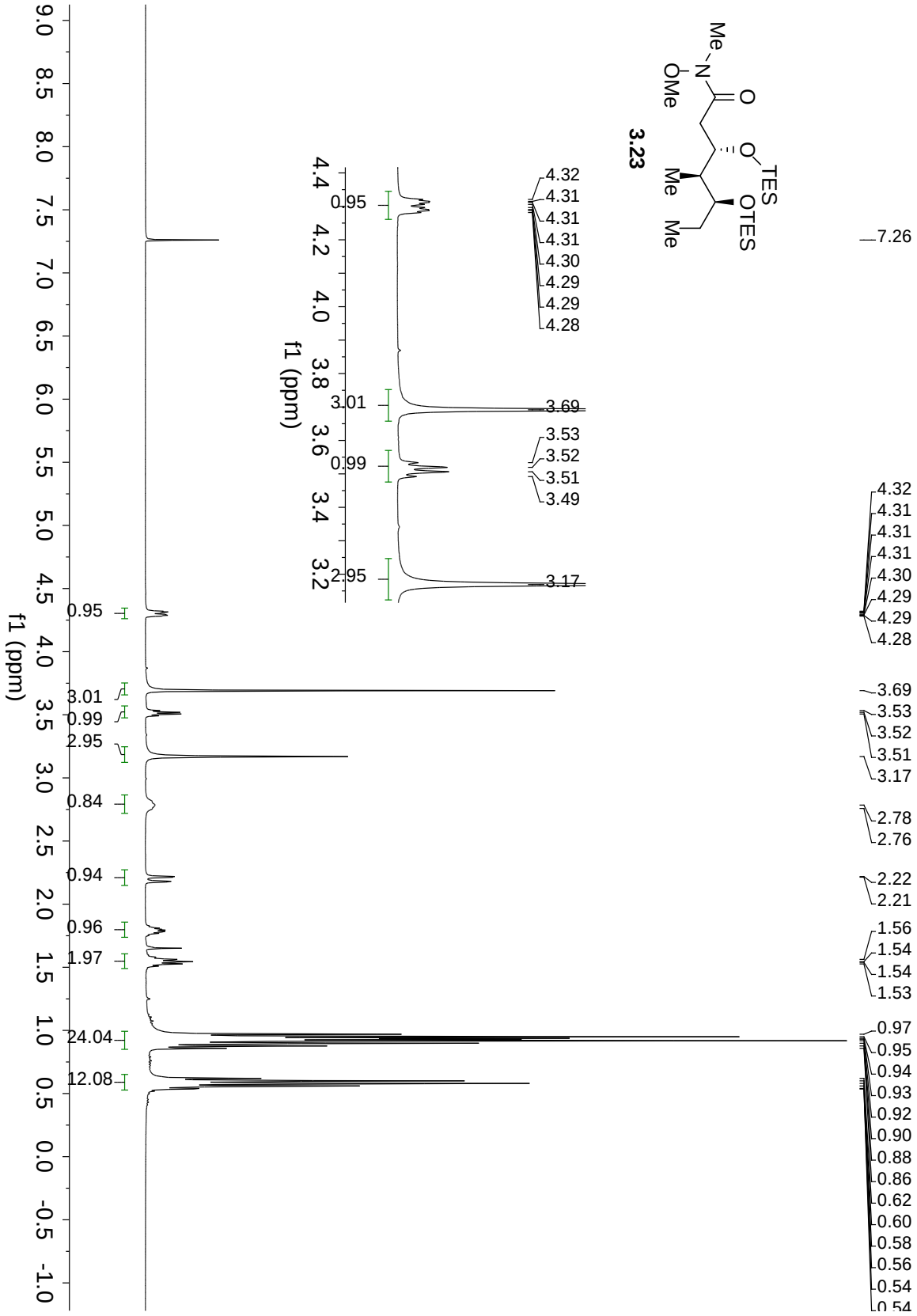
3.23
Me
N
OMe
O
O
TES
OTES
Me
Me
Me
f1 (ppm)
9.0 8.5 8.0 7.5 7.0 6.5 6.0 5.5 5.0 4.5 4.0 3.5 3.0 2.5 2.0 1.5 1.0 0.5 0.0 -0.5 -1.0
0.95
3.01
0.99
2.95
0.84
0.94
0.96
1.97
24.04
12.08
4.4 4.2 4.0 3.8 3.6 3.4 3.2
0.95
3.01
0.99
2.95
4.32
4.31
4.31
4.31
4.30
4.29
4.29
4.28
3.69
3.53
3.52
3.51
3.49
3.17
7.26
4.32
4.31
4.31
4.31
4.30
4.29
4.29
4.28
3.69
3.53
3.52
3.51
3.17
2.78
2.76
2.22
2.21
1.56
1.54
1.54
1.53
0.97
0.95
0.94
0.93
0.92
0.90
0.88
0.86
0.62
0.60
0.58
0.56
0.54
0.54

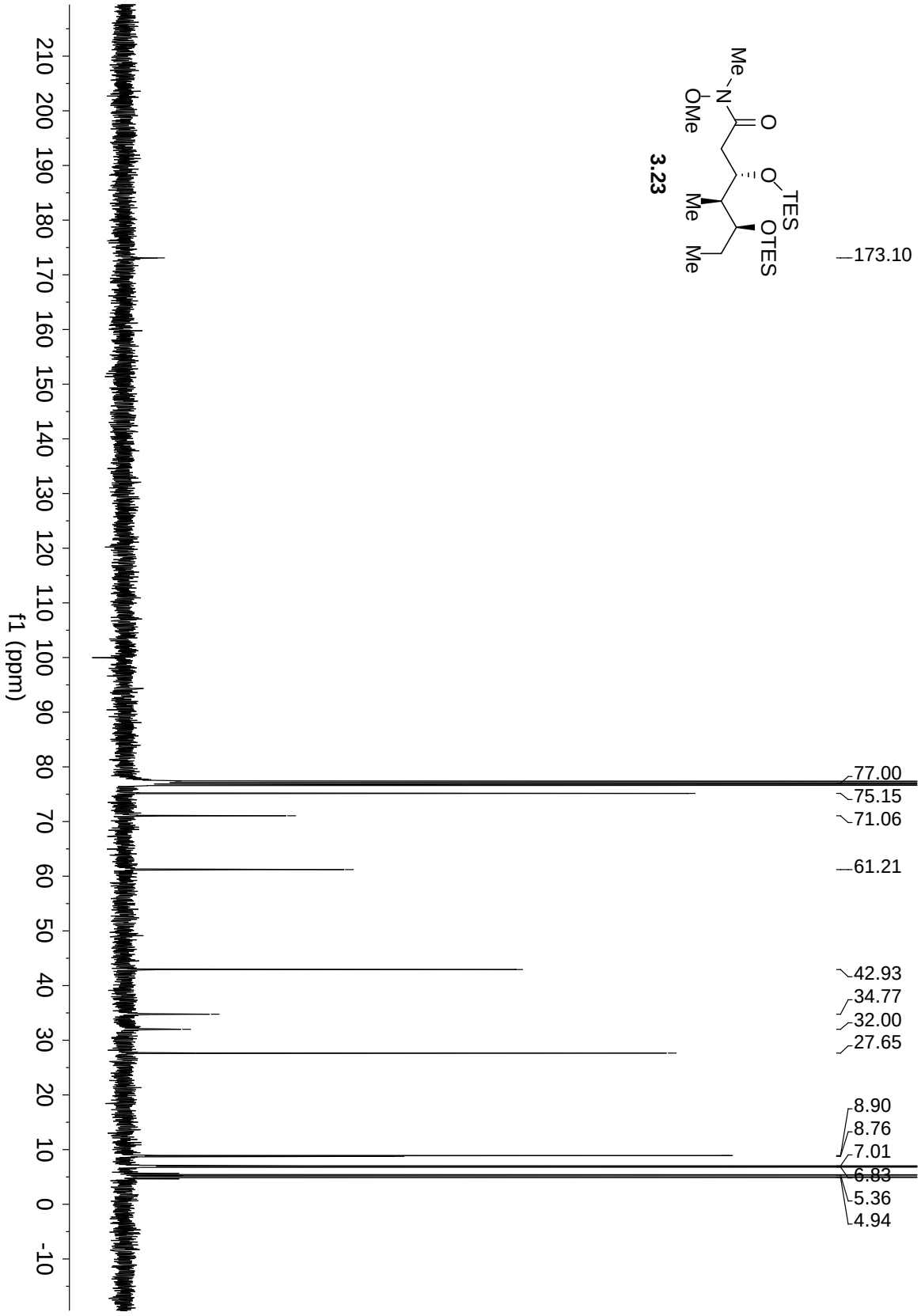
3.23
Me
N
OMe
O
O
TES
OTES
Me
Me
173.10
77.00
75.15
71.06
61.21
42.93
34.77
32.00
27.65
8.90
8.76
7.01
6.83
5.36
4.94
f1 (ppm)
210 200 190 180 170 160 150 140 130 120 110 100 90 80 70 60 50 40 30 20 10 0 -10

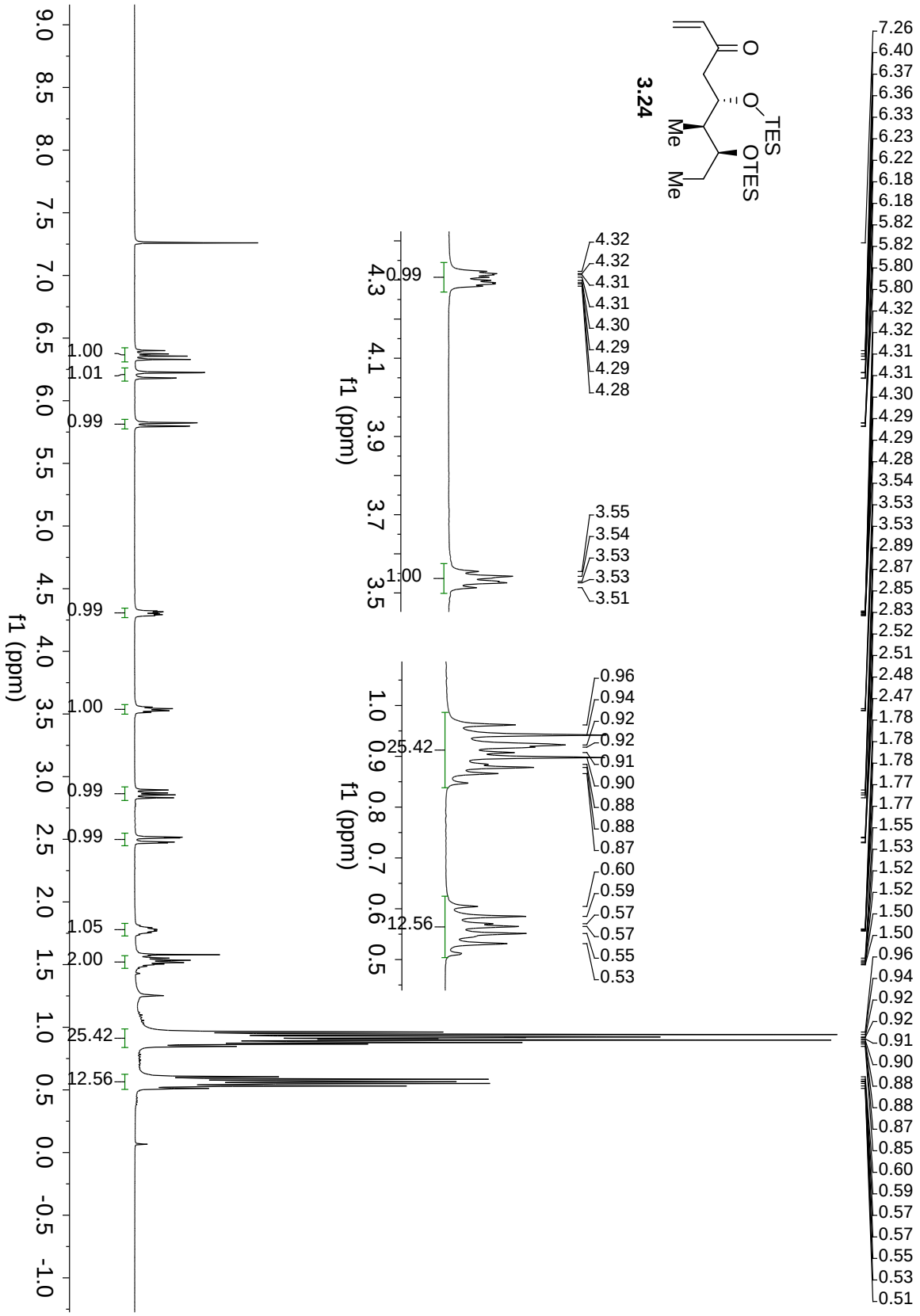
3.24
TES
OTES
Me
Me
f1 (ppm)
1.00
1.01
0.99
0.99
1.00
0.99
0.99
1.05
2.00
25.42
12.56
0.99
1.00
25.42
12.56

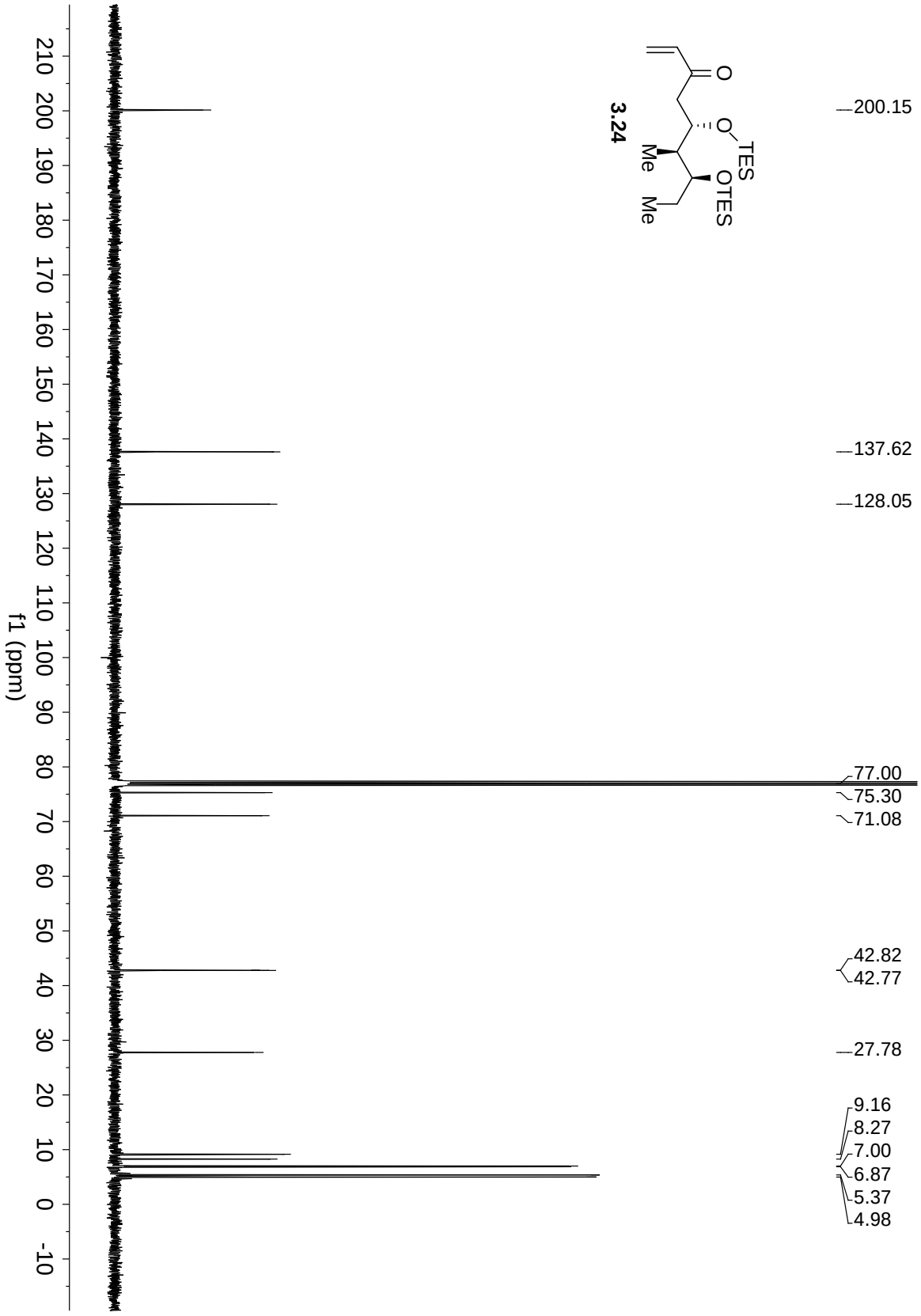
3.24
O
O
TES
OTES
Me
Me
200.15
137.62
128.05
77.00
75.30
71.08
42.82
42.77
27.78
9.16
8.27
7.00
6.87
5.37
4.98
f1 (ppm)
210 200 190 180 170 160 150 140 130 120 110 100 90 80 70 60 50 40 30 20 10 0 -10

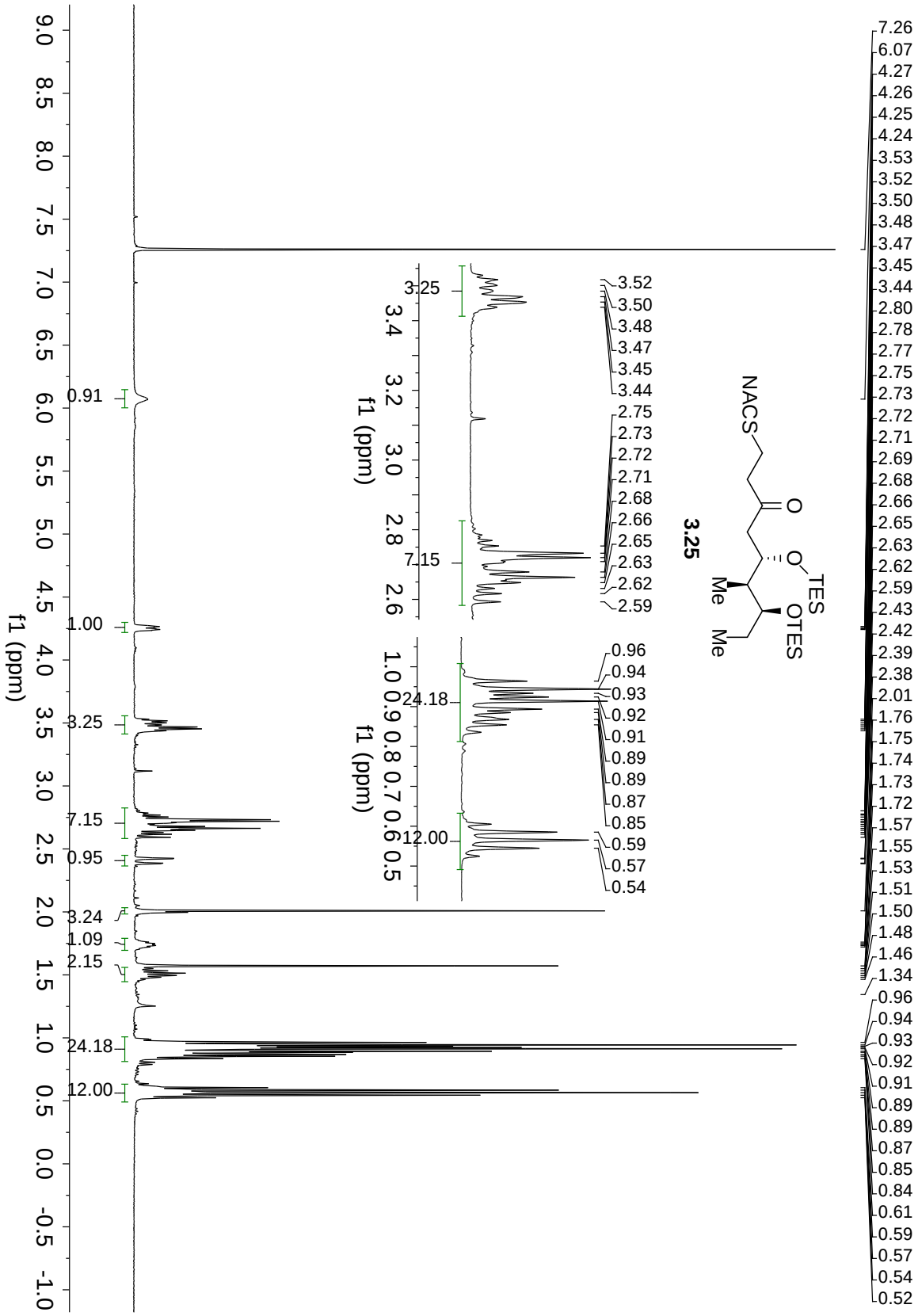
f1 (ppm)
9.0 8.5 8.0 7.5 7.0 6.5 6.0 5.5 5.0 4.5 4.0 3.5 3.0 2.5 2.0 1.5 1.0 0.5 0.0 -0.5 -1.0
0.91
1.00
3.25
7.15
0.95
3.24
1.09
2.15
24.18
12.00
3.25
7.15
3.52
3.50
3.48
3.47
3.45
3.44
2.75
2.73
2.72
2.71
2.68
2.66
2.65
2.63
2.62
2.59
24.18
12.00
0.96
0.94
0.93
0.92
0.91
0.89
0.89
0.87
0.85
0.59
0.57
0.54
NACS
O
O
TES
OTES
Me
Me
3.25
7.26
6.07
4.27
4.26
4.25
4.24
3.53
3.52
3.50
3.48
3.47
3.45
3.44
2.80
2.78
2.77
2.75
2.73
2.72
2.71
2.69
2.68
2.66
2.65
2.63
2.62
2.59
2.43
2.42
2.39
2.38
2.01
1.76
1.75
1.74
1.73
1.72
1.57
1.55
1.53
1.51
1.50
1.48
1.46
1.34
0.96
0.94
0.93
0.92
0.91
0.89
0.89
0.87
0.85
0.84
0.61
0.59
0.57
0.54
0.52

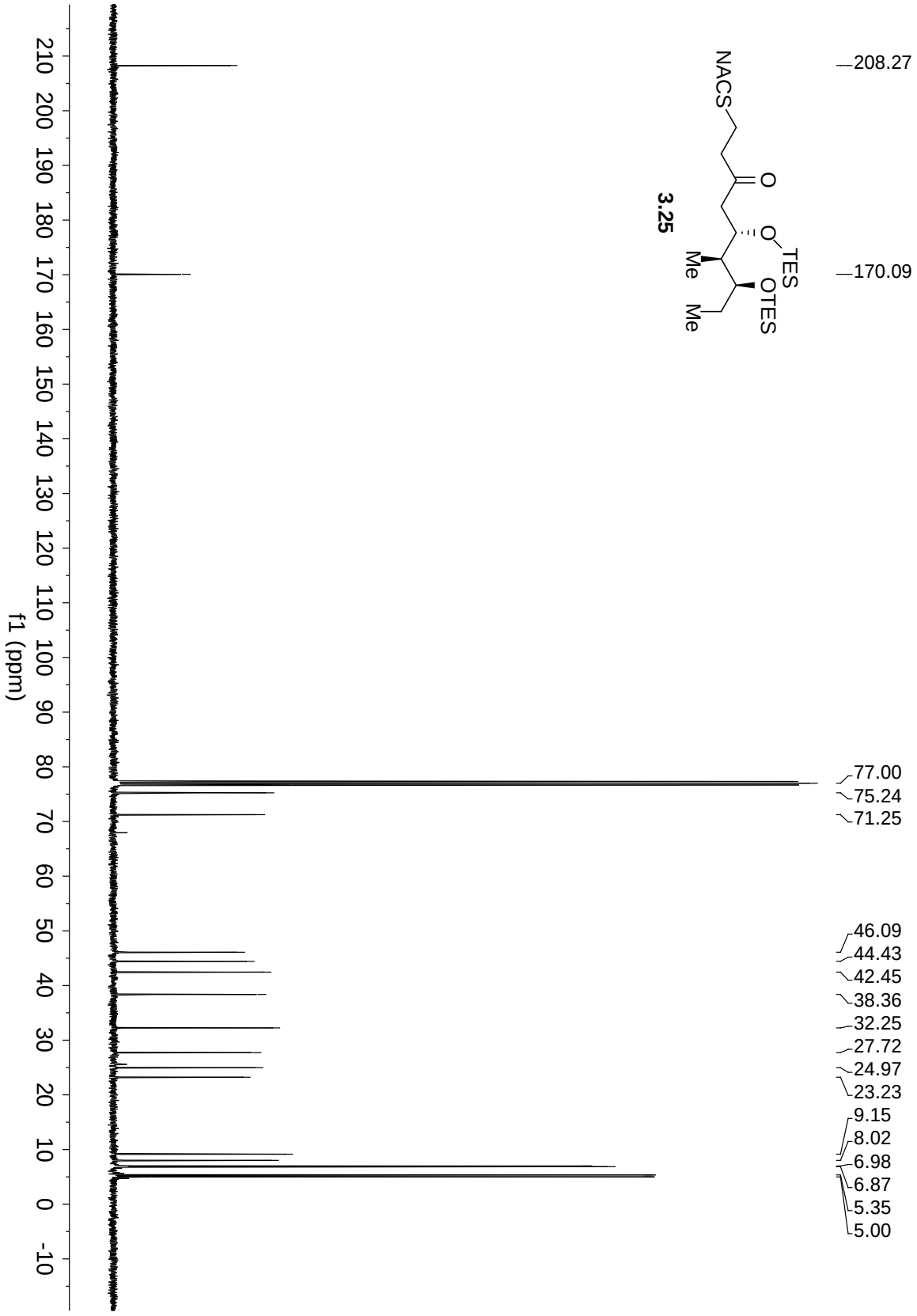
NACS
O
O
TES
OTES
Me
Me
3.25
208.27
170.09
77.00
75.24
71.25
46.09
44.43
42.45
38.36
32.25
27.72
24.97
23.23
9.15
8.02
6.98
6.87
5.35
5.00
f1 (ppm)
210 200 190 180 170 160 150 140 130 120 110 100 90 80 70 60 50 40 30 20 10 0 -10

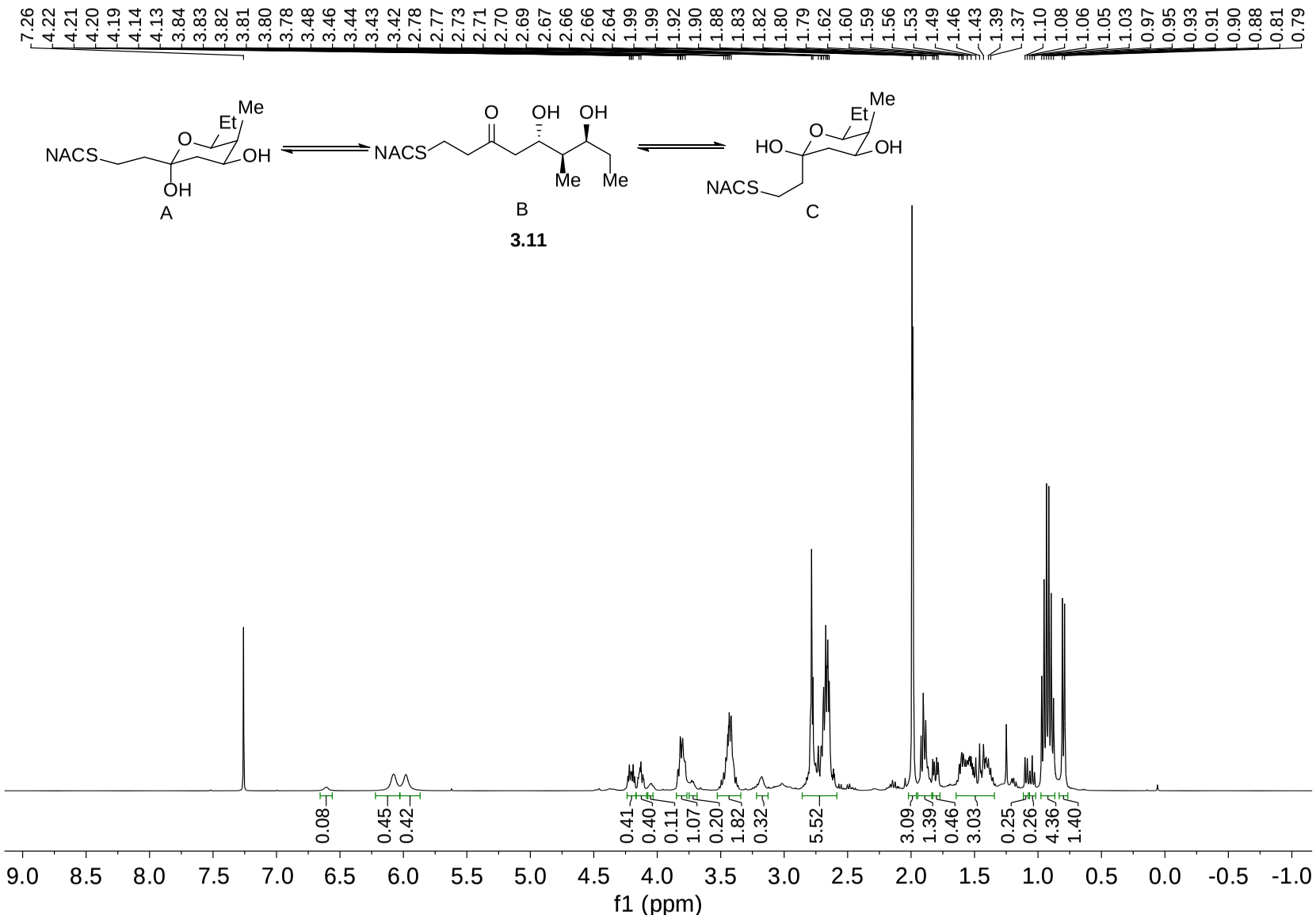
7.26 4.22 4.21 4.20 4.19 4.14 4.13 3.84 3.83 3.82 3.81 3.80 3.78 3.48 3.46 3.44 3.43 3.42 2.78 2.77 2.73 2.71 2.70 2.69 2.67 2.66 2.66 2.64 1.99 1.99 1.92 1.90 1.88 1.83 1.82 1.80 1.79 1.62 1.60 1.59 1.56 1.53 1.49 1.46 1.43 1.39 1.37 1.10 1.08 1.06 1.05 1.03 0.97 0.95 0.93 0.91 0.90 0.88 0.81 0.79
NACS
Me
Et
O
OH
OH
A
NACS
O
OH
OH
Me
Me
B
NACS
HO
Me
Et
O
OH
C
3.11
0.08 0.45 0.42 0.41 0.40 0.11 1.07 0.20 1.82 0.32 5.52 3.09 1.39 0.46 3.03 0.25 0.26 4.36 1.40
9.0 8.5 8.0 7.5 7.0 6.5 6.0 5.5 5.0 4.5 4.0 3.5 3.0 2.5 2.0 1.5 1.0 0.5 0.0 -0.5 -1.0
f1 (ppm)

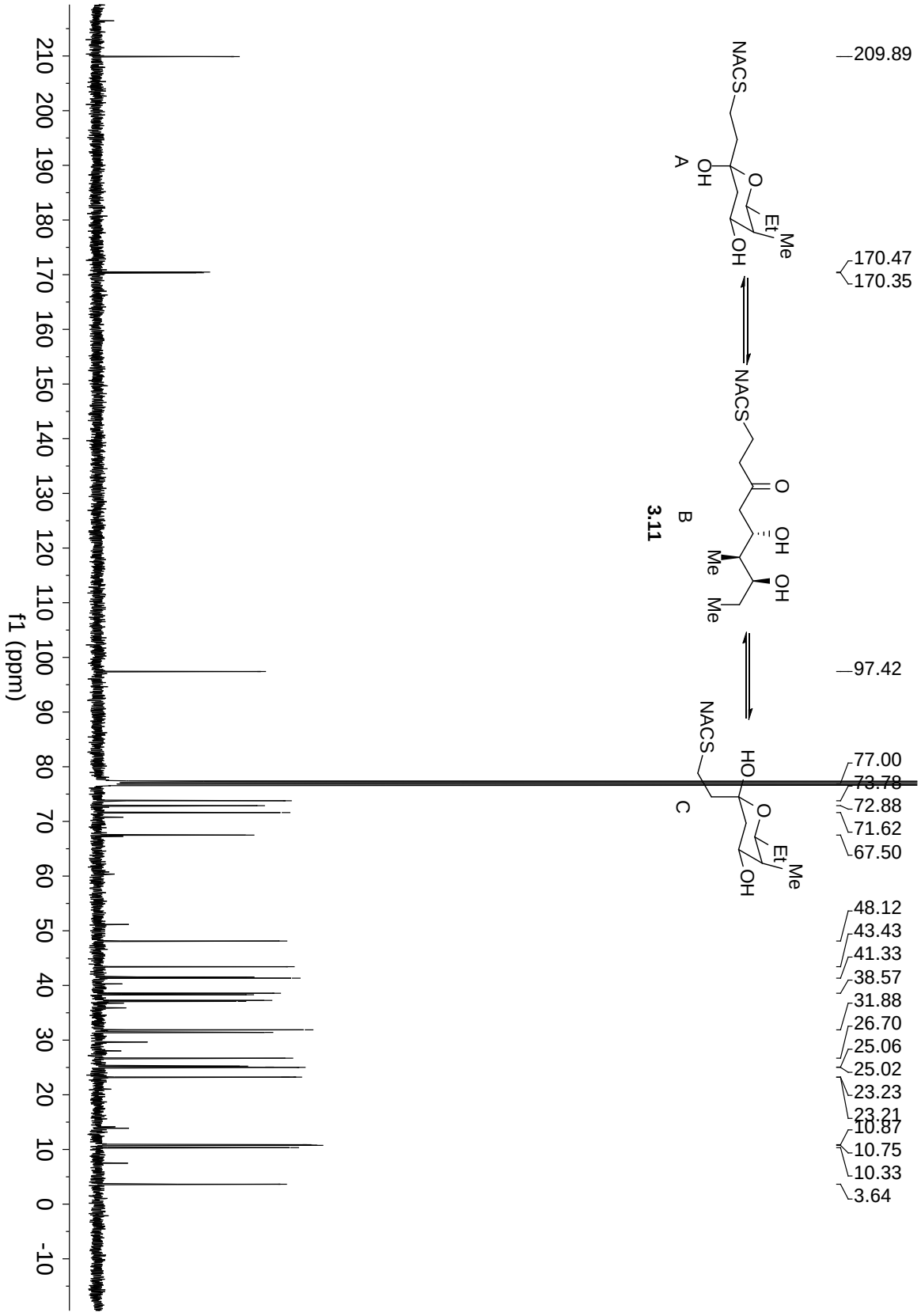
209.89
170.47
170.35
97.42
77.00
73.78
72.88
71.62
67.50
48.12
43.43
41.33
38.57
31.88
26.70
25.06
25.02
23.23
23.21
10.87
10.75
10.33
3.64
f1 (ppm)
A
B
3.11
C

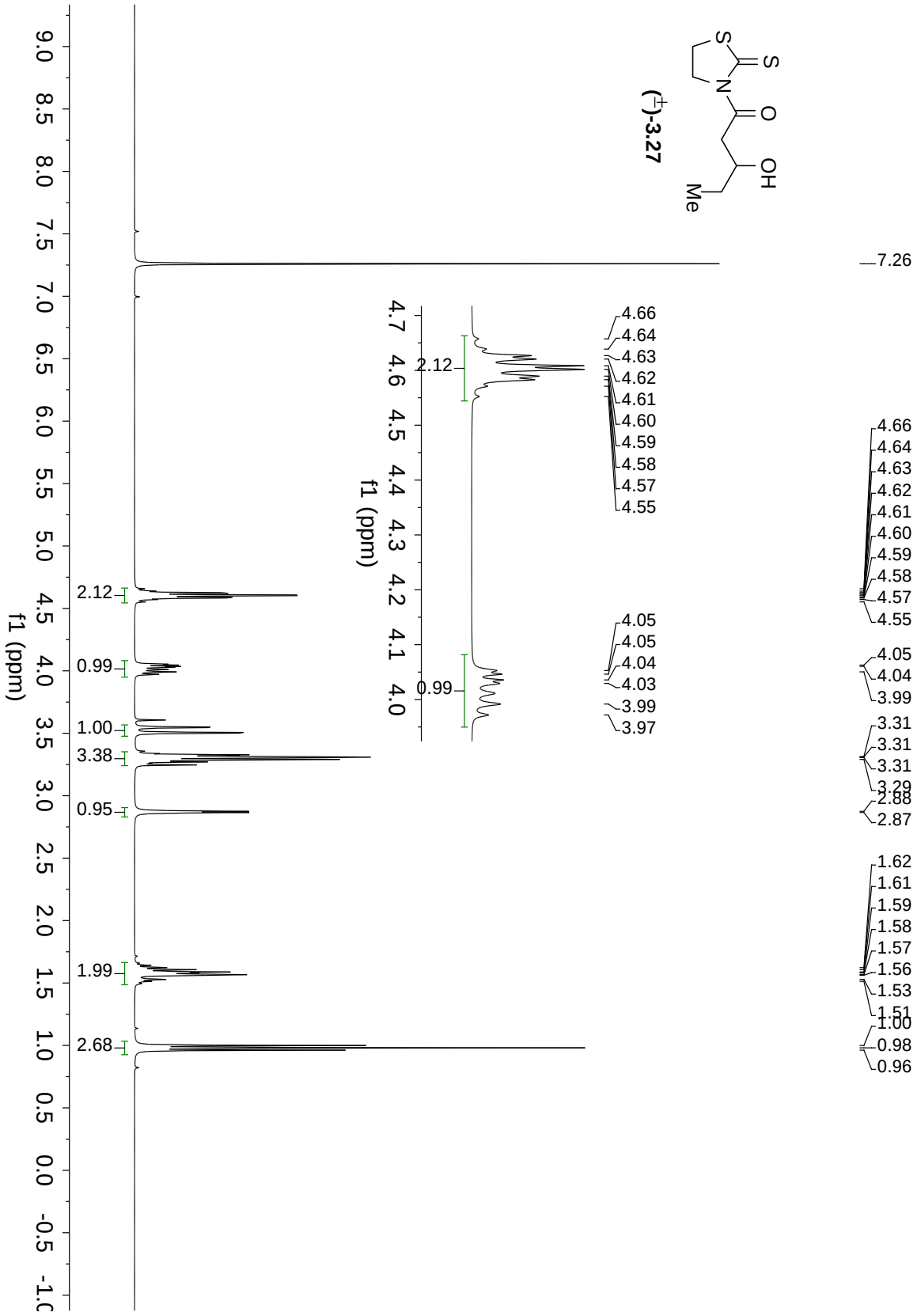
(±)-3.27
S
S
N
O
OH
Me
f1 (ppm)
9.0 8.5 8.0 7.5 7.0 6.5 6.0 5.5 5.0 4.5 4.0 3.5 3.0 2.5 2.0 1.5 1.0 0.5 0.0 -0.5 -1.0
2.12
0.99
1.00
3.38
0.95
1.99
2.68
4.7 4.6 4.5 4.4 4.3 4.2 4.1 4.0
2.12
0.99
4.66
4.64
4.63
4.62
4.61
4.60
4.59
4.58
4.57
4.55
4.05
4.05
4.04
4.03
3.99
3.97
7.26
4.66
4.64
4.63
4.62
4.61
4.60
4.59
4.58
4.57
4.55
4.05
4.04
3.99
3.31
3.31
3.31
3.29
2.88
2.87
1.62
1.61
1.59
1.58
1.57
1.56
1.53
1.51
1.00
0.98
0.96

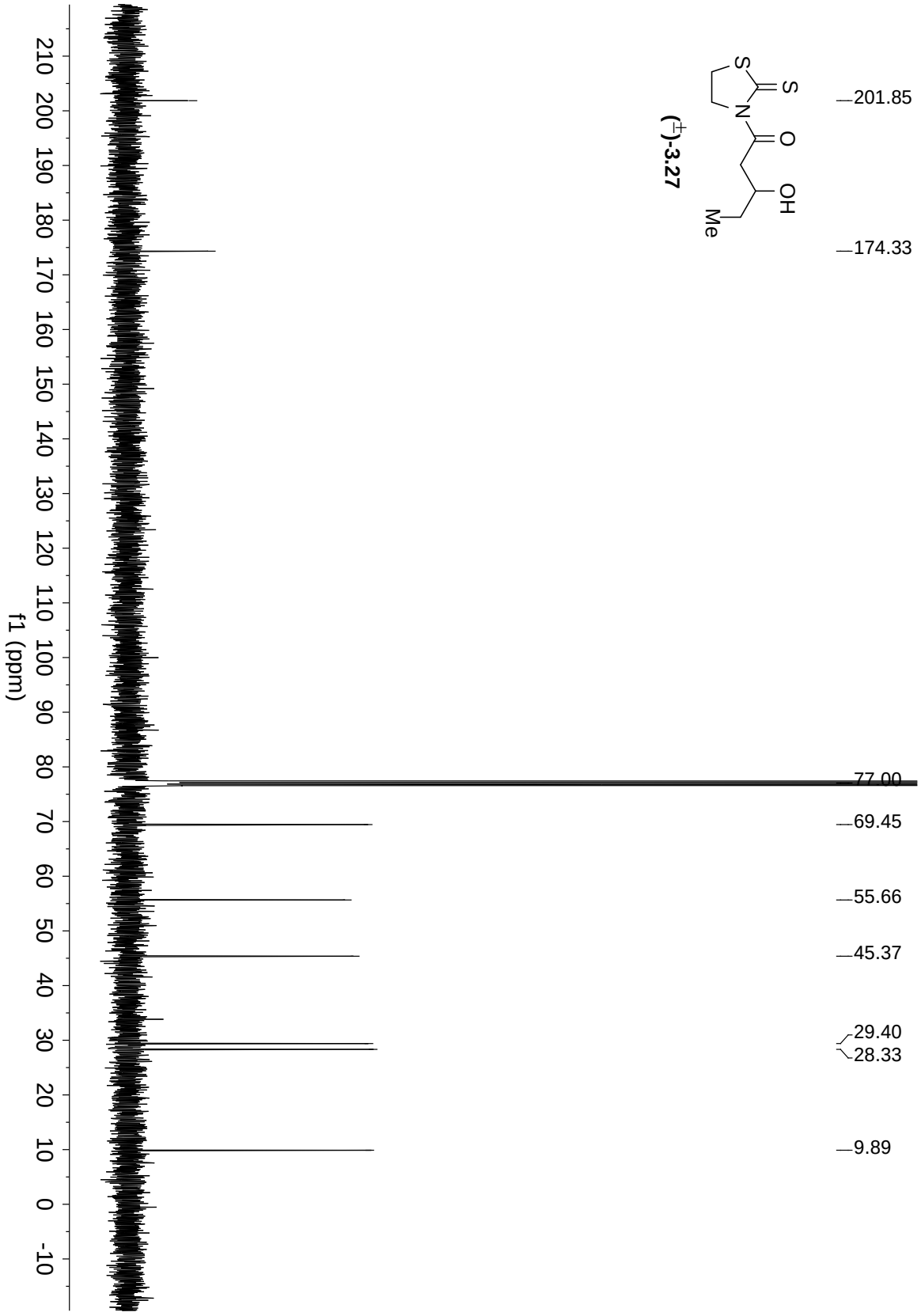
(±)-3.27
S
S
N
O
OH
Me
201.85
174.33
77.00
69.45
55.66
45.37
29.40
28.33
9.89
f1 (ppm)
210 200 190 180 170 160 150 140 130 120 110 100 90 80 70 60 50 40 30 20 10 0 -10

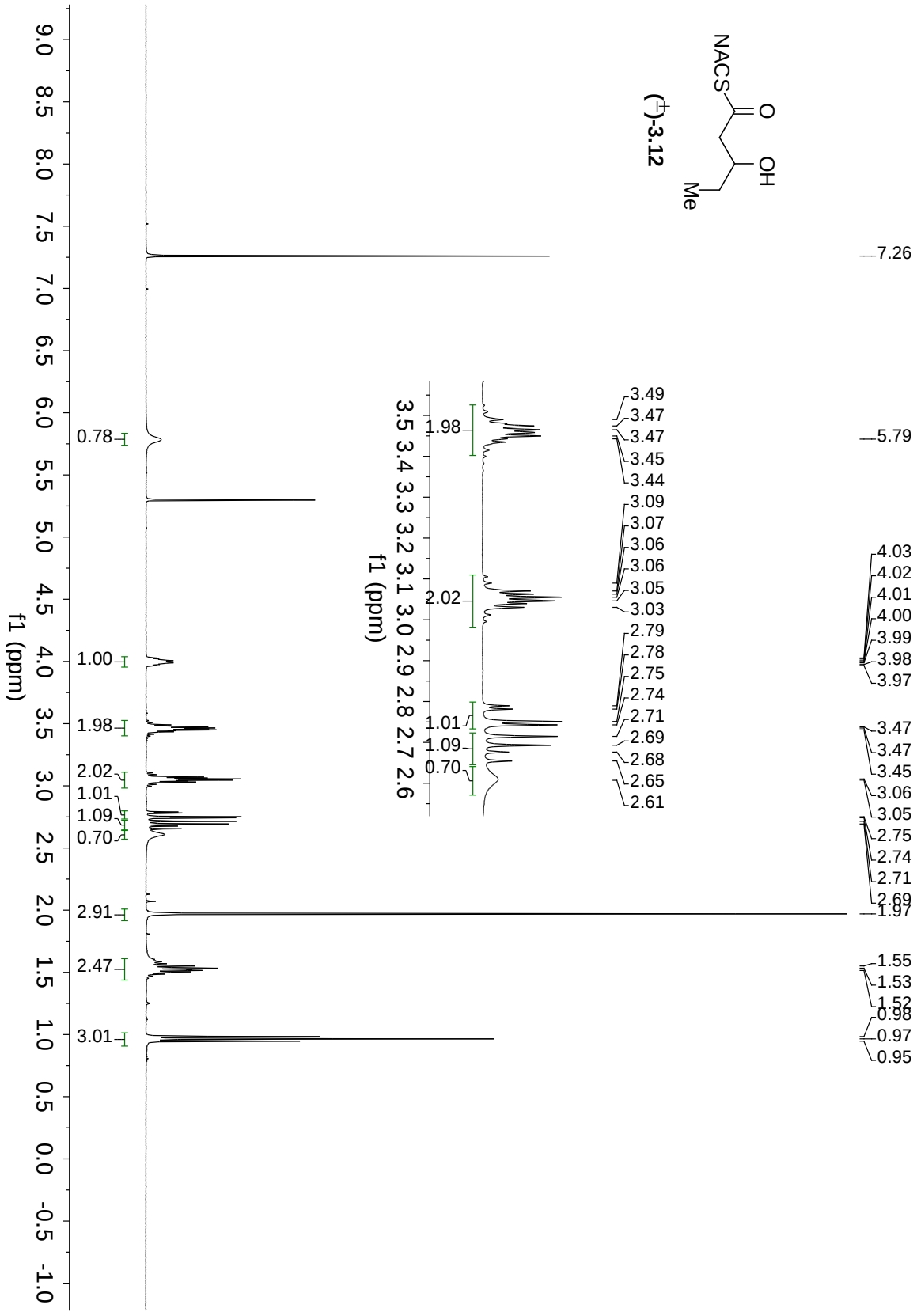
(±)-3.12
NACS
O
OH
Me
f1 (ppm)
9.0 8.5 8.0 7.5 7.0 6.5 6.0 5.5 5.0 4.5 4.0 3.5 3.0 2.5 2.0 1.5 1.0 0.5 0.0 -0.5 -1.0
0.78
1.00
1.98
2.02
1.01
1.09
0.70
2.91
2.47
3.01
3.5 3.4 3.3 3.2 3.1 3.0 2.9 2.8 2.7 2.6
1.98
2.02
1.01
1.09
0.70
3.49
3.47
3.47
3.45
3.44
3.09
3.07
3.06
3.06
3.05
3.03
2.79
2.78
2.75
2.74
2.71
2.69
2.68
2.65
2.61
7.26
5.79
4.03
4.02
4.01
4.00
3.99
3.98
3.97
3.47
3.47
3.45
3.06
3.05
2.75
2.74
2.71
2.69
1.97
1.55
1.53
1.52
0.98
0.97
0.95

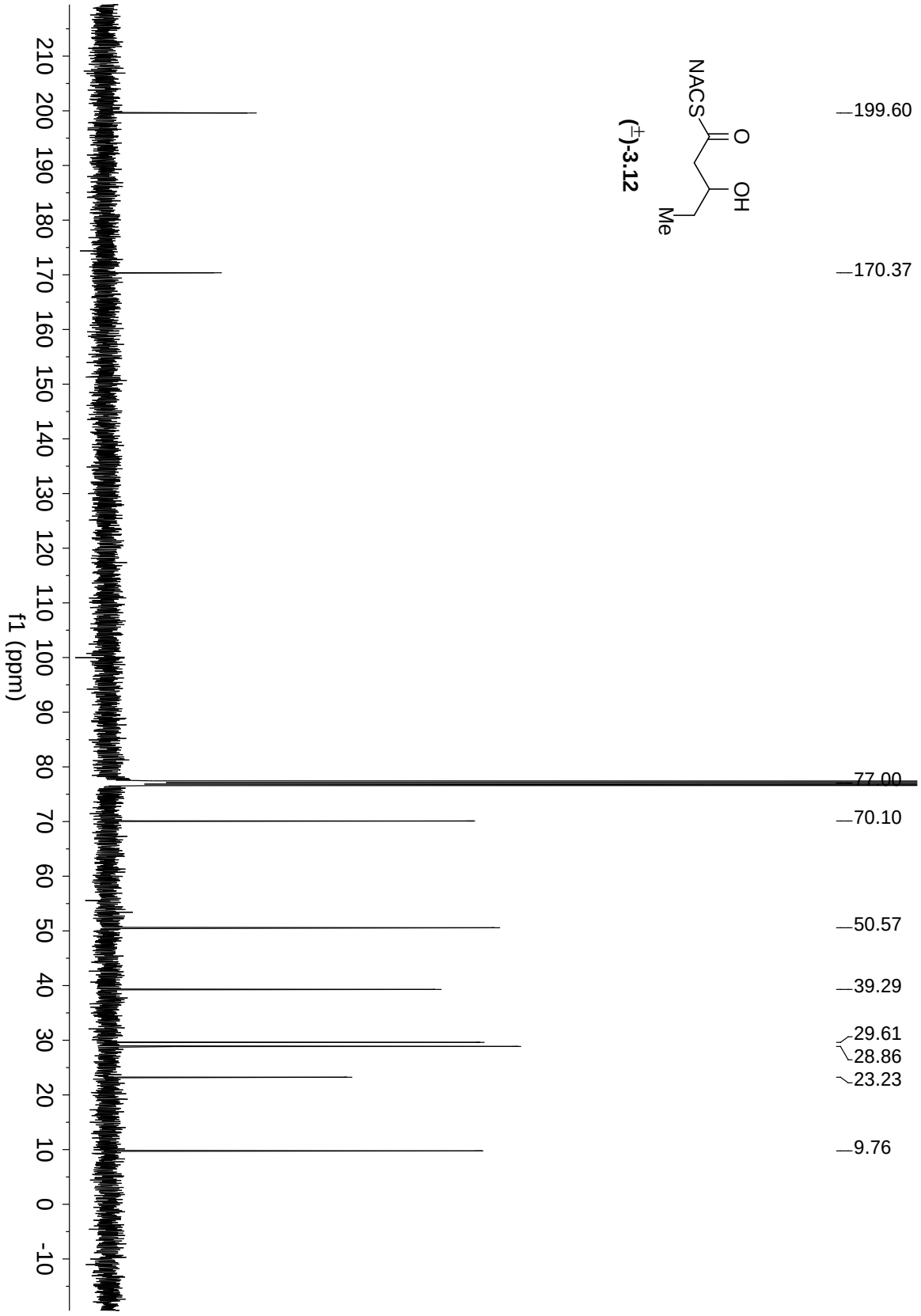
NACS
O
OH
Me
(±)-3.12
199.60
170.37
77.00
70.10
50.57
39.29
29.61
28.86
23.23
9.76
f1 (ppm)
210 200 190 180 170 160 150 140 130 120 110 100 90 80 70 60 50 40 30 20 10 0 -10

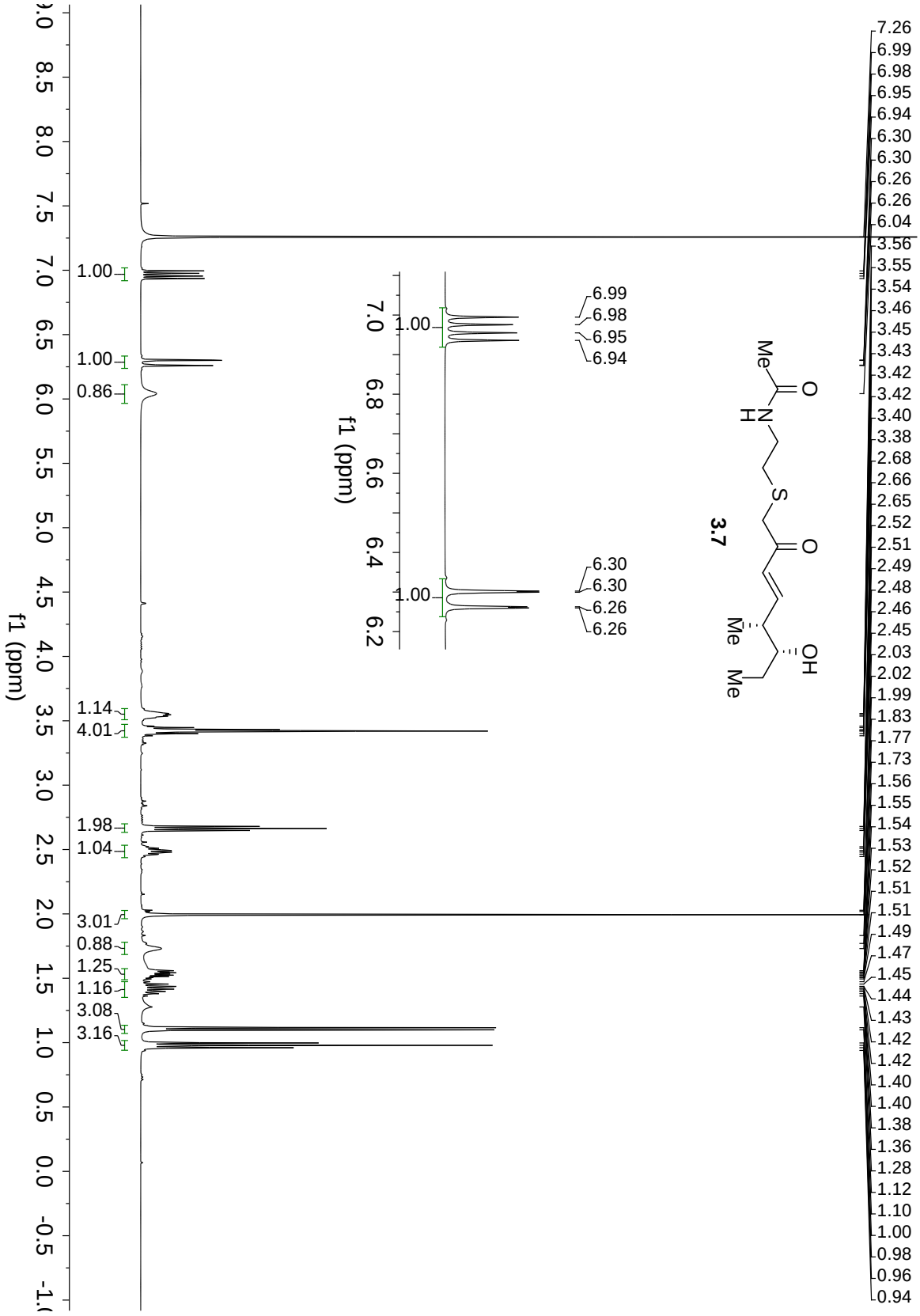
f1 (ppm)
1.00
1.00
0.86
1.14
4.01
1.98
1.04
3.01
0.88
1.25
1.16
3.08
3.16
7.26
6.99
6.98
6.95
6.94
6.30
6.30
6.26
6.26
3.56
3.55
3.54
3.46
3.45
3.43
3.42
3.42
3.40
3.38
2.68
2.66
2.65
2.52
2.51
2.49
2.48
2.46
2.45
2.03
2.02
1.99
1.83
1.77
1.73
1.56
1.55
1.54
1.53
1.52
1.51
1.51
1.49
1.47
1.45
1.44
1.43
1.42
1.42
1.40
1.40
1.38
1.36
1.28
1.12
1.10
1.00
0.98
0.96
0.94
3.7

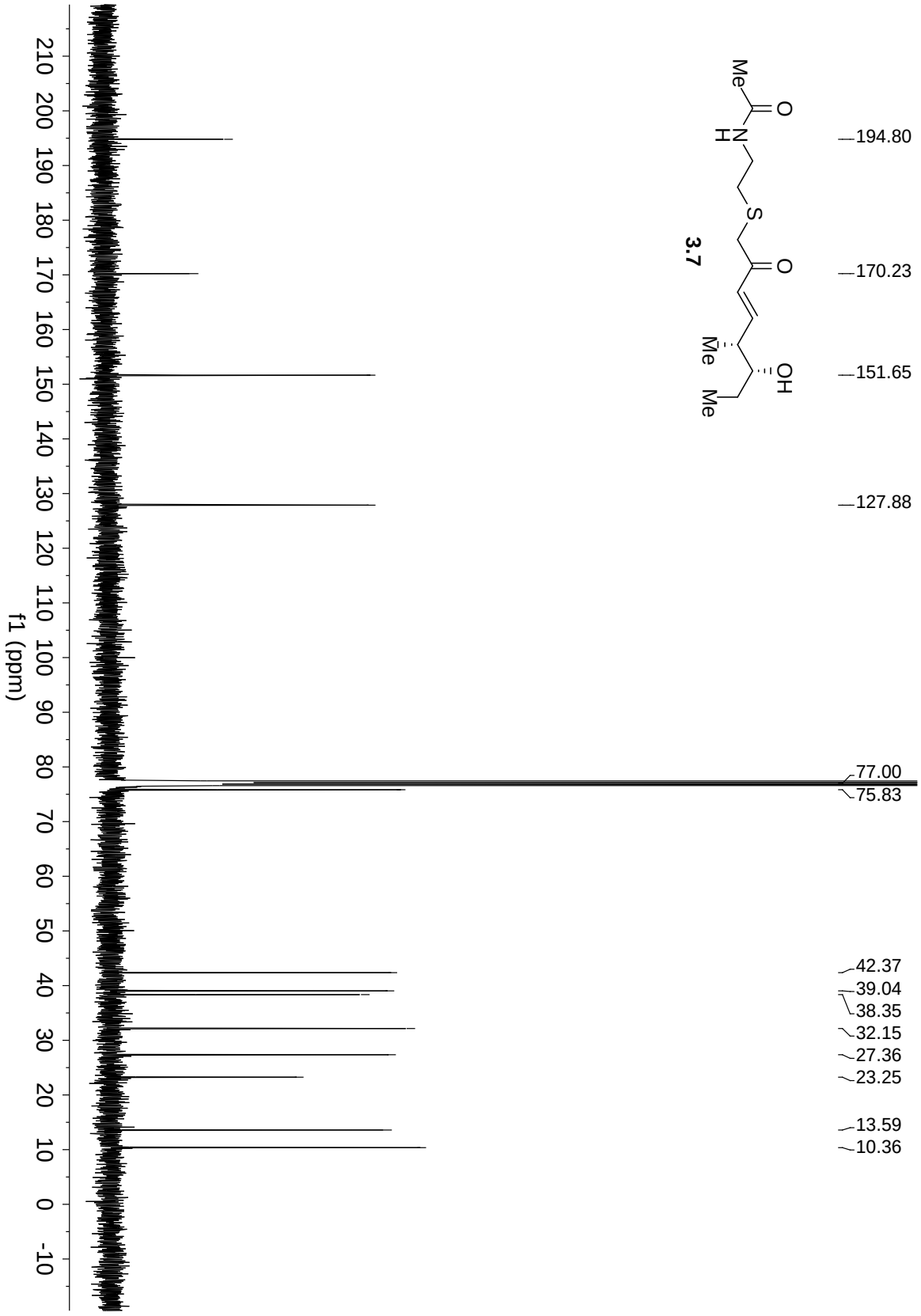
f1 (ppm)
210 200 190 180 170 160 150 140 130 120 110 100 90 80 70 60 50 40 30 20 10 0 -10
Me
O
N
H
S
O
Me
OH
Me
3.7
194.80
170.23
151.65
127.88
77.00
75.83
42.37
39.04
38.35
32.15
27.36
23.25
13.59
10.36

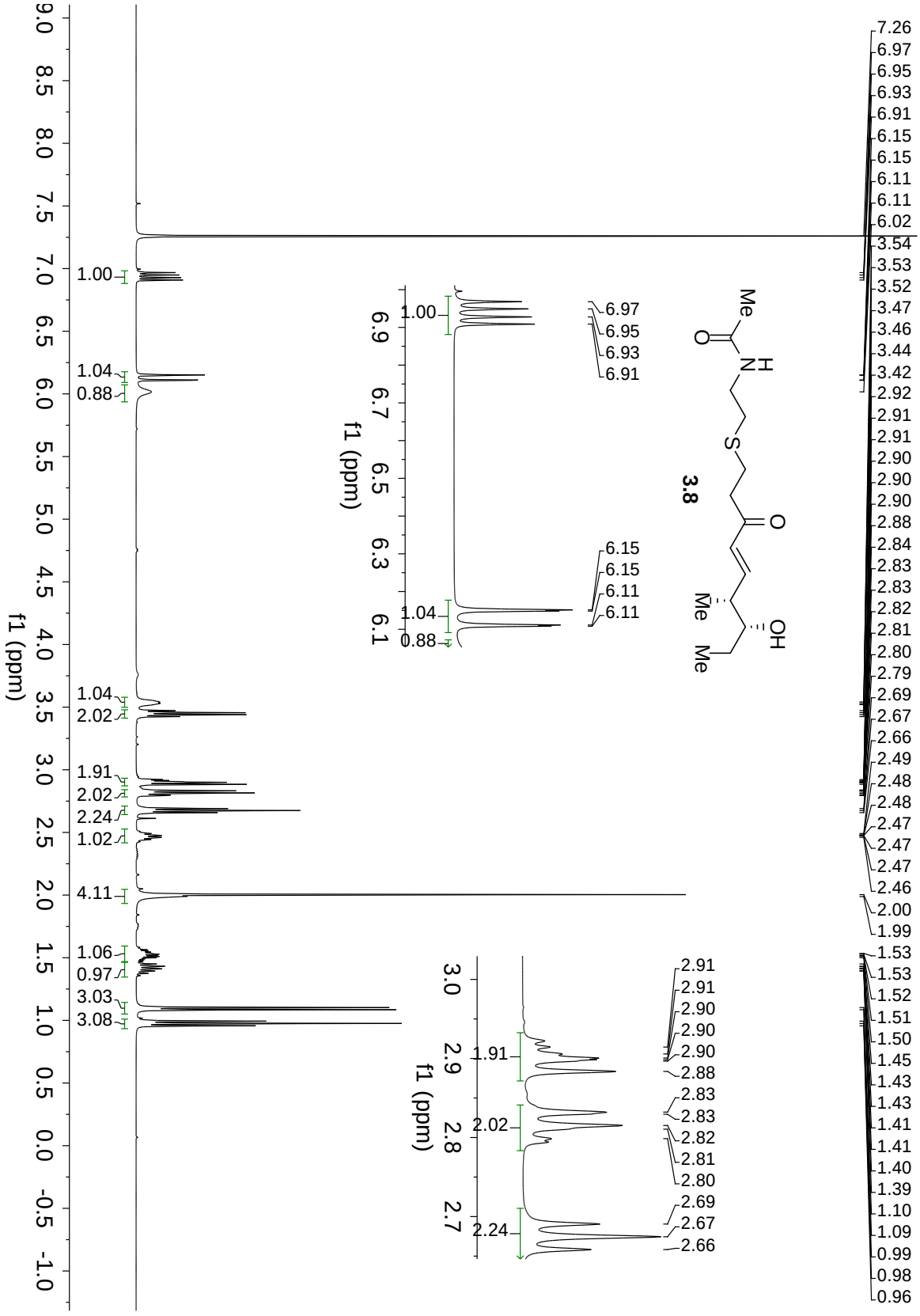
f1 (ppm)
9.0 8.5 8.0 7.5 7.0 6.5 6.0 5.5 5.0 4.5 4.0 3.5 3.0 2.5 2.0 1.5 1.0 0.5 0.0 -0.5 -1.0
1.00
1.04
0.88
1.04
2.02
1.91
2.02
2.24
1.02
4.11
1.06
0.97
3.03
3.08
7.26
6.97
6.95
6.93
6.91
6.15
6.15
6.11
6.11
6.02
3.54
3.53
3.52
3.47
3.46
3.44
3.42
2.92
2.91
2.91
2.90
2.90
2.90
2.88
2.84
2.83
2.83
2.82
2.81
2.80
2.79
2.69
2.67
2.66
2.49
2.48
2.48
2.47
2.47
2.47
2.46
2.00
1.99
1.53
1.53
1.52
1.51
1.50
1.45
1.43
1.43
1.41
1.41
1.40
1.39
1.10
1.09
0.99
0.98
0.96
Me
O
H
N
S
O
Me
OH
Me
3.8

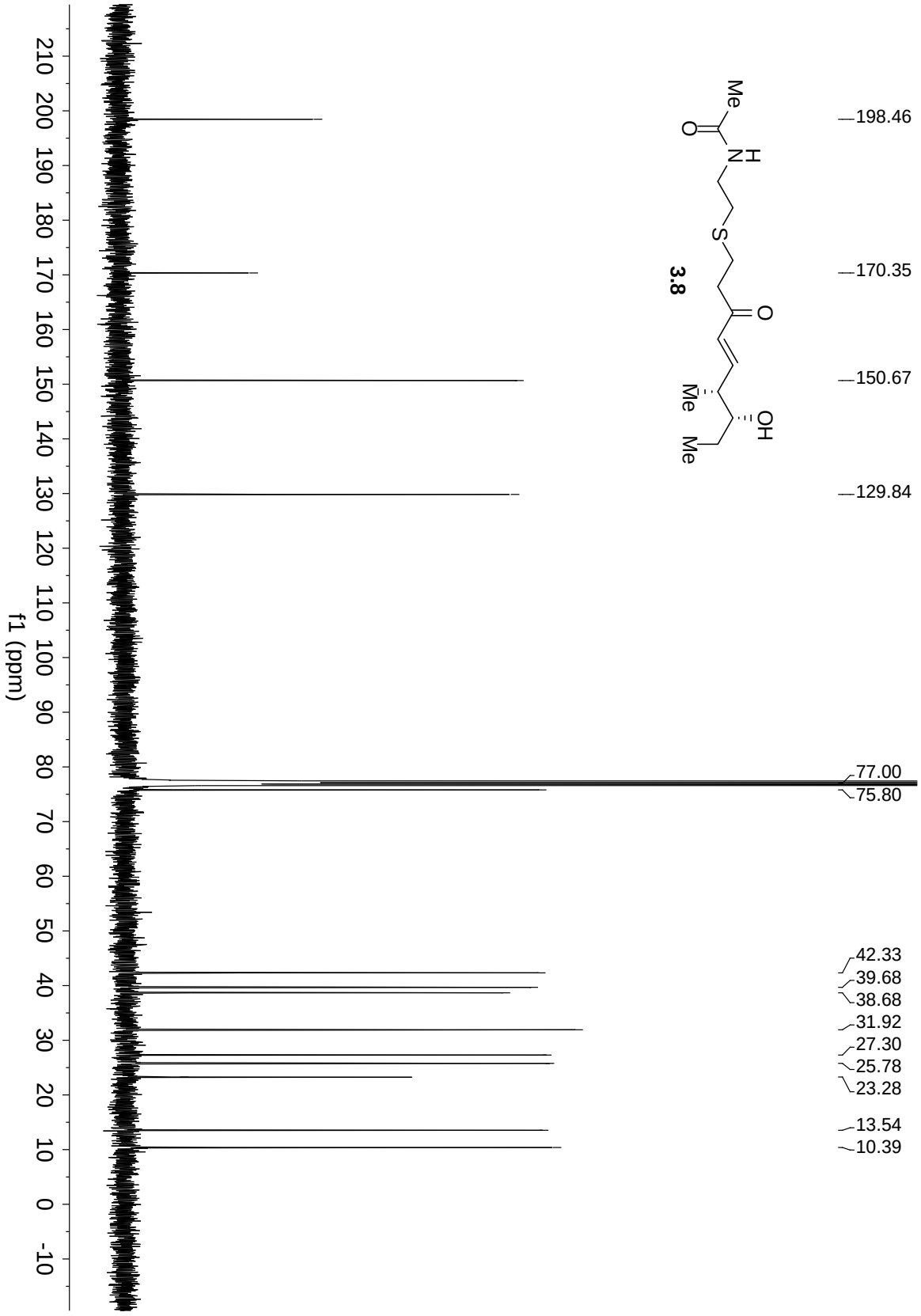
198.46
170.35
150.67
129.84
77.00
75.80
42.33
39.68
38.68
31.92
27.30
25.78
23.28
13.54
10.39
f1 (ppm)
3.8